NOVEMBER 2025
VOLUME 84
ISSUE
11

ANNALS OF THE RHEUMATIC DISEASES

THE EULAR JOURNAL

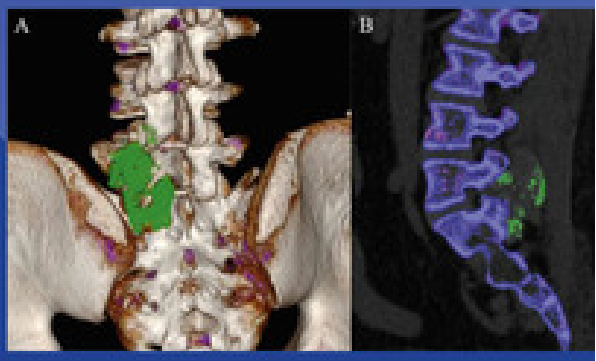

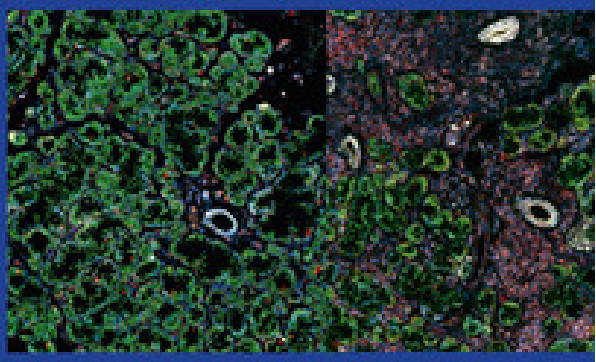

ELSEVIER

eular
EUROPEAN ALLIANCE OF ASSOCIATIONS FOR RHEUMATOLOGY

The home of innovative rheumatology research

Ann Rheum Dis 84 (2025) 1757–1759

Contents lists available at ScienceDirect

Annals of the Rheumatic Diseases

journal homepage: https://www.sciencedirect.com/journal/annals-of-the-rheumatic-diseases

Editorial

When borders impact science: what is the future of European rheumatology research?

INTRODUCTION

The beginning of 2025 has seen notable significant geopolitical developments resulting in adjustments to funding across various sectors, including scientific research. These changes have parked reflections and concerns within the scientific community, prompting the creation of the "Stand up for Science" movement in support of international research.

Long regarded as a key hub for science, education, and technology, the United States (US), similar to other countries, now appears to be adjusting its priorities with a stronger focus on domestic economic policies, including the reintroduction of trade barriers and tariffs. In addition, budgetary revisions have reportedly led to situations where previously awarded grants were withdrawn, causing certain research programs to be paused. For instance, in the US, reductions in National Institutes of Health (NIH) funding have reportedly led some laboratories to scale down or suspend projects.

This evolving situation raises questions about its impact on scientific research and international collaborations, particularly in rheumatology. The COVID-19 pandemic demonstrated the crucial value of pooling expertise to accelerate discoveries. In this context, it is worth reflecting on how the future ties between European and American rheumatology research might evolve?

THE ESSENTIAL ROLE OF INTERNATIONAL FUNDING

Scientific research, similar to many other fields, is fundamentally reliant on adequate funding. At the European level, various financial support mechanisms are available, including the Horizon 2020 framework, the Marie Skłodowska-Curie Actions —designed to support researchers at all career stages while promoting mobility and scientific excellence—and funding from the Foundation for Rheumatology Research (FOREUM) and the Assessment of SpondyloArthritis International Society (ASAS). At a national level, European countries generally offer various funding mechanisms for research, and often local rheumatology societies also offer smaller research support.

In axial spondyloarthritis (SpA) research, among the 39 clinical trials published in 2024, 15 (38%) involved collaboration between European and North American teams, highlighting the great transatlantic relationship in this particular field with various and international fundings. This trend extends across rheumatology, illustrating the mutual connections of research systems.

In 2024, the NIH budget was approximately $47 billion, of which 132 projects totalling around $74.5 million, roughly 0.15%, were allocated to researchers based in Europe. The direct consequences of NIH budget cuts on European rheumatology research remain modest but the potential indirect consequences are more substantial. Recent cutbacks to science funding risk progressively weakening transatlantic research ties, limiting opportunities for collaboration, knowledge exchange, and joint innovation.

ESSENTIAL INTERNATIONAL SCIENTIFIC COOPERATION

One of the most significant recent breakthroughs in SpA research has involved American and several European teams. The discovery of resident cells expressing the interleukin (IL)-23 receptor in entheses by Sherlock et al [1] was a pathophysiological revolution for spondyloarthritis, even if today anti-IL-23 therapies have failed to treat axial SpA. This study resulted from a collaboration between researchers from the University of Birmingham and Oxford in the United Kingdom (UK), Stanford in the USA, and the Institut Pasteur in France, emphasising the importance of international cooperation.

From a therapeutic perspective, the history of tumour necrosis factor (TNF) and its inhibition in inflammatory rheumatic diseases is another example of the impact of international partnerships in scientific research [2]. The demonstration of TNF overexpression in rheumatoid arthritis dates back to the 1980s by Brennan et al [3]. Preclinical studies conducted at the Kennedy Institute of Rheumatology in the UK [4] laid the foundation for the development of clinical research projects in rheumatology through collaboration with an American company (Centocor, which has since been acquired by Johnson & Johnson), which developed a chimeric (mouse Fv, human IgG1) neutralising antibody with high affinity for TNFα, now known as infliximab [5]. As for adalimumab, the first fully human antibody, its development also resulted from a transatlantic collaboration between Cambridge Antibody Technology, Knoll AG-BASF Pharma, and the American firm Abbott [6]. The concept of TNF neutralisation was a collaborative effort between several countries across the world.

The inhibition of IL-6 is also a prime example of international collaboration. The role of IL-6 in inflammatory diseases such as rheumatoid arthritis stems from Japanese studies [7], and the development of tocilizumab also involved European teams [8]. Finally, regarding IL-17 in spondyloarthritis, the first study highlighting increased serum IL-17 levels in spondyloarthritis came from an European (French) team [9], which led to

https://doi.org/10.1016/j.ard.2025.06.2125
Received 27 March 2025; Revised 12 June 2025; Accepted 14 June 2025

subsequent evaluation of IL-17 blockade with secukinumab in inflammatory rheumatic diseases [10,11], developed by Novartis.

All of these examples demonstrate that the development of pharmaceuticals is a global affair and the transatlantic scientific partnerships have been particularly productive in rheumatology.

The joint development of criteria and treatment recommendations by the American College of Rheumatology (ACR) and the European League Against Rheumatism (EULAR) is a clear example. This kind of international collaboration offers a stable, independent platform to support scientific progress. It has also been reinforced by joint funding mechanisms such as those between the Foundation for Research in Rheumatology and the Rheumatology Research Foundation (RRF).

WHAT COULD BE THE CONSEQUENCES OF GEOPOLITICAL CHANGES IN RHEUMATOLOGY RESEARCH?

If the current US policy changes and modifications in certain grant mechanisms, were to continue or intensify, several aspects of rheumatology research might be affected:

1. Potential reduction of transatlantic funding: a decrease in bilateral fundings opportunities could limit the scope of collaborative projects and reduce funding opportunities for European and US researchers.
2. Possible restriction on access to technology and reagents: many reagents, automated systems and biomarkers are developed by US-based firms. Any barriers to exchanges could potentially slow European research and innovation.
3. Impact on scientific mobility: young European researchers might encounter fewer opportunities for training and collaborative experience in the US, reducing their exposure to key expertise and network. In addition, visa restrictions may reshape the global scientific landscape, potentially creating new opportunities for European research centres by increasing access to a broader pool of talented international researchers for recruitment.

Given this evolving context, it seems timely to reflect on and adapt funding and collaboration strategies in Europe. Several avenues could be explored:

- Strengthening European cooperation: enhanced pooling of infrastructures and resources within the European Union could help mitigate the effects of changing geopolitical priorities. The JAK-Pot study [12] and the *EURO-SpA* registry [13] are examples of successful collaborations between European countries.
- Expanding European research funds: recent initiatives such as "Choose Europe for Science" and similar national initiatives represent essential steps in strengthening European support for scientific research in general, support from which rheumatology research could clearly benefit. Diversifying funding sources, particularly by enhancing support from private foundations and European industries, would offer valuable resilience.
- Promoting collaborative research: highlighting intercontinental cooperation models could encourage the continuation of partnerships regardless of political developments. Collaborative efforts such as the development of recommendations and classification criteria jointly endorsed by ACR and EULAR remain prime examples to support and expand.
- Supporting European and national task forces: initiatives, such as ASAS which just celebrated its 30th anniversary [14] has united researchers interested in SpA research and has accelerated both clinical and basic studies.
- Expanding new international collaborations including Canada, Australia, and Asian countries.

Rheumatology research, and medical research more broadly, can only thrive through strong international collaborations. A potential decline in international collaborations should not be seen as an inevitable setback, but as an opportunity to rethink and strengthen research strategies. Strengthening European initiatives, developing national and continental consortia, and cultivating diverse international partnerships will help secure the future of scientific innovation.

In conclusion, although shifts in global policy and funding landscapes may present challenges, they also provide an opportunity to reassess how we foster collaboration and innovation. By remaining open, constructive, and forward-looking, the scientific community can continue to build bridges across borders. Strengthening European frameworks, diversifying partnerships, and embracing flexibility will not only safeguard but also enhance the resilience and impact of rheumatology research in the years ahead.

Competing interests

The author declares no competing interests.

Patient consent for publication

Not applicable.

Provenance and peer review

Not commissioned; externally peer reviewed.

Orcid

Frank Verhoeven: http://orcid.org/0000-0003-2708-2918

Frank Verhoeven *
Rhumatologie, CHU de Besançon, Besançon, France
Université Marie et Louis Pasteur, EFS, INSERM, RIGHT (UMR 1098), F-25000 Besançon, France
CNRS, UMR 5525, T-RAIG, TIMC, Université Grenoble Alpes, Grenoble, France

Athan Baillet
CNRS, UMR 5525, T-RAIG, TIMC, Université Grenoble Alpes, Grenoble, France

Celine Demougeot
Université Marie et Louis Pasteur, EFS, INSERM, RIGHT (UMR 1098), F-25000 Besançon, France

Xavier Romand
CNRS, UMR 5525, T-RAIG, TIMC, Université Grenoble Alpes, Grenoble, France

Daniel Wendling
Rhumatologie, CHU de Besançon, Besançon, France

Axel Finckh
University of Geneva, Geneva Center for Inflammation Research (GCIR), Geneva, Switzerland
Rheumatology, Geneva University Hospital, Geneva, Switzerland

Francesco Ciccia
Department of Precision Medicine, University of Campania "L. Vanvitelli", Naples, Italy

Rik Lories
Department of Development and Regeneration at KU Leuven, Leuven, Belgium

Clement Prati
Rhumatologie, CHU de Besançon, Besançon, France
Université Marie et Louis Pasteur, EFS, INSERM, RIGHT (UMR 1098), F-25000 Besançon, France

*__Correspondence to__ Dr Frank Verhoeven, Rhumatologie, CHRU Jean Minjoz, 2 Boulevard Fleming, F-25030 Besançon, France.

REFERENCES

[1] Sherlock JP, Joyce-Shaikh B, Turner SP, Chao CC, Sathe M, Grein J, et al. IL-23 induces spondyloarthropathy by acting on ROR-γt+ CD3+CD4-CD8- entheseal resident T cells. Nat Med 2012;18(7):1069–76.
[2] Feldmann M, Maini RN. Discovery of TNF-α as a therapeutic target in rheumatoid arthritis: preclinical and clinical studies. Joint Bone Spine 2002;69:12–8.
[3] Brennan FM, Chantry D, Jackson AM, Maini RN, Feldmann M. Cytokine production in culture by cells isolated from the synovial membrane. J Autoimmun 1989;2:177–86.
[4] Elliott MJ, Maini RN, Feldmann M, Long-Fox A, Charles P, Katsikis P, et al. Treatment of rheumatoid arthritis with chimeric monoclonal antibodies to tumor necrosis factor alpha. Arthritis Rheum 1993;36:1681–90.
[5] Elliott MJ, Maini RN, Feldmann M, Kalden JR, Antoni C, Smolen JS, et al. Randomised double-blind comparison of chimeric monoclonal antibody to tumour necrosis factor alpha (cA2) versus placebo in rheumatoid arthritis. Lancet 1994;344:1105–10.
[6] Kempeni J. Preliminary results of early clinical trials with the fully human anti-TNFalpha monoclonal antibody D2E7. Ann Rheum Dis 1999;58(Suppl 1(Suppl 1)):I70–2.
[7] Miyasaka N, Sato K, Hashimoto J, Kohsaka H, Yamamoto K, Goto M, et al. Constitutive production of interleukin 6/B cell stimulatory factor-2 from inflammatory synovium. Clin Immunol Immunopathol 1989;52:238–47.
[8] Choy EH, Isenberg DA, Garrood T, Farrow S, Ioannou Y, Bird H, et al. Therapeutic benefit of blocking interleukin-6 activity with an anti-interleukin-6 receptor monoclonal antibody in rheumatoid arthritis: a randomized, double-blind, placebo-controlled, dose-escalation trial. Arthritis Rheum 2002;46:3143–50.
[9] Wendling D, Cedoz JP, Racadot E, Dumoulin G. Serum IL-17, BMP-7, and bone turnover markers in patients with ankylosing spondylitis. Joint Bone Spine 2007;74:304–5.
[10] Hueber W, Patel DD, Dryja T, Wright AM, Koroleva I, Bruin G, et al. Effects of AIN457, a fully human antibody to interleukin-17A, on psoriasis, rheumatoid arthritis, and uveitis. Sci Transl Med 2010;2(52):52ra72.
[11] Baeten D, Baraliakos X, Braun J, Sieper J, Emery P, van der Heijde D, et al. Anti-interleukin-17A monoclonal antibody secukinumab in treatment of ankylosing spondylitis: a randomised, double-blind, placebo-controlled trial. Lancet 2013;382:1705–13.
[12] Lauper K, Iudici M, Mongin D, Bergstra SA, Choquette D, Codreanu C, et al. Effectiveness of TNF-inhibitors, abatacept, IL6-inhibitors and JAK-inhibitors in 31 846 patients with rheumatoid arthritis in 19 registers from the 'JAK-pot' collaboration. Ann Rheum Dis 2022;81(10):1358–66.
[13] Ørnbjerg LM, Brahe CH, Askling J, Ciurea A, Mann H, Onen F, et al. Treatment response and drug retention rates in 24 195 biologic-naïve patients with axial spondyloarthritis initiating TNFi treatment: routine care data from 12 registries in the EuroSpA collaboration. Ann Rheum Dis 2019;78:1536–44.
[14] van der Heijde D, Navarro-Compán V, Landewé R, Sieper J, van Gaalen F, Gensler LS, et al. 1995-2025: thirty years of ASAS and its contribution to the understanding of spondyloarthritis. Ann Rheum Dis 2025;84:382–7.

Ann Rheum Dis 84 (2025) 1760–1769

Contents lists available at ScienceDirect

Annals of the Rheumatic Diseases

journal homepage: https://www.sciencedirect.com/journal/annals-of-the-rheumatic-diseases

Review

The shared debt of art and rheumatology

Alain Saraux[1,*], Dominique Le Nen[2,3], on behalf of the Brest art-lover physician group

[1] *Department of Rheumatology and Pole PHARES (Pharmacie, Recherche, Epidémiologie, Santé Publique et Santé au Travail), Université de Bretagne Occidentale (Univ Brest), CHU Brest, INSERM (U1227), LabEx IGO, Brest, France*
[2] *Department of Orthopaedic Surgery, Université de Bretagne Occidentale (Univ Brest), CHU Brest, Brest, France*
[3] *Department of History of Science and Technology (UR 1161), Brest/Nantes, France*

ARTICLE INFO

Article history:
Received 10 May 2025
Received in revised form 9 July 2025
Accepted 10 July 2025

ABSTRACT

Medicine is not part of the fine arts. However, it is the art, scientifically informed, of care. Rheumatology in particular requires the ability to observe, listen, feel and interpret with humanity to care for people with musculoskeletal diseases. This narrative review explores the reciprocal links between art, artists, and musculoskeletal systems to seek to balance the debt of rheumatology to art with the debt of art to rheumatology over time. Before the Renaissance, knowledge about rheumatology was relatively poor and was largely restricted to Hippocratic theories and animal descriptions provided by Galen, and therefore poorly represented by artists. From 1480 to 1520, painters began to establish the field of artistic anatomy, focusing on the science of external forms. Although its impact on understanding rheumatic diseases was minimal, it led to the identification of anatomical structures affected by these conditions. Thus, human anatomy was born. After 1700, poor hygiene, a lack of physical activity, and overeating by the middle class were believed to be likely external causes of joint diseases, particularly gout, which was often conflated with other arthritis. Inspired by painters who idealised thermal baths, spas and seaside facilities were developed, promoting sports, hygiene, wellness, and healthy gastronomy. This gave birth to hydrotherapy. Patients with rheumatic diseases began congregating in balneological and thermal cities, allowing physicians to better describe the nosology of musculoskeletal diseases. Thus, rheumatology was born. More than 200 musculoskeletal conditions were documented between 1800 and 2000. Art and rheumatology share a debt, and rheumatologists began to engage with patients through art.

INTRODUCTION

Homo sapiens, who emerged in Africa, utilised dance, rhythmic musical sounds, and paintings as cultural innovations with symbolic social meanings rather than merely aesthetic purposes [1]. Over time, art has allowed humans to represent their perceptions of the world, their bodies, and diseases with varying degrees of accuracy. There is no consensus definition of art, other than its recognition as such by a group of individuals. Today, art is defined as the expression or application of human creative skill and imagination, producing works appreciated for their aesthetic value or emotional power, thereby establishing a link between the artist and the spectator [2,3]. The broadest definition encompasses architecture, sculpture, visual arts

*Correspondence to Prof Alain Saraux, Rheumatology Unit, Hôpital de la Cavale Blanche, Brest, France.
E-mail address: alain.saraux@chu-brest.fr (A. Saraux).

Lou Autret, Clara Calon, Lena Eychenne, Yann Meudic, Charlotte Oleron, Benoit Rieth, Corentin Simier, and Mathilde Tomes (students in master 1), Guillaume Bronsard (professor of child psychiatry), Fréderic Dubrana (professor of orthopaedic surgery), Dominique Le Nen (professor of orthopaedic surgery) and Alain Saraux (professor of rheumatology).

Handling editor Josef S. Smolen.

https://doi.org/10.1016/j.ard.2025.07.012

(painting, drawing, photography), music, literature (poetry, dramaturgy), performing arts (theatre, dance, mime, etc.), cinema, media arts, comics and gastronomy.

Some rheumatologists are involved in various art forms through writing, drawing (anatomy description through ultrasound expansion) [4], painting, music, etc. Their example can be highlighted to maintain the necessary link between art and rheumatology, which was important in the past. For 2 years, the French Society of Rheumatology welcomed the work of rheumatologists and patients in a dedicated space called Rheum' artist. Better knowledge of history of both rheumatology and art may help to understand their interconnection.

This narrative review explores the reciprocal links between art, artists, and healthy and pathological musculoskeletal conditions over time. In other words, we seek to balance the debt of rheumatology to art with the debt of art to rheumatology. So, the research question is: What are the contributions of rheumatology to the arts, but equally, how does artistic practice affect rheumatic conditions?

For this purpose, as art is poorly represented in medical literature, we conducted distinct literature reviews on PubMed and Google using the key words 'rheumatology' or 'musculoskeletal' and the key words of various arts: 'architecture', 'sculpture', 'visual arts', 'painting', 'drawing', 'photography', 'music', 'poetry', 'dramaturgy', 'theatre', 'dance', 'mime', 'cinema', 'media arts', 'comics', and 'gastronomy'.

We selected all academic articles describing any link between these forms of art and rheumatology and classified them as debt of rheumatology to art or debt of art to rheumatology.

This review begins with a succinct account of the historical interactions between art and rheumatology. We then examine the development of rheumatology, noting its roots in the anatomical understanding cultivated by painters, the growing movement towards improved hygiene practices, and artistic conceptions of rehabilitation tailored for rheumatic patients. Finally, we explore the influence of rheumatology on artistic expression and its role in the creative achievements of artists.

THE HISTORY OF ART AND RHEUMATOLOGY IN BRIEF

No uncontroversial subsets can separate art history into periods, as artists find inspiration in time and space to make their marks. In brief [1–3], cave art, which has been found on all continents and produced during prehistoric periods, primarily depicts animals hunted (such as bison or antelope) and human symbols (such as hands and faces). The intended purpose is still unknown to us. During antiquity, cities were built where various events (religious, historical, natural phenomena) were depicted on different media by artisans or artists who could often be considered inseparable. Art became predominantly religious during the Middle Ages and linked to divine punishment. The discovery of perspective by the Florentine architect Filippo Brunelleschi (1377-1446), with Leon Battista Alberti as its first theorist [5], allowed for the gradual emergence of realism. Paintings became coherent spaces that included backgrounds, landscapes, characters, and depth created by shadows and movement. The Renaissance period in Europe aimed to represent reality based on scientific knowledge (including anatomy and perspective architecture). Western art distanced itself from the arts of other regions, which evolved independently, only to converge again with globalisation. From 1900 to 1945, neuroscience emerged in the medical field, whereas nihilism arose as a consequence of wars, the Holocaust, and inequalities stemming from colonisation and racism, leading to a loss of religious meaning. The pathologies represented during this time by expressionists and surrealists were primarily mental illnesses, psychological trauma, and psychic suffering. Contemporary art, that is, art produced from 1945 to the present, primarily addresses societal and personal themes such as ecology, terrorism, migration, gender issues, exclusion, societal anxiety, and indifference.

The majority of diseases that are recognised today did not appear at all in the arts over the time, either because their prevalence has fluctuated over time (diabetes and metabolic diseases were probably relatively rare before the Renaissance and autoimmune and allergic diseases were probably rare before industrialisation), because they were not named (cases were too rare to be categorised and studied without grouping patients into specific specialties, eg, cardiology, pneumology, etc.), because they were only visible because of their complications (many invisible diseases, such as diabetes or hypertension, are now treated preventively, with the burden being more related to the complexity of care rather than the symptoms), or because they were considered expected (posttraumatic conditions, ageing-related issues, divine punishments).

The representation on rheumatic diseases in art has been poorly studied. Most rheumatic diseases, which can affect joints, muscles, and bones, causing pain, swelling, and stiffness, potentially leading to joint deformities, were unknown and also underrepresented in art. Indeed, before the Renaissance, knowledge about rheumatology was limited and was largely based on the Hippocratic theories (AD 460-377) and descriptions provided by Galen (AD 129-216). Although arthritis suggestive of gout was recorded by Egyptians and Greeks, gouty arthritis (podagra) was clearly described by the English physician Thomas Sydenham (1624-1689) in 1683 [6]. Rheumatoid arthritis was distinguished from gout in 1800 by a French resident physician, Augustin Jacob Landre-Beauvais (1772-1840) [7], and was named as such in England by a physician, Sir Alfred Barring Garrod (1819-1907), in 1858 [8]. Various rheumatic diseases, including spondylarthritis, were recognised around 1880 by 3 neurologists: the German Adolf Von Strümpell (1853-1925), the Russian Vladimir Bekhterev (1857-1927) and the French Pierre Marie (1853-1940) [9]. Rheumatology was only fully differentiated as a distinct field during the 20th century, with most rheumatic diseases being named after 1900. Over 200 musculoskeletal conditions are currently known. They arise from various mechanisms, including overuse, genetic predisposition, infections, and autoimmunity. Common diseases treated by rheumatologists include osteoarthritis, gout, rheumatoid arthritis, and chronic back pain, including spondylarthritis, tendinitis/bursitis, and lupus, among others [10].

Rheumatology requires the ability to observe, listen, feel, and interpret and clinical examination remains the main part of evaluation in 2025, when other specialties use machines rather than clinical evaluation (eg, cardiology). Rheumatology is an art in the sense that it is more artisanal than artistic but can feed itself from the knowledge of the arts. For the philosopher André Comte-Sponville, medicine, obviously, is not part of the fine arts; its purpose is health, not beauty. However, it is an art in that its purpose (the patient's health) is part of its definition. It is, therefore, the art, scientifically informed, of care [11]. The Dutch painter Vincent van Gogh (1853-1890) [12] wrote to his brother, "The more I think about it, the more I feel that there is nothing more truly artistic than loving people".

KNOWLEDGE OF MUSCULOSKELETAL ANATOMY DUE TO PAINTERS AND SCULPTORS

The human body conceals an interiority that remained largely unknown until the Renaissance, except through the

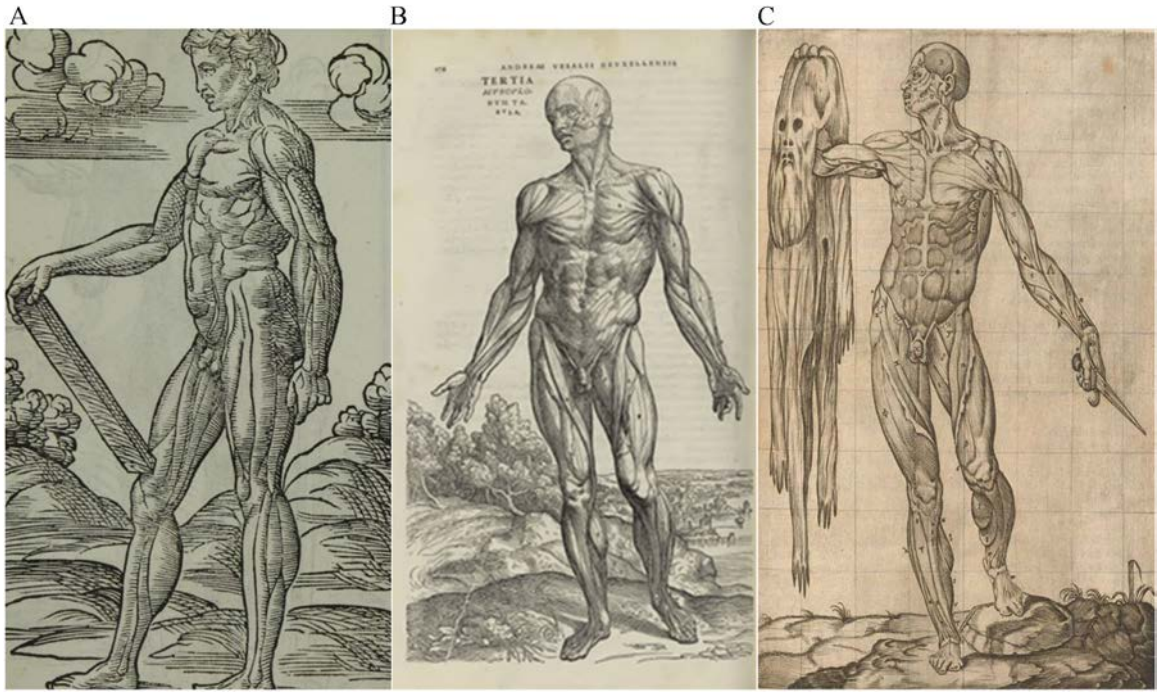

Figure 1. Anatomy during Renaissance period. (A) *Musculi exteriores laterales corporis humanis.* Berengario da Carpi Commentaria cum amplissimis additionibus super anatomia Mundini: Hieronymus de Benedictis, 1521. (B) *Musculi corporis humanis*. Andreas Vésalius Ouvrage: *De humani corporis fabrica libri septem*, Bâle, Ex officina Joannis Oporini, 1543. (C) *Tabla primera del libro, secundo.* Valverde de Amusco: *Historia de la composicion del cuerpo humano*, 1556. Source: Public domain.

writings of Galen, which have survived the centuries and are based on the work of his predecessors and animal dissection. For centuries, the observation of deep lesions in arenas or battlefields, along with the extrapolation of animal anatomy to humans, was the primary means of understanding the human body. It was only from the 13th and 14th centuries onwards that anatomists began moving beyond the superficial layers of the body to gain a better understanding of its internal structures, particularly for autopsy purposes [13]. Two anatomists are particularly associated with the first human dissections: Henri de Mondeville (1220-1316), the surgeon to French King Philippe Le Bel, and his contemporary, Mondino dei Luzzi (1270-1326), a physician at the University of Bologna in Italy [14].

By the end of the 15th century, however, anatomical references were still minimally related to musculoskeletal and joint anatomy. Three works were considered definitive at the time: Mondino dei Luzzi's *Anathomia*, first published in Pavia in 1478 and reprinted 33 times until 1541, with or without commentary; Jean de Ketham's *Fasciculus medicinae* [15], which partially reproduces *Anathomia*; and *La Grande Chirurgie* by the French Guy de Chauliac (1300-1368), a pupil of Mondino. Unfortunately, the anatomical illustrations included in these texts were rudimentary. Similarly, in early 16th century Italy—the cradle of anatomy—works by the renowned physicians Bartolomeo Compagnana, Hieronymo Manfredi, Gabriele Zerbi, Alessandro Benedetti, and Alessandro Achillini were published without iconography.

The first significant descriptions and representations of the musculoskeletal system in the form of flayed figures are attributed to Jacopo Berengario da Carpi (1457-1530) [16], who included these in his *Commentaria cum amplissimis super anatomia Mundini*, published in 1521, the first genuinely illustrated book in the history of anatomy (Fig 1A). This was followed by the *De Humani Corporis Fabrica*, published in 1543 and reprinted in 1555 [17] (Fig 1B), written by the Dutch Andreas Vésalius (1514-1564).

Alongside anatomists, artists began to develop a fascination with the human body, particularly during the High Renaissance period (1480-1520), often regarded as the golden age of anatomy [18]. The inability of anatomists to accurately depict the musculoskeletal system provided a significant opportunity for artists, some of whom collaborated with doctors to illustrate surgical studies. For example, the Italian Girolamo da Carpi (1501-1556) created 54 plates for Giovanni Battista Canano's treatise on myology around 1541. In Florence, Italy, painters belonged to the same guild as doctors and apothecaries—the *Arte dei Medici e Speziali*—contributed to this collaboration, although it was not the only factor.

As both an artist and an anatomist who practiced dissection, the Italian Leonardo da Vinci (1452-1519) is an exception. He produced drawings of remarkable accuracy and artistic value, particularly those of the musculoskeletal system, around 1510 [19,20].

Independent of medical practitioners, artists established a field known as artistic anatomy, which studied the external forms of the body (morphology) and their relationship with the deeper anatomical structures that comprise the skeleton. They elevated anatomy to the level of a subject taught in fine arts schools. The first such school, founded in 1563 under the auspices of Giorgio Vasari (1511-1574), the biographer of Italian painters, and Michelangelo (1475-1564), was the *Accademia delle Arti del Disegno* in Florence, Italy.

Artists sought knowledge of anatomy not merely as support for their creations, following the precepts of the Italian Leon Battista Alberti (1404-1472), the first theoretician of painting, who advocated for an anatomical education for artists in his *De Pictura* (published in 1435). Instead, they sought to theorise art by establishing its scientific basis and elevating painters from the status of mere craftsmen [21].

For artists, drawing, painting, or sculpting the body fuelled a desire to represent its muscular reliefs as accurately as possible.

Transitioning from the idealised form of Greek statuary to a more authentic representation in Renaissance art was not a simple task. Apart from intentionally symbolic or metaphorical representations, the results sometimes surpassed nature. This led Leonardo da Vinci to critique contemporary painters for depicting stereotypes or creating figures that looked more like bags of walnuts than human forms and more like boots of radishes than muscular nudes [17].

The study of anatomical subjects, often conducted with the assistance of doctors or through dissections performed by artists in hospitals, convents, or private settings, complemented the observations of models and Greek statuary. This Italian movement towards a 'figuration of the body', initiated by prominent artists such as Luca Signorelli (1445-1523), Leonardo da Vinci, Michelangelo, Raphaello Sanzio (1483-1520), and Baccio Bandinelli (1493-1560), thrived within the cultural revival centres of Florence—the 'City of Lilies'—and Rome, the 'Eternal City'. This evolution began at the end of the 15th century and peaked during the 16th century.

The Renaissance witnessed the emergence of a true 'cult' of the nude and the 'écorché', the *uomo scorticato*, alongside a culture of anatomical drawings that focused on torsos, arms, and legs. This was a fertile period for interactions among artists, exemplified by a drawing by the Italian Bartolomeo Passarotti (1529-1592) (in the Louvre Museum) that depicts a dissection attended solely by artists. The depiction of the naked body at the end of the Middle Ages, shifting from a biblical representation that emphasised modesty and moral beauty over physical beauty, required a paradigm shift. This transformation aimed to restore the beauty championed in ancient Greece, encompassing both pagan mythological and biblical iconography. Certain artists came to believe and assert that the representation of the nude could be achieved only through a solid understanding of anatomy.

Among the most famous 'écorchés' are the Spanish Juan Valverde's engraving of the flayed man holding his skin (Fig 1C) [22] and the Italian sculptures Flayed Man Dancing by Baccio Bandinelli, Michelangelo's own 'écorché', and Marco d'Argate's 'écorché' of Saint Bartholomew in the Duomo of Milan.

On this basis, figurative art uses knowledge of the musculoskeletal system to represent the human body authentically. In 1632, the Dutch painter and printmaker Rembrandt van Rijn (1606-1669) painted the renowned *Anatomy Lesson of Dr. Nicolaes Tulp*, depicting surgeons performing a dissection. In 1803, the French Guillaume Dupuytren (1777-1835) and René Laennec (1781-1826) founded the Society of Anatomy in Paris, France. Prominent anatomists, such as Henry Vandyke Carter (1831-1897) [23] and Frank H. Netter (1906-1991) [24], drew artistic atlases of anatomy—*Gray's Anatomy* and *Netter's Atlas*, respectively—which remain authoritative references to this day.

After 1900, many painters, such as the Italian artist Amedeo Modigliani (1884-1920), who depicted models with deliberately elongated necks (Fig 2); the French painter Chaïm Soutine (1893-1943), known for his asymmetrical faces; and contemporary artists, such as the French painter Paul Bloas (1961-), who illustrated workers at the Brest arsenal, represented disproportionate bodies to express their feelings rather than to faithfully reproduce their models (Fig 2). Similarly, sculptors such as the Italian Alberto Giacommetti (1901-1966) and Columbian Fernando Botero (1932-2023) created thin and rounded sculptures, respectively. I had the opportunity to discuss this point with Paul Bloas (personal communication), who confirmed that his objective was to create disproportionate hands in blue-collar workers. This distortion was intended to express both their manual labour and their desire for human connection, deliberately breaking with the rules of proportion depicted and systematically employed by painters from the Renaissance through the 19th century. The body deformations seen in paintings and sculptures from the Neolithic period to the Renaissance were likely due more to an imperfect knowledge of proportion than to a specific artistic intent to deform. This fact complicates the retrospective iconodiagnosis of rheumatic diseases, which were evoked in previous articles [25–29].

Figure 2. Examples of portraits that have been distorted. (A) Woman with blue eyes, Amedeo Modigliani- 1918, Musée d'art moderne, Paris. Source: Public domain. © Photo Alain Saraux (B) To our fathers, Paul Bloas- 2023, Brest museum. With permission from Paul Bloas. © Photo Alain Saraux.

A HEALTHY LIFESTYLE RECOMMENDED BY 19TH AND 20TH CENTURY ARTISTS

Anatomy has had a limited impact on understanding rheumatic diseases; however, it has facilitated identifying involved areas. Although artists were largely unaware of the mechanisms underlying rheumatic diseases, they observed a link between unhealthy lifestyles and joint swelling, leading them to advocate for lifestyle changes for patients suffering from rheumatism.

The creation of thermal and balneological architecture

Water has long been used for health recovery and therapeutic purposes across Arabic, Greek, and Roman cultures. Egyptians also utilised seawater for its therapeutic benefits. The idealisation of baths was propelled by painters such as the French Jean-Auguste-Dominique Ingres (1780-1867) and his pupil Theodore Chassériau (1819-1856), the Dutch painter Lawrence Alma-Tadema (1836-1912), and the Brazilian Pedro Weingärtner (1853-1929). This resulted in establishing health facilities in the 18th and 19th centuries, initially in England, Germany, and France, and later across Europe and the world, evolving into leisure facilities by the 20th century. Hydrotherapy, encompassing balneotherapy (drinking and/or bathing in medicinal water, as well as soaking in warm or cold water or mud) and spa therapy (drinking and/or bathing in thermal or mineral water) [30,31], emerged as curative and preventive treatments for rheumatism.

European architects created grand resorts to attract wealthy patrons from bustling cities, curists who would contribute to economic vitality. The architectural styles of the thermal baths, hotels, and casinos were characterised by the Regency, Victorian

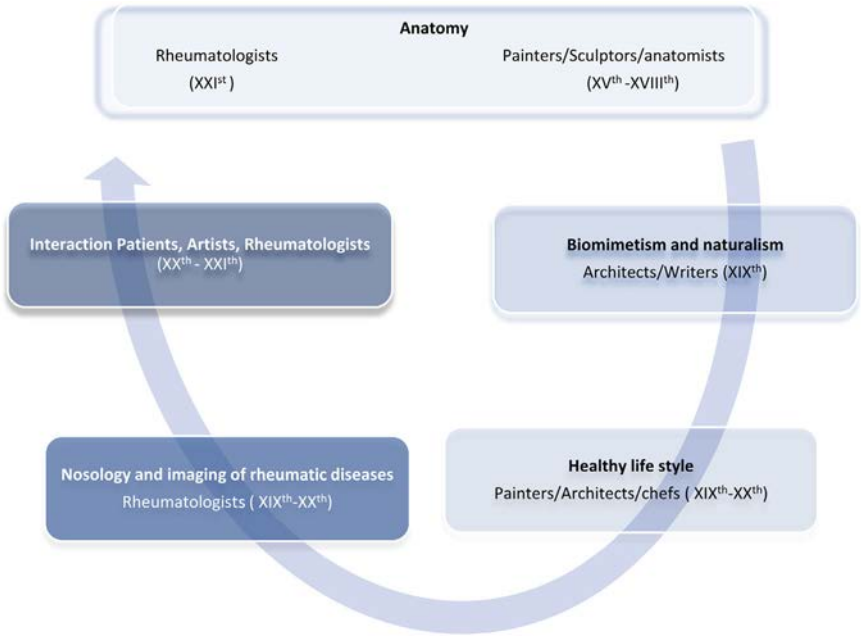

Figure 3. Respective role of artists and rheumatologists in rheumatology knowledge.

and Edwardian styles in England, the Belle Époque style, often adorned with mosaics, Art Deco elements, stucco decorations, and Neo-Byzantine influences in France, and the Neo-Renaissance style in Belgium and Germany. So, many European villages with ancient springs or thermal baths (such as Bad Ems, Baden-Baden, Bad Kissingen, Baden Bei Wien, Bath, Frantiscovi Lazne, Kalovy Vary, Marianske Lazne, Montecatini or Vichy) as well as seaside resorts (Brighton, Cabourg or Trouville, etc.) developed rapidly, attracting affluent visitors. These magnificent resorts, where the 19th-century middle class mingled with patients suffering from rheumatism and their entourages, served as a source of inspiration for many artists. Notably, the French novelist Marcel Proust (1871-1922) wrote while staying at the Grand Hotel of Cabourg (Normandy, France). Many French painters, such as Eugène Boudin (1824-1898) and René Xavier Prinet (1861-1946), as well as the Spanish Joaquin Sorrolla (1863-1923) and the American painter William Merritt Chase (1849-1916), depicted the middle class and nobility enjoying leisure time on the beaches. These artistic productions created considerable public awareness, ultimately driving an influx of patients suffering from rheumatic diseases, for which a dedicated medical specialty had yet to fully develop.

As patients with rheumatic diseases were gathered in spas and bathing establishments, a more refined nosology began to emerge, driven particularly by early pioneers of rheumatology: Vincenz Priessnitz (1799-1851) in Austria, Fortescue Fox (1858-1940) in the UK, Jacques Forestier (1890-1978) in France, and Max Hirsh (1875-1941) in Germany [32–35]. Vincenz Priessnitz established the world's first hydrotherapy institute in Grafenberg in 1822, laying the foundations for this new treatment [32]. Fortescue Fox, the founder and president of the International League against Rheumatism, played a crucial role in establishing an innovative outpatient clinic in the UK and is regarded as a founding father of British rheumatology and medical rehabilitation [33]. Jacques Forestier, an Olympic medallist and thermal physician in Aix-les-Bains, is known for describing polymyalgia rheumatica, discovering the effectiveness of gold salts in treating rheumatism, and developing advanced radiological contrast products [34,35]. He is considered the father of French rheumatology. Other thermal physicians, such as Marx Hirsh in Germany, also contributed significantly to the field [35]. The bath indices developed in the thermal city of Bath serve as criteria for monitoring spondylarthritis [36], illustrating the always active role of thermal cities in advancing rheumatological knowledge.

So, rheumatology has anatomy and hydrotherapy for parents, which have been influenced by artistic movements, confirming that both art and the field of rheumatology mutually enrich each other. Figure 3 summarises these associated legacies. Anatomy is always a pillar of rheumatology, especially through ultrasonography. Hydrotherapy has almost disappeared from rheumatological management, but physical activity, food hygiene and rehabilitation remain essential in preventive management.

The chef of kings becomes the king of chefs

During this same period, the renowned gastronomist Antonin Carême (1783-1833), a prominent head chef who worked in St. Petersburg (Russia), Vienna (Austria) and in London (England) for future King George IV, attempted to alleviate the gout of George IV through healthier cooking practices [37]. Carême personified this gastronomic paradigm in his book *L'Art de la cuisine au XIXe siècle* (1833), which outlined culinary standards that gained acclaim through his successor, Auguste Escoffier (1846-1935) [38]. Their influence was so profound that many of Carême's proposals regarding kitchen organisation and table services are still relevant today.

So, the frequency of gout cases in royal courts motivated a shift towards lighter and more varied culinary practices, initially within royal households and subsequently adopted by the broader population, due to perceived health benefits. While not traditionally categorised as an art form, gastronomy, particularly since the era of Carême, can be considered an art due to its extension beyond mere sustenance. It encompasses the creation, execution, and presentation of food as a form of artistic expression, in which chefs act as artists, using ingredients as their medium to compose complex sensory experiences that evoke emotions and cultural narratives. Like painting or sculpture, gastronomic creations require technical skill, creativity, and a discerning eye for aesthetics.

Table
Famous artists impacted by rheumatic diseases before 1950

Artist	Nationality	Birth–death	Art	Disease
Albrecht Dürer	German	1471–1528	Painter	Rheumatoid arthritis
Peter Paul Rubens	German	1577–1640	Painter	
Marquise De Sévigné	French	1626-1696	Writer	
Pierre-Auguste Renoir	French	1841–1919	Painter	
Alexej Von Jawlensky	Russian	1864–1941	Painter	
Manolo Hugué	Spanish	1872–1945	Painter, Sculptor	
Colette	French	1873–1954	Writer	
Raoul Dufy	French	1877–1953	Painter	
Barrie Cook	English	1929–2020	Painter	
Niki de Saint Phalle	French	1930–2002	Painter, Sculptor	
Aleijadinho	Brazilian	1730–1814	Sculptor	Systemic sclerosis
Paul Klee	Swiss	1879–1940	Painter, Poet	
Michelangelo	Italian	1475–1564	Painter, Sculptor	Gout
Jean-Baptiste Corot	French	1796–1875	Painter	
Max Slevogt	German	1868–1932	Painter	
Antoni Gaudí	Spanish	1852–1926	Architect, Painter	Juvenile idiopathic arthritis
Maud Lewis	Canadian	1903–1970	Painter	
Benvenuto Cellini	Italian	1500–1571	Sculptor, Writer	Reactive arthritis
Henri de Toulouse-Lautrec	French	1864–1901	Painter	Pycnodysostosis
Frida Kahlo	Mexican	1907–1954	Painter	Back pain/fibromyalgia
Paul Scarron	French	1610–1660	Writer	Spondylarthritis
Dominique Séraphin	French	1747–1800	Puppet theatre	
Alexander Pope	English	1668–1744	Writer	Cyphoscoliosis
Niccolò Paganini	Italian	1782–1840	Violinist	Marfan
Serguei Rachmaninoff	Russian	1873–1943	Pianist	Marfan (or acromegaly)

THE ARTS AS A MEANS OF COPING

Among artists living with rheumatic diseases (Table), coping with and adapting to rheumatism was effectively illustrated by Pierre-Auguste Renoir (1841-1919), a major figure of the Impressionist movement [39,40]. His rheumatoid arthritis developed around 1890 to 1895, and by 1901, he required a cane to walk; by 1908, he depended on 2 canes; and by 1912, he was confined to a wheelchair. Despite his physical limitations, Renoir's style remained unaffected by his illness (Fig 4). He adapted by devising innovative strategies to continue painting, including creating a system of cylinders and cranks to move his canvases. When he could no longer hold his brush, he secured it in his clenched hand, protected by cloth, and often painted in beloved settings, stabilising his palette with his knees. For comfort, he surrounded himself with his cats and engaged in physical exercises such as juggling to maintain hand mobility. In this way, Renoir exemplified the beginnings of occupational therapy. Other artists, including French painter Raoul Dufy (1877-1953) and Spanish artist Manolo Hugué (1872-1945) [17,41], who also suffered from rheumatoid arthritis, continued high quality painting despite rheumatoid arthritis.

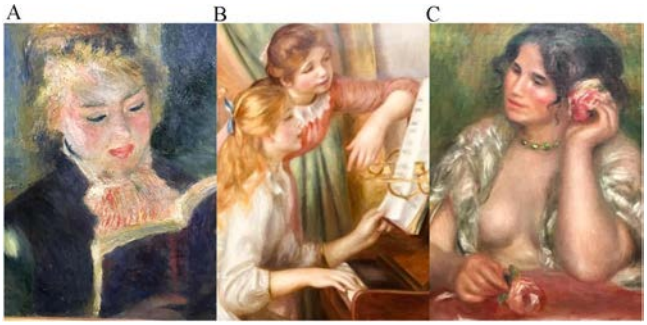

Figure 4. Example of painting of Pierre-Auguste Renoir (1841-1919), who developed rheumatoid arthritis around 1891. This figure shows paintings before (A), at the beginning (B) and after a long evolution (C). (A) The reader, 1874 Paris, Orsay museum © Photo Alain Saraux; (B) Two young girls at the piano, 1891 Paris, Orsay museum © Photo Alain Saraux (C) Gabrielle à la rose, 1911, Paris, Orsay museum. © Photo Alain Saraux. Source: Public domain.

The Swiss painter Paul Klee (1879-1940), who was afflicted with scleroderma [42,43], continued to produce art despite the progression of his disease, demonstrating a perseverance that prevented the quality of his work from diminishing. During the 5 years of his illness, he painted approximately 2500 works of art. He nevertheless modified his technique, changing the materials he used and adopting peculiarly large brushes for easier handling. In the advanced stages of the illness, he also adopted a broad, flat style characterised by heavy, black-crayon-like lines and rather dull colours [43].

Similarly, Frida Kahlo endured chronic and debilitating back pain throughout her life, stemming from a severe bus accident. She also experienced multiple miscarriages, including both spontaneous and therapeutic abortions undertaken to avert complications from her compromised pelvis. Furthermore, a positive Wassermann test suggests the possibility of concurrent antiphospholipid syndrome. She also suffered from severe fatigue, chronic neck, back, and right leg pain, weight loss, and depression [44]. Most of her paintings represented her back pain and psychological suffering [45].

Few writers have detailed the daily struggles associated with these conditions. Madame de Sévigné (1626-1696), a writer well-known for her letters to her daughter, described her experiences with polyarthritis and the treatments she attempted, including opium, quinine, and thermal baths [46]. Alexander Pope (1688-1744), a pivotal poet of the 18th century who suffered from kyphoscoliosis caused by tuberculous spondylitis, employed biting irony to mock his condition [47]. In *The Club of Little Men*, he creates the character Dick Distick, president of a fictional club for short men, portraying him as a diminutive figure dressed in black to appear even smaller, evoking haunting imagery reminiscent of a spider or a windmill. In *Epistle to Dr.*

Arbuthnot, Pope provides a transparent and satirical self-portrait, addressing his short stature and various physical imperfections. Colette (1873-1954) developed rheumatoid arthritis after 1940, and her final book, *The Blue Beacon Light*, poignantly illustrates the limitations imposed by her condition [48]. Flannery O'Connor (1925-1964), a key figure in American literature, was diagnosed with lupus in 1950 [49]. Prior to her diagnosis, she faced numerous medical misdiagnoses and underwent arduous cortisone treatments that resulted in significant complications. O'Connor's work, imbued with elements of violence and spirituality, reflects her personal experience of suffering and her worldview. She regarded illness as a source of introspection and insight, famously writing, 'Sickness, before it is a limitation, is a vocation'.

Examples of exhibitions of artistic photographs made by patients as a way of coping include *I Have Rheumatism* by Leyla Avsar (https://leylaavsar.com/i-have-rheumatism), *Exception'elles* by Barbara Grossmann (https://smileyaufeminin.fr), or https://ungareumatiker.se/unga-reumatiker-rapporten.

Regarding cinema, we may also mention some actors affected by rheumatological diseases, notably Kathleen Turner (1954-) and James Coburn (1928-2002), who, despite having rheumatoid arthritis, made a comeback on the big screen.

Many studies have been made to demonstrate the usefulness of art for coping and social interaction. Participatory theatre initiatives that enhance communication between patients and physicians are exemplified by Leung's work on systemic lupus erythematosus education [50].

INSPIRATION FROM NORMAL MUSCULOSKELETAL ANATOMY AND RHEUMATIC DISEASES

Interestingly, even during antiquity, as described by Marcus Vitruvius Pollio (about 80-15 BC) [51], architects drew inspiration from the anatomy of the human body, both aesthetically and structurally, to create innovative and functional spaces. While Leonardo da Vinci did not apply his anatomical studies directly to architecture in the modern sense, his research on musculoskeletal structures indirectly influenced architectural thought during the Renaissance and beyond. His observations of the mechanics of the human body facilitated reimagining building structures, integrating biomechanical principles for enhanced stability and efficiency. This approach paved the way for organic and functionally inspired architectural designs, influencing contemporary architects. Biomorphic architecture, which draws from organic forms (animals, plants, and the human body), was prevalent in the Art Nouveau movement of the late 19th century [52–54]. For example, the Spanish architect Antoni Gaudí (1852-1926), who suffered from idiopathic juvenile arthritis, designed the Casa Batlló and the Sagrada Família, transposing anatomical forms into architecture (Fig 5). Swiss architect Charles Édouard Jeanneret-Gris, known as Le Corbusier (1887-1965), pioneered modern architecture by developing a universal system of proportions to harmonise architectural design with the human body. His system, known as the Modulor, was based on the proportions of an idealised human figure. The Eiffel Tower, Gustave Eiffel's masterpiece designed for the 1889 World's Fair in Paris, drew inspiration from the structure of the human femur (Fig 6). Indeed, Eiffel was known for drawing inspiration from principles found in nature in his designs, such as material strength and force distribution [55].

More recently, the Spanish architect Santiago Calatrava (1951-) designed the Turning Torso in Malmö, Sweden, which resembles a spine (https://calatrava.com/projects/turning-torso-malmoe.html), the Oculus train station of the World Trade Center in New York, and the roof of the Milwaukee Art Museum (https://mam.org/info/architecture/quadracci-pavilion), which evokes the design of a rib cage.

Figure 5. Example of biomimetism. (A) The Eiffel Tower (the basis of each foot mimics a human femur, and the underlying lattice structure makes them both solid and light). Source: Public domain. © Photo Alain Saraux (B) The Sagrada Família (the structure mimics bone architecture) With permission from Sagrada familia. © Photo Sandrine Jousse-Joulin.

Figure 6. Example of media art: illustration by Sara Gironi Carnevale of the BACHELOR study (comparing baricitinib 4 mg to placebo in polymyalgia rheumatica) on the cover of issue of *The Lancet Rheumatology* published in April 2025. Reproduced with permission.

Few descriptions of rheumatic diseases were documented in literature before 1800, aside from autobiographical accounts. William Shakespeare's characters, suffering from gout [56], were an exception, despite little knowledge about the disease [57]. Even Victor Hugo (1802-1885), who wrote many books in which various diseases were described, did not evoke gout or other rheumatic diseases [58]. The first novel addressing rheumatic disease was Émile Zola's *The Joy of Living*, published in 1884, featuring Mr Chanteau, who suffered from a severe form of gout [59]. In this period, writers aimed to depict reality without embellishment. Zola likely drew from descriptions published by Alfred Baring Garrod in 1859. Mr Chanteau's gout symbolises not only his physical decline but also the moral decay of the bourgeoisie, a class unable to rejuvenate itself amid its excesses. The portrayal of the characteristics of rheumatic diseases became somewhat common in the literature only after 1950.

Today, representations of rheumatic diseases in literature are more prevalent but are frequently authored by those experiencing similar conditions (eg, fibromyalgia, back pain) [60−62]. The visibility of celebrity experiences with these ailments can be a powerful tool for raising awareness and promoting research efforts in rheumatology.

Similarly, painters rarely represented rheumatic diseases. Most reviews made by rheumatologists consider only a few paintings as likely iconodiagnoses of rheumatic disease [25−29]: camptodactyly in several paintings by Leonardo da Vinci or Dieric Bouts (1415-1475), such as *Mater Dolorosa;* hypermobility syndrome in *The Three Graces* (1638-1640) painted by Peter Paul Rubens and *Boneless Valentin* by Henri de Toulouse-Lautrec; trapeziometacarpal osteoarthritis in *Old Woman Frying Eggs* (1618) by Velásquez and *An Old Man* painted by Alma il giovane; gout in *The Gout* by James Gillray (1799) and *A Gouty Man Who is Drinking Wine and Playing the Cello* by H.W. Bunbury; giant-cell arteritis in *The Virgin with Canon Van der Paele* (1436) by Jan van Eyck and in the *Portrait of Francesco Giamberti* (1505) by Piero di Cosimo; scleroderma in *The Archangel Raphael and Bishop Francisco Domonte* (1680) by Murillo; juvenile idiopathic arthritis in *Sleeping Cupid* (1608) by Caravaggio; Paget's disease (osteitis deformans) in *A Grotesque Old Woman*, attributed to the Flemish artist Quinten Metsys (1465-1530); or osteoporosis in *Arrival of the English Ambassadors*, painted by Vittore Carpaccio in 1495. Frida Kahlo (1907-1954) painted many self-portraits that suggested her back pain.

Some films have been dedicated to the most spectacular rheumatological diseases. *The Hunchback of Notre-Dame* (Wallace Worsley, Universal Pictures, 1923) addressed social exclusion and the stigma surrounding rare diseases (scoliosis), emphasising both the psychological and physical impact of such conditions. Inflammatory rheumatic diseases are poorly represented by cinema except for gout in *The Favourite* (Yorgos Lanthimos, Film 4 production, 2018), *Falstaff* (Orson Welles, Chimes at Midnight, 1965), and *Barry Lyndon* (Stanley Kubrick, Warner Bros, 1975); juvenile arthritis in *Maudie* (Aisling Walsh, Calvary Media, 2016); rheumatoid arthritis in *Renoir* (Gilles Bourdos, Les films du fil, 2012) and *La Vie en Rose* (Olivier Dahan, La môme production, 2017); and lupus in *Standing Eight* (Brian Kazmarck Films *2007)* and *Depois do universo and in Clouds* (Mauro Schwartz, O2 filmes, 2022). Noninflammatory diseases are almost absent from these scenarios, except for osteoarthritis with ageing (*A Walk in the Woods*, Ken Kwapis, 2015; *The Straight Story,* David Lynch, 1999; and *On Golden Pond*, Mark Rydell, 1981).

Digital art is a new way to represent diseases. Artists such as Simone Rotella, Grace Russell, Chiara Vercesi, Jason Lyon, and Sara Gironi Carnevale illustrated covers of *The Lancet Rheumatology*. For example, the cover of a recent issue features our BACHELOR thesis comparing baricitinib to placebo, illustrated by Sara Gironi Carnevale (Fig. 6) [63]. If you have enjoyed the paintings on the covers of the medical journal *JAMA* since 1964, you will probably also be interested in these illustrations.

Bryan Robert Smith, a medical student studying biomedical ethics at Stanford University, creatively explored rheumatology through *Rheumatology's Animal Kingdom: A Digital Art Series* [64], an artistic study of 3 rheumatological conditions utilising animal imagery to represent specific syndromes and symptoms. This collection aims to extend the metaphor of animals in medical nomenclature and explore them through visual art.

Comics are used for education or art therapy in young patients who have juvenile idiopathic arthritis [65,66], not for entertainment.

The scarcity of main characters suffering from rheumatic diseases in artistic works by authors without these conditions suggests a hesitance to depict lesser known, less visually striking ailments compared with more dramatic afflictions such as infections or cancer. We hope that introducing representations of rheumatic diseases with new support from artworks will improve public knowledge of rheumatology.

RHEUMATIC DISEASES MAY ALSO HAVE A POSITIVE IMPACT ON ARTISTIC CAREERS

Gaudí was probably more interested in nature than other children were because juvenile arthritis limited his mobility, explaining his interest in bone architecture, which inspired biomimetics in architecture.

Some rheumatic diseases could benefit musicians, who may be susceptible to various overuse complications [67−72]. Both Niccolò Paganini (1782-1840), an Italian violinist, and Sergei Rachmaninoff (1873-1943), a Russian pianist, likely had Marfan syndrome [60,73,74]. Both artists transformed their conditions into advantages, becoming virtuosos thanks to the extreme flexibility of their fingers. Paganini's techniques, such as *bariolages, pizzicati*, and *double harmonics*, showcased the remarkable capabilities afforded by his condition. In contrast, Rachmaninoff utilised the condition's advantages, which allowed him to extend his fingers an octave and a half.

Other hypermobility syndromes may also increase the likelihood of becoming a dancer [75,76] and explain the success of Edme-Étienne-Jules Renaudin (1843-1907), nicknamed 'the boneless Valentin', who probably suffered from Ehler−Danlos disease. He was a French can-can dancer who was a star of the Moulin Rouge in the 1890s and whose memory lives in paintings and posters of the French painter Henri de Toulouse-Lautrec (1864-1901).

This is also true for actors. For example, Vincent Schiavelli (1948-2005), who also had Marfan syndrome, took advantage of his morphology in the film *One Flew Over the Cuckoo's Nest* (Milos Forman, Fantasy films, 1975).

In contrast, spondylarthritis induces axial stiffness, which results in a curved, forwards-leaning appearance, characteristic features of both French Paul Scarron (1610-1660) and Dominique Séraphin (1747-1800) [77]. Paul Scarron, a major figure of 17th-century burlesque literature who likely had spondylarthritis, wrote with irony and a strong taste for the absurd, reflecting his perspective on illness and society. Through his works, he caricatures human flaws, challenges conventions, and questions the perception of suffering bodies. Dominique Séraphin, nicknamed 'the facetious hunchback', was the founder of shadow puppetry in France. His axial deformity seemed to have contributed to its popularity.

Notably, rheumatism inspired the modern photography of the Norwegian Leyla Avsar (https://www.leylaavsar.com/i-have-rheumatism), who had rheumatoid arthritis, and the American Riva Lehrer (1958-) (https://www.rivalehrerart.com/gallery/circle-stories), who practiced digital art.

CONCLUSION

Developing a link between art and rheumatology during education, therapeutic education, and information in media, as well as through exhibitions of art produced by rheumatologists and patients, can serve as a compelling avenue for fostering this connection. Rheumatologists, like all other physicians, need both the arts and sciences to equip them with criticality and creativity

of the mind as well as aesthetic and emotional capacities [78]. Rheumatologists need special empathy because a large part of their activity relies on interrogation, listening ability, and the gift of observation of patients, especially those who are chronically in pain and worried.

Competing interests

All authors declare they have no competing interests.

CRediT authorship contribution statement

Alain Saraux: Writing – review & editing, Writing – original draft, Visualization, Validation, Supervision, Formal analysis, Data curation, Conceptualization. **Dominique Le Nen:** Writing – review & editing, Writing – original draft, Visualization, Validation, Formal analysis, Data curation, Conceptualization.

Funding

This research did not receive any specific grant from funding agencies in the public, commercial, or not-for-profit sectors.

Patient consent for publication

Not applicable.

Ethics approval

Not applicable.

Provenance and peer review

Not commissioned; externally peer reviewed.

Orcid

Alain Saraux: http://orcid.org/0000-0002-8454-7067

REFERENCES

[1] Zaidel DW. Culture and art: importance of art practice, not aesthetics, to early human culture. Prog Brain Res 2018;237:25–40.
[2] Adajian T. The definition of art. In: Zalta EN, Nodelman U, editors. Stanford Encyclopedia of Philosophy. Fall 2024 Edition. Stanford: Stanford University; 2024.
[3] Piechowski-Jozwiak B, Boller F, Bogousslavsky J. Universal connection through art: role of mirror neurons in art production and reception. Behav Sci (Basel) 2017 May 5;7:29.
[4] Alberti LB. De Pictura, praestantissima et nunquam satis laudata arte, libri tres absolutissimi Leonis Baptistae de Albertis. Basel: Thomas Venatorius; 1540.
[5] Sydenham T. *A Treatise on Gout and Dropsy*. London; 1683.
[6] AJ Landré-Beauvais. The first description of rheumatoid arthritis: the unabridged text of the doctoral dissertation presented by Landré-Beauvais in 1800. Rev Rhum 2001;68:230–8.
[7] Garrod AB. The nature and treatment of gout and rheumatic gout. London: Walton and Maberly; 1859.
[8] MARIE P. Sur la spondylose rhizomélique. Revue de Medecine (Paris) 1898;18:285–315.
[9] GBD 2021. Other Musculoskeletal Disorders Collaborators. Global, regional, and national burden of other musculoskeletal disorders, 1990-2020, and projections to 2050: a systematic analysis of the Global Burden of Disease Study 2021. Lancet Rheumatol. 2023;5:e670–82.
[10] Comte Sponville A. In: Le Nen D, Dubrana F. La médecine... Art ou science ? L'Harmarttan; 2022:9-13.
[11] Gogh Vincent Van. Lettres à son frère Theo. Grasset 1990:303.
[12] Bruyn GAW, Schmidt WA. Musculoskeletal Ultrasound for the Rheumatologist: An Introductory Guide. 3rd ed. Springer; 2023. p. 262.
[13] Perdicoyanni-Paléologou H. Anatomy and Surgery: from Antiquity to the Renaissance. Amsterdam: Adolf M. Hakkert Publishing; 2016.
[14] Wickerscheimer E. Anatomies de Mondino dei Luzzi et de Guido de Vigevano. Geneva: Slatkine Reprints; 1977.
[15] de Ketham J. Fasciculus medicinae. Venice: Joannes et Gregorius de Gregoriis; 1493.
[16] Carpi B. Commentaria cum amplissimis super anatomia Mundini. Bologna: Hyeronimus de Benedictis; 1521.
[17] Vésale A. De humani corporis fabrica libri septem. Basel: Ex officina Joannis Oporini; 1543.
[18] Le Nen D, Brioist P. Leonardo da Vinci and Anatomy: The Mechanics of Life. Paris: Skira; 2023.
[19] Clayton M, Philo R. Leonardo da Vinci: Anatomist. Royal Collection Enterprises; 2012.
[20] Laurenza D. Art and anatomy in Renaissance Italy: images from a scientific revolution. Metropolitan Museum of Art Bulletin 2012:173–9.
[21] Alberti LB. Della Pittura et della Statua. Milan: Dalla Società Tipografica de Classici Italiani; 1804.
[22] Valverde de Amusco J. Historia de la composicion del cuerpo humano. Rome: Antonio Salamanca & Antonio Lafreri; 1556.
[23] Gray H, Carter HV. Gray's Anatomy. Cosimo Classics; 2011. p. 784.
[24] Netter FH. Netter *Atlas of Human Anatomy: Classic Regional Approach with Latin Terminology: paperback + eBook*. English Edition (Netter Basic Science); 2022.
[25] Camurcu Y, Sofu H, Ucpunar H, Duman S, Cobden A. Paediatric orthopaedics through paintings. J Child Orthop 2018;12:647–51.
[26] Hinojosa-Azaola A, Alcocer-Varela J. Art and rheumatology: the artist and the rheumatologist's perspective. Rheumatology (Oxford). 2014;53:1725–31.
[27] Appelboom T. Art and history: a large research avenue for rheumatologists. Rheumatology (Oxford) 2004;43:803–5.
[28] Dequeker J. What can a rheumatologist learn from paintings? Acta Reumatol Port 2006;31:11–3.
[29] Yeap SS. Rheumatoid arthritis in paintings: a tale of two origins. Int J Rheum Dis 2009;12:343–7.
[30] van Tubergen A, van der Linden S. A brief history of spa therapy. Ann Rheum Dis 2002;61:273–5.
[31] Aribi I, Nourredine M, Giroudon C, Massy E, Lega JC, Kassai B, et al. Efficacy and safety of balneotherapy in rheumatology: a systematic review and meta-analysis. BMJ Open 2025;15:e089597.
[32] Fox RM. Hydrology, rheumatology, and rehabilitation: the campaigning of Fortescue Fox. J R Coll Physicians Edinb 2020;50:196–201.
[33] Dougados M. Jacques FORESTIER, a visionary of the clinical epidemiology in rheumatology. Ann Rheum Dis 2018;77:1097–8.
[34] Ashraf O, Channapatna Suresh S, Raju B, Jumah F, Sun H, Gupta G, et al. Jacques Forestier: forgotten contributions of a rheumatologist to spine surgery. World Neurosurg 2021;148:136–40.
[35] Keitel W, Olsson L, Matteson EL. Max Hirsch (1875-1941): his forgotten fate and contributions to the founding of modern rheumatology. Eur J Rheumatol 2016;3:101–5.
[36] Zochling J. Measures of symptoms and disease status in ankylosing spondylitis: Ankylosing Spondylitis Disease Activity Score (ASDAS), Ankylosing Spondylitis Quality of Life Scale (ASQoL), Bath Ankylosing Spondylitis Disease Activity Index (BASDAI), Bath Ankylosing Spondylitis Functional Index (BASFI), Bath Ankylosing Spondylitis Global Score (BAS-G), Bath Ankylosing Spondylitis Metrology Index (BASMI), Dougados Functional Index (DFI), and Health Assessment Questionnaire for the Spondylarthropathies (HAQ-S). Arthritis Care Res (Hoboken) 2011;63 (Suppl 11):S47–58.
[37] Del Moral RG. Gastronomic paradigms in contemporary Western cuisine: from French haute cuisine to mass media gastronomy. Front Nutr 2020;6:192.
[38] Carême A. L'art de la cuisine au XIXe siècle. Reedition BNF; 2023:472.
[39] da Mota LM, Neubarth F, Diniz LR, de Carvalho JF, dos Santos Neto LL. Pierre-Auguste Renoir (1841-1919) and rheumatoid arthritis. J Med Biogr 2012;20:91–2.
[40] Boonen A, van de Rest J, Dequeker J, van der Linden S. How Renoir coped with rheumatoid arthritis. BMJ 1997;315:1704–8.
[41] Pou MA, Díaz-Torné C, Azevedo VF. Manolo Hugué: de la escultura a la pintura a causa de la artritis [Manolo Hugué: from sculpture to painting due to arthritis]. Reumatol Clin 2011;7:135–6 Spanish.
[42] Suter H. Case report on the illness of Paul Klee (1879-1940). Case Rep Dermatol 2014;6:108–13.
[43] Wolf G. Endure!: how Paul Klee's illness influenced his art. Lancet 1999;353:1516–8.

[44] Morales Torres J, Aceves FJ, Amigo Castañeda MC, Hernández Cuevas CB. Could Frida Kahlo have had antiphospholipid syndrome? Reumatol Clin (Engl Ed) 2022;18:65–8.
[45] Romagna B. The art of resilience: a psychobiography of Frida Kahlo. Int Rev Psychiatry 2024 Feb-Mar;36(1-2):91–103.
[46] Dilleman G, Lemay R. Les médicaments de Mme de Sévigné. Rev Hist Pharm 1966;190:161–84.
[47] Veith I. This long disease, my life-postscript to "He" (Percival Pott and Alexander Pope). Perspect Biol Med 1971;15:110–4.
[48] Colette SG. Le Fanal Bleu. Editions Ferenczi; 1949. p. 241.
[49] Coles R, Flannery O. Connor's lupus: a commentary on her collected letters, The Habit of Being. JAMA 1980;244:1441–2.
[50] Leung J, Som A, McMorrow L, Zickuhr L, Wolbers J, Bain K, et al. Rethinking the difficult patient: formative qualitative study using participatory theater to improve physician-patient communication in rheumatology. JMIR Form Res 2023;7:e40573.
[51] Vitruve. Les dix livres d'architecture. Paris: Ed. Tardieu et Coussin; 1837.
[52] Chayaamor-Heil N. From bioinspiration to biomimicry in architecture: opportunities and challenges. Encyclopedia 2023;3:202–23.
[53] Aeschlimann FA, Aeschlimann AG, Laxer RM. Early onset of chronic rheumatic disease may lead to creative expression: the stories of Antoni Gaudi and Maud Lewis. J Rheumatol 2016;43:1436–43.
[54] Azevedo VF, Diaz-Torne C. The arthritis of Antoni Gaudi. J Clin Rheumatol 2008;14:367–9.
[55] Ramzy N. Sustainable spaces with psychological connotation: historical architecture as reference book for biomimetic models with biophilic qualities. Int J Archit Res Archnet 2015;9:248–67.
[56] Ehrlich GE. Shakespeare's rheumatology. Ann Rheum Dis 1967;26:562–3.
[57] d'Alembert. Venel, Jaucourt, Le Roy, Penchenier. 1st ed. L'Encyclopédie; 1757. p. 771–8.
[58] Hugo V. Les Misérables. Original ed. 1862.
[59] Zola É. La Joie de vivre. The Rougon-Macquart; 1884 Tome 12.
[60] Kamiński M, Hrycaj P. Celebrities influence on rheumatic diseases interest: a Google trends analysis. Rheumatol Int 2024;44:517–21.
[61] Rahmani G, Selena G. Lupus and the impact of celebrity health disclosure on public awareness. Lupus 2017;27:1045–6.
[62] Elsalti A, Darkhabani M, Alrifaai MA, Mahroum N. Celebrities and medical awareness-the case of Celine Dion and Stiff-Person Syndrome. Int J Environ Res Public Health 2023;20:1936.
[63] Saraux A, Carvajal Alegria G, Dernis E, Roux C, Richez C, Tison A, et al. Baricitinib in early polymyalgia rheumatica (BACHELOR): a randomised, double-blind, placebo-controlled, parallel-group trial. Lancet Rheumatol 2025;7:e233–42.
[64] Smith BR. Rheumatology's animal kingdom: a digital art series. J Rheumatol 2023;50:958–60.
[65] Moll JM. Doctor-patient communication in rheumatology: studies of visual and verbal perception using educational booklets and other graphic material. Ann Rheum Dis 1986;45:198–209.
[66] Mendelson A, Rabinowicz N, Reis Y, Amarilyo G, Harel L, Hashkes PJ, et al. Comics as an educational tool for children with juvenile idiopathic arthritis. Pediatr Rheumatol Online J 2017;15:69.
[67] Dąbrowski KP, Stankiewicz-Jóźwicka H, Kowalczyk A, Wróblewski J, Ciszek B. Morphology of sesamoid bones in keyboard musicians. Folia Morphol (Warsz) 2021;80:410–4.
[68] Rietveld ABMB. Dancers' and musicians' injuries. Clin Rheumatol 2013;32:425–34.
[69] Larsson LG, Baum J, Mudholkar GS, Kollia GD. Benefits and disadvantages of joint hypermobility among musicians. N Engl J Med 1993;329:1079–82.
[70] Bird HA. Overuse syndrome in musicians. Clin Rheumatol 2013;32:475–9.
[71] Bejjani FJ, Kaye GM, Benham M. Musculoskeletal and neuromuscular conditions of instrumental musicians. Arch Phys Med Rehabil 1996;77:406–13.
[72] Bird HA, Pinto SO. Scoliosis in musicians and dancers. Clin Rheumatol 2013;32:515–21.
[73] Sperati G, Felisati D. Nicolò Paganini (1782-1840). Acta Otorhinolaryngol Ital 2005;25:125–8.
[74] Smith RD. Paganini's hand. Arthritis Rheum 1982;25:1385–6.
[75] Scheper MC, de Vries JE, de Vos R, Verbunt J, Nollet F, Engelbert RHH. Generalized joint hypermobility in professional dancers: a sign of talent or vulnerability? Rheumatology (Oxford) 2013;52:651–8.
[76] Sun Y, Liu H. Prevalence and risk factors of musculoskeletal injuries in modern and contemporary dancers: a systematic review and meta-analysis, 12. Front Public Health; 2024:1325536.
[77] Prati C, Verhoeven F, Wendling D, Quetel E. Séraphin (1747-1800), "the facetious hunchback": how ankylosing spondylitis contributed to the success of his shadow puppet theatre. Rheumatol Int 2024;44:3113–7.
[78] Braund M, Reiss MJ. The 'Great Divide': how the arts contribute to science and science education. Can J Sci Math Technol Educ 2019;19:219–36.

Ann Rheum Dis 84 (2025) 1770–1778

Contents lists available at ScienceDirect

Annals of the Rheumatic Diseases

journal homepage: https://www.sciencedirect.com/journal/annals-of-the-rheumatic-diseases

Recommendations

ASAS recommendations on reporting axial spondyloarthritis clinical trials

Floris A. van Gaalen[1,*], Victoria Navarro-Compán[2], Xenofon Baraliakos[3], Filip van den Bosch[4,5], Lianne S. Gensler[6], Ihsane Hmamouchi[7], Robert Landewé[8,9], Pedro M. Machado[10,11], Helena Marzo-Ortega[12], Valeria Rios Rodriguez[13], Denis Poddubnyy[13,14], Sofia Ramiro[1,9], Désirée van der Heijde[1]

[1] *Department of Rheumatology, Leiden University Medical Center, Leiden, The Netherlands*
[2] *Department of Rheumatology, La Paz University Hospital, IdiPaz, Madrid, Spain*
[3] *Rheumazentrum Ruhrgebiet Herne, Ruhr-University Bochum, Herne, Germany*
[4] *VIB-UGent Center for Inflammation Research, Department of Internal Medicine and Pediatrics, Ghent University, Ghent, Belgium*
[5] *Ghent University Hospital, Department of Rheumatology, Ghent, Belgium*
[6] *Department of Medicine, Division of Rheumatology, University of California, San Francisco, California, USA*
[7] *Faculty of Medicine, Health Sciences Research Center (CReSS), International University of Rabat (UIR), Rabat, Morocco*
[8] *Amsterdam Rheumatology & Clinical Immunology Center, Amsterdam, The Netherlands*
[9] *Department of Rheumatology, Zuyderland Medical Center, Heerlen, The Netherlands*
[10] *Department of Neuromuscular Diseases and Centre for Rheumatology, University College London, London, UK*
[11] *NIHR University College London Hospitals Biomedical Research Centre, University College London Hospitals NHS Foundation Trust, London, UK*
[12] *NIHR Leeds Biomedical Research Centre, The Leeds Teaching Hospitals NHS Trust and Leeds Institute of Rheumatic and Musculoskeletal Medicine, University of Leeds, Leeds, UK*
[13] *Department of Gastroenterology, Infectiology and Rheumatology (including Nutrition Medicine), Charité – Universitätsmedizin Berlin, corporate member of Freie Universität Berlin and Humboldt – Universität zu Berlin, Berlin, Germany*
[14] *Division of Rheumatology, University of Toronto and University Health Network, Toronto, ON, Canada*

ARTICLE INFO

Article history:
Received 9 June 2025
Received in revised form 20 July 2025
Accepted 22 July 2025

ABSTRACT

Objectives: This study aims to develop recommendations on reporting baseline features and outcomes from axial spondyloarthritis (axSpA) clinical trials based on the recently updated instrument set of the Assessment of SpondyloArthritis international Society (ASAS) core outcome set (COS).

Methods: A steering group (SG) convened a workgroup (WG), consisting of 13 ASAS members including rheumatologists, methodologists, epidemiologists, and 2 Young ASAS members. Recommendations on reporting axSpA trials baseline features and outcomes were developed in 3 steps: (1) the SG identified relevant baseline features from key axSpA clinical trials and formulated a proposal on how outcomes related to the instruments in the ASAS COS should be presented. (2) The SG proposal was presented, discussed, and modified in WG meetings. (3) WG proposal was discussed and voted on by ASAS members during the 2024 annual ASAS workshop.

Results: Forty-two baseline features relevant for all axSpA clinical trials and 8 additional features for disease-modifying drug trials were defined including descriptions on how to report them. Additionally, recommendations on how to report 20 trial outcomes at baseline and follow-up

*Correspondence to Dr Floris A. van Gaalen, Department of Rheumatology, Leiden University Medical Center, Leiden, Albinusdreef 2 2333 ZA, The Netherlands.
E-mail address: f.a.van_gaalen@lumc.nl (F.A. van Gaalen).

Handling editor Josef S. Smolen.

https://doi.org/10.1016/j.ard.2025.07.017

timepoints were put forward. Finally, recommendations on how to report 11 outcomes of instruments additionally endorsed by ASAS but not in the COS were formulated. Proposals for baseline features, COS outcomes, and outcomes not in COS were approved by ASAS members (with 84%, 85%, and 93% of members in favour, respectively).
Conclusions: These ASAS-endorsed recommendations on axSpA clinical trial reporting provide a standardised approach to reporting both baseline features as well as outcomes from axSpA clinical trials.

INTRODUCTION

A clinical trial is the best method for assessing the effect of an intervention. Moreover, clinical trials are crucial for regulatory decision-making and the introduction of therapies into clinical practice. To improve the overall quality of clinical trials, Consolidated Standards of Reporting Trials (CONSORT) published the CONSORT statement providing a set of recommendations for reporting randomised trials. The statement offers a standard way for trialists to prepare reports of trial findings regardless of the disease studied. The most recent version of the Statement—the CONSORT 2010 Statement—contains a 25-item checklist focusing on reporting how the trial was designed, analysed, and interpreted and a flow diagram displaying the progress of participants through the trial [1].

Apart from initiatives to improve the general reporting of trial methodology, for many conditions including rheumatic and musculoskeletal diseases, disease-specific core outcome sets (COS) have been developed aimed at encouraging researchers to measure a consistent set of clinical endpoints in studies. A COS is an agreed standardised minimum set of outcomes that should be measured and reported in all clinical trials in a specific area and is intended to lead to research measuring relevant outcomes. In addition, the use of COS as an agreed standardised set of outcomes facilitates not only comparing trial outcomes but also combining trial data such as in meta-analyses [2].

The Assessment of SpondyloArthritis international Society −Outcome Measures for Arthritis Clinical Trials COS for ankylosing spondylitis was developed almost 3 decades ago and reflecting the progress made in the field, this original COS was recently updated into a COS for the entire axial spondyloarthritis (axSpA) spectrum. For the updated ASAS COS, first the domain set, which instructs what to measure, was updated and thereafter the instrument set, which tells how to measure, was updated [3,4]. The current core domain set includes 7 mandatory domains for all studies and 3 additional mandatory domains for studies evaluating disease-modifying antirheumatic drugs (DMARDs). In the core instrument set, 7 mandatory instruments were selected for all trials and 9 additional mandatory instruments for DMARD trials. Furthermore, 11 extra instruments were also endorsed by ASAS and can be used in addition to those included in the COS [4].

While initiatives like the CONSORT statement aid in trial methodology and the updated ASAS COS provide axSpA trialists guidance on which instruments to use in axSpA clinical trials, recommendations on how to report the outcomes of axSpA clinical trials are not available. Moreover, recommendations on which baseline features should be reported, as well as how to report them to adequately describe the study population are lacking.

The aim of this ASAS project was to develop expert recommendations on which baseline features to collect, how to report baseline features, and how to present axSpA trial outcome data in text, tables, and graphs.

METHODS

The project took place under the auspices of ASAS, the worldwide organization of SpA experts. Following project approval in September 2023, the steering group (FAvG, VN-C, and DvdH) convened a workgroup consisting of 8 additional ASAS members (XB, RL, PMM, HM-O, DP, LSG, SR, and FvdB). The workgroup was complemented by 2 Young ASAS members (IH, VRR).

The project consisted of 3 steps. First, the steering group collected a limited set of recent publications of clinical trials in axSpA covering the entire spectrum of the disease and treatment armamentarium, including trials aimed at disease modification. The aim of the scoping literature search was to provide the steering group with an overview to be used in workgroup discussion of possible relevant baseline features and examples of how baseline features and outcomes are reported. For this, a literature search was performed on 23 January 2023 in the Web of Science database using the keywords ‘spondyloarthritis’ and ‘clinical trial’ [5]. After limiting results to the last 10 years and ranking these by highest cited trials, all publications were selected until at least 2 examples of clinical trials in radiographic axSpA, 2 in nonradiographic trials, and 2 axSpA disease-modifying antirheumatic drug (DMARD) trials with imaging outcomes had been included (Supplementary Table S1).

The steering group then identified relevant baseline features based on the discussion of the literature review and made a proposal on how baseline features and outcomes can be reported as clearly and informatively as possible. As a second step, after having received the proposals prior via e-mail, the workgroup discussed and modified the proposals in 2 online meetings in November 2024.

The proposals as agreed on by the workgroup were sent to all ASAS members 1 week before the annual ASAS workshop on the 12 and 13 January 2024, in Barcelona. During the workshop, the proposals were discussed, additional proposals could be made, and final proposals were voted on by ASAS members with full membership.

RESULTS

Baseline features for all trials

Table 1 shows the recommended baseline features for all trials including DMARD trials and how to present them. Of the recommended 42 baseline features, the majority were selected by the steering group from published axSpA clinical trials (Supplementary Table S1).

The first 6 baseline features are demographics including sex and age. Smoking and body mass index were added as recommended baseline features by the workgroup. Highest level of education completed as a baseline feature was added to the steering group proposal by the ASAS members at the annual meeting (89 votes with 70% in favour, 28% against and 2% abstaining) (Supplementary Table S2).

Baseline features 7 to 20 provide details on the presence or SpA features and disease duration based on axial symptoms. As

Table 1
Baseline features for all trials including disease-modifying antirheumatic drug (DMARD) trials

Demographics	How	Comment
1. Biological sex	*n* (%)	-
2. Age	Mean years (SD)	-
3. Highest completed level of education	*n* (%) of primary, secondary, and tertiary	According to ISCED levels (see Supplementary Table 2)
4. Geographic location	*n* (%) per country	Geographic location could be text only
5. Smoking	*n* (%) current/never/past	If collected report mean (SD) pack years
6. Body mass index	Mean kg/m^2 (SD)	-
Spondyloarthritis symptoms and features	How	Comment
7. Duration axial symptoms since disease onset	Mean years (SD)	
8. Symptom duration ≤2 y	*n* (%)	According to ASAS SPa EARLy (SPEAR) definition
9. Duration since diagnosis	Mean years (SD)	-
10. History of IBP	*n* (%)	Definition according to ASAS classification criteria
11. History of peripheral arthritis	*n* (%)	According to physician
12. History of enthesitis	*n* (%)	According to physician
13. History of dactylitis	*n* (%)	According to physician
14. History of uveitis	*n* (%)	According to physician
15. History of IBD	*n* (%)	According to physician
16. History of psoriasis	*n* (%)	According to physician
17. HLA-B27 positivity	*n* (%)	-
18. Radiographic sacroiliitis (ever)	*n* (%)	Report if collected (mandatory for DMARD trials)
19. Inflammation on MRI-SIJ (ever)	*n* (%)[c]	Report if collected (mandatory for DMARD trials)
20. Structural lesions on MRI-SIJ (ever)	*n* (%)[c]	Report if collected
Previous and current treatment	How	Comment
21. Previous b or tsDMARD	*n* (%) + mean /median number per patient	-
22. Previous TNFi	*n* (%)	-
23. Previous IL-17A-i or IL-17A/F-i	*n* (%)	
24. Previous JAKi	*n* (%)	-
25. Previous 2 b/tsDMARD classes	*n* (%)	-
26. Previous 3 b/tsDMARD classes	*n* (%)	-
27. Current NSAID	*n* (%)	Report ASAS NSAID score if collected
28. Current TNFi	*n* (%)	-
29. Current IL-17A-i or IL-17A/F-i	*n* (%)	-
30. Current JAKi	*n* (%)	-
31. Current csDMARD	*n* (%)	-
Clinical and laboratory measures	How	Comment
32. ASDAS	Mean score (SD)	-
33. ASDAS disease status[a]	*n* (%) per category	-
34. Patient global disease activity	Mean (SD)	-
35. Total back pain (BASDAI Q2)	Mean (SD)	-
36. Severity/duration stiffness (BASDAI [Q5 + Q6]/2)	Mean (SD)	-
37. Fatigue (BASDAI Q1)	Mean (SD)	-
38. BASFI	Mean (SD)	-
39. ASAS health index	Mean (SD)	-
40. ASAS health index status[b]	*n* (%) per category	-
41. CRP (mg/L)	Mean (SD)	Last CRP value from clinical care may be used
42. Elevated CRP (≥5 mg/L)	*n* (%)	-

ASAS, Assessment of SpondyloArthritis international Society; ASDAS, Axial Spondyloarthritis Disease Activity Score; BASDAI, Bath Ankylosing Spondylitis Disease Activity Index; BASFI, Bath Ankylosing Spondylitis Functional Index; bDMARD, biological DMARD; CRP, C-reactive protein; csDMARD, conventional synthetic DMARD; DMARD, disease-modifying antirheumatic drug; IBD, inflammatory bowel disease; IBP, inflammatory back pain; SIJ, sacroiliac joints; NSAID, nonsteroidal anti-inflammatory drug; i, inhibitor; Q, question; tsDMARD, targeted synthetic DMARD.

[a] ASDAS categories: ≤1.3 inactive disease, >1.3 and ≤2.1 low disease, >2.1 and ≤3.5 high disease, >3.5 very high disease activity.

[b] ASAS health index categories: good ≤ 5, moderate <5 to <12, poor ≥12.

[c] Definitions according to current ASAS classification criteria.

commented in Table 1, current but also past extramusculoskeletal manifestations (EMM) such as inflammatory bowel disease and musculoskeletal manifestations like dactylitis should have been diagnosed by a physician. As baseline features, the imaging items radiographic sacroiliitis, magnetic resonance imaging (MRI) inflammation, and MRI structural lesion were already proposed mandatory by the steering group for DMARD trials but in workgroup meeting it was decided that these are also useful to be reported for trials other than DMARD trials. However, while these imaging items set as mandatory for DMARD trials (Table 2), they are optional for non-DMARD trials (ie, 'report if collected').

Eleven features (items 21-31) in Table 1 are on current and past pharmacological treatment of axial SpA with the steering and workgroup having added several items not reported in published clinical trials such as previous use of 3 biological or targeted synthetic DMARD classes and previous use of Janus kinase inhibitor (JAK) inhibitors.

Items 32 to 42 in Table 1 are baseline values of instruments like the Axial Spondyloarthritis Disease Activity Score (ASDAS), a composite index to assess disease activity, the ASAS health index (ASAS HI) for overall health and functioning, and results from C-reactive protein (CRP) laboratory test. Apart from a CRP value (≥5 mg/L), all baseline features in the 'Clinical and laboratory measures' category are also baseline values of the outcomes in Tables 3 and 4.

Additional baseline features for DMARD trials

Table 2 lists recommended extra baseline features for trials aimed at showing disease modification. In addition to the baseline features for all trials from Table 1, for DMARD trials, it is

Table 2
Additional baseline features for disease-modifying antirheumatic drug (DMARD) trials

Item	How	Comment
1. SPARCC MRI activity of the SIJ	Mean (SD)	-
2. SPARCC MRI activity of the spine	Mean (SD)	-
3. 44 swollen joint count	*n* (%) patients with ≥1 swollen joint and mean (SD) in patients with ≥1 swollen joint	-
4. MASES	*n* (%) patients with score ≥1 and mean (SD) in patients with score ≥1	-
5. Dactylitis count	*n* (%) patients with ≥1 and mean (SD) in patients with ≥1	-
6. mSASSS	Mean (SD)	-
7. Syndesmophytes	*n* (%) patients with ≥1 syndesmophyte	-
8. Radiographic sacroiliitis	*n* (%) bilateral ≥grade 2 or unilateral ≥grade 3	Grading according to modified New York criteria

MASES, Maastricht Ankylosing Spondylitis Enthesitis Score; mSASSS, modified Stoke Ankylosing Spondylitis Spinal Score; SIJ: sacroiliac joints; SPARCC, Spondyloarthritis Research Consortium of Canada.

Table 3
Reporting outcomes of instruments in the ASAS Core Outcome Set

Item	At baseline	At follow-up timepoint(s)
For all trials		
1. ASDAS	Mean (SD)	Mean (SD) and mean (SD) CFB and *n* (%) of pts with improvement of ≥1.1 (clinically important-) and ≥2.0 (major- improvement)[a]
2. ASDAS disease activity status	*n* (%) per category[b]	*n* (%) per category and *n* (%) <2.1 and ≥2.1
3. Patient global disease activity	Mean (SD)	Mean (SD) and mean (SD) CFB
4. Total back pain (BASDAI Q2)	Mean (SD)	Mean (SD) and mean (SD) CFB
5. Mean stiffness severity (BASDAI Q5) and duration (BASDAI Q6)[c]	Mean (SD)	Mean (SD) and mean (SD) CFB
6. Fatigue (BASDAI Q1)	Mean (SD)	Mean (SD) and mean (SD) CFB
7. BASFI	Mean (SD)	Mean (SD) and mean (SD) CFB
8. ASAS 20 and ASAS 40 responses	Not applicable	*n* (%)
9. ASAS health Index	Mean (SD)	Mean (SD) and mean (SD) CFB and *n* (%) of pts with improvement ≥3
10. ASAS health Index status[d]	*n* (%) per category	*n* (%) per category
Mandatory for DMARD trials only		
11. SPARCC MRI-SIJ activity	Mean (SD)	Mean (SD) and mean (SD) CFB
12. SPARCC MRI-spine activity	Mean (SD)	Mean (SD) and mean (SD) CFB
13. Acute anterior uveitis	*n* (%) with history	*n* (%) since baseline/rate per 100 pt yrs and split by pts with and without history
14. Psoriasis	*n* (%) with history	*n* (%) since baseline[e]/rate per 100 pt yrs and split by pts with and without history
15. IBD	*n* (%) with history	*n* (%) since baseline/rate per 100 pt yrs and split by pts with and without history
16. 44 swollen joint count	Mean (SD)	Mean (SD) and mean (SD) CFB[f]
17. MASES	Mean (SD)	Mean (SD) and mean (SD) CFB[f]
18. Dactylitis count	Mean (SD)	Mean (SD) and mean (SD) CFB[f]
19. mSASSS	Mean (SD)	Mean (SD) and mean (SD) CFB
20. Syndesmophytes	*n* (%) with ≥1	*n* (%) with ≥1 syndesmophyte and *n* (%) with a new syndesmophyte

ASAS, Assessment of SpondyloArthritis international Society; ASDAS, Axial Spondyloarthritis Disease Activity Score; BASFI, Bath Ankylosing Spondylitis Functional Index; CFB, change from baseline; IBD, inflammatory bowel disease; MASES, Maastricht Ankylosing Spondylitis Enthesitis Score; mSASSS, modified Stoke Ankylosing Spondylitis Spinal Score; pt, patient; Q, question; SPARCC, Spondyloarthritis Research Consortium of Canada.
[a] If flares are reported: *n* (%) of pts. with ASDAS of ≥0.9.
[b] ASDAS categories: ≤1.3 inactive disease (ASDAS-ID), >1.3 and ≤2.1 low disease (ASDAS-LDA), >2.1 and ≤3.5 high disease (ASDAS-HDA), >3.5 very high disease activity (ASDAS-VHDA).
[c] BASDAI (Q5 + Q6)/2.
[d] ASAS health index categories: good ≤5, moderate <5 to <12, poor ≥12.
[e] For psoriasis 'since baseline' is restricted to new-onset since baseline.
[f] In pts with swollen joint count>0, MASES > 0 or dactylitis count>0 at baseline.

recommended to report the 44 swollen joint count, Maastricht Ankylosing Spondylitis Enthesitis Score (MASES) and dactylitis count as baseline features. Moreover, while radiographic sacroiliitis and inflammation on MRI of the sacroiliac joint according to Table 1 are not mandatory and can be reported if collected, for DMARD trials it is recommended to report radiographic sacroiliitis with grading according to modified New York criteria and Spondyloarthritis Research Consortium of Canada (SPARCC) MRI activity score of the sacroiliac joint.

Grading according to the modified New York criteria (88 votes with 81% in favour and 19% against) was proposed by the ASAS members.

Additional imaging as a baseline feature recommended for DMARD trials is to report the mean SPARCC MRI activity score of the spine, mean modified Stoke Ankylosing Spondylitis Spinal Score (mSASSS), and the number of patients with at least 1 spinal syndesmophyte at baseline

With the exception of the number of patients with at least 1 syndesmophyte, all these baseline features are also trial outcomes. However, for swollen joint count, MASES and dactylitis count there are subtle differences in reporting. As a baseline feature, the 44 swollen joint count is recommended to be reported as the number of patients with at least 1 swollen joint plus the mean number of swollen joints in patients with at least 1 swollen joint, but as an outcome only the mean number of swollen joints in patients with at least 1 swollen joint is to be reported (Table 3). This is similar for MASES and dactylitis count.

Table 4
Reporting outcomes of instruments additionally endorsed by ASAS but not in the Core Outcome Set

<If collected present this way> *Item*	*At baseline*	*At follow-up timepoint(s)*
1. BASDAI	Mean (SD)	Mean (SD) + mean (SD) change from baseline
2. CRP (mg/L)	Mean (SD)	Mean (SD) + mean (SD) change from baseline
3. Berlin MRI-SIJ activity	Mean (SD)	Mean (SD) + mean (SD) change from baseline
4. Berlin MRI-spine activity	Mean (SD)	Mean (SD) + mean (SD) change from baseline
5. Back pain at night	Mean (SD)	Mean (SD) + mean (SD) change from baseline
6. Severity morning stiffness (BASDAI Q5)	Mean (SD)	Mean (SD) + mean (SD) change from baseline
7. Duration morning stiffness (BASDAI Q6)	Mean (SD)	Mean (SD) + mean (SD) change from baseline
8. SF-36 (PCS, MCS)	Mean (SD)	Mean (SD) + mean (SD) change from baseline
9. 66 swollen joint count[a]	Mean (SD)	Mean (SD) + mean (SD) change from baseline
10. SPARCC enthesitis[a]	Mean (SD)	Mean (SD) + mean (SD) change from baseline
11. SPARCC MRI SSS for erosion	Mean (SD)	Mean (SD) + mean (SD) change from baseline

BASDAI, Bath Ankylosing Spondylitis Disease Activity Index; CRP, C-reactive protein; MCS, mental component summary; PCS, physical component summary, Q, question; SF-36, 36-item Short Form Health Survey; SIJ, sacro-iliac joint; SPARCC, Spondyloarthritis Research Consortium of Canada; SSS, Sacroiliac joint Structural Score.
[a] In pts with swollen joint count>0, or enthesitis>0 at baseline.

Study outcomes

Table 3 presents recommendations on how outcomes from the instruments in the COS should be reported. The first 10 outcomes are for all clinical trials and the second 10 are outcomes for DMARD trials only. In the second column of the table, the outcomes are listed, in the third column how to report the outcomes at baseline, and in the fourth column how to report at 1 or more follow-up timepoints in the study. The most commonly recommended format for outcomes is to report the mean plus the SD at baseline and the mean value plus SD at other timepoints of the study while adding the mean change with SD from baseline for each timepoint. When more appropriate—for example, for outcomes with a highly skewed distribution—the geometric means may also be used.

While the recommendation to report the mean also applies to the ASDAS and the ASAS HI, it is recommended for these outcomes to also report the number and percentage of patient that achieve a specific improvement, namely a decrease of ≥1.1 (clinically important [CI]) and ≥2.0 units (major improvement [MI]) for the ASDAS and a decrease in the score of ≥3 for the ASAS HI. In addition, if disease activity flares are reported, the recommended threshold of an increase of 0.9 units for the ASDAS should be used. For both ASDAS and ASAS HI, it is recommended to also report the number and percentage of patients with specific status at each timepoint. For ASDAS, this is the number and percentage of patients with ASDAS inactive (≤1.3) (ASDAS-ID), low (>1.3 and ≤2.1) (ASDAS-LDA), high (>2.1 and ≤3.5) (ASDAS-HDA), and very high (>3.5) disease activity (ASDAS-VHDA) plus the number and percentage of patients with an ASDAS score of <2.1 (ie, ASDAS-ID or LDA) and ≥2.1 (ie, ASDAS-HDA or VHDA). For ASAS HI, the number and percentage of patients with a good (≤ 5), moderate (<5 to <12), and poor (≥12) status should be reported.

For ASAS20 and ASAS40 responses, it is recommended to report the number and percentage of patients meeting response criteria. ASAS 20 and 40 are improvement criteria than can be calculated from patient global disease activity, total back pain (Bath Ankylosing Spondylitis Disease Activity Index [BASDAI] Q2), Bath Ankylosing Spondylitis Functional Index (BASFI) and severity and duration stiffness (mean of BASDAI questions 5 and 6).

Psoriasis, acute anterior uveitis and inflammatory bowel disease are EMMs of axSpA and new occurrences or flares are recommended to be reported as the number and percentage of patients with flare or (re)occurrence since baseline plus the rate per 100 patient-years while also splitting the results by patients with and without a history of that particular EMM.

For spinal syndesmophytes, it is recommended to report the number and percentage of patients with at least 1 at baseline and outcomes plus the number and percentage of patients with a newly developed syndesmophyte which, if not scored on radiographs separately, can be derived from the mSASSS scoring with a vertebral unit over time developing an mSASSS score of 2 or 3 from a score less than 2 counting as the development of a syndesmophyte.

Table 4 lists the recommendations on how instruments additionally endorsed by ASAS but not in the COS should be reported at both baseline and at follow-up timepoints. All outcomes are recommended to be reported as mean with the SD of the mean at baseline and at follow-up timepoints the mean with the SD plus the mean changes from baseline with SD.

Voting

The final proposals were voted in by a majority of ASAS members in 3 separate votes: 85 members voting on the proposal for baseline features (Tables 1 and 2) with 84 % in favour, 11% against, and 6% abstaining, 81 members voting on the proposals for reporting outcomes of COS instruments (Table 3) with 85% in favour, 9% against, and 6% abstaining, and 85 members voting on reporting items of additional instruments not in the COS (Table 4) with 93% in favour, 2% against and 5% abstaining.

Presentation

All recommendations can be applied to reporting baseline characteristics and outcomes in text and tables but also in graphs. Figures 1-3 contain graph examples of 3 outcomes from Table 3 in a bar graph, a line graph, and a cumulative probability plot, respectively.

Figure 1 shows a bar graph of BASFI responses over time. While the use of the bars allows the reader to immediately see the difference between the 2 groups, the actual mean values can be found including the mean changes over time. Without these numbers, it would otherwise be difficult to accurately estimate the exact results by eye (or even ruler) using the height of the bars against the *Y*-axis. Apart from providing a more exact outcome, this greatly facilitates the reuse of the data into, for example, meta-analysis.

Similarly, in Figure 2, a line graph presents the mean ASDAS over 52 weeks' time in 2 groups of patients. While it is clear just by looking at the graphs that over time the mean ASDAS decreases in both groups, the exact means for each time point can be found in the box below the graphs with the change from baseline in the figure at each timepoint. Finally, Figure 3 shows cumulative probability plots of the change in mSASSS for patients receiving 2 different treatments.

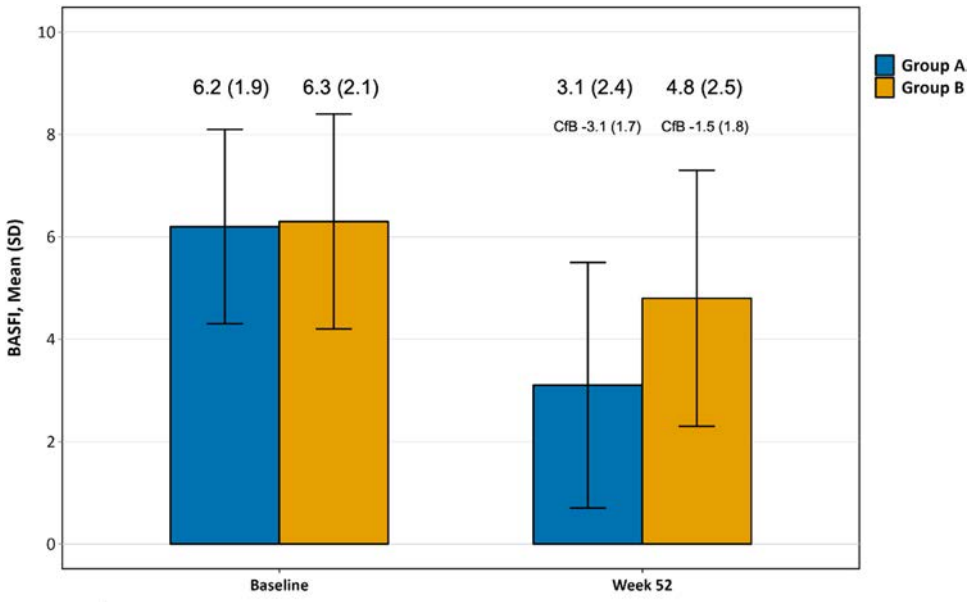

Figure 1. Bar graphs of hypothetical data showing the mean Bath Ankylosing Spondylitis Functional Index (BASFI) at baseline and 52 weeks in 2 groups of patients. For both groups the mean baseline values plus SD at baseline, 52 weeks, and the change over 52 weeks can be found directly above the graph. CfB, change from baseline.

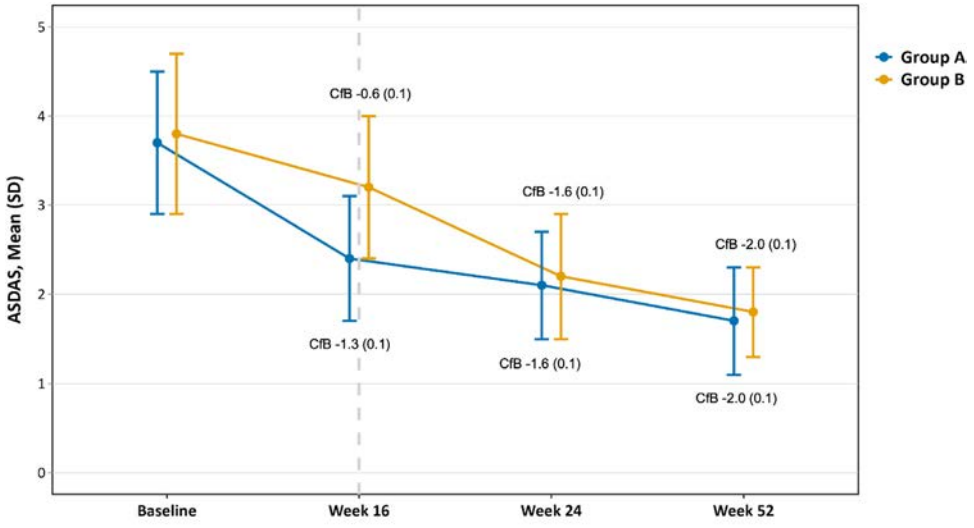

Group	Baseline	Week 16	Week 24	Week 52
Group A	3.7 (0.8)	2.4 (0.7)	2.1 (0.6)	1.7 (0.6)
Group B	3.8 (0.9)	3.2 (0.8)	2.2 (0.7)	1.8 (0.5)

Figure 2. Line graphs of hypothetical data showing the mean Axial Spondyloarthritis Disease Activity Score (ASDAS) in 2 groups of patients over time with the mean scores and SD at all timepoint in the box below the graphs with the change in ASDAS between baseline and the other timepoints in the graph itself. CfB, change from baseline.

Each symbol represents the change score of an individual patient ordered from the lowest to the highest change score by treatment group and the mean scores at baseline, mean scores at outcome, and mean change from baseline are shown in the graph.

DISCUSSION

Recommendations on reporting axSpA clinical trials based on a high degree of consensus from a large group of SpA experts are presented, consisting not only of recommendations on which baseline features to collect and how to report them but also which outcomes from instruments in the ASAS COS to present and how to present these outcomes.

While the recommendations on reporting outcomes build and expand upon the updated COS instruments set, the recommendations on the baseline features for clinical trials are novel. Baseline data should adequately describe the population in a trial including demographic variables, disease characteristics, and known factors that influence the outcomes (including past and current medications taken by participants). AxSpA is a heterogeneous disease and that is reflected in the number of clinical features listed in the baseline features table. Moreover, the relatively large number of items concerning pharmacological treatment reflect the recent increase in the number of treatments available for axSpA including whole new classes of biological and target synthetic DMARDs [6]. That said, while the number of recommended baseline features is substantial in particular

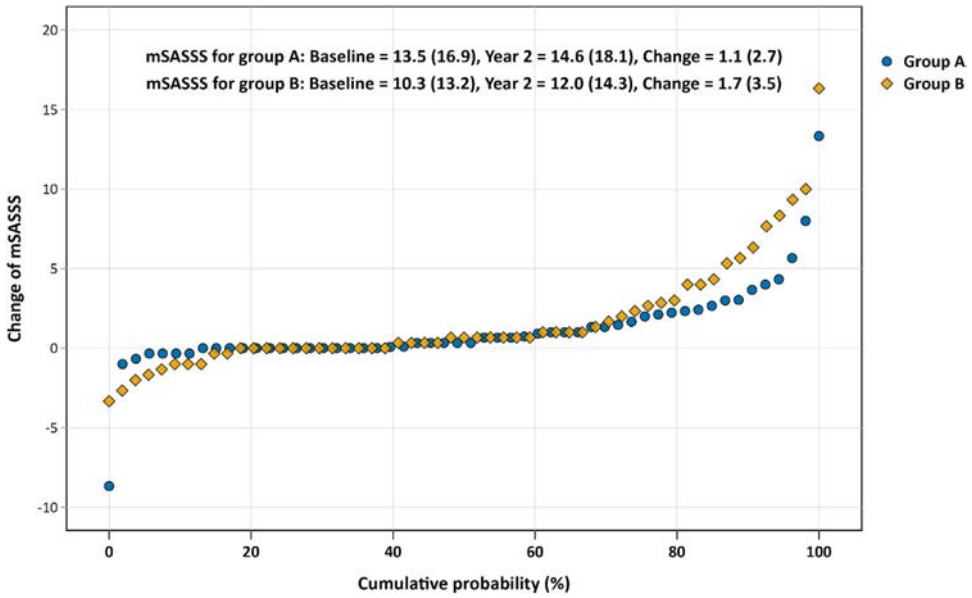

Figure 3. Cumulative probability plot of change in modified Stoke Ankylosing Spondylitis Spinal Scores (mSASSS) over 2 years in 2 groups of patients with mean scores plus SD at baseline, 2 years and the change over 2 years in the graph. Each symbol represents the change score of an individual patient ordered from the lowest to the highest change score by treatment group.

specific items describing pharmacological treatment options may not be applicable to all trials for obvious reasons, for example, previous bDMARD use in a trial aimed at bDMARD-naïve patients. However, given that information on the background of patients participating in a clinical trial is needed for correct interpretation of the results, it is important that the appropriate information on baseline features—like the study outcomes—can be found in the main manuscript and not only in an appendix.

A limitation of the process of drafting the baseline recommendations was that the number of publications consulted by the steering group was relatively small based on reviewing highly cited axSpA clinical trial publications. However, the recommendations were reviewed and commented on by a large number of experts making it unlikely that important items are missing. Nevertheless, apart from the recommended mandatory features, trialists may want to add specific baseline items and this should be analysed in future evaluations of these recommendations.

Per clear recommendation of ASAS members, educational level was added as a baseline feature. The steering group operationalized this by recommending the highest completed level of education in terms of primary, secondary, and tertiary education. The International Standard Classification of Education which offers uniform and internationally agreed definitions on education should be used to properly classify educational achievements despite substantial differences in educational systems around the world (Supplementary Table S2) [7].

The recommendation to report the number and percentage of axSpA with axial symptoms of less than 2 years as a baseline feature reflects the progress made in recent years in making earlier diagnoses. Diagnostic delay is far longer in axSpA than in other inflammatory disease and for many patients it can take years before being diagnosed. Recently, ASAS has adopted a definition of early axSpA as a duration of ≤2 years of axial symptoms and data from the SPondyloArthritis Caught Early cohort were published showing that rheumatologists are able to diagnose axSpA in patients with chronic back pain with less than 2 years of symptom duration [8,9].

In addition to for the first time providing recommendations on baseline features for axSpA trials, the project is a clear extension of the recently updated axSpA COS. The recommendations expand on the publication of the updated COS domains and instruments by advising how to actually report outcomes from the COS instruments.

Notably, while in the COS there are 16 instruments (7 mandatory instruments for all trials and 9 additional for DMARD trials), Table 3 shows 20 items to report: 10 for all trials and 10 additional items for DMARD trials. While most COS instruments correspond with 2 outcomes (eg, mean and mean change from baseline), other instruments such as ASAS HI [10] and mSASSS [11] but in particular the ASDAS inform more outcomes. Apart from a COS instrument, ASDAS is the recommended instrument for monitoring patients in clinical practice [6] and this is one of the reasons that outcomes of the ASDAS are recommended to be extensively reported including mean values at timepoints, change from baseline, patients with CI and MI and flare [12,13]. In addition, CRP, the laboratory test in the ASDAS and an objective marker of inflammation may be reported separately as an endorsed instrument but not in the COS.

Overall, these recommendations contain a substantial number of different axSpA features, definitions, and instruments. Important background information on these items including how to correct use instruments can be found in the original publications such as the ASAS20 and 40 improvement criteria [14,15] but also the ASAS handbook available on the ASAS website and which is currently in the process of being updated [16,17].

There is a growing recognition that sufficient attention must be paid to the outcomes measured and reported in clinical trials. Having a COS available as an agreed minimum standardised set of outcomes that should be measured is an important step in reducing trial heterogeneity but so is consistent and precise reporting of trial outcomes. With COSs having been developed for most major rheumatic and musculoskeletal diseases, to our knowledge not many include recommendations on reporting outcomes of clinical trials. However, recommendations on reporting clinical trials have been published before, for example,

the European Alliance of Associations for Rheumatology (EULAR)/American College of Rheumatology (ACR) collaborative recommendations on reporting disease activity in clinical trials of patients with rheumatoid arthritis and the EULAR recommendations for the reporting of clinical trial extension studies [18,19].

While this study is focused on recommendations for available data, reporting missing data in clinical trials are a critical aspect of ensuring transparency, reproducibility, and the integrity of study findings. Both the European Medicines Agency and the International Conference on Harmonization (ICH) (ICH E9) provide comprehensive guidelines on how to not only handle but also report missing data in clinical trials [20,21].

Finally, the readership of clinical trials is diverse and may include researchers, policy makers, patients, and clinicians. Therefore, ensuring clinical trial reports are accessible to readers with different training and educational backgrounds is important and may—for example—require explaining context or implications to nonclinicians and explanation of the interpretation of advanced methodology to readers with less extensive statistical training.

In summary, as the final step in updating the axSpA COS, we present ASAS-endorsed expert recommendations for collecting and reporting baseline features and presenting outcomes of axSpA clinical trials using instruments from the COS with the overall aim of improving the quality of evidence-based knowledge in axSpA. Adherence to these recommendations will standardise presentation of results and thereby provide better insight into trial outcomes and facilitate comparing outcomes across studies.

Competing interests

FAvG reports a relationship with multiple disclosures all mentioned in manuscript that include: board membership, consulting or advisory, and funding grants. VN-C reports a relationship with multiple disclosures all mentioned in manuscript that include: board membership, consulting or advisory, and funding grants. XB reports a relationship with multiple disclosures all mentioned in manuscript that include: board membership, consulting or advisory, funding grants, and speaking and lecture fees. FvdB reports a relationship with multiple disclosures all mentioned in manuscript that include: consulting or advisory. LSG reports a relationship with multiple disclosures all mentioned in manuscript that include: board membership, consulting or advisory, and funding grants. IH reports a relationship with multiple disclosures all mentioned in manuscript that include: funding grants and travel reimbursement. RL reports a relationship with multiple disclosures all mentioned in manuscript that include: board membership, consulting or advisory, and funding grants. PMM reports a relationship with multiple disclosures all mentioned in manuscript that include: board membership and consulting or advisory. HM-O reports a relationship with multiple disclosures all mentioned in manuscript that include: consulting or advisory and funding grants. VRR reports a relationship with multiple disclosures all mentioned in manuscript that include: funding grants and travel reimbursement. DR reports a relationship with multiple disclosures all mentioned in manuscript that include: board membership, consulting or advisory, and funding grants. SR reports a relationship with multiple disclosures all mentioned in manuscript that include: board membership, consulting or advisory, and funding grants. DvdH reports a relationship with multiple disclosures all mentioned in manuscript that include: board membership and consulting or advisory. If there are other authors, they declare that they have no known competing financial interests or personal relationships that could have appeared to influence the work reported in this paper.

CRediT authorship contribution statement

Floris A. van Gaalen: Writing – review & editing, Writing – original draft, Visualization, Validation, Supervision, Project administration, Methodology, Investigation, Formal analysis, Data curation, Conceptualization. **Victoria Navarro-Compán:** Writing – review & editing, Supervision, Investigation, Formal analysis, Data curation, Conceptualization. **Xenofon Baraliakos:** Writing – review & editing, Investigation, Formal analysis. **Filip van den Bosch:** Writing – review & editing, Investigation, Formal analysis. **Lianne S. Gensler:** Writing – review & editing, Investigation. **Ihsane Hmamouchi:** Writing – review & editing, Investigation, Formal analysis. **Robert Landewé:** Writing – review & editing, Investigation, Formal analysis. **Pedro M. Machado:** Writing – review & editing, Investigation, Formal analysis. **Helena Marzo-Ortega:** Writing – review & editing, Investigation, Formal analysis. **Valeria Rios Rodriguez:** Writing – review & editing, Visualization, Investigation, Formal analysis. **Denis Poddubnyy:** Writing – review & editing, Investigation, Formal analysis. **Sofia Ramiro:** Writing – review & editing, Investigation, Formal analysis. **Désirée van der Heijde:** Writing – review & editing, Supervision, Methodology, Investigation, Data curation, Conceptualization.

Acknowledgements

We would like to thank Dr Murat Torgutalp for providing the data used in Figure 3 and for helping create the graph.

Funding

HM-O is supported by the National Institute for Health Research (NIHR) Leeds Biomedical Research Centre (LBRC), The Leeds Teaching Hospitals NHS Trust. PMM is supported by the NIHR University College London Hospitals BRC, University College London Hospitals NHS Foundation Trust. The views expressed are those of the authors and not necessarily those of the (UK) National Health Service (NHS), the NIHR, or the (UK) Department of Health.

Patient consent for publication

Not applicable.

Provenance and peer review

Not commissioned; externally peer reviewed.

Ethics approval

Not applicable.

Supplementary materials

Supplementary material associated with this article can be found in the online version at doi:10.1016/j.ard.2025.07.017.

Orcid

Floris A. van Gaalen: http://orcid.org/0000-0001-8448-7407
Victoria Navarro-Compán: http://orcid.org/0000-0002-4527-852X
Xenofon Baraliakos: http://orcid.org/0000-0002-9475-9362
Filip van den Bosch: http://orcid.org/0000-0002-3561-5932
Lianne S. Gensler: http://orcid.org/0000-0001-6314-5336
Ihsane Hmamouchi: http://orcid.org/0000-0003-4402-5034
Robert Landewé: http://orcid.org/0000-0002-0577-6620
Pedro M. Machado: http://orcid.org/0000-0002-8411-7972
Helena Marzo-Ortega: http://orcid.org/0000-0002-9683-3407
Valeria Rios Rodriguez: http://orcid.org/0000-0001-5612-043X
Denis Poddubnyy: http://orcid.org/0000-0002-4537-6015
Sofia Ramiro: http://orcid.org/0000-0002-8899-9087
Désirée van der Heijde: http://orcid.org/0000-0002-5781-158X

REFERENCES

[1] Schulz KF, Altman DG, Moher D. CONSORT 2010 statement: updated guidelines for reporting parallel group randomised trials. PLOS Med 2010;7(3):e1000251.
[2] Kirkham JJ, Williamson P. Core outcome sets in medical research. BMJ Med 2022;1(1):e000284.
[3] Navarro-Compán V, Boel A, Boonen A, Mease P, Landewé R, Kiltz U, et al. The ASAS-OMERACT core domain set for axial spondyloarthritis. Semin Arthritis Rheum 2021;51(6):1342–9.
[4] Navarro-Compán V, Boel A, Boonen A, Mease PJ, Dougados M, Kiltz U, et al. Instrument selection for the ASAS core outcome set for axial spondyloarthritis. Ann Rheum Dis 2023;82(6):763–72.
[5] Web of Science. Available from: https://www.webofscience.com/wos/woscc/basic-search. Accessed September 1, 2025.
[6] Ramiro S, Nikiphorou E, Sepriano A, Ortolan A, Webers C, Baraliakos X, et al. ASAS-EULAR recommendations for the management of axial spondyloarthritis: 2022 update. Ann Rheum Dis 2023;82(1):19–34.
[7] International Standard Classification of Education ISCED 2011. Available from: https://en.wikipedia.org/wiki/International_Standard_Classification_of_Education. Accessed September 1, 2025.
[8] Marques ML, Ramiro S, van Lunteren M, Stal RA, Landewé RB, van de Sande M, et al. Can rheumatologists unequivocally diagnose axial spondyloarthritis in patients with chronic back pain of less than 2 years duration? Primary outcome of the 2-year SPondyloArthritis Caught Early (SPACE) cohort. Ann Rheum Dis 2024;83(5):589–98.
[9] Navarro-Compán V, Benavent D, Capelusnik D, van der Heijde D, Landewé RB, Poddubnyy D, et al. ASAS consensus definition of early axial spondyloarthritis. Ann Rheum Dis 2024;83(9):1093–9.
[10] Kiltz U, van der Heijde D, Boonen A, Akkoc N, Bautista-Molano W, Burgos-Vargas R, et al. Measurement properties of the ASAS Health Index: results of a global study in patients with axial and peripheral spondyloarthritis. Ann Rheum Dis 2018;77(9):1311–7.
[11] Creemers MC, Franssen MJ, van't Hof MA, Gribnau FW, van de Putte LB, van Riel PL. Assessment of outcome in ankylosing spondylitis: an extended radiographic scoring system. Ann Rheum Dis 2005;64(1):127–9.
[12] Machado P, Landewé R, Lie E, Kvien TK, Braun J, Baker D, et al. Ankylosing Spondylitis Disease Activity Score (ASDAS): defining cut-off values for disease activity states and improvement scores. Ann Rheum Dis 2011;70(1):47–53.
[13] Molto A, Gossec L, Meghnathi B, Landewé RBM, van der Heijde D, Atagunduz P, et al. An Assessment in SpondyloArthritis International Society (ASAS)-endorsed definition of clinically important worsening in axial spondyloarthritis based on ASDAS. Ann Rheum Dis 2018;77(1):124–7.
[14] Brandt J, Listing J, Sieper J, Rudwaleit M, van der Heijde D, Braun J. Development and preselection of criteria for short term improvement after anti-TNF alpha treatment in ankylosing spondylitis. Ann Rheum Dis 2004;63(11):1438–44.
[15] Anderson JJ, Baron G, van der Heijde D, Felson DT, Dougados M. Ankylosing spondylitis assessment group preliminary definition of short-term improvement in ankylosing spondylitis. Arthritis Rheum 2001;44(8):1876–86.
[16] Sieper J, Rudwaleit M, Baraliakos X, Brandt J, Braun J, Burgos-Vargas R, et al. The Assessment of SpondyloArthritis international Society (ASAS) handbook: a guide to assess spondyloarthritis. Ann Rheum Dis 2009;68(Suppl 2):ii1–44.
[17] ASAS Handbook. Available from: https://www.asas-group.org/education/asas-handbook. Accessed September 1, 2025.
[18] Aletaha D, Landewe R, Karonitsch T, Bathon J, Boers M, Bombardier C, et al. Reporting disease activity in clinical trials of patients with rheumatoid arthritis: EULAR/ACR collaborative recommendations. Ann Rheum Dis 2008;67(10):1360–4.
[19] Buch MH, Silva-Fernandez L, Carmona L, Aletaha D, Christensen R, Combe B, et al. Development of EULAR recommendations for the reporting of clinical trial extension studies in rheumatology. Ann Rheum Dis 2015;74(6):963–9.
[20] Available from: https://www.ema.europa.eu/en/missing-data-confirmatory-clinical-trials-scientific-guideline. Accessed September 1, 2025.
[21] Lewis JA. Statistical principles for clinical trials (ICH E9): an introductory note on an international guideline. Stat Med 1999;18(15):1903–42.

Ann Rheum Dis 84 (2025) 1779–1790

Contents lists available at ScienceDirect

Annals of the Rheumatic Diseases

journal homepage: https://www.sciencedirect.com/journal/annals-of-the-rheumatic-diseases

Rheumatoid arthritis

Comparative risk of incident malignancies in rheumatoid arthritis patients treated with Janus kinase inhibitors or bDMARDs: observational data from the German RABBIT register

Martin Schaefer[1,*], Alina Purschke[1], Vera Zietemann[1], Tatjana Rudi[1], Yvette Meissner[1], Adrian Richter[1,2], Sylvia Berger[3], Karin Rockwitz[4], Klaus Krüger[5], Karl Matthias Schneider[6], Anne C. Regierer[1], Anja Strangfeld[1,7]

[1] *Programme Area Epidemiology and Health Services Research, German Rheumatology Research Center, Berlin, Germany*
[2] *Department SHIP-KEF, Institute for Community Medicine, University Medical Center Greifswald, Greifswald, Germany*
[3] *Rheumatological Practice, Naunhof, Germany*
[4] *Rheumatological Practice, Goslar, Germany*
[5] *Rheumatological Practice Center, Munich, Germany*
[6] *Heinrich Heine University, Düsseldorf, Germany*
[7] *Department of Rheumatology and Clinical Immunology, Charité University Medicine Berlin, Germany*

ARTICLE INFO

Article history:
Received 14 January 2025
Received in revised form 18 May 2025
Accepted 20 May 2025

ABSTRACT

Objectives: To estimate the effects of Janus kinase inhibitors (JAKis) vs biologic disease-modifying antirheumatic drugs (bDMARDs) on the risk of incident malignancies (excluding nonmelanoma skin cancer) in patients and patient subgroups with rheumatoid arthritis.

Methods: Episodes of disease-modifying antirheumatic drug (DMARD) treatment initiated between January 2017 and December 2020 and followed up to June 2024 in RABBIT, the German register for the long-term observation of therapy with biologics and targeted disease-modifying antirheumatic drugs in adult patients with rheumatoid arthritis, were analysed. Incidence rates (IRs) per 1000 patient-years with 95% CIs were calculated, and incident malignancy risk was estimated as hazard ratios (HRs) by inverse probability weighted adjusted Cox models.

Results: Among 2285 JAKi and 4259 bDMARD treatment episodes, 88 and 135 malignancies occurred, respectively. JAKi treatments were dominated by baricitinib and tofacitinib, while most bDMARD treatments comprised tumour necrosis factor inhibitors. IRs were 11.6 (95% CI: 9.3, 14.3) in JAKi- and 8.9 (95% CI: 7.4, 10.5) in bDMARD-treated groups. The adjusted HR comparing JAKis with bDMARDs was 1.40 (95% CI: 1.09, 1.80). An increase in the malignancy risk for JAKi vs bDMARD treatment could only be observed in treatment episodes lasting longer than 16 months. The risk appeared higher in some subgroups of patients, including those who started treatment aged ≥60 years, patients with ≥3 prior conventional synthetic DMARD treatments, and patients with high disease activity.

Conclusions: In this German observational cohort study, an overall small increase in malignancy risk for JAKi vs bDMARD treatment was observed, with more pronounced risks in some subgroups of patients. The observed risk should be carefully counterbalanced to the known malignancy risk associated with insufficient disease control.

*Correspondence to Dr. Martin Schaefer, German Rheumatology Research Center, Programme Area Epidemiology and Health Services Research, Berlin, Germany.
E-mail address: martin.schaefer@drfz.de (M. Schaefer).
Handling editor Josef S. Smolen.

https://doi.org/10.1016/j.ard.2025.05.014

WHAT IS ALREADY KNOWN ON THIS TOPIC

- The Oral Rheumatoid Arthritis Trial (ORAL) Surveillance study found an increased occurrence of incident malignancies (excluding nonmelanoma skin cancer) with the Janus kinase inhibitor (JAKi) tofacitinib compared to tumour necrosis factor inhibitors in patients with rheumatoid arthritis aged ≥50 years and with ≥1 additional cardiovascular risk factor. This risk was not observed in several register and claims data studies.
- A warning was issued by the European Medicines Agency regarding the use of all JAKis in patients aged ≥65 years, cardiovascular high-risk patients, and patients with malignancy risk factors for the approved indications.

WHAT THIS STUDY ADDS

- In a comprehensive real-world analysis, an increased risk for malignancies in patients ever treated with JAKis compared to those ever treated with bDMARDs was found, with risk estimates comparable to those reported by the ORAL Surveillance trial.
- To detect this increased risk, a sufficiently long follow-up period is crucial, as the increased risk for JAKi treatment is only observed after 16 months of follow-up.

HOW THIS STUDY MIGHT AFFECT RESEARCH, PRACTICE OR POLICY

- By being informed about the specific characteristics of patients who are at a potentially increased risk of malignancy on JAKi compared to bDMARD therapy, healthcare providers can improve their treatment decisions and be guided regarding the intensity of cancer screening in patients under and after JAKi treatment.

INTRODUCTION

Patients with rheumatoid arthritis (RA) are at an increased risk of overall malignancies compared with the general population, particularly lung cancer, lymphoma, and skin cancer, whereas risks for colon cancer and breast cancer are lower [1–3]. This increased risk was shown to be partly driven by the rheumatic disease activity, especially for lymphoma, highlighting the need for appropriate treatment with disease-modifying antirheumatic drugs (DMARDs). The overall excess cancer risk associated with treatment of conventional synthetic (cs)DMARDs, mainly methotrexate, and with biologic (b)DMARDs appears to be low based on large observational studies [1,4], with a few individual analyses indicating the possibility that some bDMARDs may even have an overall protective effect [5,6].

Janus kinase inhibitors (JAKis) target Janus kinases (JAKs) within the JAK-STAT (signal transducer and activator of transcription) pathway, which transmits signals from numerous cytokines and growth factors, contributing to pleiotropic effects on innate and adaptive immune responses as well as on regulating cell growth and differentiation [7]. JAK inhibition may impair antitumour immunity and apoptosis, potentially influencing tumour progression [8,9]. On the other hand, by reducing chronic inflammation as well as targeting overexpressed JAK and/or STAT family members, tumour-promoting effects of JAK-STAT metabolism are also counteracted [10,11]. This suggests that JAK inhibition might alter malignancy risk, with unclear clinical significance so far. The Oral Rheumatoid Arthritis Trial (ORAL) Surveillance study included a risk-enriched population of RA patients with a minimum age of 50 years and ≥1 cardiovascular (CV) risk factor. It detected an overall malignancy risk (excluding nonmelanoma skin cancer [NMSC]) of 1.47 (95% CI: 1.00, 2.18) for 5 mg tofacitinib twice daily compared to tumour necrosis factor inhibitors (TNFis) [12], prompting the US Food & Drug Administration and the European Medicines Agency (EMA) to issue warnings regarding tofacitinib use [13,14].

Upon assessment of the final trial [14] and including observational study results [12,15], the EMA endorsed the safety alerts and took a precautionary approach to all JAKis currently approved for the treatment of several chronic inflammatory disorders. For patients aged ≥65 years, for current or past long-time smokers, and for patients at increased risk of major CV events or cancer, the EMA is now advising to use JAKi treatment only if no suitable treatment alternatives are available [16]. The current European Alliance of Associations for Rheumatology recommendations for the management of RA already take this into account to some extent [17].

Several studies using register or claims data of RA patients have attempted to replicate the ORAL Surveillance (OS) findings in real-world settings [18–23]. While a significant increase of cancer risk with JAKi compared to TNFi treatment has not been shown yet, the Danish register of patients with rheumatoid arthritis (DANBIO) has reported a hazard ratio (HR) of 1.41 (95% CI: 0.76, 2.37) for JAKis compared to bDMARDs, which is numerically similar to OS but with limited power due to a small number of events among patients ever treated with JAKis (n = 19) [23]. Conversely, analyses from the Antirheumatic Therapies in Sweden (ARTIS) register [18], a register from Hong Kong [21], US collaborative claims data [24] as well as Korean claims data [20,22] have all found HRs consistently close to 1, indicating no evidence of an increased or decreased risk associated with JAKi compared to TNFi treatment. In some analyses, the risk estimate was higher, although not significant, when investigating bDMARD-naïve patients or when applying a lag time beginning at treatment initiation ('latency period,' LP) during which events are not assigned to that treatment [19,20,22]. It remains largely unclear what the differences in the results of the individual studies can be attributed to.

To better understand the complex role of JAKis in cancer development in RA patients, the aim of this study was to estimate the effects of JAKis compared to bDMARDs on the risk of malignancy (excluding NMSC) in patients with RA.

METHODS

Data source

The data for this study originate from RABBIT, the German register for the long-term observation of therapy with biologics and targeted disease-modifying antirheumatic drugs in adult patients with rheumatoid arthritis. RABBIT is a nationwide prospective observational longitudinal cohort study that ascertains data from routine clinical care since 2001. Adult RA patients are continuously enrolled into the register when starting a b/tsDMARD or when starting a csDMARD after ≥1 prior DMARD therapy. Information is reported by rheumatologists and patients at regular time points for ≥5 years and ≤10 years, comprising demographics, disease and treatment characteristics, comorbidities, and patient-reported outcomes [25]. Prior to their participation, patients gave their written informed consent.

Study population

The study included patients with ≥1 follow-up and without a history of prior malignancies except NMSC who began a new JAKi or bDMARD treatment (Fig 1) between January 2017 and

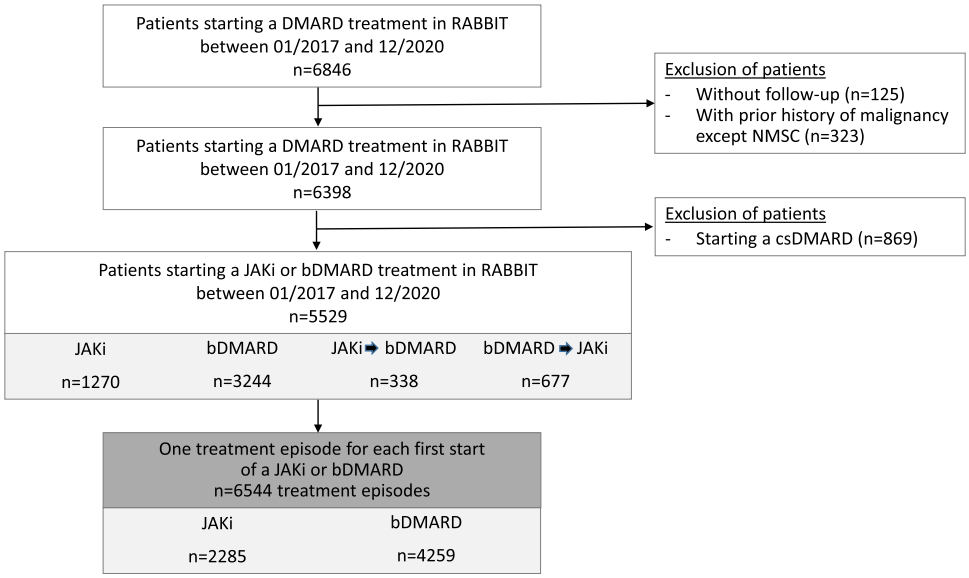

Figure 1. Flow chart of patient and treatment episode selection for overall patients. Numbers of patients starting a treatment are given for patients who only received a substance (or various substances) of 1 of the 2 compared treatment groups, as well as for patients who received substances from both treatment groups, differentiated by the order in which substances from each treatment group were given. 1270 patients received JAKis but no bDMARDs, 3244 patients received bDMARDs but no JAKis, 338 patients received first JAKis and then bDMARDs, and 677 patients received first bDMARDs and then JAKis. Thus there were 1270 + 338 + 677 = 2285 JAKi treatment episodes and 3244 + 338 + 677 = 4259 bDMARD treatment episodes. bDMARD, biologic disease-modifying antirheumatic drug; csDMARD, conventional synthetic disease-modifying antirheumatic drug; DMARD, disease-modifying antirheumatic drug; JAKi, Janus kinase inhibitor; NMSC, nonmelanoma skin cancer; RABBIT, German register for the long-term observation of therapy with biologics and targeted disease-modifying antirheumatic drugs in adult patients with rheumatoid arthritis.

December 2020 (overall patients). This period was chosen to cover the time between the European Union marketing authorisation of the first 2 JAKis and the first warnings of a potential malignancy risk associated with JAKi treatment [16]. Considering the relationship between CV risk and malignancy as well as to increase similarity with the OS cohort, an additional subgroup with a CV risk-enriched population was defined employing some OS eligibility criteria [12], selecting patients aged ≥50 years and with ≥1 CV risk factor defined as hypertension, coronary heart disease, diabetes, or hyperlipoproteinemia or current smoking at treatment start (selected patients). Patients were followed up until June 2024 or dropout, ensuring a potential follow-up time of ≥3.5 years.

Outcomes

Overall incident malignancies (excluding NMSC) were investigated as the primary outcome and individual cancer entities as secondary outcomes. For both outcomes, death from any cause except malignancy, and for the secondary outcomes, malignancies other than the one of interest, were considered as competing risks.

Assignment of treatment exposure

Treatment episodes from 2 exposure groups were evaluated in this analysis: (A) JAKis (baricitinib, filgotinib, tofacitinib, or upadacitinib) and (B) bDMARDs (abatacept, adalimumab, certolizumab, etanercept, golimumab, infliximab, rituximab, sarilumab, or tocilizumab). JAKis and bDMARDs could be applied as monotherapy or combined with a csDMARD. One patient could contribute observation time and, potentially, an event, to 1 or both exposure groups. Switching substances within an exposure group did not trigger a new treatment episode. For example, a patient who initiated adalimumab in 2017 and etanercept in 2019 contributed 1 treatment episode to group B, whereas a patient who initiated adalimumab in 2017 and baricitinib in 2019 contributed 1 treatment episode each to group A and group B. An LP of 6 months was respected to account for the slow development of malignancies as well as to deal with reverse causation and detection bias [26]. Therefore, the index date was defined as the day 6 months after the initiation of the first drug from one exposure group. Treatment exposure lasted from index date until (i) death, (ii) end of individual patient observation, (iii) end of study period, or (iv) first occurrence of a malignancy, whichever came first and regardless of subsequent switches between exposure groups (‘once exposed, always at risk’).

Statistical analyses

Patient characteristics were summarised per exposure group at the time of treatment start (baseline). Numbers of events, patient-years (PYs) at risk and crude incidence rates (IRs) per 1000 PYs including a descriptive 95% CI for the time after the index date were calculated per exposure group assuming a Poisson distribution for observed event numbers [27]. Cumulative incidence was assessed graphically. In the primary analysis, adjusted HRs with 95% CIs were calculated to investigate the risk of malignancies associated with JAKi compared with bDMARD treatment. The Fine and Gray subdistribution hazard Cox regression model [28] was employed, using robust sandwich estimates [29] and accounting for competing risks. When the event probability is low, as in this analysis, the subdistribution hazard model’s coefficients can be interpreted as odds ratios for the cumulative incidence function [30]. HRs and IRs for the competing event of death/specific malignancy entities were also calculated.

Inverse probability of treatment weighting (IPTW) was used to reduce confounding with respect to exposure, estimating the average treatment effect (ATE) [31]. Stabilised weights were calculated by logistic regression using propensity scores,

adjusting for the baseline covariates age, sex as reported by physician, smoking habits, number of prior TNFi/IL6i treatments, number of prior b/tsDMARD treatments other than TNFis/IL6is, number of prior csDMARDs, rheumatoid factor/anti-citrullinated protein autoantibody status, Disease Activity Score based on erythrocyte sedimentation rate and 28 joints (DAS28-ESR), C-reactive protein, disease duration, number of comorbidities associated with malignancy risk (lung fibrosis, chronic obstructive pulmonary disease, coronary heart disease, heart failure, stroke, diabetes, chronic kidney disease, chronic liver disease, gastrointestinal disease without ulcus duodenii/ventriculi, psoriatic arthritis, Sjögren's disease, chronic viral infection, tuberculosis, depression, obesity), concomitant glucocorticoid therapy, and concomitant csDMARD therapy (Supplementary Table S1). TNFis/IL6is and abatacept/rituximab/JAKi were grouped for assessment of prior DMARD treatments, because for TNFis and IL6is, preclinical data suggests the possibility of antitumour effects [32–35]. Propensity score distributions were assessed graphically. If a covariate showed a mean standardised difference of >0.1 or <−0.1 after weighting, indicating insufficient balance between treatment groups, it was additionally included as covariate in the Cox model. The Cox proportional hazard assumption was assessed via Schoenfeld residuals.

Ten-fold imputation of missing values via fully conditional specification [36] was applied. All analyses were conducted in SAS (version 9.4) and R (version 4.3.0).

Subgroup and secondary analyses

Subgroup analyses were stratified by different covariates (Supplementary Table S1). Due to the known effect of age and considering the results of preliminary analyses, stratifications by covariates (except age) were further applied using a binary age cutoff (≥60 years and <60 years). Several secondary analyses were performed.

1. TNFi and non-TNFi bDMARDs were considered as reference category instead of all bDMARDs.
2. In an 'on treatment' analysis employing the Andersen-Gill model [37–40], treatment episodes lasted from index date until (i) death, (ii) treatment stop (switching substances within the same exposure group did not trigger a new episode), (iii) end of individual patient observation, (iv) end of study period, or (v) first occurrence of a malignancy, whichever came first. A risk window of 6 months (12 months for rituximab) was added after treatment discontinuation.
3. An unweighted Fine and Gray Cox model was fitted, both with full covariate adjustment and adjusted only for age and sex.
4. For an intention-to-treat (ITT) analysis, only the first treatment episode of each patient was considered, reducing dependency between treatment episodes and events.
5. The model was fitted without applying a LP.
6. To assess the existence of possible change points, the observation time of treatment episodes was split at different time points and analysed in separate models.
7. Inverse probability of censoring weighting (IPCW) was carried out in addition to IPTW to adjust for different types of informative censoring, employing the IPTW set of covariates and without considering competing risks.
8. A logistic generalised estimation equations (GEE) model was fitted for comparison with the Cox model.
9. csDMARDs (without any of the treatments from exposure groups A and B) were considered as an additional treatment group and compared to bDMARDs and (stratified by prior TNFi/IL6i use) to JAKis.

Patient and public involvement

RABBIT collaborates closely with the Deutsche Rheuma-Liga, the major German patient organisation for persons affected by rheumatic and musculoskeletal disorders.

RESULTS

Between January 2017 and December 2020, a total of 6544 newly initiated treatment episodes from 5529 patients were eligible for the analysis, of which 2285 were with JAKis and 4259 with bDMARDs, corresponding to 7594 and 15,220 PYs excluding the LP, respectively (overall patients, Fig 1). Median follow-up was 47 and 50 months including the LP, respectively (Supplementary Table S2). When using the selected cohort more similar to OS inclusion criteria, 1341 and 2381 episodes with 4391 and 8237 PYs excluding the LP remained in the groups of JAKis and bDMARDs, respectively (selected patients). Unless stated otherwise, the following results refer to overall patients. The Supplementary Material also contains information on an additional treatment group with patients who received csDMARDs without parallel treatment with b/tsDMARDs (see Supplementary Section 5 for more information on this group; Supplementary Fig S1 contains an overview flow chart comprising all considered treatment comparisons).

Baseline characteristics

Age and sex distribution was comparable between the treatment groups (Table 1, Supplementary Table S3). Compared with patients starting a bDMARD, JAKi-treated patients on average had a higher number of prior TNFi or IL6i treatment failures, a slightly higher disease duration, and a slightly lower functional capacity and were considerably less likely to receive concomitant csDMARD therapy. When further stratifying by age (Supplementary Table S4), patients aged ≥60 years in both groups had a longer disease duration, more cancer-related comorbidities, and more frequent joint erosions but a lower functional capacity and were less likely to receive concomitant csDMARD therapy and to ever have smoked than younger patients. When further stratifying by prior TNFi/IL6i treatment (Supplementary Table S5), the discrepancy between JAKi- and bDMARD-treated patients regarding concomitant csDMARD therapy was notably higher among TNFi/IL6i-naïve patients than among patients with prior TNFi/IL6i treatment failures. In addition, among TNFi/IL6i-naïve patients, the prevalence of a number of comorbidities was higher in the JAKi group, while among patients with prior TNFi/IL6i treatment failures, it was higher in the bDMARD group. These comorbidities included coronary heart disease, COPD, diabetes mellitus, chronic kidney disease, chronic liver disease, chronic gastrointestinal disease, or depression. Among TNFi/IL6i-naïve patients, JAKi-treated patients had a longer disease duration than bDMARD-treated patients but not among individuals with prior TNFi/IL6i treatment failures.

Crude IRs and adjusted HRs of malignancy

Of the 190 malignancies reported, 55 events were assigned only to JAKis, 102 only to bDMARDs, and 33 to both groups.

The crude IRs per 1000 PYs for malignancies were 9.7 (95% CI: 8.3, 11.1) for both groups, and 11.6 (95% CI: 9.3, 14.3) and 8.9 (95% CI: 7.4, 10.5) for JAKis and bDMARDs, respectively (Table 2). Higher IRs were observed in the selected patient

Table 1
Patient characteristics at the time of starting treatment with JAKis and bDMARDs

Patient characteristics	#NA	JAKis 2285	#NA	bDMARDs 4259
Baricitinib at start		1077 (47.1)		
Tofacitinib at start		922 (40.4)		
Upadacitinib at start		278 (12.2)		
Filgotinib at start		10 (0.4)		
TNFi at start				2617 (61.4)
Abatacept at start				364 (8.5)
Rituximab at start				681 (16.0)
IL6i at start				605 (14.2)
Concomitant csDMARDs[a]		975 (42.7)		2416 (56.7)
Concomitant methotrexate[a]		906 (39.6)		2198 (51.6)
Treatment start 2019 or later		1149 (50.3)		1649 (38.7)
Age, y, median (IQR)		59.3 (14.8)		58.8 (15.4)
<50		411 (18.0)		951 (22.3)
≥50 to <55		349 (15.3)		579 (13.6)
≥55 to <60		428 (18.7)		786 (18.5)
≥60 to <65		407 (17.8)		656 (15.4)
≥65 to <70		262 (11.5)		530 (12.4)
≥70 to <75		180 (7.9)		318 (7.5)
≥75		248 (10.9)		439 (10.3)
Male patients		531 (23.2)		1109 (26.0)
Smoking habits				
Current smoking	*65*	616 (27.0)	*129*	1156 (27.1)
Ever smoked	*65*	1347 (58.9)	*129*	2576 (60.5)
DD, y, median (IQR)	*1*	10.1 (12.1)	*4*	9.1 (11.5)
≤2	*1*	146 (6.4)	*4*	450 (10.6)
>2 to ≤5	*1*	418 (18.3)	*4*	856 (20.1)
>5 to ≤10	*1*	575 (25.2)	*4*	1014 (23.8)
>10 to ≤15	*1*	422 (18.5)	*4*	769 (18.1)
>15	*1*	723 (31.7)	*4*	1166 (27.4)
Positive rheumatoid factor or ACPA	*104*	1725 (79.1)	*161*	3218 (78.5)
Joint erosions	*76*	1040 (47.1)	*132*	1899 (46.0)
DAS28-ESR, median (IQR)	*388*	4.2 (2.0)	*714*	4.2 (2.1)
<2.6	*388*	267 (14.1)	*714*	511 (14.4)
≥2.6 to <3.2	*388*	219 (11.5)	*714*	394 (11.1)
≥3.2 to ≤5.1	*388*	889 (46.9)	*714*	1646 (46.4)
>5.1	*388*	522 (27.5)	*714*	994 (28.0)
CDAI, median (IQR)	*229*	12.0 (13.0)	*426*	11.0 (12.0)
≤2.8	*229*	133 (6.5)	*426*	246 (6.4)
>2.8 to ≤10	*229*	809 (39.3)	*426*	1645 (42.9)
>10 to ≤22	*229*	724 (35.2)	*426*	1331 (34.7)
>22	*229*	390 (19.0)	*426*	611 (15.9)
CRP, mg/L, median (IQR)	*335*	3.1 (7.0)	*703*	3.0 (6.1)
<5	*335*	1217 (62.4)	*703*	2273 (63.9)
≥5 to ≤10	*335*	318 (16.3)	*703*	639 (18.0)
>10	*335*	415 (21.3)	*703*	644 (18.1)
Percentage of full physical function, median (IQR)	*184*	72.2 (36.1)	*340*	75 (36.1)
<60%	*184*	778 (37.0)	*340*	1241 (31.7)
Number of prior TNFis or IL6is, mean (SD)		1.4 (1.3)		0.8 (1.1)
None		640 (28)		2355 (55.3)
1		691 (30.2)		926 (21.7)
2		507 (22.2)		575 (13.5)
≥3		447 (19.6)		403 (9.5)
Number of prior b/tsbDMARDs other than TNFis/IL6is, mean (SD)		0.4 (0.6)		0.4 (0.7)
Any prior non-TNFi/IL6i bDMARD		663 (29.0)		1246 (29.3)
b/tsDMARD-naïve patients		587 (25.7)		2150 (50.5)
Number of prior csDMARDs, mean (SD)		2.2 (1.0)		2.1 (1.0)
0 or 1		504 (22.1)		1113 (26.1)
2		1041 (45.6)		1865 (43.8)
3		494 (21.6)		852 (20.0)
≥4		246 (10.8)		429 (10.1)
Concomitant corticosteroid therapy, mg/d				
None	*100*	1157 (53.0)	*130*	2233 (54.1)
<5	*100*	716 (32.8)	*130*	1282 (31.0)
5 to <10	*100*	234 (10.7)	*130*	484 (11.7)
≥10	*100*	78 (3.6)	*130*	130 (3.1)
Sum of cancer risk related comorbidities, mean (SD)	*327*	1.0 (1.1)	*507*	0.9 (1.1)
Educational attainment, y				
<10	*275*	577 (28.7)	*556*	1111 (30.0)
10	*275*	1012 (50.3)	*556*	1716 (46.3)
≥12	*275*	421 (20.9)	*556*	876 (23.7)
Enrolling institution: rheumatology clinic[b]		399 (17.5)		797 (18.7)
Dropout due to death[c]		86 (3.8)		175 (4.1)
Selective dropout due to other reasons[c]		236 (10.3)		520 (12.2)

ACPA, anti-citrullinated protein autoantibody; bDMARD, biologic disease-modifying antirheumatic drug; CDAI, Clinical Disease Activity Index; CRP, C-reactive protein; csDMARD, conventional synthetic disease-modifying antirheumatic drug; DAS28-ESR, Disease Activity Score based on erythrocyte sedimentation rate and 28 joints; DD, disease duration; IL6i, interleukin-6 inhibitor; JAKi, Janus kinase inhibitor; NA, not available; TNFi, tumour necrosis factor inhibitor; tsDMARD, targeted synthetic disease-modifying antirheumatic drug.

Results are based on treatment episodes, not patients, and are given as median (IQR) or mean (SD) for continuous variables and number (percentage) for categorical variables. '#NA' gives the number of missing values per variable, if applicable. Treatments given at start refer to all treatments given in the first month of a treatment episode from one of the exposure groups; the prescription of multiple treatments within this month is possible.

[a] Defined as ≥2 consecutive months of concomitant treatment.

[b] In contrast to rheumatology practice.

[c] Not a baseline value.

cohort with 12.8 events per 1000 PYs (95% CI: 10.8, 15.1) overall, and 15.9 (95% CI: 12.4, 20.1) and 11.5 (95% CI: 9.3, 14.1) for JAKis and bDMARDs, respectively (Table 2).

Compared with bDMARDs, the adjusted HR was 1.40 (95% CI: 1.09, 1.80) for JAKis in overall patients and 1.61 (95% CI: 1.22, 2.13) in selected patients (Table 2). In the main model, IPTW achieved well balanced groups (Supplementary Table S6). The number of PYs under or after JAKi exposure needed to observe 1 additional malignancy event, relative to bDMARDs (number needed to harm, NNH), was 368 PYs for overall patients and 227 PYs for selected patients. The estimates regarding the competing risk of death did not indicate any difference in risk between JAKis and bDMARDs (Table 2). Estimates regarding the additional treatment group of patients who received csDMARDs without parallel treatment with b/tsDMARDs are given in Supplementary Table S7.

Cumulative incidence plot and follow-up

Based on assessment of the adjusted [41] (Fig 2) and crude (Supplementary Fig S2) cumulative incidence plot and the results of the Cox models assessing potential change points (Table 2, Supplementary Table S8), the increased malignancy risk in the JAKi group compared to the bDMARD group became detectable only after 16 months of follow-up. For months 1 to 16 (considering a LP), the HR for JAKis vs bDMARDs was 0.94 (95% CI: 0.46, 1.92), while for >16 months, the HR was 1.54 (95% CI: 1.17, 2.04). Deviations from the Cox proportional hazards assumption are visible in all Schoenfeld residual plots for JAKi treatment (Supplementary Fig S3).

Table 2
Crude incidence rates and adjusted hazard ratios of malignancies estimated by Fine and Gray Cox model

	Episodes		PYs		Events		Crude incidence rate per 1000 PYs						Relative risk estimate				NNH
	JAKi	Ref.	JAKi	Ref.	JAKi	Ref.	JAKi			Reference			HR	LCL	UCL	*P*	
Considered treatment groups and model							IR	LCL	UCL	IR	LCL	UCL					
JAKis vs bDMARDs—main model, LP = 6																	
Outcome: malignancy																	
Overall patients	2285	4259	7593.7	15,219.6	88	135	11.6	9.3	14.3	8.9	7.4	10.5	1.40	1.09	1.80	.008	368
Selected patients	1341	2381	4391.0	8237.1	70	95	15.9	12.4	20.1	11.5	9.3	14.1	1.61	1.22	2.13	.001	227
Outcome: death (competing risk)																	
Overall patients	2285	4259	7593.7	15,219.6	86	175	11.3	9.1	14.0	11.5	9.9	13.3	0.95	0.73	1.22	.673	NA
Selected patients	1341	2381	4391.0	8237.1	76	146	17.3	13.6	21.7	17.7	15.0	20.8	0.94	0.71	1.24	.643	NA
JAKis vs bDMARDs—time-split (overall patients)																	
Only months 1-16, LP = 6	2285	4259	1809.0	3394.2	12	30	6.6	3.4	11.6	8.8	6.0	12.6	0.94	0.46	1.92	.868	NA
LP = 16	2048	3869	5785.5	11,829.9	76	104	13.1	10.3	16.4	8.8	7.2	10.7	1.54	1.17	2.04	.002	230
JAKis vs TNFis, LP = 6																	
Overall patients	2285	2826	7593.7	10,410.8	88	83	11.6	9.3	14.3	8.0	6.4	9.9	1.54	1.13	2.09	.007	277
Selected patients	1341	1529	4391.0	5488.6	70	57	15.9	12.4	20.1	10.4	7.9	13.5	1.82	1.29	2.57	.001	180
JAKis vs non-TNFi bDMARDs, LP = 6																	
Overall patients	2285	2180	7593.7	7381.2	88	72	11.6	9.3	14.3	9.8	7.6	12.3	1.30	0.98	1.71	.068	545
vSelected patients	1341	1262	4391.0	4125.0	70	55	15.9	12.4	20.1	13.3	10.0	17.4	1.25	0.91	1.71	.164	383
JAKis vs bDMARDs—on treatment model, LP = 6																	
Overall patients	2491	5764	5590.6	10,991.8	67	89	12.0	9.3	15.2	8.1	6.5	10.0	1.69	1.21	2.37	.002	257
Selected patients	1465	3288	3331.9	5853.0	52	63	15.6	11.7	20.5	10.8	8.3	13.8	1.75	1.19	2.58	.004	206
JAKis vs bDMARD—unweighted multivariable model, LP = 6																	
Overall patients	See main model												1.37	1.06	1.76	.016	368
Selected patients													1.57	1.18	2.08	.002	227

bDMARD, biologic disease-modifying antirheumatic drug; csDMARD, conventional synthetic disease-modifying antirheumatic drug; HR, hazard ratio; IR, incidence rate; JAKi, Janus kinase inhibitor; LCL, lower confidence limit; LP, latency period; NA, not applicable; NNH, number needed to harm in PYs; PY, patient-year; Ref., reference; TNFi, tumour necrosis factor inhibitor; UCL, upper confidence limit.
Results are for outcome malignancy unless specified otherwise. Confidence intervals for crude incidence rates are descriptive. The number needed to harm (NNH) is given as the number of patient-years of exposure to the target group (eg, JAKi) required to have 1 additional malignancy event, relative to the reference group (eg, bDMARDs). Events could be assigned to both treatment groups simultaneously. Death was considered as a competing event in Cox models. For regression models, inverse probability of treatment weighting was applied unless specified otherwise. 'Selected patients' refers to patients aged ≥50 years and with ≥1 cardiovascular risk factor defined as hypertension, coronary heart disease, diabetes, hyperlipoproteinemia, or current smoking at treatment start.

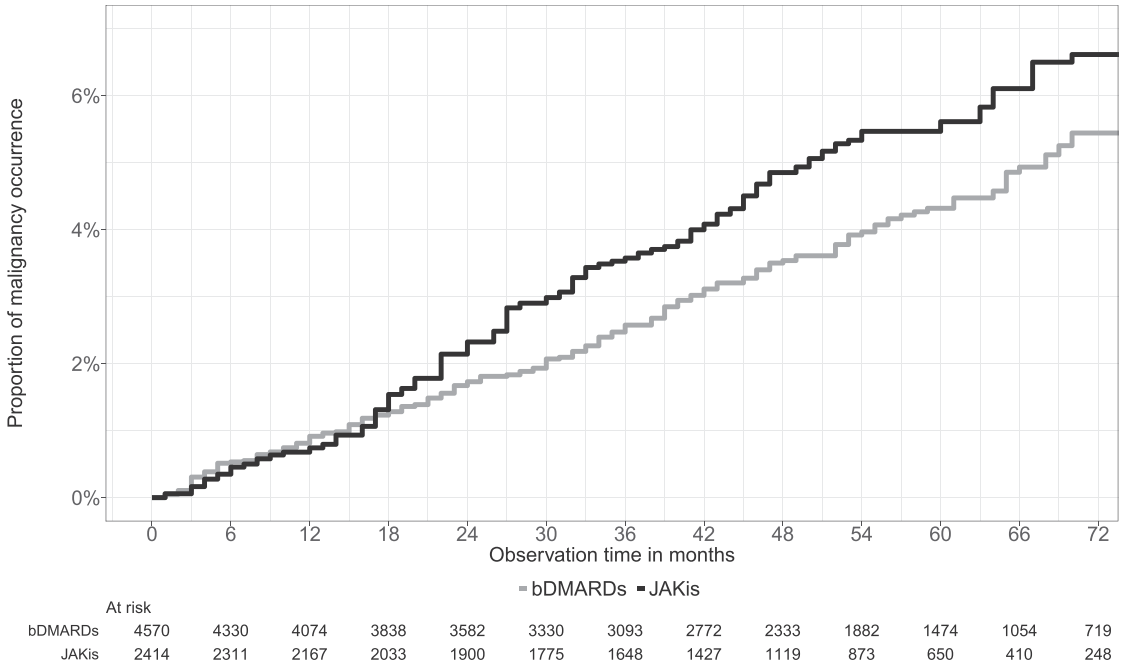

Figure 2. Adjusted cumulative incidence plot for malignancy excluding NMSC for JAKis and bDMARDs in overall patients. Adjustment was carried out by weighting, employing the weights from the main Cox model. Numbers at risk for every 6 months of observation time denote the (weighted and rounded) numbers of treatment episodes with JAKis and bDMARDs lasting at least the corresponding number of months. Observation time >72 months was not considered due to small numbers. No latency period was considered in this figure. bDMARD, biologic disease-modifying antirheumatic drug; JAKi, Janus kinase inhibitor; NMSC, nonmelanoma skin cancer.

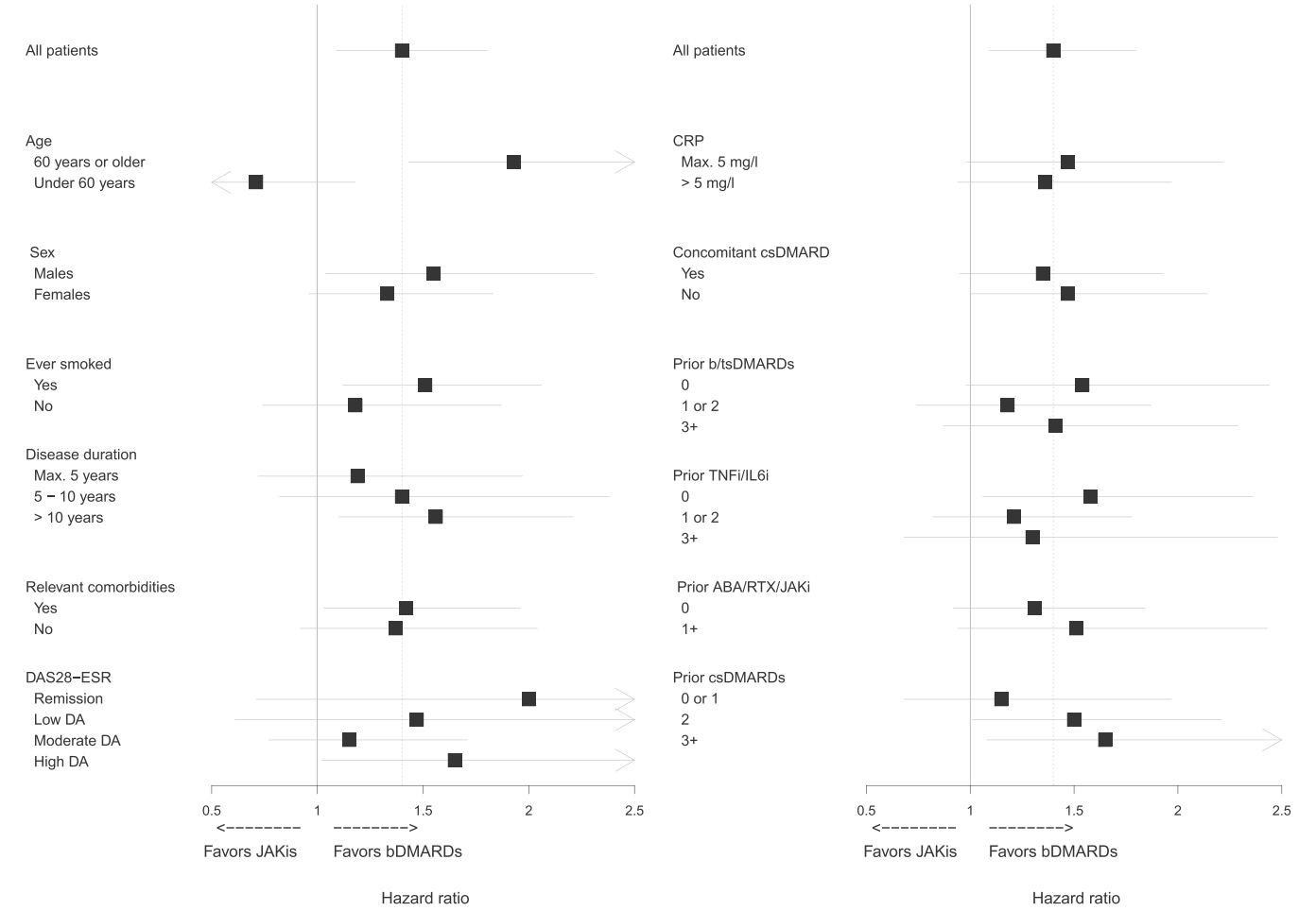

Figure 3. Stratified adjusted hazard ratios of malignancies for JAKi vs. bDMARD therapy. Hazard ratios are estimated by Fine and Gray Cox models with inverse probability of treatment weighting, following the 'once exposed, always at risk' paradigm and considering a 6-month latency period. A hazard ratio of 1 means that there is no risk difference between JAKi and bDMARDs (solid vertical line). The HR of 1.40 estimated for the overall patient cohort is marked with a dotted vertical line. ABA, abatacept; bDMARD, biologic disease-modifying antirheumatic drug; CRP, C-reactive protein; csDMARD, conventional synthetic disease-modifying antirheumatic drug; DA, disease activity; DAS28-ESR, Disease Activity Score based on erythrocyte sedimentation rate and 28 joints; IL6i, interleukin-6 inhibitor; JAKi, Janus kinase inhibitor; RTX, rituximab; TNFi, tumour necrosis factor inhibitor; tsDMARD, targeted synthetic disease-modifying antirheumatic drug. Remission is defined as DAS28-ESR <2.6, low disease activity as DAS28-ESR ≥2.6 to ≤3.2, moderate disease activity as DAS28-ESR >3.2 to ≤5.1, and high disease activity as DAS28-ESR >5.1.

Subgroup analyses

Subgroup analyses revealed that the HR of malignancy for JAKis vs bDMARDs was increased for patients who started treatment at age ≥60 years (HR: 1.93; 95% CI: 1.43, 2.60), while this could not be proven for patients starting treatment at age <60 years (Fig 3, Supplementary Tables S9-S11). Further subgroups with an increased HR included patients with ≥3 prior csDMARD treatments (HR: 1.65; 95% CI: 1.08, 2.52) and patients with high disease activity (HR: 1.65; 95% CI: 1.02, 2.70), as well as ever smokers, male patients, patients with comorbidities, patients with a disease duration >10 years, and patients without prior TNFi or IL6i treatment failures (Fig 3). The HR for patients in remission was also notably increased, although not statistically significant. Particularly high HRs were observed in most of these subgroups when combined with an age ≥60 years, whereas the risk differences between the age groups were small for patients with a disease duration ≤5 years or without prior bDMARD or JAKi treatment failures (Supplementary Tables S10 and S11). Among b/tsDMARD-naïve patients, numerically, HRs were consistently ≥1.50 across age groups. IRs were particularly elevated for male patients aged ≥60 years in both JAKi and bDMARD groups but appeared low in the absence of mentioned risk factors (Supplementary Table S10).

Secondary analyses

When employing TNFis as reference category, the HR for JAKis was 1.54 (95% CI: 1.13, 2.09) in overall and 1.82 (95% CI: 1.29, 2.57) in selected patients (see Table 2). When using non-TNFi bDMARDs as the reference, the HR for JAKis was 1.30 (95% CI: 0.98, 1.71) in overall patients (Table 2). The HR estimated by the 'on treatment' model was 1.69 (95% CI: 1.21, 2.37) for overall and 1.75 (95% CI: 1.19, 2.58) for selected patients. The IRs of the individual JAKi substances were only compared in an 'on treatment' perspective. In overall patients, 34 malignancy events occurring during JAKi therapy 'on treatment' were assigned to baricitinib (IR: 13.0; 95% CI: 9.0, 18.2), 23 to tofacitinib (IR: 12.1; 95% CI: 7.7, 18.1), and 7 to upadacitinib (IR: 8.8; 95% CI: 3.5, 18.2) (Supplementary Table S12).

Results for the multivariable, unweighted regression models are shown in Supplementary Tables S13-S16. An ITT analysis, a Cox regression model employing IPTW and IPCW, and a GEE

logistic regression model led to roughly similar results compared to the primary Cox model (Supplementary Table S8).

Secondary outcomes

For most individual cancer entities, event numbers were small (Supplementary Table S17). The most frequent malignancies were lung cancer (JAKis: 15, bDMARDs: 31), breast cancer (JAKis: 11, bDMARDs: 21), transitional cell/bladder cancer (JAKis: 8, bDMARDs: 12), prostate cancer (JAKis: 8, bDMARDs: 10), and gynaecological cancer (ovarian, endometrial, cervical, and vulva cancer; JAKis: 8, bDMARDs: 6). Compared to bDMARDs, in patients treated with JAKis, significantly increased HRs were observed for prostate cancer in male patients and gynaecological cancers in female patients, both overall and in patients aged ≥60 years (Supplementary Tables S17 and S18).

DISCUSSION

This study, which analysed a substantial number of treatment episodes started between 2017 and 2020, found a statistically significant, increased HR of malignancy in JAKi-treated patients compared to bDMARD-treated patients. Given that this HR is small, it is of interest to identify patients for whom this result may be clinically relevant. The result is consistent with the OS safety trial's results [12] and numerically similar to results from the DANBIO study [23] but differs from findings in other register and claims data studies [18–22]. The increased risk for malignancy was observed both in the overall RABBIT patient population (HR: 1.40; 95% CI: 1.09, 1.80) and in the selected cohort more similar to the trial's patient cohort with higher CV risk (HR: 1.61; 95% CI: 1.22, 2.13). The reference group for JAKis comprised all bDMARDs instead of only TNFis, as has been used elsewhere [23], because the distributions of the number of prior bDMARD failures, crucial for comparing exposure groups, are more similar between these groups. When employing TNFis as reference category, the risk observed for JAKi treatment in the overall RABBIT population and in the selected cohort was 1.54 (95% CI: 1.13, 2.09) and 1.82 (95% CI: 1.29, 2.57), respectively.

The IPTW models suggested an increased HR for JAKi therapy compared to the unweighted model, which may seem counterintuitive. This is because JAKi-treated patients on average have experienced more prior b/tsDMARD treatment failures, particularly more TNFi and IL6i failures, than bDMARD patients in RABBIT. IPTW downweights patients that are 'typical' and upweights patients that are 'atypical' within their exposure groups to calculate ATE weights. In stratified analyses, TNFi/IL6i-naïve patients presented a higher HR than nonnaïve patients but at the same time were 'atypical' within the JAKi group and were thus upweighted in our analysis to guarantee a fair comparison. Conversely, more 'typical' JAKi-treated patients with prior TNFi/IL6i treatment failures (associated with a lower risk) were downweighted. This situation causes the IPTW to increase the overall risk estimate for JAKi therapy. This is confirmed by the fact that within TNFi/IL6i-naïve patients, for which up- or downweighting due to differences regarding previous TNFi/IL6i failures does not happen, the HR for JAKi therapy estimated with the IPTW model is lower than the HR from the unweighted model, as would normally be expected (Supplementary Table S15). Differences between JAKi and bDMARD treatment groups were relatively small for most other patient characteristics, including comorbidities and disease activity.

RABBIT patients were considerably less often b/tsDMARD-naïve, more often current or past smokers, and slightly more often male than those from the OS trial. In OS, the NNH was 274 PYs of tofacitinib exposure required for 1 additional malignancy compared to TNFis, whereas in the selected patient cohort in RABBIT, this number was lower (180 PYs, or 227 PYs when comparing JAKis to bDMARDs).

We consider differences in follow-up time as the key reason for the discrepancies between results in RABBIT and other observational studies: In both OS and RABBIT, although not in DANBIO, the increased HR became evident only after 16 to 18 months [42], while the HR in ARTIS increased pronouncedly in a numerical sense for follow-up times ≥24 months. This highlights the critical importance of sufficient follow-up time under or after JAKi treatment to capture the time between cancer initiation or promotion until cancer detection [26,43,44]. As a particular strength of the RABBIT analysis, it had median follow-up times of 47 to 50 months in all exposure groups, similar to the 48 months reached by OS. Conversely, most other published studies, such as from DANBIO, ARTIS, and Safety of Tofacitinib in Routine Care Patients with Rheumatoid Arthritis (STAR-RA), had significantly shorter follow-up times for JAKi treatment, averaging 18, 23, and 10 months, respectively (Supplementary Table S19). Of note, these studies not only had shorter study periods but, unlike RABBIT, also permitted new treatment episodes to start until the end of the study period, leading to limited maximum follow-up times for the episodes started late. In contrast to several other studies, RABBIT used a 6-month LP, eg, to avoid the possibility of reverse causation [26,45], and furthermore assessed the impact of longer LP. Additionally, numerous secondary analyses strengthened our results both clinically and methodically.

Subgroup analyses revealed that the increased HRs in JAKi vs bDMARD treatments is particularly high for patients starting treatment at an age ≥60 years, for patients with ≥3 prior csDMARD failures, as well as for patients with high disease activity (Fig 3, Supplementary Tables S9 and S10). Further subgroups with increased HRs included ever smokers, men, patients with a disease duration >10 years, those with comorbidities, and those without prior TNFi and IL6i treatment. The HR for patients in remission was also pronounced, although without statistical significance. The majority of these findings are consistent with the OS results [46]. No increased HRs could be found in our study for individuals starting treatment aged <60 years. It should be noted, however, that for these patients, a numerically pronounced, elevated HR was found in the absence of prior bDMARD or JAKi failures. IRs in both the bDMARD and JAKi groups were highest in men aged ≥60 years but appeared low in the absence of the mentioned risk factors. The notably increased HRs for patients in remission was unexpected. These patients, however, are a small group and overall have a longer median disease duration than patients with moderate or high disease activity (10.7 years vs 8.8 years), so it is possible that the DAS28-ESR values at treatment start do not capture relevant prior long-term disease activity.

There are pronounced differences regarding the proportion of bDMARD-naïve patients across different studies. ARTIS, STAR-RA, and one of the Korean claims data studies [22] performed secondary analyses restricted to bDMARD-naïve patients, and their estimated malignancy risk among JAKi-treated patients was consistently higher than the overall estimate (Supplementary Table S19). In our study, compared to b/tsDMARD-naïve patients, the malignancy risk was notably lower for patients with 1 or 2 prior b/tsDMARD failures in a numerical

sense, but not as much for patients with ≥3 prior b/tsDMARD failures. This pattern could be explained by the fact that the first and second b/tsDMARDs are mostly TNFis, while the later b/tsDMARDs are mostly abatacept, rituximab, or JAKis, for which a higher IR is found.

Claims data have known disadvantages such as lack of information on disease activity and a high likelihood of incomplete data on smoking habits, as indicated by extremely low reported proportions of smokers (eg, 16% in STAR-RA). Modelling choices may also explain part of the differences: ARTIS, the Hong Kong biologics register, and one of the Korean claims data studies [20] did not employ propensity score methods and opted for a traditional multivariable Cox model; some models accounted for competing risks but others did not.

In our analyses, we have assessed the choice of different reference groups. There is no clear clinical evidence on the effect of TNFis, IL6is, or other bDMARDs on malignancy risk in RA patients, although preclinical data suggest a protective effect for TNFis and IL6is [32–35]. The HR observed for JAKis vs TNFis was numerically higher than the HRs for JAKis vs non-TNFi bDMARDs and the overall bDMARD group, indicating some degree of heterogeneity in the bDMARD group regarding malignancy risk.

These differences aside, it is important to note that the increased risk of malignancy under or after JAKi therapy compared to bDMARD therapy reflects the malignancy risk for JAKi-treated patients relative to bDMARD-treated patients but not compared to patients with an untreated chronic inflammatory disorder. Neither the OS trial nor our study were designed to assess whether patients with high disease activity lacking alternative treatment options are at lower malignancy risk with or without a JAKi (and such assessments are difficult to perform for practical and ethical reasons). Even in the presence of risk factors, patients with uncontrolled disease who have exhausted viable treatment alternatives to JAKis might possibly be better served with a JAKi than without any effective DMARD treatment due to uncontrolled disease itself being a risk factor for cancer. The JAKi numbers needed to treat for achieving treatment targets such as American College of Rheumatology response criteria have been reported as ≤10 [47], much less than the NNH for malignancies reported in this study, with 368 PYs in the overall cohort considering JAKis vs bDMARDs. In the absence of differing competing risks of death, this suggests a reasonable overall safety profile. Finally, while the JAK/STAT pathway plays a role in regulating cell growth, differentiation, apoptosis, and tumour progression, the direction of its influence cannot be inferred from preclinical data. Thus, further basic research is needed to investigate a potential protumourigenic effect of JAK inhibition in RA patients to confirm the results of an increased malignancy risk, as reported in our study.

It remains to be clarified whether the increased HR is a JAKi class effect. Selectivity for specific JAKs may influence the role of JAK inhibition in carcinogenesis, but a thorough, fair comparison of individual JAKi substances remains unfeasible in RABBIT (and other studies) at this stage due to different lengths of follow-up and the low exposure to filgotinib and, to some extent, upadacitinib. We thus only compared the individual JAKi substances by crude IRs, focusing on the 'on treatment' approach, which is probably least affected by differential follow-up. While the upadacitinib rate is numerically smaller than the rates for baricitinib and tofacitinib, further analyses based on greater follow-up times and more events are needed before inference on potential differences between specific JAKis can be undertaken.

JAKis are not associated with an increase in the risk of breast cancer compared to bDMARDs in RABBIT, consistent with the results from OS. The HR of lung cancer, surprisingly, was also not significantly increased in overall patients; however, a numerically larger signal is seen when only analysing male patients. There were only few events in each of the other cancer entities, thus results on those should be interpreted with caution. Due to the wide variations in growth rates depending on cancer and subtypes [43] and due to the small numbers for most entities, further studies with longer follow-up times are needed.

There are some limitations to our work. Exposure to 2 of the JAKi substances, as well as to abatacept, rituximab, and IL6is, was too limited to reliably estimate their associated risk, and future studies are needed to address this. In an observational study, persistence of residual confounding cannot be ruled out. Assessment of Schoenfeld residuals in our Cox models indicated some degree of violation of the proportional hazards assumption. We are aware of the time-averaged nature of the model estimates in such a case and employed a robust sandwich estimator for the variance. It has been shown that this estimate is robust to several misspecifications in the Cox model, including the lack of proportional hazards [29,48]. As an additional measure, we have looked at models partitioning the time axis [48]. We further fitted GEE logistic models for comparison, yielding similar results. While the 'on treatment' model likely does not capture all events attributable to a treatment episode due to the slow development of malignancies, in the primary 'once exposed, always at risk' model, the time between measurement of adjustment variables and outcome may be considerable. This model also leads to overlap between treatment exposures and, thus, dependency due to events potentially being assigned to several episodes. In an ITT analysis, such dependencies can be avoided, but likely at the cost of additional bias due to disregarding all treatment episodes after the first. However, results from all these models point in the same direction, supporting the stability of our results.

Disease activity may be an important driver in the development of cancer in patients with RA. IPTW adjusted for disease activity at the start of each treatment episode in our models; however, long-term disease activity between RA diagnosis and enrolment is also important but not available in RABBIT. It can be adjusted for only indirectly and imprecisely by using disease duration and the number of previous DMARD therapies as proxies.

In this study, risk differences between patients aged ≥60 years and younger patients were present. A major risk change at the age of 60 years is biologically plausible [49]. The age-related risk differences were, however, small for patients without prior b/tsDMARD treatment failures or in patients with a disease duration of ≤5 years. This raises the question of whether the strong effect modification by age may in part be owed to some kind of bias. First, this study is not primarily based on a first-ever new user design due to the low number of b/tsDMARD-naïve JAKi episodes (n = 587), so the existence of some degree of prevalent user bias cannot be ruled out, which could also be viewed as a form of collider bias [50]. However, analyses restricted to patients without prior b/tsDMARD failures support the increased risk of JAKis, so a potential prevalent user bias should not affect the main result. There might be reasons for patients to go directly from a csDMARD to a JAKi instead of to a bDMARD that imply a higher risk for malignancy but are incompletely adjusted for by the considered available covariables (residual confounding). Among TNFi/IL6i-naïve patients, JAKi-treated patients have relatively more comorbidities associated with contraindications for methotrexate than bDMARD-

treated patients compared to individuals with prior TNFi/IL6i treatment failures, eg, they have more frequently chronic renal disease and chronic liver disease. When adjusting for such individual comorbidities instead of the sum of comorbidities, however, the HR for JAKi therapy does not change (Supplementary Table S16). Second, in the OS trial, approximately 90% of patients had received no prior b/tsDMARD therapies. The OS study also found a higher risk for patients aged ≥65 years [46], although the risk difference between the 2 age categories was considerably smaller than that in this analysis.

To conclude, treatment with JAKis (predominantly baricitinib and tofacitinib) was associated with an increased HR of malignancies compared to treatment with bDMARDs in the overall study cohort, consistent with results from the OS trial. The increase in the HR could only be detected in treatment episodes with follow-up lasting longer than 16 months. Behind the overall small risk increase attributed to JAKis compared to bDMARDs, with uncertain clinical implications, a more pronounced risk increase could be detected for some patient groups, including older patients starting treatment aged ≥60 years, patients with ≥3 csDMARD failures, as well as patients with high disease activity. This can help physicians to assess the individual risk of their patients and thus strengthen precision medicine, as well as to decide which patients should be more closely monitored.

Given the risk stratification, the aforementioned clinical aspects, and the relatively high overall NNH, clinicians should carefully assess whether the described increased malignancy risk outweighs the potential risks of discontinuing a highly effective therapy like JAKis, including the known malignancy risk associated with an uncontrolled disease activity.

Competing interests

MS, AP, VZ, TR, YM, AR, and AS report financial support was provided to their institution by a joint, unconditional grant from AbbVie, Alfasigma, Amgen, BioCon, Bristol Myers Squibb, Fresenius Kabi, Hexal, Lilly, Pfizer, Samsung Bioepis, Sanofi Aventis, and UCB, and previously Celltrion, MSD, and Roche. ACR reports financial support was provided to her institution by a joint, unconditional grant from AbbVie, Amgen, BioCon, Biogen, Celltrion, Hexal, Janssen-Cilag, Lilly, MSD, Novartis, Pfizer, and UCB. VZ reports a relationship with British Association of Dermatologists' Biologic Interventions Registry that includes: board membership. YM reports a relationship with Alfasigma, Lilly, and Pfizer that includes: speaking and lecture fees. AR reports a relationship with Dachverband Osteologie e.V. (German umbrella organization for osteology) that includes: paid expert testimony. KK reports a relationship with AbbVie, Galapagos, Lilly, MSD, Pfizer, and UCB that includes: speaking and lecture fees. KK and KMS report a relationship with AbbVie that includes: travel reimbursement. KMS reports a relationship with German Society of Rheumatology (DGRh) that includes: board membership. ACR reports a relationship with Amgen, Pfizer, LAWG, and TMF that includes: speaking and lecture fees. ACR reports a relationship with TMF that includes: board membership. AS reports a relationship with AbbVie, Pfizer, Galapagos, Alfasigma, Takeda, Janssen, Lilly, and UCB that includes: speaking and lecture fees. AS reports a relationship with Fresenius Kabi that includes: travel reimbursement. AS reports a relationship with British Association of Dermatologists' Biologic Interventions Registry, German Society of Rheumatology (DGRh), and European Alliance of Associations for Rheumatology (EULAR) that includes: board membership. MS has done consulting for Janssen; payment was made to his institution. KK has discussed data (no payments). SB and KR declare that they have no known competing financial interests or personal relationships that could have appeared to influence the work reported in this paper.

Acknowledgements

We acknowledge the invaluable contributions of all participating consultant rheumatologists and their patients. In particular, we thank those rheumatologists who enrolled the highest numbers of patients. We also acknowledge the significant contributions of Peter Herzer (Munich), Jörn Kekow (Vogelsang-Gommern), Bernhard Manger (Erlangen), Angela Zink (Berlin), and Dieter Wiek (Bonn) as members of the advisory board.

Contributors

AS is responsible for the overall content as guarantor. MS had full access to all data of this study and takes responsibility for data integrity and accuracy of the analysis. Study concept and design: MS, VZ, TR, YM, and AS. Acquisition of the data: SB, KR, KK, and KMS. Analysis and interpretation of the data: MS, AP, VZ, TR, YM, AR, ACR, and AS. Drafting the manuscript: MS, AP, and VZ. Critical revision of the manuscript for important intellectual content: MS, AP, VZ, TR, YM, AR, SB, KR, KK, KMS, ACR, and AS. Obtaining funding: AS. All authors read and approved the manuscript.

Funding

RABBIT is supported by a joint, unconditional grant from AbbVie, Alfasigma, Amgen, Biocon, Bristol Myers Squibb, Fresenius Kabi, Hexal, Lilly, Pfizer, Samsung Bioepis, Sanofi Aventis, and UCB, and previously by Celltrion, MSD and Roche. Role of the funding source: The principal investigators and their team had full academic freedom in study design and conduct, data analysis, and publication of results. These stipulations were delineated in their contract with the sponsors. For the purpose of information, all funding companies received the manuscript 30 days prior to submission. Publication of this article was not contingent on their approval. The data interpretation, drafting, critical revision, and approval of the final manuscript were performed solely by the authors.

Patient consent for publication

Patients gave their written informed consent prior to their participation.

Ethics approval

The study protocol of RABBIT was approved by the ethics committee of the Charité University Medicine Berlin, Germany (EA4/123/21).

Provenance and peer review

Not commissioned; externally peer reviewed.

Data availability statement

In the RABBIT study, patients' consent does not include approval to share their data. Data therefore cannot be made available.

Supplementary materials

Supplementary material associated with this article can be found in the online version at doi:10.1016/j.ard.2025.05.014.

Orcid

Martin Schaefer: http://orcid.org/0000-0001-6487-3634
Alina Purschke: http://orcid.org/0009-0004-3458-6764
Tatjana Rudi: http://orcid.org/0000-0001-7467-7901
Yvette Meissner: http://orcid.org/0000-0003-0147-4112
Adrian Richter: http://orcid.org/0000-0002-3372-2021
Sylvia Berger: http://orcid.org/0009-0001-0919-5137
Karl Matthias Schneider: http://orcid.org/0009-0007-2106-9196
Anne C. Regierer: http://orcid.org/0000-0003-2456-4049
Anja Strangfeld: http://orcid.org/0000-0002-6233-022X

REFERENCES

[1] De Cock D, Hyrich K. Malignancy and rheumatoid arthritis: epidemiology, risk factors and management. Best Pract Res Clin Rheumatol 2018;32(6):869–86. doi: 10.1016/j.berh.2019.03.011.
[2] Parodi S, Santi I, Marani E, Casella C, Puppo A, Sola S, et al. Chronic diseases, medical history and familial cancer, and risk of leukemia and non-Hodgkin's lymphoma in an adult population: a case-control study. Cancer Causes Control 2015;26(7):993–1002. doi: 10.1007/s10552-015-0592-6.
[3] Simon TA, Thompson A, Gandhi KK, Hochberg MC, Suissa S. Incidence of malignancy in adult patients with rheumatoid arthritis: a meta-analysis. Arthritis Res Ther 2015;17(1):212. doi: 10.1186/s13075-015-0728-9.
[4] Raheel S, Crowson CS, Wright K, Matteson EL. Risk of malignant neoplasm in patients with incident rheumatoid arthritis 1980-2007 in relation to a comparator cohort: a population-based study. Int J Rheumatol 2016;2016:4609486. doi: 10.1155/2016/4609486.
[5] Cho SK, Lee J, Han M, Bae SC, Sung YK. The risk of malignancy and its incidence in early rheumatoid arthritis patients treated with biologic DMARDs. Arthritis Res Ther 2017;19(1):277. doi: 10.1186/s13075-017-1482-y.
[6] Wadström H, Frisell T, Askling J. Anti-Rheumatic Therapy in Sweden (ARTIS) Study Group. Malignant neoplasms in patients with rheumatoid arthritis treated with tumor necrosis factor inhibitors, tocilizumab, abatacept, or rituximab in clinical practice: a nationwide cohort study from Sweden. JAMA Intern Med 2017;177(11):1605–12. doi: 10.1001/jamainternmed.2017.4332.
[7] Rawlings JS, Rosler KM, Harrison DA. The JAK/STAT signaling pathway. J Cell Sci 2004;117(Pt 8):1281–3. doi: 10.1242/jcs.00963.
[8] Ghoreschi K, Jesson MI, Li X, Lee JL, Ghosh S, Alsup JW, et al. Modulation of innate and adaptive immune responses by tofacitinib (CP-690,550). J Immunol 2011;186(7):4234–43. doi: 10.4049/jimmunol.1003668.
[9] Philips RL, Wang Y, Cheon H, Kanno Y, Gadina M, Sartorelli V, et al. The JAK-STAT pathway at 30: much learned, much more to do. Cell 2022;185(21):3857–76. doi: 10.1016/j.cell.2022.09.023.
[10] O'Shea JJ, Holland SM, Staudt LM. JAKs and STATs in immunity, immunodeficiency, and cancer. N Engl J Med 2013;368(2):161–70. doi: 10.1056/NEJMra1202117.
[11] Xue C, Yao Q, Gu X, Shi Q, Yuan X, Chu Q, et al. Evolving cognition of the JAK-STAT signaling pathway: autoimmune disorders and cancer. Signal Transduct Target Ther 2023;8(1):204. doi: 10.1038/s41392-023-01468-7.
[12] Ytterberg SR, Bhatt DL, Mikuls TR, Koch GG, Fleischmann R, Rivas JL, et al. Cardiovascular and cancer risk with tofacitinib in rheumatoid arthritis. N Engl J Med 2022;386(4):316–26. doi: 10.1056/NEJMoa2109927.
[13] US Food & Drug Administration. Initial safety trial results find increased risk of serious heart-related problems and cancer with arthritis and ulcerative colitis medicine Xeljanz, Xeljanz XR (tofacitinib) [Internet]. US Food & Drug Administration; 2021. Accessed on 18 June 2025 from: https://www.fda.gov/drugs/drug-safety-and-availability/initial-safety-trial-results-find-increased-risk-serious-heart-related-problems-and-cancer-arthritis.
[14] Xeljanz (tofacitinib): initial clinical trial results of increased risk of major adverse cardiovascular events and malignancies (excluding NMSC) with use of tofacitinib relative to TNF-alpha inhibitors [Internet]. European Medicines Agency; 2021. Accessed on 18 June 2025 from: https://www.ema.europa.eu/en/documents/dhpc/direct-healthcare-professional-communication-dhpc-xeljanz-tofacitinib-initial-clinical-trial-results-increased-risk-major-adverse-cardiovascular-events-and-malignancies-excluding-nmsc-use-tofacitinib_en.pdf.
[15] Salinas CA, Louder A, Polinski J, Zhang TC, Bower H, Phillips S, et al. Evaluation of VTE, MACE, and serious infections among patients with RA treated with baricitinib compared to TNFi: a multi-database study of patients in routine care using disease registries and claims databases. Rheumatol Ther 2023;10(1):201–23. doi: 10.1007/s40744-022-00505-1.
[16] European Medicines Agency. EMA confirms measures to minimise risk of serious side effects with Janus kinase inhibitors for chronic inflammatory disorders (EMA/27681/2023) [Internet]. European Medicines Agency; 2023. Accessed on 18 June 2025 from: https://www.ema.europa.eu/en/medicines/human/referrals/janus-kinase-inhibitors-jaki.
[17] Smolen JS, Landewé RBM, Bergstra SA, Kerschbaumer A, Sepriano A, Aletaha D, et al. EULAR recommendations for the management of rheumatoid arthritis with synthetic and biological disease-modifying antirheumatic drugs: 2022 update. Ann Rheum Dis 2023;82(1):3–18. doi: 10.1136/ard-2022-223356.
[18] Huss V, Bower H, Hellgren K, Frisell T, Askling J. Behalf of the ARTIS group, et al. Cancer risks with JAKi and biological disease-modifying antirheumatic drugs in patients with rheumatoid arthritis or psoriatic arthritis: a national real-world cohort study. Ann Rheum Dis 2023;82(7):911–9. doi: 10.1136/ard-2022-223636.
[19] Khosrow-Khavar F, Desai RJ, Lee H, Lee SB, Kim SC. Tofacitinib and risk of malignancy: results from the Safety of Tofacitinib in Routine Care Patients With Rheumatoid Arthritis (STAR-RA) study. Arthritis Rheumatol 2022;74(10):1648–59. doi: 10.1002/art.42250.
[20] Min HK, Kim H, Jeong HJ, Kim SH, Kim HR, Lee SH, et al. Risk of cancer, cardiovascular disease, thromboembolism, and mortality in patients with rheumatoid arthritis receiving Janus kinase inhibitors: a real-world retrospective observational study using Korean health insurance data. Epidemiol Health 2023;45:e2023045. doi: 10.4178/epih.e2023045.
[21] Mok CC, So H, Yim CW, To CH, Lao WN, Wong SPY, et al. Safety of the JAK and TNF inhibitors in rheumatoid arthritis: real world data from the Hong Kong Biologics Registry. Rheumatology (Oxford) 2024;63(2):358–65. doi: 10.1093/rheumatology/kead198.
[22] Song YJ, Cho SK, You SH, Kim JY, Kim H, Jung SY, et al. Association between malignancy risk and Janus kinase inhibitors versus tumour necrosis factor inhibitors in Korean patients with rheumatoid arthritis: a nationwide population-based study. RMD Open 2022;8(2):e002614 10 p. doi: 10.1136/rmdopen-2022-002614.
[23] Westermann R, Cordtz RL, Duch K, Mellemkjaer L, Hetland ML, Burden AM, et al. Cancer risk in patients with rheumatoid arthritis treated with janus kinase inhibitors: a nationwide Danish register-based cohort study. Rheumatology (Oxford) 2024;63(1):93–102. doi: 10.1093/rheumatology/kead163.
[24] Khosrow-Khavar F, Kim SC, Lee H, Lee SB, Desai RJ. Tofacitinib and risk of cardiovascular outcomes: results from the Safety of TofAcitinib in Routine care patients with Rheumatoid Arthritis (STAR-RA) study. Ann Rheum Dis 2022;81(6):798–804. doi: 10.1136/annrheumdis-2021-221915.
[25] Richter A, Meißner Y, Strangfeld A, Zink A. Primary and secondary patient data in contrast: the use of observational studies like RABBIT. Clin Exp Rheumatol 2016;34(5 Suppl 101):S79–86.
[26] Hicks B, Kaye JA, Azoulay L, Kristensen KB, Habel LA, Pottegård A. The application of lag times in cancer pharmacoepidemiology: a narrative review. Ann Epidemiol 2023;84:25–32. doi: 10.1016/j.annepidem.2023.05.004.
[27] Ulm K. A simple method to calculate the confidence interval of a standardized mortality ratio (SMR). Am J Epidemiol 1990;131(2):373–5. doi: 10.1093/oxfordjournals.aje.a115507.
[28] Fine JP, Gray RJ. A proportional hazards model for the subdistribution of a competing risk. J Am Stat Assoc 1999;94(446):496–509.
[29] Lin DY, Wei LJ. The robust inference for the Cox proportional hazards model. J Am Stat Assoc 1989;84(408):1074–8.
[30] Austin PC, Fine JP. Practical recommendations for reporting Fine-Gray model analyses for competing risk data. Stat Med 2017;36(27):4391–400. doi: 10.1002/sim.7501.
[31] Austin PC. The use of propensity score methods with survival or time-to-event outcomes: reporting measures of effect similar to those used in randomized experiments. Stat Med 2014;33(7):1242–58. doi: 10.1002/sim.5984.
[32] Grivennikov S, Karin E, Terzic J, Mucida D, Yu GY, Vallabhapurapu S, et al. IL-6 and Stat3 are required for survival of intestinal epithelial cells and development of colitis-associated cancer. Cancer Cell 2009;15(2):103–13. doi: 10.1016/j.ccr.2009.01.001.

[33] Johnson DE, O'Keefe RA, Grandis JR. Targeting the IL-6/JAK/STAT3 signalling axis in cancer. Nat Rev Clin Oncol 2018;15(4):234–48. doi: 10.1038/nrclinonc.2018.8.
[34] Lebrec H, Ponce R, Preston BD, Iles J, Born TL, Hooper M. Tumor necrosis factor, tumor necrosis factor inhibition, and cancer risk. Curr Med Res Opin 2015;31(3):557–74. doi: 10.1185/03007995.2015.1011778.
[35] Propper DJ, Balkwill FR. Harnessing cytokines and chemokines for cancer therapy. Nat Rev Clin Oncol 2022;19(4):237–53. doi: 10.1038/s41571-021-00588-9.
[36] van Buuren S. Multiple imputation of discrete and continuous data by fully conditional specification. Stat Methods Med Res 2007;16(3):219–42. doi: 10.1177/0962280206074463.
[37] Cheung YB, Xu Y, Tan SH, Cutts F, Milligan P. Estimation of intervention effects using first or multiple episodes in clinical trials: the Andersen-Gill model re-examined. Stat Med 2010;29(3):328–36. doi: 10.1002/sim.3783.
[38] Guo Z, Gill TM, Allore HG. Modeling repeated time-to-event health conditions with discontinuous risk intervals. An example of a longitudinal study of functional disability among older persons. Methods Inf Med 2008;47(2):107–16.
[39] Sagara I, Giorgi R, Doumbo OK, Piarroux R, Gaudart J. Modelling recurrent events: comparison of statistical models with continuous and discontinuous risk intervals on recurrent malaria episodes data. Malar J 2014;13(1):293. doi: 10.1186/1475-2875-13-293.
[40] Andersen PK, Gill RD. Cox's regression model for counting processes: a large sample study. Ann Stat 1982;10(4):1100–20.
[41] Denz R, Klaaßen-Mielke R, Timmesfeld N. A comparison of different methods to adjust survival curves for confounders. Stat Med 2023;42(10):1461–79. doi: 10.1002/sim.9681.
[42] Curtis JR, Yamaoka K, Chen YH, Bhatt DL, Gunay LM, Sugiyama N, et al. Malignancy risk with tofacitinib versus TNF inhibitors in rheumatoid arthritis: results from the open-label, randomised controlled ORAL Surveillance trial. Ann Rheum Dis 2023;82(3):331–43. doi: 10.1136/ard-2022-222543.
[43] Little MP, Eidemüller M, Kaiser JC, Apostoaei AI. Minimum latency effects for cancer associated with exposures to radiation or other carcinogens. Br J Cancer 2024;130(5):819–29. doi: 10.1038/s41416-023-02544-z.
[44] Pottegård A, Friis S, Stürmer T, Hallas J, Bahmanyar S. Considerations for pharmacoepidemiological studies of drug-cancer associations. Basic Clin Pharmacol Toxicol 2018;122(5):451–9. doi: 10.1111/bcpt.12946.
[45] Pottegård A, Hallas J. New use of prescription drugs prior to a cancer diagnosis. Pharmacoepidemiol Drug Saf 2017;26(2):223–7. doi: 10.1002/pds.4145.
[46] Kristensen LE, Danese S, Yndestad A, Wang C, Nagy E, Modesto I, et al. Identification of two tofacitinib subpopulations with different relative risk versus TNF inhibitors: an analysis of the open label, randomised controlled study ORAL Surveillance. Ann Rheum Dis 2023;82(7):901–10. doi: 10.1136/ard-2022-223715.
[47] Strand V. RMD commentary, JAK kinase inhibitors: a preferred alternative to TNF inhibitors? RMD Open 2021;7:e001565. doi: 10.1136/rmdopen-2021-001565.
[48] Therneau TM, Grambsch PM. Modeling survival data: extending the Cox model. New York: Springer; 2000. p. 350 p.
[49] Shen X, Wang C, Zhou X, Zhou W, Hornburg D, Wu S, et al. Nonlinear dynamics of multi-omics profiles during human aging. Nat Aging 2024;4(11):1619–34. doi: 10.1038/s43587-024-00692-2.
[50] Acton EK, Willis AW, Hennessy S. Core concepts in pharmacoepidemiology: key biases arising in pharmacoepidemiologic studies. Pharmacoepidemiol Drug Saf 2023;32(1):9–18. doi: 10.1002/pds.5547.

Ann Rheum Dis 84 (2025) 1791–1800

Contents lists available at ScienceDirect

Annals of the Rheumatic Diseases

journal homepage: https://www.sciencedirect.com/journal/annals-of-the-rheumatic-diseases

Rheumatoid arthritis

Quantified intakes of key diet components and the risk of developing rheumatoid arthritis: Results from a nested case—control study

Rebecka Bäcklund[1,*], Ulf Bergström[1], Michele Compagno[1], Linnea Arvidsson[1], Emil Rydell[1], Emily Sonestedt[2,3], Carl Turesson[1]

[1] *Rheumatology, Department of Clinical Sciences, Malmö, Lund University, Malmö, Sweden*
[2] *Nutritional Epidemiology, Department of Clinical Sciences, Malmö, Lund University, Malmö, Sweden*
[3] *Food and Meal Science, Faculty of Natural Sciences, Kristianstad University, Sweden*

ARTICLE INFO

Article history:
Received 29 January 2025
Received in revised form 8 June 2025
Accepted 10 June 2025

ABSTRACT

Objectives: This nested case—control study aimed to investigate the relationship between components of the Swedish food-based dietary guidelines (SDG) from 2015 and the risk of developing rheumatoid arthritis (RA).

Methods: Data were obtained from the prospective Malmö Diet and Cancer Study (MDCS) conducted 1991—1996. Diet was assessed at baseline using a validated diet history method. Incident RA cases until 2016 were identified through register linkage, followed by a validation process through review of medical records. For each case, 4 RA-free controls, matched for age, sex, and year of inclusion in the MDCS, were selected from the cohort. Adherence to the SDG was assessed using the SDG Score (SDGS) of 5 components. Multivariable logistic regression and restricted cubic splines (RCS) were applied to analyse the relationships among the SDGS, its components, and RA.

Results: A total of 305 incident RA cases (67% rheumatoid factor/anti-cyclic citrullinated peptide positive) were identified. Recommended intakes of vegetables and fruits (>400 g/day) and red and processed meat (<500 g/week) were associated with lower risks of RA, with multivariable-adjusted odds ratios of 0.64 (95% CI 0.43—0.94) and 0.60 (95% CI 0.38—0.97), respectively. RCS revealed a positive linear association for total intake of red/processed meat with RA development and a negative association for vegetables and fruits. The risk was higher by quartile of red and processed meat intake for seropositive, but not seronegative RA.

Conclusions: Higher intake of red/processed meat associated with a higher risk of seropositive RA, whereas vegetables and fruit may reduce the risk of RA overall.

*Correspondence to Dr. Rebecka Bäcklund, Rheumatology, Department of Clinical Sciences, Malmö, Lund University, Jan Waldenströms gata 1B, 20502 Malmö, Sweden.

E-mail address: rebecka_teresia.backlund@med.lu.se (R. Bäcklund).

Handling editor Josef S. Smolen.

https://doi.org/10.1016/j.ard.2025.06.2123

WHAT IS ALREADY KNOWN ON THIS TOPIC

- The relationship between diet and the risk of rheumatoid arthritis (RA) has been investigated as a part of its multifactorial aetiology. Protective as well as disease risk promoting dietary habits have been described. However, the results are variable, and the underlying mechanisms are not fully elucidated.

WHAT THIS STUDY ADDS

- In this nested case–control study based on a prospective survey, we demonstrated a dose–response relationship between higher intakes of red and processed meat and the risk of developing seropositive but not seronegative RA, suggesting differences in the diet related pathomechanisms for these subtypes. High intakes of vegetables and fruit were associated with reduced risk of RA.

HOW THIS STUDY MIGHT AFFECT RESEARCH, PRACTICE OR POLICY

- This study provides a valuable base for furthering our understanding of the mechanisms related to RA development and for future preventative measures.

INTRODUCTION

Rheumatoid arthritis (RA) is an autoimmune, systemic disease that presents as polyarthritis [1].

The induction of the autoantibodies rheumatoid factor (RF) and antibodies to citrullinated proteins (ACPAs) is considered to be a part of the preclinical phase in RA development [2]. Furthermore, these RA-related autoantibodies are markers of poor prognosis [3].

Smoking is a major and well-established risk factor for RA [4]. Various other environmental- and lifestyle-related factors have been suggested as potential predictors [5]. Diet and its relation to RA risk have gained interest in the literature, but how the underlying mechanisms that are relevant for disease development are driven by different dietary habits is still not fully understood.

There is limited evidence suggesting protective roles for high intakes of fish, vegetables, and Mediterranean style diets [6]. Regarding meat intake, results are conflicting [6]. One study indicated an increased risk of RA development with higher consumption of red meat (7), but several other observational studies did not find any such association [8–12]. A previous study from our group demonstrated that recommended intakes of dietary fibres, but not overall diet quality, associated with a decreased risk of RA [13]. However, that study did not investigate the impact of red meat consumption, which is included in more recent Swedish dietary guidelines (SDGs) [14].

The aim of this nested case–control study was to examine the relation between adherence to the food-based SDGs, including those on limited red meat intake, and the risk of developing RA. Furthermore, this study sought to perform analyses separately for seropositive and seronegative RA, as we hypothesise that the role of diet in the development of these subtypes could differ and contribute to differences in pathomechanisms and clinical presentation.

METHODS

Study population

This case–control study was nested in the population-based Malmö Diet and Cancer Study (MDCS) cohort. Recruitment for the MDCS was carried out between January 1, 1991, and September 25, 1996. The background population included 74,138 adult individuals residing in Malmö at the time of baseline examinations and born between 1926 and 1945. The cohort was extended in 1995, to include women born between 1923 and 1950, and men born 1923–1945. Individuals with mental incapacity and inadequate Swedish language skills ($\widetilde{N}$ = 1975) were excluded. A total of 68,905 subjects met the inclusion criteria, among whom 28 098 were considered complete participants, with available data from all dietary assessments and other baseline examinations. The overall participation rate for MDCS was 41% (28 098/68 905) [15]. The expected number of incident cases of RA during the study period was estimated based on population statistics from Statistics Sweden, and using published incidence rates from the same region in 2008 [16].

Data collection

Information on lifestyle habits, socioeconomics, and previous medical history was collected using a self-administered questionnaire [17]. Leisure time physical activity was assessed using a modified questionnaire adapted from the Minnesota Leisure Time Physical Activity Questionnaire [18].

At baseline, diet was assessed using the modified diet history method, a previously validated three-part methodology [19,20], comprising a 7-day menu book, a 168-item quantitative diet questionnaire, and a complementary in-person 45–60 minute diet interview [21]. All cooked main meals, cold beverages (i.e. milk, juice, soft drinks, water, alcoholic beverages), drugs, natural remedies, and dietary supplements were described by participants in the menu book during 7 consecutive days, reflecting those meals eaten on a daily basis with daily variation. Frequency and portion size of foods consumed regularly over the prior year with low day-to-day variation (i.e. hot beverages, sandwiches, edible fats, breakfast cereals, yogurt, milk, fruits, cakes, candies, snacks) were recorded in the diet questionnaire. Additional information on details regarding cooking methods and estimations of portion sizes for meals that had been recorded in the menu book were gathered during the interview. Further, the menu books and questionnaires were reviewed for overlap and to make sure that the previously completed information seemed reasonable. All dietary data collected were converted into nutrient and energy intakes (EI) by use of the Swedish Food Database PC KOST2-93 [21].

Case and control selection

Incident cases of RA were identified from the time of study enrolment until December 2016 by linking the MDCS cohort to several national and local registers, as previously described [22]. All registered RA cases were subjected to a validation process through a structured medical records review. Validated cases were considered to have a definite diagnosis of RA according to expert opinion and fulfilled the 1987 American College of Rheumatology (ACR) [23] and/or the 2010 ACR/European League Against Rheumatism classification criteria for RA [24]. During the review process, data on RF and anti-cyclic citrullinated peptide (anti-CCP) antibody status was retrieved. For each validated RA case 4 controls were matched for sex, year of birth (±1 year), and year of inclusion (±1 year) in the MDCS. The controls were alive and free of RA when the index person was diagnosed with RA. There was no exclusion based on other incident inflammatory conditions. The choice of 4 controls per case is standard for our nested case–control studies and reflects

an established rule of thumb based on diminishing power gains with increasing number of controls [25].

Variables

The Swedish Dietary Guidelines Score

The Swedish Dietary Guidelines Score (SDGS) is a dietary index designed to portray a healthy dietary pattern according to the Swedish dietary guidelines (SDG) from 2015. The SDG from 2015 are based on the Nordic Nutrition Recommendations from 2012. According to the SDG, increasing intakes of vegetables and fruits, berries, fish and shellfish, nuts, and seeds should be encouraged. Wholegrain varieties, vegetable-based fats, and low-fat dairy products should be favoured over refined grains, butter, and high-fat dairy products. Red and processed meat, salt, sugar, and alcohol should be limited. The SDGS was developed for use in analysis based on the MDCS [26]. The 5 dietary components included in the SDGS are fibres, vegetables and fruits, fish and shellfish, added sugars, and red and processed meat. A score of 1 is assigned to each component for which the individual is compliant with the recommendation [26]. The scoring for SDGS ranges from 0 (noncompliant to all recommendations) to 5 (compliant to all recommendation).

Other variables

Based on reported smoking habits, participants were classified as regular and occasional current smokers, prior smokers, and never smokers. Level of formal education was categorised into 6 categories, as previously described [22]. Self-reported intakes of alcohol were categorised into zero-consumers (based on consumption from the questionnaire and the menu book) and sex-specific quintiles (from the menu book), and self-reported leisure time physical activity (based on questionnaire) was categorised into predefined categories expressed in hours per week of metabolic equivalent of task.

Patient and public involvement statement

A research partner, appointed by the Swedish Rheumatism Association, a national patient organisation, was involved at the stage of interpretation of the results. There was no patient or public involvement at the other stages of the study. The research partner will be involved in the dissemination of the results to the wider patient community, through collaboration on channels for such dissemination, and its format.

Statistics

The relationship for SDGS and its components with RA was explored using logistic regression analysis. A group number was given for each case and its matched controls, which was added as a categorical covariate to the regression model to consider for the matched design. Estimates were expressed as odds ratios (OR) with 95% confidence intervals (CIs).

SDGS was analysed as a continuous variable (increment per additional score) and divided into 3 categories defined as low adherence (0–1 points), moderate adherence (2–3 points), or high adherence (4–5 points) based on the total score. The odds of RA were also examined for each dietary component both dichotomously (as compliant with recommendation vs not compliant) and as a continuous variable (total intake, per SD).

In the adjusted models, all potential misreporters of total EI (defined by a ratio of EI to basal metabolic rate outside of the 95% limits of the calculated physical activity level) were excluded [27]. A separate model was run in which reported EI was added as a covariate with the purpose of examining the effect of diet separate from reported EI. The final multivariable model was further adjusted for potential confounders (smoking, alcohol, physical activity), and logistic regression analyses were conducted to evaluate the impact of these covariates on the risk of RA. To assess the robustness of results all adjusted models were performed without exclusion of potential misreporters of energy. Additionally, all dietary components were divided into quartiles, and the ORs for each category, compared with the lowest, were estimated.

All analyses described above were also stratified for seropositive (positive for RF and/or anti-CCP) and seronegative (negative for RF and anti-CCP) RA. In a post hoc analysis, we stratified by age at screening (above vs below the median).

Spline analyses were performed to examine the linearity of associations between intakes of SDGS components and outcome. Restricted cubic splines (RCS) with 3 knots were fitted to unconditional logistic regression models adjusting for matching variables (baseline age, sex) and additionally for covariates (total EI, smoking, alcohol, physical activity) excluding potential misreporters of EI.

RESULTS

Characteristics of cases and controls

A total of 305 incident RA cases were identified in the study population (76.1% women; 204 seropositive, 101 seronegative). The expected total number of incident cases of RA in Malmö during the study period was 1937. The mean age at screening was 56.8 years. The mean time from screening date at baseline to date of diagnosis was 12 years. Baseline characteristics of the pre-RA cases and controls are presented in Table 1. Baseline characteristics of seropositive and seronegative cases and their controls are presented in Supplementary Table S1. Descriptives for the SDGS and its score distributions are presented in Table 2, and those for seropositive and seronegative cases and their controls are presented in Supplementary Table S2.

Predictors of RA overall

No significant associations were shown for moderate and high SDGS adherences relative to the reference category or when analysed as a continuous variable (0 to 5) in crude and multivariable-adjusted analyses (Table 3).

When examining each dietary component separately, intakes of vegetables and fruits and red and processed meat compliant with dietary recommendations were associated with a decreased risk of RA in the crude model including all cases (OR 0.70, 95% CI 0.51–0.96; OR 0.60, 95% CI 0.41–0.87) (Table 3). For the corresponding continuous variables, an inverse association for intake of vegetables and fruits (OR per SD 0.81, 95% CI 0.69–0.95) and a positive association for higher consumption of red and processed meat (OR 1.27, 95% CI 1.09–1.49) with subsequent RA were shown (Table 3). The associations remained significant and became somewhat stronger when excluding potential misreporters and adjusting for potential confounders (Table 3). Furthermore, in comparison to the first quartile, the ORs for RA in the third and fourth quartiles of red and processed meat intakes were 1.65 (95% CI 0.96–2.84) and 1.92 (95% CI 1.11–3.35), respectively (Table 4). Compared to the lowest vegetable and fruit intake quartile, a significantly reduced risk of

Table 1
Baseline characteristics of pre-RA cases and controls

	Pre-RA cases (N = 305)	Controls (N = 1220)
Age at diagnosis (years), mean [SD]	68.9 (8.1)	NA
Age at screening (years), mean [SD]	56.8 (7.1)	56.5 (7.0)
Time from screening date at baseline to date of diagnosis/index date[a] (years), mean [SD]	12.00 (5.7)	11.65 (5.60)
Female, n [%]	232 (76.1)	928 (76.1)
RF seropositive[b], n [%]	186 (61.8)	NA
Anti-CCP seropositive[b], n [%]	111 (51.4)	NA
RF and/or anti-CCP positive [b], n [%]	204 (66.9)	NA
Formal education ≤8 years, n [%]	125 (44.3)	451 (39.8)
Current smoker at time of screening, n [%]	86 (30.4)	249 (21.9)
Total energy intake (kJ), mean [SD]	9404.5 (2770.8)	9246.7 (2602.8)
Potential misreporters of total energy intake, n [%]	55 (19.8)	204 (18.2)
Alcohol consumption, N [%]		
Zero-consumption	16 (5.7)	69 (6.1)
Quintile 1[c]	50 (17.9)	209 (18.5)
Quintile 2[c]	57 (20.4)	212 (18.8)
Quintile 3[c]	46 (16.4)	207 (18.4)
Quintile 4[c]	53 (18.9)	218 (19.3)
Quintile 5[c]	58 (20.7)	213 (18.9)
Physical activity, N [%]		
0–7.5 MET h/week	22 (7.8)	108 (9.5)
7.5–15 MET h/week	44 (15.5)	183 (16.2)
15–25 MET h/week	60 (21.2)	252 (22.2)
25–30 MET h/week	115 (40.6)	405 (35.7)
>50 MET h/week	42 (14.8)	185 (16.3)

MET, metabolic equivalent of task; NA, not applicable; RA, rheumatoid arthritis; RF, rheumatoid factor.
[a] Defined for the controls as date of diagnosis of the corresponding case.
[b] At diagnosis.
[c] Quintile 1: <0.9 g/day for women/ <3.4 g/day for men.
Quintile 2: 0.9–4.3 g/day for women/ 3.4–9.1 g/day for men.
Quintile 3: 4.3–8.1 g/day for women/ 9.1–15.7 g/day for men.
Quintile 4: 8.1–14.0 g/day for women/ 15.7–25.7 g/day for men.
Quintile 5: >14.0 g/day for women/ >25.7 g/day for men.
Missing data: current smoker at time of screening: 22 cases, 84 controls; physical activity: 22 cases, 87 controls; alcohol consumption: 25 cases, 92 controls; formal education: 23 cases, 88 controls; RF status: 4; anti-CCP status: 89.

RA was seen only for the fourth quartile of intake of this component (OR 0.44, 95% CI 0.25–0.78) (Table 4).

A higher reported total intake of fibre was associated with a decreased risk of RA in the multivariable model (adjusted OR per SD 0.80, 95% CI 0.64–0.99) (Table 3). In particular, there was a lower risk in those with fibre intake in the highest quartile (OR 0.51, 95% CI 0.29–0.92) compared to the lowest quartile, but no corresponding associations for the second and third quartiles (Table 4).

Table 2
Descriptives for Swedish Dietary Guidelines Score and its score distributions for pre-RA cases and controls

	Pre-RA cases	Controls
SDGS components, mean [SD]		
Fibre (g/MJ)	2.17 (0.61)	2.25 (0.65)
Vegetables and fruits (g/day)	363.0 (178.4)	391.5 (187.0)
Fish and shellfish (g/week)	324.9 (209.1)	300.2 (234.2)
Added sugar (E%)	10.0 (4.42)	9.75 (4.25)
Red and processed meat (g/week)	832.2 (446.0)	768.2 (394.6)
Adherence to recommendation, N [%]		
Fibre (g/MJ)	85 (30.4)	396 (35.1)
Vegetables and fruits (g/day)	99 (35.4)	468 (41.5)
Fish and shellfish (g/week)	139 (49.6)	468 (41.5)
Added sugar (E%)	155 (55.4)	653 (57.9)
Red and processed meat (g/week)	52 (18.6)	279 (24.7)
SDGS, N [%]		
0	40 (14.3)	155 (13.7)
1	81 (28.9)	302 (26.8)
2	73 (26.1)	275 (24.4)
3	47 (16.8)	216 (19.1)
4	33 (11.8)	136 (12.1)
5	6 (2.1)	44 (3.9)

E%, percent of total energy intake; RA, rheumatoid arthritis; SDGS, Swedish Dietary Guidelines Score.
Missing data for SDGS components: 25 cases and 92 controls.

Moreover, it was found that compliant intakes of fish and shellfish were significantly associated with an increased risk of RA (Table 3). However, there were no significant associations for the total intake of this food group, when analysed as a continuous variable (Table 3). In the corresponding adjusted analyses by quartile, no significant associations were seen (Table 4).

Among potential confounders adjusted for, smoking was associated with increased risk of RA, but there was no significant association with physical activity or alcohol intake (Supplementary Table S3).

In the post hoc analysis stratified by age at screening, there were significant associations with compliance with recommendations on intake of fibre, vegetables and fruit, and red/processed meat and reduced risk of RA. In addition, a corresponding association with high SDGS was noted among individuals who were younger at screening, but no such pattern among those aged ≥55.8 years when participating in the MDCS (Supplementary Table S4).

Analyses stratified by RF/anti-CCP status

Higher SDGS, analysed as a continuous variable (0 to 5), were significantly associated with a decreased risk of seropositive RA in crude and in multivariable analysis after adjustment for potential confounders, with ORs per increment of additional

Table 3
SDGS, its components, and the risk of developing RA (logistic regression)

		Crude model		Adjusted for total energy intake, smoking, alcohol (quintiles), leisure time physical activity[a]	
		OR	95% CI	OR	95% CI
SDGS components	Recommendation				
Compliant with recommendation					
Fibre (g/MJ)	≥2.4	0.78	0.56–1.09	0.69	0.45–1.06
Vegetables and fruits (g/day)	≥400	**0.70**	**0.51–0.96**	**0.64**	**0.43–0.94**
Fish and shellfish (g/week)	≥300	**1.53**	**1.13–2.08**	**1.68**	**1.15–2.45**
Added sugar (E%)	≤10	0.85	0.63–1.14	0.73	0.51–1.05
Red and processed meat (g/week)	< 500	**0.60**	**0.41–0.87**	**0.60**	**0.38–0.97**
SDGS					
0–1		1.00	(Ref)	1.00	(Ref)
2–3		0.89	0.64–1.24	0.83	0.56–1.23
4–5		0.75	0.48–1.19	0.65	0.36–1.17
Per additional score		0.91	0.81–1.02	0.88	0.76–1.02
Reported intake, per SD[b]					
Fibre		**0.85**	**0.73–0.96**	**0.80**	**0.64–0.99**
Vegetables and fruits		**0.81**	**0.69–0.95**	**0.70**	**0.57–0.87**
Fish and shellfish		1.14	0.98–1.31	1.09	0.92–1.30
Added sugar		1.10	0.95–1.27	1.17	0.98–1.41
Red and processed meat		**1.27**	**1.09–1.49**	**1.31**	**1.07–1.59**

Bold text indicates significant associations.
CI, confidence interval; E%, percent of total energy intake; OR, odds ratio; RA, rheumatoid arthritis; Ref, reference; SDGS, Swedish Dietary Guidelines Score.
[a] All potential energy misreporters excluded.
[b] SD for fibre 0.64; vegetables and fruits 185.60; fish and shellfish 229.58; added sugar 4.28; red and processed meat 406.01.

Table 4
SDGS components per quartile and the risk of developing RA (logistic regression)

	Crude model		Adjusted for total energy intake, smoking, alcohol (quintiles), leisure time physical activity[a]	
	OR	95% CI	OR	95% CI
SDGS components				
Reported intake, per quartile (range; mean)				
Fibre (g/MJ)				
Q1 (0.45–1.80; 1.51)	1.00	(Ref)	1.00	(Ref)
Q2 (1.80–2.12; 1.98)	0.90	0.60–1.35	0.83	0.52–1.35
Q3 (2.12–2.58; 2.36)	0.78	0.51–1.18	0.64	0.39–1.06
Q4 (2.58–5.63; 3.11)	**0.60**	**0.38–0.93**	**0.51**	**0.29–0.92**
Vegetables and fruits (g/day)				
Q1 (46.9–255.7; 184.0)	1.00	(Ref)	1.00	(Ref)
Q2 (255.7–356.2; 305.7)	0.86	0.57–1.31	0.83	0.50–1.38
Q3 (356.2–483.0; 416.9)	0.90	0.59–1.36	0.73	0.44–1.21
Q4 (483.0–1393.3; 636.5)	**0.57**	**0.36–0.88**	**0.44**	**0.25–0.78**
Fish and shellfish (g/week)				
Q1 (0.0–148.0; 64.3)	1.00	(Ref)	1.00	(Ref)
Q2 (148.0–266.3; 207.2)	1.47	0.95–2.28	1.24	0.73–2.11
Q3 (266.3–418.4; 335.0)	**1.69**	**1.09–2.63**	1.57	0.92–2.68
Q4 (418.4–2008.1; 614.1)	**1.69**	**1.09–2.63**	1.47	0.86–2.51
Added sugar (E%)				
Q1 (0.51–6.85; 5.03)	1.00	(Ref)	1.00	(Ref)
Q2 (6.85–9.20; 8.12)	0.80	0.52–1.24	0.59	0.34–1.01
Q3 (9.20–12.13; 10.5)	1.18	0.77–1.79	1.16	0.69–1.93
Q4 (12.13–31.61; 15.5)	1.19	0.78–1.81	1.26	0.75–2.11
Red and processed meat (g/week)				
Q1 (0.0–509.5; 350.4)	1.00	(Ref)	1.00	(Ref)
Q2 (509.5–720.5; 613.1)	1.50	0.97–2.33	1.48	0.86–2.52
Q3 (720.5–981.3; 842.7)	**1.56**	**1.01–2.41**	1.65	0.96–2.84
Q4 (981.3–3386.1; 1317.4)	**1.89**	**1.20–2.96**	**1.92**	**1.11–3.35**

Bold text indicates significant associations.
CI, confidence interval; E%, percent of total energy intake; OR, odds ratio; RA, rheumatoid arthritis; Ref, reference; SDGS, Swedish Dietary Guidelines Score.
[a] All potential energy misreporters excluded.

Table 5
SDGS, its components, and the risk of developing RA based on RF/Anti-CCP status (logistic regression)

		RF/Anti-CCP positive		RF/Anti-CCP negative	
		OR[a]	95% CI	OR[a]	95% CI
SDGS components	Recommendation				
Compliant with recommendation					
Fibre (g/MJ)	≥2.4	0.63	0.37–1.07	0.96	0.46–1.99
Vegetables and fruits (g/day)	≥400	**0.59**	**0.36–0.96**	0.75	0.40–1.42
Fish and shellfish (g/week)	≥300	**1.59**	**1.01–2.52**	**2.08**	**1.05–4.13**
Added sugar (E%)	≤10	0.81	0.52–1.26	0.52	0.27–1.00
Red and processed meat (g/week)	<500	**0.30**	**0.15–0.57**	2.03	0.91–4.52
SDGS					
0–1		1.00	(Ref)	1.00	(Ref)
2–3		0.81	0.50–1.31	0.94	0.46–1.93
4–5		0.52	0.25–1.10	1.06	0.38–2.97
Per additional score		**0.82**	**0.69–0.99**	1.03	0.80–1.32
Reported intake, per SD[b]					
Fibre		0.76	0.57–1.01	0.90	0.64–1.25
Vegetables and fruits		**0.64**	**0.48–0.85**	0.83	0.60–1.16
Fish and shellfish		1.08	0.87–1.36	1.11	0.83–1.49
Added sugar		1.24	0.99–1.55	1.03	0.75–1.43
Red and processed meat		**1.41**	**1.10–1.80**	1.13	0.81–1.59

Bold text indicates significant associations.
CI, confidence interval; E%, percent of total energy intake; OR, odds ratio; RA, rheumatoid arthritis; Ref, reference; SDGS, Swedish Dietary Guidelines Score.
[a] Adjusted for total energy intake, smoking, alcohol (quintiles), leisure time physical activity. All potential energy misreporters excluded.
[b] SD – seropositive RA and controls for fibre 0.62; vegetables and fruits 179.1; fish and shellfish 223.1; added sugar 4.31; red and processed meat 384.2. Seronegative RA and controls for fibre 0.68; vegetables and fruits 198.4; fish and shellfish 242.6; added sugar 4.21; red and processed meat 447.7.

Table 6
SDGS components per quartile and the risk of RA, by RF/Anti-CCP status (logistic regression)

	RF/Anti-CCP positive		RF/Anti-CCP negative	
	OR[a]	95% CI	OR[a]	95% CI
Reported intake, per quartile[b]				
Fibre (g/MJ)				
Q1	1.00	(Ref)	1.00	(Ref)
Q2	0.60	0.33–1.10	1.27	0.54–2.96
Q3	0.79	0.43–1.45	0.54	0.21–1.36
Q4	**0.45**	**0.22–0.93**	0.71	0.27–1.91
Vegetables and fruits (g/day)				
Q1	1.00	(Ref)	1.00	(Ref)
Q2	1.35	0.73–2.51	**0.32**	**0.12–0.84**
Q3	0.73	0.38–1.38	0.71	0.30–1.68
Q4	0.53	0.25–1.05	**0.31**	**0.12–0.82**
Fish and shellfish (g/week)				
Q1	1.00	(Ref)	1.00	(Ref)
Q2	1.24	0.65–2.36	1.64	0.60–4.50
Q3	1.64	0.86–3.14	2.22	0.8–6.04
Q4	1.36	0.70–2.65	2.18	0.79–6.03
Added sugar (E%)				
Q1	1.00	(Ref)	1.00	(Ref)
Q2	0.70	0.36–1.36	**0.38**	**0.14–0.99**
Q3	1.01	0.53–1.92	1.33	0.54–3.24
Q4	1.44	0.75–2.75	1.06	0.44–2.59
Red and processed meat (g/week)				
Q1	1.00	(Ref)	1.00	(Ref)
Q2	**2.14**	**1.07–4.27**	0.43	0.16–1.15
Q3	**2.58**	**1.28–5.19**	0.59	0.24–1.50
Q4	**3.43**	**1.69–6.96**	0.54	0.20–1.49

Bold text indicates significant associations.
CI, confidence interval; E%, percent of total energy intake; OR, odds ratio; RA, rheumatoid arthritis; Ref, reference; SDGS, Swedish Dietary Guidelines Score.
[a] Adjusted for total energy intake, smoking, alcohol (quintiles), leisure time physical activity. All potential energy misreporters excluded.
[b] For quartile limits and mean intakes per quartile, see Supplementary Table S14.

score 0.85 (95% CI 0.74–0.98) and (OR 0.82, 95% CI 0.69–0.99), respectively (Table 5).

In the multivariable analyses stratified by RF/Anti-CCP status, associations with lower risks of seropositive RA were observed for those reporting intakes adherent to the recommendations for vegetables and fruits (OR 0.59, 95% CI 0.36–0.96) and for red and processed meat (OR 0.30, 95% CI 0.15–0.57) (Table 5). A completely different pattern was observed for seronegative RA, with a trend towards reduced risk among individuals reporting intakes of red/processed meat adherent to dietary recommendations and across quartiles of red/processed meat consumption (Table 6). Further, there were associations for total intakes of vegetables and fruits and red and processed meat that remained significant throughout all models within the seropositive group but not seronegative group (Table 5, Supplementary Tables S6,S7). In comparison to the first quartile, the ORs for developing seropositive RA increased gradually for the second, third, and fourth quartile, thus suggesting a dose–response relationship (Table 6). The adjusted OR for those in the highest quartile of red/processed meat intake (about 1 kg/week or more) was 3.43 (95% CI 1.69–6.96) for seropositive RA, but 0.54 (95% CI 0.20–1.49) for seronegative RA (Table 6).

There was a trend towards decreased risk for seropositive RA with a higher intake of fibre (Table 5), which reached significance in the analysis comparing the highest quartile to the lowest (OR 0.45; 95% CI 0.22–0.93) (Table 6). No associations between fibre intake and seronegative RA were observed (Table 6).

However, compliant intakes of fish and shellfish were associated with an increased risk of seropositive and seronegative RA in the adjusted models (Table 5). The corresponding analyses by quartile of fish/shellfish intake showed no significant associations (Table 6).

Similar results were obtained in analyses adjusted for total EI only (Supplementary Tables S5-S8) and in multivariable models

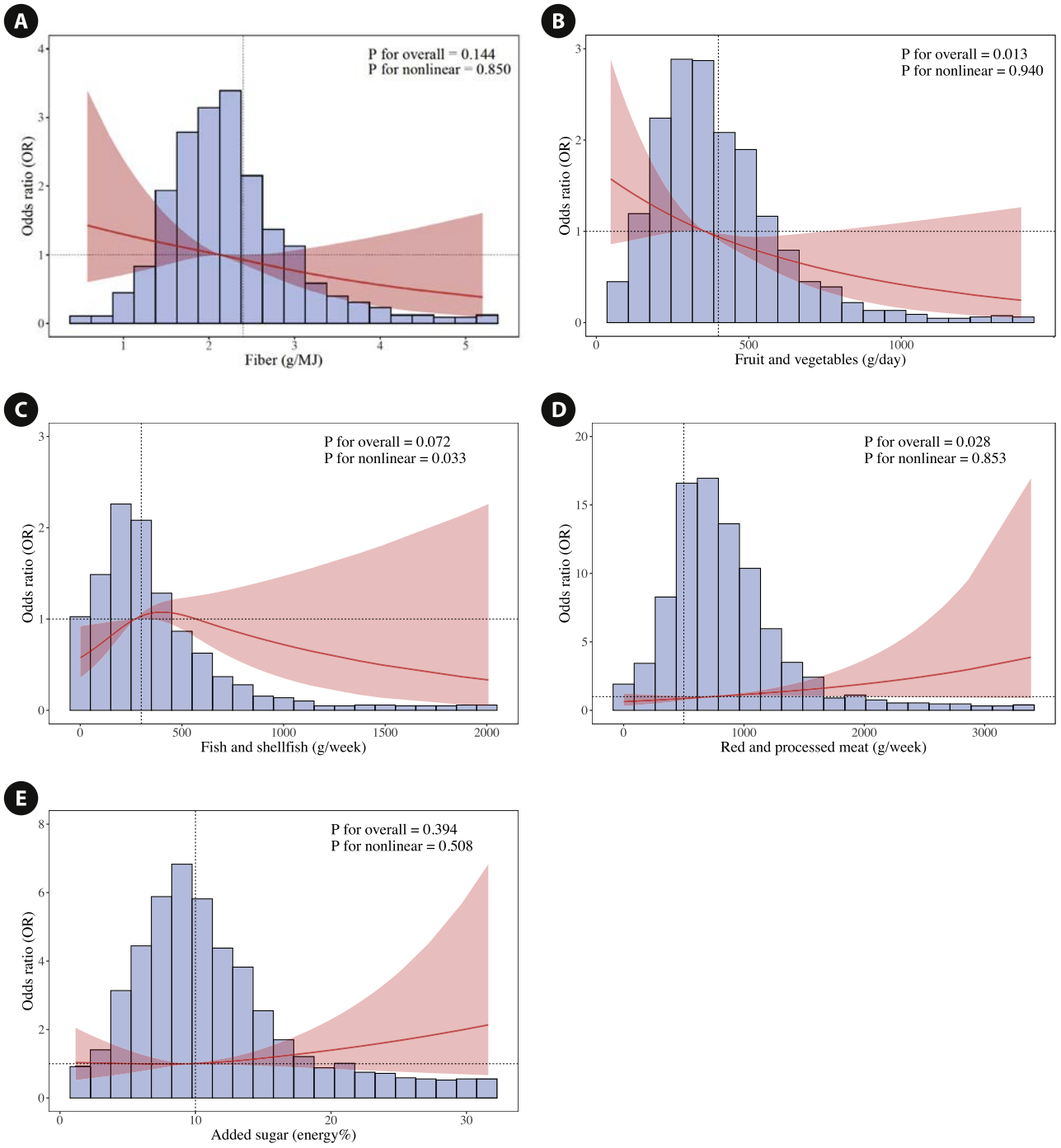

Figure. Restricted cubic spline models of intakes of fibre (A), vegetables and fruits (B), fish and shellfish (C), red and processed meats (D), and added sugars (E) and the risk of rheumatoid arthritis (RA) fitted to unconditional logistic regression models adjusted for baseline age and sex and total energy intake, smoking and physical activity, excluding energy misreporters. A–E, Histograms (blue) showing the population distribution across intake levels of the SDGS dietary components. The red solid line shows the odds ratio (OR), and the shaded red area represents the 95% CI. The horizontal reference line (dashed) indicates an OR of 1.0. The vertical reference line (dashed) indicates the recommended intake level of the dietary components. OR, odds ratio; RA, rheumatoid arthritis; SDGS, Swedish Dietary Guideline Score.

when potential misreporters of energy were not excluded (Supplementary Table S9-S14).

Restricted cubic splines

The fully adjusted RCS regression models are illustrated in Figure. For intakes of vegetables and fruits an inverse linear association was demonstrated in the fully adjusted model (*P* for overall association = 0.013). By contrast, for intakes of red and processed meat, a linear positive association was found (*P* for overall association = 0.028). For fish and shellfish, a nonlinear association was observed (*P* for nonlinear association = 0.033, *P* for overall association = 0.072). Results of the analyses adjusted for the matching variables only (Supplementary Fig S1) were largely similar to the fully adjusted models.

DISCUSSION

This nested case–control study investigated the relationship between adherence to the current food-based SDGs and the risk of developing RA. We identified a dose–response relationship between red and processed meat consumption and an increased

risk of RA, particularly seropositive RA. An opposite nonsignificant trend towards reduced risk of seronegative RA was observed for adherence to recommendations on red/processed and with increasing intakes of red/processed meat consumption. Moreover, we found an association between higher intakes of vegetables and fruits and a reduced risk of RA. Higher scores for the SDGS, indicating adherence to the current Swedish food-based dietary guidelines, were significantly associated with a decreased risk of seropositive RA only in multivariable-adjusted analysis. The effects appeared to be driven by compliance with recommendations for red and processed meat as well as vegetables and fruits and to be stronger for younger individuals. This pattern might reflect early disease mechanisms that are variable by age [28]. For example, hormone-related risk factors for RA [29,30] could be more important in older people.

Importantly, the majority of participants consumed meat and reported limited intakes of vegetables and fruit. The present study could not evaluate the impact of vegan or vegetarian diets on the risk of RA, and there are no studies on this aspect in the literature [6].

In line with our results, analyses based on the Nurses' Health Study demonstrated a significantly increased risk of RA with higher intakes of red/processed meat in women aged <55 years [7]. Further, results from a nested case–control study based on the European Prospective Investigation of Cancer in Norfolk cohort demonstrated that total meat intakes within the highest tertile compared to the lowest were significantly associated with an increased risk of developing inflammatory polyarthritis [31]. Further, a cross-sectional study based on the National Health and Nutrition Examination Survey and a 2-sample Mendelian randomisation study using data from the UK Biobank study suggested associations between higher beef intakes and increased risk of RA [32].

It should, however, be noted that these studies are not directly comparable with regards to differences in study designs, diet assessment methods, and definitions of meat. In addition, none of these studies looked into the effects of red/processed meat on seropositive and seronegative RA separately. There are several other observational studies that have examined the effect of meat on the risk of RA development, but these did not find any significant associations with RA [8–12]. To the best of our knowledge, no observational studies have suggested protective effects of red meat on RA development.

Our results demonstrated that intakes of red/processed meat were associated with an increased risk of seropositive RA. In contrast, the association with seronegative RA was in the opposite direction, although not statistically significant. These findings suggest potentially different roles of red meat on the pathogenic mechanisms behind the development of these subtypes. Early development of autoantibodies in seropositive RA is a process which has been suggested to be initiated in the lung as a result of smoking-induced protein citrullination triggering the production of ACPA, particularly in genetically predisposed individuals [33–35].

The association in models adjusted for smoking in the present study suggests that other mechanisms may also be important. Interestingly, the intestinal microbiota has been suggested to be involved in the immune dysfunction present in RA [36]. Therefore, the gut could be another relevant pathway for the production of autoantibodies, a process possibly influenced by dietary factors, as such as red and processed meats.

The impact of vegetables and fruits has been examined in several studies with various design, mainly indicating a potential protective effect [37,38]. In the present study, there was no indication of a differential effect of vegetable and fruit intakes in analyses stratified by seropositive and seronegative RA. It therefore appears that intakes of vegetables and fruits may protect against RA development in general, regardless of serostatus. Although we did not find a significant association between recommended fibre intake and RA, a decreased risk for those reporting intake in the highest quartile was noted. Hypothetically, fibres might explain part of the protective effect of vegetables and fruits as a natural part of their nutritional content.

The importance of dietary habits for different individuals may be variable. Considering the multifactorial aetiology of RA, it might be that at risk individuals, e.g. genetically predisposed and/or seropositive for RA associated antibodies without signs or symptoms of arthritis, may be particularly prone to develop RA if nonadherent to dietary guidelines. Moreover, healthy dietary habits might be associated with a higher health literacy, possibly due to higher awareness of dietary and nutritional recommendations overall.

We identified that recommended intakes of fish/shellfish associated with an increased risk of developing RA. However, contrary to intakes of red/processed meat and vegetables and fruits, the associations between fish/shellfish and RA were clearly nonlinear, indicating some uncertainty regarding its biological relevance for RA development.

In other observational studies on fish and the risk of RA, intakes appear to be mostly associated with a lower risk of RA [9,39–43]. A varying nutritional composition in fish depending on species, if wild-caught or farmed, and differences in cooking methods might influence the course of RA development differently.

Intakes of fish and shellfish 2–3 times per week is encouraged according to the current food-based SDGs [14]. As a food group, fish and shellfish are nutritious and contain a variety of different healthy micro- and macronutrients. Intake of fish and shellfish has been shown to lower the risk of cardiovascular disease and is found in diets associated with a reduced risk of obesity. In contrast, red and processed meat consumption has been associated with an increased risk of cardiovascular disease, and in higher amounts, with colorectal cancer, thereby supporting recommendations for limited use [14].

Based on a holistic approach to diet, it is reasonable to assume that some differences exist regarding the overall nutritional profiles between those consuming high amounts of red and processed meat versus those consuming high amounts of fish and shellfish, with the latter being more likely to have healthier nutritional profiles compared to those with high intakes of red meat. Therefore, given that the association we found for fish and shellfish was nonlinear, the observed unexpected association direction for those with recommended fish and shellfish intakes could be explained by residual confounding and should be interpreted with caution.

There are some limitations to consider in this study. Although diet was assessed using a validated methodology designed for MDCS, it was registered only at baseline. Hence, it is possible that participants changed their eating habits during the follow-up period assessed in this study. Moreover, it has been demonstrated that MDCS, with the primary aim of studying the relationship between diet and subsequent cancer, may introduce selection bias by attracting certain individuals with systematic differences compared to the true background population [15]. Furthermore, the participation rate in the MDCS was ~40% and the study participants were middle-aged and older at the time of dietary assessment in the 1990s, limiting the external validity.

Our results should be interpreted in light of changes in dietary guidelines over time, especially those concerning meat intake.

The classification of cases into either seropositive/seronegative was based on data collected from the cases' medical records during the validation process. Therefore, serostatus for the matched controls is unknown. Moreover, whereas the ACPA tests most commonly used in clinical practice detect anti-CCPs, alternative methods utilised mostly in research settings have been developed using other citrullinated proteins [44]. The use of retrospective data from standard tests could result in misclassification of truly seropositive cases as seronegative RA.

This study has several strengths. Its prospective design eliminates the risk of recall bias. Further, dietary assessment was performed using a validated 3-phase method. Incident RA cases were identified by register linkage with a following validation process through review of medical records. In addition to the high quality diet assessment and the adequately obtained outcome data, information on relevant confounders were available in the MDCS, enabling multivariable analyses. Despite this, the risk of residual confounding cannot be fully excluded. Consequentially to the extended follow-up period until 2016, we identified 305 incident RA cases (vs 174 cases in our prior study), enabling stratified analyses by serostatus yielding valuable information about the underlying differences between these groups. Further, by performing spline analyses, we were able to investigate linearity and shape of the relationships, preserving statistical power in the analyses, which can be compromised when categorising the exposure variable into quartiles. Finally, results were largely similar in analyses of quantified diet components when using different methods.

CONCLUSION

Our findings suggest a dose–response relationship between red/processed meat intake and the risk of seropositive, but not seronegative, RA. This study helps to improve our understanding of the effects of dietary components in RA development, particularly for red and processed meats, but the exact mechanisms behind our findings need further investigation.

Competing interests

All authors declare that they have no conflicts of interest.

CRediT authorship contribution statement

Rebecka Bäcklund: Writing – original draft, Writing – review & editing, Formal analysis, Conceptualization. **Ulf Bergström:** Writing – review & editing, Investigation, Supervision. **Michele Compagno:** Writing – review & editing, Supervision. **Linnea Arvidsson:** Writing – review & editing, Investigation. **Emil Rydell:** Writing – review & editing, Investigation. **Emily Sonestedt:** Writing – review & editing, Methodology, Data curation. **Carl Turesson:** Writing – review & editing, Supervision, Investigation, Conceptualization.

Acknowledgements

We thank Isabel Drake for her significant contribution to the work with the RCS analyses. Parts of the results of this study were presented as a poster at the American College of Rheumatology Convergence meeting on November 12, 2023 [45].

Funding

This study was supported by the Swedish Rheumatism Association, the Gustav V 80-year fund, the Greta and Johan Kock foundation, the Alfred Österlund foundation and Lund University.

Patient consent for publication

Not applicable.

Ethics approval

This study was approved by the Regional Research Ethics Committee of Lund, Sweden, record number 71/2005.

Provenance and peer review

Not commissioned; externally peer reviewed.

Supplementary materials

Supplementary material associated with this article can be found in the online version at doi:10.1016/j.ard.2025.06.2123.

Orcid

Rebecka Bäcklund: http://orcid.org/0000-0002-4878-8349
Carl Turesson: http://orcid.org/0000-0002-3805-2290

REFERENCES

[1] Scott DL, Wolfe F, Huizinga TW. Rheumatoid arthritis. Lancet 2010;376(9746):1094–108.
[2] Rantapää-Dahlqvist S, de Jong BA, Berglin E, Hallmans G, Wadell G, Stenlund H, et al. Antibodies against cyclic citrullinated peptide and IgA rheumatoid factor predict the development of rheumatoid arthritis. Arthritis Rheum 2003;48(10):2741–9.
[3] Castro C, Gourley M. Diagnostic testing and interpretation of tests for autoimmunity. J Allergy Clin Immunol 2010;125(2 Suppl 2):S238–47.
[4] Sugiyama D, Nishimura K, Tamaki K, Tsuji G, Nakazawa T, Morinobu A, et al. Impact of smoking as a risk factor for developing rheumatoid arthritis: a meta-analysis of observational studies. Ann Rheum Dis 2010;69(1):70–81.
[5] Rydell E, Forslind K, Nilsson J, Karlsson M, Åkesson KE, Jacobsson LTH, et al. Predictors of radiographic erosion and joint space narrowing progression in patients with early rheumatoid arthritis: a cohort study. Arthritis Res Ther 2021;23(1):27.
[6] Bäcklund R, Drake I, Bergström U, Compagno M, Sonestedt E, Turesson C. Diet and the risk of rheumatoid arthritis - A systematic literature review. Semin Arthritis Rheum 2023;58:152118.
[7] Hu Y, Sparks JA, Malspeis S, Costenbader KH, Hu FB, Karlson EW, et al. Long-term dietary quality and risk of developing rheumatoid arthritis in women. Ann Rheum Dis 2017;76(8):1357–64.
[8] Pedersen M, Stripp C, Klarlund M, Olsen SF, Tjønneland AM, Frisch M. Diet and risk of rheumatoid arthritis in a prospective cohort. J Rheumatol 2005;32(7):1249–52.
[9] Shapiro JA, Koepsell TD, Voigt LF, Dugowson CE, Kestin M, Nelson JL. Diet and rheumatoid arthritis in women: a possible protective effect of fish consumption. Epidemiology 1996;7(3):256–63.
[10] Sundström B, Ljung L, Di Giuseppe D. Consumption of meat and dairy products is not associated with the risk for rheumatoid arthritis among women: a population-based cohort study. Nutrients 2019;11(11):2825.
[11] Benito-Garcia E, Feskanich D, Hu FB, Mandl LA, Karlson EW. Protein, iron, and meat consumption and risk for rheumatoid arthritis: a prospective cohort study. Arthritis Res Ther 2007;9(1):R16.
[12] Rubin KH, Rasmussen NF, Petersen I, Kopp TI, Stenager E, Magyari M, et al. Intake of dietary fibre, red and processed meat and risk of late-onset Chronic Inflammatory Diseases: A prospective Danish study on the "diet, cancer and health" cohort. Int J Med Sci 2020;17(16):2487–95.

[13] Bäcklund RT, Drake I, Bergström U, Compagno M, Sonestedt E, Turesson C. Adherence to dietary guidelines, and the risk of developing rheumatoid arthritis: results from a nested case-control study. Rheumatology (Oxford) 2024;63(2):407–13.
[14] Livsmedelsverket. Swedish dietary guidelines - risk and benefit management report 2015. Accessed June 8, 2025. Available from: https://www.fao.org/3/az907e/az907e.pdf
[15] Manjer J, Carlsson S, Elmståhl S, Gullberg B, Janzon L, Lindström M, et al. The Malmö Diet and Cancer Study: representativity, cancer incidence and mortality in participants and non-participants. Eur J Cancer Prev 2001;10(6):489–99.
[16] Englund M, Jöud A, Geborek P, Felson DT, Jacobsson LT, Petersson IF. Prevalence and incidence of rheumatoid arthritis in southern Sweden 2008 and their relation to prescribed biologics. Rheumatology (Oxford) 2010;49(8):1563–9.
[17] Drake I, Gullberg B, Ericson U, Sonestedt E, Nilsson J, Wallström P, et al. Development of a diet quality index assessing adherence to the Swedish nutrition recommendations and dietary guidelines in the Malmö Diet and Cancer cohort. Public Health Nutr 2011;14(5):835–45.
[18] Li C, Aronsson CA, Hedblad B, Gullberg B, Wirfält E, Berglund G. Ability of physical activity measurements to assess health-related risks. Eur J Clin Nutr 2009;63(12):1448–51.
[19] Riboli E, Elmståhl S, Saracci R, Gullberg B, Lindgärde F. The Malmö Food Study: validity of two dietary assessment methods for measuring nutrient intake. Int J Epidemiol 1997;26(Suppl 1):S161–73.
[20] Elmstahl S, Riboli E, Lindgärde F, Gullberg B, Saracci R. The Malmö Food Study: the relative validity of a modified diet history method and an extensive food frequency questionnaire for measuring food intake. Eur J Clin Nutr 1996;50(3):143–51.
[21] Wirfält E, Mattisson I, Johansson U, Gullberg B, Wallström P, Berglund G. A methodological report from the Malmö Diet and Cancer study: development and evaluation of altered routines in dietary data processing. Nutr J 2002;1:3.
[22] Bergström U, Jacobsson LT, Nilsson J, Wirfält E, Turesson C. Smoking, low formal level of education, alcohol consumption, and the risk of rheumatoid arthritis. Scand J Rheumatol 2013;42(2):123–30.
[23] Arnett FC, Edworthy SM, Bloch DA, McShane DJ, Fries JF, Cooper NS, et al. The American Rheumatism Association 1987 revised criteria for the classification of rheumatoid arthritis. Arthritis Rheum 1988;31(3):315–24.
[24] Kay J, Upchurch KS. ACR/EULAR 2010 rheumatoid arthritis classification criteria. Rheumatology (Oxford) 2012;51(Suppl 6) vi5-9.
[25] Gail M, Williams R, Byar DP, Brown C. How many controls? J Chronic Dis 1976;29(11):723–31.
[26] González-Padilla E, Tao Z, Sánchez-Villegas A, Álvarez-Pérez J, Borné Y, Sonestedt E. Association between adherence to Swedish dietary guidelines and Mediterranean diet and risk of stroke in a Swedish population. Nutrients 2022;14(6):1253.
[27] Mattisson I, Wirfält E, Aronsson CA, Wallström P, Sonestedt E, Gullberg B, et al. Misreporting of energy: prevalence, characteristics of misreporters and influence on observed risk estimates in the Malmö Diet and Cancer cohort. Br J Nutr 2005;94(5):832–42.
[28] Takanashi S, Kaneko Y. Unmet needs and current challenges of rheumatoid arthritis: difficult-to-treat rheumatoid arthritis and late-onset rheumatoid arthritis. J Clin Med 2024;13(24):7594.
[29] Pikwer M, Bergström U, Nilsson J, Jacobsson L, Turesson C. Early menopause is an independent predictor of rheumatoid arthritis. Ann Rheum Dis 2012;71(3):378–81.
[30] Pikwer M, Giwercman A, Bergström U, Nilsson JÅ, Jacobsson LT, Turesson C. Association between testosterone levels and risk of future rheumatoid arthritis in men: a population-based case-control study. Ann Rheum Dis 2014;73(3):573–9.
[31] Pattison DJ, Symmons DP, Lunt M, Welch A, Luben R, Bingham SA, et al. Dietary risk factors for the development of inflammatory polyarthritis: evidence for a role of high level of red meat consumption. Arthritis Rheum 2004;50(12):3804–12.
[32] Chen W, Liu K, Huang L, Mao Y, Wen C, Ye D, et al. Beef intake and risk of rheumatoid arthritis: Insights from a cross-sectional study and two-sample Mendelian randomization. Front Nutr 2022;9:923472.
[33] Sparks JA, Karlson EW. The roles of cigarette smoking and the lung in the transitions between phases of preclinical rheumatoid arthritis. Curr Rheumatol Rep 2016;18(3):15.
[34] Källberg H, Ding B, Padyukov L, Bengtsson C, Rönnelid J, Klareskog L, et al. Smoking is a major preventable risk factor for rheumatoid arthritis: estimations of risks after various exposures to cigarette smoke. Ann Rheum Dis 2011;70(3):508–11.
[35] Makrygiannakis D, Hermansson M, Ulfgren AK, Nicholas AP, Zendman AJ, Eklund A, et al. Smoking increases peptidylarginine deiminase 2 enzyme expression in human lungs and increases citrullination in BAL cells. Ann Rheum Dis 2008;67(10):1488–92.
[36] Zaiss MM, Joyce Wu HJ, Mauro D, Schett G, Ciccia F. The gut-joint axis in rheumatoid arthritis. Nat Rev Rheumatol 2021;17(4):224–37.
[37] Cerhan JR, Saag KG, Merlino LA, Mikuls TR, Criswell LA. Antioxidant micronutrients and risk of rheumatoid arthritis in a cohort of older women. Am J Epidemiol 2003;157(4):345–54.
[38] Linos A, Kaklamani VG, Kaklamani E, Koumantaki Y, Giziaki E, Papazoglou S, et al. Dietary factors in relation to rheumatoid arthritis: a role for olive oil and cooked vegetables? Am J Clin Nutr 1999;70(6):1077–82.
[39] Rosell M, Wesley AM, Rydin K, Klareskog L, Alfredsson L. Dietary fish and fish oil and the risk of rheumatoid arthritis. Epidemiology 2009;20(6):896–901.
[40] Linos A, Kaklamanis E, Kontomerkos A, Koumantaki Y, Gazi S, Vaiopoulos G, et al. The effect of olive oil and fish consumption on rheumatoid arthritis—a case control study. Scand J Rheumatol 1991;20(6):419–26.
[41] Di Giuseppe D, Wallin A, Bottai M, Askling J, Wolk A. Long-term intake of dietary long-chain n-3 polyunsaturated fatty acids and risk of rheumatoid arthritis: a prospective cohort study of women. Ann Rheum Dis 2014;73(11):1949–53.
[42] Nguyen Y, Salliot C, Gelot A, Gambaretti J, Mariette X, Boutron-Ruault MC, et al. Mediterranean diet and risk of rheumatoid arthritis: findings from the French E3N-EPIC Cohort Study. Arthritis Rheumatol 2021;73(1):69–77.
[43] Sparks JA, O'Reilly É J, Barbhaiya M, Tedeschi SK, Malspeis S, Lu B, et al. Association of fish intake and smoking with risk of rheumatoid arthritis and age of onset: a prospective cohort study. BMC Musculoskelet Disord 2019;20(1):2.
[44] Rönnelid J, Turesson C, Kastbom A. Autoantibodies in rheumatoid arthritis - laboratory and clinical perspectives. Front Immunol 2021;12:685312.
[45] Bäcklund R, Drake IU, Bergström U, Compagno M, Sonestedt E, Turesson C. Higher intakes of red meat are associated with an increased risk of developing seropositive but not seronegative rheumatoid arthritis – results from a nested case-control study. Arthritis Rheumatol 2023;75(suppl 9) Accessed June 8, 2025. Available from: https://acrabstracts.org/abstract/higher-intakes-of-red-meat-are-associated-with-an-increased-risk-of-developing-seropositive-but-not-seronegative-rheumatoid-arthritis-results-from-a-nested-case-control-study/.

Ann Rheum Dis 84 (2025) 1801–1810

Contents lists available at ScienceDirect

Annals of the Rheumatic Diseases

journal homepage: https://www.sciencedirect.com/journal/annals-of-the-rheumatic-diseases

Systemic lupus erythematosus

SLE classification criteria item relationships: implications on SLE as a disease entity

Martin Aringer[1,*], Franziska Szelinski[2], Thomas Dörner[2], Karen H. Costenbader[3], Sindhu R. Johnson[4,5]

[1] *Division of Rheumatology, Department of Medicine III, and interdisciplinary University Center for Autoimmune and Rheumatic Entities (UCARE), University Medical Center and Faculty of Medicine TU Dresden, Dresden, Germany*
[2] *Department of Rheumatology and Clinical Immunology, Charité – Universitätsmedizin Berlin, Corporate member of Freie Universität Berlin, Humboldt-Universität zu Berlin, and Deutsches Rheumaforschungszentrum (DRFZ), Berlin, Germany*
[3] *Division of Rheumatology, Inflammation and Immunity, Department of Medicine, Brigham and Women's Hospital, Harvard Medical School, Boston, Massachusetts, USA*
[4] *Division of Rheumatology, Department of Medicine, Toronto Western Hospital, Mount Sinai Hospital, Toronto, ON, Canada*
[5] *Institute of Health Policy, Management and Evaluation, University of Toronto, Toronto, ON, Canada*

ARTICLE INFO

Article history:
Received 23 February 2025
Received in revised form 10 July 2025
Accepted 27 July 2025

ABSTRACT

Objectives: This study aims to analyse potential relationships between European Alliance of Associations for Rheumatology (EULAR)/American College for Rheumatology (ACR) classification criteria domains and individual criteria items in a large systemic lupus erythematosus (SLE) patient cohort. Previous findings showed meaningful associations only within organ systems, but not across them. We seek to validate these findings and expand on them.

Methods: Cluster analysis was performed on the EULAR/ACR criteria domains in a cohort of 1196 patients with SLE. Criteria items were analysed as binary variables (ever present = 1, always absent = 0) and tested for associations using network analysis.

Results: The cluster analysis resulted in 10 clusters, but with no convincing patterns beyond antibody-organ relationships. Relevant correlations between items were found within the domains, but some associations between items of different domains still showed significant, if mostly weak associations with *r* values of 0.10 to 0.26. These included correlations between antibodies to double-stranded DNA and Sm, low complements and lupus nephritis, and between antiphospholipid antibodies and thrombocytopenia. Anti-Sm antibodies were also associated with alopecia and leukopenia, autoimmune haemolysis with seizures, and serositis with fever. Joint involvement was negatively correlated with lupus nephritis and thrombocytopenia. The network analysis showed fever and serositis detached from the other items, with items within organ domains grouped.

Conclusions: This comprehensive analysis of relationships between the domains and items of the EULAR/ACR SLE classification criteria underlines the relevance of the domain structure. Overall, the data are more compatible with chance distribution than with fixed subsets of SLE.

*Correspondence to Dr. Martin Aringer, Rheumatology, Medicine III, University Medical Center TU Dresden, Fetscherstrasse 74, Dresden 01307, Germany. (M. Aringer).

E-mail address: martin.aringer@uniklinikum-dresden.de (M. Aringer).

Handling editor Josef S. Smolen.

https://doi.org/10.1016/j.ard.2025.07.024

WHAT IS ALREADY KNOWN ON THIS TOPIC

- During the development of the European Alliance of Associations for Rheumatology (EULAR)/American College for Rheumatology (ACR) classification criteria for systemic lupus erythematosus (SLE), meaningful associations between items were found within organ systems only
- These findings led to the domain structure of the EULAR/ACR classification criteria.

WHAT THIS STUDY ADDS

- Classification criteria domains and items both followed distributions reminiscent of Gaussian curves, not of several peaks.
- Clustering of the domains resulted in 10 clusters, but without an indication of defined subsets.
- A network analysis of items found relevant associations within domains only; additional weak positive and negative associations were mostly reflective of known SLE pathophysiology.

HOW THIS STUDY MIGHT AFFECT RESEARCH, PRACTICE OR POLICY

- The findings together suggest important random elements in combinations of autoantibodies and clinical items, rather than fixed subsets, and are in line with SLE as 1 disease.
- The associations within organ systems in this large cohort with mostly long-standing SLE support the domain structure of the EULAR/ACR SLE classification criteria.

INTRODUCTION

Systemic lupus erythematosus (SLE) is a highly variable autoimmune disease, which, due to a range of autoantibodies and ensuing immune complexes, can afflict essentially any organ [1–3]. Before the development of the European Alliance of Associations for Rheumatology (EULAR)/American College for Rheumatology (ACR) SLE classification criteria [4,5], potential associations between manifestations (criteria items) had not been systematically investigated in any of the previous classification criteria approaches.

Within the EULAR/ACR classification criteria development work, the SLE international expert panel suggested grouping items that are clinically or physiologically related [6]. Analysis of data from an early SLE cohort [7] and from the EuroLupus cohort [8] led to the recognition of several associations occurring between items within organ-specific domains. However, these analyses did not reveal any meaningful connections between criteria items belonging to different criteria domains [9].

As a result, the EULAR/ACR SLE classification criteria items were organised into 10 domains, in each of which only the highest-scoring item contributed to the sum score [10]. This is also highly relevant for the ongoing discussion on whether SLE is a single disease entity or a syndrome consisting of several distinct subdiseases. The latter would be expected to result in reproduced fixed combinations of criteria items and well-defined clusters.

To address this question, the current study examined the distribution of SLE classification criteria items, representing SLE-specific manifestations, and evaluated potential associations between any of these items, both within and across organ-specific domains. In addition, we employed network visualisation of the relationships between clinical features to evaluate for the presence of disease subsets, and performed state-of-the-art cluster analysis in the combined SLE cohort established in the classification criteria project, which represents more than 14,000 years of SLE disease duration, and thus the full array of manifestations for most patients.

This study also serves as an important test of the appropriateness of the cohort structure of the criteria, since the items exactly match the criteria items in this cohort. In addition, even weak associations between items in a large, well-defined cohort may help to find clinical relationships.

PATIENTS AND METHODS

Cohort

Data on the presence or absence of EULAR/ACR SLE classification criteria items were collected for 1196 patients with SLE that were contributed by 21 expert SLE centres worldwide [4,11]. The diagnosis of SLE was based on physician judgement and adjudicated by 3 independent SLE experts regardless of whether the patient's classification score met the threshold for classification.

Distribution

The number of positive domains and the number of positive items were counted for each patient, and the ensuing distribution analysed.

Association

To assess the strength of associations between binary clinical features, phi-coefficients were also calculated using the psych package in R. The resulting phi-coefficient matrix provided a pairwise measure of the association between the features. Fisher's exact tests assessed the statistical significance of these associations. *P* values were adjusted using the Benjamini-Hochberg procedure to control for false discovery rates. Significant pairs of features were identified by applying a significance level threshold of 0.05.

Subset analysis

Multiple correspondence analysis (MCA) was performed on the 10 classification criteria domains, using R (version 4.3.2) and the FactoMineR (version 2.11) package. Consensus clustering was performed using the ConsensusClusterPlus package (Version 1.66.0), to formally investigate whether the EULAR/ACR domains define patient clusters. The consensus cumulative distribution function (CDF) was used to evaluate the stability of clustering solutions across a range of possible cluster numbers (k) in our dataset. The double angle identity of the cosine function (Cos2) values of the MCA plot was examined, which indicates the degree of association between the domains and the first 2 dimensions. In addition, a Scree plot was created to examine the proportion of the variance explained by increasing numbers of organ system domains.

Associations between individual items were analysed in an unbiased approach. In this 23 × 23 table, associations were accordingly tested for 529 pairs, and corrected by means of Benjamini-Hochberg-adjusted phi-coefficients. In addition, Bonferroni's correction for multiple comparisons was employed, with significance defined as a P value of lower than .05 divided by 529, or $P < 9.45e^{-5}$, independent of the r value.

Additionally, a network was constructed based on significant associations identified from that pairwise analyses. Using the tidygraph software package, a network was constructed with clinical features as nodes and significant correlations as edges.

The feature domains were incorporated as node attributes, allowing each node to be assigned to its respective clinical category. The network was visualised using the graph package with a Fruchterman-Reingold layout to achieve a clear spatial arrangement. Edge thickness was proportional to the strength of the correlation, and the edges were coloured red for positive correlations and blue for negative correlations. Only edges with correlation coefficients greater than 0.1 were plotted to ensure that the visualisation focused on the most relevant and meaningful relationships. This network visualisation provided an intuitive representation of the relationships between clinical features, with domain-based colouring of nodes, and edges reflecting the strength and direction of associations.

Patient and public involvement

Patients or the general public were not actively involved in this work.

RESULTS

Numbers of items and domains

The combined cohort included 1054 female and 142 male patients with SLE, with a median age of 44 years (range 14-93) and a median disease duration of 10 years (range 1-56), representing 14,032 years of cumulative SLE experience. Since classification criteria apply to the rule that the occurrence of a criterion on at least 1 occasion is sufficient, the data show cumulated fulfilment of criteria items, and do not include data on activity or therapy.

These patients fulfilled a minimum of 1 and a maximum of 9 of the 10 domains (Fig 1), with a median of 4. On the item levels, patients fulfilled a range of 1 to 15 of the 23 items, with a median of 6 (Fig 1B). The distribution was slightly skewed, with at least 100 patients each fulfilling 3, 4, 5, 6, 7, and 8 items. Both the item and the domain curves were suggestive of a random distribution. In particular, there was no indication of 2 or more peaks (Fig 1).

Distribution and relationships between the different EULAR/ACR domains

More than two-thirds of the patients had ever fulfilled criteria items within the domain SLE-specific antibodies (n = 955, 79.8%), the mucocutaneous (n = 862, 72.0%) and musculoskeletal (n = 861, 71.9%) domains, and complements (n = 857, 71.6%). The hematologic and renal domains, as well as the antiphospholipid antibody domain, were more equally distributed. Less frequently involved were the constitutional (n = 256, 21.4%) and serosal (n = 211, 17.6%) domains, and least common was the neuropsychiatric domain (n = 82, 6.9%) (Fig 2A). Domains affected did not change relevantly over time (Supplementary Table).

Using MCA to further analyse and visualise the relationships between the different EULAR/ACR domains, the first 2 dimensions of the lower-dimensional space collectively explained 28.2% of the data variability (Fig 2B). Dimension 1 (Dim1) accounted for 16.4%, dimension 2 (Dim2) for 11.8% of the variability (Supplementary Fig S1A).

In the MCA biplot of variables (Fig 2B and Supplementary Fig S1B), the positioning of the clinical features along the 2 dimensions revealed their relationships. The constitutional, musculoskeletal, and serosal domains clustered together, indicating that these 3 domains were positively correlated and contributed significantly to the second dimension. These domains separated from domains including renal domain, complement levels, and SLE-specific antibodies, which clustered together along the first dimension (Fig 2B and Supplementary Fig S1B). The proximity of 3 domains, antiphospholipid antibodies, mucocutaneous, and neuropsychiatric, to the origin of the plot suggested that these manifestations are of lesser discriminative value (Fig 2B).

Cos2 values revealing the degree of association between the domains and the first 2 dimensions of the MCA are shown in Supplementary Figure S1B. For most domains, the presence (indicated with a '1' designation, eg, 'Renal_1') demonstrated a higher quality of representation on the MCA dimensions than absence ('0' designation). This suggests that the presence of these clinical features shapes the multivariate pattern observed in SLE. The most prominent exceptions are the musculoskeletal and low complement domains, where absence ('0') had higher representation than presence. Of note, antiphospholipid antibodies and the mucocutaneous and neuropsychiatric domains have Cos2 values <0.2, indicating that neither their presence nor their absence had a relevant impact on the MCA model.

These data may indicate that patients tend to either present with a pattern of constitutional, musculoskeletal, and serosal domain manifestations, or with preferential renal domain involvement, low complements, and SLE-specific antibodies. However, the distribution of individual patients based on the first 2 dimensions was not reflective of a relevant separation of the cohort within those 2 dimensions (Fig 2C).

Consensus clustering based on the EULAR/ACR domains

Clustering became increasingly stable up to a plateau at $k=10$, suggesting that the increase in stability was marginal beyond this number of clusters (Fig 3A). The delta area curve also levelled off at $k=10$, indicating that $k>10$ did not yield significant improvements in stability (Fig 3B).

The heatmap in Figure 3C illustrates the clustering results, where the rows represent EULAR/ACR domains, and the columns represent the identified clusters. In this analysis, co-occurrence of clinical features does not refer to simultaneous manifestation at a single point in time but rather reflects the cumulative presence of these features throughout the entire disease duration of an individual patient. The bar chart above the heatmap shows the size of clusters.

Most patients fell into cluster 5, where patients exhibited musculoskeletal involvement as well as laboratory findings of SLE-specific antibodies and low complements. Cluster 3 showed a similar pattern, but with more common serositis and a complete absence of antiphospholipid antibodies. Musculoskeletal involvement was also prominent in cluster 2, differing from clusters 5 and 3 by lower prevalence of renal or serosal involvement or low complements.

Patients in cluster 6, the second largest cluster, exhibited SLE-specific antibodies and low complements similar to cluster 5, but in combination with renal involvement, often mucocutaneous, serosal, and haematological involvement, and reduced rates of arthritis. Patients with nephritis without mucocutaneous and serosal involvement were grouped in cluster 10.

Clusters 7 and 8 were prominent for mucocutaneous symptoms, combined with musculoskeletal involvement in cluster 7 and with low complements in cluster 8. The remaining small group of patients fell into cluster 9, with fever and serositis, but no renal, musculoskeletal, or hematologic involvement and with normal complements.

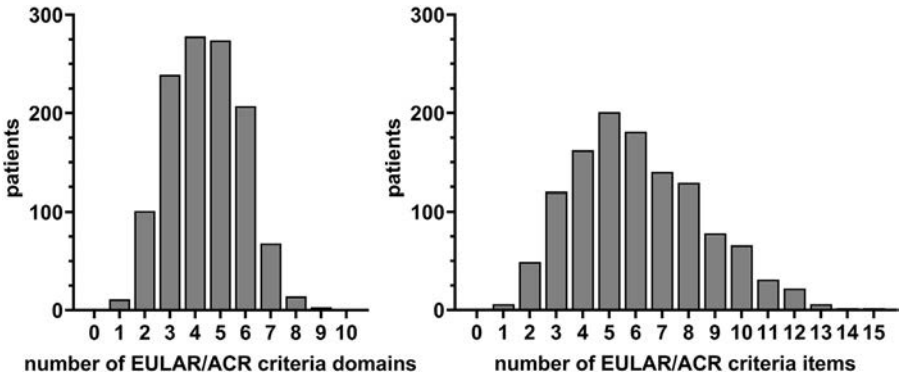

Figure 1. Distribution of EULAR/ACR criteria domains and items per patient. Depicted are absolute numbers of patients (of a total 1197) ever having fulfilled the respective number of individual EULAR/ACR domains (left) and EULAR/ACR classification criteria items (right). ACR, American College for Rheumatology; EULAR, European Alliance of Associations for Rheumatology.

Associations between items

While only the domains could be considered independent, a detailed analysis of the classification criteria items within each domain still seemed worthwhile, particularly to reconfirm associations within domains. The lifetime prevalence of the items ranging between 0.4% for delirium and 75.6% for anti-dsDNA antibodies has already been published [12]. Figure 4 shows the *r* values of the significant Benjamini-Hochberg-adjusted phi-coefficients of all 529 pairs of potential associations. A total of 51 pairwise correlations remained significant, with the *r* values of the 46 significant positive associations ranging from 0.07 to 0.54 and those of the 11 significant negative associations ranging from −0.08 to −0.16. Of note, the items C3 AND C4 low and C3 OR C4 would be mutually exclusive, by definition, but C3 significantly correlated with C4 ($r = 0.48$), as expected.

Only correlations within organ domains had *r* values of 0.3 or higher. Four significant negative *r* values lower than −0.10 were found between joint involvement and either thrombocytopenia or any of proteinuria, class II or V nephritis, or class III or IV nephritis. Outside organ domains, associations with *r* values ≥0.10 were found (1) between SLE-specific autoantibodies and low complements and proteinuria, (2) between antibodies to dsDNA and class III or IV nephritis, (3) between anti-Sm

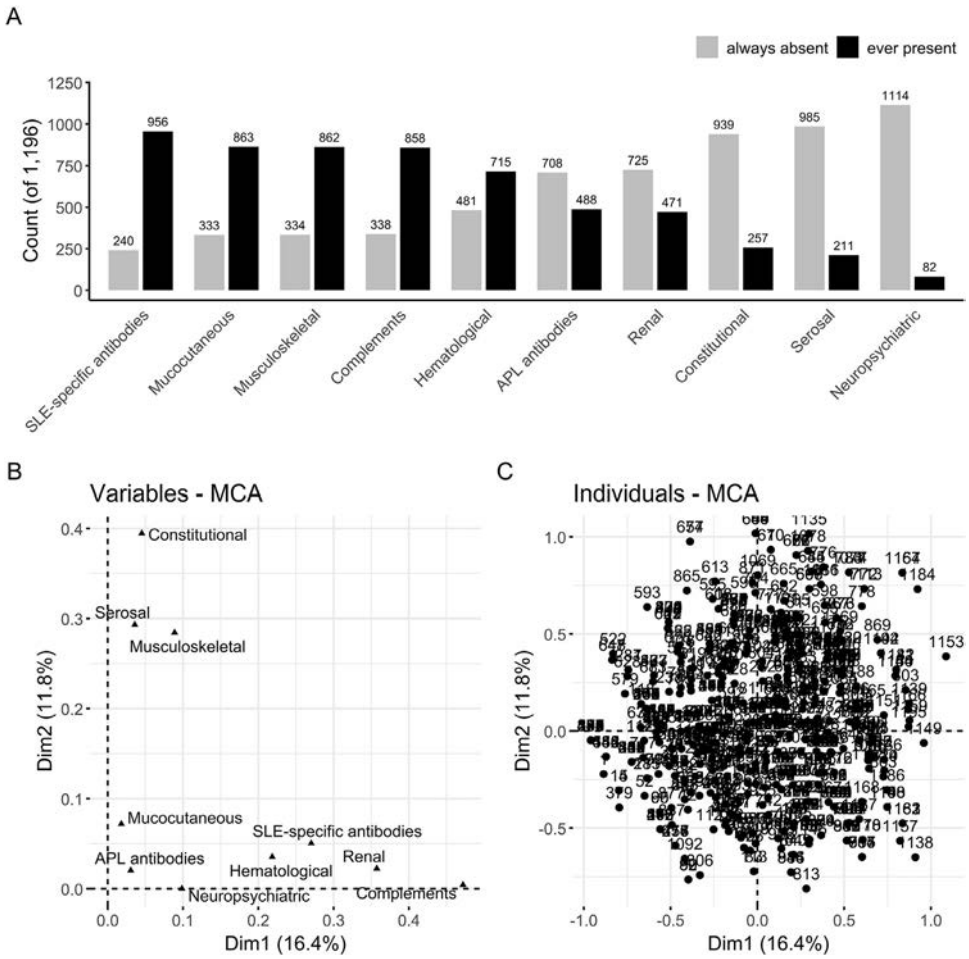

Figure 2. Distribution and relationships between the different EULAR/ACR domains. (A) Bar plots showing items ever present (black bars) or always absent (grey bars) within each of the 10 EULAR/ACR classification criteria domains in the combined (derivation plus validation) EULAR/ACR criteria cohort of 1197 patients with SLE. (B) MCA biplot for variables, showing the relationship and contribution of different clinical variables to the first 2 dimensions (Dim1 and Dim2). Dim1 and Dim2 explain 16.4% and 11.8% of the total variance, respectively. (C) MCA plot showing the distribution of individuals (patients) on the first 2 dimensions (Dim1 and Dim2). Each dot and number represent an individual. ACR, American College for Rheumatology; EULAR, European Alliance of Associations for Rheumatology; MCA, multiple correspondence analysis; SLE, systemic lupus erythematosus.

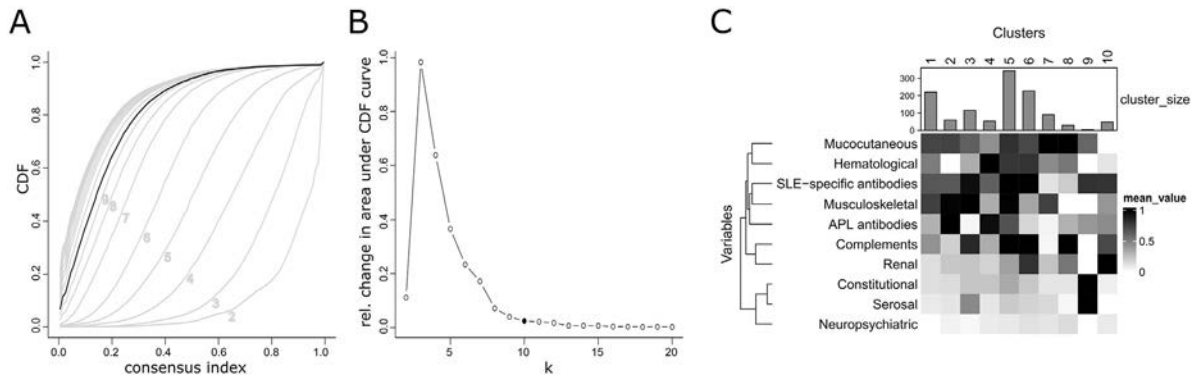

Figure 3. Consensus clustering of domains. (A) The cumulative distribution function (CDF) plot illustrates the consensus CDFs for a range of cluster numbers (*k*) from 2 to 20. The CDF represents the proportion of item pairs consistently clustered across multiple subsampling runs. A flatter CDF curve suggests better clustering stability for the corresponding k value, indicating more robust and consistent clustering. (B) The Delta area plot visualises the relative change in the area under the CDF curve for a range of cluster numbers (*k*) from 2 to 20. Each point on the plot corresponds to a specific *k* value, with the vertical axis representing the relative change in area from each k to the next. A peak in the plot suggests the most significant gain in cluster stability before diminishing returns on further increasing k. (C) The heatmap represents the presence (ever) of the 10 EULAR/ACR domains across the 10 identified clusters. Darker shades represent higher prevalence. The bar plot on top shows the size of each cluster, the dendrogram on the left groups the variables. ACR, American College for Rheumatology; EULAR, European Alliance of Associations for Rheumatology.

antibodies and nonscarring alopecia as well as leukopenia, (4) between antiphospholipid antibodies and thrombocytopenia, (5) between low complements and haematological cytopenias, alopecia, proteinuria, or class III or IV nephritis, (6) between haemolytic anaemia and both proteinuria and seizures and (7) between fever and effusion. A somewhat more conservative analysis with Bonferroni correction showed 31 significant associations with the same pattern (Supplementary Fig 2). Of note, the criteria items C3 and C4 low and C3 or C4 low behaved similarly, except for autoimmune haemolytic anaemia, which was significantly associated with C3 and C4 low ($r = 0.19$), but not C3 or C4 low ($r = 0.10$)

Pairwise comparisons of autoantibodies and low complements

To better understand the associations, we investigated the relationships of the significantly associated pairs in detail. Figure 5 presents the autoantibody associations, except for the likewise significant associations between antibodies to dsDNA or Sm and low C3 or C4. Most of these associations, including anti-dsDNA with proliferative nephritis and proteinuria as well as anti-phospholipid antibodies with thrombocytopenia, were expected. Not as clearly expected was the association between anti-Sm antibodies and nonscarring alopecia. Almost half of the 23.6% anti-Sm positive, but less than a third of the 76.4% anti-Sm negative patients had nonscarring hair loss. This still means that about two-thirds of the patients with SLE with nonscarring alopecia were anti-Sm negative.

In Figure 6, the significant associations between clinical items are depicted. These include the (weak) negative associations of joint involvement with thrombocytopenia, proteinuria, and both proliferative and class II or V lupus nephritis. The lower panel shows the associations of haemolytic anaemia with seizure and proteinuria, as well as the expected association of

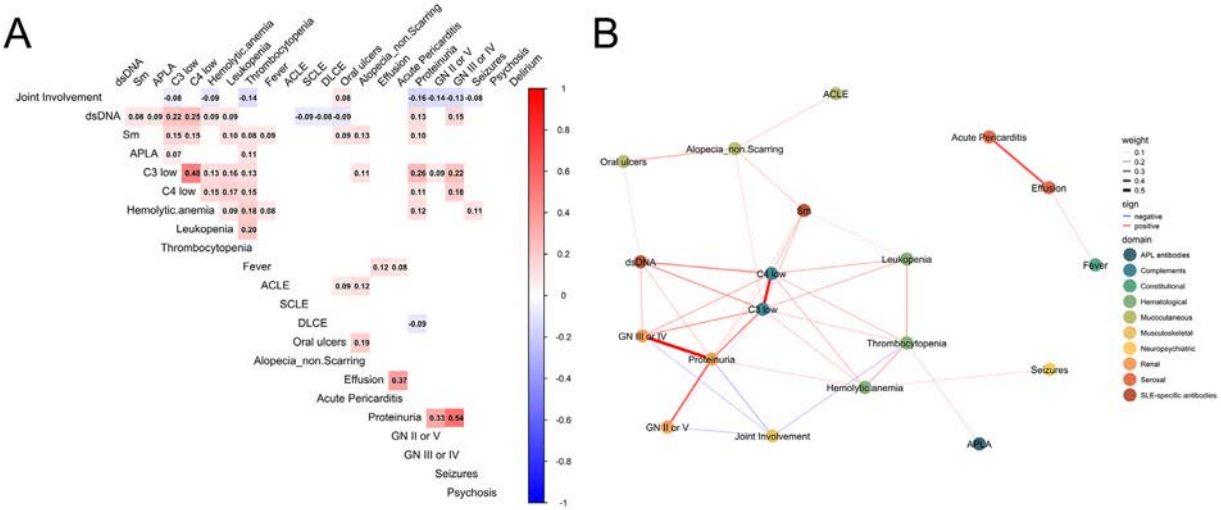

Figure 4. Correlation and network analysis of items of the domains. (A) Correlation matrix depicting significant phi-coefficients (Benjamini-Hochberg adjusted *P* value of Fisher's exact test < .05). Positive correlations are indicated in red, negative correlations in blue, and nonsignificant correlations were left blank to emphasise statistically meaningful associations. (B) Network plot of the phi-correlation analysis. Nodes of the items are colour-coded according to domains. Positive correlations are indicated by red edges, and negative correlations by blue edges. The weight of the line represents the phi-coefficient only significant correlations above an absolute weight threshold of 0.1 are plotted.

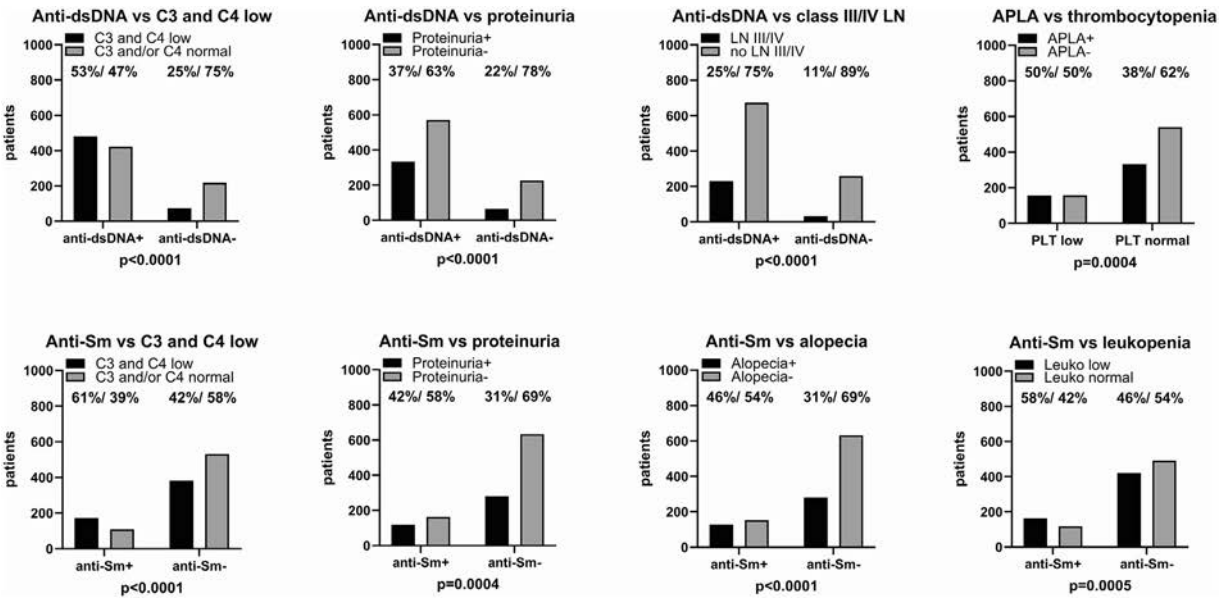

Figure 5. Autoantibody associations. For full representation of the data, absolute numbers of patients are shown for each column. Percentages within the subsets indicated on the *x*-axis are shown above the bars for easier comparison. *P* values derived from Fisher's exact tests are uncorrected and nominal only.

pleural or pericardial effusion and fever. Of note, none of the associations are even close to being perfect, and combinations of items are found throughout the spectrum.

DISCUSSION

In this study, we evaluated potential associations between items and clusters within a multinational cohort of close to 1200 patients with SLE with mostly long-standing disease.

Above confirming the criteria domain structure, these analyses have implications on how we perceive SLE, that is, whether we see it as one variable disease entity or as a syndrome of several disease phenotypes. In combination, they reflect the first comprehensive effort to fully address the question of potential fixed disease subsets in a well-defined, large SLE cohort.

The analysis of both the numbers of criteria domains and criteria items per patient showed that the per-patient numbers peaked at 4 domains and 5 criteria items, with few patients fulfilling less than 2 or more than 12 criteria items. The distributions of either items or domains resulted in rather typical Gaussian distribution curves. This part is similar to a project by Lupus Europe, the European SLE patient association, where the number of symptoms per patient also resulted in a conventional Gaussian curve [13]. We would interpret these findings as

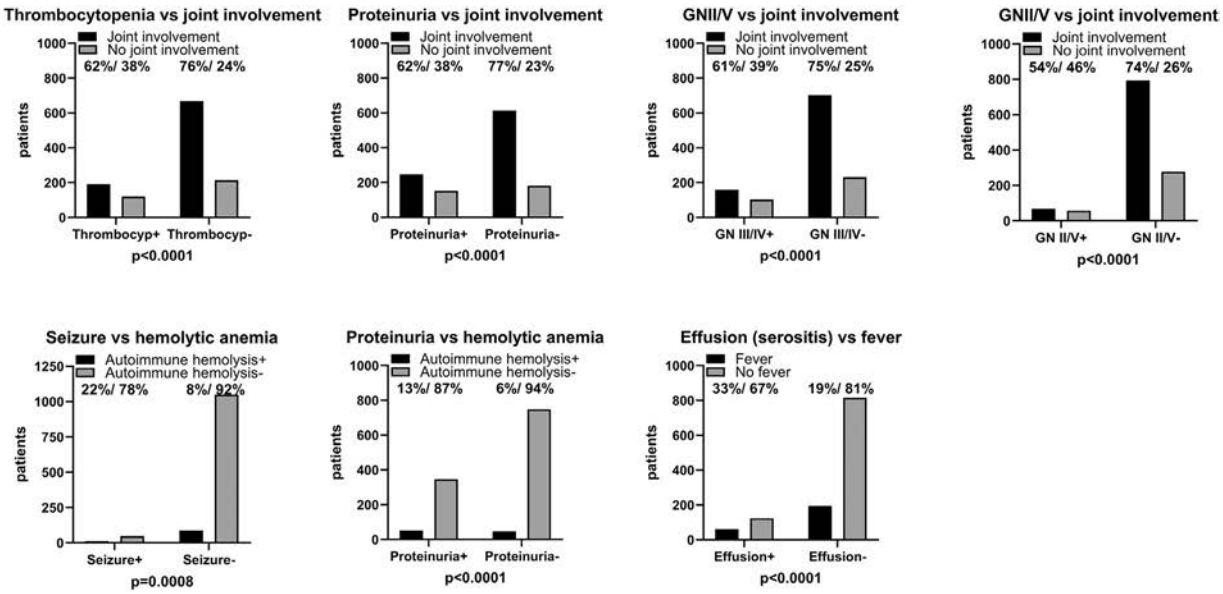

Figure 6. Negative and positive associations between organ manifestations. Negative associations are depicted in the upper, and positive associations in the lower row. For full representation of the data, absolute numbers of patients are shown for each column. Percentages within the subsets indicated on the *x*-axis (Thrombocyp thrombocytopenia) are shown above the bars for easier comparison. *P* values derived from Fisher's exact tests are uncorrected and nominal only. Note that the *y*-axis of the left lower panel (seizure vs haemolytic anaemia) has a different range (0-1250) than the other panels.

suggestive of stochastic processes being at work, that is, in line with a chance distribution, rather than fixed combinations of items.

Looking at the individual domains, it is apparent that most patients had involvement within the mucocutaneous and musculoskeletal domains, reflective of patient populations most often included in randomized controlled SLE trials [14–21]. Likewise, most patients had SLE-specific antibodies, that is, antibodies to dsDNA, or less commonly to Sm. On the other end of the spectrum, only a small group of patients had any of the 3 items within the neuropsychiatric domain (seizures, psychosis, or delirium). Fever and serositis were also relatively uncommon. In the mid-range, around 40%, involvement in the haematological and renal domains, as well as antiphospholipid antibodies, was found.

The MCA analysis of the domains suggested some separation of 2 groups, namely serositis, fever, and joint involvement on the one hand, on dimension 1, and renal domain with low complements and SLE-specific antibodies on the other, on dimension 2, with the remainder of domains close to the origin of the plot. The analysis of all individuals in the first 2 dimensions, however, did not indicate meaningful clustering.

Both the CDF curves and the differences in area under the curve (delta area plot) suggested saturation at $k = 10$ clusters. The resulting cluster structure resulted in 3 larger clusters, cluster 5, and slightly smaller clusters 1 and 6, as well as 7 smaller ones. Both cluster 5 and 6 scored high in the SLE-specific antibody and low complement domains, but patients in these clusters also commonly had involvement in the mucocutaneous and haematological domains. Looking at the overall distribution, however, none of these features were specific. SLE-specific antibodies were also prominent in clusters 3, 9, and 10, low complements also in clusters 3 and 8, and mucocutaneous and haematological involvement was even more prominent in clusters 7 and 8, and 4, respectively.

While the interpretation is different, in that we do not see meaningful subsets, the data do not relevantly differ from those of cluster analyses other groups previously performed in SLE [22–26], with similar methodology, but different kinds of input, from the ACR criteria via a large set of 29 items mostly derived from the EULAR/ACR and Systemic Lupus International Collaborating Clinics (SLICC) criteria to laboratory values, autoantibodies and cytokines, and anti-nuclear antibody (ANA) patterns and subsets. Three of these analyses found 3 clusters each, 2 had a fourth cluster [23,25]. However, despite the similarity in cluster count, the defined clusters were not consistent across the studies. Rather, all these studies showed associations between autoantibodies and manifestations, with some overlap with disease severity.

Given that the previous analysis within the EULAR/ACR criteria project had shown correlations within domains, our approach had an advantage by analysing domains rather than single items, which should reduce the risk of increasing the weight of domains with co-occurring items. Still, the overall outcome of consensus clustering failed to convincingly separate SLE in defined subsets, thus being more consistent with the idea that SLE is 1 disease entity comprising various inflammatory organ manifestations rather than several.

For the examination of associations between items, both for completing the analysis on possible SLE subtypes and to potentially detect associations relevant for disease pathology, we next analysed the whole set of 23 items against each other. Based on the Benjamini-Hochberg procedure, this approach at least led to 57 associations that were statistically significant, 37 of which had an r value of at least 10 or −10. Eleven of these associations were between items of the same domain, as were all associations with an r value of higher than 0.3, as expected [9]. Associations with an r value of at least 0.2 were also found between 4 pairs of items in different domains, namely between low complements and anti-dsDNA antibodies, proliferative lupus nephritis, or proteinuria. These associations were likewise expected, given the well-established link between anti-dsDNA immune complexes, complement activation, and proliferative lupus nephritis [27].

With lower r values of 0.13 to 0.17, low complements are also associated with leukopenia, thrombocytopenia, and haemolytic anaemia. Lupus cytopenias are probably due to direct autoantibody effects, not to immune complexes [28,29]. Nevertheless, SLE activity is usually not limited to 1 organ system, and some link via general SLE activity would indeed be expected. Autoimmune haemolytic anaemia with its low frequency of only 4.4% also showed weak associations with proteinuria and seizure, likely in the wake of general SLE activity.

In contrast, the association between antiphospholipid antibodies and thrombocytopenia is probably causal—mild thrombocytopenia is now included in the new ACR/EULAR classification criteria for antiphospholipid syndrome [30]. Associations found between pleural or pericardial effusion and fever as well as between nonscarring alopecia and anti-Sm antibodies are also in line with published evidence: An association of acute, febrile SLE manifestations with serositis is well established [31,32] and in line with clinical experience. Associations of anti-Sm with both nonscarring [33] and scarring alopecia [34] were previously reported from large Chinese cohorts. Inverse relations with an r value of −0.1 or lower were found for joint involvement only, namely with lupus nephritis, again in line with published results [35], as well as with thrombocytopenia ($r = -0.14$). While some of these associations are interesting confirmations, they are rather weak, which is also apparent from the respective column blots.

Taken together, the various data sets offer evidence for SLE being 1 disease entity instead of a syndrome of several diseases with typical sets of SLE manifestations. Both the number of items and the number of domains ever active followed distributions that were suggestive of chance events. Our attempts to subgroup the SLE population by domains gave no consistent patterns that would be meaningful. Rather, positivity for items in each of the 10 domains differed greatly, but associations between domains were found across the range. Moreover, meaningful associations between items were found within domains only, confirming the data within the project leading to the criteria [9]. Additional weak associations were found between immune parameters and clinical findings well known to be mechanistically linked. All other, additional associations are weak. We thus interpret the body of data as indicative of a mostly random distribution of manifestations within the SLE spectrum.

It is important to stress again that these data refer to manifestations that the individual patients have ever had. By the criteria definition, criteria need not occur simultaneously, and occurrence on at least 1 occasion is sufficient [4]. The intraindividual pattern commonly remains stable and so does the prevalence of manifestations in this cohort over time. However, the data capture the overall disease manifestations of a patient, and not the direct interaction in 1 episode of SLE activity. This fact may have implications for the interpretation of the data, and in this sense is a limitation of the current study. An additional weakness is the absence of a broad array of possible additional symptoms and laboratory results and demographic information, which were not collected for this cohort. Within the criteria framework, however, strengths of the study include the data-

driven approach, the completeness of the data set, and the robust amount of data.

In conclusion, this study of associations between SLE criteria items within a well-characterised, multinational SLE cohort supports the classification criteria domain structure. Moreover, findings are compatible with the concept of SLE as a single disease with a propensity to generate multiple autoantibodies and distinct systemic organ manifestations, the exact nature of which may highly depend on random events. This has implications for the ongoing discussion on whether SLE is 1 disease entity or a syndrome of several autoantibody-mediated disorders.

Competing interests

All authors declare they have no competing interests.

CRediT authorship contribution statement

Martin Aringer: Writing – review & editing, Writing – original draft, Visualization, Validation, Supervision, Formal analysis, Data curation, Conceptualization. **Franziska Szelinski:** Writing – review & editing, Writing – original draft, Visualization, Methodology, Formal analysis. **Thomas Dörner:** Writing – review & editing, Writing – original draft, Validation, Supervision, Conceptualization. **Karen H. Costenbader:** Writing – review & editing, Supervision, Methodology. **Sindhu R. Johnson:** Writing – review & editing, Supervision, Methodology, Conceptualization.

Acknowledgements

The authors wish to again thank all other investigators of the EULAR/ACR classification criteria project, on which this study built: Branimir Anic MD, Division of Clinical Immunology and Rheumatology, University of Zagreb School of Medicine and University Hospital Centre Zagreb, Zagreb, Croatia; Florence Assan MD, Université Paris-Saclay, INSERM, CEA, Centre de recherche en Immunologie des infections virales et des maladies auto-immunes, AP-HP. Université Paris Saclay, Hôpital Bicêtre, Rheumatology, 94270, Le Kremlin Bicêtre, France; George Bertsias MD, Rheumatology, Clinical Immunology and Allergy, University of Crete Medical School, Heraklion, Greece; and Institute of Molecular Biology-Biotechnology, Foundation for Research and Technology - Hellas (FORTH), Heraklion, Greece; Dimitrios Boumpas MD, Medical School, National and Kapodestrian University of Athens, and Biomedical Research Foundation of the Athens Academy, Athens, Greece; Medical School, University of Cyprus, Nicosia, Cyprus; Ricard Cervera MD PhD FRCP, Department of Autoimmune Diseases, Hospital Clínic, University of Barcelona, Barcelona, Catalonia, Spain; Tak Mao Chan MD, University of Hong Kong, Hong Kong; Ann E. Clarke MD MSc, Division of Rheumatology, Cumming School of Medicine, University of Calgary, Calgary, Alberta, Canada; Nathalie Costedoat-Chalumeau, MD PhD AP-HP, Cochin Hospital, Internal Medicine Department, Centre de référence maladies auto-immunes et systémiques rares d'île de France, Paris, France, Université Paris Descartes-Sorbonne Paris Cité, Paris, France, INSERM U 1153, Center for Epidemiology and Statistics Sorbonne Paris Cité (CRESS), Paris, France; Mary K. Crow MD, Hospital for Special Surgery, New York, NY, USA; László Czirják MD, University of Pécs, Medical School, Pécs, Hungary; Betty Diamond MD, Feinstein Institute, Manhasset, NY, United States; Andrea Doria MD, Rheumatology Unit, Department of Medicine (DIMED), University of Padova, Padova, Italy; Marvin J Fritzler PhD MD, Faculty of Medicine, Cumming School of Medicine, University of Calgary, Calgary, AB, Canada; Dafna D. Gladman, MD FRCPC, Division of Rheumatology, Department of Medicine, Toronto Western Hospital, University of Toronto, Toronto, Ontario, Canada; Winfried B. Graninger MD, Medical University of Graz, Graz, Austria; Bevra H Hahn MD, University of California at Los Angeles, Los Angeles, CA, USA; Bernadett Halda-Kiss MD, University of Pécs, Medical School, Pécs, Hungary; Sarfaraz Hasni MD, NIAMS, NIH, Bethesda, MD; Falk Hiepe MD, Charité – Universitätsmedizin Berlin, Corporate member of Freie Universität Berlin, Humboldt-Universität zu Berlin, and Berlin Institute of Health, Department of Rheumatology and Clinical Immunology, Berlin, Germany; Bimba F. Hoyer MD, Department of Rheumatology and Clinical Immunology, University Hospital of Schleswig-Holstein at Kiel, Kiel, Germany; Peter Izmirly MD, New York University School of Medicine, New York, New York, USA; Søren Jacobsen MD DMSc, Copenhagen Lupus and Vasculitis Clinic, Rigshospitalet, Copenhagen University Hospital, Copenhagen, Denmark; David Jayne MD FRCP FRCPE FMedSci, Department of Medicine, University of Cambridge, United Kingdom; Michelle Jung, University of Calgary, Calgary, Alberta, Canada; Diane L. Kamen MD MSCR, Medical University of South Carolina, Charleston, SC, USA; Dinesh Khanna MD MS, University of Michigan, Ann Arbor, MI, USA; Gábor Kumánovics MD, University of Pécs Medical School, Pécs, Hungary; Kirsten Lerstrøm, Lupus Europe, co-opted trustee for research, Essex, UK; Nicolai Leuchten MD, University Medical Center and Faculty of Medicine Carl Gustav Carus, TU Dresden, Dresden, Germany; Xavier Mariette MD PhD, Université Paris-Saclay, INSERM, CEA, Centre de recherche en Immunologie des infections virales et des maladies auto-immunes, AP-HP, Université Paris Saclay, Hôpital Bicêtre, Rheumatology, 94270, Le Kremlin Bicêtre, France; Elena Massarotti MD, Brigham and Women's Hospital, Boston MA; Harvard Medical School, Boston, USA; W. Joseph McCune MD, University of Michigan, Ann Arbor, MI, USA; Pier Luigi Meroni MD, Clinical Immunology and Rheumatology Unit, IRCCS Istituto Auxologico Italiano, Milan, Italy; Marta Mosca MD PhD, University of Pisa, Pisa, Italy; Ray P. Naden MB ChB FRACP, Department of Medicine, McMaster University, Hamilton, Ontario, Canada; Ivan Padjen MD, Division of Clinical Immunology and Rheumatology, University of Zagreb School of Medicine and University Hospital Centre Zagreb, Zagreb, Croatia; José M. Pego-Reigosa MD PhD, Department of Rheumatology, University Hospital of Vigo, IRIDIS Group, Instituto de Investigación Sanitaria Galicia Sur (IISGS), Vigo, Spain; Guillermo Ruiz-Irastorza MD PhD, Autoimmune Diseases Research Unit, Department of Internal Medicine, Biocruces Bizkaia Health Research Institute, Hospital Universitario Cruces, UPV/EHU, Bizkaia, The Basque Country, Spain; Jorge Sanchez-Guerrero MD MSc, Division of Rheumatology, Department of Medicine Mount Sinai Hospital/University Health Network, University of Toronto, Toronto, Ontario, Canada; and Instituto Nacional de Ciencias Médicas y Nutrición Salvador Zubirán, Mexico City, Mexico; Gabriela Schmajuk MD MS, University of California at San Francisco and the VA Medical Center, San Francisco, USA; Raphaèle Seror MD, PhD, Université Paris-Saclay, INSERM, CEA, Centre de recherche en Immunologie des infections virales et des maladies auto-immunes, AP-HP. Université Paris Saclay, Hôpital Bicêtre, Rheumatology, 94270, Le Kremlin Bicêtre, France; Matthias Schneider MD, Policlinic and Hiller Research Unit for Rheumatology, Medical Faculty, Heinrich-Heine-University, Düsseldorf, Germany; Josef S. Smolen MD, Medical University of Vienna, Austria; Georg Stummvoll MD,

Medical University of Vienna, Vienna, Austria; Yoshiya Tanaka MD PhD, University of Occupational & Environmental Health, Kitakyushu, Japan; Chiara Tani MD, Rheumatology Unit, Azienda Ospedaliero Universitaria Pisana, University of Pisa, Pisa, Italy; Sara K. Tedeschi MD MPH, Brigham and Women's Hospital, Harvard Medical School, Boston, MA, USA; Maria G. Tektonidou MD PhD, Medical School, National and Kapodistrian University of Athens, Athens, Greece; Zahi Touma, MD PhD, Division of Rheumatology, Department of Medicine, Toronto Western Hospital, Institute of Health Policy, Management and Evaluation, University of Toronto, Toronto, Ontario, Canada; Murray B. Urowitz MD, Division of Rheumatology, Department of Medicine, Toronto Western Hospital, University of Toronto, Toronto, Ontario, Canada; Carlos Vasconcelos MD PhD, Centro Hospitalar do Porto, ICBAS, UMIB, University of Porto, Porto, Portugal; Edward M Vital MRCP PhD, Leeds Institute of Rheumatic and Musculoskeletal Medicine, University of Leeds; NIHR Leeds Biomedical Research Centre, Leeds Teaching Hospitals NHS Trust, Leeds, United Kingdom; Daniel J. Wallace MD, Cedars-Sinai, Los Angeles, CA, USA; David Wofsy MD, Russell/Engleman Rheumatology Research Center, University of California at San Francisco, San Francisco, USA; and Sule Yavuz MD, Istanbul Bilim University, Istanbul Florence Nightingale Hospital, Istanbul, Turkey.

Funding

There was no direct funding for this study, but the classification criteria project was supported by both EULAR and the ACR.

Patient consent for publication

For the EULAR/ACR criteria project, patient consent was obtained as by local regulations.

Ethics approval

For the EULAR/ACR criteria project, ethics committee approval was obtained as by local regulations.

Provenance and peer review

Not commissioned; externally peer reviewed.

Supplementary materials

Supplementary material associated with this article can be found in the online version at doi:10.1016/j.ard.2025.07.024.

Orcid

Martin Aringer: http://orcid.org/0000-0003-4471-8375
Thomas Dörner: http://orcid.org/0000-0002-6478-7725
Karen H. Costenbader: http://orcid.org/0000-0002-8972-9388

REFERENCES

[1] Crow MK. Pathogenesis of systemic lupus erythematosus: risks, mechanisms and therapeutic targets. Ann Rheum Dis 2023;82(8):999–1014.
[2] Caielli S, Wan Z, Pascual V. Systemic lupus erythematosus pathogenesis: interferon and beyond. Annu Rev Immunol 2023;41:533–60.
[3] Gómez-Bañuelos E, Fava A, Andrade F. An update on autoantibodies in systemic lupus erythematosus. Curr Opin Rheumatol 2023;35(2):61–7.
[4] Aringer M, Costenbader K, Daikh D, Brinks R, Mosca M, Ramsey-Goldman R, et al. 2019 European League Against Rheumatism/American College of Rheumatology classification criteria for systemic lupus erythematosus. Ann Rheum Dis 2019;78(9):1151–9.
[5] Aringer M, Costenbader K, Daikh D, Brinks R, Mosca M, Ramsey-Goldman R, et al. 2019 European League Against Rheumatism/American College of Rheumatology classification criteria for systemic lupus erythematosus. Arthritis Rheumatol 2019;71(9):1400–12.
[6] Johnson SR, Khanna D, Daikh D, Cervera R, Costedoat-Chalumeau N, Gladman DD, et al. Use of consensus methodology to determine candidate items for systemic lupus erythematosus classification criteria. J Rheumatol 2019;46(7):721–6.
[7] Mosca M, Costenbader KH, Johnson SR, Lorenzoni V, Sebastiani GD, Hoyer BF, et al. Brief report: how do patients with newly diagnosed systemic lupus erythematosus present? A multicenter cohort of early systemic lupus erythematosus to inform the development of new classification criteria. Arthritis Rheumatol 2019;71(1):91–8.
[8] Cervera R, Khamashta MA, Font J, Sebastiani GD, Gil A, Lavilla P, et al. Morbidity and mortality in systemic lupus erythematosus during a 5-year period. A multicenter prospective study of 1,000 patients. European Working Party on Systemic Lupus Erythematosus. Medicine (Baltimore). 1999;78(3):167–75.
[9] Touma Z, Cervera R, Brinks R, Lorenzoni V, Tani C, Hoyer BF, et al. Associations between classification criteria items in systemic lupus erythematosus. Arthritis Care Res 2020;72(12):1820–6.
[10] Tedeschi SK, Johnson SR, Boumpas D, Daikh D, Dörner T, Jayne D, et al. Developing and refining new candidate criteria for systemic lupus erythematosus classification: an international collaboration. Arthritis Care Res(Hoboken) 2018;70(4):571–81.
[11] Johnson SR, Brinks R, Costenbader KH, Daikh D, Mosca M, Ramsey-Goldman R, et al. Performance of the 2019 EULAR/ACR classification criteria for systemic lupus erythematosus in early disease, across sexes and ethnicities. Ann Rheum Dis 2020;79(10):1333–9.
[12] Aringer M, Brinks R, Dörner T, Daikh D, Mosca M, Ramsey-Goldman R, et al. European League Against Rheumatism (EULAR)/American College of Rheumatology (ACR) SLE classification criteria item performance. Ann Rheum Dis 2021;80(6):775–81.
[13] Aringer M, Mosca M. SLE criteria are by necessity still based on clinical (and immunological) criteria items. Expert Rev Clin Immunol 2024;20(3):305–11.
[14] Navarra SV, Guzmán RM, Gallacher AE, Hall S, Levy RA, Jimenez RE, et al. Efficacy and safety of belimumab in patients with active systemic lupus erythematosus: a randomised, placebo-controlled, phase 3 trial. Lancet 2011;377(9767):721–31.
[15] Furie R, Petri M, Zamani O, Cervera R, Wallace DJ, Tegzová D, et al. A phase III, randomized, placebo-controlled study of belimumab, a monoclonal antibody that inhibits B lymphocyte stimulator, in patients with systemic lupus erythematosus. Arthritis Rheum 2011;63(12):3918–30.
[16] Stohl W, Schwarting A, Okada M, Scheinberg M, Doria A, Hammer AE, et al. Efficacy and safety of subcutaneous belimumab in systemic lupus erythematosus: a fifty-two-week randomized, double-blind, placebo-controlled study. Arthritis Rheumatol 2017;69(5):1016–27.
[17] Ordi-Ros J, Saez-Comet L, Perez-Conesa M, Vidal X, Mitjavila F, Castro SA, et al. Enteric-coated mycophenolate sodium versus azathioprine in patients with active systemic lupus erythematosus: a randomised clinical trial. Ann Rheum Dis 2017;76(9):1575–82.
[18] Furie RA, Morand EF, Bruce IN, Manzi S, Kalunian KC, Vital EM, et al. Type I interferon inhibitor anifrolumab in active systemic lupus erythematosus (TULIP-1): a randomised, controlled, phase 3 trial. Lancet Rheumatol 2019;1(4):e208–19.
[19] Morand EF, Furie R, Tanaka Y, Bruce IN, Askanase AD, Richez C, et al. Trial of anifrolumab in active systemic lupus erythematosus. N Engl J Med 2020;382(3):211–21.
[20] Morand EF, Vital EM, Petri M, van Vollenhoven R, Wallace DJ, Mosca M, et al. Baricitinib for systemic lupus erythematosus: a double-blind, randomised, placebo-controlled, phase 3 trial (SLE-BRAVE-I). Lancet 2023;401(10381):1001–10.
[21] Petri M, Bruce IN, Dörner T, Tanaka Y, Morand EF, Kalunian KC, et al. Baricitinib for systemic lupus erythematosus: a double-blind, randomised, placebo-controlled, phase 3 trial (SLE-BRAVE-II). Lancet 2023;401(10381):1011–9.
[22] Mariette F, Le Guern V, Nguyen Y, Yelnik C, Morel N, Hachulla E, et al. Cluster analysis of clinical manifestations assigns systemic lupus erythematosus-phenotype subgroups: a multicentre study on 440 patients. Joint Bone Spine 2024;91(6):105760.
[23] Choi MY, Chen I, Clarke AE, Fritzler MJ, Buhler KA, Urowitz M, et al. Machine learning identifies clusters of longitudinal autoantibody profiles predictive of systemic lupus erythematosus disease outcomes. Ann Rheum Dis 2023;82(7):927–36.

[24] Jung JY, Lee HY, Lee E, Kim HA, Yoon D, Suh CH. Three clinical clusters identified through hierarchical cluster analysis using initial laboratory findings in Korean patients with systemic lupus erythematosus. J Clin Med 2022;11(9):2406.
[25] Diaz-Gallo LM, Oke V, Lundström E, Elvin K, Ling Wu Y, Eketjäll S, et al. Four systemic lupus erythematosus subgroups, defined by autoantibodies status, differ regarding HLA-DRB1 genotype associations and immunological and clinical manifestations. ACR Open Rheumatol 2022;4(1):27–39.
[26] To CH, Mok CC, Tang SS, Ying SK, Wong RW, Lau CS. Prognostically distinct clinical patterns of systemic lupus erythematosus identified by cluster analysis. Lupus 2009;18(14):1267–75.
[27] Goilav B, Putterman C. The role of anti-DNA antibodies in the development of lupus nephritis: a complementary, or alternative, viewpoint? Semin Nephrol 2015;35(5):439–43.
[28] Neely J, von Scheven E. Autoimmune haemolytic anaemia and autoimmune thrombocytopenia in childhood-onset systemic lupus erythematosus: updates on pathogenesis and treatment. Curr Opin Rheumatol 2018;30(5):498–505.
[29] Fayyaz A, Igoe A, Kurien BT, Danda D, James JA, Stafford HA, et al. Haematological manifestations of lupus. Lupus Sci Med 2015;2(1):e000078.
[30] Barbhaiya M, Zuily S, Naden R, Hendry A, Manneville F, Amigo MC, et al. 2023 ACR/EULAR antiphospholipid syndrome classification criteria. Ann Rheum Dis 2023;28:1258–70.
[31] Olivieri G, Ceccarelli F, Perricone C, Ciccacci C, Pirone C, Natalucci F, et al. Fever in systemic lupus erythematosus: associated clinical features and genetic factors. Clin Exp Rheumatol 2022;40(11):2141–6.
[32] Liang Y, Leng RX, Pan HF, Ye DQ. The prevalence and risk factors for serositis in patients with systemic lupus erythematosus: a cross-sectional study. Rheumatol Int 2017;37(2):305–11.
[33] Hu C, Li M, Liu J, Qian J, Xu D, Zhang S, et al. Anti-SmD1 antibodies are associated with renal disorder, seizures, and pulmonary arterial hypertension in Chinese patients with active SLE. Sci Rep 2017;7(1):7617.
[34] Xiang Y, Li M, Luo H, Wang Y, Duan X, Zhao C, et al. Chinese SLE Treatment and Research Group Registry (CSTAR) XIII: Prevalence and risk factors for chronic scarring alopecia in patients with systemic lupus erythematosus. Arthritis Res Ther 2021;23(1):20.
[35] Hanly JG, O'Keeffe AG, Su L, Urowitz MB, Romero-Diaz J, Gordon C, et al. The frequency and outcome of lupus nephritis: results from an international inception cohort study. Rheumatology (Oxford) 2016;55(2):252–62.

Ann Rheum Dis 84 (2025) 1811–1821

Contents lists available at ScienceDirect

Annals of the Rheumatic Diseases

journal homepage: https://www.sciencedirect.com/journal/annals-of-the-rheumatic-diseases

Systemic lupus erythematosus

Genetically modified CD19-targeting IL-15 secreting NK cells for the treatment of systemic lupus erythematosus

Yakai Fu[1,2,#], Zupeng Xu[3,#], Chunmei Wu[1,#], Fangjie Gao[3], Pengyu Huang[3], Fuwei Jiang[3], Chuxuan Hu[4], Nick Patsoukis[4], Yiyang Wang[1,5], Zejin Cui[5], Limin Wen[3], Peiying Li[6], Chong Wang[5,##], Shuang Ye[1,##], Zhuoxiao Cao[3,##], Qiong Fu[1,5,*]

[1] *Department of Rheumatology, Renji Hospital, Shanghai Jiaotong University School of Medicine, Shanghai, China*
[2] *UMR_S INSERM 1109, Immunorhumatologie Moléculaire, Strasbourg, France*
[3] *R&D Department, Shanghai Simnova Biotechnology Co., Ltd., Shanghai, China*
[4] *R&D Department, Simcere Zaiming, Inc., Boston, MA, USA*
[5] *Shanghai Immune Therapy Institute, Renji Hospital, Shanghai Jiaotong University School of Medicine, Shanghai, China*
[6] *Clinical Research Unit, Renji Hospital, Shanghai Jiaotong University School of Medicine, Shanghai, China*

ARTICLE INFO

Article history:
Received 17 May 2025
Received in revised form 9 July 2025
Accepted 31 July 2025

ABSTRACT

Objectives: Given the efficacy of B-cell depletion therapy in systemic lupus erythematosus (SLE) treatment and the capacity of engineered natural killer (NK) cells in B-cell elimination, we explored the potential of genetically modified NK cells to target CD19 for the treatment of SLE.
Methods: Peripheral blood-derived NK cells were engineered with CAR.CD19/interleukin (IL)-15 (XB-19.15) or CAR.CD19 alone. *In vitro* assays tested cytotoxicity, proliferation (Ki-67), and cytokine release (IL-15/interferon-gamma [IFN-γ]] against CD19+ cells (Raji, Nalm6, SLE B-cell). *In vivo* models included Nalm6-luc xenografts, humanised CD34+ mice, and SLE peripheral blood mononuclear cells xenografts to assess efficacy, persistence, and safety. A phase 1 trial enrolled 3 patients with refractory SLE receiving XB-19.15 as a proof-of-concept study.
Results: XB-19.15 showed superior cytotoxicity, sustained IL-15 secretion, and enhanced proliferation *in vitro*. In the mouse model, XB-19.15 showed significant dose-dependent tumour regression of Nalm-6 and B-cell depletion of humanised mice with long-term persistence in various lymphoid organs. The total levels of hIgG and anti-dsDNA antibodies were decreased in XB-19.15-treated groups with deep clearance of B-cell and plasma cells of bone marrow and spleen in the SLE xenograft model, indicating potential attenuation of SLE. Three patients received XB-19.15 achieved improvement in disease activity and reset of B-cell repertoires without severe adverse events.
Conclusions: XB-19.15 enables potent, durable B-cell depletion and immune resetting in SLE with off-the-shelf utility and favourable safety. Preclinical and early clinical data support further trials to optimise dosing and confirm long-term efficacy.

*Correspondence to Qiong Fu, Department of Rheumatology, Renji Hospital, School of Medicine, Shanghai Jiaotong University, 2000 Jiang Yue Road, Shanghai 201112, China.
E-mail address: fuqiong5@163.com (Q. Fu).
Handling editor Josef S. Smolen.
# These authors have contributed equally to this work.
These authors share senior authorship.

https://doi.org/10.1016/j.ard.2025.07.028

What is already known on this topic?

- Systemic lupus erythematosus (SLE) is a chronic autoimmune disease characterized by autoantibodies and autoreactive B-cells, while B-cell elimination therapy, such as monoclonal antibodies, offers benefits. Autologous anti-CD19 chimeric antigen receptor (CAR)-T cell therapy has shown promise in deep clearance of autoreactive B-cell and inducing remission in refractory SLE but faces challenges including high cost, manufacturing delays, poor T-cell quality in patients with SLE, and potential toxicities. Universal allogeneic CAR-natural killer (NK) cells would be a more scalable alternative to overcome these obstacles.

WHAT THIS STUDY ADDS

- This study demonstrates, for the first time, the clinical feasibility and safety of peripheral blood mononuclear cells-derived anti-CD19 CAR-NK cells (XB-19.15) in treating refractory SLE. By incorporating IL-15 into the CAR construct, the engineered NK cells showed enhanced expansion, persistence, and cytotoxicity both *in vitro* and *in vivo*. In a pilot clinical trial, XB-19.15 achieved rapid and sustained B-cell depletion, symptom improvement, and preserved immune homeostasis without severe toxicities.

HOW THIS STUDY MIGHT AFFECT RESEARCH, PRACTICE OR POLICY

- This study could shift the therapeutic landscape for autoimmune diseases by supporting CAR-NK cells as a safer, more accessible alternative to CAR-T therapy. It may prompt further clinical trials to validate efficacy, inform the development of standardised, off-the-shelf cell therapy products, and influence treatment guidelines to incorporate CAR-NK approaches in refractory SLE.

INTRODUCTION

Systemic lupus erythematosus (SLE) is a severe, life-threatening autoimmune disease that affects approximately 0.1% of the general population [1,2]. It is characterised by widespread immune activation, pathogenic autoantibody production, immune complex-mediated inflammation, and subsequent multiorgan dysfunction. Despite significant advances in SLE management, achieving a complete drug-free remission remains a formidable challenge. Autoreactive B-cells play a pivotal role in SLE pathogenesis by producing autoantibodies and presenting self-antigens to autoreactive T-cells, making B-cell-targeted therapy a promising treatment strategy [3]. Monoclonal antibodies directed against B-cell activating factor or B lymphocyte stimulator and CD20 have demonstrated partial efficacy in some patients with SLE [4,5]. However, the limited depletion of certain B-cell subsets and poor tissue penetration can reduce the effectiveness of this approach.

Cell therapy, particularly CD19 chimeric antigen receptor (CAR) T-cells, has been a milestone in treating B-cell lymphoid malignancies [3,6]. This approach has also been extended to autoimmune diseases due to its potential for deep B-cell depletion and a profound reset of the B-cell repertoire. Recently, autologous anti-CD19 CAR-T cells have demonstrated sustained remission in patients with SLE and other autoimmune diseases involving autoreactive B-cells, including idiopathic inflammatory myositis and systemic sclerosis [7–9]. Although further controlled clinical trials with larger patient cohorts are necessary to confirm their efficacy and safety, preliminary clinical data suggest new therapeutic possibilities for controlling SLE disease activity through autologous anti-CD19 CAR-T cells [10,11]. However, several obstacles limit the widespread adoption of autologous anti-CD19 CAR T cells in SLE treatment. First, the high cost poses a significant economic burden for patients and society [1]. Background therapy of glucocorticoids in SLE treatment would significantly affect the manufacture of autologous anti-CD19 CAR T cells [12]. Additionally, the production time of the autologous CAR-T cells would limit the application in severe patients with SLE who could not wait for manufacturing [13]. Cytokine release syndrome (CRS) and immune effector cell-associated neurotoxicity syndrome (ICANS), well documented in haematological disorders, have not been well addressed in SLE [14,15].

To overcome these limitations, allogeneic CAR-natural killer (NK) cells therapy is becoming an attractive choice due to its off-the-shelf convenience, superior safety profile, and excellent potency in depleting target cells [16]. Anti-CD19 CAR-NK cells have been validated for their efficacy in treating relapsed or refractory B-cell lymphoid malignancies and have indicated their potential in SLE [17]. However, expansion and killing efficiency would be a challenge for allogeneic CAR-NK cell therapy [18]. Interleukin (IL)-15 can enhance the expansion and persistence of CAR-NK cells. In this study, we genetically modified NK cells with targeted CD19 CAR as well as soluble intrinsic IL-15 and investigated its underlying efficacy for SLE.

MATERIALS AND METHODS

Patients and healthy peripheral blood mononuclear cell donors

Peripheral blood from healthy donors was obtained from Shanghai Xuanfeng Biotech Co., Ltd., with ethical approval granted by the Clinical Research Ethics Committee of Xuanfeng Biotech Co., Ltd. Peripheral blood from autoimmune disease patients was obtained from Renji Hospital, Shanghai Jiaotong University School of Medicine, with informed consent following the Declaration of Helsinki. Ethical approval was granted by the Clinical Research Ethics Committee of Renji Hospital. Peripheral blood mononuclear cells (PBMCs) were isolated by density gradient centrifugation, and B-cells were purified using the EasySep human B-cell isolation kit (StemCell Technologies; 17954) according to the instructions.

Cell lines and cell cultures

Raji-luc, Nalm6-luc, and K562 cell lines were obtained from the American Type Culture Collection. These cells were cultured in RPMI 1640 medium supplemented with 10% foetal bovine serum (FBS) and 1% penicillin/streptomycin (Pen/Strep).

Construction of CAR-NK cells

Primary human NK cells were isolated from the peripheral blood of healthy donors with informed consent and purified using the EasySep Human NK Cell Isolation Kit (StemCell Technologies; 17955). On day 0, purified NK cells were stimulated with irradiated K562-41BBL-IL21-B2M-KO feeder cells at a 2:1 ratio and expanded in NK MACS medium (Miltenyi Biotec, 130-114-429) supplemented with 10% heat-inactivated FBS (Gibco, 10099-141C), 1% Pen/Strep, and 400 IU/mL of recombinant human IL-2 (Sihuan, S20040008) for 6 days. After expansion,

primary human NK cells were transduced with retroviral particles containing supernatants in RetroNectin (TaKaRa, T202) coated plates at 37°C for 2 hours. Retrovirus particles were produced in HEK293T cells by transfecting with the transfer vector along with the 2 auxiliary packaging plasmids. The required volume of virus was added to each well and pelleted by centrifugation at 1000 *g* for 60 minutes at 32 °C (Multiplicity of infection = 10). After aspirating the virus completely, NK cells were replated, centrifuge at 500 *g* for 5 minutes at room temperature and incubated. On day 13, CAR-NK cells were harvested for downstream use. The CAR expression was determined by flow cytometry, measuring CD56, CD19-CAR expression with fluorescein isothiocyanate-labelled human-CD19 protein (ACRO, CD9-HF251), PE-cy7-CD56 antibody (Biolegend, 362510), and Brilliant Violet 421 anti-human CD3 antibody (Biolegend, 317344). The IL-15 levels were quantified using the human IL-15 quantikine enzyme-linked immunosorbent assay (ELISA) kit (R&D Systems, D1500) following the manufacturer's instructions.

CAR-NK cell killing assay

The XB-19.15 or mock NK cells were coincubated with Raji-luc, K562, and human primary B-cells to assess cytotoxicity using single-round (4 hours at different effector-to-target ratios [E/T]) coculture assays. Multiround stimulation was performed using Nalm6-luc cells (luciferase-expressing) at decreasing E/T ratios (4:1 for 24 hours, 2:1 for 48 hours, 2:1 for 72 hours). B-cells derived from healthy donors and patients with SLE received 2 cycles of stimulation (24 and 48 hours) at an E/T ratio of 1:1. The cytotoxicity was determined by luciferase activity using the following formula: (luminescence of target cells alone − sample luminescence)/target luminescence) × 100 for Raji-luc and Nalm-luc cell lines. For killing potency in K562 cells, residual cells were stained with PE-cy7-CD56 antibody (BD, 557747), and K562 cells were gated on the CD56-negative population. The killing efficiency on human primary B-cells was calculated by PE/Cyanine7 anti-human CD19 antibody (Biolegend, 363012) using flow cytometry results.

CAR-NK cells proliferation

To evaluate proliferation, XB-19.15/XB-19.0 and mock NK cells were cocultured with Nalm6-Luc cells in 2 sequential rounds: first at a 2:1 E/T ratio for 72 hours, followed by replating with fresh target cells at the same ratio for 48 h. Proliferation was assessed using flow cytometry by measuring CD56, CD19-CAR, and Ki-67 expression with PE-labelled human-CD19 protein (ACRO, CD9-HP2H3), PE-cy7-CD56 antibody (BD, 557747), and Ki-67 monoclonal antibody (Thermo Fisher, 350514, 10-fold dilution with phosphate-buffered saline) through flow cytometry (BD FACSCanto II).

In vitro cytokine production

XB-19.15/XB-19.0 and mock NK cells were cocultured with Nalm6-Luc cells in 2 sequential rounds: first at a 2:1 E/T ratio for 72 hours, followed by replating with fresh target cells at the same ratio for 48 hours. Supernatants from both rounds were collected. The IL-15 levels were quantified using the human IL-15 quantikine ELISA kit (R&D Systems, D1500) following the manufacturer's instructions. Interferon-gamma (IFN-γ) levels were quantified by BD OptEIA human IFN-γ ELISA set (BD, 555142) following the manufacturer's instructions.

In vivo functional studies of XB-19.15 CAR-NK cells in xenografted mice

The efficacy of XB-19.15 was evaluated across multiple *in vivo* models. In NOD.Cg-Prkdc^{scid} IL-2rg^{tm1sug}/JicCrl mice (NOG), xenografts were established by intravenous (IV) injection of 2.5E5 Nalm6-Luc cells/mice to create Nalm6-luc-bearing NOD mice. In Nalm6 xenograft studies, efficacy and biodistribution were assessed: tumour-bearing mice received IV XB-19.15 (2×10^6–8×10^6 cells/mouse) or controls, with bioluminescence imaging (D-luciferin) tracking tumour regression. Biodistribution in NOG mice injected with 1×10^7 XB-19.15 cells revealed persistence of CAR DNA in blood and tissues up to 56 days post injection, as determined by quantitative polymerase chain reaction using primers/probes targeting the CAR transgene.

In immune-humanised NOD.CB17-Prkdc^{scid} Il2rg^{tm1Bcgen} Il15$^{tm1(IL15)\ Bcgen}$/Bcgen (NDG) mice (CD34+ stem cell-engrafted), the human immune system was reconstituted by transplanting human CD34 stem cells into immunodeficient mice. The XB-19.15 (1×10^7–2×10^7 cells/mouse) were IV injected into the animals. Peripheral blood was collected from each mouse to detect B-cell depletion and CAR-NK persistence in peripheral blood by flow cytometry.

SLE PBMC xenograft models (NOD.Cg-Prkdc^{scid}H2-K1$^{b\text{-}tm1Bpe}$H2-Ab1$^{g7\text{-}em1Mvw}$H2-D1$^{b\text{-}tm1Bpe}$Il2rg^{tm1Wjl}/SzJ, NOD scid gamma (NSG)-MHC I/II DKO mice) indicated dose-dependent B-cell reduction (CD19+/CD20+ flow panels) and reduced serum immunoglobulin G (IgG)/anti-dsDNA levels (ELISA). The PBMC were injected into the NSG-MHC I/II DKO mice. The XB-19.15 (1.5×10^7 cells/mouse) were IV injected into the animals. Blood was collected from each mouse to detect IgG/anti-dsDNA levels. At the study's endpoint, part of the spleen and bone marrow cell suspensions were prepared from the mice for flow cytometry analysis. Detailed methods are provided in the supplementary methods.

Toxicity study

Tumorigenicity was assessed using *in vitro* soft agar assays, indicating no colony formation by XB-19.15 cells compared to Hela/2BS controls. *In vivo* subcutaneous injection in NOG mice (1×10^7 cells/mouse) indicated no tumour formation over 112 days, as confirmed by histopathological analysis. Repeat-dose toxicity testing (NOG mice, 4 weekly IV doses of 1.5×10^7 XB-19.15 cells/mouse) revealed nonsignificant histopathological changes or cytokine storm, as determined using a LEGENDplex panel (IL-2, IFN-γ, and Granzyme B).

Clinical trial design and patient eligibility

This phase 1 clinical trial was approved by the Ethics Committees of Renji Hospital, Shanghai Jiaotong University School of Medicine (approval number: LY-2023-222C) and registered at ClinicalTrials.gov (NCT06208280). The trial enrolled patients aged 18-65 years with moderate-to-severe active SLE, diagnosed according to the 2019 American College of Rheumatology and the European Alliance of Associations for Rheumatology classification criteria. The full eligibility criteria are present in the supplementary methods. The dose-limiting toxicity (DLT) and adverse events (AEs) were measured as the primary outcome. Patients were required to have discontinued rituximab for at least 6 months, and belimumab or telitacicept for at least 1 month before lymphodepletion. Additionally, all conventional

immunosuppressants were withheld for at least 1 week before CAR-T cell infusion. Patient 1 was in the low-dosage group receiving 0.5×10^9 CAR-NK cells while patients 2 and 3 received 3×10^9 after lymphodepletion using fludarabine (25-30 mg/m^2 for 3 days) and cyclophosphamide (250-300 mg/m^2 for 3 days). The primary outcome measures were the incidence of DLT up to 4 weeks and the proportion of subjects with AEs and serious AEs. The secondary outcome measures were efficacy and cellular kinetics.

Statistical analysis

All data were analysed using GraphPad Prism software (version 10.4.0). Group differences were analysed by 1-way or 2-way analysis of variance, with post hoc multiple comparisons (Tukey's Honestly Significant Difference, Bonferroni, or Dunnett's test) as appropriate. A $P < 0.05$ was considered statistically significant.

RESULTS

Construction of anti-CD19 CAR-NK cells with IL-15 secretion

We successfully constructed anti-CD19 CAR-NK cells with (XB-19.15) or without coexpressing IL-15 (XB-19.0) in PBMC-derived NK cells. The structural genes for XB-19.15 and XB-19.0 were inserted between the long terminal repeats of the retroviral vector (Fig 1A). The CAR construct included an extracellular single-chain variable fragment domain, a transmembrane domain, and intracellular signalling domains combining CD28 and CD3ζ-C termini, with soluble IL-15 added to enhance NK cell function (Fig 1B). Flow cytometry analysis demonstrated a high transduction efficiency, with a significant percentage of CAR-positive NK cells in both XB-19.15 and XB-19.0 groups (Fig 1C). Additionally, ELISA-based quantification confirmed IL-15 secretion in the supernatant of XB-19.15 cells (Fig 1D).

XB-19.15 exerted strong cytotoxic activity against CD19+ cells in vitro

To assess the cytotoxicity of XB-19.15, we cocultured it with various cell lines, including Raji, K562, Nalm6, and B-cells derived from patients with SLE. In the CD19+ Raji cell line, XB-19.15 displayed significantly enhanced cytotoxicity compared to the mock NK cells across different E/T ratios from 0.5:1 to 4:1 (Fig 2A). In contrast, XB-19.15 did not increase cytotoxicity against CD19-negative K562 cell across all E/T ratios as expected (Fig 2B), indicating its specific killing effect to targeted cells. Furthermore, continuous killing potency was elucidated by multiround coincubation in Nalm6 cell lines with XB-19.15 or XB-19.0. Although both exhibited increased cytotoxicity in the first round compared to mock NK cells, XB-19.15 indicated a stronger killing efficiency than XB-19.0 in the second and third round (Fig 2C). As expected, XB-19.15 released high level IL-15 in supernatants during coculture while no IL-15 secretion was detected from XB-19.0 or mock NK cells (Fig 2D). The IFN-γ release was increased in both CAR-NK cells compared to mock NK cells but was more enhanced in XB-19.15 (Fig 2E). Following antigen stimulation by Nalm6 cells, all NK cells with or without CAR indicated a higher Ki-67 positive proportion from XB-19.15 system than XB-19.0 and mock NK in both 2 round coculture (Fig 2F). These suggested that IL-15 significantly enhanced the proliferation capability of total NK cells and bolstered the persistence of CAR-NK cells cytotoxicity.

Subsequently, the efficacy of XB-19.15 for human primary cells was validated *in vitro*. In the 4-h killing assay and continuous killing assay, XB-19.15 exhibited significantly higher killing efficacy than mock NK groups in different E/T ratios and 2 rounds of coculture with B-cells derived from healthy donors (Fig 2G) and patients with SLE (Fig 2H), indicating the potential value in SLE treatment.

XB-19.15 indicated robust clearance of CD19-positive cells and long-term persistence in vivo

To investigate the *in vivo* efficacy of XB-19.15 on depleting CD19 positive cells, Nalm6-luc-bearing NOD mice model was created and treated with vehicle control, mock NK, and different dosages of XB-19.15 (2×10^6, 4×10^6, 8×10^6/mice for low, medium, and high doses, respectively) at 1 day post Nalm6 injection ($n = 10$ for each group). Bioluminescence imaging was used to evaluate the growth of Nalm6 in mice model (Fig 3A). In this xenograft model derived from a human B-cell malignancy, mice treated with vehicle or mock NK cells indicated rapid tumour expansion, but XB-19.15 significantly inhibited Nalm6 growth in mice model with dosage dependence (Fig 3B, C). In the high-dose group, XB-19.15 would also

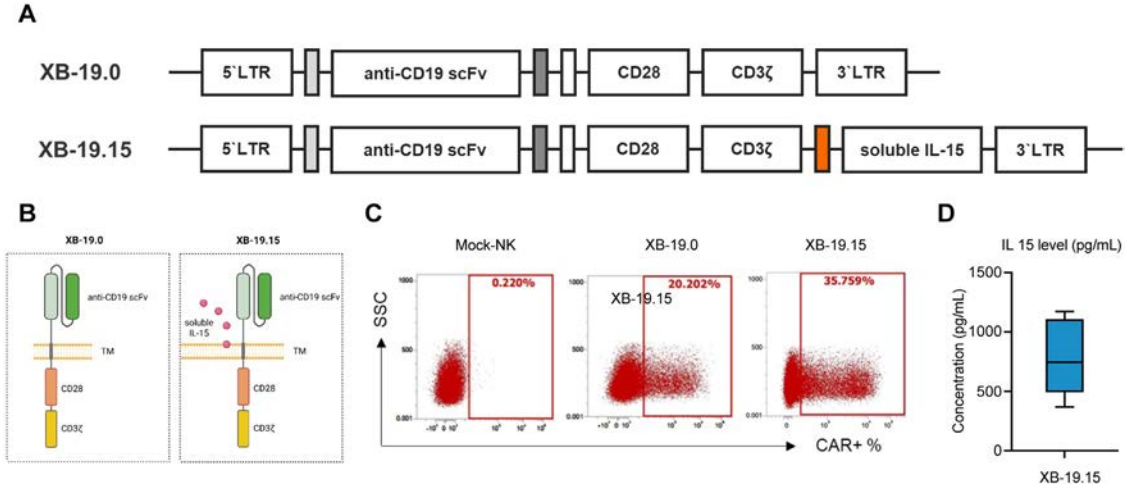

Figure 1. Construction of chimeric antigen receptor (CAR)-natural killer (NK) cells. (A,B) Schematic representation of XB-19.15 and XB-19.0. (C) Representative flow cytometry plots showing CD19 CAR expression (D) enzyme-linked immunosorbent assay (ELISA)-based quantification of interleukin (IL)-15 in culture supernatant of XB-19.15 without stimulation.

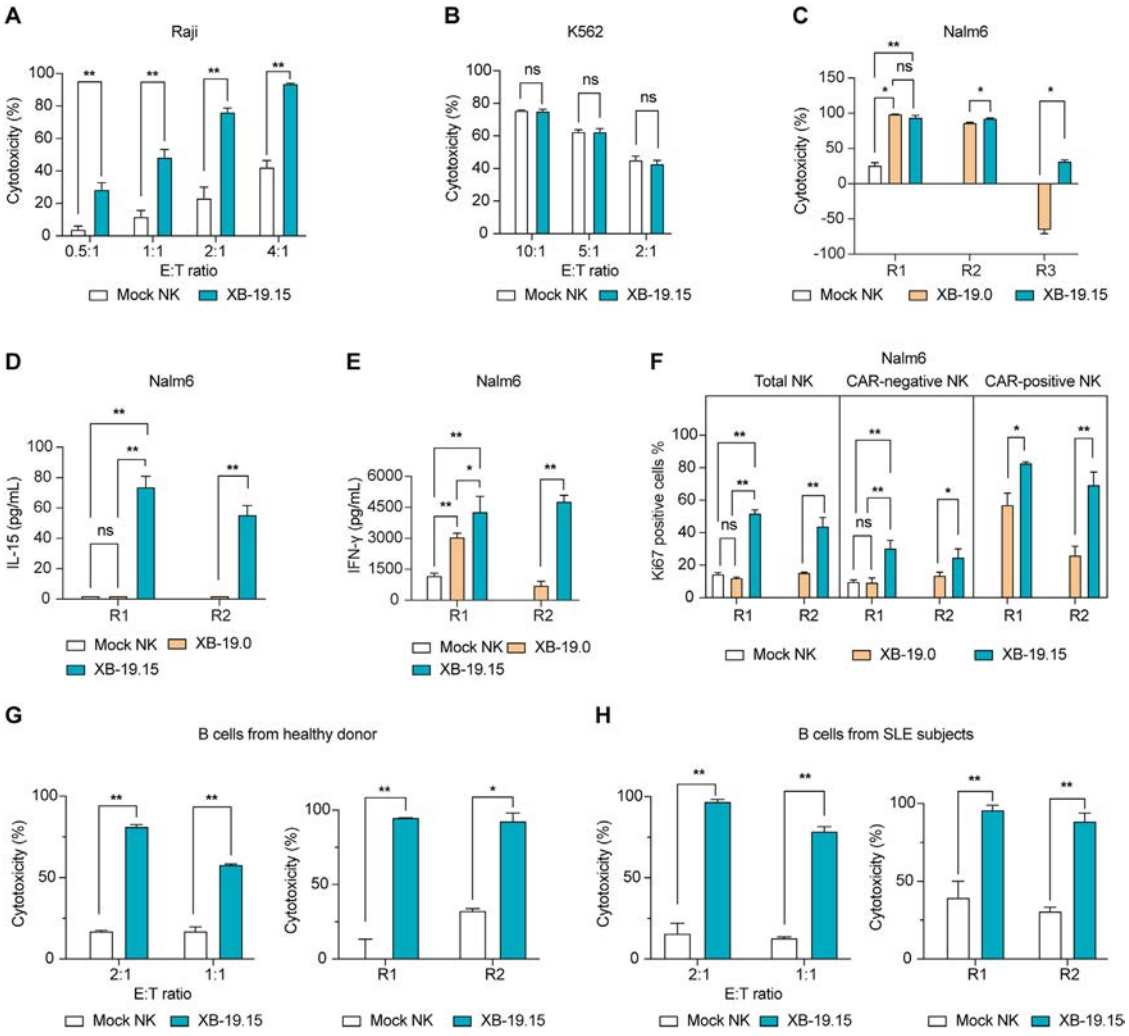

Figure 2. *In vitro* function evaluation of XB-19.15. Short-term cytotoxicity assay of XB-19.15 against Raji cells (A) and K562 cells (B) at different E:T ratios. (C) Multiple rounds of cytotoxicity assay of XB-19.15 and XB-19.0 against Nalm6 cell. Mock natural killer (NK) was removed as less than 50% killing efficiency at the first round. Interleukin (IL)-15 concentration (D) and interferon-gamma (IFN-γ) (E) in the first and second round coculture supernatant were analysed by enzyme-linked immunosorbent assay (ELISA). (F) Proliferation of NK in the first and second round coculture. Ki67 positive percentage in total NK, chimeric antigen receptor (CAR) negative NK, and CAR-positive NK were analysed. Short-term and multiple cytotoxicity assay of XB-19.15 against B-cells from healthy donor (G) and patients with systemic lupus erythematosus (SLE) (H) at different E:T ratios ($n = 3$ for each group). A 2-way analysis of variance (ANOVA) was performed, followed by Bonferroni's or Tukey's multiple comparisons test. *$P < .05$; **$P < .01$ versus Mock NK; #$P < .05$; ##$P < .01$ versus XB-19.0.

prolong the survival and decrease body weight loss, indicating the reduction of disease activity (Supplementary Figs S1A,B). To further assess long-term effect and tissue distribution of XB-19.15, we analysed CAR DNA copies in peripheral blood, bone marrow, spleen, and lymph nodes at days 8, 29, 43, and 56 post infusion ($n = 10$ for each timepoint; Fig 3D). CAR DNA copies increased during the first 4 weeks and remained stable through 8 weeks in both peripheral blood and lymphoid organs (Fig 3E), suggesting the long-term persistence and well tissue penetration of XB-19.15.

Moreover, we evaluated the *in vivo* function of XB-19.15 in a CD34+ haematopoietic stem cell (HSC) humanised NDG xenograft model. NDG mice with humanised CD45+ HSC greater than 25% in peripheral blood were selected and randomised into 3 groups which received vehicle, low-dosage (1×10^7 cells), and high-dosage (2×10^7 cells) XB-19.15 in day 0, respectively ($n = 5$ for each group) (Fig 3F). In initiation, CD45+ cells indicated nonsignificant difference among these 3 groups (Supplementary Fig S1C). After infusion, both treatment groups exhibited sustained B-cell depletion until day 14, with high-dosage group indicating more robust B-cell clearance on day-1 and day-4 than low-dosage group (Fig 3G). At day 21, B-cell reconstitution occurred in both groups that received CAR-NK cells. XB-19.15 cells were also monitored during the follow-up. From day 7, XB-19.15 was detected to gradually decrease in peripheral blood and turned negative on day 21, consistent with previous results of B-cell recovery (Fig 3H).

Safety and tumorigenicity evaluation of XB-19.15

To address the long-term safety concern of XB-19.15, we conducted a tumorigenicity evaluation both *in vitro* and in *vivo*. In the soft agar colony formation assay, no colony formation was observed in both low-, middle-, or high-dose group until day 21, while Hela cells in the positive control group indicated clear colony proliferation (Supplementary Fig S2A). Furthermore, a subcutaneous tumorigenicity assay was performed via a single injection of XB-19.15 into NOG mice. Over a 112-day observation, no tumour formation was observed in various tissues

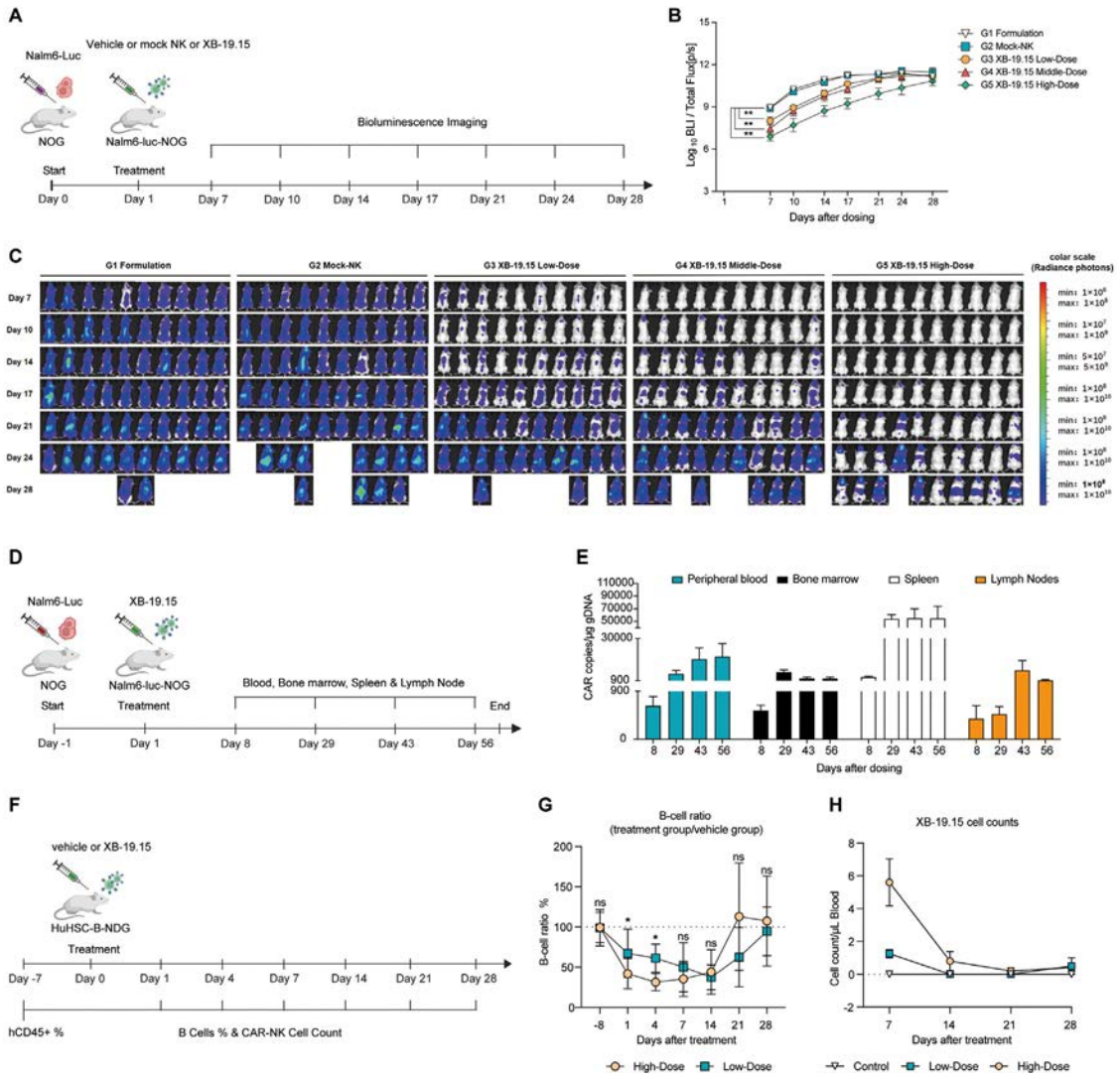

Figure 3. *In vivo* CD19+ cells clearance of XB-19.15. (A) Schematic of the experimental design to test XB-19.15 efficacy on Nalm6 depletion. (B,C) Bioluminescence imaging of different groups over time ($n = 10$ for each group) versus formulation. (D) Schematic of the biodistribution experimental design. (E) *In vivo* chimeric antigen receptor (CAR) natural killer (NK) expansion and persistence were measured by a quantitative polymerase chain reaction (qPCR) assay according to the number of CAR transgene copies per microgram of genomic DNA in blood, bone marrow, spleen and lymph nodes samples on days 8, 29, 43, and 56 after dosing. $n = 10$ at each time point. (F) Schematic of the experimental design to test XB-19.15 efficacy on immune-humanised with CD34+ hematopoietic stem cells NOD.CB17-Prkdc^{scid} Il2rg^{tm1Bcgen} Il15$^{tm1(IL15)\ Bcgen}$/Bcgen (B-NDG) xenograft model. (G) Percentage of B-cells over time after dosing in mice treated with XB-19.15 compared to mice in vehicle control group ($n = 5$ for each group). (H) XB-19.15 cell counts per microliter of blood over time after dosing. *$P < .05$; **$P < .01$.

through histopathological examination in the XB-19.15 group (Supplementary Fig S2B).

XB-19.15 indicated promising therapeutic benefits in the SLE PBMC xenograft model

To evaluate the therapeutic efficacy of XB-19.15 cells in SLE, PBMC from active patients with SLE were injected into NSG mice to establish a xenograft model. The NSG mice were divided into 3 groups: vehicle control, single-dose group, and delayed double-dose group; $n = 5$ for each group. The control and single-dose group received an infusion 1 day after establishing the mouse model. To fully understand the efficacy of XB-19.15 during disease activity accumulation, we also set delayed double-dose group which would have injection at days 7 and 11 (Fig 4A). During the follow-up, both single and delayed double group indicated decreased total IgG level compared to control (Fig 4B,C), as well as anti-dsDNA antibodies (Fig 4D,E), which indicated XB-19.15 would inhibit the disease burden of SLE xenograft model. At the endpoint, CD19+ B-cells, CD38+CD27+ plasmablasts, and CD138+ plasma cells of XB-19.15 treatment groups were significantly decreased in bone marrow (Figs 4F-H) and spleen (Figs 4I-K). These results suggested that XB-19.15 exhibited a well penetration and deep depletion of B-cells in lymphoid tissue.

Clinical efficacy of XB-19.15 in patients with refractory SLE

A phase 1 multicentre, open-label clinical trial was conducted to evaluate the safety and tolerability of F01 (XB-19.15 CAR-NK cells injection) in patients with autoimmunity disease. Three patients with refractory SLE who received at least 2 standard regimens for SLE and biologic agents before enrolment were included in this study (Table). One patient was allocated to the initial low-dosage group (0.5×10^9 cells) while the other 2 patients were escalated to the high-dosage group (3×10^9 cells) due to the absence of DLT (Fig 5A). Most AEs were mild and manageable, including lymphodepletion-related cytopenia and

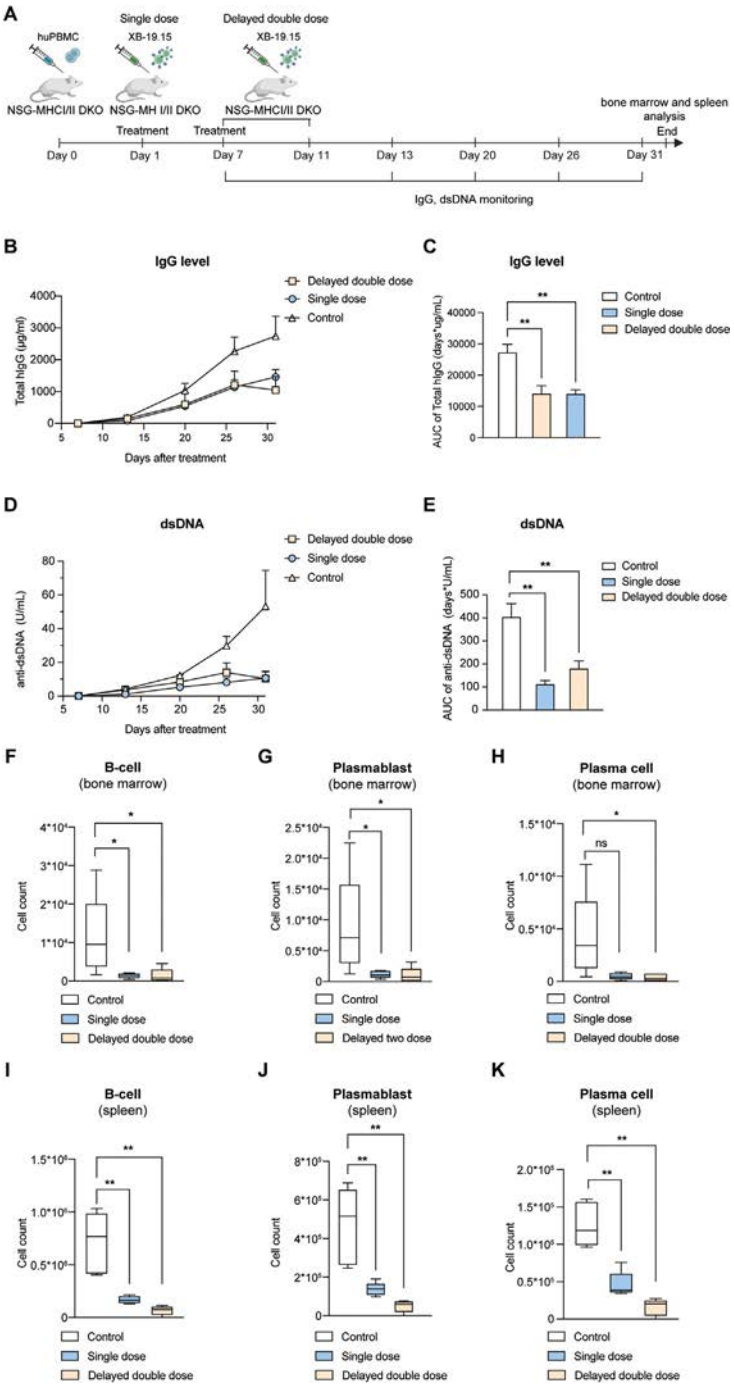

Figure 4. XB-19.15 effectively inhibited disease burden in systemic lupus erythematosus (SLE) peripheral blood mononuclear cells (PBMC) xenograft model. (A) Schematic of the experimental design ($n = 5$ for each group). Dynamitic changes of concentration of total IgG (B) and area under the curve (AUC). (C) in different groups during follow-up. Dynamitic changes of concentration anti-dsDNA (D) and AUC (E) in different groups during follow-up. Count of bone marrow $CD19^+$ B-cells (F), $CD38^+CD27^+$ plasmablast (G) and $CD138^+$ plasma cells (H) at endpoint. Count of spleen $CD19^+$ B-cells (I), $CD38^+CD27^+$ plasmablast (J) and $CD138^+$ plasma cells (K) at endpoint. $^*P < .05$; $^{**}P < .01$.

postinfusion fever. Patient 1 experienced a COVID-19 infection 1 month after treatment but recovered promptly. No other infection was recorded in these 3 patients (Supplementary Table S1). Patients 1 and 2 had long-term lupus nephritis, and patient 3 experienced thrombocytopenia at baseline. No CRS or ICANS was observed in any patient. Peripheral blood test revealed that CAR transgene copies peaked at 8 h post infusion and decreased to below the limit of quantification within 3 days (Fig 5B). Despite multiple CAR-NK infusions, no anti-CAR antibody was detected during the follow-up (Supplementary Fig S3A). Complete B-cell depletion was achieved by week 4, with reconstitution occurring on approximately 12 weeks in all 3 patients (Fig 5C). T-cells and NK cells were stable during the treatment (Fig 5D,E). As expected, serum IL-15 has a synchronous trend of CAR-NK cell copies during follow-up as well as IFN-γ (Fig 5F and Supplementary Fig S3B). In reconstitution of B-cell repertoires, plasmablast and memory B-cells significantly decreased while naive and transitional B-cells were the majority compared to baseline (Fig 5G). Meanwhile, decreased proportions of naive T-cells were accompanied by increased proportions of effector T-cells within both CD4 and CD8 compartments. Specifically, $CD8^+$ TEMRA cells were elevated relative to baseline levels (Supplementary Figs S4A-C).

All 3 patients achieved SRI-4 (SLE responder index-4) response, with decreased SLEDAI-2000 score and an improvement in cutaneous symptoms (Fig 5H and Supplementary Fig S5). Two patients discontinued glucocorticoids after infusion and remained steroid-free for approximately 6 months during follow-up. One patient reached a lupus low disease activity state at 4 months and Definitions Of Remission In SLE remission at 6 months after treatment (Supplementary Table S2). Patient 3, who had baseline thrombocytopenia, indicated a rapid increase

Table
Baseline characteristics of patients with systemic lupus erythematosus treated with XB-19.15

	Patient 1	Patient 2	Patient 3
Demographics			
Age (y)	31	25	27
Sex	Female	Female	Female
Disease duration (y)	18	9	6
SLEDAI-2K	10	8	11
SELENA-SLEDAI	6	8	11
Dose level	$0.5*10^9$ cells	$3*10^9$ cells	$3*10^9$ cells
Laboratory values			
White blood cells(10^9/L)	4.19	6.69	4.59
Lymphocytes (10^9/L)	0.83	1.46	1.87
Platelets (10^9/L)	239	340	70
Haemoglobin (g/L)	127	114	123
IgG (mg/dL)	8.41	14.20	15.90
C3 (g/L)	0.865	0.83	0.915
Antinuclear antibodies	1:320	1:1280	1:320
Anti-dsDNA (IU/mL)	144.7	47.63	192.6
Other autoantibodies	SSA-Ro60, Histone	AnuA, SSA60, Histone, b2-GP1	AnuA, SSA-Ro52, SSA-Ro60, RiP, b2GP1
Proteinuria (mg/24 h)	2926.4	1829.8	51.5
Previous treatments			
Glucocorticoid pulses	+	+	+
Hydroxychloroquine	+	+	+
Mycophenolate mofetil	+	+	+
Cyclophosphamide	+	+	+
Tacrolimus	+	+	+
Belimumab	+	+	+
Telitacicept	+	–	–
Rituximab	+	–	–
Outcome			
SIR-4 at 4 mo	Response	Response	LLDAS
SIR-4 at 6 mo	Response	Response	DORIS

DORIS, Definitions Of Remission In SLE; LLDAS, Low Lupus Disease Activity State; SELENA-SLEDAI, Safety of Estrogens in Lupus Erythematosus National Assessment – Systemic Lupus Erythematosus Disease Activity Index; SLEDAI-2K, Systemic Lupus Erythematosus Disease Activity Index 2000; SRI-4, Systemic Lupus Erythematosus Responder Index-4.

in platelet count within 4 weeks (Fig 5I). Although proteinuria did not completely resolve, patients 1 and 2 demonstrated a gradual reduction in proteinuria during the follow-up (Supplementary Fig S3C). Notably, the serum IgG and C3 levels remained in normal range after infusion, indicating a good tolerance of XB-19.15 (Fig 5J,K). Concurrently, no substantial decline in protection and vaccine antibody responses was observed during follow-up (Supplementary Figs S6A-F).

DISCUSSION

In this study, we investigated the therapeutic potential of PBMC-derived CAR-NK cells targeting CD19, with or without IL-15 coexpression (designated XB-19.15 and XB-19.0, respectively), for treating SLE *in vitro* and *in vivo*. Our results demonstrated that CAR-NK cells, particularly XB-19.15, exhibit enhanced cytotoxic activity, robust immune function, and sustained *in vivo* persistence. These findings were supported by efficient B-cell clearance from peripheral blood and secondary lymphoid tissues, and detectable NK cell presence for approximately 56 days post infusion in NOG xenograft models. These preclinical results justified the translation of XB-19.15 into a first-in-human clinical trial, where treatment of 3 patients with refractory SLE demonstrated a favourable safety profile, rapid B-cell depletion, symptom alleviation, and reduced disease activity.

Autologous CD19-targeted CAR-T cell therapy has indicated promise in treating autoimmune diseases such as SLE by eliminating autoreactive B-cells and potentially inducing long-term remission [19–21]. However, broader clinical implementation is limited by complex and time-consuming manufacturing and high cost [22–25]. Universal allogeneic CAR-NK cells offer a potentially transformative alternative [26]. As 'off-the-shelf' products derived from healthy donors, CAR-NK cells eliminate the need for individualised cell production, improve batch consistency, reduce costs, and allow for flexible dosing and repeat administration. NK cells seldom trigger graft-versus-host disease and are associated with minimal CRS or ICANS compared to autologous CAR-T cells [27,28]. Furthermore, CAR-NK cells exert cytotoxicity via both CAR-dependent and innate mechanisms. Clinically, allogeneic CAR-NK cells have indicated encouraging preliminary efficacy in patients who had been heavily pretreated in B-cell lymphoma with minimal immune-related toxicities [18,29–31]. These early data underscore the therapeutic potential and safety of CAR-NK strategies and support their exploration in several ongoing clinical trials of autoimmune diseases [32,33].

In current clinical studies and investigational therapies, NK cells used for infusion, particularly in CAR-NK, are predominantly derived from cord blood or induced pluripotent stem cells that are more amenable to transduction, while PBMC-derived NK cells offer critical practical advantages, including easier accessibility, better scalability, and tighter quality control in manufacturing [34]. Our data confirmed that PBMC-derived NK cells (XB-19.15) can be effectively transduced with a CD19-specific CAR and expanded to clinical scale. Notably, comparative analyses indicated that PBMC-derived CAR-NK cells possess potent cytotoxicity, supporting their use as a viable and potentially superior platform for immunotherapy development [35]. Furthermore, tissue infiltration studies demonstrated effective

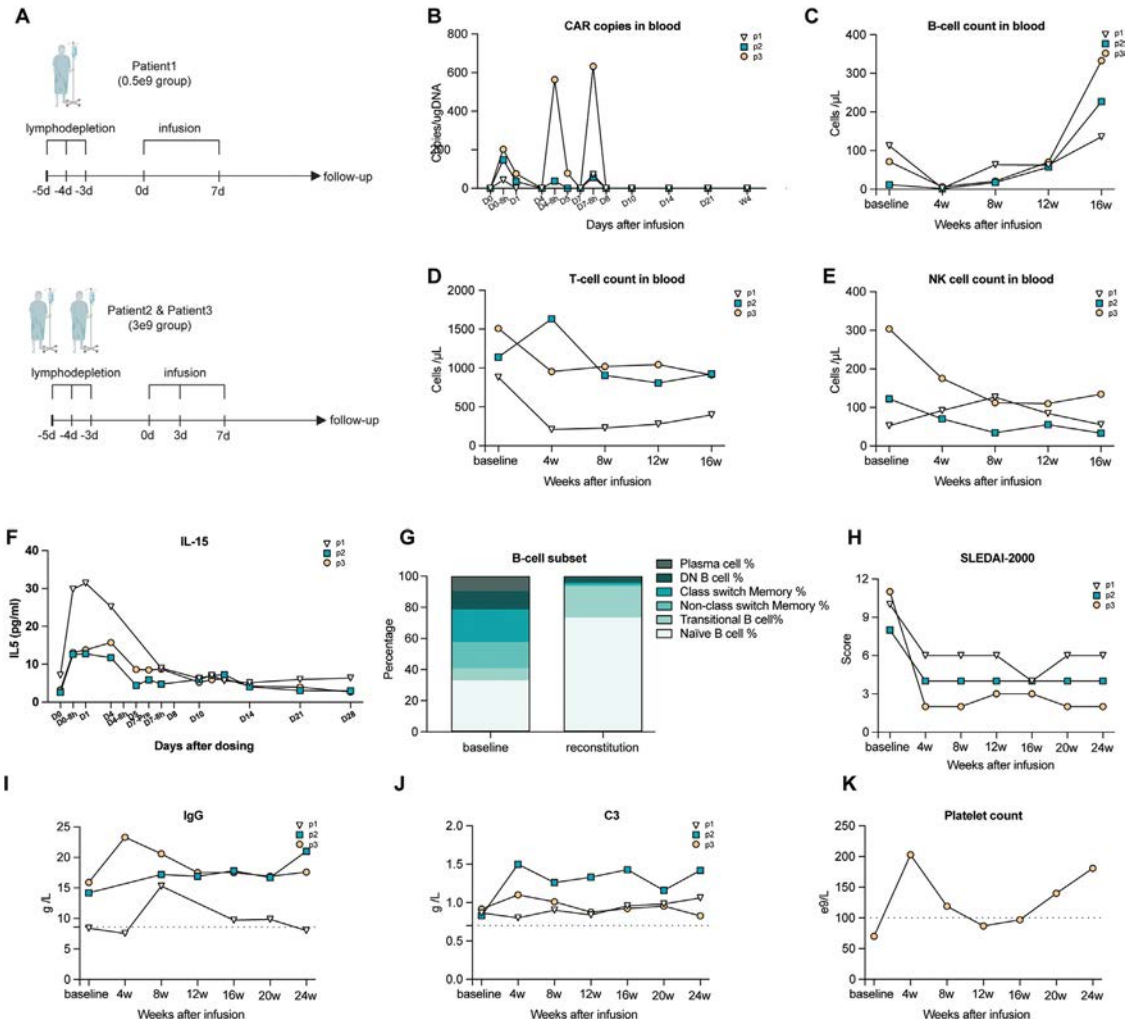

Figure 5. Patients with refractory systemic lupus erythematosus (SLE) treated with XB-19.15. (A) Schematic of treatment design. (B) Chimeric antigen receptor (CAR) copies in treated patients over time. (C) The absolute number of circulating B-cell, (D) T-cell, and (E) natural killer (NK) cells over time. (F) The secretion of interleukin (IL)-15 in serum after infusion. (G) B-cell repertoires between baseline and reconstitution. (H) Dynamic changes of Systemic Lupus Erythematosus Disease Activity Index (SLEDAI)-2000 after treatment in 3 patients. (I) Platelet count changes of patient 3 after treatment. (J) Serum IgG and (K) C3 quantification levels over time.

biodistribution of XB-19.15 to lymphoid organs, supporting their role in systemic B-cell depletion—a crucial therapeutic goal in SLE [27]. Given the short *in vivo* lifespan of NK cells, we incorporated IL-15 into the CAR construct to enhance expansion and persistence. IL-15 is known to support NK cell survival and proliferation [36], and our findings confirmed that its inclusion significantly enhanced cytotoxicity and persistence of XB-19.15 *in vitro* and *in vivo*, particularly under repeated stimulation assays. This strategy may address one of the key limitations of NK cell-based therapies and further improve their therapeutic window [37].

To our knowledge, this is one of the first reports describing the clinical application of CAR-NK cells in patients with refractory SLE. Treatment with XB-19.15 resulted in rapid B-cell depletion, accompanied by improvements in clinical symptoms and disease activity scores. Importantly, lymphocyte reconstitution was rapid, and IgG remained within the physiological range, suggesting that immune homeostasis was preserved. B-cell recovery was observed approximately 12 weeks posttreatment, mirroring kinetics reported in CAR-T-treated patients with SLE [38]. Considering the small sample size of our study, further investigations with larger cohorts and more advanced techniques such as single-cell ribonucleic acid sequencing are needed to provide a comprehensive understanding of the reconstitution of B-cells and the dynamic impact of the T-cell compartment. These findings suggest that dose-escalation or repeat infusion may further enhance efficacy and prolong remission.

Despite these encouraging findings, several limitations must be addressed. First, the clinical sample size was small, and long-term follow-up is needed to evaluate the durability of response and safety over time. Second, the optimal dose and treatment schedule for XB-19.15 remain to be defined. Future trials should explore dose-escalation strategies, multiple infusion regimens, and combination approaches with immunomodulatory agents to enhance efficacy and extend remission.

In conclusion, our preclinical and early-phase clinical data support the feasibility, safety, and therapeutic potential of PBMC-derived CAR-NK cells, particularly XB-19.15, in targeting autoreactive B-cells in SLE. This approach offers a novel, scalable, and potentially safer alternative to autologous CAR-T therapy and paves the way for broader development of off-the-shelf CAR-NK cell therapy for autoimmune diseases. Continued investigation in larger clinical trials is warranted to optimise therapeutic protocols and fully define the clinical utility of this emerging platform.

Competing interests

ZX, FG, PH, FJ, CH, NP, LW, and ZC were employed by Shanghai Simnovia Biotechnology Co., Ltd. The remaining authors declare that the research was conducted in the absence of any commercial or financial relationships that could be constructed as a potential conflict of interest.

CRediT authorship contribution statement

Yakai Fu: Writing – original draft, Visualization, Validation, Software, Resources, Project administration, Formal analysis, Data curation, Conceptualization. **Zupeng Xu:** Writing – original draft, Investigation, Formal analysis. **Chunmei Wu:** Writing – original draft, Resources, Investigation, Data curation. **Fangjie Gao:** Resources, Investigation. **Pengyu Huang:** Investigation. **Fuwei Jiang:** Resources, Investigation. **Chuxuan Hu:** Resources, Investigation. **Nick Patsoukis:** Resources, Investigation. **Yiyang Wang:** Investigation. **Zejin Cui:** Investigation. **Limin Wen:** Investigation. **Peiying Li:** Supervision, Resources. **Chong Wang:** Resources, Investigation, Conceptualization. **Shuang Ye:** Writing – review & editing, Validation, Supervision, Conceptualization. **Zhuoxiao Cao:** Writing – review & editing, Supervision, Funding acquisition, Conceptualization. **Qiong Fu:** Writing – review & editing, Writing – original draft, Supervision, Investigation, Funding acquisition, Formal analysis, Data curation, Conceptualization.

Acknowledgements

The authors sincerely thank all the patients for participation in this study. Their extraordinary fortitude and dedication would pave the way for the application of unproven but promising therapy. We would like to thank Ying An and Pingping Hou from the Core Facility of the Shanghai Immune Therapy Institute for assistance in flow cytometry.

Contributors

QF, ZC, SY, and CW designed the research. YF, ZX, and CW analysed the data and wrote the manuscript. YF, CW, LW, and PL performed clinical practice and data collection. ZX, FG, PH, FJ, CH, NP, YW, and ZC performed cells and animal experiments, designed the study. QF funded the project. QF is the guarantor.

Funding

This research is supported by grants from National Natural Science Foundation of China (92474112, 82371805, and 82471822), Shanghai Hospital Development Center (SHDC) (SHDC2023CRD012), Shanghai Municipal Science and Technology Fund (21ZR1438800, 22Y11902400), Science and Technology Commission of Shanghai Municipality (24S11901100), Pudong New Area Science Technology and Economy Commission (PKX2024-S10).

Patient consent for publication

Not applicable.

Ethics approval

This study was approved by the ethics committees of Renji Hospital, Shanghai Jiao Tong University School of Medicine (LY2023-222-C).

Provenance and peer review

Not commissioned; externally peer reviewed.

Data availability statement

The corresponding authors will take charge of any data sharing inquiries.

Supplementary materials

Supplementary material associated with this article can be found in the online version at doi:10.1016/j.ard.2025.07.028.

Orcid

Qiong Fu: http://orcid.org/0000-0001-5873-6422

REFERENCES

[1] Durcan L, O'Dwyer T, Petri M. Management strategies and future directions for systemic lupus erythematosus in adults. Lancet 2019 Jun;393 (10188):2332–43.
[2] Tsokos GC. Systemic lupus erythematosus. N Engl J Med 2011 Dec;365 (22):2110–21.
[3] Li M, Zhang Y, Jiang N, Ning C, Wang Q, Xu D, et al. Anti-CD19 CAR T cells in refractory immune thrombocytopenia of SLE. N Engl J Med 2024 Jul;391 (4):376–8.
[4] Lee DSW, Rojas OL, Gommerman JL. B cell depletion therapies in autoimmune disease: advances and mechanistic insights. Nat Rev Drug Discov 2021 Mar;20(3):179–99.
[5] Abeles I, Palma C, Meednu N, Payne AS, Looney RJ, Anolik JH. B cell-directed therapy in autoimmunity. Annu Rev Immunol 2024 Jun;42(1):103–26.
[6] Mackensen A, Muller F, Mougiakakos D, Boltz S, Wilhelm A, Aigner M, et al. Anti-CD19 CAR T cell therapy for refractory systemic lupus erythematosus. Nat Med 2022 Oct;28(10):2124–32.
[7] Muller F, Taubmann J, Bucci L, Wilhelm A, Bergmann C, Volkl S, et al. CD19 CAR T-cell therapy in autoimmune disease—a case series with follow-up. N Engl J Med 2024 Feb;390(8):687–700.
[8] Wang X, Wu X, Tan B, Zhu L, Zhang Y, Lin L, et al. Allogeneic CD19-targeted CAR-T therapy in patients with severe myositis and systemic sclerosis. Cell 2024 Sep;187(18) 4890-904.e4899.
[9] Sosnoski HM, Posey Jr. AD. Therapeutic intersections: expanding benefits of CD19 CAR T cells from cancer to autoimmunity. Cell Stem Cell 2024 Apr;31:437–8.
[10] Albelda SM. CAR T cell therapy for patients with solid tumours: key lessons to learn and unlearn. Nature reviews Clin Oncol 2024 Jan;21(1):47–66.
[11] Zhang P, Zhang G, Wan X. Challenges and new technologies in adoptive cell therapy. J Hematol Oncol 2023 Aug;16(1):97.
[12] Luijten RK, Fritsch-Stork RD, Bijlsma JW, Derksen RH. The use of glucocorticoids in systemic lupus erythematosus. After 60 years still more an art than science. Autoimmun Rev 2013 Mar;12(5):617–28.
[13] Beccastrini E, D'Elios MM, Emmi G, Silvestri E, Squatrito D, Prisco D, et al. Systemic lupus erythematosus: immunopathogenesis and novel therapeutic targets. Int J Immunopathol Pharmacol 2013;26(3):585–96 Jul-Sep.
[14] Kennedy LB, Salama AKS. A review of cancer immunotherapy toxicity. CA Cancer J Clin 2020 Mar;70(2):86–104.
[15] Morris EC, Neelapu SS, Giavridis T, Sadelain M. Cytokine release syndrome and associated neurotoxicity in cancer immunotherapy. Nat Rev Immunol 2022 Feb;22(2):85–96.
[16] Baker DJ, June CH. Off-the-shelf CAR-T cells could prove paradigm shifting for autoimmune diseases. Cell 2024 Sep;187(18):4826–8.
[17] Zhong Y, Liu J. Emerging roles of CAR-NK cell therapies in tumor immunotherapy: current status and future directions. Cell Death Discov 2024 Jul;10 (1):318.

[18] Marin D, Li Y, Basar R, Rafei H, Daher M, Dou J, et al. Safety, efficacy and determinants of response of allogeneic CD19-specific CAR-NK cells in CD19 (+) B cell tumors: a phase 1/2 trial. Nat Med 2024 Mar;30(3):772–84.
[19] Schett G, Müller F, Taubmann J, Mackensen A, Wang W, Furie RA, et al. Advancements and challenges in CAR T cell therapy in autoimmune diseases. Nat Rev Rheumatol 2024 Sep;20(9):531–44.
[20] Mougiakakos D, Krönke G, Völkl S, Kretschmann S, Aigner M, Kharboutli S, et al. CD19-targeted CAR T cells in refractory systemic lupus erythematosus. N Engl J Med 2021 Aug;385(6):567–9.
[21] Cavallo MC, Cavazza M, Bonifazi F, Casadei B, Cutini I, Tonietti B, et al. Cost of implementing CAR-T activity and managing CAR-T patients: an exploratory study. BMC Health Serv Res 2024 Jan;24(1):121.
[22] Haghikia A, Schett G. Mougiakakos D. B cell-targeting chimeric antigen receptor T cells as an emerging therapy in neuroimmunological diseases. Lancet Neurol 2024;23(6):615–24.
[23] Brudno JN, Kochenderfer JN. Current understanding and management of CAR T cell-associated toxicities. Nat Rev Clin Oncol 2024 Jul;21(7):501–21.
[24] Schubert ML, Schmitt M, Wang L, Ramos CA, Jordan K, Muller-Tidow C, et al. Side-effect management of chimeric antigen receptor (CAR) T-cell therapy. Ann Oncol 2021 Jan;32(1):34–48.
[25] Epperla N, Feng L, Shah NN, Fitzgerald L, Shah H, Stephens DM, et al. Outcomes of patients with secondary central nervous system lymphoma following CAR T-cell therapy: a multicenter cohort study. J Hematol Oncol 2023 Nov;16(1):111.
[26] Heipertz EL, Zynda ER, Stav-Noraas TE, Hungler AD, Boucher SE, Kaur N, et al. Current Perspectives on "Off-The-Shelf" allogeneic NK and CAR-NK cell therapies. Front Immunol 2021;12:732135.
[27] Ruggeri L, Capanni M, Urbani E, Perruccio K, Shlomchik WD, Tosti A, et al. Effectiveness of donor natural killer cell alloreactivity in mismatched hematopoietic transplants. Science (New York, NY) 2002 Mar;295 (5562):2097–100.
[28] Lamers-Kok N, Panella D, Georgoudaki AM, Liu H, Özkazanc D, Kučerová L, et al. Natural killer cells in clinical development as non-engineered, engineered, and combination therapies. J Hematol Oncol 2022 Nov;15 (1):164.
[29] Ghobadi A, Bachanova V, Patel K, Park JH, Flinn I, Riedell PA, et al. Induced pluripotent stem-cell-derived CD19-directed chimeric antigen receptor natural killer cells in B-cell lymphoma: a phase 1, first-in-human trial. Lancet 2025 Jan;405(10473):127–36.
[30] Lei W, Liu H, Deng W, Chen W, Liang Y, Gao W, et al. Safety and feasibility of 4-1BB co-stimulated CD19-specific CAR-NK cell therapy in refractory/relapsed large B cell lymphoma: a phase 1 trial. Nat Cancer 2025 May;6 (5):786–800.
[31] Liu E, Marin D, Banerjee P, Macapinlac HA, Thompson P, Basar R, et al. Use of CAR-transduced natural killer cells in CD19-positive lymphoid tumors. N Engl J Med 2020 Feb;382(6):545–53.
[32] Jorgensen LV, Christensen EB, Barnkob MB, Barington T. The clinical landscape of CAR NK cells. Exp Hematol Oncol 2025 Mar;14(1):46.
[33] Yu J, Yang Y, Gu Z, Shi M, La Cava A, Liu A. CAR immunotherapy in autoimmune diseases: promises and challenges. Front Immunol 2024; 15:1461102.
[34] Nazarpour R, Zabihi E, Alijanpour E, Abedian Z, Mehdizadeh H, Rahimi F. Optimization of Human peripheral blood mononuclear cells (PBMCs) cryopreservation. Int J Mol Cell Med 2012 Spring;1(2):88–93.
[35] Liu W, Zhao Y, Liu Z, Zhang G, Wu H, Zheng X, et al. Therapeutic effects against high-grade glioblastoma mediated by engineered induced neural stem cells combined with GD2-specific CAR-NK. Cell Oncol (Dordr) 2023;46 (6):1747–62.
[36] Aggarwal S, Pittenger MF. Human mesenchymal stem cells modulate allogeneic immune cell responses. Blood 2005 Feb;105(4):1815–22.
[37] Hirayama AV, Chou CK, Miyazaki T, Steinmetz RN, Di HA, Fraessle SP, et al. A novel polymer-conjugated human IL-15 improves efficacy of CD19-targeted CAR T-cell immunotherapy. Blood Adv 2023 Jun;7(11):2479–93.
[38] Scherlinger M, Nocturne G, Radic M, Launay D, Richez C, Bousso P, et al. CAR T-cell therapy in autoimmune diseases: where are we and where are we going? Lancet Rheumatol 2025 Jun;7(6):e434–47.

Ann Rheum Dis 84 (2025) 1822–1835

Contents lists available at ScienceDirect

Annals of the Rheumatic Diseases

journal homepage: https://www.sciencedirect.com/journal/annals-of-the-rheumatic-diseases

Sjögren's syndrome

Transcriptomic profiling of Sjögren's disease salivary glands identifies signatures associated with both follicular and extrafollicular responses linked to rheumatoid factor and anti-La/SSB seropositivity

Elena Pontarini[1,*], Davide Lucchesi[1], Elisabetta Sciacca[1], Giulia Cavallaro[2], Qingxuan Song[3], David Galbraith[3], Elizabeth Thomas[3], Annalisa Marino[4], Nurhan Sutcliffe[5], Anwar R. Tappuni[5,6], Roberto Giacomelli[4], Alfredo Pulvirenti[7], Simon J. Bowman[8], Ling-Yang Hao[3], Kathy Sivils[3], Costantino Pitzalis[1,5], Myles J. Lewis[1,5], Michele Bombardieri[1,5]

[1] *Department of Experimental Medicine and Rheumatology, William Harvey Research Institute, Queen Mary University of London, London, UK*
[2] *Istituto Oncologico Mediterraneo, Viagrande, Catania, Italy*
[3] *Janssen Pharmaceuticals, Immunology Translational Science Division, Spring House, PA, USA*
[4] *Rheumatology and Immunology Unit, Department of Medicine, Campus Biomedico, Rome, Italy*
[5] *Barts Health NHS Trust, London, UK*
[6] *Centre of Oral Immunobiology and Regenerative Medicine, Institute of Dentistry, Queen Mary University of London, London, UK*
[7] *Department of Clinical and Experimental Medicine, Bioinformatics Unit, University of Catania, Catania, Italy*
[8] *Rheumatology Department, University Hospitals Birmingham NHS Foundation Trust, Birmingham, UK*

ARTICLE INFO

Article history:
Received 11 March 2025
Received in revised form 20 July 2025
Accepted 22 July 2025

Handling editor Josef S Smolen

ABSTRACT

Objectives: This study aims to identify salivary gland (SG) transcriptomic signatures associated with peripheral and histological biomarkers of disease activity and lymphoma risk factors to inform on Sjögren's disease (SjD) stratification.

Methods: Bulk RNA-sequencing of labial SG from exploratory Queen Mary University of London (QMUL) cohort (SjD [$n = 55$] and non specific-chronic-sialadenitis [sicca, $n = 44$]) and trial for anti-B-cell therapy in Sjogren's syndrome (TRACTISS)validation cohort (SjD, $n = 29$) analysed integrating transcriptomic, clinical, serological, and histological data.

Results: Unsupervised gene clustering confirmed clear transcriptome segregation between sicca and SjD. The most differentially expressed genes were either common to all SjD's versus sicca or specific to SjD's glands with lymphocytic infiltrates with features of ectopic lymphoid structures (ELS). In SjD, principal component analysis identified a significant proportion of variability associated with rheumatoid factor (RF)-seropositivity, exceeding that associated with SG-ELS and anti-Ro/Sjögren's syndrome antigen-A (SSA) seropositivity. Transcriptomes of SjD-SG with ELS from patients with positivity for either RF, anti-Ro/SSA, and anti-La/SSB showed mainly genes associated with germinal centre formation. Conversely, SG without ELS from patients with

*Correspondence to Dr Elena Pontarini.
E-mail address: e.pontarini@qmul.ac.uk (E. Pontarini).
Elena Pontarini and Davide Lucchesi contributed equally to this work as first authors.
Myles J. Lewis and Michele Bombardieri contributed equally to this work as senior authors.

https://doi.org/10.1016/j.ard.2025.07.021

either RF or double anti-Ro (SSA)/anti-La (SSB) seropositivity (unlike patients with seronegative or single anti-Ro/SSA seropositivity) displayed a unique extrafollicular B-cell gene set associated with type-I interferon (IFN), through the retinoic acid-inducible gene-I (RIG-1) endogenous RNAs (including viral) sensing pathway and E3-ubiquitin ligases. The identified IFN genes showed strong positive correlations with serum RF levels in 2 independent cohorts (QMUL and TRACTISS).

Conclusions: Comprehensive SG bulk-RNA sequencing provided the first transcriptomic evidence of distinct RF and anti-La/SSB-driven SG transcriptomic signatures in patients with SjD with and without ELS. These findings suggest that both classical follicular and extrafollicular viral-associated responses contribute to the selection of autoreactive B-cells in the glands of patients with SjD.

INTRODUCTION

Sjögren's disease (SjD) is a systemic autoimmune disease that targets preferentially the exocrine glands, in particular lacrimal and salivary glands (SG) [1], leading to dry mouth and dry eyes. Besides exocrine symptoms, SjD can cause systemic manifestations and confer an increased risk to develop mucosa-associated lymphoid tissue B-cell lymphoma (MALT-L) [1]. Together with circulating autoantibodies, focal lymphocytic infiltrates in the SG, which can acquire features of ectopic lymphoid structures (ELS), are the hallmarks of the disease [2]. The disease pathobiology and the mechanisms leading to ELS formation and MALT-L are still poorly understood [3–6]. In addition to classical clinical predictors of lymphomagenesis, the presence of circulating rheumatoid factor (RF), anti-La/SSB, and the development of ELS forming ectopic germinal centres (GCs) are independent risk factors for lymphoma [7–9] with at least 40% of parotid MALT-L arising from RF-producing B-cells [10]. While the prevalence of RF-seropositivity is higher in patients with SjD with ectopic GC [11], there is evidence from experimental models of autoimmunity that RF-producing B-cells can be activated also at extrafollicular sites [12,13]. The definition of ELS and ectopic GCs is based on the histopathological assessment of SG biopsies, which is prone to the intrinsic bias of interpretation [14]; conversely, bulk transcriptomic profiling of SG biopsies has recently emerged as a powerful tool to better elucidate the molecular diversity underlying the pathogenesis of SjD [15–22]. However, currently published studies are limited by the relatively small number of SG biopsies analysed [23,24].

Here, we report a comprehensive analysis of the largest SG RNAseq of SjD and non-specific-chronic-sialadenitis (sicca) to date. By integrating peripheral and histological biomarkers, including independent lymphoma risk factors, we identified novel molecular endotypes of SjD underlying disease heterogeneity with the potential to redefine disease taxonomy.

MATERIAL AND METHODS

Patients' samples

Labial SG biopsies were collected after informed consent from patients with non-specific-chronic-sialadenitis (sicca) (n = 44) or SjD (n = 55), according to the 2016 American College of Rheumatology (ACR)/European League Against Rheumatism (EULAR) classification criteria [25]. The study was approved by the ethics committee: REC 05/Q0702/1-Rheumatology/Oral medicine clinic-Queen Mary University of London (QMUL). The demographic, clinical, and histological characteristics are summarised in Table. Of the 99 SG samples, 6 were excluded (5 due to buccal tissue contamination and 1 due to a diagnosis of lymphoma). The histology/bulk RNAseq from baseline SG labial biopsies (n = 29) from the TRACTISS randomised clinical trial cohort was used as a validation cohort [26].

Histological assessment of labial SGs

For histological analysis, formalin-fixed and paraffin-embedded tissue sections were used (3 μm). Focus score was calculated on haematoxylin/eosin staining using digital image analysis as previously described [27]. The inflammatory infiltrate identification and organisation were based on the immunohistochemistry/fluorescence staining for B-cells (CD20+), T-cells (CD3+),

Table
Demographic, clinical, and laboratory parameters

Cohort	Sicca (n = 42)	Sjögren (n = 52)	*Sjogren*	
			Sjögren ELS POS (n = 25)	Sjögren ELS NEG (n = 23)
Sex (F/M)	37F 5M	44F 8M	21F 4M	19F 4M
Age (y), mean (median) (SD)	56.62 (56.50) 13.02	55.04 (55.00) 13.26	54.88 (56.00) 14.36	54.70 (52.00) 12.23
Disease duration (y), mean (median) (SD)	4.65 (2.00) 5.34	7.26 (6.00) 6.13	5.30 (4.00) 4.70	9.00 (7.00) 7.22
ESSDAI at biopsy, mean (median) (SD)	/	6.07 (5.00) 5.03	6.77 (5.50) 5.77	5.95 (5.50) 4.16
Serology				
Anti-Ro (Ro/SSA) positive of total (%)	0/42 (0%)	33/52 (63.46%)	15/25 (60.00%)	16/23 (69.57%)
Anti-La (La/SSB) positive of total (%)	0/42(0%)	22/52 (42.31%)	11/25 (44.00%)	9/23 (39.13%)
Rheumatoid factor (RF-IgM) positive of total (%)	2/37 (5.41%)	26/48 (54.17%)	16/23 (69.57%)	7/21 (33.33%)
Antinuclear antibody (ANA) positive of total (%)	12/41 (29.27%)	30/38 (78.95%)	20/22 (90.91%)	9/14 (64.29%)
Serum IgG (g/L), mean (median) (SD)	11.01 (11.20) 2.57	15.73 (14.00) 7.20	16.38 (14.55) 8.71	14.69 (13.50) 5.45
Serum IgA (g/L), mean (median) (SD)	2.75 (2.30) 2.83	2.94 (2.43) 1.63	3.17 (2.23) 1.97	2.77 (2.59) 1.31
Serum IgM (g/L), mean (median) (SD)	1.30 (1.06) 0.80	1.72 (1.18) 2.31	1.91 (1.22) 3.09	1.26 (1.06) 0.64
Serum C3 (g/L), mean (median) (SD)	1.29 (1.31) 0.21	1.23 (1.20) 0.28	1.14 (1.14) 0.23	1.31 (1.25) 0.33
Serum C4 (g/L), mean (median) (SD)	0.29 (0.27) 0.09	0.25 (0.26) 0.11	0.24 (0.23) 0.10	0.27 (0.26) 0.13
Histology				
Focus score	/	1.09 (0.86) 0.99	1.72 (1.37) 1.00	0.49 (0.43) 0.49
ELS negative/positive/NA	/	23/25/4	/	/

ELS, ectopic lymphoid structures; ESSDAI, EULAR Sjögren's syndrome disease activity index; NA, not available; NEG, negative; POS, positive; SSA, Sjögren's syndrome antigen A; SSB Sjögren's syndrome antigen B.

follicular dendritic cell network (FDCs) (CD21+), and plasma cells (CD138+), as previously described [26,28].

RNA isolation and RNA-sequencing

Labial SG lobules, stored in RNAlater solution, were extracted with RNeasy Micro Kit (Qiagen), quantified, and checked for integrity using Qubit-2.0 Fluorometer (Invitrogen) and TapeStation (Agilent Technologies), respectively. Total RNA (500 ng per sample) was outsourced for bulk mRNA sequencing.

RNA-sequencing libraries were prepared with KAPA Stranded RNA-Seq Kits with RiboErase (HMR) for NovaSeq platform. mRNA was first enriched with Oligod(T) beads, fragmented for 15 minutes at 94°C, following first-strand and second-strand cDNA synthesis; cDNA fragments were end-repaired and adenylated at 3'ends, and universal adapters were ligated to cDNA fragments, followed by index addition and library enrichment by PCR with limited cycles. The sequencing library was validated on TapeStation and quantified with Qubit 2.0 Fluorometer and quantitative PCR (KAPA Biosystems). Libraries were sequenced on Illumina NovaSeq 6000, using 2 × 100 bp paired-end configuration, 50 million reads/sample. One mismatch was allowed for index sequence identification.

Transcriptomic analysis: differentially expressed gene, pathway analysis, enrichment, and estimating cell-type enrichment analyses

RNA-sequencing (RNA-seq) data were analysed with R (v.4.2.1) within RStudio (v1.2.5042). Principal component analysis (PCA) was performed with PCAtools (v2.8.0) and pcaExplorer (v2.22.0), identifying the most influential loadings using linear regression for continuous variables and analysis of variance test for categorical variables. The DESeq2 R-pipeline (v1.36.0) was used to extract differentially expressed genes (DEGs) between sicca and SjD and within SjD subgroups (eg, ELS±, RF±). Only protein-coding genes were kept for the analysis, and the linear model was adjusted using gender as a covariate, as for previous evidence of gender-driven differences in SjD-SG transcriptomic [26]. Variance stabilising transform normalised gene expression levels were used to draw heatmaps and volcano plots, via the ComplexHeatmap (v2.6.2) and ggplot2 (V3.3.6) R packages, respectively. Pathways and gene ontologies (GO) associated with DEGs were derived through EnrichR (v3.0) [29] from the GO/pathway library GO_Biological_Processes_2018. Co-expressed module genes were identified via CEMItool (v1.20.0), using it for plotting module expression heatmaps, interaction networks, and pathways. Cell-type abundance in the SG was determined using xCell package (v1.1.0) [30]. The radial volcano plots were generated as previously reported [31]. Relative log expression counts were *Z*-score normalised and mean *Z*-scores calculated for the 3 pathotype groups (ELS+, ELS−, sicca) for each gene. This 3-dimensional data were reduced to 2-dimensional polar coordinate system analogous to colour space conversion of red, green, blue colour space to hue, saturation, value allowing the mapping of ELS+, ELS−, and sicca vectors to 3 axes in the horizontal plane. Genes with false discovery rate (FDR)-adjusted *P* value for likelihood ratio test <.05 were considered significant. Significant genes were colour-coded based on pairwise statistical tests using the minimum group mean as reference. Gene signature scores were calculated using the hacksig package (v0.1.2) [32].

Data sharing statement

The RNA-seq data generated and analysed for the current study are available on an interactive web interface for direct data exploration: https://sjogren.hpc.qmul.ac.uk/. The datasets can be downloaded from https://doi.org/10.6084/m9.figshare.29211473.

RESULTS

Transcriptomic profile distinguishes sicca and Sjögren's SG

Transcriptomic profiles of labial SG biopsies from patients with SjD and sicca were first compared, looking at the potential molecular disease drivers. The DEGs analysis between SjD and sicca SGs (Supplementary Table S1) identified 1749 genes upregulated and 698 downregulated in SjD versus sicca (adjusted *P* value < .01). In Figure 1A, the top upregulated (adjusted *P* value $< 10^{-14}$ and log2 [fold-change] > 2, coloured in gold) and downregulated (adjusted *P* value $< 10^{-5}$ and log2 [fold-change] < 0, coloured in blue) genes for each group are annotated. As expected, SjD-SGs showed an upregulation of genes associated with recruitment of immune cells, such as chemokine receptors and their ligands (*CCR7-CXCL9, CXCL13-CXCR5*), and adaptive immune cell activation (eg, *CD19, CR2, FCRL3, FCRL4*, IL21R, *MS4A1, PAX5, SLAMF6, TLR10*), when compared to sicca SG (Fig 1A). Activated CD4+ T-cells upregulate CCR7 expression facilitating infiltration to the SG, where they differentiate into Th1, Th17 cells, and T-follicular helper cells (Tfh) upon interaction with B-cells (expressing *CD19*, and *MS4A1* encoding for CD20) recruited to the gland via the CXCL13/CXCR5 axis. Tfh cells are pivotal to the local GC reaction that leads to B-cell maturation and plasma cell differentiation (*IL21R, PAX5, CR2, CXCR5*) [33] within SG.

When performing over-representation analysis on the top upregulated genes in SjD-SG transcriptome compared to sicca (adjusted *P* value < .05, log2[fold-change] > 0), we found an enrichment in pathways involving T and B-cells activation (Fig 1B), confirming a strong immunomediated response taking place in SjD-SG, in line with previous published RNAseq analysis in SjD and sicca SGs [23,24]. In particular, over-representation analysis confirmed the activation of pathways associated with immune responses initiated by antigen-presentation via major histocompatibility complex (MHC) molecules, which induces lymphocytes proliferation and differentiation with mainly CD4 + T-cell activation. Risk *loci* in HLA-DR and HLA-DQ regions are known to be associated with SjD [34] and have been linked to a loss of tolerance to self-antigens in the context of autoimmunity. In our cohort as well, *HLA-DRA, HLA-DRB5, HLA-DRB1, HLA-DQA1, HLA-DQB1*, and *HLA-DQB2* genes were all upregulated in SjD versus sicca SG (adjusted *P* value <.001 and log2 [fold-change] > 1.2) (Supplementary Table S1). We also found IL-17-related pathways among the most enriched in SjD, in line with the role of Th17 cells in the formation/maturation of ectopic GCs [35,36].

Genes with higher DEG in sicca group (ie, downregulated in the SjD vs sicca comparison, adjusted *P* value <.05 and log2 [fold-change] < 0) were enriched in pathways associated with negative regulation of cell-cell adhesion, O-glycan processing, and glycoprotein metabolic processes which are necessary for proper SG function including host-mediated defence mechanisms but devoid of immune-related biological functions (Supplementary Fig S1). The unsupervised clustering of the SG transcriptomic profile, selecting genes with adjusted *P* value

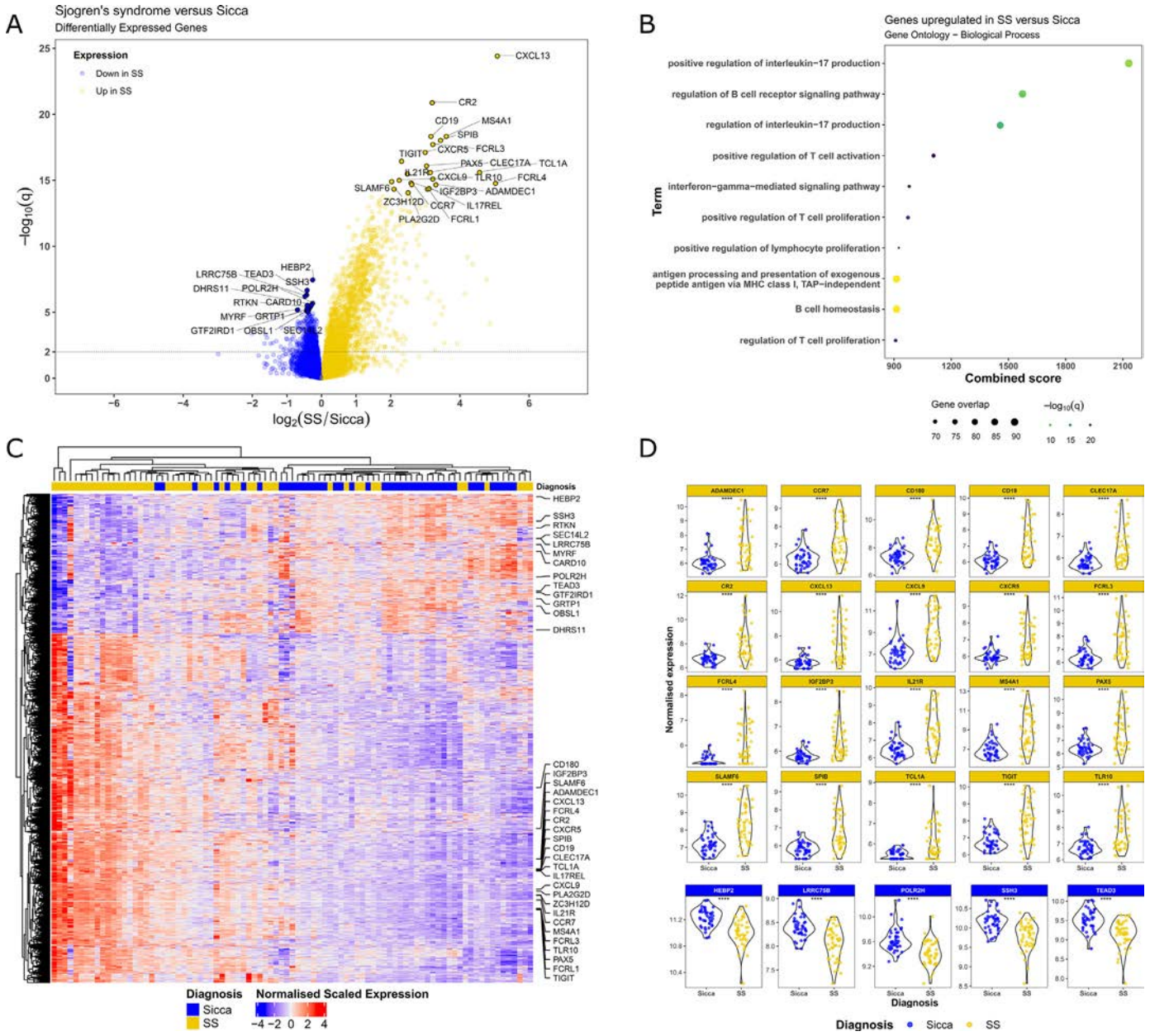

Figure 1. (A) Volcano plots showing differentially expressed genes (DEGs) between sicca (n = 42) and Sjögren's disease (SjD) (n = 51) salivary gland (SG) biopsies. Gold-coloured dots represent genes upregulated in SjD versus sicca (blue-coloured dots). Top upregulated (adjusted P value $< 10^{-14}$, log2 [fold-change] > 2) and downregulated genes (adjusted P value $<10^{-5}$, log2 [fold-change] < 0) are annotated. The dotted line corresponds to adjusted P value = .01. (B) Enricher over-representation pathway analysis using top upregulated genes in the SjD versus sicca comparison (adjusted P value <.05) against the gene ontology (GO)-biological process database. Resulting enriched pathways were filtered for an enrichment-adjusted P value < .01 (colour coded). Dot sizes are proportional to the overlap between the number of pathway-matching genes queried and those included in the pathway. (C) Unsupervised heatmap of the most DEGs (adjusted P value <.01) from the SjD versus sicca comparison (annotated genes as in panel A), and (D) their expression level (adjusted P value <.0001 marked as ****, as calculated by DeSeq2).

<.01, shows a clear segregation between the 2 diagnoses (Fig 1C). The same most upregulated and downregulated genes in SjD compared to sicca annotated in Figure 1A were reported in the heatmap in Figure 1C and the expression of selected individual genes in Figure 1D.

Overall, these results confirm that transcriptomics profiling involving key immune activation pathways can clearly distinguish SjD from sicca SGs.

Sjögren-specific genes in SG with and without ELS

The SjD-SGs were classified based on the histological evidence of ELS, defined as large periductal *foci* (over 50 lymphocytes) displaying clear B and T-cell segregation and CD21 + FDC network within the B-cell aggregates (Fig 2A), as originally described by Barone et al [28]. To confirm and further quantify differences in the SG cell infiltrate at the transcriptomic level in sicca, SjD -ELS−, and SjD -ELS+ groups we used XCell cell-enrichment analysis, as previously described [26]. As expected, the SjD-ELS+ group exhibited substantial immune cell enrichment compared to both sicca and SjD-ELS− SG, whereas the SjD-ELS− group showed only minimal immune cell enrichment relative to sicca. Notably, the enrichment of T-helper cells observed in SjD-ELS+ was accompanied by increased memory class-switched B-cells and activated DC, along with associated plasma cell enrichment (Fig 2B, Supplementary Fig S2A). This pattern reflects the development of functional GCs that support the maturation of autoreactive plasma cells. These findings

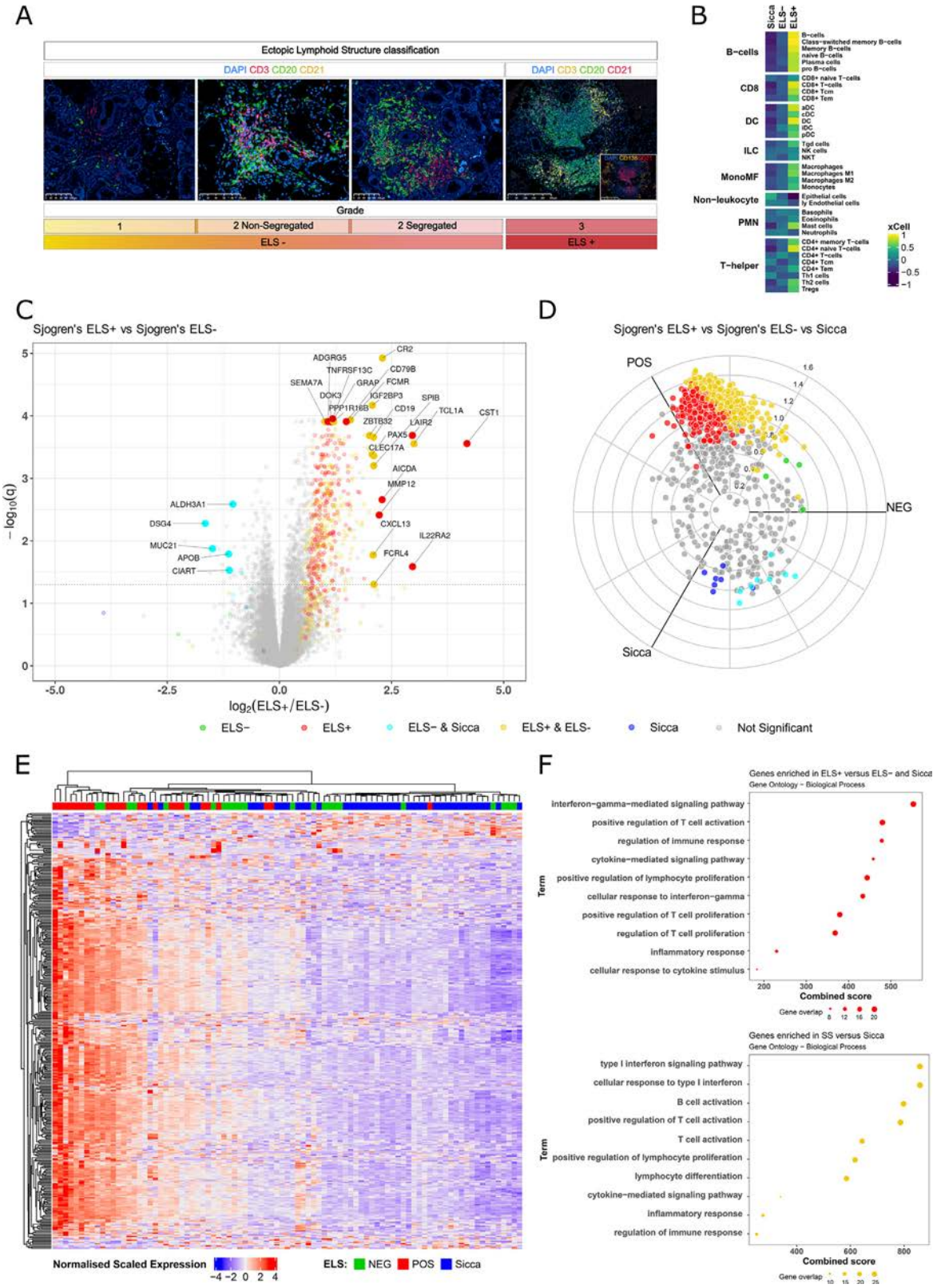

Figure 2. (A) Representative histological images showing semiquantitative grading for the evaluation of the aggregate organisation for the ectopic lymphoid structures (ELS) classification. (B) Heatmap for the average xCell-score for each immune cell types for sicca, Sjögren's disease (SjD)-ELS+, and ELS− salivary glands (SGs). (C) Volcano plot showing differentially expressed genes (DEGs) in SjD between ELS− and ELS+ SG biopsies. DEGs in ELS+ versus ELS− are shown above the dotted line corresponding to adjusted *P* value = .05. In addition, significant genes were colour-coded based on pairwise statistical tests using the minimum group mean as reference. Genes which were significantly upregulated in one group alone were coloured using red for SjD-ELS+ (n = 22), green for SjD-ELS− (n = 21) and blue for sicca (n = 42). Genes upregulated in 2 groups compared to the minimum reference group were depicted using gold for 'SjD-ELS+ & ELS-' (vs sicca) and cyan for 'SjD-ELS− & sicca' (vs SjD-ELS+). Nonsignificant genes were coloured in grey. Significant genes for the pairwise tests with adjusted *P* value <.05 and |log2(fold-change)| > 1 were annotated and plotted in solid colours. (D) Three-way volcano plot of DEGs between ELS+ SG, ELS− SG and sicca groups. Vectors for pathotype mean *Z*-score per gene were projected onto a polar coordinate space. SjD-ELS+, SjD-ELS− and sicca SG vectors are mapped to 3 axes (POS, NEG, and Sicca, respectively), using polar coordinates in the horizontal plane. Colour-coding as described in (A). (E) Unsupervised heatmap with DEGs (adjusted *P* value < .05, fold change

confirm the expected cellular infiltration between ELS+ and ELS− SjD SG [2], further validating the reliability of transcriptomic cell-enrichment analysis.

We then compared the SG transcriptomic profile of the 3 groups (SjD-ELS+, SjD-ELS− and sicca) using FDR-adjusted likelihood ratio test and pairwise group tests for differential expression, as previously reported [31]. In Figure 2C, DEGs between SjD-ELS+ and ELS− are visualised using a standard volcano plot and colour-coded based on the multiple pairwise comparison (ELS+ vs sicca and ELS− vs sicca volcano plots are reported in Supplementary Fig S2B). However, due to the 3-way nature of the analysis, visualisation on 2 axes makes data interpretation difficult. In alternative, a radial geometry was used to visualise the 3-way comparison. By doing so, the polar angle of each gene directly conveys the degree to which a gene is associated with one or more groups (SjD-ELS+, SjD-ELS−, and sicca, DEGs for each pairwise comparison in Supplementary Table S2). This analysis showed that only few genes were specific for ELS− SjD-SG, whereas a greater number of genes were specifically associated to ELS+ SjD glands (Fig 2D). Interestingly, a substantial number of genes were jointly upregulated in both ELS+ and ELS− comparisons, highlighting the presence of a gradient in the level of inflammation within the SjD-SG progressing from sparse unorganised infiltrates (ELS-) to fully formed ectopic GCs. This is also evident when plotting the heatmap for the DEGs for the various pairwise comparisons (adjusted *P* value <.05 and |log2(fold-change)|>1), where the ELS+ and sicca SG form separate clusters with ELS− SG lying between the 2 (Fig 2E).

When running the over-representation analysis using the most DEGs for the various pairwise comparisons among SjD-ELS+, SjD-ELS−, and sicca, we observed further evidence of this 'continuum' among SjD biopsies. Genes differentially upregulated in SjD-ELS+ versus SjD-ELS− and sicca indicated an enrichment in the type-II interferon (IFN-γ) pathway, along with T-cell recruitment and activation associated with a Th1 polarisation (Fig 2F). Type-II interferons were reported alone and/or in combination with IL-21 in SG of patients with SjD by T-follicular helper and T-peripheral helper cells in ELS+ SjD-SG [5]. However, the pathways upregulated in SjD (ELS+ and ELS−), compared to sicca, confirmed the role of type-I interferons as initiator of innate immune response in SjD-SG. In fact, the type-I interferon (IFNα and IFNβ) pathways were the most upregulated in SjD. Type-I interferons are produced by all body cells upon interaction with microbial or self-nucleic acids with membrane-bound or cytosolic pattern-recognition receptors, driving T-cell recruitment and activation first, followed by B-cells, a process well known from the histological [26] and transcriptomic analyses of SjD-SG [23,24].

Of note, when comparing the SG transcriptomic profile of the SjD groups using the focus score (FS), to compare the degree of similarity with the ELS classification, only a partial overlap in the DEGs was observed. As previously reported [11], ELS+ SjD-SG displayed significantly higher FS values compared to ELS− SjD (Table and Supplementary Fig S3A). As expected, although an enrichment in B-cell related gene expression was observed with the increasing FS (Supplementary Fig S3B-E), GC-related genes were better captured by the ELS classification (Fig 2C) compared to the FS classification reflecting the different nature of the 2 classifications with the FS purely assessing focal aggregation while ELS classification also assessing B/T-cell positioning and development of ectopic GC.

We next used the CEMItool R-package to perform weighted Gene Co-expression Network Analysis across the 3 groups (sicca, SjD-ELS− and SjD-ELS+) to identify unique and/or shared gene modules across the spectrum of the SjD and sicca SGs. CEMItool-identified 7 modules across the dataset (Fig 3A), and an interaction network graph analysis was run for the modules specifically associated with SjD-ELS+ (M1), SjD (ELS+ and ELS-) (M7), and sicca (M6) SGs (Fig 3B). Network analysis of module M1 (SjD-ELS+) showed interactions among genes involved in B and T-cell receptor signalling and maturation (eg, *CD79A, CD79B, CARD11, SCIMP*, and *TIGIT*). In module M7, enriched in both ELS− and ELS+ SjD-SG compared to sicca, network analysis highlighted several interactions associated with antiviral response and type-I interferon-related genes (eg, *IRF7, MX1, DDX58, DDX60, OAS1-3*, and *TRIM22*). For module M6, specific to sicca SG, the top interactions were with genes linked to epithelial damage (eg, *LCN2, S100A2*) and homeostasis (eg, *TGFB2, MUC1, ERMP1*, and *CLDN1*). The identified gene modules were run against the gene ontology (GO) biological process database using E*nrichr*. Over-representation analysis further confirmed the activation of type-I interferon and antiviral responses pathways for module M7, whereas for module M1, enriched exclusively in SjD-ELS+ SG, the analysis highlighted pathways linked to adaptive immune response activation. The modules enriched in sicca (eg, M6) were associated with pathways linked to the mechanisms regulating the secretory capacity (Fig 3C). These findings align with the DEGs analyses shown in Figure 2.

Sjogren's patients seropositive for RF show a distinctive SG transcriptomic profile

The transcriptome analysis was next restricted to the SjD-SGs only. The PCA was performed to assess the strength of association of clinical, laboratory and histopathology features with the principal components generated from the SjD-SG dataset. Of note, the analysis identified a significant association between serum RF positivity (*IgM isotype*) and the first principal component (PC1, accounting for 34.2% of the variation in the data). Conversely, anti-Ro/SSA positivity was significantly associated with PC4, which contributed only 5% of the variation (Fig 4A). Neither the presence of ELS nor FS grading significantly influenced SG transcriptomic PCs. PCA loading analysis for PC1 showed that the top loading genes were linked to B-cell recruitment, differentiation and activation in the GC reaction (eg, *PAX5, CXCL13*, and *MS4A1*), and to type-I IFN activation (Fig 4B, left side) upon mononuclear cell infiltration (eg, *FCRL1, 2, 3* and *5, MMP9, PARP15*) [37]. Fc-receptor ligands (FCRL) are preferentially expressed in mature B-cells, with FCRL 2, 3, and 5 mainly upregulated on clonal CD21−/low marginal-zone B-cells. Matrix metalloproteinase-9 (MMP-9) was described as upregulated in SjD-SGs, where an imbalance between MMPs

> 1) from the 3-way comparisons between sicca, SjD-ELS− and SjD-ELS+. The distance between cluster pairs is defined as the Euclidean distance, complete clustering. (F) Enricher over-representation pathway analysis using top upregulated genes (FDR-adjusted *P* value <.05, log2FC > 1) in ELS+ and ELS− group (top) and in ELS+ only group (bottom) against the gene ontology (GO)-biological process database. Resulting enriched pathways were filtered for an enrichment-adjusted *P* value < .01 (colour coded). Dot sizes are proportional to the overlap between the number of pathway-matching genes queried and those included in the pathway.

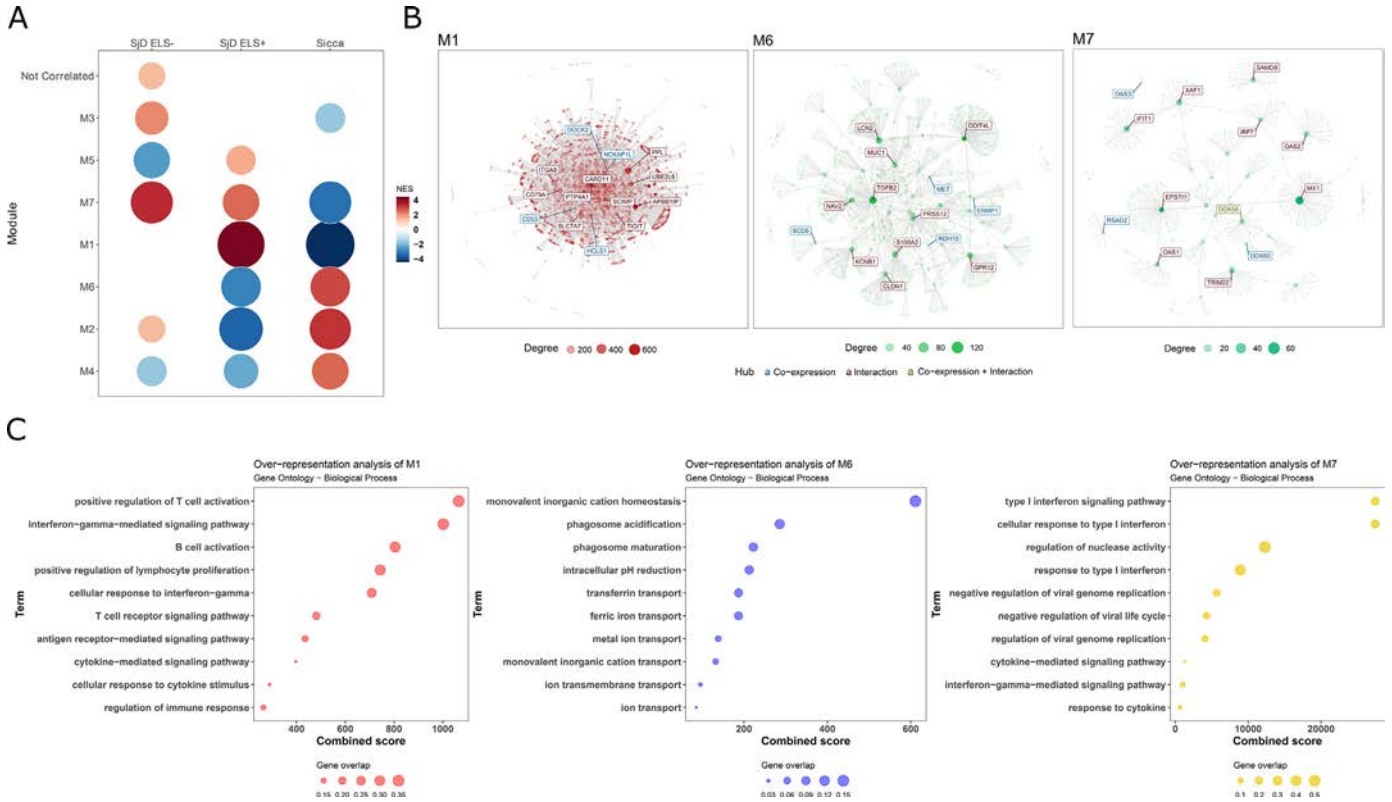

Figure 3. (A) Plot of the normalised enrichment score (NES) for expressed gene modules as generated by CEMItool in sicca and patients with Sjögren's disease (SjD) with histological presence (POS) or absence (NEG) of ectopic lymphoid structures within salivary gland (SG) biopsy (size and colour of the dots proportional to the NES). (B) Interaction network graph for selected modules (M1, M6, M7). Labelled genes represent the most connected genes (hubs). Blue labels genes are those originally part of the module, while red labels indicate adjacent genes connected by network interaction. The size of the node is proportional to its degree of connectedness. (C) Enricher over-representation pathway analysis using CEMItool-identified module genes against the gene ontology (GO)-biological process database. Resulting enriched pathways were filtered for an enrichment-adjusted *P* value < .01 (colour coded). Dot sizes are proportional to the overlap between the number of pathway-matching genes queried and those included in the pathway.

and their inhibitors is associated with acinar damage [38]. Additionally, type-I IFN has been reported to induce PARP9 expression, which, along with PARP15, stimulates CXCL10, thereby promoting mononuclear cell infiltration in SjD [39]. PCA loading analysis for PC4 and their expression level are reported in Figure 4B (right side), and Supplementary Fig S4A.

Furthermore, the genes identified as top loadings of PC1 were significantly upregulated in SG of RF-seropositive versus seronegative SjD patients (Fig 4C), but not in Ro/SSA or La/SSB seropositive versus seronegative patients (Fig 4D). Interestingly, and in line with the findings above, RF seropositivity appeared to better cluster the PCA plot when compared to histological positivity for ELS in the SG, or anti-Ro/SSA and anti-La/SSB autoantibodies (Fig 4E and Supplementary Fig S4B).

Autoantibody seropositivity and ELS define SG gene signatures of functional GC and extrafollicular responses

Building on the above observations, we sought to understand whether seropositivity for RF and other SjD-associated autoantibodies was dependent on the SG-ELS or if both ELS-dependent and ELS-independent gene signatures could be identified in the SjD-SG.

Notably, in the present cohort, 40% of patients with SjD exhibit overlapping seropositivity for RF, anti-Ro/SSA, and anti-La/SSB, with complete overlap between anti-Ro/SSA and anti-La/SSB positivity. Most of these patients show reactivity to both anti-Ro52 and anti-Ro60 (Fig 5A,B, Supplementary Table S3).

We analysed the gene expression of patients with SjD stratified by the combined ELS and autoantibody seropositivity. The RF seropositivity and histological evidence of ELS defined 4 groups: ELS+/RF+, ELS-/RF+, ELS−/RF−, and ELS+/RF−. The same was applied for anti-Ro/SSA and anti-La/SSB seropositivity (Fig 5C,D).

The average expression of selected genes identified through interaction analysis (top interactor for modules M1 and M7 in Fig 3), as well as genes associated with humoral response, B/T-cell interaction, and GC formation, was plotted across the SjD subgroups. The number of DEGs identified from these group comparisons is summarised in Supplementary Figure S5A,B.

Within the ELS+ subset, a gene signature typical of functional GC (eg, IL21, CD4, CR2, LTB, CXCR5, AICDA, CD40) clustered with RF seropositivity (also observed with anti-Ro/SSA alone and, to a lesser extent, dual anti-La/SSB and anti-Ro/SSA seropositivity) (Fig 5C,D, Supplementary Fig S5C). Notably, cell-enrichment analysis showed the highest cellular enrichment (primarily DC, T-helper and class-switched memory B-cells) in patient with SjD with both RF seropositivity and ELS within SGs, compared to those with either ELS or RF alone (Supplementary Fig S5D,E). This supports the association between RF positivity and ectopic GC activity within ELS+ SGs.

By contrast, RF-seropositive SjD patients without ELS exhibited a distinct gene signature characterised by the overexpression of genes involved in endogenous RNAs (including viral) sensing through the retinoic acid-inducible gene-I (RIG-I) pathway (DDX58, DHX58), activation of E3 ubiquitin ligase activity (TRIM25, TRIM56, TRIM22), and downstream interferon-

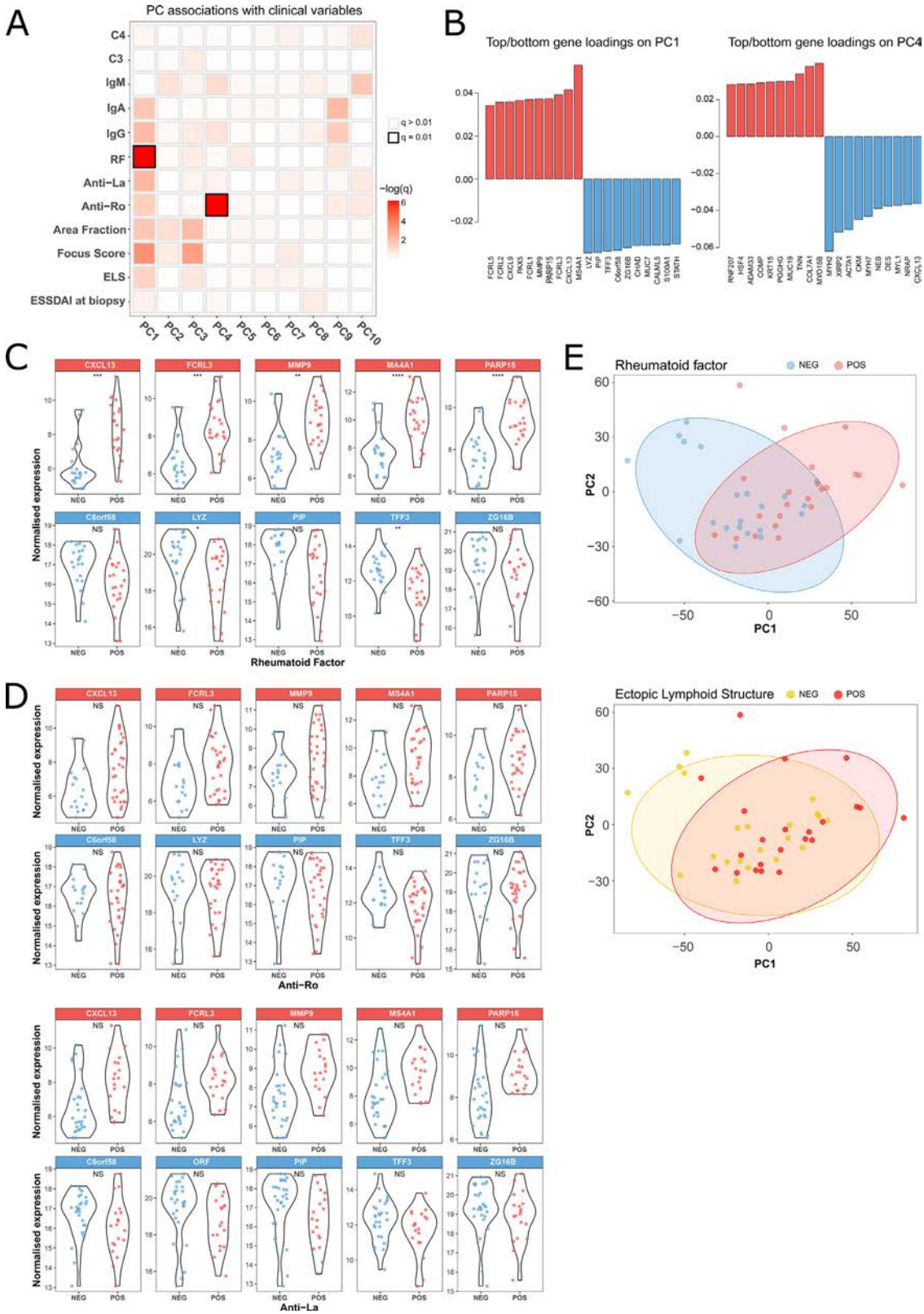

Figure 4. (A) Tile plot displaying the association between the top 10 principal components (PCs) of transcriptomic data and clinical variables. Black outlined tiles show significant correlations (adjusted *P* value<.01). (B) Top (red) and bottom (blue) loadings plot for the 20 genes that have the largest effect on PC1 and PC4. (C, D) Boxplot for the normalised expression levels of the top 5 (red) and bottom 5 (blue) loading genes for PC1 in patients with SjD, compared by rheumatoid factor (RF) seropositivity (C) or anti-Ro/SSA and anti-La/SSB seropositivity (D). Adjusted *P* value, as calculated by DeSeq2, is shown (* = adjusted *P* <.05, ** = adjusted *P* <.01, *** = adjusted *P* <.001, *** = adjusted *P* <.0001, ns = not significant). (E) Scatterplot for PC1 and PC2 colouring by groups for RF-seropositivity (top panel) or ectopic lymphoid structures (ELS) presence (bottom panel). Ellipses show 95% confidence interval of the distribution of every group.

induced antiviral responses (IRF7, STAT2, PARP14, OAS3, RSAD2, MX2, and RNF213) (Fig 5C,F, Supplementary Fig S5C). Cell-enrichment analysis showed an intermediate SG transcriptomic profile, marked by the enrichment of both activated DCs and switched memory B-cell compartments, suggesting an alternative RF-driven response independent of ELS (Supplementary Fig S5D-E). Consistently, type-I IFN gene module was closely associated with RF positivity, irrespectively from ELS status,

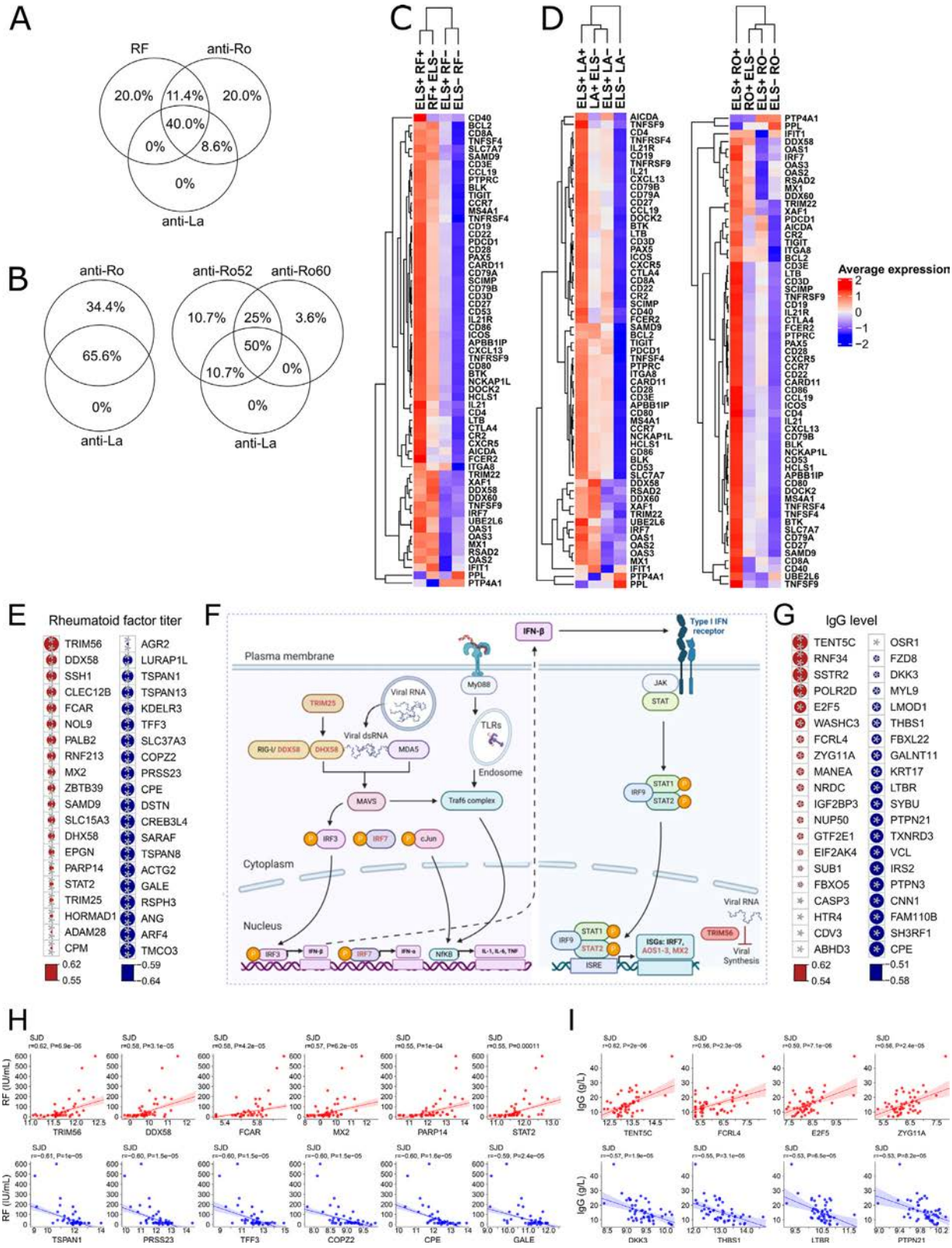

Figure 5. Venn diagram showing the seropositivity overlap of (A) rheumatoid factor (RF) with anti-Ro/SSA and anti-La/SSB, (B) anti-Ro/SSA and anti-La/SSB, and between anti-Ro52, anti-Ro60 and anti-La/SSB. (C, D) Heatmaps for the average normalised expression of genes upregulated in Sjögren's disease (SjD)-salivary glands (SGs) and the most connected genes from CEMItool modules M1 and M7 interaction analysis, grouped by histological evidence of ectopic lymphoid structures (ELS) combined with RF seropositivity (C) or anti-La/SSB and anti-Ro/SSA seropositivity (D). Correlation matrix of the top 20 genes (false discovery rate [FDR] < 0.05) correlating positively and negatively with (E) serum RF titre and (G) IgG level. The size of the circle encodes for the magnitude of each correlation, while the colour of the dot denotes the value of the Pearson's correlation coefficient (*r*). The *P* values are adjusted for multiple testing with FDR correction and are shown within the dots, when statistically significant. (F) Graphical representation of genes (highlighted in red the genes from correlations in [E]) involved in viral sensing through the retinoic acid-inducible gene-I (RIG-I) pathway and downstream activation of type-I interferon (IFN)-induced and type-I IFN-regulating genes. (H, I) Representative plots of selected correlations (positive correlations in red and negative correlations in blue) shown in the correlation matrixes (E, G).

while type-II IFN gene module appears to be influenced primarily by the presence of ELS (Supplementary Fig S6A,B).

Stratifying patients according to the combined RF seropositivity and ELS presence uncovered a previously undescribed SG gene signature strongly associated with RF or dual anti-La/SSB and anti-Ro/SSA seropositivity, but not anti-Ro/SSA alone, which appeared entirely independent from ELS.

To confirm the identified genes linked to a follicular and extrafollicular autoreactive B-cell responses, an unbiased approach was applied. We looked for the top 20 genes with the strongest positive and the negative correlation with serum RF titre and with IgG level (Fig 5E-I). The interferon-regulating antiviral response genes (DDX58 and its homologue DHX58, MX2, TRIM25) showed the strongest correlation with serum RF titre (Fig 5E,H). Conversely, TENT5C and FCLR4, which primarily drive T-cell independent B-cell response, emerged as the most positively correlated with circulating IgG levels (Fig 5G,I), further supporting the identification of an extrafollicular intra-SG B-cell activation, alongside the classical follicular response in ectopic GCs.

Validation in an independent cohort

To validate the above findings from the single-centre QMUL cohort, we performed a similar analysis in a validation cohort, looking at patients with SjD recruited in the multicentre TRACTISS trial for which SG transcriptomic (bulk RNAseq) from baseline (ie, pretreatment) SG biopsies was available (extended TRACTISS-bulk RNAseq cohort's details are published in [26]). Because anti-Ro/SSA positivity was an inclusion criterion in the TRACTISS trial, the analysis focused on confirming the association/correlation of the identified SG genes with RF titres, IgG levels, and dual anti-La/SSB and anti-Ro/SSA seropositivity. The positive correlation between interferon-regulating antiviral response genes (TRIM25, DDX58, PARP14, IRF7, and OAS3), as well as genes associated with interferon-induced, toll-like receptor (TLR)-mediated extrafollicular B-cell response (TENT5C and FCRL4), with RF titres, anti-La/SSB seropositivity, and IgG (but not IgA or IgM) levels was independently confirmed (Fig 6A-C).

DISCUSSION

The transcriptome of target tissues in autoimmune disorders, including SG biopsies in SjD, has the potential to elucidate the heterogeneity underlying the pathophysiological processes leading to the typical histopathological lesions observed during autoimmune responses [23,24]. Hereby portraying the transcriptomic profile of labial SG biopsies stratifying patients for the degree of lymphoid aggregates organisation and the presence of typical circulating autoantibodies, we identified previously unreported transcriptomic clusters selectively associated with clinically relevant peripheral and histological biomarkers.

The pathophysiological role of ELS as local niches for maturation and differentiation of autoreactive B-cells in autoimmune conditions, such as SjD, is well recognised [2]. In SjD, ELS formation within SG and their functional maturation in ectopic GCs correlate with B-cell hyperactivity, local autoimmunity, and a potentially pathogenic humoral immune response. The definition of ELS and their association with circulating autoantibodies in SjD has so far relied on SG histopathology [11], which bears significant limitations which have hindered its clinical relevance as a reliable tool for patients' stratification [14]. Conversely, molecular pathology analysis through bulk RNA-sequencing applied to rheumatic conditions such as rheumatoid arthritis (RA) synovial tissue proved vastly superior to histopathology in defining disease heterogeneity and taxonomy [31] as well as informing clinical response to targeted therapies through molecular pathology stratification [40,41].

The present transcriptomic analysis (bulk RNA-sequencing) of 99 SG tissues was first performed using 3-way comparison of the sicca and SjD-SGs, with the SjD group further subclassified on the histological evidence of ELS (absence or presence), then combined with autoantibody seropositivity. Of note, only few genes emerged differentially expressed specifically in SjD-SGs without ELS compared to patients with sicca, whereas a greater number of DEG in SG with ELS were jointly upregulated in both, showing a gradient of increased expression from absence to a proper organisation of the inflammatory aggregates into ELS in SjD-SGs. This likely reflects the progressing evolution from sparse T-cells to highly organised B-cell rich follicles typical of ELS [26]. Despite any attempt at a dichotomic classification for the presence or absence of ELS, each group bears inevitably a certain degree of heterogeneity; accordingly, the application of the marker-gene-based approach that we reported here confirmed the variability in the relative content of infiltrating immune cell subsets in line with a gradient of immune cell organisation which is difficult to appreciate by SG histopathology.

Surprisingly, when we restricted our analysis to SjD-SGs to identify drivers of transcriptional heterogeneity, the PCA identified serum RF as the variable responsible for the largest variance in the SjD-SG transcriptomic, rather than FS, ELS or other serological markers (eg, anti-Ro/SSA). This suggested that the nature of the autoreactivity of the infiltrating cells, rather than their histological organisation, defined either as total aggregation (FS) or as lymphoid organisation (ELS), is a primary driver of molecular heterogeneity. Looking at the genes responsible for most of the variance (PC1 loadings), the genes were mainly linked to B-cell differentiation, recruitment, and activation (PAX5, CXCL13, MS4A1), alongside Fc receptor-like (FCRL1, FCRL2, FCRL3, FCRL5) proteins. While FCRL proteins are preferentially and differently expressed in mature B-cells at various differentiation stages, FCRL proteins 2, 3, and 5 are increased on clonal CD21$^{neg/low}$ marginal-zone B-cells [42]. This is of particular interest, as MALT lymphoma in SjD arises from post-GC B-cells with a marginal-zone phenotype often bearing RF autoreactivity [10]. RF seropositivity was also associated with the highest cellular enrichment (dendritic cells (DC), T-helper, and class-switched memory B-cells) and a cluster of GC-related genes in patients with SjD with combined RF seropositivity and ELS. This evidence confirms previous meta-analysis identifying RF seropositivity as the main peripheral biomarkers associated with ectopic GCs in SjD-SG [43]. When analysing the ELS+ population further stratified for autoantibody seropositivity, we demonstrated that ELS+ with either RF, anti-Ro/SSA alone and to a lesser extent dual anti-La/SSB and anti-Ro/SSA seropositivity show a strong expression of genes typically involved in functional T-cell dependent ectopic GC responses (IL21, CR2, LTB, CXCR5, AICDA, CD40, and CD4). On contrary, seronegative SjD with ELS displayed a SG gene profile compatible with immature follicular responses. Whether these represent evolutionary stages of ELS remains unclear and would require longitudinal studies.

The most novel and interesting observation of our studies was the identification of an SG gene signature strongly associated with RF and anti-La/SSB seropositivity which appears independent from follicular B-cell response and driven by a unique set of genes associated with endogenous RNAs (including viral) sensing through the RIG-I pathway and downstream activation

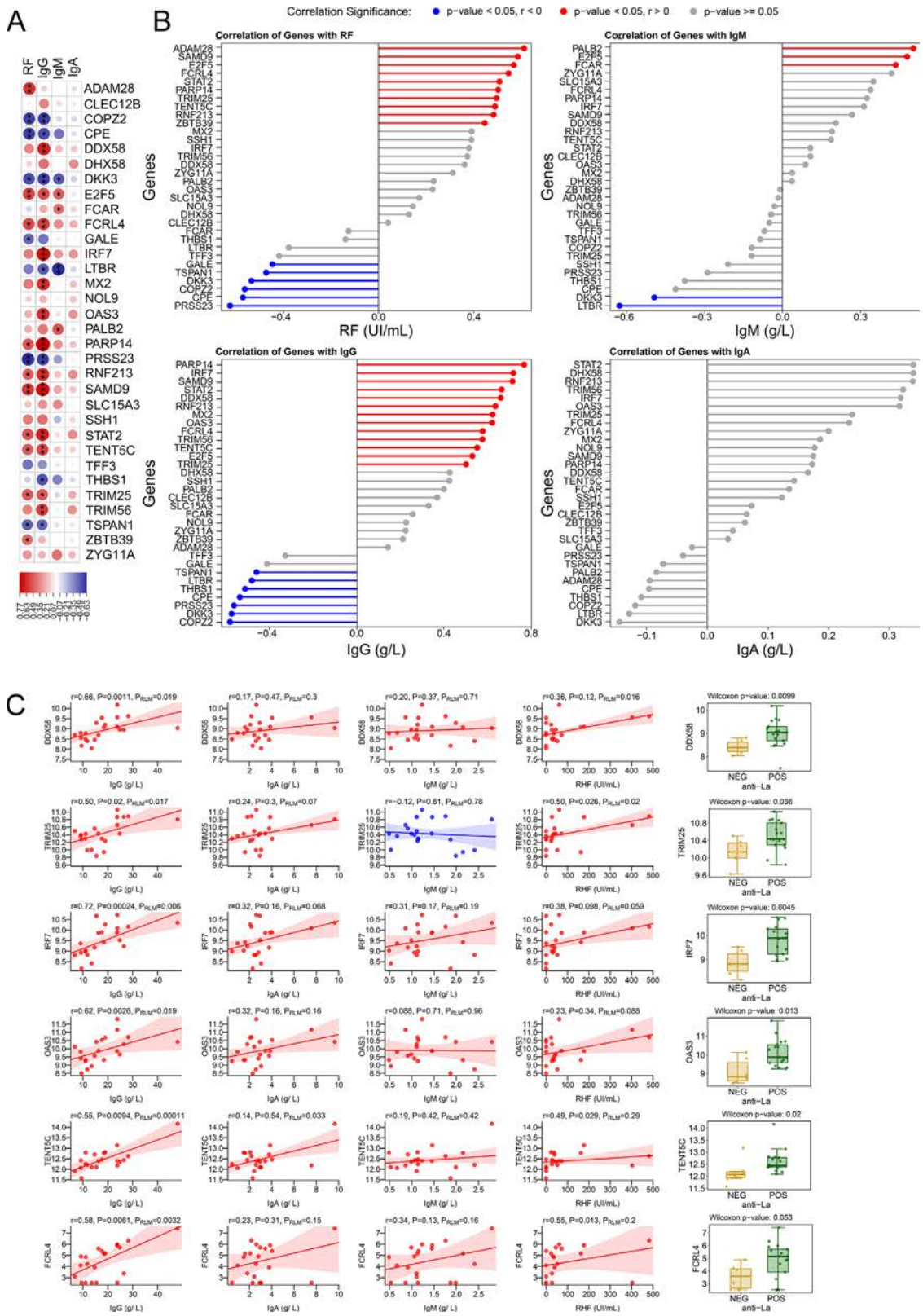

Figure 6. TRACTISS-validation cohort. (A) Correlation matrix and (B) lollipop plots showing the correlation of salivary gland (SG) gene expression with serum rheumatoid factor (RF) titre, IgG, IgM, and IgA level. In the correlation matrix, the size of the circle encodes for the magnitude of each correlation, while the colour of the dot denotes the value of the Pearson's correlation coefficient (*r*). The *P* values are adjusted for multiple testing with false discovery rate (FDR) correction and are shown within the dots, when statistically significant. (C) Individual correlation plots of selected genes and serum RF titre, IgG, IgA, and IgM level. Pearson correlation coefficient (*r*), *P* value, and the *P* value for regression linear model are shown. The boxplots show the median values for each gene in SjD-SGs segregated for anti-La seropositivity. The vertical size of the boxes is the interquartile range (IQR). The *P* value of unpaired Wilcoxon tests is shown on top of each boxplot.

of type-I IFN-induced/regulating genes. Although virus-driven responses could not be directly assessed, the RIG-I pathway is involved in sensing endogenous RNAs and also plays a role in viral RNA recognition, with viral involvement considered a potential factor in SjD pathology. RIG-I and its homologue (encoded by DDX58 and DHX58 genes, respectively, both highly correlated with RF and anti-La/SSB), together with MDA5 and LGP2, is part of a family of key cytosolic sensors of virus

infection recognising primarily viral RNAs by sensing 5' triphosphate groups through the helicase and carboxy-terminal domains [44,45]. RIG-I is strongly expressed in epithelial and infiltrating immune cells in the SG of patients with SjD [46] and mediates the downstream transcriptional activation of type-I IFN and other genes involved in the antiviral host response through activation of its aminoterminal CARD domain [47]. Remarkably, several genes encoding key proteins downstream of the RIG-I signalling pathway were also selectively upregulated in the SG of patients with SjD with seropositivity for RF or anti-La/SSB. Among these, DExD/H-box helicase 60 (DDX60) promotes RIG-I-dependent antiviral IFN and IFN-stimulated genes induction [48], while tripartite motif 25 (TRIM25), an E3 ubiquitin ligase, is required for the K63-linked ubiquitylation of the RIG-I CARD [49], necessary for downstream signalling via TBK1/IKKε leading to activation and nuclear translocation of IRF3 and IRF7 and the transcription of type-I IFNs and other IFN-stimulated genes [47]. Closely linked to RIG-I, we showed a strong association between RF and double anti-La/SSB and anti-Ro/SSA seropositivity with oligoadenylate synthetases (OAS)1 and OAS3, which, upon activation by cytosolic dsRNA, catalyses the synthesis of 2'-5'- oligoadenylates, which activates the viral restriction endoribonuclease RNaseL [50]. The association among extrafollicular responses, upregulation of type-I IFN, and an RF-driven signature in the SjD-SG is of particular interest since RF+ B-cells are strongly activated by dual engagement (cross-linking) between the B-cell receptor (BCR) and TLR7/TLR9 leading to increased B-cell proliferation and autoantibody production [51] and type-I IFN is able to enhance TLR7 and TLR9 expression and responsiveness in normal and autoreactive B-cells via the IFNAR2 receptor [52,53]. The presence of extrafollicular pathways driving B-cell autoreactivity in SjD SG is further demonstrated by the strong correlation between circulating autoreactive IgG responses with TENT5C and FcRL4 gene expression in both QMUL and TRACTISS SG-RNAseq datasets. Both gene are intimately involved in BCR-mediated and extrafollicular B-cell responses whereby TENT5C promotes antibody production by the polyadenylation and stabilisation of immunoglobulin mRNAs [54], and is strongly upregulated by selective TLR signalling. Accordingly, knocking-out of TENT5C in B-cells leads to decreased serum IgG concentrations and diminished humoral responses upon immunisation with thymus-independent antigens [55]. FcRL4 is expressed by a subset of memory B-cells located in close association with epithelial cells at mucosal sites which typically fail to proliferate in response to BCR ligation [56]. Interestingly, FcRL4 is strongly upregulated upon TLR9 signalling and enhances TLR-mediated activation upon binding of soluble IgA, thus, switching from adaptive to innate signalling in response to chronic antigenic stimulation [57]. In SjD-SG, the majority, if not all, of the intraepithelial B-cells, including those in advanced prelymphomatous lymphoepithelial lesions express FcRL4, indicating a possible role in driving early stages of B-cell lymphomagenesis in SjD.

In summary, our work suggests that molecular classification of SjD-SG, combined with known peripheral and histological biomarkers, can refine SjD disease taxonomy highlighting novel and heterogeneous molecular pathways driving disease in different subsets of patients. Using this approach, we provided the first transcriptomic-based evidence at the molecular level of the coexistence of follicular and an extrafollicular responses driving autoreactive B-cells within the SG of patients with SjD. While, as expected, follicular responses in patients with seropositive SjD were associated with functional GC gene signatures, we unravelled a novel disease endotype characterised by extrafollicular responses strongly and selectively linked to RIG-I endogenous (including viral) RNAs sensing and downstream type-I IFN activation which appear to drive ELS-independent RF and anti-La/SSB humoral autoimmunity. These novel molecular portraits, which appear strongly linked to known independent lymphoma risk factors, once validated in longitudinal cohorts and in response to therapeutic intervention may inform patient stratification and prediction of disease evolution and response to treatment.

Contributors

EP, DL, and MB designed the study. EP, DL, and Janssen team (QS, DG, ET) performed the experiments. EP, DL, ES, and GC analysed the transcriptomic data. EP, MB, NS, and ART facilitated the recruitment and collection of samples. MB, SJB, and CP, together with Janssen team (LY-H, KS) provided scientific insight. MB and CP provided resources for the study. All authors had full access to the data, interpreted the results, contributed to manuscript writing, critically revised the article, had final responsibility for the decision to submit for publication, and approved the final submitted version.

Funding

This work was supported by project grants from versus Arthritis UK (grant 20089 to MB and grant 21753 to EP), the William Harvey Research Foundation (to MB), Medical Research Council (grant MRC MR/T016736/1 and MR/N003063/1 to MB). Part of SJB salary comes through the Birmingham Biomedical Research Centre. This work forms part of the research portfolio of the National Institute for Health and Care Research Barts Biomedical Research Centre (NIHR203330); a delivery partnership of Barts Health NHS Trust, Queen Mary University of London, St George's University Hospitals NHS Foundation Trust and St George's University of London. The views expressed are those of the author(s) and not necessarily those of the NIHR or the Department of Health and Social Care. The TRACTISS dataset analysis was also supported by the Innovative Medicines Initiative 2 Joint Undertaking (JU) NECESSITY (grant 806975). The JU receives support from the European Union's Horizon 2020 research and innovation program and the European Federation of Pharmaceutical Industries and Associations. The present article reflects only the authors' views, and the JU is not responsible for any use that may be made of the information it contains.

Competing interests

MB reports financial support was provided by Janssen Pharmaceutical Companies of Johnson & Johnson. MB reports a relationship with GSK, UCB, Ono Pharmaceutical, Amgen, Novartis that includes: consulting or advisory. EP reports a relationship with GSK that includes: consulting or advisory. SJB reports a relationship with Amgen, Argenx, Aurinia, Bain, BMS, EcoR1, Igvia, Janssen J&J, Kiniksa & Novartis AbbVie Inc that includes: consulting or advisory. QS, DG, ET, L-YH, and KS are employees of Janssen Pharmaceuticals. If there are other authors, they declare that they have no known competing financial interests or personal relationships that could have appeared to influence the work reported in this paper.

Patient consent for publication

All patients consented for publication of data generated throught the use of the biological samples collected for research.

Provenance and peer review

Not commissioned research article, submitted for editorial and external peer-review.

Ethics approval

The study was approved by the ethics committee NRES Committee London-Westmister (REC 05/Q0702/1).

Data availability statement

Data are available on reasonable request. All data relevant to the study are included in the article or uploaded as online supplementary information. The data that support the findings of this study are available from the corresponding authors on reasonable request.

Patient and public involvement

Patients were involved in the reporting and dissemination of this research.

CRediT authorship contribution statement

Elena Pontarini: Writing – review & editing, Writing – original draft, Supervision, Project administration, Investigation, Formal analysis, Data curation, Conceptualization. **Davide Lucchesi:** Writing – review & editing, Visualization, Formal analysis, Data curation. **Elisabetta Sciacca:** Visualization, Formal analysis. **Giulia Cavallaro:** Visualization, Formal analysis. **Qingxuan Song:** Formal analysis. **David Galbraith:** Visualization, Formal analysis. **Elizabeth Thomas:** Formal analysis, Data curation. **Annalisa Marino:** Writing – review & editing, Writing – original draft, Data curation. **Nurhan Sutcliffe:** Supervision, Resources. **Anwar R. Tappuni:** Supervision, Resources. **Roberto Giacomelli:** Writing – review & editing, Supervision. **Alfredo Pulvirenti:** Writing – review & editing, Supervision. **Simon J. Bowman:** Writing – review & editing, Writing – original draft, Resources. **Ling-Yang Hao:** Supervision, Resources, Project administration. **Kathy Sivils:** Supervision, Resources, Project administration, Conceptualization. **Costantino Pitzalis:** Resources, Funding acquisition. **Myles J. Lewis:** Writing – review & editing, Software. **Michele Bombardieri:** Writing – review & editing, Writing – original draft, Supervision, Resources, Project administration, Funding acquisition, Conceptualization.

Supplementary materials

Supplementary material associated with this article can be found, in the online version, at doi:10.1016/j.ard.2025.07.021.

Orcid

Elena Pontarini: http://orcid.org/0000-0003-0439-0344
Davide Lucchesi: http://orcid.org/0000-0002-8019-556X
Elisabetta Sciacca: http://orcid.org/0000-0001-7525-1558
Giulia Cavallaro: http://orcid.org/0009-0000-1212-8368
Elizabeth Thomas: http://orcid.org/0000-0003-2311-1240
Nurhan Sutcliffe: http://orcid.org/0000-0002-8150-6446
Anwar R. Tappuni: http://orcid.org/0000-0002-5370-2423
Roberto Giacomelli: http://orcid.org/0000-0003-0670-9638
Alfredo Pulvirenti: http://orcid.org/0000-0002-9764-0295
Simon J. Bowman: http://orcid.org/0000-0001-9880-9948
Costantino Pitzalis: http://orcid.org/0000-0003-1326-5051
Myles J. Lewis: http://orcid.org/0000-0001-9365-5345
Michele Bombardieri: http://orcid.org/0000-0002-3878-5216

REFERENCES

[1] Baldini C, Fulvio G, La Rocca G, Ferro F. Update on the pathophysiology and treatment of primary Sjögren syndrome. Nat Rev Rheumatol 2024;20:473–91.
[2] Bombardieri M, Lewis M, Pitzalis C. Ectopic lymphoid neogenesis in rheumatic autoimmune diseases. Nat Rev Rheumatol 2017;13:141–54.
[3] Wieczorek G, Bigaud M, Pfister S, Ceci M, McMichael K, Afatsawo C, et al. Blockade of CD40-CD154 pathway interactions suppresses ectopic lymphoid structures and inhibits pathology in the NOD/ShiLtJ mouse model of Sjögren's syndrome. Ann Rheum Dis 2019;78:974–8.
[4] Lucchesi D, Coleby R, Pontarini E, Prediletto E, Rivellese F, Hill DG, et al. Impaired IL-27 mediated control of CD4+ T cell function impacts on ectopic lymphoid structure formation in patients with Sjögren's syndrome. Arthritis Rheumatol 2020;10 art.41289.
[5] Pontarini E, Murray-Brown WJ, Croia C, Lucchesi D, Conway J, Rivellese F, et al. Unique expansion of IL-21+ Tfh and Tph cells under control of ICOS identifies Sjögren's syndrome with ectopic germinal centres and MALT lymphoma. Ann Rheum Dis 2020;79:1588–99.
[6] Barone F, Nayar S, Campos J, Cloake T, Withers DR, Toellner KM, et al. IL-22 regulates lymphoid chemokine production and assembly of tertiary lymphoid organs. Proc Natl Acad Sci U S A 2015;112:11024–9.
[7] Nocturne G, Pontarini E, Bombardieri M, Mariette X. Lymphomas complicating primary Sjögren's syndrome: from autoimmunity to lymphoma. Rheumatology 2021;60:3513–21.
[8] Kapsogeorgou EK, Voulgarelis M, Tzioufas AG. Predictive markers of lymphomagenesis in Sjögren's syndrome: from clinical data to molecular stratification. J Autoimmun 2019;104:102316.
[9] Quartuccio L, Isola M, Baldini C, Priori R, Bartoloni Bocci E, Carubbi F, et al. Biomarkers of lymphoma in Sjögren's syndrome and evaluation of the lymphoma risk in prelymphomatous conditions: results of a multicenter study. J Autoimmun 2014;51:75–80.
[10] Bende RJ, Aarts WM, Riedl RG, de Jong D, Pals ST, van Noesel CJ. Among B cell non-Hodgkin's lymphomas, MALT lymphomas express a unique antibody repertoire with frequent rheumatoid factor reactivity. J Exp Med 2005;201:1229–41.
[11] Risselada AP, Looije MF, Kruize AA, Bijlsma JW, van Roon JA. The role of ectopic germinal centers in the immunopathology of primary Sjögren's syndrome: a systematic review. Semin Arthritis Rheum 2013;42:368–76.
[12] Sang A, Niu H, Cullen J, Choi SC, Zheng YY, Wang H, et al. Activation of rheumatoid factor-specific B cells is antigen dependent and occurs preferentially outside of germinal centers in the lupus-prone NZM2410 mouse model. J Immunol 2014;193:1609–21.
[13] Ols ML, Cullen JL, Turqueti-Neves A, Giles J, Shlomchik MJ. dendritic cells regulate extrafollicular autoreactive B cells via T cells expressing fas and fas ligand. Immunity 2016;45:1052–65.
[14] Kroese FGM, Haacke EA, Bombardieri M. The role of salivary gland histopathology in primary Sjögren's syndrome: promises and pitfalls. Clin Exp Rheumatol 2018;36:S222–33.
[15] Devauchelle-Pensec V, Cagnard N, Pers JO, Youinou P, Saraux A, Chiocchia G. Gene expression profile in the salivary glands of primary Sjögren's syndrome patients before and after treatment with rituximab. Arthritis Rheum 2010;62:2262–71.
[16] Tasaki S, Suzuki K, Nishikawa A, Kassai Y, Takiguchi M, Kurisu R, et al. Multiomic disease signatures converge to cytotoxic CD8 T cells in primary Sjögren's syndrome. Ann Rheum Dis 2017;76:1458–66.
[17] Vitali C, Dolcino M, Del Papa N, Minniti A, Pignataro F, Maglione W, et al. Gene expression profiles in primary Sjögren's syndrome with and without systemic manifestations. ACR Open Rheumatol 2019;1:603–13.
[18] Zhang L, Xu P, Wang X, Zhang Z, Zhao W, Li Z, et al. Identification of differentially expressed genes in primary Sjögren's syndrome. J Cell Biochem 2019;120:17368–77.

[19] Visser A, Verstappen GM, van der Vegt B, Vissink A, Bende RJ, Bootsma H, et al. Repertoire analysis of B-cells located in striated ducts of salivary glands of patients with Sjögren's syndrome. Front Immunol 2020;11:1486.
[20] Verstappen GM, Ice JA, Bootsma H, Pringle S, Haacke EA, de Lange K, et al. Gene expression profiling of epithelium-associated FcRL4+ B cells in primary Sjögren's syndrome reveals a pathogenic signature. J Autoimmun 2020;109:102439.
[21] James JA, Guthridge JM, Chen H, Lu R, Bourn RL, Bean K, et al. Unique Sjögren's syndrome patient subsets defined by molecular features. Rheumatology (Oxford) 2020;59:860–8.
[22] Min HK, Moon SJ, Park KS, Kim KJ. Integrated systems analysis of salivary gland transcriptomics reveals key molecular networks in Sjögren's syndrome. Arthritis Res Ther 2019;21:294.
[23] Verstappen GM, Gao L, Pringle S, Haacke EA, van der Vegt B, Liefers SC, et al. The transcriptome of paired major and minor salivary gland tissue in patients with primary sjögren's syndrome. Front Immunol 2021;12:681941.
[24] Oyelakin A, Horeth E, Song E-AC, Min S, Che M, Marzullo B, et al. Transcriptomic and network analysis of minor salivary glands of patients with primary Sjögren's syndrome. Front Immunol 2021;11:606268.
[25] van Nimwegen JF, van Ginkel MS, Arends S, Haacke EA, van der Vegt B, Sillevis Smitt-Kamminga N, et al. Validation of the ACR-EULAR criteria for primary Sjögren's syndrome in a Dutch prospective diagnostic cohort. Rheumatology 2018;57:818–25.
[26] Pontarini E, Sciacca E, Chowdhury F, Grigoriadou S, Rivellese F, Murray-Brown WJ, et al. Serum and tissue biomarkers associated with composite of relevant endpoints for Sjögren syndrome (CRESS) and Sjögren tool for assessing response (STAR) to B cell-targeted therapy in the trial of anti-B cell therapy in patients with primary Sjögren syndrome. Arthritis Rheumatol 2024;76:763–76.
[27] Lucchesi D, Pontarini E, Donati V, Mandarano M, Sidoni A, Bartoloni E, et al. The use of digital image analysis in the histological assessment of Sjögren's syndrome salivary glands improves inter-rater agreement and facilitates multicentre data harmonisation. Clin Exp Rheumatol 2020;38(Suppl 1):180–8.
[28] Barone F, Bombardieri M, Manzo A, Blades MC, Morgan PR, Challacombe SJ, et al. Association of CXCL13 and CCL21 expression with the progressive organization of lymphoid-like structures in Sjögren's syndrome. Arthritis Rheum 2005;52:1773–84.
[29] Chen EY, Tan CM, Kou Y, Duan Q, Wang Z, Meirelles GV, et al. Enrichr: Interactive and collaborative HTML5 gene list enrichment analysis tool. BMC Bioinformatics 2013;14:128.
[30] Aran D, Hu Z, Butte AJ. xCell: Digitally portraying the tissue cellular heterogeneity landscape. Genome Biol 2017;18:220.
[31] Lewis MJ, Barnes MR, Blighe K, Goldmann K, Rana S, Hackney JA, et al. Molecular portraits of early rheumatoid arthritis identify clinical and treatment response phenotypes. Cell Rep 2019;28:2455–70 .e5.
[32] Carenzo A, Pistore F, Serafini MS, Lenoci D, Licata AG, De Cecco L. Hacksig: a unified and tidy R framework to easily compute gene expression signature scores. Bioinformatics 2022;38:2940–2.
[33] Pontarini E, Coleby R, Bombardieri M. Cellular and molecular diversity in Sjogren's syndrome salivary glands: towards a better definition of disease subsets. Semin Immunol 2021;58:101547.
[34] Lessard CJ, Li H, Adrianto I, Ice JA, Rasmussen A, Grundahl KM, et al. Variants at multiple loci implicated in both innate and adaptive immune responses are associated with Sjögren's syndrome. Nat Genet 2013;45:1284–92.
[35] Bisoendial R, Lubberts E. A mechanistic insight into the pathogenic role of interleukin 17a in systemic autoimmune diseases. Mediators Inflamm 2022;2022:1–14.
[36] Verstappen GM, Corneth OBJ, Bootsma H, Kroese FGM. Th17 cells in primary Sjögren's syndrome: pathogenicity and plasticity. J Autoimmun 2018;87:16–25.
[37] Fehr AR, Singh SA, Kerr CM, Mukai S, Higashi H, Aikawa M. The impact of PARPs and ADP-ribosylation on inflammation and host–pathogen interactions. Genes Dev 2020;34:341–59.
[38] Hulkkonen J. Matrix metalloproteinase 9 (MMP-9) gene polymorphism and MMP-9 plasma levels in primary Sjogren's syndrome. Rheumatology 2004;43:1476–9.
[39] Tian Q, Zhao H, Ling H, Sun L, Xiao C, Yin G, et al. Poly(ADP-Ribose) polymerase enhances infiltration of mononuclear cells in primary sjögren's syndrome through interferon-induced protein with tetratricopeptide repeats 1-mediated up-regulation of CXCL10. Arthritis Rheumatol 2020;72:1003–12.
[40] Humby F, Durez P, Buch MH, Lewis MJ, Rizvi H, Rivellese F, et al. Rituximab versus tocilizumab in anti-TNF inadequate responder patients with rheumatoid arthritis (R4RA): 16-week outcomes of a stratified, biopsy-driven, multicentre, open-label, phase 4 randomised controlled trial. Lancet (London, England) 2021;397:305–17.
[41] Rivellese F, Surace AEA, Goldmann K, Sciacca E, Çubuk C, Giorli G, et al. Rituximab versus tocilizumab in rheumatoid arthritis: synovial biopsy-based biomarker analysis of the phase 4 R4RA randomized trial. Nat Med 2022;28:1256–68.
[42] Terrier B, Nagata S, Ise T, Rosenzwajg M, Pastan I, Klatzmann D, et al. CD21−/low marginal zone B cells highly express Fc receptor-like 5 protein and are killed by anti-Fc receptor-like 5 immunotoxins in hepatitis C virus-associated mixed cryoglobulinemia vasculitis. Arthritis Rheumatol 2014;66:433–43.
[43] Berardicurti O, Ruscitti P, Di Benedetto P, D'Andrea S, Navarini L, Marino A, et al. Association between minor salivary gland biopsy during Sjögren's syndrome and serologic biomarkers: a systematic review and meta-analysis. Front Immunol 2021;12:686457.
[44] Pichlmair A, Schulz O, Tan CP, Näslund TI, Liljeström P, Weber F, et al. RIG-I-mediated antiviral responses to single-stranded RNA bearing 5'-phosphates. Science 2006;314:997–1001.
[45] Hornung V, Ellegast J, Kim S, Brzózka K, Jung A, Kato H, et al. 5'-Triphosphate RNA is the ligand for RIG-I. Science 2006;314:994–7.
[46] Maria NI, Steenwijk EC, IJpma AS, van Helden-Meeuwsen CG, Vogelsang P, Beumer W, et al. Contrasting expression pattern of RNA-sensing receptors TLR7, RIG-I and MDA5 in interferon-positive and interferon-negative patients with primary Sjögren's syndrome. Ann Rheum Dis 2017;76:721–30.
[47] Rehwinkel J, Gack MU. RIG-I-like receptors: their regulation and roles in RNA sensing. Nat Rev Immunol 2020;20:537–51.
[48] Miyashita M, Oshiumi H, Matsumoto M, Seya T. DDX60, a DEXD/H Box helicase, is a novel antiviral factor promoting RIG-I-Like receptor-mediated signaling. Mol Cell Biol 2011;31:3802–19.
[49] Gack MU, Shin YC, Joo C-H, Urano T, Liang C, Sun L, et al. TRIM25 RING-finger E3 ubiquitin ligase is essential for RIG-I-mediated antiviral activity. Nature 2007;446:916–20.
[50] Li Y, Banerjee S, Wang Y, Goldstein SA, Dong B, Gaughan C, et al. Activation of RNase L is dependent on OAS3 expression during infection with diverse human viruses. Proc Natl Acad Sci U S A 2016;113:2241–6.
[51] Sweet RA, Cullen JL, Shlomchik MJ. Rheumatoid factor B cell memory leads to rapid, switched antibody-forming cell responses. J Immunol 2013;190:1974–81.
[52] Poovassery JS, Bishop GA. Type I IFN receptor and the B cell antigen receptor regulate TLR7 responses via distinct molecular mechanisms. J Immunol 2012;189:1757–64.
[53] Thibault DL, Graham KL, Lee LY, Balboni I, Hertzog PJ, Utz PJ, et al. Type I interferon receptor controls B-cell expression of nucleic acid-sensing toll-like receptors and autoantibody production in a murine model of lupus. Arthritis Res Ther 2009;11:R112.
[54] Herrero AB, Quwaider D, Corchete LA, Mateos MV, García-Sanz R, Gutiérrez NC. FAM46C controls antibody production by the polyadenylation of immunoglobulin mRNAs and inhibits cell migration in multiple myeloma. J Cell Mol Med 2020;24:4171–82.
[55] Bilska A, Kusio-Kobiałka M, Krawczyk PS, Gewartowska O, Tarkowski B, Kobyłecki K, et al. Immunoglobulin expression and the humoral immune response is regulated by the non-canonical poly(A) polymerase TENT5C. Nat Commun 2020;11:2032.
[56] Ehrhardt GRA, Hsu JT, Gartland L, Leu CM, Zhang S, Davis RS, et al. Expression of the immunoregulatory molecule FcRH4 defines a distinctive tissue-based population of memory B cells. J Exp Med 2005;202:783–91.
[57] Sohn HW, Krueger PD, Davis RS, Pierce SK. FcRL4 acts as an adaptive to innate molecular switch dampening BCR signaling and enhancing TLR signaling. Blood 2011;118:6332–41.

Ann Rheum Dis 84 (2025) 1836–1851

Contents lists available at ScienceDirect

Annals of the Rheumatic Diseases

journal homepage: https://www.sciencedirect.com/journal/annals-of-the-rheumatic-diseases

Myositis

Discovery of tissue-specific proteomic signatures in juvenile dermatomyositis highlights pathways reflecting persistent disease activity, clinical heterogeneity, and myositis-specific autoantibody subtype

Jessica Neely[1,*], Sara E. Sabbagh[2,†], Jeffrey Dvergsten[3,†], Chioma Madubata[1,†], Celine C. Berthier[4,†], Zilan Zheng[1,†], Christine Goudsmit[5,†], Sophia Matossian[5], Sean P. Ferris[6], Gabriela K. Fragiadakis[7], Marina Sirota[8], J. Michelle Kahlenberg[9], Hanna Kim[10,‡], Jessica L. Turnier[5,‡], for the CARRA Registry Investigators and CARRA Translational Medicine for Juvenile Myositis Working Group

[1] *Department of Pediatrics, Division of Rheumatology, University of California, San Francisco, San Francisco, CA, USA*
[2] *Department of Pediatrics, Division of Rheumatology, The Medical College of Wisconsin, Milwaukee, WI, USA*
[3] *Department of Pediatrics, Division of Rheumatology, Duke University, Durham, NC, USA*
[4] *Department of Internal Medicine, Division of Nephrology, University of Michigan, Ann Arbor, MI, USA*
[5] *Department of Pediatrics, Division of Rheumatology, University of Michigan, Ann Arbor, MI, USA*
[6] *Department of Pathology, University of Michigan, Ann Arbor, MI, USA*
[7] *Department of Medicine, Division of Rheumatology, University of California, San Francisco, San Francisco, CA, USA*
[8] *Bakar Computational Health Science Institute, University of California, San Francisco, San Francisco, CA, USA*
[9] *Department of Internal Medicine, Division of Rheumatology, University of Michigan, Ann Arbor, MI, USA*
[10] *Juvenile Myositis Pathogenesis and Therapeutics Unit, National Institute of Arthritis Musculoskeletal and Skin Diseases (NIAMS), National Institutes of Health (NIH), Bethesda, MD, USA*

ARTICLE INFO

Article history:
Received 3 March 2025
Received in revised form 18 July 2025
Accepted 23 July 2025

ABSTRACT

Objectives: Juvenile dermatomyositis (JDM) is a heterogeneous autoimmune condition needing targeted treatment approaches and improved understanding of molecular mechanisms driving clinical phenotypes. We utilised exploratory proteomics from a longitudinal North American cohort of patients with new-onset JDM to identify biological pathways at disease onset and follow-up, tissue-specific disease activity, and myositis-specific autoantibody (MSA) status.

Methods: We measured 3072 plasma proteins (Olink panel) in 56 patients with JDM within 12 weeks of starting treatment (from the Childhood Arthritis and Rheumatology Research Alliance Registry and 3 additional sites) and 8 paediatric controls. Twenty-four patients with JDM who had 6-month follow-up samples were assessed. We identified differentially expressed

*Correspondence to Dr. Jessica Neely, UCSF Benioff Children's Hospital, San Francisco, CA, USA.
E-mail address: Jessica.Neely@ucsf.edu (J. Neely).

The GEO accession number is: GSE308711. The Github code can be found at: https://github.com/jessicaneely/JDM-Olink-Explore-Proteomics-/tree/main.

Handling editor Josef S. Smolen.

† Sara Sabbagh, Jeff Dvergsten, Chioma Madubata, Celine C Berthier, Zilan Zheng, and Christine Goudsmit contributed equally.
‡ Hanna Kim and Jessica L. Turnier contributed equally.

https://doi.org/10.1016/j.ard.2025.07.020

proteins (DEPs) between groups by fitting linear mixed effects models and associated DEPs with validated disease activity measures. We assessed for cell/tissue specificity using the Human Protein Atlas and JDM muscle single nuclei and skin single-cell transcriptomic datasets. Differences within MSA subgroups were also analysed.

Results: We uncovered persistent dysregulation of innate immune activation, cell death, and redox signalling at 6 months despite multidrug immunosuppression. By leveraging tissue and cell-specific proteomes, we identified overrepresentation of circulating endothelial proteins associated with disease activity and verified endothelial cell marker expression in JDM muscle and skin. We discovered pathways associated with MSA subtypes that reflect JDM phenotypes. NXP2+ JDM-associated proteins reflected angiogenesis and extracellular matrix remodelling and were expressed in endothelial cells and fibroblasts. MDA5+ JDM was associated with circulating type III interferon and surfactant proteins.

Conclusions: These proteomic findings will inform future biomarker and treatment development considering the unique tissue- and autoantibody-associated inflammation in JDM.

WHAT IS ALREADY KNOWN ON THIS TOPIC

- There are multiple emerging inflammatory and interferon-related disease activity biomarkers in juvenile dermatomyositis (JDM); however, there is still a limited understanding of molecular mechanisms underlying disease heterogeneity and organ-specific inflammation as well as a limited repertoire of biomarkers to monitor lower levels of disease activity and vascular health in patients with JDM posttreatment.

WHAT THIS STUDY ADDS

- This exploratory proteomics study in a diverse, multicentre North American cohort of 56 newly diagnosed patients with JDM with 24 paired 6-month follow-up samples uncovered multiple persistently dysregulated biological pathways not targeted by current treatments, including redox, innate immune, proteasomal, cell death, and DNA damage repair signalling. By leveraging JDM single-cell datasets, candidate tissue and cell-specific proteins were identified for muscle, skin and endothelial cells, with endothelial-specific markers being over-represented in the group of global disease activity-associated proteins. Through analysing patient samples by myositis-specific autoantibody status, specific proteomic signatures were identified for NXP2+ and MDA5+ JDM reflective of clinical phenotypes.

HOW THIS STUDY MIGHT AFFECT RESEARCH, PRACTICE OR POLICY

- These findings highlight the complex, multiorgan biological pathway dysregulation contributing to JDM disease heterogeneity, tissue-specific inflammation, and persistent disease activity, laying the groundwork for alternate treatment targets and biomarkers as well as precision medicine care for patients with JDM.

INTRODUCTION

Juvenile dermatomyositis (JDM) is a heterogeneous immune-mediated disease characterised by muscle weakness, rash, and vasculopathy. Children with JDM often have refractory disease, with patients experiencing chronic muscle weakness, persistent rashes, and long-term disability [1]. Reliable, individual, and tissue-specific biomarkers to monitor disease activity are lacking. Currently, blood biomarkers used to assess clinical disease activity, such as creatinine kinase (CK) and lactate dehydrogenase, reflect only muscle involvement and are often unreliable [2,3]. Other clinically available biomarkers, including von Willebrand factor antigen and neopterin, have variable prevalence and myositis-specific autoantibody (MSA) association [4–7]. While many studies have demonstrated a high interferon (IFN) signature in JDM [8–12] associated with increased disease activity [8,10,11,13], these IFN markers may not accurately reflect ongoing inflammation in patients with chronic/treatment-refractory disease or low disease activity [9,14]. A subset of patients also has an incomplete response to IFN-pathway targeting [15]. To improve outcomes for children with JDM, identification of biomarkers reflective of biological pathways that encompass the complexity of JDM multiorgan pathophysiology and also a personalised approach to disease management linking disease pathophysiology to phenotype is imperative.

The peripheral blood transcriptome does not generally reflect tissue-specific information [16]; thus, several groups have utilised proteomics to investigate candidate disease activity markers [17–19]. These studies have corroborated serum biomarkers associated with systemic inflammation, such as CXCL10 and CXCL11 [17,20–22], identified galectin-9, CXCL10, and TNFR11 as predictors of poor treatment response [21,22], and found anti-MDA5 specific upregulation of type I IFN and proteasome pathways [18]. Investigations of endothelial-specific proteins have also identified VCAM-1, ANGPT2, and sVEGFR-1 (FLT-1) as disease activity biomarkers [21,22]. Recently, proteomic analysis utilising a larger, multiplexed immunoassay of 282 proteins in JDM serum detected high expression of MMP3 and GDF15 and identified IL1RL1 as a candidate global disease activity biomarker [19]. Another study applying a combined transcriptomic and proteomic analysis identified a prominent neutrophil degranulation signature in JDM [23].

Although these studies provide important clues to JDM pathophysiology, they were often constrained by low sample size, geographic homogeneity, low disease activity state with concurrent immunosuppression, or analysis of a limited number of proteins. Furthermore, contextualising the cell- and tissue-specific origin of these biomarkers and pathways has not been possible. To overcome prior limitations, we utilised an exploratory proteomics approach to assess 3072 plasma proteins in a multicentre North American cohort of 56 newly diagnosed patients with JDM and 24 paired patient samples at 6-month follow-up. We uncovered pathways not targeted by existing treatments and discovered disease activity-associated proteins that exhibit tissue- and cell-specificity in JDM muscle and skin. We revealed unique proteins underlying clinical heterogeneity by MSA phenotypes. Together, these results identify persistent dysregulation of innate immune, cell death, and redox pathways, provide a window into endothelial cell dysfunction in JDM, and highlight pathway differences by MSA.

METHODS

Patients

Subjects diagnosed with JDM by a paediatric rheumatologist (n = 56) and paediatric controls (CTL, n = 8) were recruited

from the University of Michigan (U-M) (JDM n = 7, CTL n = 4), Duke University (JDM n = 9), the University of California San Francisco (JDM n = 12, CTL n = 4), and the Childhood Arthritis and Rheumatology Research Alliance (CARRA) Registry and Biobank (JDM n = 28). The CARRA Registry is a North American rheumatologic disease registry that enrols patients from 72 sites in the United States and Canada with JDM diagnosed within 6 months and no more than 12 weeks of treatment. No patients met criteria for another autoimmune disease. Controls were recruited from paediatric and rheumatology clinics who had no evidence of autoimmune disease, and samples were processed the same as patients with JDM at the respective sites. Institutional Review Board (IRB) approval was granted from each site and the CARRA Registry and Biobank. All subjects provided informed consent and assent as appropriate. Of 56, 24 patients had follow-up samples 6 months into treatment (CARRA n = 20 and Duke n = 4). At each visit, International Myositis Assessment and Clinical Studies Group core consensus data set components [24] were collected, including the Physician's Global Activity Assessment (PGA), an overall assessment of disease activity on a 0 to 10 visual analogue scale (VAS).

Proteomic analysis

We utilised the multiplexed Olink Explore 3072 Proximity Extension Assay platform to measure proteins in plasma samples (www.olink.com). The OlinkAnalyze R Package (v3.7.0) was used for downstream analyses. Protein expression in Olink data is provided as normalised protein expression (NPX) values, Olink's arbitrary unit, on a log2 scale. After removing proteins that were designated with an assay warning by Olink (did not pass Olink's quality control n = 175), we analysed a total of 2897 proteins (2879 unique). A principal component analysis (PCA) plot revealed a potential for site-specific effects necessitating the use of linear mixed effects (lme) models to account for site (Supplementary Fig S1). In each model, proteins with duplicate measures within the Olink Explore panel were included, and downstream results were then either averaged or filtered for the greatest estimate. To identify differentially expressed proteins (DEPs), lme models were fit to each protein using the 'olink_lmer' function with 'site' as a random effect and 'individual' as a random effect in models when longitudinal timepoints were included. In each model, Benjamini-Hochberg adjusted *P* values were reported and those meeting a threshold of *P*-adj < .05 were included in a post-hoc analysis using the 'olink_lmer_posthoc' function to quantify the direction and magnitude of the protein association accounting for the random effects. Significance threshold was a post-hoc *P*-adj of <.05. A lme model analysis was used for baseline (BL) vs CTL samples, follow-up (FU) longitudinal vs CTL samples, and association of PGA VAS in all JDM samples. A paired *t*-test with 'olink_ttest' function was used for longitudinal samples (n = 24) (*P*-adj < .05).

Tissue-specific analyses

The Human Protein Atlas (HPA) tissue-specific proteome tool was utilised to identify protein lists that were 'tissue-enriched' and 'tissue-enhanced' for muscle and skin [25]. The HPA cell-specific proteome tool was used to identify 'cell type enriched' and 'cell type enhanced' endothelial cell proteins. To identify tissue- and cell-associated proteins, we evaluated the intersection of these lists with disease activity-associated proteins. To determine tissue-specific markers of organ-associated clinical assessments, the intersection of the HPA tissue lists and the Olink data set (n = 243 proteins) was used to fit lme models to Childhood Health Assessment Questionnaire (CHAQ), physician muscle VAS (0-10), and physician skin VAS (0-10), with both site and individual included as random effects as above.

MSA analysis

All MSA testing was performed using the 'comprehensive myositis autoantibody panel' at Oklahoma Medical Research Foundation on a clinical or research basis (omrf.org/research-faculty/core-facilities/myositis-testing/). MSA-associated proteins were identified by fitting a lme to each protein in BL (n = 55, 1 sample overlapping between 2 sites but obtained at different time points was excluded) samples for anti-TIF1γ, anti-NXP2, and anti-MDA5. Only BL samples were assessed to minimise confounding by medication. One patient tested positive for both anti-NXP2 and anti-TIF1γ on 2 occasions and was included in both models. To increase discovery of MSA-associated proteins in a smaller number of patients, proteins reaching a *P*-adj < .1 were included in a post-hoc analysis. Those with post-hoc *P*-adj < .05 were deemed significant.

Pathway enrichment analyses, heatmap and dot plot generation

MetaCore (www.clarivate.com) software, V24.3.71800, was used to identify the 'process networks' or 'Gene Ontology Biological Process' (GOBP) enriched in each set of DEP. Pathways with false discovery rate (FDR)<0.05 were considered significant. Heatmaps were generated using the Morpheus visualisation software from the Broad Institute (https://software.broadinstitute.org/morpheus), using the 'transform values: subtract row mean, divide by row standard deviation' option (which generates colour intensity based on the Row *Z*-score).

Single-cell data

Single nuclei RNAseq data were generated from JDM (n = 6) and histopathologically normal CTL (n = 7) frozen muscle multiplexed in 2 batches using the 10 × Genomics multiome kit. A technical replicate from 1 patient was included in both batches. Freemuxlet was used to genetically demultiplex samples (https://github.com/statgen/popscle). DoubletFinder was used to remove heterotypic doublets [26]. Low-quality cells were filtered. SoupX was used for ambient RNA filtering [27]. Libraries were merged, scaled, and integrated using Harmony [28] and variable features. Single-cell RNAseq data using archival formalin-fixed, paraffin-embedded skin blocks from lesional JDM biopsies (n = 12) and CTL skin (n = 4) were generated using the 10 × Genomics Fixed RNA Profiling kit with 'Chromium Human Transcriptome Probe Set v1.0.1'. Low-quality cells were removed. Doublet removal was performed using DoubletFinder [26], and SoupX was used for ambient RNA filtering [27]. For both datasets, Seurat (v4.3) was used to create uniform manifold approximation and projection (UMAP) embeddings and clusters were identified with the Leiden algorithm and manual annotation. Both datasets were subset to include only tissue-specific proteins of interest to evaluate cell-type-specific gene expression. N = 3 skin biopsies and n = 3 muscle biopsies were from patients in the proteomics cohort; however, sampling was not obtained at the same time.

Patient and public involvement

Patients with JDM and their families were involved in the discussion of research priorities that led to this study. This

project proposal was reviewed by a parent of a child with rheumatic disease within CARRA. Interim results were presented to patients with JDM and their families at a Cure Juvenile Myositis Town Hall.

RESULTS

Clinical cohort characteristics

An overview of the study design is represented in Figure 1. The patient cohort included 56 patients with JDM from a broad geographic area (Fig 1A). Patients with JDM had demographic and clinical characteristics (Table 1) similar to that reported in other registries [29,30] and moderate disease activity (median BL PGA = 6.0, IQR 5.0-7.0) (Table 2). At BL visit, 86% of patients with JDM were treatment naïve, and all had received <6 weeks of immune suppression. All but 1 patient had improvement in PGA by 6 months (Table 2). The CTL group was 50% female sex, with a median age of 7.5 years, not significantly different from the JDM group (Table 1).

JDM proteome at disease onset and posttreatment demonstrates IFN and innate immune activation signatures

To identify biological pathways associated with disease onset, we applied a linear mixed effects model comparing BL JDM and CTL, which identified 1186 proteins (1172 unique) DEPs, including 1126 increased and 46 decreased proteins (Fig 2A, Supplementary Table S1). The top DEPs by greatest NPX difference in BL JDM were CXCL10, TNNI3, GBP1, TLR2, RAD51, CCL7, MYOM2, and MYL3 (Fig 2B). BL DEP were enriched in several inflammatory pathways and networks bridging innate and adaptive immunity, including IFN signalling, cell adhesion and chemotaxis, neutrophil activation, interleukin and Th17-derived cytokine signalling, and cell death signalling (Fig 2C, Supplementary Table S1). The same model was then used to compare 6-month FU JDM to CTL, which identified 232 DEP, including 222 increased and 10 decreased proteins (Fig 2D, Supplementary Table S2). The top DEPs at 6-month FU included DOCK9, TLR2, BCL2, IGDCC3, STAT5B, PTEN, IL1B and SMAD2 (Fig 2E). Pathway and network analysis of the DEP at 6-month FU highlighted multiple shared pathways at both BL and FU, including persistently activated inflammatory pathways such as Th17-derived cytokine and IFN signalling, neutrophil activation and chemotaxis, as well as oxidative stress, cell death, and ubiquitin-proteasome pathway activation (Fig 2C, Supplementary Table S2). Due to few number of CTL samples (n = 8) in these analyses, PCA plots comparing site and disease effects with all proteins to only those significant in the analyses were compared visually and by analysis of variance of PC1 and PC2, which suggested DEPs were driven more by biological rather than site-specific effects (Supplementary Figs S2 and S3).

Posttreatment JDM proteome highlights persistent dysregulation of innate immune, cell death, and redox signalling

To identify proteins persistently dysregulated at 6 months posttreatment, we compared the intersection of DEP from BL vs

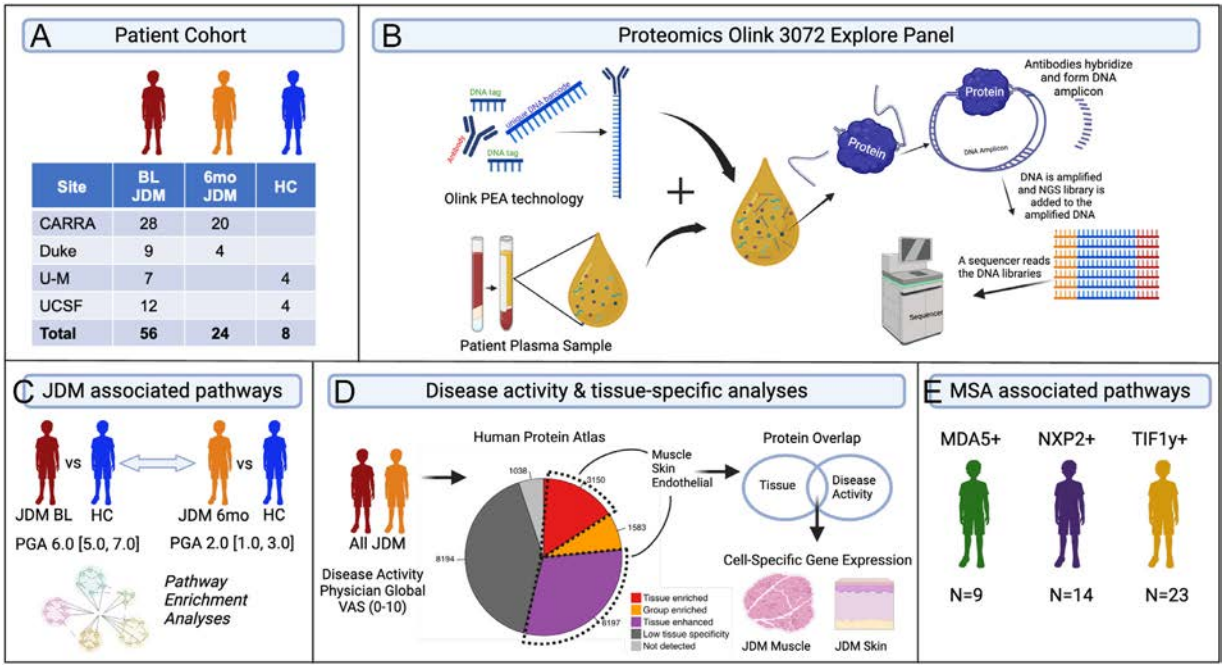

Figure 1. Study design overview. (A) Patient cohort details describing the number of patients with juvenile dermatomyositis (JDM) with baseline (BL) and 6-mo follow-up (6 mo) plasma samples and number of paediatric controls (CTL). (B) The Olink proximity extension assay (PEA) Explore 3072 Panel was utilised for simultaneous measurement of 3072 proteins in JDM and CTL plasma samples. Olink PEA technology harnesses antibodies labelled to DNA oligonucleotides followed by hybridisation, extension, and quantitative PCR amplification for protein quantification. Linear mixed effects model analysis identified: (C) proteins and biological pathways enriched in JDM BL or JDM 6-mo groups as compared to CTL. It also lists the physician global activity (median [IQR]), which is an overall disease activity measure on a 0 to 10 visual analogue scale (VAS). (D) Proteins associated with the global activity (PGA) in all patients with JDM at both time points. Proteins were also evaluated for either muscle, skin, or endothelial-enrichment/enhancement based on the Human Protein Atlas and evaluated for cell-type specificity in JDM muscle and skin single-nuclei and single-cell transcriptomic datasets. (E) Proteins were associated with myositis-specific autoantibody (MSA) subtype (MDA5, NXP2, TIF1γ) in BL patients with JDM. CARRA, Childhood Arthritis and Rheumatology Research Alliance; HC, healthy control; MDA5, melanoma differentiation-associated protein 5; NGS, next-generation sequencing; NXP2, nuclear matrix protein 2; PCR, polymerase chain reaction; TIF1-γ, transcription intermediary factor 1-gamma; UCSF, University of California San Francisco; U-M, University of Michigan.

Table 1
Baseline demographics and autoantibody testing of participants

Characteristic	All JDM (N = 56)[a]	Healthy control (N = 8)[a]	JDM paired (N = 24)[a]
Age (y)	7.0 (4.0, 11.3)	7.5 (4.5, 11)	7.5 (6.0, 11.5)
Time from symptom onset to diagnosis (mo)	3.1 (1.6, 5.3)		2.77 (1.56, 6.23)
Sex assigned at birth	**N = 56**[b]	**N = 8**[b]	**N = 24**[b]
Female	39 (70%)	4 (50%)	16 (66.7%)
Male	17 (30%)	4 (50%)	8 (33.3%)
Race and ethnicity			
White	31 (55.4%)	5 (62.5%)	15 (62.5%)
Hispanic or Latino	9 (16.1%)	0 (0.0%)	2 (8.3%)
2+ Race	8 (14.3%)	1 (12.5%)	3 (12.5%)
Black or African American	3 (5.4%)	0 (0.0%)	1 (4.2%)
Middle eastern	2 (3.6%)	0 (0.0%)	1 (4.2%)
Other race	2 (3.6%)	0 (0.0%)	1 (4.2%)
American Indian or Alaskan Native	1 (1.8%)	0 (0.0%)	1 (4.2%)
Native Hawaiian or Other Pacific Islander	0 (0.0%)	1 (12.5%)	0 (0.0%)
Asian	0 (0.0%)	1 (12.5%)	0 (0.0%)
Treatment naïve	48 (85.7%)		16 (67%)
Myositis-specific antibodies[c]	**All JDM (N = 56)**[b]		**JDM paired (N = 24)**[b]
Anti-TIF1-γ (formerly p155)	23/56 (41.0%)	–	9 (37.5%)
Anti-NXP2 (formerly MJ)	14/56 (25.0%)	–	5 (20.8%)
Anti-MDA5	9/56 (16.0%)	–	6 (25.0%)
Anti-Mi2	12/56 (21.4%)	–	6 (25.0%)
MSA negative	8/56 (14.3%)	–	4 (16.7%)
Myositis-associated antibodies[c]		–	
ANA	32/49 (65.3%)	–	13 (54.6%)
Anti-Ro (SSA)	8/56 (14.3%)	–	4 (16.7%)
Anti-PMSCL	2/56 (3.6%)	–	0 (0.0%)

ANA, anti-nuclear antibody; BL, baseline; HMGCR, 3-hydroxyl-3-methyl-glutaryl-coenzyme A reductase; JDM, juvenile dermatomyositis; MDA5, melanoma differentiation-associated protein 5; MSA, myositis-specific autoantibody; NXP2, nuclear matrix protein 2; PMSCL, polymyositis scleroderma; SRP, signal recognition peptide; SSA, Sjögren's syndrome-related antigen A; SSB, Sjögren's syndrome-related antigen B; TIF1-γ, transcription intermediary factor 1-gamma.
Bold font is used within the table to emphasise sections.
[a] Median (IQR).
[b] n (%).
[c] Anti-Jo1, SRP, HMGCR, La (SSB), and Ku are excluded because no patients were positive for these antibodies.

CTL and from FU vs CTL, which revealed that 83% (976/1172) of BL DEP were no longer differentially expressed at FU. However, 84% (196/232) of the 6-month FU DEP were also differentially expressed at BL (Fig 3A), highlighting persistent dysregulation of some DEP. Whereas many proteins related to muscle structure (MYOM2, MYL3) and IFN signalling (IFIT3, IFNL1) normalised at 6 months, those related to innate immunity (TLR2, IL1RN, IL6), oxidation-reduction (redox) enzymes (PRDX5/6, SOD1/2), protein processing (PSME1/2, UBE2B) and DNA damage repair (RAD23B, PARP1), remained differentially expressed (Fig 3B). There was also a shift in the expression ratio of specific proteins at FU with opposing roles within biological pathways. For instance, in the IL1 signalling pathway, IL1B was newly differentially expressed at FU, with IL1RN (IL1 receptor antagonist) decreasing (Fig 3B). There were similar shifts in cell death signalling proteins: at 6-month FU, the proapoptotic protein, BAX, was no longer increased, whereas the anti-apoptotic protein BCL2 further increased [31] (Fig 3B). We also noted an inverse shift in chemotactic proteins (CCL5 further increasing whereas CCL7 was decreasing) (Fig 3B). The increase in IL1B at 6 months was intriguing, so we further evaluated IL1B expression in the public peripheral blood mononuclear cell (PBMC) single-cell RNAseq dataset to leverage the longitudinal nature of this dataset finding that, in fact, IL1B expression, which is restricted to CD14+ monocytes, is increased in inactive patients with JDM compared to treatment-naïve JDM (Supplementary Fig S4). To determine if patients treated more aggressively might have different profiles, we performed a sensitivity analysis removing 5 patients who received either mycophenolate or cyclophosphamide, which did not significantly change the results (Supplementary Fig S5).

JDM paired proteome analysis at disease onset and posttreatment reveals persistent inflammation and angiogenesis

To determine if similar DEP changes occurred within individuals, we next used the 1186 DEP (1172 unique) identified in BL JDM vs CTL in a paired analysis with BL vs 6-month FU (n = 24) (Supplementary Table S3), which revealed similar shifts in dysregulated pathways at an individual level. Fifty-eight per cent (691/1186) of DEP from the prior BL JDM vs CTL analysis showed differential expression at 6-month FU within individuals, with nearly all showing decreased expression (97%, 669/691). Notably, 42% (499/1186) of proteins had no significant change at 6-month FU in individuals, despite ongoing treatment. Enrichment analysis of the 496 unique, nonsignificant or unchanged proteins within individuals between BL and FU highlighted many of the same pathways identified in the prior analysis, such as Th17-derived cytokine signalling, neutrophil activation, protein folding and processing, cell death, endothelial-immune cell interactions, and regulation of angiogenesis (Fig 3C,D), supporting the findings using the entire dataset.

Disease activity-associated proteins reflect IFN signalling, muscle inflammation, cell death, and endothelial-immune cell interaction

Next, we fit a model to identify proteins associated with global disease activity by PGA of 80 JDM samples, including

Table 2
Clinical data for patients with JDM at BL and for paired JDM samples at BL and FU

Clinical characteristics	All JDM at BL (N = 56)[a]	Paired JDM at BL (N = 24)[a]	Paired JDM at FU (N = 24)[a]
Physician global VAS	6.0 (5.0, 7.0)/0	6.0 (5.0, 7.0)/0	3.0 (1.0, 3.25)/0
Muscle VAS	4.0 (3.0, 6.25)/4	4.0 (3.0, 6.0)/3	1.0 (0.0, 3.0)/3
Skin VAS	5.0 (3.0, 6.0)/4	5.0 (3.0, 6.0)/3	2.0 (0.6, 2.4)/2
Patient/parent global VAS	5.0 (4.0, 7.0)/6	6.0 (3.75, 7.0)/0	3.0 (1.0, 3.8)/2
CHAQ	1.0 (0.375, 2.125)/8	0.875 (0.375, 2.127)/1	0.125 (0.0, 0.625)/3
CDASI Activity Score	12 (6.0, 17.5)/13	11 (6.8, 16.50)/8	2.0 (1.0, 4.0)/5
CMAS	31.5 (24.3, 45.0)/30	38.5 (22.5, 48.5)/6	47.0 (43.5, 50.5)/9
MMT8	66 (49.5, 73.8)/30	71.5 (53.5, 79.3)/14	79.5 (69.75, 80.0)/8
Laboratory tests (U/L)			
CK	309 (82, 949)/2	115 (51, 701)/1	47.5 (34.8, 87.8)/4
LDH	520 (349, 1086)/5	551 (350, 1201)/2	578 (267, 663)/3
Aldolase	15.9 (9.10, 33.975)/8	10.7 (9.0, 30.5)/5	6.9 (5.7, 9.5)/9
AST	75 (51.00, 132.75)/1	61.0 (33.0, 126.5)/1	38.5 (25.5, 52.5)/2
ALT	41 (20.75, 98.75)/1	31.0 (17.5, 78.5)/1	21.0 (16.0, 32.0)/1
History	**N = 56**[b]	**N = 24**[b]	**N = 24**[b]
Elevated muscle enzymes	49 (87.5%)	20 (83.3%)	–
Proximal muscle weakness	50 (89.2%)	21 (87.5%)	–
Rash consistent with JDM	50 (89.3%)	21 (87.5%)	–
Glucocorticoids/steroids	6 (10.7%)	4 (16.7%)	–
Immune suppressants[c]	5 (8.9%)	3 (12.5%)	–
Symptoms due to JDM			
Fever	11 (20.0%)	5 (20.8%)	0 (0.0%)
Fatigue	41 (75.9%)	16 (66.7%)	4 (16.7%)
Weight loss (>5%)	9 (17.0%)	20 (83.3%)	0 (0.0%)
Arthritis	20 (36.4%)	10 (41.7%)	2 (8.3%)
Respiratory muscle weakness	3 (5.7%)	1 (4.2%)	1 (4.2%)
Interstitial lung disease	1 (2.0%)	0 (0.0%)	2 (8.3%)
Gottron's papules or sign	48 (85.7%)	20 (83.3%)	12 (50.0%)
Heliotrope rash	42 (76.4%)	18 (75.0%)	4 (16.7%)
Cutaneous ulceration	5 (9.1%)	3 (12.5%)	1 (4.2%)
Periungual capillary loop changes	43 (78.2%)	16 (66.7%)	14 (58.3%)
Current calcinosis	1 (3.4%)	1 (0.0%)	0 (0.0%)
Current medications			
Glucocorticoids/steroids	–	–	22 (91.7%)
Oral steroid dose (mg)	–	–	16.6 (9.9, 24.4)
Methotrexate	–	–	21 (87.5%)
IVIG	–	–	14 (58.3%)
MMF/MPA	–	–	3 (12.5%)
Cyclophosphamide	–	–	2 (8.3%)
Rituximab	–	–	0 (0.0%)

ALT, alanine aminotransferase; AST, aspartate aminotransferase; BL, baseline; CDASI, Cutaneous Dermatomyositis Disease Area and Severity Index Score; CHAQ, Childhood Health Assessment Questionnaire; CK, creatine kinase; CMAS, Childhood Myositis Assessment Scale; FU, follow-up; IVIG, intravenous immunoglobulin; JDM, juvenile dermatomyositis; LDH, lactate dehydrogenase; MMF, mycophenolate mofetil; MMT8, Manual Muscle Testing and a Subset of Eight Muscles; MPA, mycophenolic acid; VAS, visual analogue scale.
Bold font is used within the table to emphasise sections.
[a] Median (IQR)/# missing data.
[b] n positive (% positive); percentage is out of those with complete data; history items only collected at BL; current medications assessed at FU.
[c] Methotrexate (n = 5), IVIG (n = 2), plaquenil (n = 3); note that plaquenil monotherapy (n = 1) was not considered systemic immune suppressant therapy.

paired measurements of the same individual. We identified 1075 proteins (1062 unique) associated with PGA (Fig 4A, Supplementary Table S4). Many top proteins associated with PGA reflected IFN signalling (GBP1, IFNL1, CXCL10) and muscle structure and function (MYOM2, MYL3, MYBPC1) (Fig 4A). Top enriched pathways included endothelial cell interactions, IFN signalling, NK cytotoxicity, Th17-derived cytokine signalling, apoptosis, chemotaxis, and proteolysis (Fig 4B). Because the initial analysis revealed that many DEP normalise by 6 months, we investigated potential markers of lower disease activity. To do this, we identified the intersection of proteins associated with disease activity also differentially expressed at 6-month FU compared to CTL, identifying CXCL10, PARP1, IL1RN, SOD2, and IL6 as candidate markers that can potentially detect not only higher baseline disease activity but also lower persistent disease activity (Fig 4C).

Candidate markers of tissue-specific disease activity reflect endothelial cell dysfunction

To identify putative tissue-specific or cell-specific disease activity markers, we found the intersection of PGA-associated proteins with the HPA [25] 'tissue enriched' and 'tissue enhanced' protein lists for muscle, skin, and endothelial cells (Fig 5A,B, full list of HPA proteins included in Supplementary Table S5). We identified 30 muscle, 20 skin, and 46 endothelial cell-specific disease activity-associated proteins (Fig 5A,B, Supplementary Table S5). A hypergeometric test was performed for each tissue, which revealed that only endothelial cell-specific proteins were over-represented among disease activity-associated proteins ($P = .04$, uncorrected) (Fig 5B).

To validate protein specificity within JDM target tissues and investigate gene expression at the single-cell level, we utilised a

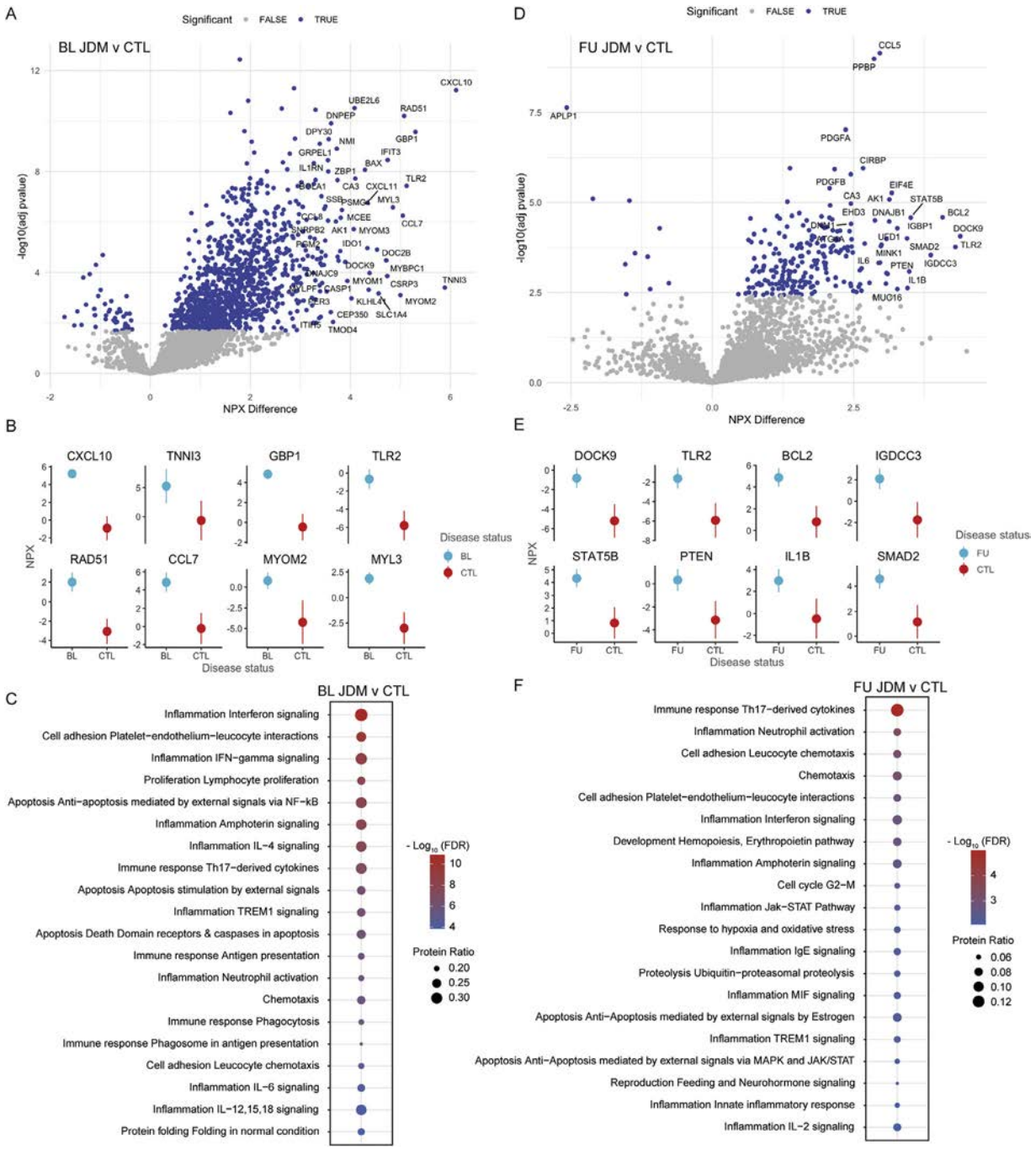

Figure 2. (A) Volcano plot displaying differentially expressed proteins (DEP) in baseline (BL) juvenile dermatomyositis (JDM) compared to control (CTL) using a linear mixed effects model with site as a covariate. Significance was defined as *P*-adj < .05 in the linear mixed effects model and *P*-adj < .05 in the post-hoc test. (B) Point range plots of the top 8 proteins with the greatest normalised protein expression (NPX) difference. The dots represent the fixed effect NPX estimate and the line the 95% CI summarising the NPX difference between BL JDM and CTL accounting for site effect. (C) Dot plot representing the top 20 Metacore process networks enriched at BL JDM vs CTL DEP, where dot size represents the protein ratio of DEP within each pathway and the colour of the dot represents significance defined by the FDR (false discovery rate). (D-F) Same as A-C, except for follow-up (FU) compared to CTL analyses. IFN, interferon; IL, interleukin; NF-kB, nuclear factor kappa B.

single nuclei RNAseq muscle dataset (n = 6 JDM, n = 7 CTL, 26,638 total nuclei) and a single-cell RNAseq skin dataset (n = 12 JDM, n = 4 CTL, 91,216 cells) generated by our group. Several disease activity-associated proteins exhibited tissue- and cell-specific gene expression (Fig 5C,D). *MYL3* was specifically expressed in type 1 muscle fibres, whereas *CAPN3* and *ANK2* were more broadly expressed in multiple muscle fibre types (Fig 5C). Skin-related markers were primarily expressed in keratinocytes (Fig 5D). Interestingly, endothelial-related genes, including *FLT1*, also known as vascular endothelial growth factor receptor 1 (*VEGFR1*), were expressed in both muscle and skin endothelial cells (Fig 5C,D).

To determine if tissue-specific proteins associated with clinical muscle and skin measures, we fit models using the tissue- or cell-specific proteins from HPA also represented in the Olink panel (n = 243 proteins, Supplementary Table S6). While muscle-specific proteins are most strongly associated with muscle

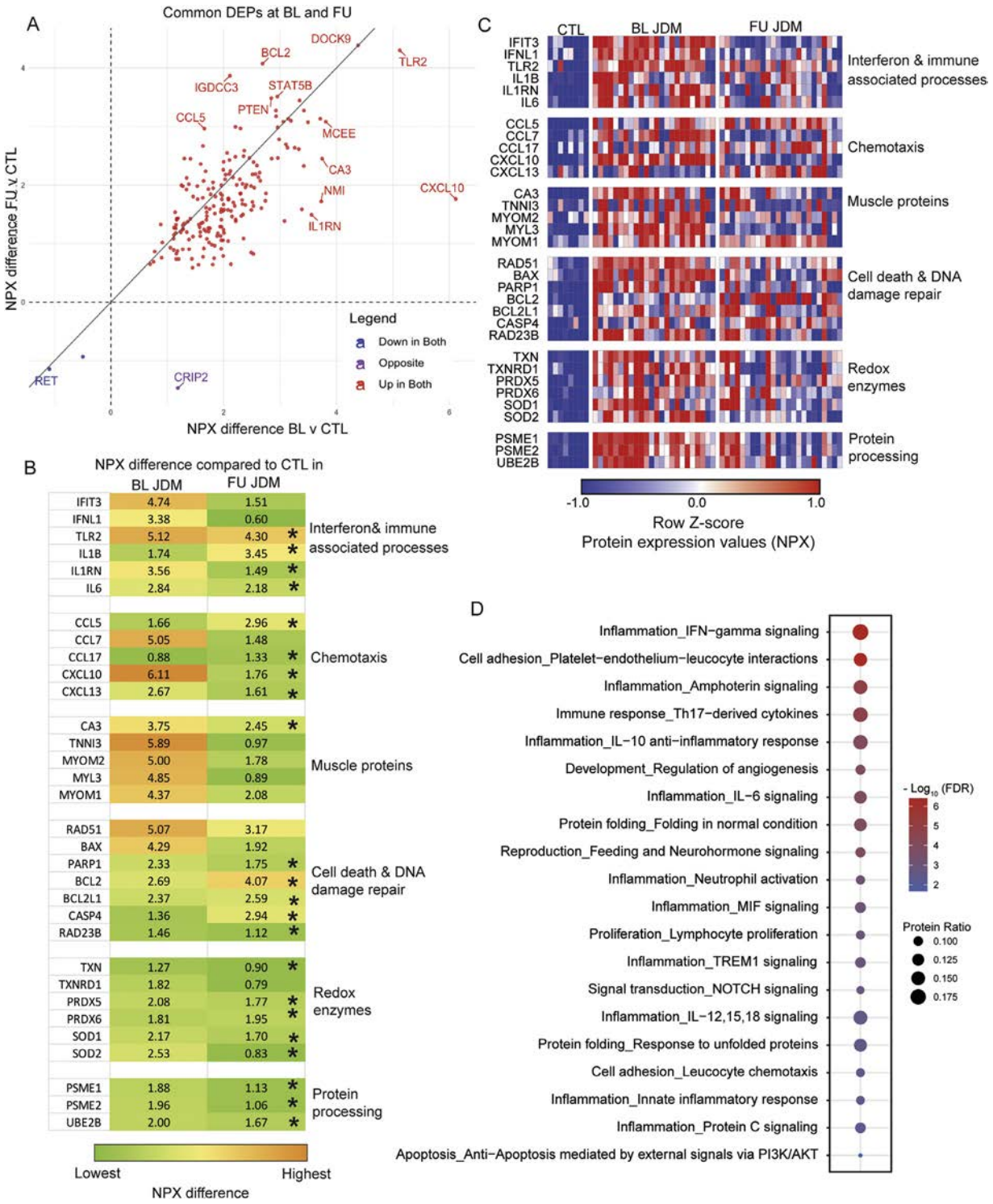

Figure 3. (A) Scatter plot comparing NPX difference of 196 common DEPs in BL compared to CTL (x-axis) and FU compared to CTL (y-axis). (B) Heatmap displaying the NPX difference between BL JDM and CTL and FU JDM and CTL for select DEPs at BL JDM of interest grouped by biological processes to highlight change in these proteins from BL to FU. Asterisks are used to indicate significance for the FU compared to CTL analysis. Of note, IL1B is not differentially expressed in BL JDM but was included to highlight the increase in NPX difference at 6 months. (C) Heatmap displaying NPX *z*-score expression of select proteins in 24 paired samples (and 8 CTL samples) grouped by biological pathways of interest. (D) Dot plot representing Metacore process networks enriched in the set of nonsignificant proteins in a paired analysis of n = 24 samples with BL and FU measurements, where dot size represents the protein ratio of DEP within each pathway and the colour of the dot represents significance as defined by the FDR (false discovery rate). BL, baseline; CTL, control; DEP, differentially expressed protein; FU, follow-up; IFN, interferon; IL, interleukin; JDM, juvenile dermatomyositis; NPX, normalised protein expression.

disease measures (CHAQ, muscle VAS) (Fig 5D), a similar number of endothelial-specific proteins significantly associated with these outcomes (Supplementary Table S6). Only 3 proteins were significantly associated with physician skin VAS, including IL34, a skin-specific marker, as the top associated protein (Fig 5D). CK and aldolase, clinical muscle enzymes, demonstrated low Spearman correlation with PGA, with CK being particularly poor at FU (Fig 5E), highlighting the need for improved markers of tissue inflammation, particularly with lower disease activity.

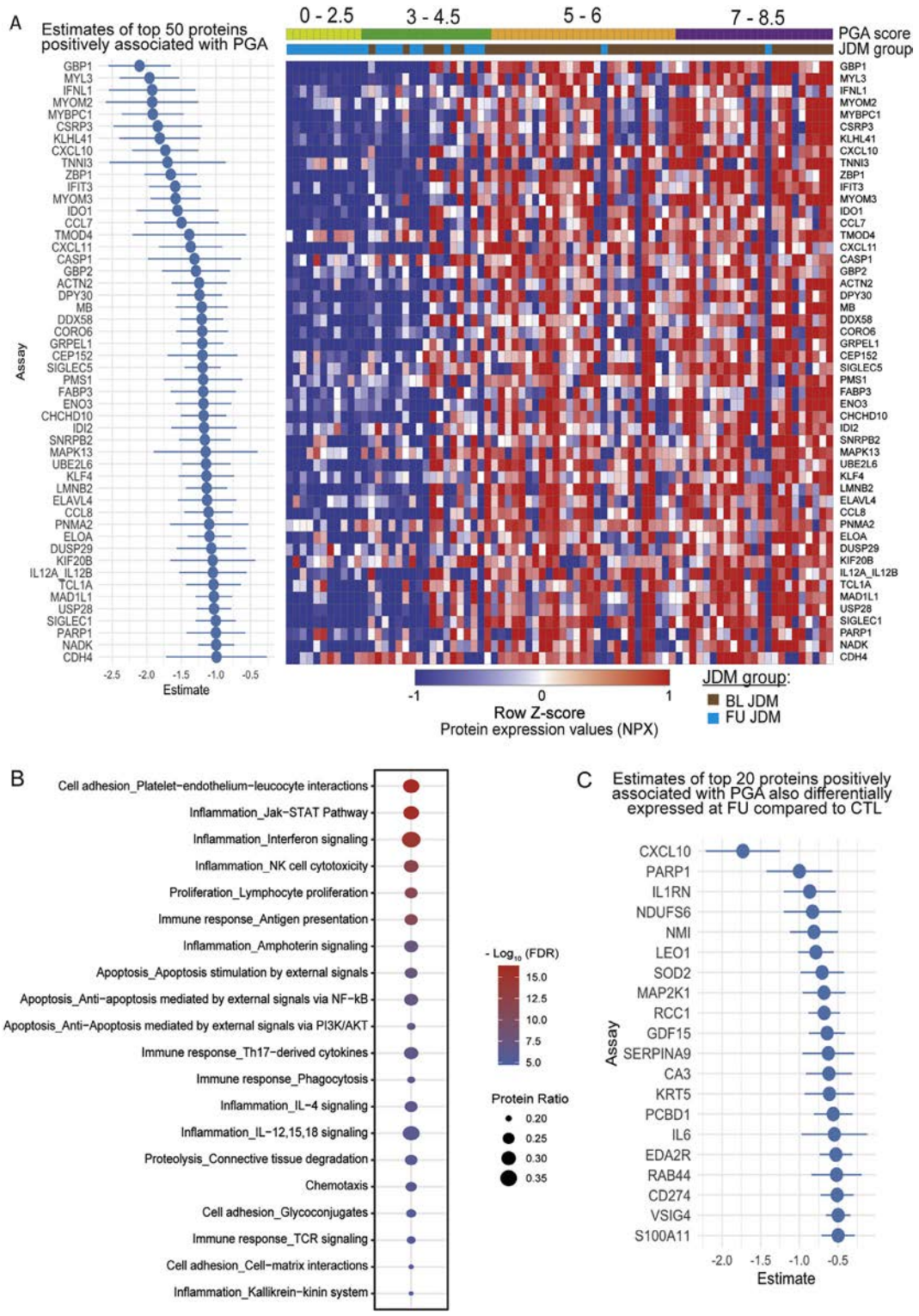

Figure 4. (A) (Left) Point range plot of the top 50 proteins with the greatest estimates in a linear mixed effects model with post-hoc testing evaluating the association with disease activity measured by the physician global assessment (PGA) and (right) a heatmap of individual-level z-score NPX expression of this set of proteins. The dot represents the fixed effect NPX estimate, and the line the 95% CI summarising the association with PGA, accounting for site effect and individual, where negative estimates represent proteins positively associated with PGA. A PGA score of 8.5 was the maximum value in the cohort. (B) Dot plot representing Metacore process networks enriched in PGA-associated proteins where dot size represents the percentage of DEPs within that pathway and colour represents significance defined by the FDR (false discovery rate). (C) Point range plot displaying the top 20 proteins with the greatest estimates from the PGA analysis that are also differentially expressed in the FU compared to CTL analysis. BL, baseline; CTL, control; DEP, differentially expressed protein; IL, interleukin; FU, follow-up; JDM, juvenile dermatomyositis; NF-kB, nuclear factor kappa B; NK, natural killer; NPX, normalised protein expression; TCR, T cell receptor.

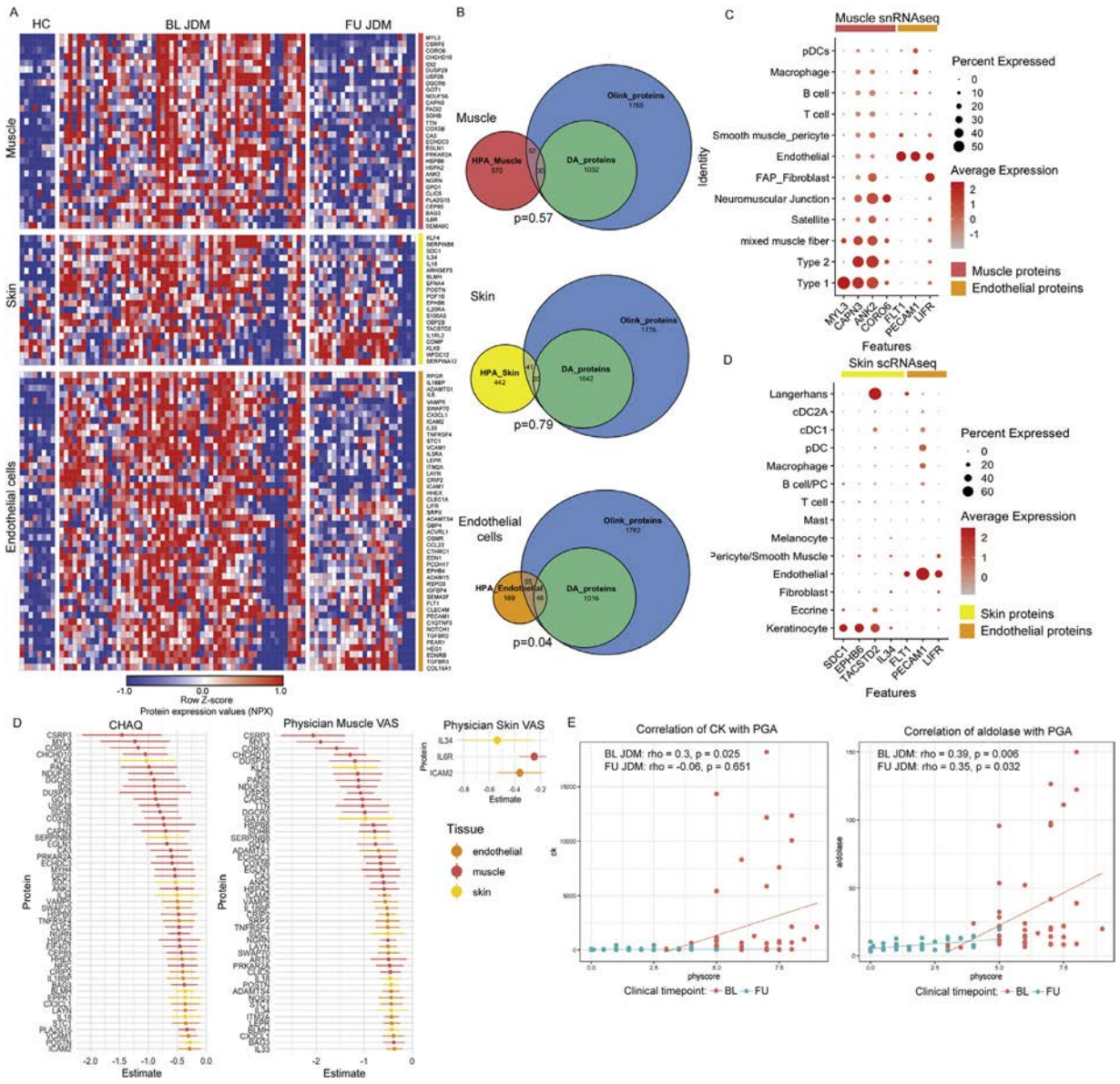

Figure 5. (A) Heatmap displaying individual-level *Z*-score normalised protein expression (NPX) expression of disease activity-associated proteins overlapping with tissue-specific proteome lists from the Human Protein Atlas (HPA) organised by tissue and ordered by decreasing estimates within each tissue. (B) Euler diagrams showing the overlap between tissue-specific lists from HPA, disease activity (DA) associated proteins (n = 1075) and the complete Olink protein dataset (n = 2897). *P* values represent the significance of a hypergeometric test to assess for enrichment of the tissue-specific lists within the intersection of these lists. (C, D) Dotplots displaying average gene expression (indicated by colour) and per cent of cells (indicated by size of dot) expression for select markers in (C) single nuclei RNA sequencing data from muscle (n = 6 JDM, n = 7 control, 26,638 total nuclei) and (D) single-cell RNA sequencing data from skin (n = 12 JDM, n = 4 control, 91,216 total cells). (D) Point range plots displaying the top proteins associated with Child Health Assessment Questionnaire (CHAQ), physician muscle visual analogue score (VAS), or physician skin VAS from linear mixed effects models associating with tissue-specific markers as defined by HPA represented in the Olink dataset where the dot represents the fixed effect NPX estimate and the line represents the 95% CI summarising the association with each outcome. Proteins are coloured by the associated tissue. (E) Scatter plots demonstrating the Spearman correlation (rho) between creatinine kinase (CK) (left) and aldolase (right) and the PGA score for BL samples and FU samples. BL, baseline; HC, healthy control; FU, follow-up; JDM, juvenile dermatomyositis; PGA, physician global assessment.

Anti-NXP2 JDM is associated with endothelial and fibroblast-associated proteins and angiogenesis and extra-cellular matrix remodelling pathways

To determine proteomic signatures associated with MSA subtype, we fit a model to proteins from BL JDM samples for 3 MSA groups (n = 14 anti-NXP2, n = 23 anti-TIF1γ, n = 9 anti-MDA5). Clinical data stratified by MSA subtype are presented in Supplementary Tables S7-S9, which revealed higher skin disease activity and fewer constitutional symptoms in the TIF1y+ group, higher muscle disease and less skin disease activity in the NXP2+ group, and higher transaminase elevation and skin ulceration in the MDA5+ group. There were 11 proteins associated with anti-NXP2, no proteins associated with anti-TIF1γ, and 99 proteins associated with anti-MDA5 (*P*-adj < .1 in lmer, *P*-adj < .05 in post-hoc lmer, Fig 6A,E, Supplementary Tables S10, S11). There was also a higher distribution of anti-NXP2+ patients from U-M; however, PCA analyses of DEPs in each group suggested that DEPs were driven more by MSA group differences than site differences (Supplementary Figs S6-S8). Despite a small number of DEP, anti-NXP2 associated proteins were significantly enriched in processes related to 'angiogenesis', 'vascular development', and 'extracellular matrix organisation' (Fig 6A,B, Supplementary Table S10).

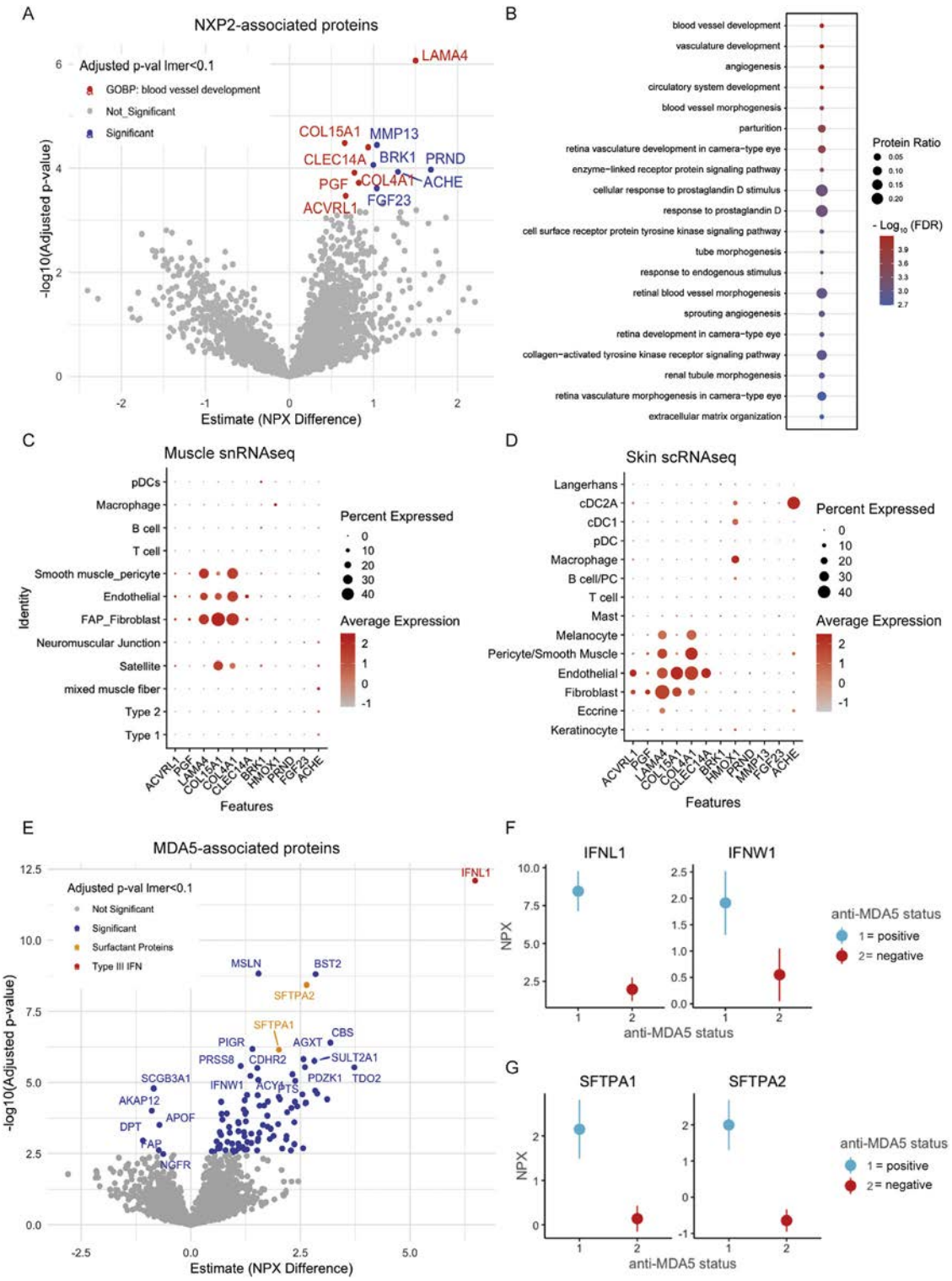

Figure 6. (A) Volcano plot displaying proteins differentially expressed in n = 14 patients with anti-NXP2 antibodies at baseline (BL) using a linear mixed effects (lme) model with post-hoc testing. Significance was defined as *P*-adj < .1 in the lmer and *P*-adj < .05 in post-hoc lme. Colour represents significance and red indicates proteins falling within the GOBP (Gene Ontology Biological Process) term 'blood vessel development'. (B) Dotplot displaying pathway enrichment analysis terms associated with NXP2-associated proteins using GOBP references where dot size represents the percentage of DEPs within that term and colour represents significance defined by the FDR (false discovery rate). (C, D) Dotplots displaying normalised gene expression (indicated by colour) and per cent of cells (indicated by size of dot) expressing the genes of NXP2-associated proteins from (C) single nuclei RNA sequencing from muscle (n = 7 JDM, n = 6 CTL, 26,638 total nuclei) and from (D) single-cell RNA sequencing from skin (n = 12 JDM, n = 4 control, 91,216 total cells). (E) Volcano plot displaying proteins differentially expressed in n = 9 patients with MDA5 antibodies at BL using an lme model with post-hoc testing. Significance was defined as *P*-adj < .1 in the lme and *P*-adj < .05 in post-hoc lme. Colour represents significance and type III IFN proteins are in red and surfactant proteins in yellow for emphasis. (F) Point range plots of IFN proteins where the dot represents the fixed effect NPX estimate and the line the 95% CI summarised the NPX difference between JDM BL patients positive for MDA5 antibodies and those negative for MDA5 antibodies. (G) Same plots as E but for surfactant proteins. DEP, differentially expressed proteins; IFN, interferon; JDM, juvenile dermatomyositis; MDA5, melanoma differentiation-associated protein 5; NPX, normalised protein expression; NXP2, nuclear matrix protein 2.

These proteins corresponded to specific cell types in JDM muscle and skin single-cell gene-expression datasets related to these processes: endothelial cells, pericytes, and fibroblasts (Fig 6C, D), which is intriguing given anti-NXP2 is associated with severe muscle disease, vasculopathy, and calcinosis [32]. LAMA4, a structural component of the endothelial cell basement membrane [33] with a role in trans-endothelial migration [34], was the top protein associated with anti-NXP2 JDM.

Anti-MDA5 JDM is associated with circulating IFNL1 and surfactant proteins

Patients with anti-MDA5 antibodies had strikingly high expression of circulating IFNL1 (Fig 6E,F), a type III IFN, whose receptor is more restricted to epithelial surfaces in the lung, gut, and skin than type I IFN receptors, which are ubiquitously expressed [35]. IFNW1, a type I IFN, was also significant. Anti-MDA5 DEP were enriched in numerous metabolic processes, including oxidative stress responses (Supplementary Table S11). To our surprise, anti-MDA5 patients also had higher surfactant-related proteins SFTPA1 and SFTPA2 (Fig 6F), primarily expressed by lung type II pneumocytes. Only 1 anti-MDA5 patient had known lung disease at sampling identified by computed tomography imaging through routine screening.

DISCUSSION

Using exploratory plasma proteomics in a multicentre North American JDM longitudinal cohort, we identified biological pathways persistently dysregulated at 6 months despite treatment, including multiple innate immune (IL1, IL6, TLR2), redox (SOD2), proteasomal (PSME1/2, UBE2B), cell death (BCL2, CASP4) and DNA damage repair (RAD23B, PARP1) pathways. In addition to highlighting some less traditional pathways linked to JDM pathogenesis, this study also independently validated inflammatory and IFN-related proteins previously reported in JDM, including CXCL10 [17,21] and CCL7 [23]. By integrating tissue data from the HPA and JDM organ-specific single-cell datasets, we defined circulating tissue and cell-type-specific disease activity-associated proteins, including MYL3 (muscle) and IL34 (skin). We also highlighted overrepresentation of endothelial cell-specific markers, including FLT1, in proteins associated with disease activity, emphasising the central role of vasculopathy in JDM. We further described distinctive proteomic signatures of NXP2 and MDA5 JDM subgroups, laying the groundwork for better understanding JDM disease heterogeneity.

Leveraging longitudinal analysis, we uncovered proteins and pathways with subtle but persistent dysregulation that might be obscured using other research designs. Notably, redox and proteasomal signalling emerged as top dysregulated pathways, suggesting ongoing oxidative stress and antigen processing posttreatment. These findings are consistent with other studies describing proteasomal upregulation [36], oxidative stress [37], and mitochondrial dysfunction [38,39] in JDM. We also observed shifts in IL1B, CCL5, and BCL2, which appear to rise at 6 months posttreatment, raising questions regarding the role of these proteins in inflammation vs repair. Elevated circulating CCL5, an immunoregulatory chemokine, has been described not only in autoimmune myositis but also in hereditary muscle disorders and may arise from chronic muscle damage or myokine secretion [40]. CCL5 is a chemoattractant and can promote angiogenesis, revascularisation, and muscle regeneration [41]. IL1B has been previously described in JDM with low disease activity states [14], posing hypotheses of chronic muscle damage, especially as related to mitochondrial dysfunction [42,43]. Overall, these findings highlight multiple pathways with persistent dysregulation that may represent alternate treatment targets.

This study reinforces and expands upon emerging candidate markers of JDM disease activity. While proteins related to IFN signalling and muscle structure/function are most strongly associated with disease activity, disease activity-associated DEP at 6-month FU represented diverse biological processes. This suggests that alternate proteins, or a combination of proteins, may be useful to assess lower levels of disease activity. Notably, both SOD2 and PARP1 function in response to cellular injury and oxidative stress. Although SOD2 traditionally facilitates the production of reactive oxygen species (ROS), it may also buffer ROS effects under the mitochondrial unfolded protein response [44]. Notably, low SOD levels have been associated with poor prognosis and exacerbation of interstitial lung disease (ILD) in adult anti-MDA5 DM [45]. PARP1 similarly has dual roles, both as an enhancer of ROS generation and a modulator of DNA repair. Future longitudinal studies validating these biomarkers in a range of disease activity states should be prioritised, especially considering limitations of IFN and muscle-related biomarkers that may normalise more rapidly with treatment.

We also identified candidate markers reflecting organ-specific disease activity that could be useful in distinguishing disease activity from damage and monitoring of organ-specific disease activity. We found cell-type-specific muscle markers, including MYL3 for type I fibres. We identified IL-34 as a skin marker and FLT1, LIFR, and PECAM1 as endothelial markers. Endothelial-associated markers were over-represented among disease activity-associated proteins, including FLT1 (VEGFR1). Interestingly, soluble FLT1 acts as a decoy receptor, serving to inhibit rather than promote angiogenesis like the membrane-bound form [46]. Thus, FLT1 elevation in plasma and its association with disease activity may reflect impaired angiogenesis and vascular repair in target tissues. These findings support a central role for vascular dysregulation in JDM pathogenesis [21,22] and emphasise the critical need for vascular markers for JDM disease monitoring.

MSAs define clinical subgroups, and we found unique proteins and pathways for specific MSAs. Within anti-NXP2 JDM, we noted enrichment for angiogenesis and extracellular matrix remodelling proteins, including LAMA4. LAMA4, a laminin subunit which promotes migration of cells to inflamed tissue and regulates angiogenesis [47], showed gene expression in endothelial cells and fibroblasts in both JDM skin and muscle. It is possible that elevated LAMA4 levels may reflect more severe vasculopathy and could serve as a candidate marker of ongoing vasculopathy in anti-NXP2 JDM. In anti-MDA5 JDM, we identified high circulating levels of IFNL1, a type III IFN, which is highly expressed in lung, gut, and skin epithelium [35], all of which are clinically affected tissues in anti-MDA5 disease. IFNL1 signals with JAK1 and TYK2, making JAK inhibitors an attractive treatment for MDA5 JDM [15,35]. Small studies have indicated that anti-MDA5 JDM may have higher type I IFN-regulated gene expression in blood and muscle [10,48]; however, type I and type III IFN activate similar gene responses, so without proteomic resolution, the IFN source or type may be unclear [35]. We also identified elevated surfactant proteins (SFTPA1, SFTPA2) in anti-MDA5 JDM, despite the lack of clinically apparent lung disease. Surfactant protein A has been reported as a serum marker of nonmyositis-associated ILD [49]. Surfactant protein D is a prognostic marker for mortality in adult MDA5-

ILD [50]. Since ILD is more common in anti-MDA5 JDM, higher circulating surfactant proteins may indicate subclinical lung inflammation in anti-MDA5 JDM.

A strength of our study is the inclusion of JDM plasma samples from multiple sites including CARRA Registry and Biobank; however, we had to account for site differences and not all patients had FU samples, overall decreasing power in the models. Given cost and sample constraints, we included a limited number of controls from 2 sites, but the primary focus of our study was to compare proteomic signatures between JDM samples, and we used strict cutoffs with multiple hypothesis testing and emphasised only individual proteins with large effect sizes. We had missing data for clinical disease activity measures in several patients, including the Cutaneous Dermatomyositis Disease Area and Severity Index Score activity, Manual Muscle Testing and a Subset of Eight Muscles and Childhood Myositis Assessment Scale scores, and relied on multiple physicians to score clinical measures, which may have impacted those analyses. While we were able to utilise the HPA to define tissue/cell-specific expression and used separate JDM tissue datasets to validate expression at a single-cell level in muscle and skin, we have not yet validated candidate plasma proteins in an independent JDM cohort due to limited sample availability. There were also relatively small numbers of individuals by MSA group, and we were unable to detect proteins associated with the TIF1y group, which may be due to statistical power or potentially clinical differences of systemic disease in this cohort, as skin disease activity markers may not be as represented in plasma, highlighting areas for further study. Future studies should focus on validation of markers in an independent JDM cohort and longitudinal assessments of candidate biomarkers beyond 6 months, to further support the clinical utility of these findings. Mechanistic studies to assess the role of persistently dysregulated pathways highlighted here, as well as the MSA-associated pathways, will help establish their roles in JDM pathogenesis.

By highlighting the multifaceted JDM disease biology and heterogeneity through a proteomic lens, we lay the groundwork for the development of a multiprotein biomarker panel for JDM disease monitoring. We identify key persistently dysregulated pathways in JDM despite treatment, highlight tissue and cell-type-specific markers of disease activity, and define MSA-associated proteins in anti-NXP2 and anti-MDA5 patients with JDM that may serve to distinguish disease endotypes. These findings are a key step towards the beginnings of precision medicine in JDM.

Competing interests

JLT and JN report financial support was provided by CARRA Inc. JLT, JN, JMK, SPF, and GKF report financial support was provided by The Chan Zuckerberg Initiative. JLT, JN, HK, JMK, GKF, and MS report financial support was provided by National Institutes of Health. JN and JD report financial support was provided by Cure JM Foundation. HK reports a relationship with Cabaletta Bio Inc that includes: consulting or advisory. JLT reports a relationship with Cabaletta Bio Inc that includes: consulting or advisory. HK reports a relationship with Bristol Myers Squibb Co that includes: nonfinancial support. JMK reports a relationship with Q32 Bio that includes: funding grants. JMK reports a relationship with Bristol Myers Squibb Co that includes: consulting or advisory and funding grants. JMK reports a relationship with Ventus Therapeutics Inc that includes: consulting or advisory and funding grants. JMK reports a relationship with ROME Therapeutics that includes: consulting or advisory and funding grants. JMK reports a relationship with Janssen Therapeutics that includes: funding grants. JMK reports a relationship with AstraZeneca that includes: consulting or advisory. JMK reports a relationship with Biogen that includes: consulting or advisory. JMK reports a relationship with Eli Lilly that includes: consulting or advisory. JMK reports a relationship with EMD Serrano that includes: consulting or advisory. JMK reports a relationship with Gilead Sciences that includes: consulting or advisory. JMK reports a relationship with GlaxoSmithKline Inc that includes: consulting or advisory. JMK reports a relationship with Aurinia Pharmaceuticals Inc that includes: consulting or advisory. HK reports a relationship with Eli Lilly and Company that includes: nonfinancial support. JD consults for Rare Disease Research. If there are other authors, they declare that they have no known competing financial interests or personal relationships that could have appeared to influence the work reported in this paper.

CRediT authorship contribution statement

Jessica Neely: Writing – review & editing, Writing – original draft, Visualization, Resources, Investigation, Funding acquisition, Formal analysis, Data curation, Conceptualization. **Sara E. Sabbagh:** Writing – review & editing, Writing – original draft, Investigation, Conceptualization. **Jeffrey Dvergsten:** Writing – review & editing, Resources, Investigation, Conceptualization. **Chioma Madubata:** Writing – review & editing, Visualization, Formal analysis, Data curation. **Celine C. Berthier:** Writing – review & editing, Visualization, Formal analysis, Data curation. **Zilan Zheng:** Writing – review & editing, Project administration, Formal analysis, Data curation. **Christine Goudsmit:** Writing – review & editing, Project administration, Methodology, Investigation. **Sophia Matossian:** Writing – review & editing, Project administration, Data curation. **Sean P. Ferris:** Resources, Methodology, Investigation. **Gabriela K. Fragiadakis:** Writing – review & editing, Visualization, Supervision, Investigation. **Marina Sirota:** Writing – review & editing, Visualization, Supervision, Investigation. **J. Michelle Kahlenberg:** Writing – review & editing, Visualization, Supervision, Investigation. **Hanna Kim:** Writing – review & editing, Writing – original draft, Visualization, Resources, Investigation, Data curation, Conceptualization. **Jessica L. Turnier:** Writing – review & editing, Writing – original draft, Visualization, Resources, Investigation, Funding acquisition, Formal analysis, Data curation, Conceptualization.

Acknowledgements

This work could not have been accomplished without the patients who generously shared their samples for our work. This study utilized data and biospecimens collected in the CARRA Registry. The views expressed are the authors' and do not necessarily represent the view of CARRA. We want to thank all participants and hospital sites that recruited patients for the CARRA Registry. We thank the University of Michigan and C.S. Mott juvenile myositis patient and family advisory committee for advising the research study. We thank patients and families who participated in the UCSF JuMP Study and the U-M JDM registry and biobank. This work could also not have been accomplished without the aid of the following organisations: The Childhood Arthritis and Rheumatology Research Association (CARRA), the NIH's National Institute of Arthritis and Musculoskeletal and Skin Diseases (NIAMS), George M. O'Brien Michigan Kidney Translational Resource Center (MKTC) funded by NIH/NIDDK

grant U54DK137314, the Arthritis Foundation, and the Cure JM Foundation (Cure JM). The authors thank the following CARRA Registry site principal investigators, subinvestigators and research coordinators: R. Aamir, K. Abulaban, A. Adams, C. Aguiar Lapsia, H. Ahmed, S. Akoghlanian, A. AlBijadi, E. Allenspach, M. Alpizar, G. Amarilyo, M. Amoruso, S. Angeles-Han, S. Ardoin, S. Armendariz, N. Aviran Dagan, I. Balboni, S. Balevic, S. Ballinger, S. Baluta, L. Barillas-Arias, L. Barillas-Arias, M. Basiaga, K. Baszis, M. Becker, A. Begezda, E. Beil, H. Bell-Brunson, H. Benham, S. Benseler, L. Bermudez-Santiago, W. Bernal, T. Bigley, C. Bingham, B. Binstadt, C. Black, B. Blackmon, M. Blakley, J. Bohnsack, A. Boneparth, H. Bradfield, J. Bridges, E. Brooks, M. Brothers, D. Brown, H. Brunner, L. Buckley, Mary Buckley, Meredith Buckley, H. Bukulmez, D. Bullock, A. Cancino, S. Canna, L. Cannon, S. Canny, V. Cartwright, E. Chalom, Johanna Chang, Joyce Chang, M. Chang, A. Chang-Hoftman, A. Chen, P. Chiraseveenuprapund, K. Ciaglia, M. Cidon, D. Co, E. Cohen, R. Connor, K. Cook, A. Cooper, J. Cooper, K. Corbin, C. Correll, R. Cron, M. Curry, A. Dagci, A. Dalrymple, E. Datyner, T. Davis, D. De Ranieri, J. Dean, C. DeCoste, F. Dedeoglu, M. DeGuzman, N. Delnay, E.L. DeSantis, R. Devine, M. Dhalla, A. Dhanrajani, D. Dissanayake, B. Dizon, J. Drew, K. Driest, Q. Du, E. Duncan, K. Dunnock, D. Durkee, J. Dvergsten, A. Eberhard, K. Ede, B. Edelheit, C. Edens, M. Elder, Y. Elzaki, C. Failing, D. Fair, L. Favier, B. Feldman, J. Fennell, I. Ferguson, P. Ferguson, C. Figueroa, E. Flanagan, L. Fogel, E. Fox, M. Fox, L. Franklin, R. Fuhlbrigge, J. Fuller, T. Futch-West, S. Gagne, M. Geiszler, D. Gerstbacher, M. Gilbert, A.C. Gironella, D. Glaser, I. Goh, S. Gorry, N. Goswami, B. Gottlieb, T. Graham, S. Grevich, T. Griffin, A. Grim, A. Grom, M. Guevara, L. Guzman, T. Hahn, O. Halyabar, E. Hammelev, T. Hammond, S. Haro, J. Harris, O. Harry, J. Hausmann, A. Hay, K. Hays, K. Hayward, L. Henderson, M. Henrickson, A. Hersh, L. Hiraki, M. Hiskey, P. Hobday, C. Hoffart, M.J. Holland, M. Hollander, S. Hong, D. Horton, J. Hsu, A. Huber, J. Huggins, J. Hui-Yuen, M. Ibarra, A. Imlay, L. Imundo, C. Inman, A. Jackson, K. James, G. Janow, Y. Jiang, L. Johnson, N. Johnson, J. Jones, D. Kafisheh, K. Kaidar, S. Kasinathan, R. Kaur, E. Kessler, B. Kienzle, S. Kim, Y. Kimura, D. Kingsbury, M. Kitcharoensakkul, J. Klauss, K. Klein, M. Klein-Gitelman, A. Knight, L. Kovalick, D. Krajewski, C. Kremer, T. LaFlam, B. Lang, S. Lapidus, B. Lapin, A. Lasky, E. Lawson, R. Laxer, A. Lee, Patricia Lee, Pui Lee, T. Lee, E. Leisinger, L. Lentini, M. Lerman, Y. Levinsky, D. Levy, S. Li, S. Lieberman, L. Lim, E. Limenis, C. Lin, N. Ling, G. Lionetti, R. Livny, M. Lo, A. Long, M. Lopez-Peña, D. Lovell, S. Lvovich, A. Lytch, M. Ma, A. Machado, J. MacMahon, J. Madison, M. Mannion, C. Manos, L. Mansfield, B. Marston, K. Marzan, T. Mason, S. Matossian, L. McAllister, K. McBrearty, D. McCurdy, K. McDaniels, J. McDonald, L. McIntosh, E. Meidan, E. Mellins, Z. Mian, P. Miettunen, M. Miller, D. Milojevic, R. Mitacek, R. Modica, S. Mohan, K. Moore, T. Moore, L. Moorthy, J. Moreno, E. Morgan, A. Moyer, B. Murante, A. Murphy, E. Muscal, O. Mwizerwa, A. Najafi, K. Nanda, L. Nassi, S. Nativ, M. Natter, J. Neely, L. Newhall, A. Nguyen, P. Nigrovic, J. Nocton, B. Nolan, A. Nowakowski, K. Nowicki, R. Oakes, E. Oberle, S. OgbonnayaWhittesley, E. Ogbu, M. Oliver, R. Olveda, K. Onel, A. Orandi, J. Padam, N. Pan, J. Pandya, S. Panupattanapong, A. Pappo Toledano, J. Patel, P. Patel, A. Patrick, S. Patrizi, S. Paul, J. Perfetto, M. Perron, M. Peskin, C. Pinotti, L. Ponder, R. Pooni, S. Prahalad, M. Quinlan-Waters, J. Rafko, H. Rahimi, S. Ramsey, R. Randell, L. Ray, Ann Reed, Annelle Reed, H. Reid, D. Reiff, I. Reyhan, B. Richard, M. Riebschleger, E. Rife, M. Riskalla, A. Robinson, L. Robinson, L. Rodgers, M. Rodriquez, D. Rogers, T. Ronis, A. Rosado, M. Rosenkranz, N. Rosenwasser, H. Rothermel, D. Rothman, E. Rothschild, K. Rouster - Stevens, T. Rubinstein, N. Ruth, S. Sabbagh, R. Sadun, L. Santiago, V. Saper, A. Sarkissian, L. Scalzi, J. Schahn, K. Schikler, A. Schlefman, B. Schlichting, H. Schmeling, E. Schmitt, G. Schulert, C. Schutt, C. Seper, B. Shaham, R. Sheets, A. Shehab, S. Shenoi, M. Sherman, J. Shirley, M. Shishov, N. Singer, V. Sivaraman, E. Sloan, C. Smith, J. Smith, E. Smitherman, J. Soep, M.B. Son, C. Spencer, L. Spiegel, J. Spitznagle, H. Srinivasalu, H. Stapp, A. Stephens, Y. Sterba Rakovchik, S. Stern, B. Stevens, R. Stevenson, C. Stingl, M. Stoll, E. Stringer, S. Sule, J. Sullivan, R. Sundel, M. Sutter, C. Swaffar, N. Swayne, T. Symington, G. Syverson, A.M. Szymanski, S. Taber, R. Tal, A. Tambralli, A. Taneja, T. Tanner, S. Tarvin, A. Taxter, M. Tesher, T. Thakurdeen, A. Theisen, G. Thieroff, B. Thomas, L. Thomas, N. Thomas, L. Timmerman, T. Ting, C. Todd, D. Toib, K. Torok, H. Tory, M. Toth, E. Treemarcki, S. Tse, T. Tse, C. Tsin, J. Twachtman-Bassett, M. Twilt, T. Valcarcel, R. Valdovinos, A. Vallee, H. Van Mater, S. Vandenbergen, C. Varghese, N. Vasquez, P. VegaFernandez, J. Verbsky, R. Verstegen, E. von Scheven, S. Vora, L. Wagner-Weiner, D. Wahezi, S. Wakefield, B. Walker, S. Wallgren, H. Walters, M. Waterfield, J. Weiss, P. Weiss, E. Wershba, V. Westheuser, K. Widrick, C. Williams, S. Wong, S. Wooldridge, L. Woolnough, T. Wright, E. Wu, A. Yalcindag, R. Yeung, K. Yomogida, A. Zeft, Y.J. Zhang, Y.D. Zhao, Z. Zheng, A. Zhu, C. Zic. This study utilised data and biospecimens collected in the Childhood Arthritis and Rheumatology Research Alliance (CARRA) Registry. The views expressed are the authors' and do not necessarily represent the view of CARRA.

Funding

This work was funded by a CARRA Large Grant and a Chan Zuckerberg Patient-Partnered Collaboration for Single-Cell Analysis of Rare Inflammatory Pediatric Disease.

JLT is supported by a NIAMS K23 Career Development Grant (K23AR080789). HK: This work was supported by the Intramural Research Program of the National Institute of Arthritis and Musculoskeletal and Skin Diseases of the National Institutes of Health (AR041215). SS is supported by a CTSI KL2 Child Health Mentored Research (KL2 TR001438). JN is supported by a NIAMS K08 Career Development Grant (K08AR081983) and the Cure JM Foundation Center of Excellence Award. JMK received support from NIAMS K24AR076975 for this work. JD is supported by the Cure JM Foundation Center of Excellence Award. GKF, MS: This work was additionally supported by UCSF Precision Medicine in Rheumatology (PREMIER; NIAMS P30-AR070155).

Patient consent for publication

All participants provided written informed consent and assent when applicable.

Ethics approval

Studies were approved by the institutional review board at University of California, San Francisco, University of Michigan, and Duke University. The CARRA Registry was reviewed by Duke University institutional review board and local institutional review boards for participating sites.

Provenance and peer review

Not commissioned; externally peer reviewed.

Data availability statement

Data will be deposited in NCBI Gene Expression Omnibus, an open public repository, at time of publication. Code will be available on a public GitHub repository.

Supplementary materials

Supplementary material associated with this article can be found in the online version at doi:10.1016/j.ard.2025.07.020.

Orcid

Jessica Neely: http://orcid.org/0000-0003-0420-7933

REFERENCES

[1] Mathiesen P, Hegaard H, Herlin T, Zak M, Pedersen FK, Nielsen S. Long-term outcome in patients with juvenile dermatomyositis: a cross-sectional follow-up study. Scand J Rheumatol 2012;41:50–8.
[2] Wienke J, Deakin CT, Wedderburn LR, van Wijk F, van Royen-Kerkhof A. Systemic and tissue inflammation in juvenile dermatomyositis: from pathogenesis to the quest for monitoring tools. Front Immunol 2018;9:2951.
[3] Pachman LM, Abbott K, Sinacore JM, Amoruso L, Dyer A, Lipton R, et al. Duration of illness is an important variable for untreated children with juvenile dermatomyositis. J Pediatr 2006;148:247–53.
[4] Gibbs E, Khojah A, Morgan G, Ehwerhemuepha L, Pachman LM. The von Willebrand factor antigen reflects the juvenile dermatomyositis disease activity score. Biomedicines 2023;11:552.
[5] Guzmán J, Petty RE, Malleson PN. Monitoring disease activity in juvenile dermatomyositis: the role of von Willebrand factor and muscle enzymes. J Rheumatol 1994;21:739–43.
[6] Khojah A, Morgan G, Pachman LM. Clues to disease activity in juvenile dermatomyositis: neopterin and other biomarkers. Diagnostics (Basel) 2021;12:8.
[7] Peng QL, Zhang YM, Liang L, Liu X, Ye LF, Yang HB, et al. A high level of serum neopterin is associated with rapidly progressive interstitial lung disease and reduced survival in dermatomyositis. Clin Exp Immunol 2020;199:314–25.
[8] Baechler EC, Bauer JW, Slattery CA, Ortmann WA, Espe KJ, Novitzke J, et al. An interferon signature in the peripheral blood of dermatomyositis patients is associated with disease activity. Mol Med 2007;13:59–68.
[9] Neely J, Hartoularos G, Bunis D, Sun Y, Lee D, Kim S, et al. Multi-modal single-cell sequencing identifies cellular immunophenotypes associated with juvenile dermatomyositis disease activity. Front Immunol 2022;13:902232.
[10] Kim H, Gunter-Rahman F, McGrath JA, Lee E, de Jesus AA, Targoff IN, et al. Expression of interferon-regulated genes in juvenile dermatomyositis versus Mendelian autoinflammatory interferonopathies. Arthritis Res Ther 2020;22:69.
[11] Moneta GM, Pires Marafon D, Marasco E, Rosina S, Verardo M, Fiorillo C, et al. Muscle expression of type I and type II interferons is increased in juvenile dermatomyositis and related to clinical and histologic features. Arthritis Rheumatol 2019;71:1011–21.
[12] Turnier JL, Pachman LM, Lowe L, Tsoi LC, Elhaj S, Menon R, et al. Comparison of lesional juvenile myositis and lupus skin reveals overlapping yet unique disease pathophysiology. Arthritis Rheumatol 2021;73:1062–72.
[13] Weiden C, Saers M, Schwarz T, Hinze T, Wittkowski H, Kessel C, et al. Type 1 interferon-stimulated gene expression and disease activity in pediatric rheumatic diseases: no composite scores needed? ACR Open Rheumatol 2023;5:652–62.
[14] Roberson EDO, Mesa RA, Morgan GA, Cao L, Marin W, Pachman LM. Transcriptomes of peripheral blood mononuclear cells from juvenile dermatomyositis patients show elevated inflammation even when clinically inactive. Sci Rep 2022;12:275.
[15] Wallwork RS, Paik JJ, Kim H. Current evidence for janus kinase inhibitors in adult and juvenile dermatomyositis and key comparisons. Expert Opin Pharmacother 2024;25:1625–45.
[16] Sparks R, Rachmaninoff N, Lau WW, Hirsch DC, Bansal N, Martins AJ, et al. A unified metric of human immune health. Nat Med 2024;30:2461–72.
[17] Tawalbeh SM, Marin W, Morgan GA, Dang UJ, Hathout Y, Pachman LM. Serum protein biomarkers for juvenile dermatomyositis: a pilot study. BMC Rheumatol 2020;4:52.
[18] Sato H, Inoue Y, Kawashima Y, Konno R, Ohara O, Kuwana M, et al. In-depth proteomic analysis of juvenile dermatomyositis serum reveals protein expression associated with muscle-specific autoantibodies. Rheumatology (Oxford) 2023;62:3501–6.
[19] Sparling AC, Ward JM, Sarkar K, Schiffenbauer A, Farhadi PN, Smith MA, et al. Neutrophil and mononuclear leukocyte pathways and upstream regulators revealed by serum proteomics of adult and juvenile dermatomyositis. Arthritis Res Ther 2024;26:196.
[20] Kishi T, Chipman J, Evereklian M, Nghiem K, Stetler-Stevenson M, Rick ME, et al. Endothelial activation markers as disease activity and damage measures in juvenile dermatomyositis. J Rheumatol 2020;47:1011–8.
[21] Wienke J, Pachman LM, Morgan GA, Yeo JG, Amoruso MC, Hans V, et al. Endothelial and inflammation biomarker profiles at diagnosis reflecting clinical heterogeneity and serving as a prognostic tool for treatment response in two independent cohorts of patients with juvenile dermatomyositis. Arthritis Rheumatol 2020;72:1214–26.
[22] Wienke J, Mertens JS, Garcia S, Lim J, Wijngaarde CA, Yeo JG, et al. Biomarker profiles of endothelial activation and dysfunction in rare systemic autoimmune diseases: implications for cardiovascular risk. Rheumatology (Oxford) 2021;60:785–801.
[23] Ward JM, Ambatipudi M, O'Hanlon TP, Smith MA, de Los Reyes M, Schiffenbauer A, et al. Shared and distinctive transcriptomic and proteomic pathways in adult and juvenile dermatomyositis. Arthritis Rheumatol 2023;75:2014–26.
[24] McCann LJ, Pilkington CA, Huber AM, Ravelli A, Appelbe D, Kirkham JJ, et al. Development of a consensus core dataset in juvenile dermatomyositis for clinical use to inform research. Ann Rheum Dis 2018;77:241–50.
[25] Omenn GS, Lane L, Lundberg EK, Overall CM, Deutsch EW. Progress on the HUPO draft human proteome: 2017 metrics of the human proteome project. J Proteome Res 2017;16:4281–7.
[26] McGinnis CS, Murrow LM, Gartner ZJ. DoubletFinder: doublet detection in single-cell RNA sequencing data using artificial nearest neighbors. Cell Syst 2019;8 329-37.e4.
[27] Young MD, Behjati S. SoupX removes ambient RNA contamination from droplet-based single-cell RNA sequencing data. Gigascience 2020;9:giaa151.
[28] Korsunsky I, Millard N, Fan J, Slowikowski K, Zhang F, Wei K, et al. Fast, sensitive and accurate integration of single-cell data with Harmony. Nat Methods 2019;16:1289–96.
[29] McCann LJ, Juggins AD, Maillard SM, Wedderburn LR, Davidson JE, Murray KJ, et al. The Juvenile Dermatomyositis National Registry and Repository (UK and Ireland)—clinical characteristics of children recruited within the first 5 yr. Rheumatology (Oxford) 2006;45:1255–60.
[30] Shah M, Mamyrova G, Targoff IN, Huber AM, Malley JD, Rice MM, et al. The clinical phenotypes of the juvenile idiopathic inflammatory myopathies. Medicine (Baltimore) 2013;92:25–41.
[31] Wei MC, Zong WX, Cheng EH, Lindsten T, Panoutsakopoulou V, Ross AJ, et al. Proapoptotic BAX and BAK: a requisite gateway to mitochondrial dysfunction and death. Science 2001;292:727–30.
[32] Rider LG, Shah M, Mamyrova G, Huber AM, Rice MM, Targoff IN, et al. The myositis autoantibody phenotypes of the juvenile idiopathic inflammatory myopathies. Medicine (Baltimore) 2013;92:223–43.
[33] Knöll R, Postel R, Wang J, Krätzner R, Hennecke G, Vacaru AM, et al. Laminin-alpha4 and integrin-linked kinase mutations cause human cardiomyopathy via simultaneous defects in cardiomyocytes and endothelial cells. Circulation 2007;116:515–25.
[34] Zegeye MM, Matic L, Lengquist M, Hayderi A, Grenegård M, Hedin U, et al. Interleukin-6 trans-signaling induced laminin switch contributes to reduced trans-endothelial migration of granulocytic cells. Atherosclerosis 2023;371:41–53.
[35] Lazear HM, Schoggins JW, Diamond MS. Shared and distinct functions of type I and type III interferons. Immunity 2019;50:907–23.
[36] Ghannam K, Martinez-Gamboa L, Spengler L, Krause S, Smiljanovic B, Bonin M, et al. Upregulation of immunoproteasome subunits in myositis indicates active inflammation with involvement of antigen presenting cells, CD8 T-cells and IFNΓ. PLoS One 2014;9:e104048.
[37] Wilkinson MGL, Moulding D, McDonnell TCR, Orford M, Wincup C, Ting JYJ, et al. Role of CD14+ monocyte-derived oxidised mitochondrial DNA in the inflammatory interferon type 1 signature in juvenile dermatomyositis. Ann Rheum Dis 2023;82:658–69.
[38] Zhong D, Wu C, Bai J, Xu D, Zeng X, Wang Q. Co-expression network analysis reveals the pivotal role of mitochondrial dysfunction and interferon signature in juvenile dermatomyositis. PeerJ 2020;8:e8611.
[39] Duvvuri B, Pachman LM, Hermanson P, Wang T, Moore R, Ding-Hwa Wang D, et al. Role of mitochondria in the myopathy of juvenile dermatomyositis and implications for skeletal muscle calcinosis. J Autoimmun 2023;138:103061.
[40] De Paepe B, Bracke KR, De Bleecker JL. An exploratory study of circulating cytokines and chemokines in patients with muscle disorders proposes

CD40L and CCL5 represent general disease markers while CXCL10 differentiates between patients with an autoimmune myositis. Cytokine X 2022;4:100063.
[41] Zhang Z, Wang Q, Yao J, Zhou X, Zhao J, Zhang X, et al. Chemokine receptor 5, a double-edged sword in metabolic syndrome and cardiovascular disease. Front Pharmacol 2020;11:146.
[42] Jabaut J, Ather JL, Taracanova A, Poynter ME, Ckless K. Mitochondria-targeted drugs enhance Nlrp3 inflammasome-dependent IL-1beta secretion in association with alterations in cellular redox and energy status. Free Radic Biol Med 2013;60:233–45.
[43] Cohen TV, Many GM, Fleming BD, Gnocchi VF, Ghimbovschi S, Mosser DM, et al. Upregulated IL-1beta in dysferlin-deficient muscle attenuates regeneration by blunting the response to pro-inflammatory macrophages. Skelet Muscle 2015;5:24.
[44] He C, Hart PC, Germain D, Bonini MG. SOD2 and the mitochondrial UPR: partners regulating cellular phenotypic transitions. Trends Biochem Sci 2016;41:568–77.
[45] Huang W, Chen D, Wang Z, Ren F, Luo L, Zhou J, et al. Evaluating the value of superoxide dismutase in anti-MDA5-positive dermatomyositis associated with interstitial lung disease. Rheumatology (Oxford) 2023;62:1197–203.
[46] Failla CM, Carbo M, Morea V. Positive and negative regulation of angiogenesis by soluble vascular endothelial growth factor receptor-1. Int J Mol Sci 2018;19:1306.
[47] Stenzel D, Franco CA, Estrach S, Mettouchi A, Sauvaget D, Rosewell I, et al. Endothelial basement membrane limits tip cell formation by inducing Dll4/Notch signalling in vivo. EMBO Rep 2011;12:1135–43.
[48] Hou C, Durrleman C, Periou B, Barnerias C, Bodemer C, Desguerre I, et al. From diagnosis to prognosis: revisiting the meaning of muscle ISG15 overexpression in juvenile inflammatory myopathies. Arthritis Rheumatol 2021;73:1044–52.
[49] Ohnishi H, Yokoyama A, Kondo K, Hamada H, Abe M, Nishimura K, et al. Comparative study of KL-6, surfactant protein-A, surfactant protein-D, and monocyte chemoattractant protein-1 as serum markers for interstitial lung diseases. Am J Respir Crit Care Med 2002;165:378–81.
[50] Lyu W, Zhou Y, Zhuang Y, Liu Y, Cao M, Xin X, et al. Surfactant protein D is associated with 3-month mortality of anti-MDA5 antibody-interstitial lung disease. Clin Exp Rheumatol 2020;38:1068–74.

Ann Rheum Dis 84 (2025) 1852–1864

Contents lists available at ScienceDirect

Annals of the Rheumatic Diseases

journal homepage: https://www.sciencedirect.com/journal/annals-of-the-rheumatic-diseases

Systemic sclerosis

Spatially informed phenotyping by cyclic-in-situ-hybridisation identifies novel fibroblast populations and their pathogenic niches in systemic sclerosis

Yi-Nan Li[1,2,*], Tim Filla[1,2], Andrea-Hermina Györfi[1,2,3], Minrui Liang[1,2,4], Veda Devakumar[1,2], Alexandru Micu[1,2], Hongtao Chai[1,2], Christina Bergmann[5,6], Ann-Christin Pecher[7], Jörg Henes[7], Pia Moinzadeh[8], Suzan Al-Gburi[8], Thomas Krieg[9,10,11], Alexander Kreuter[12], Jiucun Wang[4,13,14], Georg Schett[5,6], Bernhard Homey[15], Sascha Dietrich[16], Jörg H.W. Distler[1,2,3,*], Alexandru-Emil Matei[1,2,3,*]

[1] *Department of Rheumatology, University Hospital Düsseldorf, Heinrich Heine University, Düsseldorf, Germany*
[2] *Hiller Research Center, University Hospital Düsseldorf, Heinrich Heine University, Düsseldorf, Germany*
[3] *Fraunhofer Institute for Translational Medicine and Pharmacology ITMP, and Fraunhofer Cluster of Excellence for Immune Mediated Diseases CIMD, Frankfurt am Main, Germany*
[4] *Department of Rheumatology, Huashan Hospital, Fudan University, Shanghai, P. R. China*
[5] *Department of Internal Medicine 3, Rheumatology and Clinical Immunology, Friedrich-Alexander-University Erlangen-Nürnberg (FAU) and University Hospital Erlangen, Erlangen, Germany*
[6] *Deutsches Zentrum Immuntherapie (DZI), FAU Erlangen-Nürnberg and University Hospital Erlangen, Erlangen, Germany*
[7] *Department of Internal Medicine II, Hematology, Oncology, Clinical Immunology, and Rheumatology, University Hospital Tübingen, Tübingen, Germany*
[8] *Department of Dermatology, University Hospital Cologne, Cologne, Germany*
[9] *Center for Molecular Medicine Cologne (CMMC), University of Cologne, Cologne, Germany*
[10] *Translational Matrix Biology, Faculty of Medicine, University Hospital Cologne, Cologne, Germany*
[11] *Cologne Excellence Cluster on Cellular Stress Responses in Ageing-Associated Diseases (CECAD), University of Cologne, 50931, Cologne, Germany*
[12] *Department of Dermatology, Venereology and Allergology, Helios St. Elisabeth Klinik Oberhausen, Duisburg, Germany*
[13] *State Key Laboratory of Genetic Engineering, Collaborative Innovation Center for Genetics and Development, School of Life Sciences, and Human Phenome Institute, Fudan University, Shanghai, P. R. China*
[14] *Research Unit of Dissecting the Population Genetics and Developing New Technologies for Treatment and Prevention of Skin Phenotypes and Dermatological Diseases (2019RU058), Chinese Academy of Medical Sciences, Shanghai, P. R. China*
[15] *Department of Dermatology, University Hospital Düsseldorf, Heinrich Heine University, Düsseldorf, Germany*
[16] *Department of Hematology, Oncology and Clinical Immunology, University Hospital Düsseldorf, Heinrich Heine University, Düsseldorf, Germany*

*Correspondence to Prof. Jörg H.W. Distler, Dr. Alexandru-Emil Matei and Dr. Yi-Nan Li, Department of Rheumatology and Hiller Research Center, University Hospital Düsseldorf, Heinrich Heine University Düsseldorf, Düsseldorf, Germany.

E-mail addresses: yi-nan.li@med.uni-duesseldorf.de (Y.-N. Li), joerg.distler@med.uni-duesseldorf.de (J.H.W. Distler), Alexandru-Emil.Matei@med.uni-duesseldorf.de (A.-E. Matei).

Yi-Nan Li, Jörg H W Distler, and Alexandru-Emil Matei contributed equally.

Handling editor Josef S. Smolen.

https://doi.org/10.1016/j.ard.2025.06.002

ARTICLE INFO

Article history:
Received 10 January 2025
Received in revised form 30 May 2025
Accepted 1 June 2025

ABSTRACT

Objectives: Spatially nonresolved transcriptomic data identified several functionally distinct populations of fibroblasts in health and disease. However, in-depth transcriptional profiling *in situ* at the single-cell resolution has not been possible so far. We thus aimed to profile these populations by single-cell spatial transcriptomics using cyclic in situ hybridisation (cISH).

Methods: We studied fibroblast subpopulations in the skin of systemic sclerosis (SSc) patients and heathy individuals using cISH as a novel approach for transcriptional phenotyping with subcellular resolution. Clustering was performed using Building Aggregates with a Neighbourhood Kernel and Spatial Yardstick (BANKSY) as a novel approach for spatially informed transcriptional phenotyping. The findings were further validated by integration with single-cell RNA sequencing in distinct SSc cohorts.

Results: BANKSY-based spatially informed clustering identified 9 fibroblast (FB) subpopulations, with SFRP2+ reticular dermis (RetD) FB and CCL19+ nonperivascular (nonPV) FBs as novel subpopulations that reside in specific cellular niches and display unique gene expression profiles. SFRP2+ RetD FBs and CCL19+ nonPV FBs as well as COL8A1+ FBs display altered frequencies in SSc skin and play specific, disease-promoting roles for extracellular matrix release and leukocyte recruitment as revealed by their transcriptional profile, their cellular interactions, and ligand–receptor analyses. The frequencies of COL8A1+ FBs and their interactions with monocytic cells and B cells are associated with the progression of skin fibrosis in SSc.

Conclusions: Our cISH-based, spatially resolved transcriptomic approach identified novel fibroblast subpopulations deregulated in SSc skin with specific pathogenic roles. COL8A1+ FBs and their immune interactions may also have potential as biomarkers for future progression of skin fibrosis.

WHAT IS ALREADY KNOWN ON THIS TOPIC

- Single-cell RNA sequencing studies revealed that fibroblasts are a heterogenous population of cells with functionally diverse subpopulations. However, these studies lack spatial context and did not enable characterisation of the local niches and the cellular interactions *in situ*.

WHAT THIS STUDY ADDS

- We provide the first cyclic *in situ* hybridisation (cISH)-based characterisation of fibroblast subpopulations and their microenvironment in systemic sclerosis (SSc) and control skin.
- Using cISH in conjunction with a novel clustering approach that considers spatial localisation, we identify 9 subpopulations of fibroblasts, with recovery of previously described populations and identification of several novel subpopulations of fibroblasts.
- SFRP2+ reticular dermis (RetD), CCL19+ nonperivascular (nonPV), and COL8A1+ fibroblasts are numerically altered in SSc, reside in specific niches, and display unique cellular functions in SSc.
- SFRP2+ RetD, CCL19+ nonPV, and COL8A1+ fibroblasts display specific profibrotic, proinflammatory or dual profibrotic and proinflammatory roles in SSc skin.
- The frequencies of COL8A1+ fibroblasts and their interactions with monocytic cells or B cells are associated with progression of skin fibrosis.

HOW THIS STUDY MIGHT AFFECT RESEARCH, PRACTICE OR POLICY

- The newly identified fibroblast subpopulations may offer potential for selective targeting of SFRP2+ RetD, CCL19+ perivascular, and COL8A1+ fibroblasts as disease-promoting fibroblast subsets.
- COL8A1+ fibroblast counts and cellular interactions may offer potential as biomarkers for progression of skin fibrosis in SSc.

INTRODUCTION

Systemic sclerosis (SSc) is a connective disease characterised by autoimmunity and inflammation, which promote extensive fibrotic remodelling of the skin and various internal organs [1]. The progressive accumulation of the extracellular matrix (ECM) in affected tissues impairs organ function and commonly leads to organ failure, resulting in high morbidity and mortality of SSc patients [2]. Fibroblasts are the key effector cells for release of the ECM in fibrosis [2–5]. However, fibroblasts are a heterogenous population of cells with specific, functionally distinct subpopulations. Understanding fibroblast heterogeneity, particularly in the context of specific diseases, is still in its early stages. Moreover, we are lacking information on the organisation of fibroblast subpopulations *in vivo* and the intricate cellular interactions that occur within their native tissue environment.

Single-cell omics allows for the study of cellular subpopulations at previously unattainable resolution. To date, nonspatially resolved single-cell RNA sequencing (scRNA-seq) has been predominantly used to phenotype cellular changes in rheumatic diseases. scRNA-seq revealed that fibroblasts constitute a heterogenous population of cells with distinct transcriptional patterns and functions [6]. scRNA-seq data from SSc skin revealed between 6 and 10 distinct subpopulations of fibroblasts [7–9]. However, scRNA-seq, like other existing single cell techniques, requires tissue disaggregation and single cell separation. As a result, these approaches cannot provide information on the spatial localisation of cells inside the tissue, and they cannot characterise tissue niches and the cellular interplay that occurs within them. Spatial sequencing approaches overcome the lack of spatial context, but approaches published so far have a modest resolution of around 100 µm and are thus not able to resolve individual cells [7]. Here, we aimed to overcome these limitations using cyclic *in situ* hybridisation as a spatial transcriptomic approach with subcellular resolution of 120 nm.

METHODS

Patient and public involvement

Patients and/or the public were not involved in the design, conduct, reporting, or dissemination plans of our study.

Statistics

Data are presented as dot plots with the median ± IQR. Each dot represents one biological replicate, unless indicated otherwise in the figure legend. Protein expression levels are shown as heatmaps representing the mean of the Z score-normalised values. GraphPad Prism 8 was used to generate dot plots and to perform statistical analyses. Heatmaps were generated using the imcRtools R package [10]. Mann–Whitney *U* tests were applied for the comparison between 2 groups, if not indicated otherwise. Sensitivity analyses of fibroblast population frequencies were conducted using beta regression models with sex and age included as covariates using the betareg R package. Statistical analysis of activity scores was performed by linear mixed modelling fitted with donor-specific random intercepts using lmerTest R package. The comparison between SSc and controls was based on the estimated marginal means obtained from the linear mixed model using the emmeans R package.

RESULTS

Study design and identification of major cell types in SSc and control skin by cISH

We performed cISH from skin samples of SSc patients enriched for early, diffuse cutaneous involvement, with clinically active disease and sex-matched and age-matched healthy controls (Fig 1A; Supplementary Tables S1, S2, and Figure S1). We recovered a total of 20,979 cells (patients with SSc: 9876 cells; healthy individuals: 11,103 cells) (Fig 1A-C). These single cells included 3764 fibroblasts, identified by their high expression levels of *COL1A1, COL1A2, COL3A1*, and *DCN* (Fig 1B,D). We further identified other major cell populations from human skin, including keratinocytes (expressing *KRT1, KRT10, KRT14*, and *KRT15*), immune cells (expressing the panleukocyte gene *PTPRC* and specific genes for immune cells from the lymphoid and myeloid lineages such as *CD4, CD68, CD163*, and *LYZ*), endothelial cells (expressing *PECAM1, CDH5, ENG,* and *VWF*), and vascular smooth muscle cells (expressing *TAGLN, ACTA2,* and *MYL9*) (Fig 1D). These cell types had the expected spatial distribution in human skin, further validating their identity (Fig 1E).

Spatially informed phenotyping of fibroblasts in SSc and control skin identifies new fibroblast subpopulations

Using Building Aggregates with a Neighbourhood Kernel and Spatial Yardstick (BANKSY) as an algorithm that leverages the spatial information to perform clustering based not only on the own gene expression, but also on the average expression and expression gradients among each cell's neighbours [11], we identified 9 subpopulations of fibroblasts and annotated them based on their differential marker expression and on the spatial localisation. In accordance with previous studies [6–9], we identified COL8A1+ FBs, PI16+ FBs, ACKR3+ FBs, GSN+ FBs, and DUSP+ FBs, thus confirming the validity of this approach (Fig 2).

In addition, BANKSY-based clustering identified novel subpopulations that were not resolved using nonspatial approaches (Supplementary Fig S2). Two of the BANKSY-based clusters corresponded to the SFRP2+ FBs as defined by nonspatial clustering (Supplementary Fig S3A-C). In addition, 1 of the 2 SFRP2+ populations was located in spatial proximity to the epidermal layer and was thus termed SFRP2+ papillary dermis (PapD) FB. The other SFRP2+ population was located deeper in the dermis and was thus termed SFRP2+ reticular dermis (RetD) FB (Supplementary Fig S3D). The average expression and expression gradients of the keratinocyte markers *KRT14* and *KRT5* were higher among the neighbouring cells of SFRP2+ FB RetD than those of the SFRP2+ FB PapD (Supplementary Fig S3F), further confirming their distinct spatial distribution.

BANKSY-based clustering also identified 2 subpopulations of the previously described CCL19+ FB cluster as defined by nonspatial clustering (Supplementary Fig S3A-C). One of the CCL19+ FB clusters that we termed CCL19+ perivascular (PV) FBs was located around endothelial cells and consistently had a higher expression of the endothelial cell marker *PECAM1* and the pericyte marker *RGS5* among its neighbours than the CCL19+ nonperivascular (nonPV) FBs (Supplementary Fig S3E, G). The latter subpopulation was diffusely distributed in the dermis without enrichment in a particular dermal compartment (Supplementary Fig S3E).

Of particular note, the SFRP2+ RetD and the CCL19 PV FBs are not only distinct from the SFRP2+ PapD and the CCL19 nonPV FBs, respectively, with regards to their spatial location, but also with regards to their own gene expression, demonstrating functional differences of these newly identified subpopulations. For example, SFRP2+ RetD expressed higher levels of *COL1A1* and *COL3A1* than SFRP2+ PapD FBs. CCL19+ nonPV expressed higher levels of *CXCL12* and *PTGDS* than the CCL19+ PV FBs (Fig 2D).

In contrast, the other 5 subpopulations of fibroblasts defined by nonspatial clustering were homogenous not only regarding their own gene expression, but also to their spatial distribution (Fig 2D, Supplementary Fig S3A-C).

Integration with 2 scRNA-seq datasets, i.e. GSE138669 [6] and GSE195452 [8], demonstrated that neither of the label transfer-based annotations from the scRNA-seq to the cISH dataset could reliably distinguish between the SFRP2+ PapD and RetD FBs or between the CCL19+ PapD and RetD FBs, respectively (Supplementary Figs S4, S5). This finding highlights that the spatially informed BANKSY-based annotation can refine the fibroblast phenotyping performed with previous methods.

Changes in frequencies of fibroblast subpopulations in SSc skin

SFRP2+ RetD FBs and the COL8A1+ FBs had significantly higher frequencies in SSc, whereas PI16+ FBs, DUSP+ FBs, and CCL19+ PV FBs had modestly lower frequencies in SSc (Fig 3). These changes in the frequencies of COL8A1+ FBs and PI16+ FBs are consistent with those reported by scRNA-seq-based studies [6–9]. Of note, the populations resolved only by BANKSY clustering demonstrated distinct changes in SSc. SFRP2+ PapD FBs were numerically decreased in frequency in SSc, whereas SFRP2+ RetD FBs were increased. In addition, CCL19+ nonPV FBs were numerically increased in SSc, whereas CCL19+ PVs were decreased (Fig 3A,C,E). As cell composition may be influenced by donor sex and age, we performed a sensitivity analysis including these variables as covariates. This analysis excluded those variables as major confounders for the frequencies of fibroblasts in SSc (Supplementary Table S3).

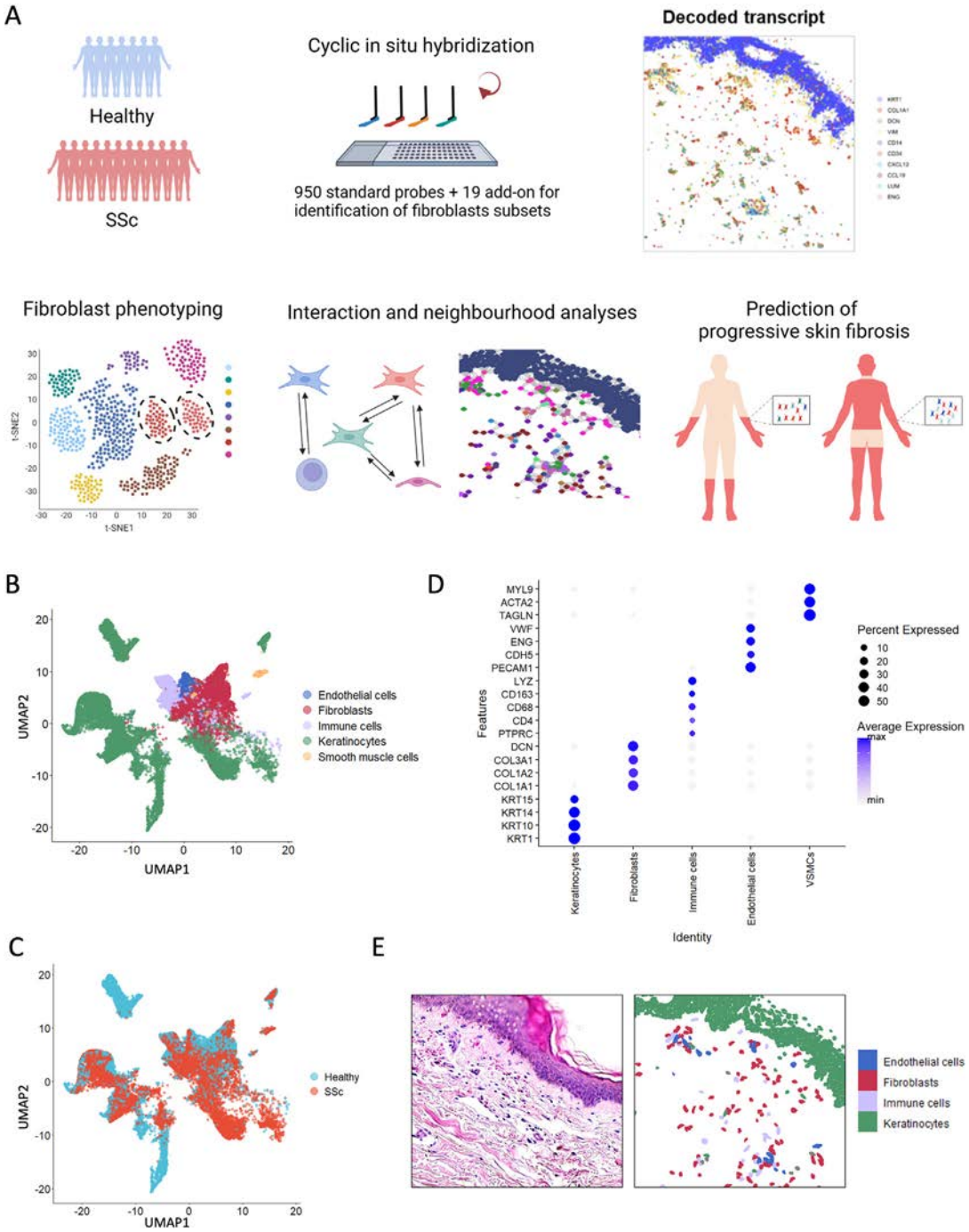

Figure 1. Characterisation of skin tissue organisation in SSc using cISH. A, Schematic overview of the experimental and analytic workflow. The transcriptomic profiles of skin tissue from healthy and SSc donors were analysed with imaging-based spatial transcriptomics using cISH. The cell populations in the skin were characterised based on the transcriptional profile. Taking advantage of spatial information, we performed cellular interaction analysis and evaluated whether changes in cell frequencies or spatial relationships might predict progression of skin fibrosis. B, UMAP plot showing 20,979 cells detected in the skin samples. The plot is coloured by the major cell types within the skin tissue. C, UMAP plot showing the cells detected in the skin samples obtained from healthy donors and SSc patients. D, Dot plot indicating marker gene expression of the major cell populations in the skin tissue. The size of the dot represents the percentage of the cells that expressed the specified gene. The dots were coloured by levels of the expression of specified gene. E, Representative images of HE staining and distribution of cISH-detected cells in the skin tissue. This figure was created with BioRender.com. cISH, cyclic *in situ* hybridisation; HE, haematoxylin and eosin; SSc, systemic sclerosis; UMAP, uniform manifold approximation and projection.

We next performed pseudotime analysis on the spatially informed fibroblast subsets using Monocle [12]. We defined PI16+ FBs as the root (starting point) of the pseudotime because they were previously described as a fibroblast subset with stem cell properties that can differentiate into specialised fibroblasts [13,14]. The pseudotime analysis revealed 3 differentiation trajectories: one trajectory going through SFRP2+ PapD FBs and ending with DUSP+ FBs; one trajectory going through CCL19+ PV FBs, then through CCL19+ nonPV FBs, and ending with GSN+ FBs; and a third trajectory going through ACKR3+ FBs, followed by SFRP2+ RetD FBs, and ending with COL8A1+ FBs (Supplementary Fig S6). The latter differentiation trajectory started from a fibroblast subset with decreased frequency in SSc and ended with 2 subsets that are highly enriched in SSc. This suggests that the fibroblast subsets enriched in SSc are terminally differentiated from precursor fibroblasts (among

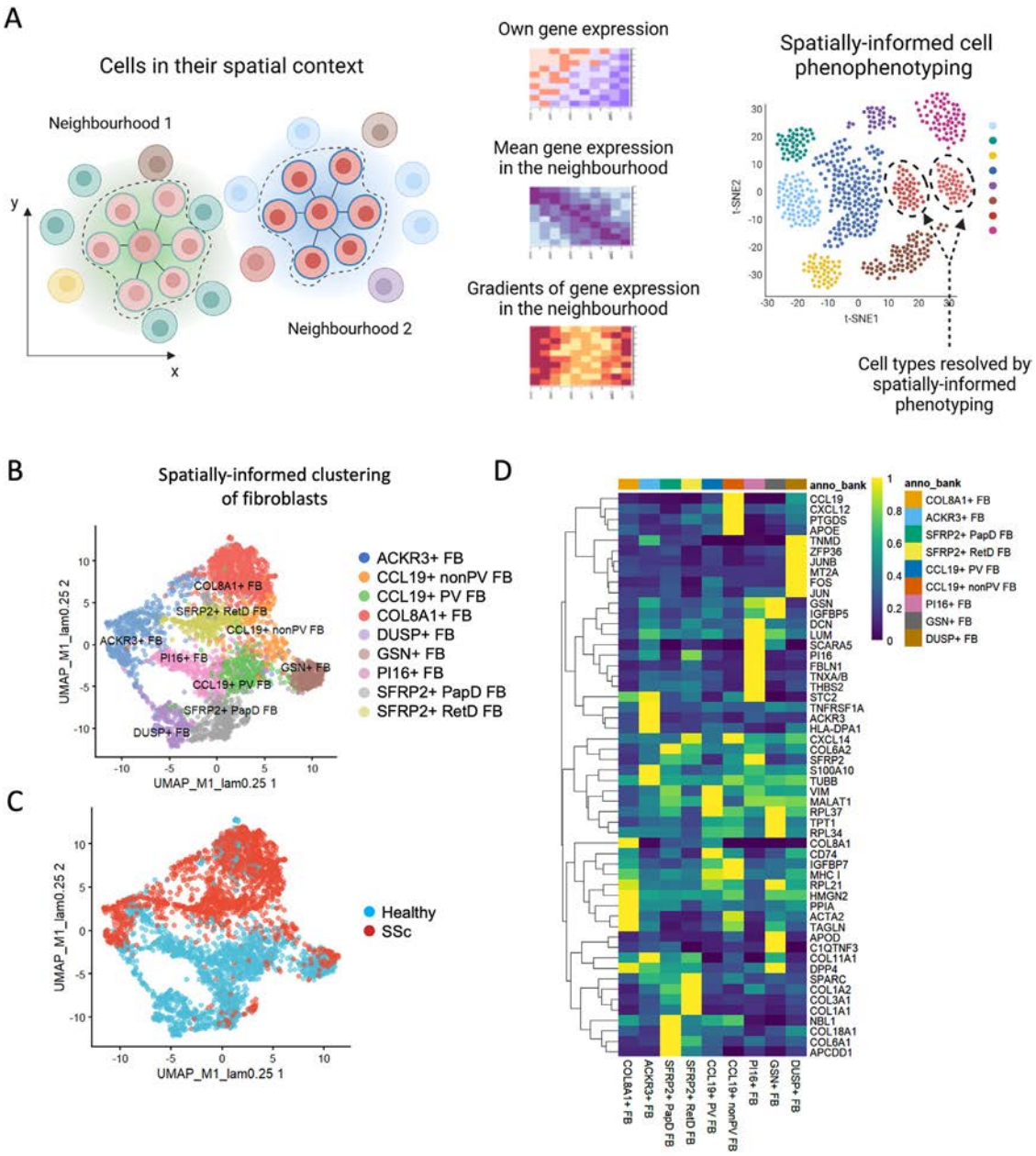

Figure 2. Fibroblasts populations identified by spatially informed clustering. A, An illustration showing the workflow for spatially informed cell phenotyping using BANKSY-based spatial clustering. In addition to the expression matrix of the cell of interest, the transcriptional profiles of the local environment, including averaged expression and the expression gradient of neighbouring cells, were computed using BANKSY and subjected to phenotyping by clustering. B, UMAP showing fibroblast populations identified by spatially informed clustering using BANKSY. C, UMAP showing the BANSY-identified populations from healthy and SSc donors. D, Expression heatmap of the marker genes for the BANKSY-identified populations. This figure was created with BioRender.com. BANKSY, Building Aggregates with a Neighbourhood Kernel and Spatial Yardstick; SSc, systemic sclerosis; UMAP, uniform manifold approximation and projection.

other cell types), in line with previous publications [13–15]. Of note, while the CCL19+ PV FB and CCL19+ nonPV FB subsets aligned along one trajectory and are thus likely developmentally related, the SFRP2+ PapD FB and the SFRP2+ RetD FB subsets were located along 2 distinct trajectories.

Functional heterogeneity of the spatially informed fibroblast subsets

We next aimed to further characterise the functional of spatially resolved subpopulations. We first computed an ECM module score, as well as scores for different ECM components with the gene sets curated in the Matrisome project (Fig 4A, Supplementary S7A) [16]. The SFRP2+ RetD FB subpopulation had the highest ECM score and collagen score of all fibroblast subpopulations (Fig 4A), while the PI16+ FBs had the highest glycoproteins and proteoglycans scores (Supplementary Fig S7A), pointing to specific roles in ECM production for the different subsets. Transforming growth factor (TGF) β pathway activity inferred using Pathway Responsive Genes for Activity Inference signatures [17] was most enriched in SFRP2+ RetD FBs (Supplementary Fig S7B). Comparison of fibroblast populations in SSc and normal skin revealed higher ECM and collagen scores and TGFβ activity for several fibroblast populations in SSc skin, including in SFRP2+ PapD FBs and CCL19+ nonPV FBs (Supplementary Fig S7C).

To validate these findings, we performed 2 complementary computational approaches. We first applied the algorithm CytoSPACE [18] to map to the cISH dataset 2 publicly available scRNA-seq datasets of SSc and healthy skin (GSE195452 and

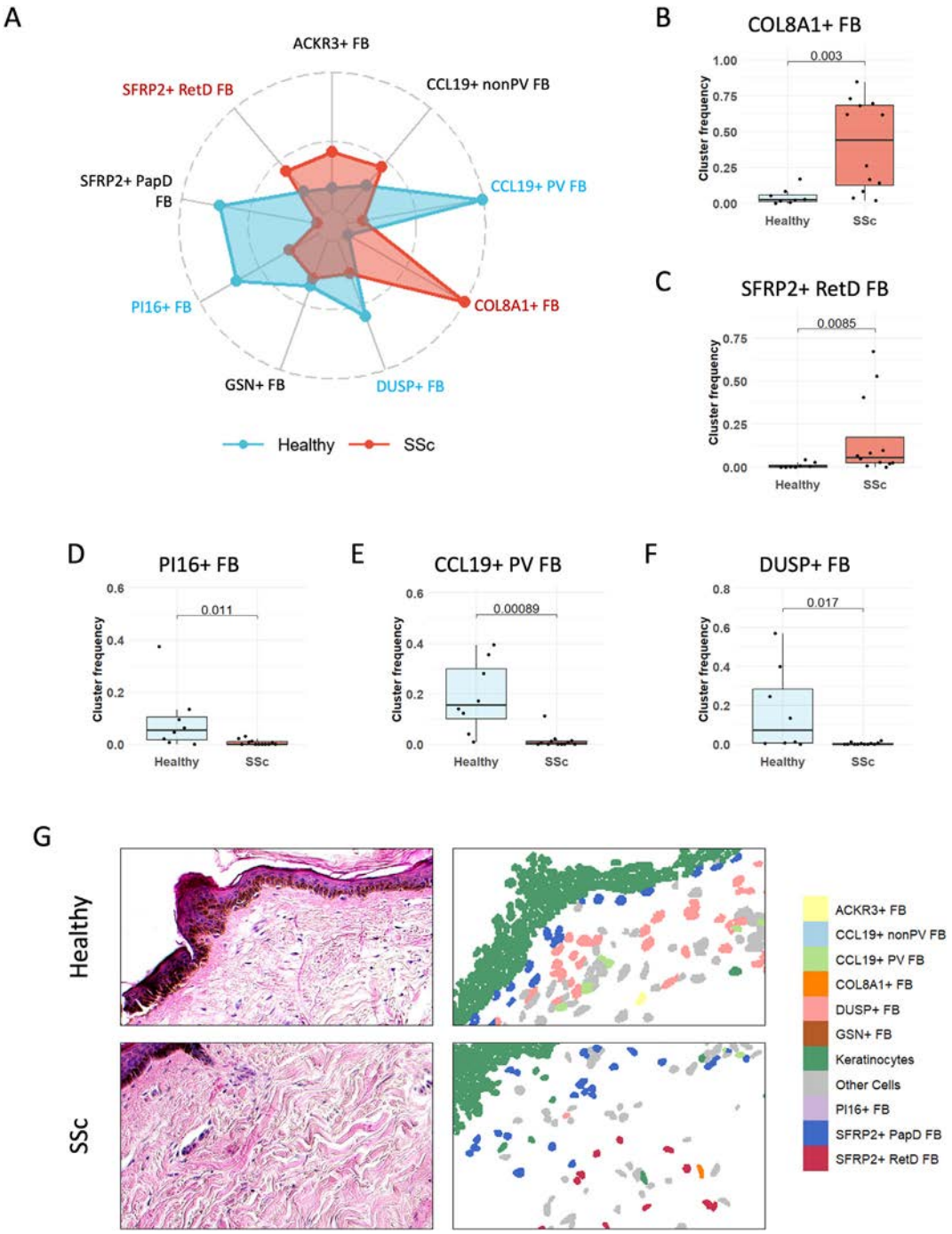

Figure 3. Changes in frequencies of fibroblast subsets identified by spatially informed phenotyping in SSc. A, An overview of the changes in the abundance of BANKSY-identified fibroblast populations. The abundance was quantified by the proportion of the specified population within the fibroblast component. Z score-normalised median proportions were plotted on the radar chart. The statistically significant changes were highlighted in red (increased in SSc) and blue (increased in healthy). B-F, Changes in frequencies of COL8A1+ FB (B), SFRP2+ RetD FB (C), PI16+ FB (D), CCL19+ PV FB (E), and DUSP+ FB (F) in SSc compared to control skin. G, Representative images of BANKSY-identified populations in the skin tissue, along with HE stainings of the corresponding regions. The statistical significance was determined by the Mann–Whitney *U* test. *P* values below 0.05 were considered significant. BANKSY, Building Aggregates with a Neighbourhood Kernel and Spatial Yardstick; HE, haematoxylin and eosin; SSc, systemic sclerosis.

GSE249279 [7,8]). The ECM and collagens scores as well as the TGFβ pathway activity computed from the enhanced cISH dataset were enriched in SFRP2+ RetD FBs (Supplementary Fig S8A), whereas the glycoproteins and proteoglycans scores were enriched in PI16+ FBs (Supplementary Fig S8B).

We next performed functional enrichment analysis using the fast gene set enrichment analysis and the univariate linear model (ULM) methods via decoupleR [19]. Both methods revealed that the fibroblast subsets have both shared and distinct biological functions (Fig 4B, Supplementary Fig S9A). The SFRP2+ RetD FBs are profibrotic, ECM-producing fibroblasts. They demonstrated the highest enrichment scores for pathways related to fibrosis, such as 'collagen formation', 'response to TGFβ', and 'positive regulation of WNT signalling pathway' (Fig 4B, Supplementary Fig S9A). In contrast, 'response to mechanical stimulus' was specifically enriched in SFRP2+ RetD FBs (Supplementary Fig S9A). SFRP2+ PapD FBs demonstrated enriched pathways specific for this population, i.

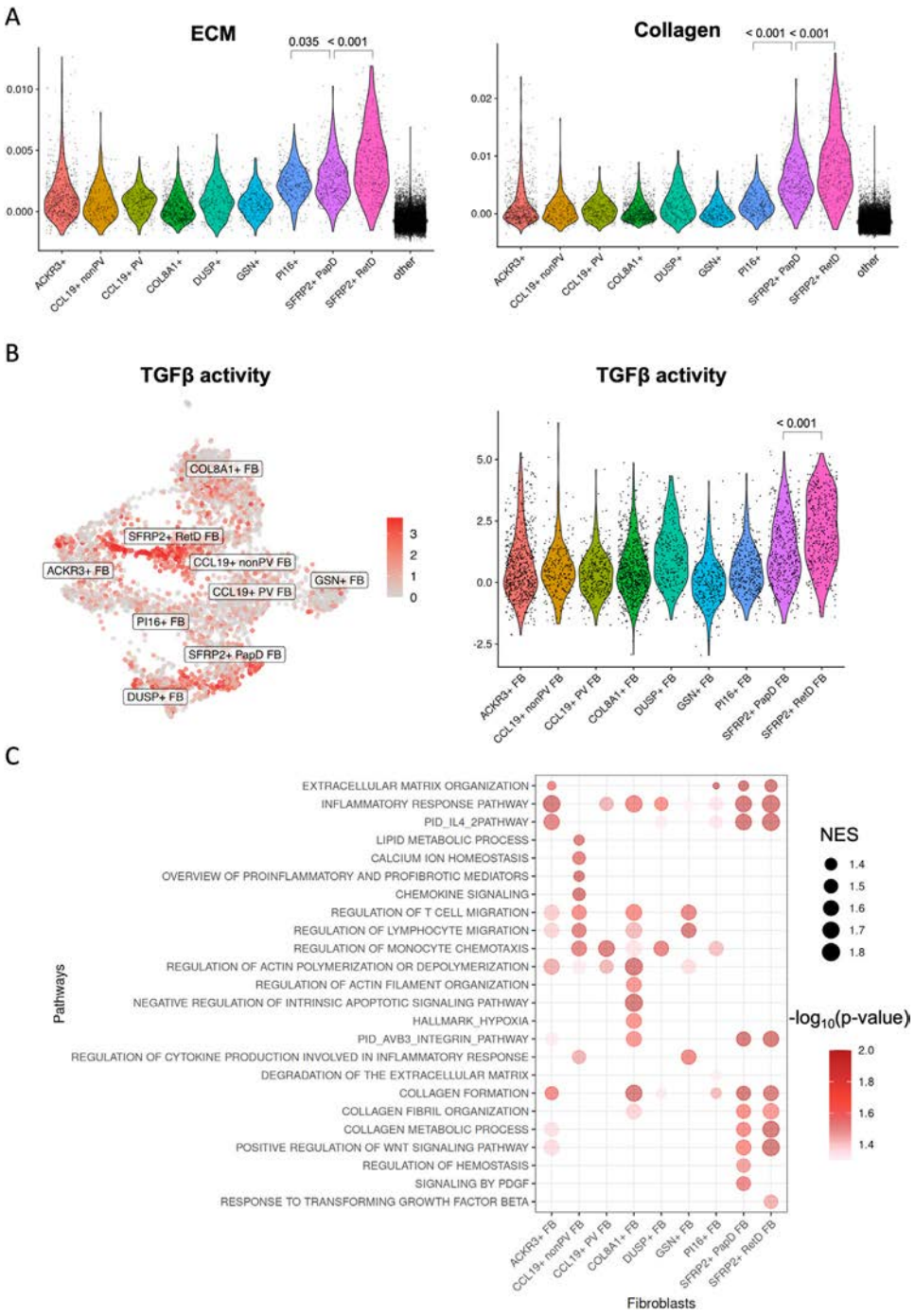

Figure 4. Distinct biological functions of spatially identified fibroblast populations. A, Violin plots showing the ECM module scores of components obtained from the Matrisome project across fibroblast populations detected in SSc and control skin. Nonfibroblast populations were labelled as 'other' in the violin plots. B, UMAP and violin plots illustrating TGFβ activities inferred using PROGENy signatures across fibroblast populations. C, Dot plot showing the pathway enrichment scores across fibroblasts populations computed by FGSEA for pathways with a P value < .05. The pathway enrichment analysis was performed using decoupleR R package using the pseudo-bulk expression matrix that contained averaged expression for each fibroblast subpopulation. Statistical significance was assessed by comparing estimated marginal means from linear mixed models including donor-specific random intercepts. P values are shown above each comparison. ECM, extracellular matrix; FGSEA, fast gene set enrichment analysis; NES, normalised enrichment score; PROGENy, Pathway Responsive Genes for Activity Inference; TGFβ, tumour growth factor β; UMAP, uniform manifold approximation and projection.

e. 'signalling by platelet-derived growth factor (PDGF)', and de-enriched for 'immune response' (Fig 4B and Supplementary Fig S9A). CCL19+ nonPV FBs are an inflammatory fibroblast population. Shared functions of CCL19+ PV and nonPV FBs included several terms related to cytokine production and immune responses. Specific functions of CCL19+ PV FB included a high enrichment score on 'regulation of monocyte chemotaxis' and de-enrichment of 'immune system process' compared to the enrichment of 'calcium ion homeostasis' and 'lipid metabolic process' in CCL19+ nonPV FBs (Fig 4B, Supplementary Fig S9A). These differences highlight that the fibroblasts populations separated by BANKSY clustering are not only distinct with regards to their spatial location in their differentiation trajectories, but also with regards to their function.

The COL8A1+ FBs may have broad spectrum of roles in modulating fibrotic and inflammatory responses as

demonstrated enrichment in pathways related to collagen organisation, but also in pathways such as 'regulation of lymphocyte migration' and 'regulation of monocyte chemotaxis' (Fig 4B, Supplementary Fig S9A). Furthermore, COL8A1+ FBs demonstrated specific enrichment of 'negative regulation of apoptotic signalling pathway', suggesting resistance to apoptosis. Of note, we detected stronger activity of terms related to immune and fibrotic modulation in these fibroblast populations in SSc compared to healthy controls (Fig S7B, Supplementary Fig S9B).

Multicellular spatial domains in SSc skin

Given the profound effects of crosstalk with neighbouring cells on cellular phenotype and function, we next aimed to characterise the local microenvironment of individual subpopulations of fibroblasts. We first annotated immune subpopulations by label transfer, using the scRNA-seq dataset GSE195452 as a reference (Supplementary Fig S10).

Identification of multicellular spatial domains, or cellular neighbourhoods (CNs), by clustering cells based on the composition of their neighbouring cells yielded 14 CNs (Supplementary Fig S11). We annotated the CNs according to their composition, i.e. to the cell population with the highest relative frequency inside each CN. Some of these CNs recovered histologically defined domains of the skin, e.g. the epithelium in the epithelial CN or the vascular region in the endothelial CN (Supplementary Fig S11). Most of the other CNs were mainly defined by the predominant fibroblast population, e.g. CCL19 nonPV CN, COL8 CN, SFRP2 CN, PI16 CN or CCL19 PV CN. SFRP2+ PapD FBs but not SFRP2+ RetD FBs were enriched in the subepithelial CN, whereas the CCL19+ PV FBs but not the CCL19+ nonPV FBs were enriched in the endothelial CN, confirming the spatial segregation of these populations with a distinct method (Supplementary Fig S11).

The composition of several CNs were remarkably different in SSc compared to normal skin, with an enrichment of immune cell subsets in the CCL19 nonPV CN, COL8 CN, and SFRP2 CN and with a de-enrichment of immune cells in the PI16 CN and CCL19 PV CN (Fig 5A). Furthermore, PI16+ FB were enriched in COL8 CN and SFRP2 CN in SSc and thus in spatial proximity to SFRP2+ RetD and COL8A1+ FBs. This indirectly supports the hypothesis that PI16+ FBs can differentiate to profibrotic fibroblast subsets in SSc (Fig 5A).

We reasoned that the changes in the composition of CNs in SSc can lead to functional changes within the local niches. Indeed, functional enrichment analysis demonstrated that fibroblast-enriched CNs, such as CCL19 nonPV CN, CCL19 PV CN, SFRP2 CN, PI16 CN, or COL8 CN, are functionally distinct in SSc compared to normal skin with changes in disease-relevant pathway enrichment scores (Fig 5B). Changes in SSc included the enhanced antiapoptotic and antigen processing activities in the CCL19 nonPV CN and COL8 CN in SSc. Activation of lymphocyte-mediated killing, including CD8 TCR signalling and apoptosis, was detected in CCL19+ PV CN in SSc. The SFRP2 CN was present exclusively in SSc skin and exhibited the highest scores in pathways related to ECM remodelling among the fibroblast-enriched CNs. These findings support the concept that the CNs identified are functional units within the skin that undergo pathologic changes in SSc.

Cell–cell interaction and communication networks in SSc skin

We next aimed to unravel changes in cell–cell interaction networks. Pairwise interaction analysis revealed distinct cellular interaction networks in SSc skin (Fig 5C, Supplementary Fig S12). CCL19+ nonPV FBs demonstrated increased interactions with several immune cell subsets, whereas CCL19 PV FBs showed decreased interactions with mast cells, B cells, and plasma cells in SSc compared to normal skin (Fig 5C). COL8A1+ FBs transitioned from an immune-inert state, as shown by the lack of interactions or even avoidance of immune cells, to an immune-engaging state, interacting with macrophages, dendritic cells, natural killer (NK) cells, and plasma cells in SSc (Fig 5C). In SSc skin, SFRP2+ PapD FBs interacted with T cells, and SFRP2+ RetD FBs interacted with mast cells and NK cells. These interactions were not observed in normal skin (Supplementary Fig S12).

We further performed spatially informed cell–cell communication analysis using CellChat [20]. This analysis revealed profound changes in the patterns of ligand-receptor (L–R) interactions in SSc compared to control skin (Fig 6, Supplementary Figs S13, S14). SFRP2+ RetD FBs demonstrated L–R interactions with several other fibroblast subsets and with mast cells, NK cells, or dendritic cells in SSc, whereas in control skin they were only communicating with other SFRP2+ RetD FBs (Fig 6A). In contrast, the SFRP2+ PapD FBs lost communication with multiple cell types in SSc (Fig 6A). Of note, CellChat analysis without spatial distance constraints, which did not account for spatial information, did not resolve these differences between SSc and normal skin and showed comparable L–R interactions for both SFRP2+ FB subsets (Supplementary Fig S13A).

At the signalling level, SFRP2+ RetD FB in SSc demonstrated an increased relative strength for outgoing, but a decreased strength for incoming signals for collagen and fibronectin1 compared to normal skin, which may point towards a reduced capacity for ECM sensing in SSc (Fig 6B, Supplementary Fig S13B). Indeed, further analysis indicated decreased ECM signals received by CD44, a receptor with well-characterised roles in ECM sensing [21], on SFRP2+ RetD FBs compared to other fibroblast populations in SSc (Supplementary Fig S14A). Furthermore, the CCL19+ nonPV FBs demonstrated an increased relative strength for outgoing signals for CXCL12 in SSc, suggesting a higher chemotactic capacity (Fig 5C, Supplementary Fig S14B). PDGF signalling also demonstrate subpopulation-specific differences in SSc skin:fibroblast subsets with increased frequency in SSc. For example, SFRP2+ RetD and COL8A1+ FBs started to receive PDGF signals in SSc. In contrast, in control skin, only fibroblast subsets with lower frequencies in SSc, such as SFRP2+ PapD and CCL19+ PV FBs, received PDGF signals, indicating a switch from homeostatic to pro-fibrotic roles of PDGF signalling in SSc (Supplementary Fig S13C). Furthermore, PDGF signals were sent by endothelial cells in SSc and by monocytes/macrophages in control skin.

These spatially resolved analyses demonstrate major changes in signalling between distinct fibroblast subsets and other cells in SSc skin that could not be resolved in nonspatial datasets.

Predictors of progression of skin fibrosis in SSc

We investigated whether the frequencies of fibroblast subpopulations—either on their own or stratified by their interaction partners—at the time of biopsy could predict the progression of skin fibrosis at follow-up. Patients with progression of skin fibrosis at follow-up had a higher frequency of COL8A1+ FBs than those with stable skin fibrosis (Fig 7A). Other fibroblast populations were not significantly different between the 2 groups (Supplementary Fig S15). Furthermore, COL8A1+ FBs in close

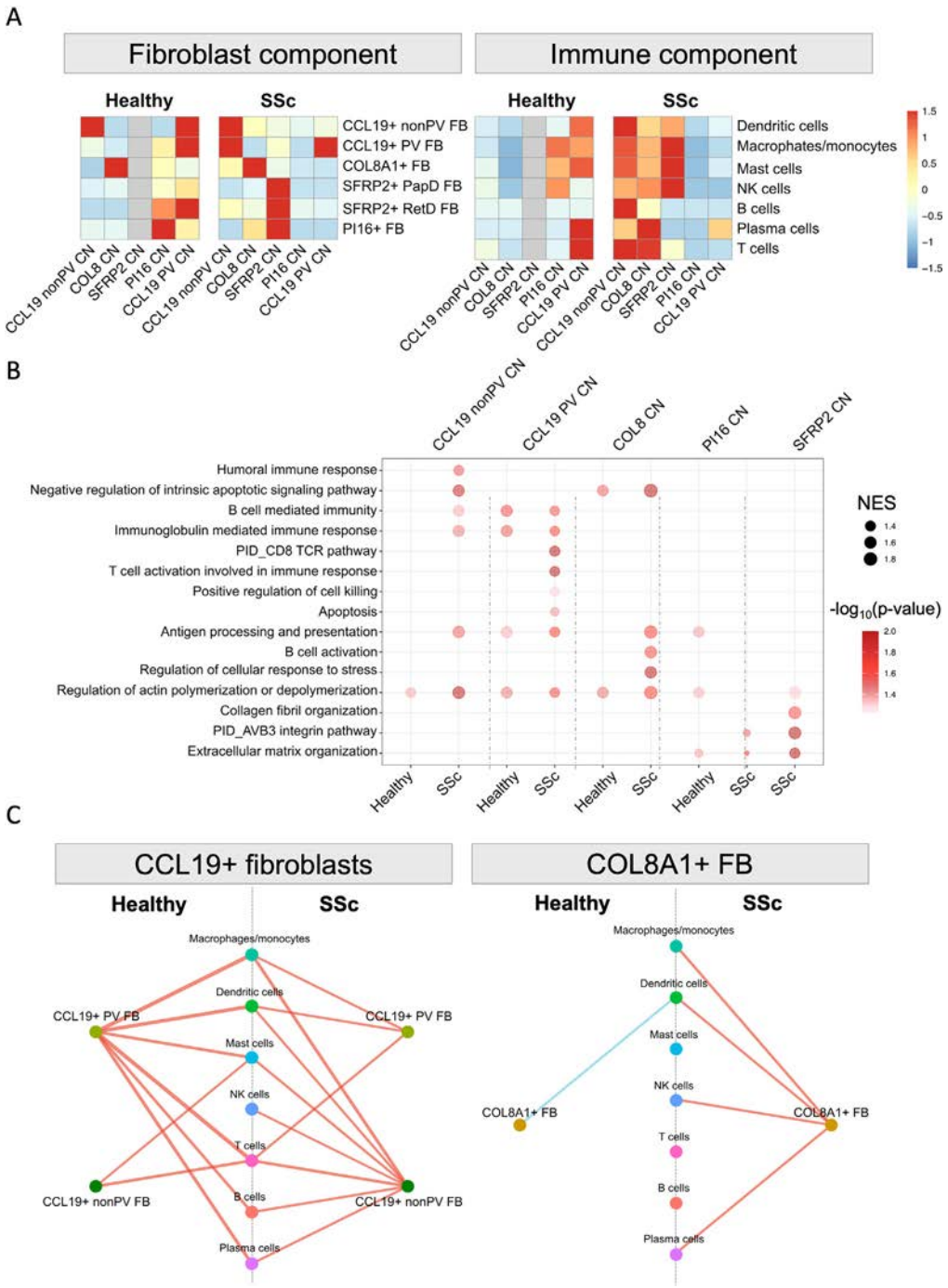

Figure 5. Changes in the cellular neighbourhoods in SSc skin. A, Heatmaps highlighting the shift in the cellular composition within the fibroblast CNs in healthy and SSc skin. The number of cells were normalised for each cell type across all CNs. SFRP2 CN was not detected in healthy samples and is shown in grey in the heatmap. B, Dot plot showing the activation of immuno- and matrix remodelling pathways within fibroblast CNs in SSc compared to healthy controls. The activation of the pathways was analysed by pseudo-bulk FGSEA. The size of the dot represents the NES, and the colour represents the *P* value. C, Network visualisation showing the immune interaction of indicated fibroblast populations in healthy and SSc skin by pairwise interaction analysis based on the cellular distribution in the tissue. Cellular attraction (red) and avoidance (blue) are indicated in the plots. The width of the lines represents the proportion of samples exhibiting statistically significant interaction. B-C, The statistical significance was determined by FGSEA (B) or using the permutation test (C). Results that did not reach statistical significance ($P < .05$) were excluded from the visualisations for clarity. CN, cellular neighbourhood; FGSEA, fast gene set enrichment analysis; NES, normalised enrichment score; SSc, systemic sclerosis.

spatial proximity to macrophages/monocytes, mast cells, or B cells had significantly higher frequencies in patients with progression of skin fibrosis, whereas COL8A1+ FBs with spatial proximity to other immune cell populations demonstrated only milder differences between the 2 groups (Fig 7B-D, Supplementary Fig S16A-D).

We further generated 2 least absolute shrinkage and selection operator predictive regression models with progression of skin fibrosis at follow-up as outcome. The first model that included the frequencies of the fibroblast subsets with shifts in frequencies in SSc skin as predictors for progression of skin fibrosis performed with a moderate accuracy and with an area under the curve (AUC) of 81% (Supplementary Fig S17). In a second model, we included the frequencies of COL8A1+ FBs with spatial proximity to macrophages/monocytes, mast cells, or B cells instead of the frequencies of all COL8A1+ FBs, while keeping

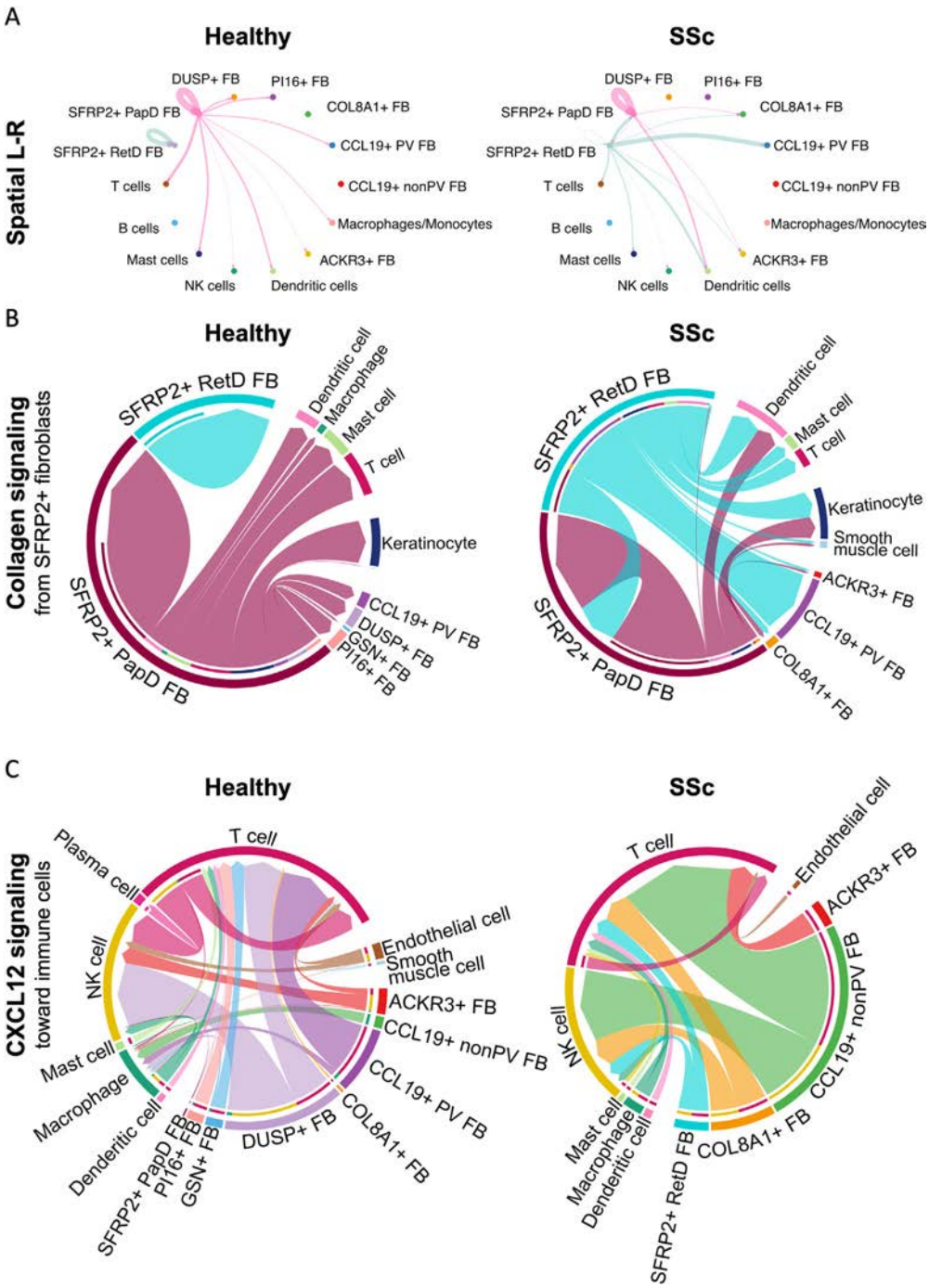

Figure 6. Distinct cell–cell communication in SSc identified by spatially informed ligand–receptor analysis. A, Representative circle plots showing the interaction of SFRP2-expressing fibroblasts in healthy and SSc skin by spatial ligand–receptor analysis using CellChat. The distance constraints were set to 250 μm for secreted signalling and 20 μm for contact-dependent signalling. Interaction routes are represented by lines, with line width indicating interaction strength as computed using CellChat. B, Chord diagrams showing the collagen signalling from the SFRP2-expressing fibroblasts. C, Chord diagrams showing the CXCL12 signalling received by immune cells and their source. In chord diagrams (B and C), the thinner inner bars represent the signalling strength received by the indicated targets. L–R, ligand–receptor analysis; SSc, systemic sclerosis.

the other predictors unchanged. This model demonstrated improved prediction accuracy, allowing a better separation between the predicted progressors and predicted stable patients, with an AUC of 95% (Fig 7E-H). The frequency of COL8A1+ in proximity to monocytes/macrophages was the most important feature of the second model, and increases in their frequency were predictors of progression. The frequency of PI16+ fibroblasts was the second most important feature, and increases in their frequency were associated with stable skin fibrosis (Fig 7E, F). This finding suggests an active differentiation through the trajectory starting from PI16+ FBs and ending at COL8A1+ FBs during the early stages of progression of skin fibrosis. These findings highlight that incorporation of spatial information can improve the prediction of skin fibrosis compared to analysing changes in cell frequencies alone.

DISCUSSION

We present herein a novel approach for identification and functional characterisation of cell populations based on

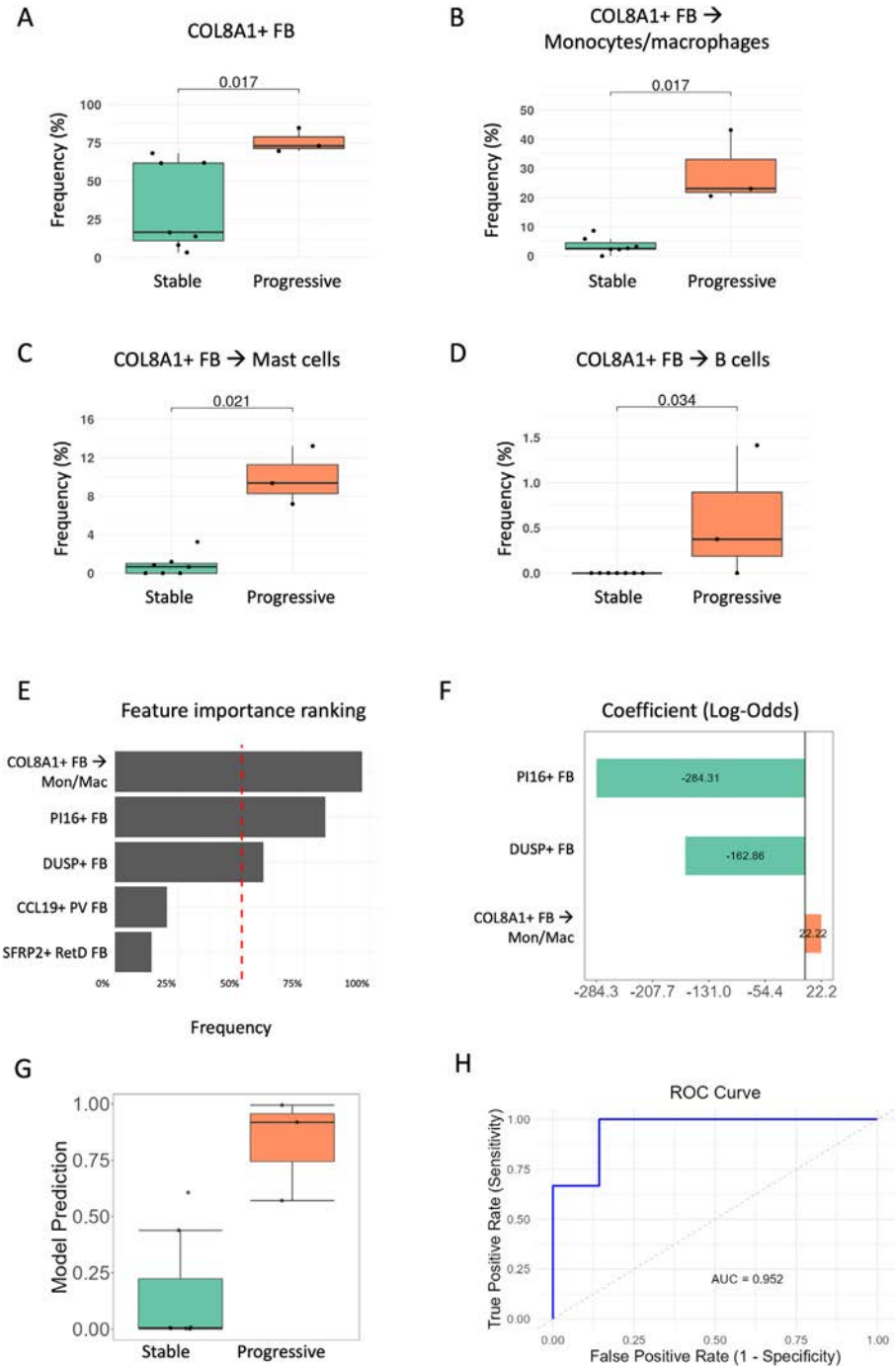

Figure 7. Predictors of progression of skin fibrosis in SSc. A-D, Frequencies of all COL8A1 + FBs (A) and of COL8A1 + FBs in spatial proximity to monocytes/macrophages (B), mast cells (C) or B cells (D) among all dermal cells. E, Top highly ranked features predictive of progression of skin fibrosis after bootstrapping with LASSO regression, starting from the frequencies of COL8A1 + FBs in spatial proximity to monocytes/macrophages, mast cells, or B cells, along with the frequencies of SFRP2 + RetD FBs, PI16 + FBs, DUSP + FBs, and CCL19 + PV FBs as predictors. (F) Increased frequencies of COL8A1 + fibroblasts in close spatial proximity to monocytes/macrophages were associated with a higher likelihood of progressive skin fibrosis, whereas elevated frequencies of PI16 + FBs and DUSP + FBs were linked to a decreased likelihood of fibrosis progression. (G) Model prediction results for each donor. (H) ROC curve and its AUC for evaluation of model performance. AUC, area under the curve; FB, fibroblasts; LASSO, least absolute shrinkage and selection operator; RetD, reticular dermis; ROC, receiver operating characteristic.

transcriptional profiles as well as on spatial localisation using cISH as an emerging technique, in conjunction with novel bioinformatical pipelines. We demonstrate the validity of this approach by confirming deregulation of previously identified subpopulations of fibroblasts [6,7,9]. Moreover, we complement the cISH-based approach with analysis of a spatial transcriptomics dataset from a second cohort of SSc patients and controls and with integration with publicly available scRNA-seq datasets from further SSc cohorts to combine the strengths of these different approaches.

Analyses of our cISH data using the BANKSY algorithm, which considers expression levels as well as spatial information, enabled us to identify 9 different fibroblast subpopulations in SSc and control skin. Our spatial phenotyping approach segregated SFRP2 + FBs and CCL19 + FBs into 4 distinct populations. We validated the distinct spatial localisation of these populations using 2 complementary methods, i.e. by spot deconvolution of the Visium dataset and by the neighbourhood analysis.

Of note, these spatially separated fibroblast populations do not only show differences in spatial localisation but are also functionally distinct. First, the spatially resolved fibroblast populations show differences in the expression levels of fibrosis-relevant genes and enrichment of distinct functional terms. For example, in SFRP2 + PapD FBs, the regulation of haemostasis was specifically enriched. However, in SFRP2 + RetD FBs, the response to mechanical stimulus was specifically enriched, and TGFβ signalling was stronger than that noted in SFRP2 + PapD FBs. The 2 populations of CCL19 + FBs also showed profound differences in the enrichment of functional terms relevant to fibrotic remodelling. Second, these pairs of fibroblasts segregated by spatially informed phenotyping differed with regards

to cellular interactions. SFRP2+ RetD FBs interacted with a wide range of immune cells. On the other hand, only a small proportion of dendritic cells were found in the surroundings of SFRP2+ PapD FBs. Third, these populations also displayed clear differences in ligand–receptor interactions. For example, ECM sensing by CD44 was specifically decreased in SFRP2+ RetD in SSc; furthermore, only CCL19+ nonPV FBs, but not CCL19+ PV FBs, signalled to NK cells via CXCL12–ACKR3. Fourth, the developmental trajectory differs for SFRP2+ PapD FBs and SFRP2+ RetD FBs, as these populations were located on 2 distinct trajectories. Fifth, these populations also show specific alterations in SSc skin. Together, these findings highlight that the novel, spatially defined populations of SFRP2+ RetD and SFRP2+ PapD FBs as well as CCL19+ PV and CCL19+ nonPV FBs are functionally clearly distinct with unique roles in the pathogenesis of SSc.

Our study also provides clear evidence that the profibrotic phenotype of fibroblasts in SSc is the result of the combined effects of different processes: (1) Our study demonstrates changes in the frequencies of fibroblast populations with increased frequencies in profibrotic populations. These changes include the elevated abundance of SFRP2+ RetD FB, which had demonstrated the highest collagen expression in our dataset. Shift towards profibrotic subsets have also been reported in non-spatially resolved scRNA-seq studies in SSc [6–9,22]. The changes in frequencies might be partially caused by a shift in the differentiation trajectory of precursor fibroblasts, particularly PI16+ FB, towards profibrotic subsets. (2) In addition, several individual populations are further biased towards a more profibrotic phenotype in SSc skin with upregulation of profibrotic genes and pathways, including TGFβ, Wingless/Int-1 (WNT), and ECM-modulating pathways. (3) The local neighbourhoods change drastically in SSc, thereby providing a microenvironment that fosters development of profibrotic fibroblasts. We detected upregulation of immune cell subsets with potential profibrotic roles such as monocytes/macrophages, mast cells, or plasma cells in the CCL19+ nonPV, COL8, and SFRP2 CNs in SSc. These changes in the interactions with immune cells are not a simple reflection of increased leukocyte counts in SSc skin, as the mentioned interactions are specific for certain leukocyte subsets and occur only with certain fibroblast populations. In contrast, other fibroblast subsets such as CCL19+ PV FBs demonstrate decreased interactions with immune cells in SSc.

We also provide first evidence that the frequencies of 2 fibroblast populations and their interactions with immune cells may help to predict the future course of skin fibrosis. The frequencies of COL8A1+ FBs were associated with future progression of skin fibrosis, whereas PI16+ FBs were associated with stable disease. This correlates well with the functional role of these 2 fibroblast subpopulations and their developmental trajectory. COL8A1+ FBs demonstrate enrichment in numerous pathways related to both fibrosis and inflammation. COL8A1+ FBs are also the end stage of differentiation of PI16+ FBs through a trajectory that involved SFRP2+ RetD FBs, another population with altered frequencies in SSc. This suggests that the active differentiation of PI16+ FBs towards COL8A1+ FBs, with potential recruitment of immune cells by COL8A1+ FBs, might drive progression of skin fibrosis. In line with this, the frequency of COL8A1+ FBs interacting with monocytes/macrophages provided an improved predictive power compared to the frequencies of all COL8A1+ FBs alone. Thus, by providing spatial information, our approach could provide an improved risk stratification than that based on evaluation of cell frequencies alone.

Our study has limitations. Although the SSc and control samples were matched for sex and age, the SSc biopsies were taken from the forearm, whereas the control samples were in part obtained from other locations such as the trunk and the lower extremities. Although our study provides extensive *in silico* validation of our findings, further experimental validation remains to be performed in follow-up studies. These might, for example, aim at confirming our findings at protein level by integration of our data with spatially resolved multiplexed protein data in SSc skin [23,24] or further functional studies on isolated subpopulations *in vitro*. The clinical relevance of our findings should be confirmed by performing cISH-based phenotyping on a higher number of SSc samples stratified by progression of skin fibrosis.

In summary, we used cISH in conjunction with novel bioinformatical pipelines that consider spatial context to identify 4 novel fibroblast subpopulations and to study the microenvironment and cellular interactions of fibroblasts in SSc and normal skin. We characterise SFRP2+ RetD FBs as s prototypical profibrotic, ECM-producing population that resides within a specific inflammatory niche, CCL19+ nonPV FBs as a proinflammatory population that attracts and activates immune cells, and COL8A1+ FBs as a population with roles in both ECM remodelling as well as immune cell recruitment that is associated with progression of skin fibrosis. These results may provide a rationale for specific therapeutic targeting of SFRP2+ RetD-, CCL19+ nonPV-, and COL8A1+ fibroblasts as disease-promoting fibroblast subsets and may stimulate follow-up studies to confirm the potential of COL8A1+ FB counts as a marker for fibrosis progression.

Competing interests

AHG received lecture fees from Boehringer Ingelheim. JHWD has consultancy relationships with Active Biotech, Anamar, ARXX, AstraZeneca, Bayer Pharma, Boehringer Ingelheim, Callidatas, Celgene, Galapagos, GSK, Inventiva, Janssen, Kyverna, Novartis, Pfizer, Quell Therapeutics and UCB; has received research funding from Anamar, ARXX, BMS, Bayer Pharma, Boehringer Ingelheim, Cantargia, Celgene, CSL Behring, Exo Therapeutics, Galapagos, GSK, Incyte, Inventiva, Kiniksa, Kyverna, Lassen Therapeutics, Mestag, Sanofi-Aventis, RedX, UCB and ZenasBio; and is CEO of 4D Science and scientific lead of FibroCure.

Acknowledgements

We thank Christoph Liebel, Philipp Steinbrecher, and Lukas Sokolowski for excellent technical assistance. We thank Michael Bailey, Trieu My Van, and Michael Leon from NanoString Technologies (now Bruker Spatial Biology) for supporting the CosMx runs.

Contributors

YNL, JHWD, and AEM designed the study. YNL, TF, AHG, ML, VD, AM, HC, and AEM were involved in acquisition and analysis of data. YNL, TF, AHG, ML, CB, ANP, TK, JH, AK, GS, SD, JHWD, and AEM were involved in interpretation of data. ML, CB, ACP, TK, JH, AK, and GS provided essential samples. All authors were involved in manuscript preparation and proofreading.

Funding

The project was supported by the following grants: Grants DI 1537/17-1, DI 1537/20-1, DI 1537/22-1, and DI 1537/23-1 of

the German Research Foundation; an unrestricted research grant from the Hiller Foundation (JHWD); MA 9219/2-1 of the German Research Foundation (AEM); a grant funded by the Deutsche Forschungsgemeinschaft (DFG, German Research Foundation) - 493659010 (AEM); grants 2021_EKEA.03 (AEM) and 2022_EKMS.02 (AEM) of the Else-Kröner-Fresenius-Foundation; The Edith Busch and World Scleroderma Foundation Research Grant Programme 2022-2023 (AEM); and the Research Committee of the Medical Faculty of the Heinrich-Heine University Düsseldorf (Forschungskommission; ID 2022-18, ID 2023-33, and ID 2023-31 to AHG, AEM, and JHWD, respectively).

Our analysis was supported by a de.NBI Cloud project (YNL) within the German Network for Bioinformatics Infrastructure (de.NBI) and ELIXIR-DE (Forschungszentrum Jülich and W-de.NBI-001, W-de.NBI-004, W-de.NBI-008, W-de.NBI-010, W-de.NBI-013, W-de.NBI-014, W-de.NBI-016, and W-de.NBI-022).

Patient consent for publication

All patients and control donors included in this study signed an informed concent, which has been reviewed by the local ethics committee.

Ethics approval

This stuty is approved by the ethics committee of the Medical Faculty of Heinrich Heine University Düsseldorf.

Provenance and peer review

Not comissioned; externally peer reviewed.

Supplementary materials

Supplementary material associated with this article can be found in the online version at doi:10.1016/j.ard.2025.06.002.

Orcid

Yi-Nan Li: http://orcid.org/0000-0001-8934-9361
Alexandru Micu: http://orcid.org/0000-0002-0154-1760
Ann-Christin Pecher: http://orcid.org/0000-0003-0201-0686
Jörg Henes: http://orcid.org/0000-0002-8385-6861
Pia Moinzadeh: http://orcid.org/0000-0002-8784-8615
Suzan Al-Gburi: http://orcid.org/0000-0002-1104-4784
Thomas Krieg: http://orcid.org/0000-0001-5616-8476
Alexander Kreuter: http://orcid.org/0000-0003-2275-499X
Jörg H.W. Distler: http://orcid.org/0000-0001-7408-9333
Alexandru-Emil Matei: http://orcid.org/0000-0003-1248-3145

REFERENCES

[1] Gabrielli A, Avvedimento EV, Scleroderma Krieg T. N Engl J Med 2009;360(19):1989–2003.
[2] Distler JHW, Györfi AH, Ramanujam M, Whitfield ML, Königshoff M, Lafyatis R. Shared and distinct mechanisms of fibrosis. Nat Rev Rheumatol 2019;15(12):705–30.
[3] Hinz B, Lagares D. Evasion of apoptosis by myofibroblasts: a hallmark of fibrotic diseases. Nat Rev Rheumatol 2020;16(1):11–31.
[4] Garrett SM, Baker Frost D, Feghali-Bostwick C. The mighty fibroblast and its utility in scleroderma research. J Scleroderma Relat Disord 2017;2(2):69–134.
[5] Györfi AH, Matei AE, Distler JHW. Targeting TGF-beta signaling for the treatment of fibrosis. Matrix Biol 2018;68-69:8–27.
[6] Zhu H, Luo H, Skaug B, Tabib T, Li YN, Tao Y, et al. Fibroblast subpopulations in systemic sclerosis: functional implications of individual subpopulations and correlations with clinical features. J Invest Dermatol 2024;144(6) 1251-61.e13.
[7] Ma F, Tsou PS, Gharaee-Kermani M, Plazyo O, Xing X, Kirma J, et al. Systems-based identification of the Hippo pathway for promoting fibrotic mesenchymal differentiation in systemic sclerosis. Nat Commun 2024;15(1):210.
[8] Gur C, Wang SY, Sheban F, Zada M, Li B, Kharouf F, et al. LGR5 expressing skin fibroblasts define a major cellular hub perturbed in scleroderma. Cell 2022;185(8) 1373-88.e20.
[9] Tabib T, Huang M, Morse N, Papazoglou A, Behera R, Jia M, et al. Myofibroblast transcriptome indicates $SFRP2^{hi}$ fibroblast progenitors in systemic sclerosis skin. Nat Commun 2021;12(1):4384.
[10] Windhager J, Zanotelli VRT, Schulz D, Meyer L, Daniel M, Bodenmiller B, et al. An end-to-end workflow for multiplexed image processing and analysis. Nat Protoc 2023;18(11):3565–613.
[11] Singhal V, Chou N, Lee J, Yue Y, Liu J, Chock WK, et al. BANKSY unifies cell typing and tissue domain segmentation for scalable spatial omics data analysis. Nat Genet 2024;56(3):431–41.
[12] Trapnell C, Cacchiarelli D, Grimsby J, Pokharel P, Li S, Morse M, et al. The dynamics and regulators of cell fate decisions are revealed by pseudotemporal ordering of single cells. Nat Biotechnol 2014;32(4):381–6.
[13] Buechler MB, Pradhan RN, Krishnamurty AT, Cox C, Calviello AK, Wang AW, et al. Cross-tissue organization of the fibroblast lineage. Nature 2021;593(7860):575–9.
[14] Merrick D, Sakers A, Irgebay Z, Okada C, Calvert C, Morley MP, et al. Identification of a mesenchymal progenitor cell hierarchy in adipose tissue. Science 2019;364(6438):eaav2501.
[15] Correa-Gallegos D, Ye H, Dasgupta B, Sardogan A, Kadri S, Kandi R, et al. $CD201^{+}$ fascia progenitors choreograph injury repair. Nature 2023;623(7988):792–802.
[16] Naba A, Clauser KR, Hoersch S, Liu H, Carr SA, Hynes RO. The matrisome: in silico definition and in vivo characterization by proteomics of normal and tumor extracellular matrices. Mol Cell Proteomics 2012;11(4) M111.014647.
[17] Schubert M, Klinger B, Klünemann M, Sieber A, Uhlitz F, Sauer S, et al. Perturbation-response genes reveal signaling footprints in cancer gene expression. Nat Commun 2018;9(1):20.
[18] Vahid MR, Brown EL, Steen CB, Zhang W, Jeon HS, Kang M, et al. High-resolution alignment of single-cell and spatial transcriptomes with CytoSPACE. Nat Biotechnol 2023;41(11):1543–8.
[19] Badia-I-Mompel P, Vélez Santiago J, Braunger J, Geiss C, Dimitrov D, Müller-Dott S, et al. decoupleR: ensemble of computational methods to infer biological activities from omics data. Bioinform Adv 2022;2(1):vbac016.
[20] Jin S, Plikus MV, Nie Q. CellChat for systematic analysis of cell-cell communication from single-cell transcriptomics. Nat Protoc 2025;20(1):180–219.
[21] Govindaraju P, Todd L, Shetye S, Monslow J, Puré E. CD44-dependent inflammation, fibrogenesis, and collagenolysis regulates extracellular matrix remodeling and tensile strength during cutaneous wound healing. Matrix Biol 2019;75-76:314–30.
[22] Valenzi E, Bulik M, Tabib T, Morse C, Sembrat J, Trejo Bittar H, et al. Single-cell analysis reveals fibroblast heterogeneity and myofibroblasts in systemic sclerosis-associated interstitial lung disease. Ann Rheum Dis 2019;78(10):1379–87.
[23] Rius Rigau A, Liang M, Devakumar V, Neelagar R, Matei AE, Györfi AH, et al. Imaging mass cytometry-based characterisation of fibroblast subsets and their cellular niches in systemic sclerosis. Ann Rheum Dis 2024.
[24] Rius Rigau A, Li YN, Matei AE, Györfi AH, Bruch PM, Koziel S, et al. Characterization of vascular niche in systemic sclerosis by spatial proteomics. Circ Res 2024;134(7):875–91.

Ann Rheum Dis 84 (2025) 1865–1876

Contents lists available at ScienceDirect

Annals of the Rheumatic Diseases

journal homepage: https://www.sciencedirect.com/journal/annals-of-the-rheumatic-diseases

Systemic sclerosis

Matrix stiffness regulates profibrotic fibroblast differentiation and fibrotic niche activation in systemic sclerosis

Ludwig Ueberall[1,2], Hashem Mohammadian[1,2], Richard Demmler[1,2], Yuko Ariza[1,2], Philipp Tripal[3], Charles Gwellem Anchang[1,2], Stefanie Weber[1,2], Mario Raphael Angeli[1,2], Maria Gabriella Raimondo[1,2], Jiyang Chang[1,2], Kaiyue Huang[1,2], Jörg H.W. Distler[4], Oliver Distler[5], Simon Rauber[1,2], Georg Schett[1,2], Andreas Ramming[1,2,*], Alina Mihaela Ramming[1,2]

[1] *Department of Internal Medicine 3 –Rheumatology and Immunology, Friedrich-Alexander-Universität Erlangen-Nürnberg and Universitätsklinikum Erlangen, Erlangen, Germany*
[2] *Deutsches Zentrum für Immuntherapie (DZI), Friedrich-Alexander-Universität Erlangen-Nürnberg and Universitätsklinikum Erlangen, Erlangen, Germany*
[3] *Optical Imaging Competence Centre (OICE), Friedrich-Alexander-Universität Erlangen-Nuremberg, Erlangen, Germany*
[4] *Department of Rheumatology, University Hospital Düsseldorf, Medical Faculty of Heinrich Heine University; Düsseldorf, Germany*
[5] *Department of Rheumatology, University Hospital Zurich, University of Zurich, Zurich, Switzerland*

ARTICLE INFO

Article history:
Received 6 February 2025
Received in revised form 15 April 2025
Accepted 21 May 2025

ABSTRACT

Objectives: Fibrosis progression in systemic sclerosis (SSc) has been attributed to matrix stiffness. Despite extensive research on fibroblast heterogeneity and subset imbalances in fibrotic disorders, the interplay between biomechanical cues and fibroblast dynamics remains largely unexplored. Here, we investigate how matrix stiffness alters fibroblast transcriptional state and influences lineage specification in fibrotic skin.

Methods: We employed a collagen I-based 3-dimensional culture system to expose fibroblasts to varying levels of matrix stiffness, followed by RNA sequencing to identify stiffness-responsive gene expression signature. We integrated single-cell RNA sequencing data from SSc and healthy skin samples to identify fibroblast subsets associated with this signature. Spatial transcriptomic analyses were performed to localise these fibroblasts and their associations with the fibrotic niche.

Results: Fibroblasts subjected to increased matrix stiffness exhibited a distinct transcriptional signature, amplified in SSc patients and enriched in *PI16*$^+$ progenitor-like cells within the *SFRP2*$^+$ fibrotic compartment. Further analysis indicated that *PI16*$^+$ fibroblasts are predisposed to *SFRP2*$^+$ *COMP*$^+$ PU.1$^+$ myofibroblasts differentiation, whereas blocking mechanotransduction by focal adhesion kinase inhibition disrupts this process, suggesting that matrix stiffness is a key driver of this lineage transition. Spatial mapping revealed colocalisation of the *PI16*$^+$ and *COMP*$^+$ subsets in extracellular matrix-dense regions, highlighting the functional relevance of this relationship in fibrotic progression.

Conclusions: Our findings suggest that increased matrix stiffness promotes fibroblast precursor differentiation into *SFRP2*$^+$ *COMP*$^+$ PU.1$^+$ myofibroblasts, thereby sustaining the vicious cycle

*Correspondence to Dr. Andreas Ramming, Department of Internal Medicine 3, Rheumatology and Immunology, Universitätsklinikum Erlangen, Erlangen, Germany.
E-mail address: andreas.ramming@uk-erlangen.de (A. Ramming).
Ludwig Ueberall and Hashem Mohammadian contributed equally and are considered as joint first authors.
Handling editor Josef S. Smolen.

https://doi.org/10.1016/j.ard.2025.05.016

of persistent fibrosis in absence of inflammatory triggers. These insights reveal new aspects of fibrosis pathogenesis and highlight biomechanical signals as therapeutic targets in SSc.

WHAT IS ALREADY KNOWN ON THIS TOPIC

- The heterogeneity of fibroblasts, their differentiation trajectories and subpopulation imbalances have been investigated through various transcriptomic and proteomic profiling techniques.
- Matrix stiffness is considered as critical factor for fibroblast activation; however, the interaction between biomechanical signals and the activation of specific fibroblast subsets are underexplored.

WHAT THIS STUDY ADDS

- We identify a distinct transcriptional signature in fibroblasts exposed to elevated matrix stiffness, with a more pronounced response observed in systemic sclerosis (SSc) fibroblasts compared to controls.
- Our findings reveal that this signature is enriched in a progenitor-like fibroblast subset and provide evidence that this subset differentiates into a fibrosis associated fibroblast subset during myofibroblast formation.
- Using spatial data analysis, we demonstrate the preferential localisation of these fibroblast subsets in regions with high extracellular matrix density.
- Our study establishes a connection between matrix stiffness and specific fibroblast subpopulations, elucidating their lineage relationships.

HOW THIS STUDY MIGHT AFFECT RESEARCH, PRACTICE OR POLICY

- This research underscores the potential of targeting matrix stiffness-related pathways as therapeutic targets for modulating fibroblast differentiation and myofibroblast activation in SSc.

INTRODUCTION

Systemic sclerosis (SSc) is a chronic fibroinflammatory disease marked by the excessive accumulation of extracellular matrix (ECM) components in connective tissue, leading to structural alterations, increased tissue stiffness and potentially life-threatening organ dysfunction [1,2]. While current therapies primarily target the inflammatory aspects of the disease, these approaches offer limited success as they fail to sufficiently inhibit fibroblast activation, which is critical for effective tissue remodelling [3–5]. The pathogenesis of SSc begins with the disruption of endothelial integrity, sparking inflammation and initiating excessive tissue repair mechanisms [5,6]. Although early inflammatory features subside as the disease progresses, persistently active myofibroblasts sustain the fibrotic process. Substantial understanding has been gained regarding the initial mechanisms of fibrosis, yet the processes that drive its progression following initial injury remain less clear. Although a variety of anti-fibrotic agents have shown promise in slowing disease progression during the early stages, later phases of SSc are often resistant to these treatments, allowing disease advancement despite minimal inflammatory stimuli [3,5–7].

Myofibroblasts are recognised as key contributors to this process of disease progression, as they generate excessive ECM that results in skin thickening [1,8]. Recent single-cell RNA sequencing (scRNAseq) studies have identified specific subtypes of myofibroblasts associated with heightened ECM production, especially in SSc [9–12]. Notably, the transcription factor *SPI1* (PU.1) has emerged as a critical driver of the differentiation of ECM-producing fibrotic fibroblasts, with end-differentiated fibrotic fibroblasts characterised by *COMP* expression, marking them as significant enhancers of fibrosis [13]. However, the persistence of *COMP*$^+$ fibroblasts within the fibrotic niche remains an area of active investigation.

ECM, once seen merely as a pathological by-product of persistent myofibroblast activation, is fundamentally important for organ architecture. Composed primarily of collagen, the ECM forms a dense, organised meshwork of complex macromolecules, including proteins and polysaccharides secreted by resident cells such as fibroblasts. Beyond its structural role, the ECM serves as a microenvironment that regulates various cellular behaviours, such as the proliferation, differentiation and metabolism of parenchymal cells. The physical properties of the ECM, particularly its stiffness, are sensed through cell surface receptors and transduced intracellularly, activating downstream signalling cascades that ultimately lead to transcriptional changes and alterations in cellular behaviour [1,14–17].

Emerging evidence underscores the crucial role of ECM biomechanical properties in modulating cellular function and maintaining homeostasis. In fibrotic conditions, increased matrix stiffness appears to be critically associated with the persistence and chronic activation of myofibroblasts, creating a feedback loop where elevated stiffness sustains myofibroblast activation [1,8,14–16]. Although research into the transcriptomic and proteomic heterogeneity of fibroblasts and the imbalances among their subpopulations in fibrotic disorders has provided new insights, the intricate interactions between matrix stiffness and fibroblast functional states have not been thoroughly examined [9,11,18,19]. Consequently, the interplay between biomechanical signals and fibroblast subset dynamics remains largely unexplored.

Here, we adopted a hybrid approach that involved utilising a collagen I-based 3-dimensional (3D) cell culture model to analyse gene expression profiles of fibroblasts exposed to various levels of matrix stiffness through RNA sequencing. Concurrently, we employed scRNAseq and spatial transcriptomic analyses of skin samples from SSc patients to identify fibroblast subsets and their lineages associated with stiffness-related gene signatures. This integrative strategy allowed us to elucidate the connections between biomechanically induced gene expression profiles and fibroblast subset dynamics, thereby advancing our understanding of the fibrotic mechanisms underlying SSc.

METHODS

Sample collection and cell culture

Skin biopsies from forearm were obtained from patients with SSc according to the 2013 American College of Rheumatology/European League Against Rheumatism criteria [20]. Written informed consent was obtained from all participants. The study was approved by the Ethics Committee of the Universitätsklinikum Erlangen. Fibroblasts were isolated from punch biopsies by enzymatic digestion with Dispase II (Boehringer-Mannheim) for 3 hours at 37 °C, followed by filtration through a 70 µm filter, centrifugation, and subsequent cell culture, as described in Supplementary Methods.

Surface preparation and 3D cell culture

The cell culture dishes (Ibidi glass bottom µ-dishes 35mm) were coated with (3-aminopropyl) triethoxysilane (Sigma-Aldrich), followed by treatment with glutaraldehyde (Carl Roth) as described in Supplementary Methods.

Then, 10× Dulbecco's modified Eagle medium (DMEM) (Sigma-Aldrich) and cells resuspended in 1× DMEM containing supplements (**4-(2-hydroxyethyl)-1-piperazineethanesulfonic acid (**HEPES), amphotericin B, penicillin, streptomycin, L-glutamine, fetal calf serum) (all Thermo Fisher Scientific) were added to the collagen type I mass (Corning Collagen I Rat Tail, concentration: 10.98 mg mL^{-1}). One batch of collagen solution was used throughout the entire experiment. Supplements were added in quantities that resulted in the same final concentrations in the collagen matrices as were present in the 2-dimensional preculture. Final collagen concentration was 3 mg mL^{-1}. Each matrix contained 100,000 cells. To prevent premature polymerisation of the collagen, the experiment was conducted on ice at acidic pH until the intended polymerisation step, which was initiated by adjusting the pH to neutral.

To create collagen matrices with increasing stiffness, 300 µL of the collagen−medium−cell suspension were polymerised in coated microdishes for 1 hour at 16°C, 27°C or 37°C. To ensure sample comparability one matrix of each stiffness/polymerisation temperature was prepared from one batch of ready pipetted collagen−medium−cell suspension. Following polymerisation, the matrices were overlaid with DMEM/F12 and incubated at 37°C in 90% humidity and 5% CO_2 for 48 hours. Preparation of 3D cell cultures was described by Doyle et al [21] with minor modifications. Briefly, noncommercial rat tail collagen I was isolated and used to prepare a stock solution on ice with 10× DMEM and a reconstitution buffer (200 mM HEPES, 262 mM $NaHCO_3$). After adjusting the pH to 7.4 using 1N NaOH, cells were added to achieve a final gel concentration of 3 mg mL^{-1}. Matrices, consisting of 150 µL of the cell−matrix−collagen solution, were cast in 35-mm MatTek dishes and polymerised at varying temperatures. These matrices were then used to observe cell migration and adhesion dynamics of single cells [21].

3D. matrix microscopy and characterisation

The matrices were stained with Carboxytetramethylrhodamin, Succinimidylester (TAMRA-SE;Invitrogen), as described in the Supplementary Methods. Images were obtained with a Leica Stellaris 8 confocal microscope. Fiji [22] was used to quantify fibre diameter and porosity, as described in the Supplementary Methods.

High-resolution visualisation of the collagen was obtained using stimulated emission depletion microscopy with an Abberior stimulated emission depletion (STED) facility line microscope. Collagen fibres were stained with STAR 580, N-Hydroxysuccinimide ester (Abberior). The protocol for staining the matrices corresponded to the protocol for staining with TAMRA-SE.

Viability examinations

Cell viability was assessed based on the morphology of phalloidin-stained cells within the tissues in z-stack images, as described in the Supplementary Methods.

Survival conditions and temperature exposure effect were assessed in the RNA sequencing data and are provided in the supplementary method.

Visualisation of mechanical forces

To highlight cell-driven mechanical forces, their macroscopic visibility was demonstrated by cultivating matrices on uncoated and coated surfaces. As control, matrices without cells were cast on uncoated glass. All matrices were polymerised at 27°C for 1 hour. Images of matrices were captured on days 1 and 3. On day 3, the collagen fibres were visualised using the second-harmonic generation (SHG) signal (Zeiss NLO-880 2 photon microscope).

RNA isolation from collagen matrices

The collagen matrices were dissolved in RA1 lysis buffer provided with the NucleoSpin RNA isolation kit (Macherey-Nagel). RNA was isolated according to the manufacturer's protocol. RNA concentration and purity were determined using NanoDrop (Thermo Fisher Scientific).

Bulk RNA-seq generation and analysis

Library preparation, quality control, 150PE Illumina sequencing, alignment to reference genome (hisat2 v2.0.5 to the reference GRCH38 p12) and quantification (FeatureCounts v1.5.0-p3) were provided by the external provider Novogene in accordance with the encyclopedia of DNA elements (ENCODE) guidelines for RNA-seq (revised version 2016). Count matrix was converted to DESeq2 (1.42.0) objects [23]. Genes with expression more or equal to 10 in at least 3 of the samples were kept for further analysis. Counts were normalised and 'rlog' transformed using DESeq2. More details about the quality control of the samples and DESeq2 differential gene expression analysis is provided in the Supplementary Methods and Supplementary Fig S1.

Single-cell RNA-seq preprocessing and integration

ScRNAseq datasets were obtained from GSE214088 [24], GSE138669 [10] and GSE167339 [25]. Count matrices were imported into R (4.3.2), converted to Seurat (5.1.0) objects and subjected to quality control. More details about the quality control, normalisation and integration is provided in the Supplementary Methods. GSE264508 was provided as a preprocessed Seurat object. Annotation of fibroblasts for GSE138669 and GSE264508 using GSE214088 as the reference was done with a repeated Seurat's reciprocal principal component analysis (RPCA) integration followed by 'FindTransferAnchors' and 'TransferData' with default parameters.

Single-cell RNA-seq trajectory analysis

Potential of heat-diffusion for affinity-based trajectory embedding (PHATE) dimension reduction was generated using Harmony embeddings from the scRNAseq dataset of skin fibroblasts using the 'phate' function from phateR (1.0.7) package [26]. Slingshot (2.10.0) [27] using the PHATE embeddings and *PI16*$^{+}$ cluster as the start cluster was used for trajectory and pseudotime identification.

Single-cell RNA-seq cluster similarity analysis

To identify transcriptional similarity among the fibroblasts subclusters, first markers of each cluster were identified using Seurat's 'FindAllMarker' function. Top 100 genes from each

cluster were selected based on highest log fold changes. Average expression for each cluster and for each of the selected genes was calculated using the 'AverageExpression' function, followed by Pearson correlation estimation using the 'cor' function. Distance matrix (1-correlation matrix) was subject to hierarchical clustering using the 'hclust function in R with the method set to 'ward D2'.

Single-cell RNA-seq meta cell generation

Meta cells (representative samples generated from summarised count of transcriptionally similar cells) were generated using hdWGCNA (0.3.03) [28]. Seurat's identified top 2000 variable features were used and the nondefault parameters for the 'MetacellsByGroups' function were as follows: 'k' = 5, 'max_shared' = 4 and 'min_cells' = 10.

Spatial transcriptomic preprocessing and cluster alignment

Visium spatial transcriptomics datasets from skin of 4 SSc patients were acquired from GSE249279 [12]. Each dataset was separately imported into R and preprocessed using BayesSpace (1.12.0) [29]. More details about the quality control and preprocessing is provided in the supplementary method. Clusters identified in the scRNAseq dataset of SSc skin (GSE214088) (Supplementary Fig S2) were aligned to the spots in each of the Visium datasets using cytospace (1.1.0) [30] on python (3.9.19), by running the pipeline with default parameters.

Statistical analysis

Statistical analysis of transcriptomic data is described in detail above. For all other analysis, parametric and nonparametric analyses as well as paired and nonpaired testing were applied as appropriate, with significance defined as $P < .05$. Adjustments for multiple testing were performed when necessary. *P* values are indicated in the figures, exact statistical test in the figure legend.

Data availability

Bulk RNA-seq dataset generated in this study is available from ArrayExpress with accession number: E-MTAB-14804.

RESULTS

3D. collagen matrix model recapitulates in vivo ECM architecture

To investigate transcriptional changes in fibroblasts induced by altering the mechanical properties of the surrounding ECM, we developed type I collagen-based 3D matrices with varying stiffness, following the methodology described Doyle et al [21]. Our goal was to maximise differences in matrix stiffness while maintaining physiologically relevant conditions. Using polymerisation temperatures of 16°C, 27°C, and 37°C, we conducted structural and functional analyses to ensure that our adapted methodology replicated previously reported matrix characteristics. Confocal and SHG imaging of TAMRA-SE-labelled collagen matrices confirmed consistent polymerisation and revealed distinct variations in matrix architecture (Fig 1B, Supplementary Fig S3A) with significant variations in fibre diameter and matrix porosity with decreasing polymerisation temperature (Fig 1C, D). We then used super-resolution STED microscopy to further elucidate the fibrous network, validating the larger fibres formed from smaller fibrils as previously described (Fig 1E) [21]. Given that these properties are consistent with previous findings and that matrices containing fibres with increased bundle thickness have been reported to result in elevated fibril-associated stiffness, we concluded that additional elasticity measurements were not required for our intended applications [21].

To assess matrix contractility, we cultured matrices with and without fibroblasts. Macroscopic examination revealed notable contraction in fibroblast-containing matrices, while acellular counterparts remained intact over time (Supplementary Fig S3B). Fibroblast-seeded matrices on uncoated surfaces detached from the substrate as a result of cellular contraction forces, leading to greater contraction compared to matrices on coated surfaces, which remained stably attached for at least 3 days. SHG imaging demonstrated that collagen fibres in nonanchored matrices transitioned from their initial linear alignment to a wavy configuration upon contraction, highlighting the enhanced resistance of anchored matrices to cellular contraction forces, which are considered essential for cellular mechanotransduction (Supplementary Fig S3B). Importantly, fibroblast viability remained stable despite variations in cell density (Supplementary Fig S3C). Furthermore, earlier studies have proven physiological relevance of the matrix model, as they demonstrated the fibres of all bundle diameters to be present in vivo in mouse back skin [21].

Fibroblast gene expression is responsive to matrix stiffness

To investigate the transcriptomic dynamics of fibroblasts in response to varying matrix stiffness, we performed bulk RNA sequencing on fibroblasts isolated from skin of both patients with SSc and healthy donors, cultured across the 3 stiffness levels described above (Fig 1A, 2A). After adjusting for disease-unrelated covariates, we identified significant transcriptional changes in fibroblasts exposed to stiff matrices, irrespective of their origin (Fig 2B). Notably, genes related to fibrotic processes and mechanotransduction pathways, such as *RACK1* and *LGALS1*, were significantly upregulated in these conditions [31–37].

Identification of stiffness-responsive fibroblast subtypes in SSc skin

To investigate how stiffness is associated with cellular heterogeneity in fibroblasts at the single-cell level during fibrosis, we derived a transcriptional signature based on the differential expressed genes in response to stiffness in our bulk RNA-seq experiment and integrated it with scRNAseq data. Specifically, we applied this signature to a publicly available scRNAseq dataset of whole skin tissue from 5 SSc patients and 6 normal controls (GSE214088) [24] (Fig 2A). Fibroblasts were isolated from these datasets, and clustering at a low resolution revealed 4 major fibroblast clusters including *SFRP2*$^+$, *CXCL12*$^+$, *TNN*$^+$ and *CLDN1*$^+$ (Fig 2C). Increasing clustering resolution identified 6 further subtypes within these clusters in line with previous reports [9,12,24], including *SFRP2*$^+$ *PI16*$^+$, *SFRP2*$^+$ *COMP*$^+$, *CXCL12*$^+$ *CCL19*$^+$, *CXCL12*$^+$ *FMO2*$^+$, *TNN*$^+$ *ASPN*$^+$ and *TNN*$^+$ *POSTN*$^+$ (Fig 2C).

Using UCell [38], fibroblast subtypes were evaluated for stiffness-associated response. The *PI16*$^+$ cluster within the *SFRP2*$^+$ fibroblast compartment exhibited the highest stiffness-response score (Fig 2A,D). *PI16*$^+$ fibroblasts also showed the highest

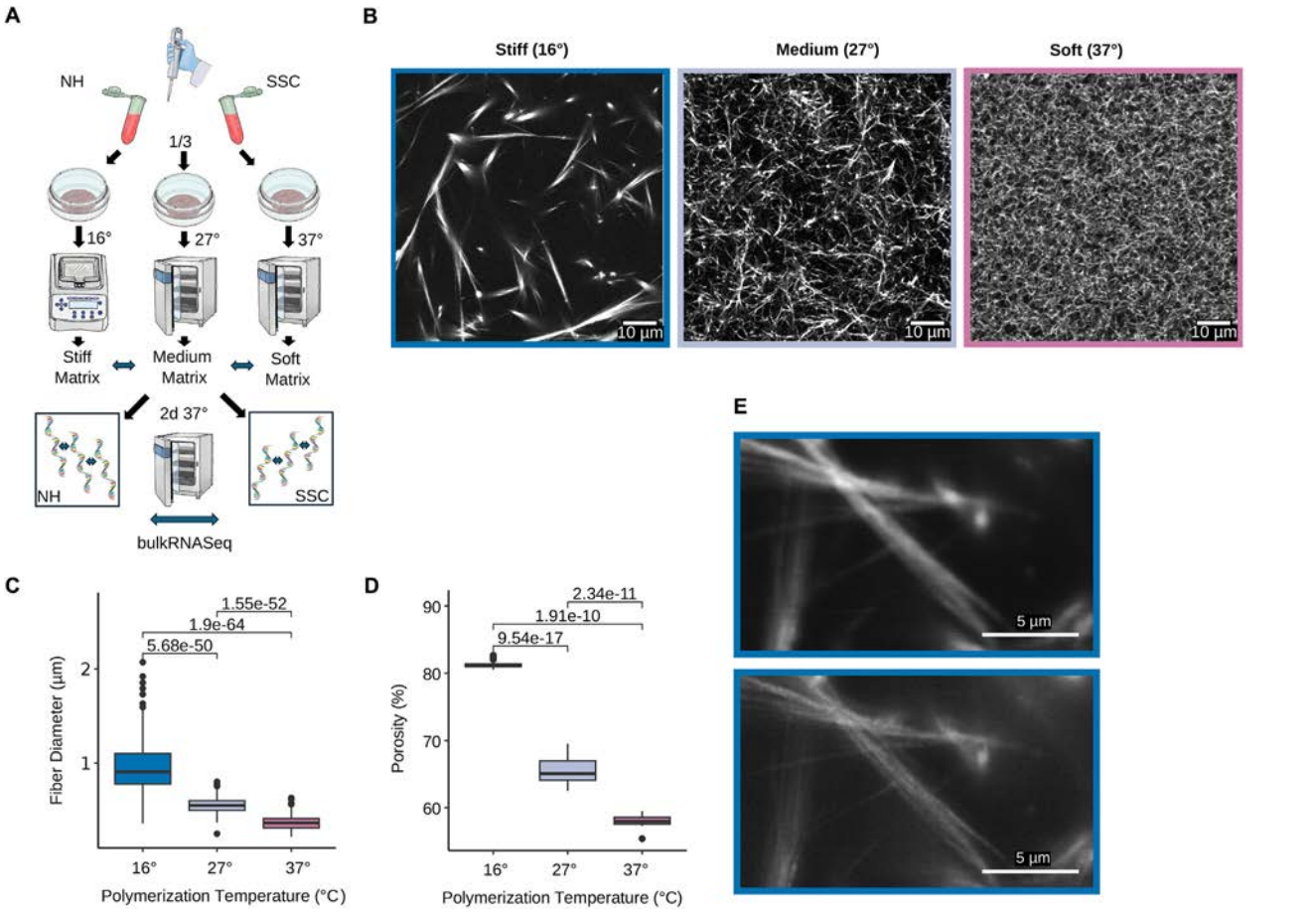

Figure 1. Polymerisation temperature-dependent microstructure variations in collagen matrices: multimodal imaging and quantitative analysis. A, Experimental workflow for studying the effect of collagen matrix stiffness on fibroblast behaviour: A cell-collagen suspension was divided into 3 portions and polymerised at 16°C, 27°C or 37°C to create stiff, medium, and soft matrices. NHDF or SSc cells were embedded, cultured for 48 hours at 37°C, and RNA was extracted for bulk RNA-Seq. B, Representative immunofluorescence images acquired using confocal microscopy of collagen matrices with varying stiffness (stiff, medium and soft), polymerised at 16°C, 27°C and 37°C, respectively, and stained with TAMRA-SE dye (white). C-D, Quantification of fibre diameters and matrix porosity in collagen matrices polymerised at 16°C, 27°C and 37°C; *P* values were calculated using Wilcoxon rank sum test and corrected for multiple testing using (Benjamini-Hochberg) BH method. Median, quartiles, min−max and outliers are shown. E, High-resolution images of individual collagen fibres stained with Abberior STAR 580 dye, captured using confocal microscopy and super-resolution STED imaging. BH, Benjamini-Hochberg; NHDF, normal human dermal fibroblasts; RNA-Seq, RNA sequencing; SSc, systemic sclerosis; TAMRA-SE, Carboxytetramethylrhodamin, Succinimidylester; STED, stimulated emission depletion.

increase of the stiffness-response score in SSc from the base line when compared to the other fibroblast subclusters indicating their high sensitivity to mechanistic properties of the ECM. Analysis of 2 additional scRNAseq datasets from fibrotic skin diseases (GSE138669) [39] and (GSE264508) [40] revealed similar heightened sensitivity to stiffness in the *PI16*$^+$ cells (Supplementary Fig S4A,B,D,E). To further support this, we evaluated the expression of *PIEZO1* and *PIEZO2*, which are mechanosensitive ion channels critical for sensing mechanical forces [41,42]. Furthermore, it has been shown that PIEZO-mediated sensing of mechanical stress promotes myofibroblast activation [43,44]. Both genes were more highly expressed in *PI16*$^+$ fibroblasts (Fig 2E), supporting their increased sensitivity to mechanical forces in stiffened matrices.

SFRP2$^+$ PI16$^+$ *fibroblasts differentiate into myofibroblasts in SSc*

Fibroblasts expressing *PI16* are previously identified as universal precursor fibroblasts capable of specialising under perturbations, particularly into fibrosis associated fibroblast [18,45,46]. Given their highest sensitivity to stiffness and their association with myofibroblast differentiation in SSc, we hypothesised that *SFRP2*$^+$ *PI16*$^+$ fibroblasts differentiate into myofibroblasts during SSc progression. To test this, transcriptional similarities between fibroblast subclusters were examined using gene expression correlations followed by hierarchical clustering, assuming that differentiated cells retain a high degree of overall similarity with their precursor population. High similarity was observed between *PI16*$^+$ cells and *COMP*$^+$ fibroblasts, another subtype within the *SFRP2*$^+$ compartment (Fig 3A). Differential abundance analysis revealed a significant decrease in the *PI16*$^+$*/COMP*$^+$ ratio in SSc, consistent with active transdifferentiation of the *PI16*$^+$ into *COMP*$^+$ cells (Fig 3B).

To model this potential differentiation during SSc, we applied the "potential of heat-diffusion for affinity-based trajectory embedding" (PHATE) [26] dimensionality reduction to the *SFRP2*$^+$ compartment. PHATE was chosen as it preserves both local and global transcriptional relationships, making it particularly well-suited for visualising differentiation processes. The resulting PHATE embedding revealed a linear trajectory of *PI16*$^+$ cells transitioning into a larger cluster of *COMP*$^+$ cells, strongly suggesting a differentiation pathway (Fig 3C). We then implemented slingshot [27] on the PHATE embedding for trajectory analysis. The resulting pseudotime estimation confirmed a trajectory wherein *PI16*$^+$ cells transitioned to *COMP*$^+$ cells, where

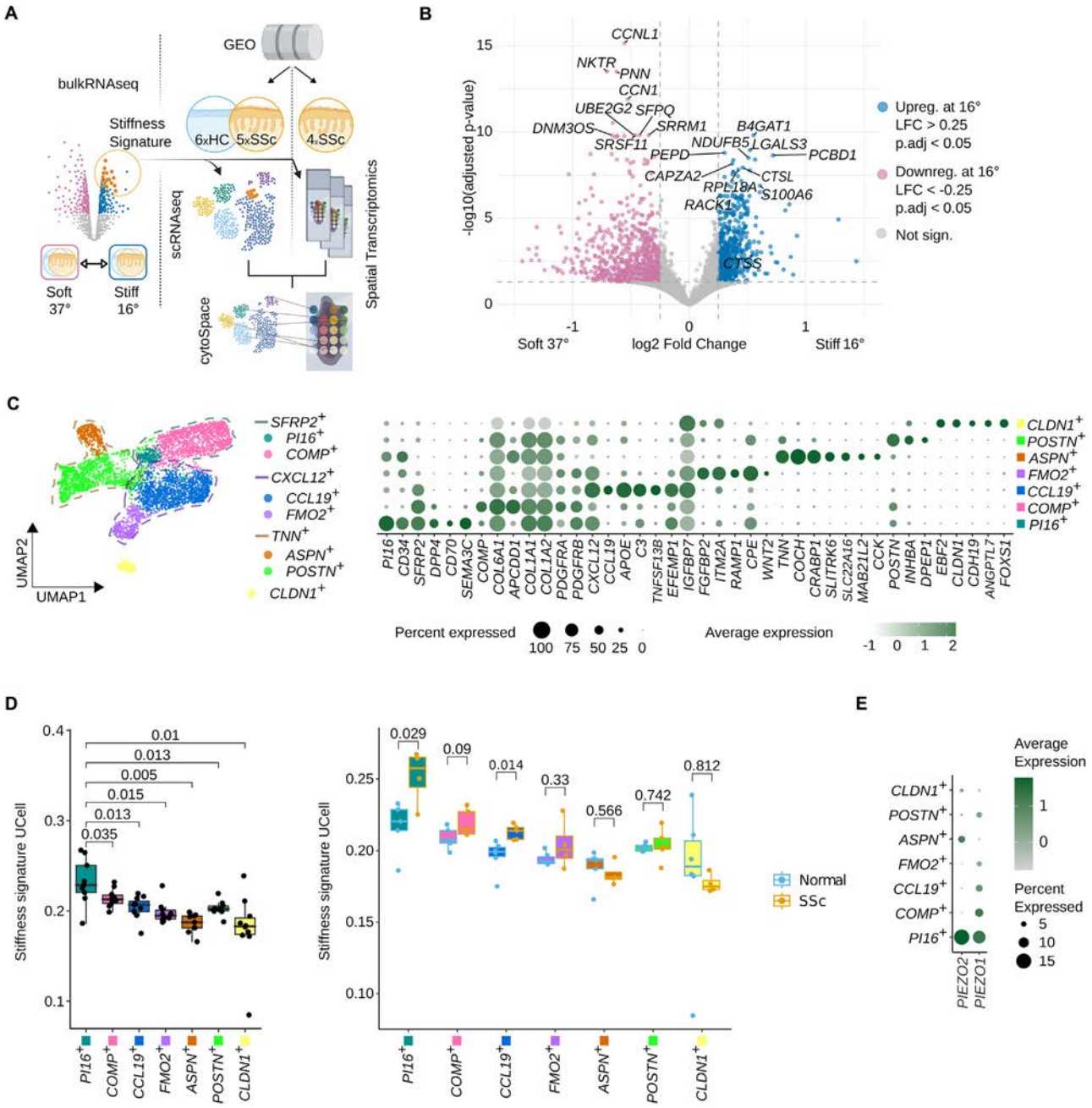

Figure 2. *PI16*$^+$ fibroblasts show the strongest response to matrix stiffness among fibroblasts subsets in SSc. A, Analysis workflow for characterisation of stiffness responsive fibroblasts in SSc: stiffness response signature was extracted from the bulk RNAseq experiment. ScRNAseq (GSE214088) and spatial transcriptomic datasets (GSE249279) from healthy and SSc skin acquired from previous publications (GEO: Gene Expression Omnibus) and analysed to identify stiffness response fibroblasts and their dynamics as well as their spatial localisation in the tissue (Created with BioRender.com) B, Volcano plot of differential gene expression (DGE) between cells at 16°C and 37°C, adjusted for covariates. Top upregulated and downregulated genes are highlighted. DGE was performed with DESeq2 and BH correction for multiple testing. C, (right) Uniform manifold approximation and projection for dimension reduction (UMAP) plot of fibroblasts major clusters (cluster borders indicated with coloured dashed lines) and their subclusters (indicated by point colour) in the skin scRNAseq dataset on normal and SSc skin (N = 5 SSc, N = 6 normal). (left) Expression of top markers of fibroblasts subclusters. D, UCell stiffness signature scores compared across fibroblast subclusters, averaged per cluster per replicate (N = 11; 5 SSc, 6 normal). *P* values were calculated with the Wilcoxon rank-sum test and BH correction. Median, quartiles and min−max are shown. (right) Comparison of UCell stiffness scores between fibroblast subclusters and disease states, averaged per cluster per replicate (N = 5 SSc, 6 normal). *P* values were calculated using the Wilcoxon rank-sum test with BH correction. Median, quartiles, and min−max are shown. E, Expression of *PIEZO2* and *PIEZO1* on fibroblasts subclusters. BH, Benjamini-Hochberg; GEO, Gene Expression Omnibus; scRNASeq, single-cell RNA sequencing; SSc, systemic sclerosis; UMAP, uniform manifold approximation.

gradient of expression of *PI16* and *CD34* were evident (Fig 3C). Analysis of 2 additional scRNAseq datasets from fibrotic skin diseases revealed similar trends (Supplementary Fig S4C,F).

To validate the activation of myofibroblast pathways along this differentiation trajectory, we scored *SFRP2*$^+$ fibroblasts using transcriptional signatures of transforming growth factor β- or interleukin 4-stimulated fibroblasts, based on a method established in a previous study [12]. Scores for these profibrotic signatures were elevated in *COMP*$^+$ cells and progressively increased along the trajectory (Fig 3D), indicating that *PI16*$^+$ differentiation is towards a myofibroblasts state. Moreover, pseudobulk differential gene expression analysis on the *COMP*$^+$ cells in SSc confirmed significant upregulation of genes associated with myofibroblast activation including *COL1A1* and

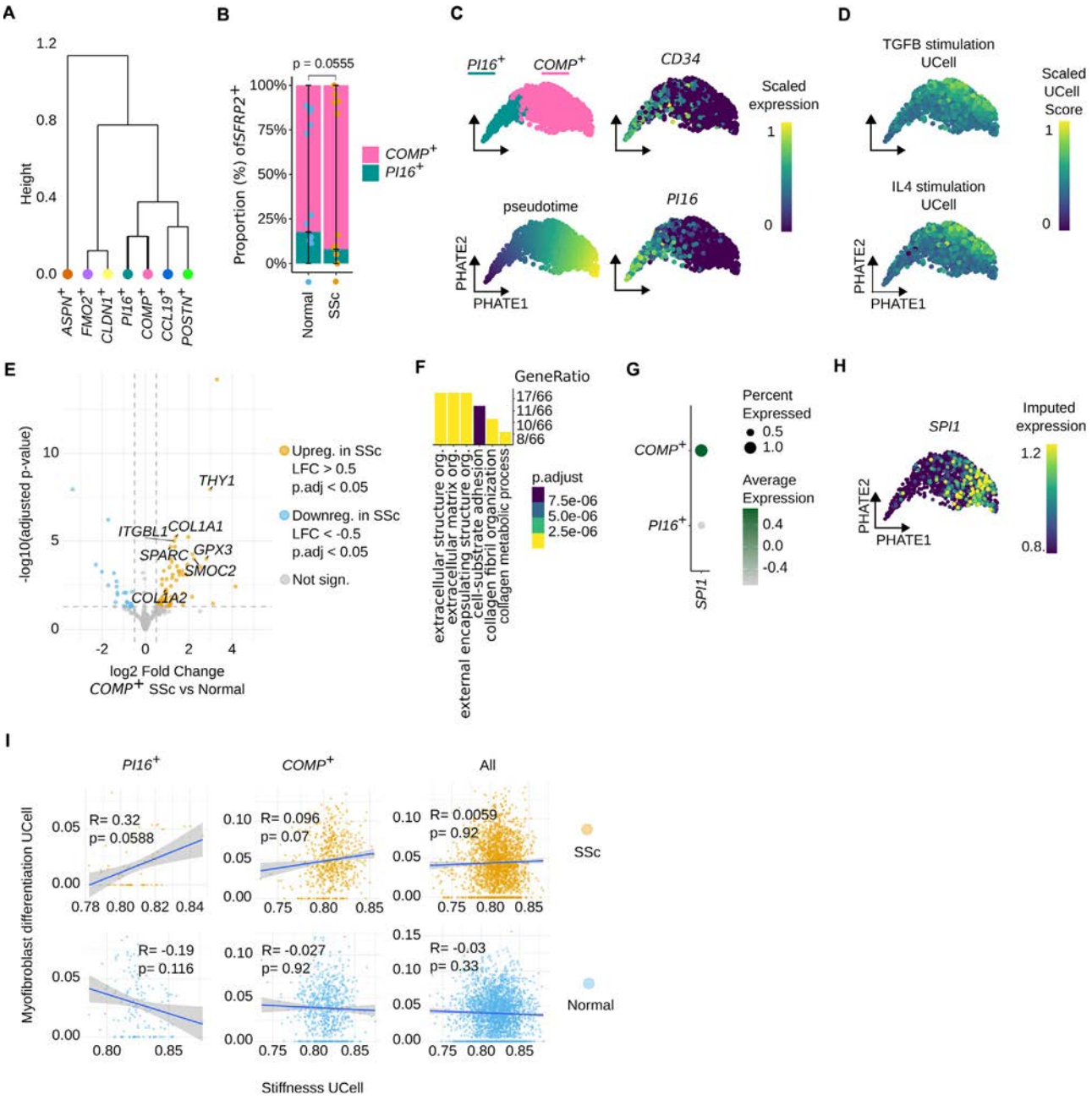

Figure 3. Increased matrix stiffness induces myofibroblasts transdifferentiation of the *PI16*$^+$ fibroblasts. A, Hierarchical clustering tree created from the transcriptional correlation between different subclusters of fibroblast in the skin scRNAseq dataset of SSc and healthy patients. B, Comparison of ratio of subclusters of *SFRP2*$^+$ fibroblasts between SSc and normal skin (SSc N = 5, normal N = 6). *P* value is calculated using 2-sided Wilcoxon rank sum test. Median is shown. C, Various parameters shown on the PHATE embeddings of the *SFRP2*$^+$ fibroblasts compartment: subclusters of *SFRP2*$^+$ fibroblasts (top left). Pseudotime values identified using slingshot (bottom left). Expression of *CD34* and *PI16* (right). D, UCell score for gene signatures of transforming growth factor (TGF)*β* (top) and interleukin (IL)4 stimulations (bottom) on *SFRP2*$^+$ fibroblasts subtypes. E, Volcano plot of DGE on *COMP*$^+$ fibroblasts between SSc and normal (SSc N = 5, normal N = 6). Top upregulated and downregulated genes are highlighted. DGE was performed on pseudobulk with DESeq2 and BH correction for multiple testing. F, GOBP pathways significantly upregulated in the *COMP*$^+$ cells in SSc. p-vales are calculated using ClusterProfiler's 'enrichGO' function and corrected for multiple testing using BH method. G, Expression of *SPI1* on *SFRP2*$^+$ fibroblasts. H, ALRA imputed expression of *SPI1* on *SFRP2*$^+$ fibroblasts. I, Scatter plots showing the GOBP myofibroblast differentiation UCell score versus stiffness signature scores on hdWGCNA-generated meta cells of *PI16*$^+$, *COMP*$^+$ or all fibroblasts in normal or SSc skin scRNAseq dataset. Correlation is calculated using 2-sided Spearman's method, and *P* values are corrected for multiple testing using BH. Blue lines show the linear fit, and the grey region shows the CI. ALRA, adaptively-thresholded low rank approximation; BH, Benjamini-Hochberg; DGE, differential gene expression; GOBP, gene ontology biological process; scRNA-Seq, single-cell RNA sequencing; SSc, systemic sclerosis; PHATE, potential of heat diffusion for affinity-based transition embeddings

COL1A2 as well as significant activation of pathways consistent with the functional characteristics of myofibroblasts including ECM production, remodelling and adhesion dynamics (Fig 3E,F).

To further characterise the differentiation of *PI16*$^+$ fibroblasts into myofibroblasts, we analysed the expression of *SPI1* (PU.1), a transcription factor implicated in fibrotic polarisation of fibroblasts [13]. *SPI1* expression was higher in *COMP*$^+$ compared to *PI16*$^+$ fibroblasts, although both the percentage and expression levels were low (Fig 3G), likely due to the challenges of detecting transcription factors in scRNAseq data [47]. Using adaptively-thresholded low rank approximation imputation (ALRA) [48], we improved signal recovery and confirmed higher *SPI1* expression in *COMP*$^+$ fibroblasts, showing a

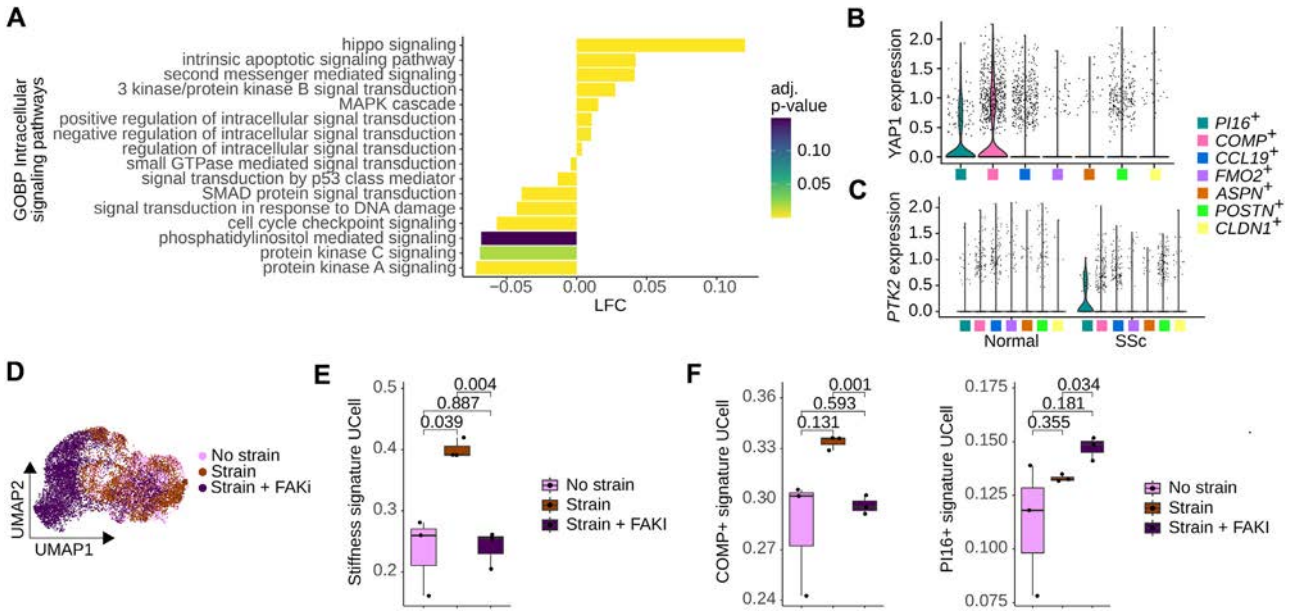

Figure 4. Inhibition of mechanotransduction pathway blocks stiffness-induced myofibroblasts activation. A, Bar plot showing the log2 fold changes of averaged UCell scores for subterms of GOBP 'intracellular signal transduction GO:0035556' pathway in *SFRP2*$^+$ fibroblasts when compared to other fibroblasts in the scRNAseq dataset of SSc and normal skin (GSE214088). *P* values are calculated using the Wilcoxon rank sum test with BH correction. B, Expression level of *YAP1* among the sub cluster of skin fibroblasts from a. C, Expression level of *PTK2* among the sub clusters of skin fibroblast from a, compared between normal and SSc skin. D, UMAP plot of fibroblasts in the human dermal scRNAseq dataset of fibroblasts cultured in 3D collagen scaffolds with either no strain, strain or strain + FAK inhibition (FAKI) (GSE138669). E and F, Comparison of stiffness-response (E) *COMP*$^+$ and *PI16*$^+$ signature (F) UCell score between fibroblasts from d. *P* values are calculated using t-test with BH correction. Median, quartiles and min−max are shown. BH, Benjamini-Hochberg; FAK, focal adhesion kinase, FAKI, focal adhesion kinase inhibitor; GOBP, gene ontology biological process; scRNASeq, single-cell RNA sequencing; SSc, systemic sclerosis; UMAP, uniform manifold approximation; LFC, log2 fold changes.

gradient increase in the later stages of myofibroblast differentiation (Fig 3H).

To assess whether the myofibroblast differentiation of the *PI16*$^+$ cells is associated with increased stiffness in SSc we evaluated the correlation of stiffness signature with the gene ontology biological processes (GOBPs) myofibroblast differentiation (GO:0036446) score. To overcome the potential errors due to scRNAseq sparsity the correlation analysis was done on meta cells generated using hdWGCNA [28]. A significant positive correlation was observed between stiffness score and myofibroblasts differentiation score in the SSc-derived *PI16*$^+$ fibroblasts but not in the normal skin *PI16*$^+$ fibroblasts, or in other subtypes of fibroblasts in the skin (Fig 3I).

Inhibition of mechanotransduction pathway blocks stiffness-induced SFRP2$^+$ COMP$^+$ *myofibroblasts differentiation*

To characterise the intracellular signalling mechanisms of myofibroblast differentiation in the *SFRP2*$^+$ compartment, we performed pathway scoring analysis using all sub terms from the GOBP 'intracellular signal transduction GO:0035556'. Consistent with prior findings [12], we observed significant upregulation of the Hippo pathway (Fig 4A). As a key component of Hippo signalling in mechanotransduction [49], the YAP/TAZ axis was notably upregulated, with increased *YAP1* expression (Fig 4B).

To further explore the role of YAP/TAZ signalling in matrix-driven myofibroblast activation, we analysed a scRNAseq dataset from a dermal wound healing culture system (GSE167339) [25], where mechanotransduction was modulated by focal adhesion kinase (FAK/*PTK2*) inhibition. Notably, *PTK2* was upregulated in *PI16*$^+$ fibroblasts in SSc (Fig 4C). Reanalysis of this dataset revealed that mechanical strain induced our stiffness-response signature, which was reversed by FAK inhibition (Fig 4D,E). Moreover, strain increased the *COMP*$^+$ fibroblast signature, whereas FAK inhibition restored *COMP*$^+$ and *PI16*$^+$ signatures (Fig 4F). These findings confirm mechanotransduction as a driver of *PI16*$^+$ to *COMP*$^+$ myofibroblast transition in response to matrix stiffness.

Spatial colocalisation of PI16$^+$ *and* COMP$^+$ *fibroblasts in stiffness-associated regions*

To further investigate the spatial distribution of *SFRP2*$^+$ *PI16*$^+$ precursor cells and their differentiated *COMP*$^+$ myofibroblasts state we analysed a publicly available spatial transcriptomic dataset of skin SSc samples (GSE249279) [12]. We implemented cytospace [30] to align the entire single-cell clusters (Supplementary Fig S1B) to their corresponding spots in the spatial transcriptomics data. Our analysis revealed that *PI16*$^+$ and *COMP*$^+$ fibroblasts populations colocalised within the tissue (Fig 5A,B). Hierarchical clustering of cytospace identifying relative abundances among all fibroblasts subsets further confirmed this observation by showing distinct clustering of precursor and *COMP*$^+$ myofibroblast populations (Fig 5C). Furthermore, we scored the spatial spots using our stiffness-associated gene signature, as well as with previously suggested ECM score [12] based on GOBP term for collagen containing extracellular matrix (GO:0062023) as a measure of ECM deposition resulting from ongoing fibrosis. We observed a significant correlation between stiffness scores and ECM scores across the tissue regions (Fig 5D, E). Notably, these scores were higher in regions where *PI16*$^+$ and differentiated myofibroblasts colocalised, indicating that increased stiffness and ECM remodelling are associated with the myofibroblasts differentiation of the *PI16*$^+$ cells. The correlation between stiffness and ECM scores suggests that these 2 factors

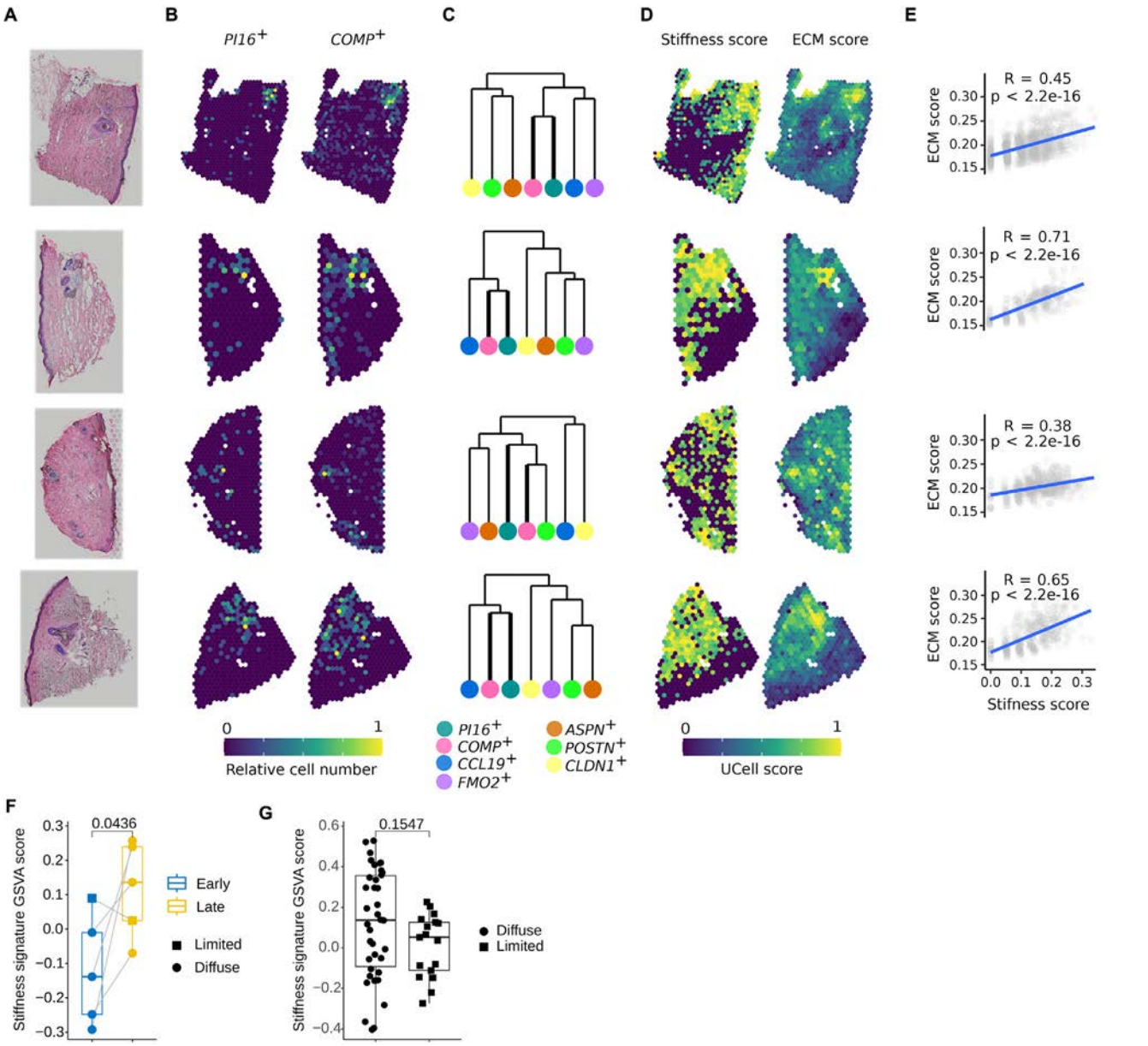

Figure 5. *PI16*$^+$ and *COMP*$^+$ fibroblasts colocalise within fibrotic niches characterised with increased matrix stiffness. A, Visium slide of human skin tissue from patients with SSc (N = 4 patients, 7 technical replicates); one representative tissue section per patient is shown. B, Spatial distribution of the relative cell number of *PI16*$^+$ and *COMP*$^+$ fibroblasts on Visium spots identified using cytospace mapped from the scRNAseq dataset of normal and SSc skin tissues. C, Hierarchical clustering tree created from the relative cell number correlation over Visium spots between different subclusters of fibroblast. D, Stiffness signature (right) and extracellular matrix (ECM) (left) UCell score visualised on Visium spots. E, Scatter plots showing the ECM vs stiffness signature UCell score across Visium spots. Correlation is calculated using 2-sided Spearman's method. Blue line shows the linear fit. F and G, Comparison of stiffness-response GSVA scores between paired early and late stage (F) and between late diffuse and late limited (G) SSc skin fibrosis patients from the GENISOS (GSE58095) cohort. *P* values are calculated using limma while accounting for covariates. Median, quartiles and min–max are shown. (N = 5 paired early-late, 38 late diffuse, 17 late limited). scRNASeq, single-cell RNA sequencing; SSc, systemic sclerosis; GSVA, gene set variation analysis.

may act synergistically in driving fibrosis. Consistent with this, data from early- and late-stage SSc patients (GSE58095) [50] showed increased expression of our stiffness signature in late-stage disease (Fig 5F), reflecting ECM accumulation and tissue stiffening in advanced skin fibrosis. No significant difference was observed between diffuse and limited disease (Fig 5G). This was expected as disease distribution does not directly impact stiffness levels.

DISCUSSION

In this study, we examined the complex relationship between matrix stiffness and fibroblast dynamics in SSc, a debilitating condition characterised by excessive skin and organ fibrosis and the consequent decline of organ function. Our findings provide significant insights into the role of biomechanical cues in modulating fibroblast behaviour and highlight specific cellular subtypes that could serve as therapeutic targets to alleviate disease progression.

One of the main results of our study was the successful establishment of a collagen-based 3D matrix model that mimics the ECM architecture *in vivo*. This model allowed us to investigate the cellular responses of fibroblasts subjected to varying stiffness levels, reflecting the pathological changes observed in SSc. The evident structural differences in fibre architecture and properties of our matrices, confirmed through advanced imaging techniques, underline the importance of matrix properties in regulating fibroblast activity. Our data align with previous

research indicating that ECM stiffness is a significant modulator of cellular behaviours, influencing processes, such as proliferation, differentiation and gene expression [1,8,14–17].

Through bulk RNA sequencing, we identified significant transcriptional changes in fibroblasts exposed to stiff matrix, including genes associated with mechanotransduction pathways and fibrotic processes. This underlines the concept that fibroblasts are finely adjusted to their mechanical microenvironment. Particularly notable was the identification of stiffness-responsive fibroblast subtypes, including the *SFRP2*$^+$ *PI16*$^+$ population, which exhibited heightened responsiveness to matrix stiffness. This finding highlights the heterogeneity within the fibroblast population in SSc and supports the idea that specific fibroblast subtypes may have differential roles in disease pathogenesis [9].

The significant correlation between increased matrix stiffness and the differentiation of *SFRP2*$^+$ *PI16*$^+$ precursor fibroblasts into myofibroblasts provides a compelling explanation about the mechanistic pathways behind fibrosis in SSc. Our trajectory analyses demonstrated a clear differentiation pathway within the *SFRP2*$^+$ compartment, suggesting that *PI16*$^+$ fibroblasts are predisposed to develop myofibroblast characteristics in response to mechanical cues. Moreover, our analysis revealed spatial colocalisation of *PI16*$^+$ fibroblasts and *COMP*$^+$ myofibroblasts in regions characterised by high stiffness and ECM remodelling. This spatial arrangement suggests a localised mechanotransduction signalling that may further reinforce the activation of myofibroblast pathways that challenges the conventional understanding of fibrosis as a uniformly distributed process. Collectively these findings reinforce the idea of a pathological positive feedback loop where heightened matrix stiffness contributes to persistent myofibroblast activation and ongoing ECM deposition, thereby sustaining fibrosis [14,16,17].

These findings not only deepen our understanding of the cellular mechanisms behind fibrosis in SSc but also present new opportunities for therapeutic intervention. However, to enhance the critical evaluation of our study, it is essential to acknowledge that the *in vitro* nature of our experiments, along with the specific methods employed for matrix preparation, may not fully capture the complexities of the *in vivo* microenvironment. In an effort to address this limitation, we compared our findings with various existing datasets derived from *in vivo* studies and *ex vivo* tissues, which serve as valuable references for validating our results. Nevertheless, this comparative analysis has its own constraints and may not encompass all relevant biological nuances, highlighting the necessity for future investigations to rigorously explore these variables and alternative explanations. Such efforts will contribute to a more comprehensive understanding of the interplay between matrix stiffness and fibroblast dynamics. In light of these insights, targeting the biomechanical properties of the ECM and their associated fibroblast-specific signalling pathways could pave the way for developing novel antifibrotic strategies. For instance, pharmacologic modulation of matrix stiffness or direct targeting of specific fibroblast subtypes that are predisposed to differentiation under stiff matrix could offer potential in reducing fibrosis progression and improving patient outcomes. Furthermore, therapeutic approaches such as RNA interference targeting specific genes involved in the transdifferentiation of *PI16*$^+$ fibroblasts into *COMP*$^+$ myofibroblasts, along with the use of integrin antagonists to disrupt fibroblast-ECM interactions, require further evaluation to enhance their efficacy in clinical applications.

In conclusion, our study elucidates the critical role of matrix stiffness in orchestrating fibroblast dynamics and myofibroblast differentiation in SSc. By revealing the interactions between mechanical cues and fibroblast heterogeneity, we advance our understanding of the pathogenesis of SSc and highlight potential ways for therapeutic exploration. As our knowledge of ECM biology and fibroblast behaviour evolves, it may provide the foundation for more effective strategies to combat fibrosis and its associated complications in SSc and other related disorders. Future studies should aim to further dissect the molecular mechanisms governing these processes and explore the interplay between mechanical signals and inflammatory pathways in fibrosis progression.

Competing interests

Financial support by German Research Foundation does not imply competing interest. German Research Foundation is a neutral funding agency from the German Government. There are no competing interests declared.

Acknowledgements

We thank M Rose and KT Yang for excellent technical assistance. We acknowledge the FAU OICE core facility for imaging assistance. The present work was performed in fulfilment of the requirements for obtaining the degree Dr. Med and partial fulfilment of the requirements for obtaining the degree Dr. Rer. Biol. Hum. at the FAU Erlangen-Nürnberg.

Contributors

LU, HM, AR and AMR were involved in the design of the study; LU, HM, RD, YA, PT, CAG, SW, MRA, MGR, JC, KH, SR, AR and AMR were involved in the acquisition of data; LU, HM, RD, YA, PT, CAG, SW, MRA, MGR, JC, KH, JHWD, OD, SR, GS, AR and AMR were involved in interpretation of data; JHWD, OD, AR and AMR were involved in support of material; and LU, HM, SR, GS, AR and AMR were involved in paper preparation.

Funding

The work was supported by the German Research Foundation (DFG) to AMR (SO 1735/2-1), AR (RA 2506/4-1, RA 2506/4-2, RA 2506/6-1, RA 2506/7-1), Clinician Scientist Program NOTICE-493624887 to MGR and AR and SCHE 1583/7-1 to GS; CRC1181 to GS (projects A01/Z03) and AR (project C06); CRC/TRR 369 DIONE to GS and AR; Gottfried Wilhelm Leibniz Prize 2023 to GS. The work was supported by the European Research Council (853508 BARRIER BREAK) to AR and EC project Nanoscope 4D to GS. The work was supported by the Federal Ministry of Education and Research (BMBF) to TK, GS and AR (MASCARA). This work was supported by the Innovative Medicines Initiative projects RTCure and HIPPOCRATES to GS and AR. The work was supported by the Interdisciplinary Centre for Clinical Research (IZKF) Erlangen (D034 to AR, P049 and J106 to MGR, J107 to SR). Confocal microscopy was enabled on a Leica Stellaris 8 laser scanning microscope funded by Deutsche Forschungsgemeinschaft (DFG, German Research Foundation; project 441730715). Multiphoton microscopy was performed on a Zeiss LSM880 NLO Intravital Microscope, funded by Deutsche Forschungsgemeinschaft (DFG, German Research Foundation; project 261193037). Super-resolution stimulated emission depletion (STED) microscopy was enabled on an Abberior STED facility line instrument, funded by Deutsche Forschungsgemeinschaft (DFG, German Research Foundation; project 263718168).

Patient consent for publication

Written informed consent was obtained from all participants.

Ethics approval

The study was approved by the Ethics Committee of the Universitätsklinikum Erlangen (Number: 30_19B).

Provenance and peer review

Not commissioned

Supplementary materials

Supplementary material associated with this article can be found, in the online version, at doi:10.1016/j.ard.2025.05.016.

Orcid

Ludwig Ueberall: http://orcid.org/0009-0002-2895-5565
Hashem Mohammadian: http://orcid.org/0000-0003-2565-2702
Philipp Tripal: http://orcid.org/0000-0003-0568-1725
Stefanie Weber: http://orcid.org/0000-0001-8592-2810
Mario Raphael Angeli: http://orcid.org/0000-0002-2911-4269
Oliver Distler: http://orcid.org/0000-0002-0546-8310
Simon Rauber: http://orcid.org/0000-0001-8306-9334
Andreas Ramming: http://orcid.org/0000-0002-7003-501X

REFERENCES

[1] Ho YY, Lagares D, Tager AM, Kapoor M. Fibrosis—a lethal component of systemic sclerosis. Nat Rev Rheumatol 2014;10:390–402. doi: 10.1038/nrrheum.2014.53.
[2] Denton CP, Khanna D. Systemic sclerosis. Lancet 2017;390:1685–99. doi: 10.1016/S0140-6736(17)30933-9.
[3] Denton CP. Systemic sclerosis: from pathogenesis to targeted therapy. Clin Exp Rheumatol 2015;33:S3–7.
[4] Nihtyanova SI, Ong VH, Denton CP. Current management strategies for systemic sclerosis. Clin Exp Rheumatol 2014;32:156–64.
[5] Varga J, Abraham D. Systemic sclerosis: a prototypic multisystem fibrotic disorder. J Clin Invest 2007;117:557–67. doi: 10.1172/JCI31139.
[6] Rosendahl A, Schönborn K, Krieg T. Pathophysiology of systemic sclerosis (scleroderma). Kaohsiung J Med Sci 2022;38:187–95. doi: 10.1002/kjm2.12505.
[7] Zhao M, Wang L, Wang M, Zhou S, Lu Y, Cui H, et al. Targeting fibrosis, mechanisms and clinical trials. Signal Transduct Target Ther 2022;7:206. doi: 10.1038/s41392-022-01070-3.
[8] Tai Y, Woods EL, Dally J, Kong D, Steadman R, Moseley R, et al. Myofibroblasts: function, formation, and scope of molecular therapies for skin fibrosis. Biomolecules 2021;11:1095. doi: 10.3390/biom11081095.
[9] Zhu H, Luo H, Skaug B, Tabib T, Li YN, Tao Y, et al. Fibroblast subpopulations in systemic sclerosis: functional implications of individual subpopulations and correlations with clinical features. J Invest Dermatol 2024;144:1251–1261.e13. doi: 10.1016/j.jid.2023.09.288.
[10] Tabib T, Huang M, Morse N, Papazoglou A, Behera R, Jia M, et al. Myofibroblast transcriptome indicates SFRP2hi fibroblast progenitors in systemic sclerosis skin. Nat Commun 2021;12:4384. doi: 10.1038/s41467-021-24607-6.
[11] Deng C-C, Hu Y-F, Zhu D-H, Cheng Q, Gu JJ, Feng QL, et al. Single-cell RNA-seq reveals fibroblast heterogeneity and increased mesenchymal fibroblasts in human fibrotic skin diseases. Nat Commun 2021;12:3709. doi: 10.1038/s41467-021-24110-y.
[12] Ma F, Tsou P-S, Gharaee-Kermani M, Plazyo O, Xing X, Kirma J, et al. Systems-based identification of the Hippo pathway for promoting fibrotic mesenchymal differentiation in systemic sclerosis. Nat Commun 2024;15:210. doi: 10.1038/s41467-023-44645-6.
[13] Wohlfahrt T, Rauber S, Uebe S, Luber M, Soare A, Ekici A, et al. PU.1 controls fibroblast polarization and tissue fibrosis. Nature 2019;566:344–9. doi: 10.1038/s41586-019-0896-x.
[14] Leask A. The hard problem: mechanotransduction perpetuates the myofibroblast phenotype in scleroderma fibrosis. Wound Repair Regen 2021;29:582–7. doi: 10.1111/wrr.12889.
[15] Leask A, Naik A, Stratton RJ. Back to the future: targeting the extracellular matrix to treat systemic sclerosis. Nat Rev Rheumatol 2023;19:713–23. doi: 10.1038/s41584-023-01032-1.
[16] Santos A, Lagares D. Matrix stiffness: the conductor of organ fibrosis. Curr Rheumatol Rep 2018;20:2. doi: 10.1007/s11926-018-0710-z.
[17] Wang K, Wen D, Xu X, Zhao R, Jiang F, Yuan S, et al. Extracellular matrix stiffness-the central cue for skin fibrosis. Front Mol Biosci 2023;10:1132353. doi: 10.3389/fmolb.2023.1132353.
[18] Buechler MB, Pradhan RN, Krishnamurty AT, Cox C, Calviello AK, Wang AW, et al. Cross-tissue organization of the fibroblast lineage. Nature 2021;593:575–9. doi: 10.1038/s41586-021-03549-5.
[19] Rius Rigau A, Liang M, Devakumar V, Neelagar R, Matei AE, Györfi AH, et al. Imaging mass cytometry-based characterisation of fibroblast subsets and their cellular niches in systemic sclerosis. Ann Rheum Dis 2024 ard-2024-226336. doi: 10.1136/ard-2024-226336.
[20] Van Den Hoogen F, Khanna D, Fransen J, Johnson SR, Baron M, Tyndall A, et al. 2013 classification criteria for systemic sclerosis: an American College of Rheumatology/European League Against Rheumatism collaborative initiative. Arthritis Rheum 2013;65:2737–47. doi: 10.1002/art.38098.
[21] Doyle AD, Carvajal N, Jin A, Matsumoto K, Yamada KM. Local 3D matrix microenvironment regulates cell migration through spatiotemporal dynamics of contractility-dependent adhesions. Nat Commun 2015;6:8720. doi: 10.1038/ncomms9720.
[22] Schindelin J, Arganda-Carreras I, Frise E, Kaynig V, Longair M, Pietzsch T, et al. Fiji: an open-source platform for biological-image analysis. Nat Methods 2012;9:676–82. doi: 10.1038/nmeth.2019.
[23] Love MI, Huber W, Anders S. Moderated estimation of fold change and dispersion for RNA-seq data with DESeq2. Genome Biol 2014;15:550. doi: 10.1186/s13059-014-0550-8.
[24] Odell ID, Steach H, Gauld SB, Reinke-Breen L, Karman J, Carr TL, et al. Epiregulin is a dendritic cell–derived EGFR ligand that maintains skin and lung fibrosis. Sci Immunol 2022;7:eabq6691. doi: 10.1126/sciimmunol.abq6691.
[25] Chen K, Kwon SH, Henn D, Kuehlmann BA, Tevlin R, Bonham CA, et al. Disrupting biological sensors of force promotes tissue regeneration in large organisms. Nat Commun 2021;12:5256. doi: 10.1038/s41467-021-25410-z.
[26] Moon KR, van Dijk D, Wang Z, Gigante S, Burkhardt DB, Chen WS, et al. Visualizing structure and transitions in high-dimensional biological data. Nat Biotechnol 2019;37:1482–92. doi: 10.1038/s41587-019-0336-3.
[27] Street K, Risso D, Fletcher RB, Das D, Ngai J, Yosef N, et al. Slingshot: cell lineage and pseudotime inference for single-cell transcriptomics. BMC Genomics 2018;19:477. doi: 10.1186/s12864-018-4772-0.
[28] Morabito S, Reese F, Rahimzadeh N, Miyoshi E. Swarup V. hdWGCNA identifies co-expression networks in high-dimensional transcriptomics data. Cell Rep Methods 2023;3:100498. doi: 10.1016/j.crmeth.2023.100498.
[29] Zhao E, Stone MR, Ren X, Guenthoer J, Smythe KS, Pulliam T, et al. Spatial transcriptomics at subspot resolution with BayesSpace. Nat Biotechnol 2021;39:1375–84. doi: 10.1038/s41587-021-00935-2.
[30] Vahid MR, Brown EL, Steen CB, Zhang W, Jeon HS, Kang M, et al. High-resolution alignment of single-cell and spatial transcriptomes with CytoSPACE. Nat Biotechnol 2023;41:1543–8. doi: 10.1038/s41587-023-01697-9.
[31] Ortega-Ferreira C, Soret P, Robin G, Speca S, Hubert S, Le Gall M, et al. Antibody-mediated neutralization of galectin-3 as a strategy for the treatment of systemic sclerosis. Nat Commun 2023;14:5291. doi: 10.1038/s41467-023-41117-9.
[32] Margadant C, van den Bout I, van Boxtel AL, Thijssen VL, Sonnenberg A. Epigenetic regulation of galectin-3 expression by β1 integrins promotes cell adhesion and migration. J Biol Chem 2012;287:44684–93. doi: 10.1074/jbc.M112.426445.
[33] Peiró T, Alonso-Carpio M, Ribera P, Almudéver P, Roger I, Montero P, et al. Increased expression of galectin-3 in skin fibrosis: evidence from in vitro and in vivo studies. Int J Mol Sci 2022;23:15319. doi: 10.3390/ijms232315319.
[34] Jia D, Duan F, Peng P, Sun L, Liu X, Wang L, et al. Up-regulation of RACK1 by TGF-β1 promotes hepatic fibrosis in mice. PLoS One 2013;8:e60115. doi: 10.1371/journal.pone.0060115.
[35] Lee HS, Millward-Sadler SJ, Wright MO, Nuki G, Al-Jamal R, Salter DM. Activation of integrin—RACK1/PKCα signalling in human articular chondrocyte mechanotransduction. Osteoarthritis Cartilage 2002;10:890–7. doi: 10.1053/joca.2002.0842.

[36] Keen AN, Payne LA, Mehta V, Rice A, Simpson LJ, Pang KL, et al. Eukaryotic initiation factor 6 regulates mechanical responses in endothelial cells. J Cell Biol 2022;221:e202005213. doi: 10.1083/jcb.202005213.
[37] Bao Q, Wang A, Hong W, Wang Y, Li B, He L, et al. The c-Abl-RACK1-FAK signaling axis promotes renal fibrosis in mice through regulating fibroblast-myofibroblast transition. Cell Commun Signal 2024;22:247. doi: 10.1186/s12964-024-01603-z.
[38] Andreatta M, Carmona SJ. UCell: robust and scalable single-cell gene signature scoring. Comput Struct Biotechnol J 2021;19:3796–8. doi: 10.1016/j.csbj.2021.06.043.
[39] Xue D, Tabib T, Morse C, Yang Y, Domsic RT, Khanna D, et al. Expansion of Fcγ receptor iiia-positive macrophages, ficolin 1-positive monocyte-derived dendritic cells, and plasmacytoid dendritic cells associated with severe skin disease in systemic sclerosis. Arthritis Rheumatol 2022;74:329–41. doi: 10.1002/art.41813.
[40] Hutchins T, Sanyal A, Esencan D, Lafyatis R, Jacobe H, Torok KS. Characterization of endothelial cell subclusters in localized scleroderma skin with single-cell RNA sequencing identifies NOTCH signaling pathway. Int J Mol Sci 2024;25:10473. doi: 10.3390/ijms251910473.
[41] Woo S-H, Lukacs V, de Nooij JC, Zaytseva D, Criddle CR, Francisco A, et al. Piezo2 is the principal mechanotransduction channel for proprioception. Nat Neurosci 2015;18:1756–62. doi: 10.1038/nn.4162.
[42] Ranade SS, Woo S-H, Dubin AE, Moshourab RA, Wetzel C, Petrus M, et al. Piezo2 is the major transducer of mechanical forces for touch sensation in mice. Nature 2014;516:121–5. doi: 10.1038/nature13980.
[43] He J, Cheng X, Fang B, Shan S, Li Q. Mechanical stiffness promotes skin fibrosis via Piezo1-Wnt2/Wnt11-CCL24 positive feedback loop. Cell Death Dis 2024;15:84. doi: 10.1038/s41419-024-06466-3.
[44] He J, Fang B, Shan S, Xie Y, Wang C, Zhang Y, et al. Mechanical stretch promotes hypertrophic scar formation through mechanically activated cation channel Piezo1. Cell Death Dis 2021;12:226. doi: 10.1038/s41419-021-03481-6.
[45] Pu X, Zhu P, Zhou X, He Y, Wu H, Du L, et al. CD34+ cell atlas of main organs implicates its impact on fibrosis. Cell Mol Life Sci 2022;79:576. doi: 10.1007/s00018-022-04606-6.
[46] Gao Y, Li J, Cheng W, Diao T, Liu H, Bo Y, et al. Cross-tissue human fibroblast atlas reveals myofibroblast subtypes with distinct roles in immune modulation. Cancer Cell 2024;42:1764–1783.e10. doi: 10.1016/j.ccell.2024.08.020.
[47] Pokhilko A, Handel AE, Curion F, Volpato V, Whiteley ES, Bøstrand S, et al. Targeted single-cell RNA sequencing of transcription factors enhances the identification of cell types and trajectories. Genome Res 2021;31:1069–81. doi: 10.1101/gr.273961.120.
[48] Linderman GC, Zhao J, Roulis M, Bielecki P, Flavell RA, Nadler B, et al. Zero-preserving imputation of single-cell RNA-seq data. Nat Commun 2022;13:192. doi: 10.1038/s41467-021-27729-z.
[49] Dupont S, Morsut L, Aragona M, Enzo E, Giulitti S, Cordenonsi M, et al. Role of YAP/TAZ in mechanotransduction. Nature 2011;474:179–83. doi: 10.1038/nature10137.
[50] Farutin V, Kurtagic E, Pradines JR, Capila I, Mayes MD, Wu M, et al. Multiomic study of skin, peripheral blood, and serum: is serum proteome a reflection of disease process at the end-organ level in systemic sclerosis? Arthritis Res Ther 2021;23:259. doi: 10.1186/s13075-021-02633-5.

Ann Rheum Dis 84 (2025) 1877–1887

Contents lists available at ScienceDirect

Annals of the Rheumatic Diseases

journal homepage: https://www.sciencedirect.com/journal/annals-of-the-rheumatic-diseases

Vasculitis

A glossary of signs and symptoms of giant cell arteritis

Medha L. Soowamber[1], Milena Bond[2], Zahi Touma[3], Carol Langford[4], Catalina Sanchez-Alvarez[5], Andy Abril[6], Sibel Zehra Aydin[7], Frank Buttgereit[8], Dario Camellino[9], Maria C. Cid[10], Peter C. Grayson[11], Bernhard Hellmich[12], William Lichliter[13], Tanaz A. Kermani[14], Nader A. Khalidi[15], Sarah L. Mackie[16,17], Eric L. Matteson[18], Mehrdad Maz[19], Peter A. Merkel[20], Paul A. Monach[21], Lorna Neill[22], Cristina Ponte[23,24], Carlo Salvarani[25,26], Wolfgang A. Schmidt[27], Peter M. Villiger[28], Kenneth J. Warrington[29], Madeline Whitlock[30], Sofia Ramiro[31,32], Christian Dejaco[2,33,*]

[1] *Mount Sinai Hospital, Toronto, Ontario, Canada*
[2] *Department of Rheumatology, Hospital of Bruneck (ASAA-SABES), Teaching Hospital of the Paracelsius Medical University, Brunico, Italy*
[3] *Schroeder Arthritis Institute, Krembil Research Institute, University Health Network, University of Toronto, Toronto, Ontario, Canada*
[4] *Department of Rheumatic and Immunologic Diseases, Cleveland Clinic, Cleveland, Ohio, USA*
[5] *Division of Rheumatology, Mayo Clinic, Rochester MN, USA and courtesy appointment at the Division of Rheumatology, University of Florida, Gainesville, FL, USA*
[6] *Rheumatology, Mayo Clinic, Jacksonville, FL, USA*
[7] *Rheumatology, University of Ottawa Faculty of Medicine, Ottawa Hospital Research Institute, Ottawa, ON, Canada*
[8] *Department of Rheumatology and Clinical Immunology, Charité Universitätsmedizin Berlin, Berlin, Germany*
[9] *Division of Rheumatology, "La Colletta" Hospital, Azienda Sanitaria Locale 3 Genovese, Arenzano, Italy*
[10] *Department of Autoimmune Diseases, Hospital Clínic, University of Barcelona, Institut d'Investigacions Biomèdiques August Pi i Sunyer (IDIBAPS), Barcelona, Spain*
[11] *National Institutes of Health/NIAMS, Bethesda, MD, USA*
[12] *Department of Internal Medicine, Rheumatology, Pulmonology, Nephrology and Diabetology, Medius Kliniken Kirchheim/Teck, University Tübingen, Kirchheim-Teck, Germany*
[13] *Patient, Vienna, Austria*
[14] *Rheumatology, David Geffen School of Medicine, University of California, Los Angeles, CA, USA*
[15] *St. Joseph's Healthcare Hamilton, McMaster University, Hamilton, Canada*
[16] *Leeds Institute of Rheumatic and Musculoskeletal Medicine, University of Leeds, Leeds, UK*
[17] *Leeds Biomedical Research Centre, Leeds Teaching Hospitals NHS Trust, Leeds, UK*
[18] *Division of Rheumatology, Mayo Clinic College of Medicine and Science, Rochester, MN, USA*
[19] *Division of Allergy, Clinical Immunology, and Rheumatology, Department of Medicine, University of Kansas Medical Center, Kansas City, KS, USA*
[20] *Division of Rheumatology, Department of Medicine, Division of Epidemiology, Department of Biostatistics, Epidemiology, and Informatics, University of Pennsylvania, Philadelphia, PA, USA*
[21] *VA Boston Healthcare System, Boston, MA*
[22] *A trustee of the Scottish Charitable Incorporated Organisation, PMR-GCA Scotland, Nethy Bridge, UK*
[23] *Rheumatology, Unidade Local de Saúde de Santa Maria, Lisbon, Portugal*
[24] *Rheumatology Research Unit, Instituto de Medicina Molecular, Faculdade de Medicina, Universidade de Lisboa, Lisbon, Portugal*

*Correspondence to Dr. Christian Dejaco.
E-mail address: christian.dejaco@gmx.net (C. Dejaco).
Handling editor Josef S. Smolen.

https://doi.org/10.1016/j.ard.2025.06.2126

[25] *Unit of Rheumatology, Azienda Unità Sanitaria Locale-IRCCS, Reggio Emilia, Italy*
[26] *Department of Surgery, Medicine, Dentistry and Morphological Sciences with Interest in Transplant, Oncology and Regenerative Medicine, University of Modena and Reggio Emilia, Modena, Italy*
[27] *Rheumatology, Immanuel Krankenhaus Berlin, Berlin-Buch, Berlin, Germany*
[28] *Rheumatology and Clinical Immunology, Medical Center Monbijou, Bern, Switzerland*
[29] *Division of Rheumatology, Department of Medicine, Mayo Clinic, Rochester, MN, USA*
[30] *Rheumatology, Southend University Hospital, Southend, UK*
[31] *Department of Rheumatology, Leiden University Medical Center, The Netherlands*
[32] *Department of Rheumatology, Zuyderland Medical Center, The Netherlands*
[33] *Department of Rheumatology, Medical University of Graz, Graz, Austria*

ARTICLE INFO

Article history:
Received 30 March 2025
Received in revised form 12 June 2025
Accepted 14 June 2025

ABSTRACT

Objectives: This study seeks to create consensus-based definitions of signs and symptoms of giant cell arteritis (GCA) for use by health care professionals, primarily in research settings.
Methods: Core definitions of signs and symptoms of GCA were extracted from 11 randomised controlled trials of GCA previously reviewed in a systematic literature review conducted in the context of the development of response criteria for GCA. This information was supplemented by definitions from other sources, such as rheumatology textbooks. A 2-round Delphi was performed within an international task force (32 members from 11 countries). The first round aimed to obtain consensus on the descriptive terms defining each sign or symptom, and round 2 rated the importance of these terms. Based on the Delphi study method, preliminary definitions were developed. In 4 online meetings, results of the Delphi were reviewed, and a consensus was achieved on final definitions.
Results: Twenty-nine signs and symptoms of GCA were reviewed. Six signs or symptoms of GCA had previously been defined in the literature. A high level of agreement was reached on the definition of 23 signs and symptoms with the following 12 considered characteristic of GCA: headache, temporal artery abnormalities, scalp tenderness, scalp necrosis, jaw claudication, tongue claudication, tongue necrosis, amaurosis fugax, permanent vision loss, fever, limb claudication, and blood pressure inequality.
Conclusions: A glossary of definitions for 23 signs and symptoms of GCA was developed through a consensus process involving international experts.

WHAT IS ALREADY KNOWN ON THIS TOPIC

- The paucity of standardised definitions for clinical manifestations of giant cell arteritis (GCA) leads to variable interpretations in research settings. Thus, there is an unmet need to establish uniform definitions of signs and symptoms of GCA to ensure standardised patient enrolment into clinical trials and characterisation of patients in clinical studies.

WHAT THIS STUDY ADDS

- This study defined 23 signs and symptoms of GCA. Of these, 12 were considered characteristic of GCA and are as follows: headache, temporal artery abnormalities, scalp tenderness, scalp necrosis, jaw claudication, tongue claudication, tongue necrosis, amaurosis fugax, permanent vision loss, fever, limb claudication, and blood pressure inequality.

HOW THIS STUDY MIGHT AFFECT RESEARCH, PRACTICE OR POLICY

- These 23 definitions can complement inclusion criteria in clinical trials and other clinical studies, allow precise application of classification criteria, and lay the groundwork for developing response criteria for GCA.

INTRODUCTION

Giant cell arteritis (GCA) is a large vessel vasculitis and the most common form of vasculitis in adults over the age of 50 [1,2]. There are no standardised definitions of the clinical manifestations of GCA in the literature. Classification criteria related manuscripts usually include definitions of individual parameters (for example, classification criteria for spondyloarthritis), whereas the classification criteria for GCA do not comprehensively include definitions for all signs and symptoms [3–5]. This lack of standardised definitions might lead to inconsistency in application in research settings. Furthermore, the diagnostic and therapeutic landscapes of GCA are rapidly expanding [6,7]. Inconsistent definitions of GCA features hinder the validity of the data and the inclusion of a homogeneous group of patients into clinical trials, thereby affecting the results and limiting the comparability of studies.

An international task force supported by the European Alliance of Associations for Rheumatology (EULAR) and the American College of Rheumatology (ACR) was established to develop response criteria for GCA. For the development of these criteria, a multistep approach is followed that includes but is not limited to a systematic literature review and a Delphi exercise to evaluate candidate descriptors in the response criteria [8]. During the Delphi, features of GCA (for example, jaw claudication) were defined to allow consistent interpretation when doing this exercise. While defining those signs and symptoms of GCA, it was noted that there were no standardised definitions in the literature. Therefore, it was decided to create a glossary of signs and symptoms of GCA. This glossary is intended to be used in research settings by health care professionals as a resource to facilitate the recruitment of patients into clinical trials by standardising the definitions of commonly used features of GCA.

METHODS

Initial development of the definitions of signs and symptoms of GCA

An international task force endorsed by EULAR and ACR to develop new response criteria for GCA conducted the current glossary project [8]. The 32 task force members consisted of 28 rheumatologists, 1 internist, 1 health professional in rheumatology, and 2 patient research partners from 11 countries (Austria, Canada, France, Germany, Italy, Netherlands, Portugal, Spain, Switzerland, United States of America, United Kingdom).

Two patient research partners were involved in each step of this study including but not limited to the Delphi study and consensus meetings.

Seven members (CAL, CD, ZT, SR, MS, MB, and CS-A) formed the Steering Committee, 3 of which are fellows (MS, MB, and CS-A). Using the systematic literature review (SLR) conducted in the context of the response criteria for GCA project as a basis, the fellows extracted definitions of the signs and symptoms of GCA from 11 randomised controlled trials (RCTs) (Supplementary Table S1) [8]. To ensure comprehensiveness, this information was supplemented by definitions from other sources, including rheumatology textbooks [9–11], the 2022 ACR/EULAR classification criteria for GCA [4], the ACR 1990 classification criteria for GCA [12], and a Delphi exercise prepared as part of the GCA response criteria project (which was different from the Delphi described below) (Fig).

For each sign and symptom of GCA, keywords or features (termed 'descriptors' in this paper) were extracted from each definition (for example, 'new onset') by 2 of the fellows (MS and MB). Descriptors that were frequently mentioned in the above sources (for example, 'new onset,' was mentioned in most RCTs) were incorporated into the potential new definition, whereas the other descriptors that were infrequently mentioned were kept as potential options. A model was created with a basic phrase that includes the common descriptors of the signs and symptoms of GCA that cannot be changed and several descriptors that can be added to make the definition comprehensive (Supplementary Fig S1). The information retrieved during this step was used as a basis for the subsequent Delphi exercise.

Delphi

The preliminary descriptors for each sign and symptom of GCA were refined via a 2-round Delphi performed among the task force members.

During round 1, participants were asked to select the descriptors that most appropriately matched each feature of GCA. Participants were also allowed to propose new descriptors.

Any descriptive term with ≥70% consensus was added to the definition of the respective sign/ symptom. Descriptors with <30% agreement were excluded. Descriptors with 30% to 70% agreement were reassessed in a second Delphi survey. The goal of round 2 was to rate the importance of the descriptors that most appropriately matched the features of GCA. The rating was as follows: 0–3 = not important, 4–6 = important, and 7–9 = critically important (Supplementary Fig S2).

Based on the results of the 2 Delphi rounds, a preliminary definition of each feature of GCA was developed by the Steering Committee as follows: those descriptors rated as critically important by ≥70% of participants were included in the preliminary definition. The rest of the descriptors were shown to task force members during subsequent meetings (below). The preliminary definitions were discussed and refined by the Steering Committee via e-mail and in online meetings until a final proposal was achieved, which was then presented to the task force.

Based on the Delphi results, the Steering Committee identified fundamental overarching principles essential for contextualising and interpreting the definitions of the features of GCA. These were also proposed to task force members.

Consensus meetings

The results of the Delphi exercise and preliminary definitions were presented to the task force members during 4 online meetings (Supplementary Fig S3).

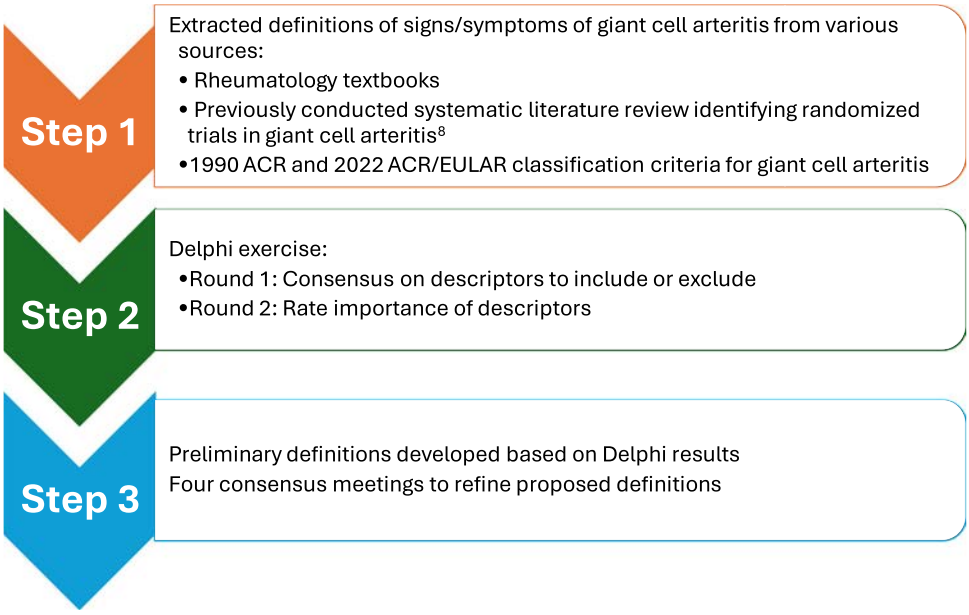

Figure. Flow chart of the study process. The steps taken to develop the glossary of signs and symptoms of giant cell arteritis. ACR, American College of Rheumatology; EULAR, European Alliance of Associations for Rheumatology.

During the meetings, task force members discussed the Delphi results and the proposed definitions. Consensus among task force members was achieved through an online live voting process. Agreement was reached if at least 70% of participants concurred on a definition. If consensus was not achieved, the definition under consideration was rediscussed. In the second round, consensus was accepted if >67% of the members voted in favour of the revised definition, and in the third round, >50% was accepted.

Finally, each task force member anonymously indicated the level of agreement (LoA) via an online survey (LoA, 0–10 numeric rating scale with 0 = do not agree and 10 = fully agree). The mean and SD of the LoA, as well as the percentage of task force members with an agreement ≥8, are presented.

RESULTS

A total of 29 out of 32 (92%) and 27 out of 32 (84%) task force members participated in rounds 1 and 2 of the Delphi exercise, respectively. Attendance by members at online meetings was >75% (meeting 1, 81%; meeting 2, 87%; meeting 3, 87%; meeting 4, 78%).

Overarching principles and definitions of signs/symptoms of GCA

The task force formulated 2 overarching principles forming a framework for all the definitions of signs and symptoms of GCA (Table 1).

Twenty-nine items were reviewed. Four were not defined (polymyalgia rheumatica [13], stroke [14], transient ischaemic attack [15], and myocardial infarction [16]) because they are clinical diagnoses with established definitions in the literature. Similarly, 2 other signs or symptoms (digital ulcers [17] and fatigue [18]) were not defined due to their accepted definitions in the literature. During online meetings, out of the 23 signs and symptoms left to define, 12 were considered characteristic for GCA, whereas 11 were regarded as self-explanatory or not highly specific for GCA. Three online meetings were dedicated to defining those 12 signs and symptoms of GCA, and 1 online meeting was used for the remaining 11 signs and symptoms.

The 12 signs and symptoms of GCA with their definitions are listed in Table 1 (including LoA) and discussed below. All statements obtained a high LoA, ranging from 8.7 to 9.9. The remaining 11 definitions of the symptoms considered self-explanatory or not highly specific for GCA are reported in Table 2 (including LoA), whereas the respective discussion points are included in Supplementary Table S2.

Overarching principles

Overarching principle 1: All the definitions from this glossary refer to signs or symptoms not better explained by other clinical conditions (that is, they are primarily attributed to GCA)

The first principle emphasises that the definitions provided in the glossary are specifically tailored to recognise signs or symptoms of GCA. This principle clarifies that these definitions are most relevant when other clinical conditions cannot better explain the symptoms, ensuring that the focus remains on identifying GCA-related signs and symptoms.

All signs or symptoms described generally represent a new occurrence (ie, not chronic). Additionally, signs and symptoms that self-resolve or resolve with conventional treatments (eg, headache responding to acetaminophen) are generally not attributable to GCA.

Table 1
Overarching principles and definitions of 12 signs and symptoms of giant cell arteritis

Overarching principles		**LoA (0–10) Mean (SD)**	**% with LoA ≥8**
1.	All the definitions from this glossary refer to signs or symptoms not better explained by other clinical conditions (that is, they are primarily attributed to GCA).	9.8 (0.5)	100
2.	The glossary should not serve to prevent patients who do not completely fit these definitions from receiving the necessary diagnostic procedures or therapies.	9.9 (0.4)	100
Signs or symptoms of GCA	**Definitions**		
Headache	New-onset pain localised to the head, not typical of headaches the patient previously experienced. The pain is usually persistent, continuous, and not easily alleviated by analgesics.	9.4 (0.8)	96.4
Temporal artery abnormalities	Any of the following features of a temporal artery: thick, firm, tender, or with a diminished or absent pulse.	9.6 (0.6)	100
Scalp tenderness	Pain/discomfort on touching the scalp, occurring on one or both sides, often elicited by brushing or combing hair.	9.7 (0.5)	100
Scalp necrosis	Ischaemic damage to the scalp marked by altered colour and compromised integrity of the skin.	9.5 (0.8)	96.4
Jaw claudication	Pain, fatigue, or discomfort in jaw muscles occurring when chewing and resolving shortly after chewing stops.	9.6 (0.7)	100
Tongue claudication	Pain, fatigue, or discomfort in the tongue when chewing or talking that resolves after chewing or talking stops.	9.5 (0.8)	100
Tongue necrosis	Ischaemic damage to the tongue marked by altered colour and compromised integrity of the mucosa.	9.3 (1.0)	92.9
Amaurosis fugax	Transient loss of vision in one or both eyes, without associated ocular pain, that is usually sudden and resolves within minutes or rarely hours.	9.3 (1.09)	96.4
Permanent loss of vision	Sudden and irreversible, partial, or complete, loss of sight in one or both eyes.	9.7 (0.6)	100
Fever	Temperature ≥38°C (100.4°F).	8.7 (1.6)	78.6
Limb claudication	Pain, fatigue, or discomfort in limb muscles that occurs with use and is relieved by rest.	9.17 (1.5)	89.3
Blood pressure inequality	A difference of ≥20 mm Hg in systolic blood pressure between contralateral limbs.	9.4 (0.9)	92.9

GCA, giant cell arteritis; LoA, level of agreement.
Numbers in the columns 'LoA' indicate the mean and SD (in parenthesis) of the LoA (assessed on a scale from 0 = no agreement to 10 = full agreement), and the proportion of task force members with a score of at least 8/10.

Table 2
Definitions of 11 additional signs and symptoms of giant cell arteritis

Additional signs or symptoms of GCA	Definitions	LoA (0–10) Mean (SD)	% with LoA ≥8
Abdominal angina	Recurrent pain or discomfort in the abdomen, usually occurring or worsening after eating, considered due to vascular insufficiency.	9.3 (1.1)	89.3
Anorexia	Diminished desire to eat.	9.2 (1.4)	89.3
Blurry vision	A visual disturbance in which objects appear unclear, making it difficult to see things sharply. *Typically sudden in onset.*	9.3 (1.3)	92.9
Carotidynia	Pain or tenderness over one or both carotid arteries.	9.8 (0.5)	100
Diplopia	Transient or persistent visual disturbance in which an object is seen partially or fully in duplicate.	9.6 (0.7)	96.4
Dry cough	A type of cough not accompanied by expectorated phlegm, mucus or blood.	9.6 (0.8)	96.4
Hearing loss	Partial or complete inability to hear sounds in one or both ears. *Typically rapidly progressive.*	9.1 (1.2)	92.9
Odynophagia	Pain or discomfort with swallowing.	9.7 (0.7)	100
Peripheral arthralgia	Pain or discomfort in the joints of the extremities.	9.3 (1.4)	92.9
Pulse abnormalities	Pulse that is difficult to detect or feels faint when palpating arteries in the extremities.	9.0 (1.2)	89.3
Weight loss	Reduction of body weight of at least 5%.	8.4 (2.4)	78.6

GCA, giant cell arteritis; LoA, level of agreement.
Numbers in the columns 'LoA' indicate the mean and SD (in parenthesis) of the LoA (assessed on a scale from 0 = no agreement to 10 = full agreement), and the proportion of task force members with a score of at least 8/10.

Overarching principle 2: The glossary should not serve to prevent patients who do not completely fit these definitions from receiving necessary diagnostic procedures or therapies

The second principle ensures that the glossary definitions do not hinder access to appropriate diagnostic procedures and treatment for patients whose symptoms may not fully align with the defined signs or symptoms. This principle acknowledges the variability in how diseases present and emphasises the importance of clinical flexibility and discretion. It underlines that the glossary serves as a guide, mainly for research, advocating for comprehensive patient care regardless of predefined signs or symptoms.

Definitions of signs and symptoms of GCA

Headache

Definition: New-onset pain localised to the head, not typical of headaches the patient previously experienced. The pain is usually persistent, continuous, and not easily alleviated by analgesics.

The concepts of new-onset (previously not experienced by the patient) and atypical headache were commonly noted for patients included in clinical trials [19–24] as well as in the ACR 1990 classification criteria for GCA [12]. However, aside from a few research papers [21,23], the medical literature offered limited additional information to further characterise a GCA-related headache. These 2 concepts were thus included in the initial potential headache definition and other descriptors extracted from the literature and textbooks were added as options for the task force members to choose from (Supplementary Fig S1).

Task force members agreed that the definition should aim to characterise the type of headache that makes a health care provider concerned about GCA rather than defining any type of headache. The headache definition had to strike a balance between avoiding oversimplification akin to other headache definitions and not being overly restrictive, which can limit inclusion of patients in clinical trials; it should thus provide some flexibility.

In contrast to the International Headache Society definition of GCA-related headache [25], which emphasises the inclusion of other symptoms of GCA (eg, scalp tenderness), it was decided that such an association should not be incorporated in the definition. The task force was reluctant to combine different features of GCA into a single definition, maintaining a distinct concept of GCA-related headache specifically for research purposes and independent of the presence of other symptoms of GCA.

The appropriateness of including a specification regarding headache characteristics such as inflammation (eg, heightened intensity during the night or in the early morning) was also discussed. However, to maintain broad inclusivity, it was decided to omit such specifications due to the heterogeneous nature of headaches across patients and disease courses.

There was a debate about whether to include the lack of response to treatment (ie, no or little improvement of headache by analgesics) as there might be a subgroup of patients who do not, or cannot, take analgesics. The addition of the adverbs 'usually' and 'not easily' in the definition was intended to accommodate such exceptions, whereas the definition also aimed to include descriptors typically associated with a GCA-related headache, such as 'persistent' and 'continuous'. Although new onset is mentioned, the task force agreed that the definition can also be extended to a patient who is relapsing if the character of headache is referencing to the initial presentation of GCA.

Temporal artery abnormalities

Definition: Any of the following features of a temporal artery: thick, firm, tender, or with a diminished or absent pulse.

Distinct features of temporal artery abnormalities that were agreed upon include thickness, firmness, tenderness and a diminished or absent pulse. Tenderness is pain elicited by touching the temporal artery. When discussing the difference between thickness and firmness, thickness was felt to incorporate the concept of being dense and not completely compressible, while firmness would be synonymous to hard or cord-like. 'Any' was intentionally added to have the flexibility of only having 1 abnormality, such as diminished pulse, and therefore increase sensitivity. However, the more abnormalities that are present, the higher the likelihood of being related to GCA. Particular care was taken in the wording of pulse palpation: 'absent pulse' was chosen to convey a lack of prior knowledge regarding the temporal artery's condition in contrast to 'loss of pulse', which implies previous awareness. The interpretation of the temporal artery pulse should be considered in the absence of a prior temporal artery biopsy, as the latter may alter the pulse characteristics. When assessing the temporal artery for signs of GCA, the

examiner should have adequate experience with the anatomy of the temporal artery and with GCA to ensure that the appropriate amount of pressure is applied for evaluating tenderness, firmness, and pulse characteristics. The task force did not include bruits as a possible abnormality of the temporal artery because auscultation of this artery is rarely conducted in clinical practice and has not been mentioned as a possible descriptor in the literature (in contrast to bruits of extracranial arteries to indicate vessel stenosis).

Scalp tenderness

Definition: Pain/discomfort on touching the scalp, occurring on one or both sides, often elicited by brushing or combing hair.

The term 'discomfort' was introduced as an option to encompass nuances related to tenderness when touching the scalp, ranging from mild discomfort to pain. Hyperesthesia was also discussed but finally not added, as the task force believed that pain/discomfort touching the scalp catches the essence of the definition. The definition included the adjective 'often' to allow room for exceptions. Similar to the discussion on temporal artery abnormalities, interpretation should be considered in the absence of a prior temporal artery biopsy.

Scalp necrosis

Definition: Ischaemic damage to the scalp marked by altered colour and compromised integrity of the skin.

There was initial discussion on whether it should be defined given it is such a rare occurrence but on the other hand, it is a very specific feature of GCA and was thus included [26]. Ischaemia means diminished or absent blood flow. Gangrene, a possible consequence of ischaemia was initially included in the definition of scalp necrosis but ultimately omitted, given its definition is restricted to the end-stage result of an ischaemic process. The term 'ischaemic damage' provides greater flexibility in the definition given that it encompasses altered colour and integrity of the skin, as well as gangrene. The task force also emphasised that a change of colour alone is not enough for this process of ischaemic damage to happen. Usually, the subcutaneous tissue also undergoes damage. It would be exceptional that necrosis occurred without also damaging the skin.

Jaw claudication

Definition: Pain, fatigue, or discomfort in jaw muscles occurring when chewing and resolving shortly after chewing stops.

The challenge was formulating a definition that effectively differentiated jaw claudication from other pathologies such as temporomandibular joint disorders. The task force agreed that the essence of the definition is that jaw claudication happens with prolonged (usually minutes) chewing and resolves once chewing stops. It does not typically occur with the first bites or with the initiation of chewing. The task force decided against including the word 'prolonged' into the definition given that its interpretation could be heterogenous with no specific cut-off in the literature. Discussing the meaning of 'prolonged' as part of the definition would introduce substantial complexity. It is important to note that GCA patients can express several jaw-related symptoms, but jaw claudication was chosen to be defined given its high diagnostic specificity [27]. Jaw muscle was added rather than simply jaw to emphasise that this phenomenon happens in the muscles of mastication and not elsewhere. Fatigue and discomfort were added to the definition because jaw claudication is not always perceived as pain by patients.

Tongue claudication

Definition: Pain, fatigue, or discomfort in the tongue when chewing or talking, that resolves after chewing or talking stops.

The task force aimed for this definition to align with the same conceptual framework as that of jaw claudication. Therefore, the essence of the meaning of claudication was kept, where the tongue pain, fatigue, or discomfort happens with activity (chewing or talking) and resolves once the activity stops.

Tongue necrosis

Definition: Ischaemic damage to the tongue marked by altered colour and compromised integrity of the mucosa.

The task force wanted this definition to mirror the same underlying principles as that of scalp necrosis. The fundamental concept of necrosis was maintained by utilising the phrase 'ischaemic damage' characterised by changes in colour and compromised mucosal integrity.

Amaurosis fugax

Definition: Transient loss of vision in one or both eyes, without associated ocular pain, that is usually sudden and resolves within minutes or rarely hours.

In defining amaurosis fugax, the task force advocated for inclusivity by specifying that this GCA feature can involve one or both eyes. Although predominantly unilateral, the less frequent bilateral presentation was retained for the benefit of a larger audience, aiming to be as inclusive as possible when recruiting patients for trials. The central debate revolved around the necessity of explicitly specifying the painlessness of vision loss itself. Cranial GCA is typically characterised by a headache, amaurosis fugax, and painless loss of vision in general (ie, patients do not experience any pain in the eye) [28]. Moreover, the task force wanted to highlight another crucial characteristic of this symptom, which is its reversibility in a short time frame in most cases [28]. However, for the sake of inclusiveness, the rare circumstance where amaurosis resolves within hours is also reported in the definition.

Permanent vision loss

Definition: Sudden and irreversible, partial or complete, loss of sight in one or both eyes.

The task force advocated for the explicit inclusion of the sudden onset and irreversibility of this feature. Vision loss in GCA is an ischaemic complication occurring in 15% to 35% of patients, almost exclusively before the start of treatment with glucocorticoids, and it may be preceded by amaurosis fugax but may also occur as the first manifestation of disease [28–30]. Visual loss encompasses a wide spectrum of visual impairment. Although some individuals may notice specific areas of visual defects, such as blind spots or scotomas, affecting their ability to perceive objects in certain areas of their visual field, others may suffer more severe impairment or blindness, importantly impacting their daily activities and quality of life [31]. Most task force members argued against the necessity of specifying the ischaemic cause in the definition, contending that the assumption of relevance to GCA covers all potential causes, as specified in the overarching principles.

Fever

Definition: Temperature of ≥38°C (100.4°F).

There was extensive discussion about whether this term warranted definition, as a few task force members deemed it self-explanatory. Although fever is defined by the Centers for Disease Control and Prevention (CDC) as measured temperature of

≥38°C [32], some experts expressed concerns that a proportion of patients with GCA may have a temperature that is only slightly higher than their baseline body temperature yet abnormal for that patient and that these low-grade temperatures might differ between individuals.

To capture the concept of low-grade fever, proposals discussed were 2 above-normal measurements or an elevation of at least 0.5°C above the patient's usual baseline temperature. The debate extended to whether patients are even aware of their normal temperature and whether they regularly measure it. However, no agreement on these aspects was reached. The minimum consensus among the task force was, therefore, to adopt the definition of fever used by the CDC as a temperature of ≥38°C and not to formulate a definition for low-grade fever. Nevertheless, all task force members acknowledged that a patient with active GCA may have a body temperature that is slightly higher than their usual baseline but not exceeding 38°C. Finally, fever in GCA is typically not relapsing and remitting, but generally persistent.

Limb claudication

Definition: Pain, fatigue, or discomfort in limb muscles that occurs with use and is relieved by rest.

Limb claudication occurs in patients with extracranial vessel involvement may affect upper and lower limbs, and symptoms may vary from mild to severe based on the degree of vascular involvement and concomitant factors, such as (pre-existent) atherosclerosis, heart failure, or anaemia. The reported definition emphasises the muscular site of the symptoms and notes that limb claudication is typically triggered by prolonged movements (of at least several seconds to minutes) and rapidly reverses with rest. These characteristics help distinguish it from other non-ischaemic conditions such as osteoarthritis, muscle injury, or tendinopathy.

Blood pressure inequality

Definition: A difference of ≥20 mm Hg in systolic blood pressure between contralateral limbs.

Although the task force voted for a ≥20 mm Hg difference in systolic blood pressure between contralateral limbs, respective cut-offs varied markedly in the literature [33–35]. This choice of the task force was influenced by the recently published classification criteria for Takayasu arteritis, which proposed the same cut-off for blood pressure difference [36]. In GCA, such inequality in blood pressure is usually observed in the upper extremities. The task force also stressed the importance of clarifying that the comparison of blood pressures should be between the 2 upper or the 2 lower limbs, not between 1 upper and 1 lower limb. Finally, accurate measurement of blood pressure is key, and guidelines on proper blood pressure measurements (for example, the American College of Cardiology and American Heart Association guidelines on blood pressure measurement [37]) should be followed.

DISCUSSION

To the authors' knowledge, this glossary reflects the first collaborative effort to establish comprehensive definitions for fundamental symptoms and signs of GCA. The task force agreed on 23 definitions for a more precise application of classification criteria and outcome assessments in clinical trials, including remission, relapse, and response to treatment. Despite these definitions being consensus based, there was substantial agreement among both experts and patient representatives.

No definition alone is assumed to possess the requisite sensitivity and specificity to diagnose a patient with GCA in clinical practice. Instead, these definitions are intended to be incorporated in inclusion criteria for research studies, standardise the application of classification criteria (even though this effort was not part of the classification criteria project), and serve as a basis for the development of the new criteria for response to treatment in GCA. Although not primarily intended for use in clinical practice, these definitions and the detailed accompanying qualifying discussions by the task force members provide useful information about the nuances of clinical features commonly associated with GCA to health care providers who may have less experience with this disease.

Obtaining clarity and homogeneity of definitions has been an exercise performed by several groups to facilitate the development of classification criteria in the field of rheumatology. For example, the third phase of the development of the classification criteria for systemic lupus erythematosus was dedicated to an in-depth examination and refinement of definitions [38]. Similarly, a glossary of definitions was incorporated in several classification criteria (eg, spondyloarthritis) to improve the validity and reliability of the final classification system [3,5]. Previous definitions were mostly based on literature review and consensus by the working group, whereas this GCA glossary included multiple rounds of refinement through iterative processes, encompassing 2 Delphi rounds and 4 consensus meetings of an international task force. In contrast to classification criteria, however, this glossary for GCA concentrated solely on clinical signs and symptoms as definitions of imaging and biopsy findings in GCA have already been described.

One potential limitation of this study is the lack of comprehensive definitions in the literature for certain signs and symptoms of GCA (eg, limb claudication), whereas several definitions are available for other features (eg, headache). Consequently, the absence of initial components could have hindered the definition-building process. Therefore, a few definitions were proposed and discussed by the task force members based on clinical expertise (eg, tongue necrosis). Another limitation of this study is that the generation of definitions was based on a SLR focused on RCTs measuring treatment response and disease activity changes in GCA. Although a dedicated SLR would have been appropriate, the task force believed it would be redundant because all relevant GCA trials had already been identified [19–24,39–43]. Because RCTs include descriptions of GCA signs and symptoms as part of the inclusion criteria, they were considered the most important data source. To enhance completeness for the generation of definitions, multiple resources, including GCA classification criteria, were also incorporated.

In conclusion, an international group of specialists in GCA formulated a glossary of definitions for 23 signs and symptoms occurring in GCA using a consensus process. These definitions are designed for research purposes. Applying these definitions should facilitate uniform characterisation of the features of GCA and harmonise the patient populations enrolled into clinical trials in GCA and outcome assessment.

CRediT authorship contribution statement

Medha L. Soowamber: Writing – review & editing, Writing – original draft, Methodology, Formal analysis, Data curation, Conceptualization. **Milena Bond:** Writing – original draft, Data curation, Conceptualization. **Zahi Touma:** Writing – review & editing, Supervision, Methodology, Conceptualization. **Carol Langford:** Writing – review & editing, Supervision,

Methodology, Conceptualization. **Catalina Sanchez-Alvarez:** Writing – review & editing, Conceptualization. **Andy Abril:** Writing – review & editing. **Sibel Zehra Aydin:** Writing – review & editing. **Frank Buttgereit:** Writing – review & editing. **Dario Camellino:** Writing – review & editing. **Maria C. Cid:** Writing – review & editing. **Peter C. Grayson:** Writing – review & editing. **Bernhard Hellmich:** Writing – review & editing. **William Lichliter:** Writing – review & editing. **Tanaz A. Kermani:** Writing – review & editing. **Nader A. Khalidi:** Writing – review & editing. **Sarah L. Mackie:** Writing – review & editing. **Eric L. Matteson:** Writing – review & editing. **Mehrdad Maz:** Writing – review & editing. **Peter A. Merkel:** Writing – review & editing. **Paul A. Monach:** Writing – review & editing. **Lorna Neill:** Writing – review & editing. **Cristina Ponte:** Writing – review & editing. **Carlo Salvarani:** Writing – review & editing. **Wolfgang A. Schmidt:** Writing – review & editing. **Peter M. Villiger:** Writing – review & editing. **Kenneth J. Warrington:** Writing – review & editing. **Madeline Whitlock:** Writing – review & editing. **Sofia Ramiro:** Writing – review & editing, Supervision, Methodology, Formal analysis, Conceptualization. **Christian Dejaco:** Writing – review & editing, Supervision, Methodology, Formal analysis, Data curation, Conceptualization.

Acknowledgements

The authors would like to thank Drs A. Mahr and B. Dasgupta for their contributions during the Delphi phase of the project.

Funding

This research did not receive any specific grant from funding agencies in the public, commercial, or not-for-profit sectors.

Competing interests

Medha Soowamber reports a relationship with AbbVie Inc that includes: consulting or advisory and speaking and lecture fees. Medha Soowamber reports a relationship with Fresenius Kabi Canada Ltd that includes: speaking and lecture fees. Medha Soowamber reports a relationship with Boehringer Ingelheim that includes: funding grants. Milena Bond reports a relationship with AbbVie Inc that includes: consulting or advisory and travel reimbursement. Milena Bond reports a relationship with Novartis Pharmaceuticals that includes: travel reimbursement. Milena Bond reports a relationship with Galapagos NV that includes: travel reimbursement. Carol Langford reports a relationship with Bristol Myers Squibb Co that includes: funding grants. Carol Langford reports a relationship with AstraZeneca Pharmaceuticals LP that includes: funding grants. Carol Langford reports a relationship with GlaxoSmithKline Inc that includes: funding grants. Sibel Aydin reports a relationship with AbbVie Inc that includes: consulting or advisory, funding grants, and speaking and lecture fees. Sibel Aydin reports a relationship with Eli Lilly and Company that includes: consulting or advisory, funding grants, and speaking and lecture fees. Sibel Aydin reports a relationship with Janssen Pharmaceuticals Inc that includes: consulting or advisory, funding grants, and speaking and lecture fees. Sibel Aydin reports a relationship with Novartis Pharmaceuticals Corporation that includes: consulting or advisory, funding grants, and speaking and lecture fees. Sibel Aydin reports a relationship with Pfizer Inc that includes: consulting or advisory, funding grants, and speaking and lecture fees. Sibel Aydin reports a relationship with UCB Inc that includes: consulting or advisory, funding grants, and speaking and lecture fees. Frank Buttgereit reports a relationship with Novartis that includes: consulting or advisory and speaking and lecture fees. Frank Buttgereit reports a relationship with Sanofi that includes: consulting or advisory and speaking and lecture fees. Frank Buttgereit reports a relationship with AbbVie Inc that includes: speaking and lecture fees and travel reimbursement. Frank Buttgereit reports a relationship with Pfizer Inc that includes: travel reimbursement. Dario Camellino reports a relationship with Boehringer Ingelheim GmbH that includes: consulting or advisory. Dario Camellino reports a relationship with AstraZeneca that includes: consulting or advisory. Dario Camellino reports a relationship with Janssen Pharmaceuticals Inc that includes: consulting or advisory. Dario Camellino reports a relationship with Abiogen Pharma SpA that includes: speaking and lecture fees. Dario Camellino reports a relationship with GSK that includes: speaking and lecture fees and travel reimbursement. Dario Camellino reports a relationship with UCB Inc that includes: travel reimbursement. Maria C Cid reports a relationship with Ministerio de Ciencia, Innovación y Universidades that includes: funding grants. Maria C Cid reports a relationship with AbbVie Inc that includes: board membership and consulting or advisory. Maria C Cid reports a relationship with AstraZeneca that includes: board membership, consulting or advisory, and speaking and lecture fees. Maria C Cid reports a relationship with GSK that includes: board membership, consulting or advisory, and speaking and lecture fees. Maria C Cid reports a relationship with CSL-Vifor that includes: consulting or advisory, speaking and lecture fees, and travel reimbursement. Bernhard Hellmich reports a relationship with AbbVie Inc that includes: consulting or advisory and speaking and lecture fees. Bernhard Hellmich reports a relationship with Novartis that includes: consulting or advisory and speaking and lecture fees. Tanaz A Kermani reports a relationship with CRA that includes: speaking and lecture fees. Tanaz A Kermani reports a relationship with Rheumatology Association of Nevada that includes: speaking and lecture fees. Tanaz A Kermani reports a relationship with Emirates Rheumatology Academy that includes: speaking and lecture fees. Tanaz A Kermani reports a relationship with Mayo Clinic that includes: speaking and lecture fees. Nader Khalidi reports a relationship with AbbVie Inc that includes: consulting or advisory and funding grants. Nader Khalidi reports a relationship with Sanofi that includes: funding grants. Nader Khalidi reports a relationship with NS Pharma Inc that includes: funding grants. Nader Khalidi reports a relationship with Roche that includes: consulting or advisory. Nader Khalidi reports a relationship with Otsuka Pharmaceutical Co Ltd that includes: speaking and lecture fees. Nader Khalidi reports a relationship with GSK that includes: speaking and lecture fees. Nader Khalidi reports a relationship with Mallinckrodt LLC that includes: speaking and lecture fees. Sarah Mackie reports a relationship with National Institute for Health and Care Research that includes: funding grants. Sarah Mackie reports a relationship with University of Leeds that includes: funding grants. Sarah Mackie reports a relationship with Fresenius Kabi that includes: speaking and lecture fees. Sarah Mackie reports a relationship with Roche Diagnostics GmbH that includes: consulting or advisory and speaking and lecture fees. Sarah Mackie reports a relationship with Pfizer Inc that includes: consulting or advisory, speaking and lecture fees, and travel reimbursement. Sarah Mackie reports a relationship with UCB that includes: speaking and lecture fees. Sarah Mackie reports a relationship with Vifor Pharma Inc that includes: speaking and lecture fees. Sarah

Mackie reports a relationship with Novartis that includes: speaking and lecture fees. Sarah Mackie reports a relationship with AstraZeneca AB that includes: consulting or advisory. Sarah Mackie reports a relationship with Sanofi that includes: consulting or advisory. Eric L Matteson reports a relationship with Boehringer Ingelheim GmBH that includes: consulting or advisory and speaking and lecture fees. Eric L Matteson reports a relationship with National Institutes of Health that includes: board membership. Eric L Matteson reports a relationship with Amgen Inc that includes: board membership. Eric L Matteson reports a relationship with HorizonTherapeutics that includes: board membership. Peter A Merkel reports a relationship with AbbVie Inc that includes: consulting or advisory and funding grants. Peter A Merkel reports a relationship with Alpine Physician Partners LLC that includes: consulting or advisory. Peter A Merkel reports a relationship with Amgen Inc that includes: consulting or advisory and funding grants. Peter A Merkel reports a relationship with Argenx Us, Inc. that includes: consulting or advisory. Peter A Merkel reports a relationship with AstraZeneca that includes: consulting or advisory and funding grants. Peter A Merkel reports a relationship with Boehringer Ingelheim that includes: consulting or advisory and funding grants. Peter A Merkel reports a relationship with Bristol-Myers Squibb Co that includes: consulting or advisory and funding grants. Peter A Merkel reports a relationship with GlaxoSmithKline Inc that includes: consulting or advisory and funding grants. Peter A Merkel reports a relationship with CSL Behring that includes: consulting or advisory. Peter A Merkel reports a relationship with Hibio, Inc. that includes: consulting or advisory. Peter A Merkel reports a relationship with iCell that includes: consulting or advisory. Peter A Merkel reports a relationship with InflaRx NV that includes: consulting or advisory and funding grants. Peter A Merkel reports a relationship with Eicos Sciences Inc that includes: funding grants. Peter A Merkel reports a relationship with Electra that includes: funding grants. Peter A Merkel reports a relationship with Forbius that includes: consulting or advisory. Peter A Merkel reports a relationship with Genentech that includes: funding grants. Peter A Merkel reports a relationship with Neutrolis that includes: funding grants. Peter A Merkel reports a relationship with Takeda Pharmaceutical Company Limited that includes: consulting or advisory and funding grants. Peter A Merkel reports a relationship with Janssen Pharmaceuticals Inc that includes: consulting or advisory. Peter A Merkel reports a relationship with Kinevant Sciences Inc that includes: consulting or advisory. Peter A Merkel reports a relationship with Kyverna Therapeutics that includes: consulting or advisory. Peter A Merkel reports a relationship with Metagenomia that includes: consulting or advisory. Peter A Merkel reports a relationship with Novartis that includes: consulting or advisory. Peter A Merkel reports a relationship with NS Pharma Inc that includes: consulting or advisory. Peter A Merkel reports a relationship with Q32 Bio that includes: consulting or advisory. Peter A Merkel reports a relationship with Regeneron Pharmaceuticals Inc that includes: consulting or advisory. Peter A Merkel reports a relationship with Sanofi that includes: consulting or advisory. Peter A Merkel reports a relationship with Sparrow Pharmaceuticals Inc that includes: consulting or advisory. Peter A Merkel reports a relationship with Visterra Inc that includes: consulting or advisory. Paul Monach reports a relationship with Genentech Inc that includes: speaking and lecture fees. Paul Monach reports a relationship with HI-bio that includes: consulting or advisory. Paul Monach reports a relationship with Clarivate Analytics that includes: consulting or advisory. Cristina Ponte reports a relationship with CSL Vifor that includes: board membership, consulting or advisory, funding grants, speaking and lecture fees, and travel reimbursement. Cristina Ponte reports a relationship with AbbVie Inc that includes: board membership, consulting or advisory, funding grants, speaking and lecture fees, and travel reimbursement. Cristina Ponte reports a relationship with Novartis that includes: funding grants and speaking and lecture fees. Cristina Ponte reports a relationship with GSK that includes: consulting or advisory and speaking and lecture fees. Cristina Ponte reports a relationship with Pfizer Inc that includes: speaking and lecture fees. Cristina Ponte reports a relationship with Viatris that includes: travel reimbursement. Peter M Villiger reports a relationship with AbbVie Inc that includes: travel reimbursement. Peter M Villiger reports a relationship with GSK that includes: speaking and lecture fees. Peter M Villiger reports a relationship with Vifor Pharma Inc that includes: speaking and lecture fees. Peter M Villiger reports a relationship with Roche that includes: speaking and lecture fees. Peter M Villiger reports a relationship with AstraZeneca that includes: consulting or advisory. Peter M Villiger reports a relationship with MSD that includes: consulting or advisory. Kenneth J Warrington reports a relationship with Amgen Inc that includes: consulting or advisory and speaking and lecture fees. Kenneth J Warrington reports a relationship with Sanofi that includes: consulting or advisory. Kenneth J Warrington reports a relationship with Kiniksa Pharmaceuticals Ltd that includes: funding grants. Kenneth J Warrington reports a relationship with Eli Lilly and Company that includes: funding grants. Kenneth J Warrington reports a relationship with Bristol Myers Squibb Co that includes: funding grants. Sofia Ramiro reports a relationship with AbbVie Inc that includes: consulting or advisory, funding grants, and speaking and lecture fees. Sofia Ramiro reports a relationship with Galapagos NV that includes: consulting or advisory, funding grants, and speaking and lecture fees. Sofia Ramiro reports a relationship with Merck Sharp & Dohme Corp that includes: consulting or advisory, funding grants, and speaking and lecture fees. Sofia Ramiro reports a relationship with Novartis that includes: consulting or advisory, funding grants, and speaking and lecture fees. Sofia Ramiro reports a relationship with Pfizer that includes: consulting or advisory, funding grants, and speaking and lecture fees. Sofia Ramiro reports a relationship with UCB Inc that includes: consulting or advisory, funding grants, and speaking and lecture fees. Sofia Ramiro reports a relationship with Sanofi that includes: consulting or advisory and speaking and lecture fees. Sofia Ramiro reports a relationship with Eli Lilly and Company that includes: consulting or advisory, speaking and lecture fees, and travel reimbursement. Christian Dejaco reports a relationship with AbbVie Inc that includes: consulting or advisory, funding grants, speaking and lecture fees, and travel reimbursement. Christian Dejaco reports a relationship with Novartis that includes: consulting or advisory, funding grants, speaking and lecture fees, and travel reimbursement. Christian Dejaco reports a relationship with Eli Lilly and Company that includes: consulting or advisory, speaking and lecture fees, and travel reimbursement. Christian Dejaco reports a relationship with Janssen Pharmaceuticals Inc that includes: consulting or advisory, speaking and lecture fees, and travel reimbursement. Christian Dejaco reports a relationship with Sparrow Pharmaceuticals Inc that includes: consulting or advisory and speaking and lecture fees. Christian Dejaco reports a relationship with Pfizer that includes: consulting or advisory, speaking and lecture fees, and travel reimbursement. Christian Dejaco reports a relationship with Roche that includes: consulting or advisory, speaking and lecture fees, and travel reimbursement. Christian Dejaco reports a

relationship with Galapagos that includes: consulting or advisory, speaking and lecture fees, and travel reimbursement. Christian Dejaco reports a relationship with Sanofi that includes: consulting or advisory and speaking and lecture fees. If there are other authors, they declare that they have no known competing financial interests or personal relationships that could have appeared to influence the work reported in this paper.

Patient consent for publication

Not applicable.

Ethics approval

Not applicable.

Provenance and peer review

Not commissioned; externally peer reviewed.

Data availability statement

Not applicable.

Supplementary materials

Supplementary material associated with this article can be found in the online version at doi:10.1016/j.ard.2025.06.2126.

Orcid

Medha L. Soowamber: http://orcid.org/0009-0003-3458-1608
Milena Bond: http://orcid.org/0000-0002-5400-2955
Zahi Touma: http://orcid.org/0000-0001-5177-2076
Carol Langford: http://orcid.org/0000-0001-9498-321X
Catalina Sanchez-Alvarez: http://orcid.org/0000-0002-6287-2213
Sibel Zehra Aydin: http://orcid.org/0000-0001-8792-4449
Frank Buttgereit: http://orcid.org/0000-0003-2534-550X
Dario Camellino: http://orcid.org/0000-0001-6384-6458
Maria C. Cid: http://orcid.org/0000-0002-4730-0938
Bernhard Hellmich: http://orcid.org/0000-0002-8014-1801
Tanaz A. Kermani: http://orcid.org/0000-0002-7335-7321
Nader A. Khalidi: http://orcid.org/0000-0002-8270-2617
Sarah L. Mackie: http://orcid.org/0000-0003-2483-5873
Eric L. Matteson: http://orcid.org/0000-0002-9866-0124
Mehrdad Maz: http://orcid.org/0000-0002-3594-0508
Peter A. Merkel: http://orcid.org/0000-0001-9284-7345
Paul A. Monach: http://orcid.org/0000-0003-4937-0515
Cristina Ponte: http://orcid.org/0000-0002-3989-1192
Carlo Salvarani: http://orcid.org/0000-0001-5426-5133
Peter M. Villiger: http://orcid.org/0000-0001-7831-8738
Kenneth J. Warrington: http://orcid.org/0000-0001-7708-2487
Sofia Ramiro: http://orcid.org/0000-0002-8899-9087
Christian Dejaco: http://orcid.org/0000-0002-0173-0668

REFERENCES

[1] Pugh D, Karabayas M, Basu N, Cid MC, Goel R, Goodyear CS, et al. Large-vessel vasculitis. Nat Rev Dis Primers 2022;7(1):93. doi: 10.1038/s41572-021-00327-5.
[2] Berti A, Dejaco C. Update on the epidemiology, risk factors, and outcomes of systemic vasculitides. Best Pract Res Clin Rheumatol 2018;32(2):271–94. doi: 10.1016/j.berh.2018.09.001.
[3] Rudwaleit M, van der Heijde D, Landewé R, Listing J, Akkoc N, Brandt J, et al. The development of Assessment of SpondyloArthritis International Society classification criteria for axial spondyloarthritis (part II): validation and final selection. Ann Rheum Dis 2009;68(6):777–83. doi: 10.1136/ard.2009.108233.
[4] Ponte C, Grayson PC, Robson JC, Suppiah R, Gribbons KB, Judge A, et al. 2022 American College of Rheumatology/EULAR classification criteria for giant cell arteritis. Arthritis Rheumatol 2022;74(12):1881–9. doi: 10.1002/art.42325.
[5] Aringer M, Costenbader K, Daikh D, Brinks R, Mosca M, Ramsey-Goldman R, et al. 2019 European League Against Rheumatism/American College of Rheumatology classification criteria for systemic lupus erythematosus. Ann Rheum Dis 2019;78(9):1151–9. doi: 10.1136/annrheumdis-2018-214819.
[6] Nepal D, Putman M, Unizony S. Giant cell arteritis and polymyalgia rheumatica: treatment approaches and new targets. Rheum Dis Clin North Am 2023;49(3):505–21. doi: 10.1016/j.rdc.2023.03.005.
[7] Prieto-González S, Espígol-Frigolé G, García-Martínez A, Alba MA, Tavera-Bahillo I, Hernández-Rodríguez J, et al. The expanding role of imaging in systemic vasculitis. Rheum Dis Clin North Am 2016;42(4):733–51. doi: 10.1016/j.rdc.2016.07.009.
[8] Sanchez-Alvarez C, Bond M, Soowamber M, Camellino D, Anderson M, Langford CA, et al. Measuring treatment outcomes and change in disease activity in giant cell arteritis: a systematic literature review informing the development of the EULAR-ACR response criteria on behalf of the EULAR-ACR response criteria in giant cell arteritis task force. RMD Open 2023;9(2):e003233. doi: 10.1136/rmdopen-2023-003233.
[9] Firestein GS, Gabriel SE, McInnes IB, O'Dell JR. Kelley & Firestein's Textbook of Rheumatology. 10th ed. Philadelphia, PA: Elsevier; 2017.
[10] Hochberg MC, Silman AJ, Smolen JS, Weinblatt ME, Weisman MH, Gravallese E, editors. Rheumatology. 7th ed. Philadelphia, PA: Elsevier, Inc.; 2019.
[11] Loscalzo J, Fauci A, Kasper D, Hauser S, Longo D, Jameson J. Harrison's Principles of Internal Medicine. 21st ed. New York: McGraw Hill; 2022.
[12] Hunder GG, Bloch DA, Michel BA, Stevens MB, Arend WP, Calabrese LH, et al. The American College of Rheumatology 1990 criteria for the classification of giant cell arteritis. Arthritis Rheum 1990;33(8):1122–8. doi: 10.1002/art.1780330810.
[13] Dasgupta B, Cimmino MA, Maradit-Kremers H, Schmidt WA, Schirmer M, Salvarani C, et al. 2012 provisional classification criteria for polymyalgia rheumatica: a European League Against Rheumatism/American College of Rheumatology Collaborative Initiative. Ann Rheum Dis 2012;71(4):484–92. doi: 10.1136/annrheumdis-2011-200329.
[14] Sacco RL, Kasner SE, Broderick JP, Caplan LR, Connors JJ, Culebras A, et al. An updated definition of stroke for the 21st century: a statement for healthcare professionals from the American Heart Association/American Stroke Association. Stroke. 2013;44(7):2064–89. doi: 10.1161/STR.0b013e318296aeca.
[15] Easton JD, Saver JL, Albers GW, Alberts MJ, Chaturvedi S, Feldmann E, et al. Definition and evaluation of transient ischemic attack: a scientific statement for healthcare professionals from the American Heart Association/American Stroke Association Stroke Council; Council on Cardiovascular Surgery and Anesthesia; Council on Cardiovascular Radiology and Intervention; Council on Cardiovascular Nursing; and the Interdisciplinary Council on Peripheral Vascular Disease. The American Academy of Neurology affirms the value of this statement as an educational tool for neurologists. Stroke. 2009;40(6):2276–93. doi: 10.1161/STROKEAHA.108.192218.
[16] Thygesen K, Alpert JS, Jaffe AS, Chaitman BR, Bax JJ, Morrow DA, et al. Fourth universal definition of myocardial infarction (2018). Circulation 2018;138(20):e618–51. doi: 10.1161/CIR.0000000000000617.
[17] Hughes M, Tracey A, Bhushan M, Chakravarty K, Denton CP, Dubey S, et al. Reliability of digital ulcer definitions as proposed by the UK scleroderma study group: a challenge for clinical trial design. J Scleroderma Relat Disord 2018;3(2):170–4. doi: 10.1177/2397198318764796.
[18] Maxwell LJ, Jones C, Bingham CO, Boers M, Boonen A, Choy E, et al. Defining domains: developing consensus-based definitions for foundational domains in OMERACT core outcome sets. Semin Arthritis Rheum 2024;66:152423. doi: 10.1016/j.semarthrit.2024.152423.
[19] Hoffman GS, Cid MC, Hellmann DB, Guillevin L, Stone JH, Schousboe J, et al. A multicenter, randomized, double-blind, placebo-controlled trial of adjuvant methotrexate treatment for giant cell arteritis. Arthritis Rheum 2002;46(5):1309–18. doi: 10.1002/art.10262.
[20] Villiger PM, Adler S, Kuchen S, Wermelinger F, Dan D, Fiege V, et al. Tocilizumab for induction and maintenance of remission in giant cell arteritis: a phase 2, randomised, double-blind, placebo-controlled trial. Lancet 2016;387(10031):1921–7. doi: 10.1016/S0140-6736(16)00560-2.

[21] Stone JH, Tuckwell K, Dimonaco S, Klearman M, Aringer M, Blockmans D, et al. Trial of tocilizumab in giant-cell arteritis. N Engl J Med 2017;377 (4):317–28. doi: 10.1056/NEJMoa1613849.
[22] Schmidt WA, Dasgupta B, Luqmani R, Unizony SH, Blockmans D, Lai Z, et al. A multicentre, randomised, double-blind, placebo-controlled, parallel-group study to evaluate the efficacy and safety of sirukumab in the treatment of giant cell arteritis. Rheumatol Ther 2020;7(4):793–810. doi: 10.1007/s40744-020-00227-2.
[23] Langford CA, Cuthbertson D, Ytterberg SR, Khalidi N, Monach PA, Carette S, et al. A randomized, double-blind trial of abatacept (CTLA-4Ig) for the treatment of giant cell arteritis. Arthritis Rheumatol 2017;69(4):837–45. doi: 10.1002/art.40044.
[24] Cid MC, Unizony SH, Blockmans D, Brouwer E, Dagna L, Dasgupta B, et al. Efficacy and safety of mavrilimumab in giant cell arteritis: a phase 2, randomised, double-blind, placebo-controlled trial. Ann Rheum Dis 2022;81 (5):653–61. doi: 10.1136/annrheumdis-2021-221865.
[25] Headache Classification Committee of the International Headache Society (IHS) The International Classification of Headache Disorders, 3rd edition. Cephalalgia 2018;38(1):1–211. doi: 10.1177/0333102417738202.
[26] Chehem Daoud Chehem F, de Mornac D, Feuillet F, Liozon E, Samson M, Bonnotte B, et al. Giant cell arteritis associated with scalp, tongue or lip necrosis: a French multicenter case control study. Semin Arthritis Rheum 2024; 64:152348. doi: 10.1016/j.semarthrit.2023.152348.
[27] Lim J, Dures E, Bailey LF, Almeida C, Ruediger C, Hill CL, et al. Jaw claudication and jaw stiffness in giant cell arteritis: secondary analysis of a qualitative research dataset. Rheumatol Adv Pract 2024;8(1) rkad082. doi: 10.1093/rap/rkad082.
[28] Dejaco C, Duftner C, Buttgereit F, Matteson EL, Dasgupta B. The spectrum of giant cell arteritis and polymyalgia rheumatica: revisiting the concept of the disease. Rheumatology (Oxford) 2017;56(4):506–15. doi: 10.1093/rheumatology/kew273.
[29] Patil P, Williams M, Maw WW, Achilleos K, Elsideeg S, Dejaco C, et al. Fast track pathway reduces sight loss in giant cell arteritis: results of a longitudinal observational cohort study. Clin Exp Rheumatol 2015;33(2 Suppl 89) S-103-6.
[30] Diamantopoulos AP, Haugeberg G, Lindland A, Myklebust G. The fast-track ultrasound clinic for early diagnosis of giant cell arteritis significantly reduces permanent visual impairment: towards a more effective strategy to improve clinical outcome in giant cell arteritis? Rheumatology (Oxford) 2016;55(1):66–70. doi: 10.1093/rheumatology/kev289.
[31] Vodopivec I, Rizzo 3rd JF. Ophthalmic manifestations of giant cell arteritis. Rheumatology (Oxford, England) 2018;57(suppl_2):ii63–72. doi: 10.1093/rheumatology/kex428.
[32] Centers for Disease Control and Prevention, National Center for Emerging and Zoonotic Infectious Diseases (NCEZID), Division of Global Migration Health (DGMH). Fever. https://www.cdc.gov/. Accessed January 28, 2024.
[33] Chen Y, Dong H, Li HW, Zou YB, Jiang XJ. Characteristics of four-limb blood pressure and brachial-ankle pulse wave velocity in Chinese patients with Takayasu arteritis. Blood Press 2022;31(1):146–54. doi: 10.1080/08037051.2022.2091513.
[34] Singh S, Sethi A, Singh M, Khosla K, Grewal N, Khosla S. Simultaneously measured inter-arm and inter-leg systolic blood pressure differences and cardiovascular risk stratification: a systemic review and meta-analysis. J Am Soc Hypertens 2015;9(8) 640-50.e12. doi: 10.1016/j.jash.2015.05.013.
[35] Clark CE, Campbell JL, Powell RJ. The interarm blood pressure difference as predictor of cardiovascular events in patients with hypertension in primary care: cohort study. J Hum Hypertens 2007;21(8):633–8. doi: 10.1038/sj.jhh.1002209.
[36] Grayson PC, Ponte C, Suppiah R, Robson JC, Gribbons KB, Judge A, et al. 2022 American College of Rheumatology/EULAR classification criteria for Takayasu arteritis. Ann Rheum Dis 2022;81(12):1654–60. doi: 10.1136/ard-2022-223482.
[37] Whelton PK, Carey RM, Aronow WS, Casey Jr DE, Collins KJ, Dennison Himmelfarb C, et al. 2017 ACC/AHA/AAPA/ABC/ACPM/AGS/APhA/ASH/ASPC/NMA/PCNA guideline for the prevention, detection, evaluation, and management of high blood pressure in adults: a report of the American College of Cardiology/American Heart Association task force on clinical practice guidelines. J Am Coll Cardiol 2018;71(19):e127–248. doi: 10.1016/j.jacc.2017.11.006.
[38] Tedeschi SK, Johnson SR, Boumpas D, Daikh D, Dörner T, Jayne D, et al. Developing and refining new candidate criteria for systemic lupus erythematosus classification: an international collaboration. Arthritis Care Res (Hoboken) 2018;70(4):571–81. doi: 10.1002/acr.23317.
[39] Seror R, Baron G, Hachulla E, Debandt M, Larroche C, Puéchal X, et al. Adalimumab for steroid sparing in patients with giant-cell arteritis: results of a multicentre randomised controlled trial. Ann Rheum Dis 2014;73(12):2074–81. doi: 10.1136/annrheumdis-2013-203586.
[40] Hoffman GS, Cid MC, Rendt-Zagar KE, Merkel PA, Weyand CM, Stone JH, et al. Infliximab for maintenance of glucocorticosteroid-induced remission of giant cell arteritis: a randomized trial. Ann Intern Med 2007;146(9):621–30. doi: 10.7326/0003-4819-146-9-200705010-00004.
[41] Mazlumzadeh M, Hunder GG, Easley KA, Calamia KT, Matteson EL, Griffing WL, et al. Treatment of giant cell arteritis using induction therapy with high-dose glucocorticoids: a double-blind, placebo-controlled, randomized prospective clinical trial. Arthritis Rheum 2006;54(10):3310–8. doi: 10.1002/art.22163.
[42] Spiera RF, Mitnick HJ, Kupersmith M, Richmond M, Spiera H, Peterson MG, et al. A prospective, double-blind, randomized, placebo controlled trial of methotrexate in the treatment of giant cell arteritis (GCA). Clin Exp Rheumatol 2001;19(5):495–501.
[43] Jover JA, Hernández-García C, Morado IC, Vargas E, Bañares A, Fernández-Gutiérrez B. Combined treatment of giant-cell arteritis with methotrexate and prednisone. A randomized, double-blind, placebo-controlled trial. Ann Intern Med 2001;134(2):106–14. doi: 10.7326/0003-4819-134-2-200101160-00010.

Ann Rheum Dis 84 (2025) 1888–1899

Contents lists available at ScienceDirect

Annals of the Rheumatic Diseases

journal homepage: https://www.sciencedirect.com/journal/annals-of-the-rheumatic-diseases

Vasculitis

Two-year efficacy and safety of anti-interleukin-5/receptor therapy for eosinophilic granulomatosis with polyangiitis

Peter A. Merkel[1,*], Parameswaran K. Nair[2], Nader Khalidi[2], Benjamin Terrier[3], Bernhard Hellmich[4], Arnaud Bourdin[5], David R.W. Jayne[6], David J. Jackson[7,8], Florence Roufosse[9], Christian Pagnoux[10], Ulrich Specks[11], Lena Börjesson Sjö[12], Calvin N. Ho[13], Maria Jison[13], Christopher McCrae[14], Sofia Necander[12], Eva Rodríguez-Suárez[15], Anat Shavit[16], Claire Walton[17], Michael E. Wechsler[18], on behalf of the MANDARA Study Group

[1] *Division of Rheumatology, Department of Medicine, University of Pennsylvania, Philadelphia, PA, USA*
[2] *Department of Medicine, McMaster University, St Joseph's Healthcare Hamilton, Hamilton, ON, Canada*
[3] *Department of Internal Medicine, National Referral Center for Rare Systemic Autoimmune Diseases, Hospital Cochin, Université Paris Cité, Paris, France*
[4] *Klinik für Innere Medizin, Rheumatologie, Pneumologie, Nephrologie und Diabetologie, Medius Kliniken, Akademisches Lehrkrankenhaus der Universität Tübingen, Kirchheim unter Teck, Germany*
[5] *Department of Respiratory Diseases, Montpellier University Hospitals, Arnaud de Villeneuve Hospital, Montpellier, France*
[6] *Department of Medicine, University of Cambridge, Cambridge, UK*
[7] *Guy's Severe Asthma Centre, Guy's and St Thomas' NHS Foundation Trust, London, UK*
[8] *School of Immunology and Microbial Sciences, King's College London, London, UK*
[9] *Department of Internal Medicine, Hôpital Erasme, Université Libre de Bruxelles, Brussels, Belgium*
[10] *Mount Sinai Hospital, University Health Network, Toronto, ON, Canada*
[11] *Thoracic Diseases Research Unit, Division of Pulmonary and Critical Care Medicine, Department of Medicine, Mayo Clinic College of Medicine and Science, Rochester, MN, USA*
[12] *Late-stage Respiratory & Immunology, BioPharmaceuticals R&D, AstraZeneca, Gothenburg, Sweden*
[13] *Late-stage Respiratory & Immunology, BioPharmaceuticals R&D, AstraZeneca, Gaithersburg, MD, USA*
[14] *Translational Science and Experimental Medicine, Early Respiratory & Immunology, BioPharmaceuticals R&D, AstraZeneca, Gaithersburg, MD, USA*
[15] *Translational Science and Experimental Medicine, Early Respiratory & Immunology, BioPharmaceuticals R&D, AstraZeneca, Cambridge, UK*
[16] *BioPharmaceutials Medical, AstraZeneca, Cambridge, UK*
[17] *Late-stage Respiratory & Immunology, BioPharmaceuticals R&D, AstraZeneca, Cambridge, UK*
[18] *Department of Medicine, National Jewish Health, Denver, CO, USA*

*Correspondence to Dr. Peter A. Merkel.
E-mail address: pmerkel@upenn.edu (P.A. Merkel).
Handling editor Josef S Smolen.

https://doi.org/10.1016/j.ard.2025.06.2131

ARTICLE INFO

Article history:
Received 11 March 2025
Received in revised form 19 June 2025
Accepted 20 June 2025

ABSTRACT

Objectives: To summarise the efficacy and safety of 2 years of anti-interleukin-5/receptor (anti-IL-5/R) therapy in patients with eosinophilic granulomatosis with polyangiitis (EGPA).

Methods: Patients were randomised 1:1 to receive benralizumab or mepolizumab every 4 weeks during the 52-week double-blind period of the MANDARA trial. Patients entered an open-label extension (OLE) in which they continued benralizumab (benralizumab/benralizumab) or switched from mepolizumab to benralizumab (mepolizumab/benralizumab). Remission (Birmingham Vasculitis Activity Score = 0 and oral glucocorticoid [OGC] dose ≤4 mg/d), OGC use, relapse, blood eosinophil count (bEOS), and safety up to year 2 (week 104) were reported.

Results: A total of 128 patients entered the OLE period (n = 66 benralizumab/benralizumab; n = 62 mepolizumab/benralizumab). At week 104, 41 (62.1%) benralizumab/benralizumab patients and 42 (67.7%) mepolizumab/benralizumab patients were in remission. During OLE year 1, 51 (77.3%) benralizumab/benralizumab patients and 42 (67.7%) mepolizumab/benralizumab patients had no relapses. By weeks 49 to 52, 27 (40.9%) benralizumab/benralizumab patients and 16 (25.8%) mepolizumab/benralizumab patients had withdrawn from OGCs, increasing to 29 (43.9%) and 27 (43.5%) at weeks 101 to 104, respectively; the median cumulative OGC dose was 950 mg and 791 mg during OLE year 1, respectively. The median bEOS among benralizumab/benralizumab-treated patients was 20 cells/μL (at weeks 52 and 100), and in mepolizumab/benralizumab-treated patients, it decreased from 70 cells/μL to 20 cells/μL 4 weeks after switching. Adverse events/serious adverse events were reported in 97.0%/22.7% of benralizumab/benralizumab and 100%/35.5% of mepolizumab/benralizumab patients.

Conclusions: In patients with EGPA, treatment for 2 years with anti-IL-5/R therapies is associated with durable rates of remission, discontinuation of OGCs, bEOS depletion, and low relapse rates. Switching from mepolizumab to benralizumab enhances bEOS depletion and OGC sparing.

WHAT IS ALREADY KNOWN ON THIS TOPIC

- Eosinophilic inflammation is a key pathogenic driver in eosinophilic granulomatosis with polyangiitis (EGPA).
- Current first-line treatment for EGPA includes oral glucocorticoids (OGCs) and other immunosuppressive drugs, which are associated with adverse effects and dose-dependent toxicity. Relapses are frequently seen during, and especially at tapering, of these medications.
- The anti-interleukin-5/receptor therapies mepolizumab and benralizumab are effective in inducing remission in some patients with EGPA.

WHAT THIS STUDY ADDS

- Two-year efficacy and safety data of (1) continued treatment with benralizumab, and (2) switching from mepolizumab to benralizumab in adults with relapsing and/or refractory EGPA.
- Two years of treatment with anti-interleukin-5/receptor therapies in patients with EGPA demonstrated a durable, favourable impact on remission rates, withdrawal of OGCs, relapse rates, and blood eosinophil depletion.
- Additional bEOS depletion and OGC sparing were seen in those switching from mepolizumab to benralizumab.
- No new safety signals were seen during the longer-term follow-up period.

HOW THIS STUDY MIGHT AFFECT RESEARCH, PRACTICE OR POLICY

- These findings provide evidence of the efficacy and safety of benralizumab over 2 years in patients with EGPA, and the efficacy and safety of switching from mepolizumab to benralizumab.

INTRODUCTION

Eosinophilic granulomatosis with polyangiitis (EGPA) is a rare inflammatory disorder, characterised by blood and tissue hypereosinophilia, necrotising small- to medium-vessel vasculitis, extravascular granulomas, and the presence of asthma [1–3]. Long-term treatment with oral glucocorticoids (OGCs) and other immunosuppressive therapies is considered standard of care for the treatment of EGPA, although these drugs are associated with toxicity, and relapses are common when treatment is tapered [4–9]. In most patients with EGPA, the disease follows a relapsing/remitting course, with high glucocorticoid exposure. Hence, there is a need for more effective, targeted, and better-tolerated treatments that allow patients to withdraw or reduce OGCs, thereby reducing treatment-related toxicity.

The monoclonal antibodies mepolizumab and benralizumab have demonstrated efficacy and safety when used to treat EGPA in clinical trials [10,11] and real-world settings [12–16]. Mepolizumab targets interleukin-5 (IL-5) and inhibits eosinophil activation and differentiation [17]; it was the first targeted therapy approved in the US and Europe for the treatment of EGPA [18,19]. International guidelines recommend the use of mepolizumab in patients with non–organ- or life-threatening relapsing and/or refractory disease [9,20]. Benralizumab inhibits the IL-5 signalling cascade by binding to the α-subunit of the IL-5 receptor expressed on eosinophils and depletes eosinophils via antibody-dependent cell-mediated cytotoxicity [21]; it was approved in 2024 in the US, Europe, and Japan for the treatment of EGPA [22–24].

In the double-blind period of the head-to-head phase 3 MANDARA trial, the efficacy and safety of benralizumab vs mepolizumab were compared over 52 weeks, and benralizumab was shown to be noninferior to mepolizumab in adults with relapsing or refractory EGPA, with almost 60% of the patients achieving remission [11]. At the end of the double-blind period, more benralizumab-treated than mepolizumab-treated patients completely withdrew their OGC use [11].

This report, based on the combined 2-year data from the 1-year double-blind period and the first year of the open-label

extension (OLE) period, describes the extended safety profile and efficacy of benralizumab, as well as the response among patients switching from mepolizumab to benralizumab.

METHODS

Study design

MANDARA (NCT04157348) was a randomised, double-blind, parallel-group, multicentre, 52-week, phase 3, noninferiority, head-to-head study comparing benralizumab (1 × 30 mg) and mepolizumab (3 × 100 mg) administered by subcutaneous injection every 4 weeks (Fig 1A). The study was conducted at 50 sites across 9 countries. The trial design and primary results from the double-blind period were published previously [11].

At the end of the 1-year double-blind period, patients were invited to continue in the OLE period (planned to last up to 4 years in total), during which they all received benralizumab 1 × 30 mg administered by subcutaneous injection every 4 weeks. This report includes data from the double-blind period (through week 52) and the first year (through week 104) of the ongoing OLE. The data cutoff date for this analysis was August 28, 2024.

The trial was conducted in accordance with the ethical principles of the Declaration of Helsinki and is consistent with the International Council for Harmonisation Good Clinical Practice guidelines, the applicable regulatory requirements, and the AstraZeneca policy on bioethics. All patients provided written informed consent [11].

Patients and treatment

The study population comprised adults aged ≥18 years who had been diagnosed with EGPA at least 6 months before screening, based on medical history or the presence of asthma and blood eosinophilia (>1.0 × 10^9/L and/or >10% of leukocytes), plus ≥2 additional features of EGPA and a history of relapsing/refractory disease on OGCs (≥7.5 mg/d) with or without stable non-OGC immunosuppressive therapy. Patients with ongoing organ- or life-threatening EGPA were excluded, as previously described [11]. From week 4 of the double-blind period onwards, investigators were encouraged to taper OGCs according to standard of care practice and clinical judgement if there

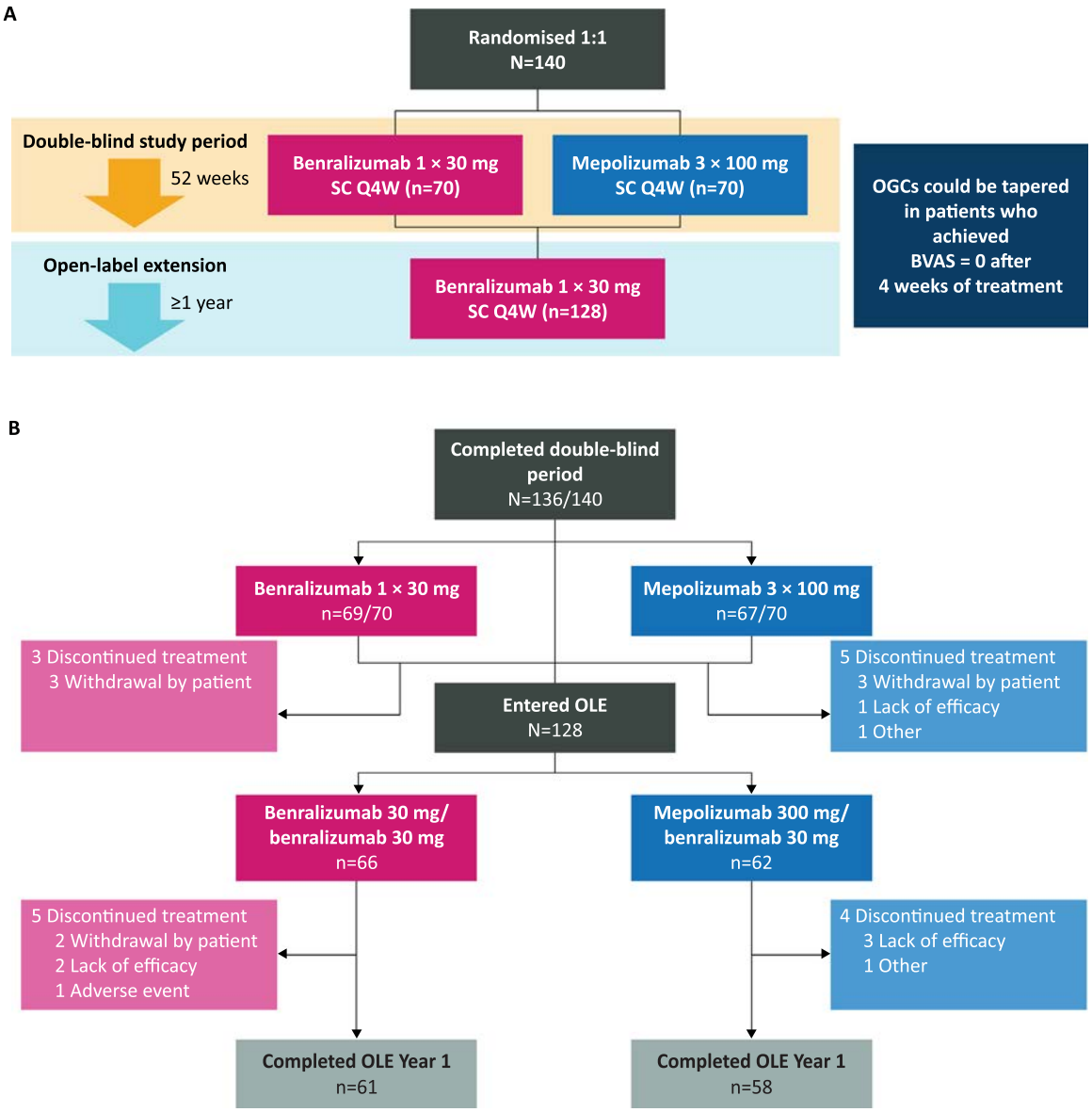

Figure 1. (A) Study design and (B) patient disposition in the double-blind and open-label extension periods. BVAS, Birmingham Vasculitis Activity Score; OGC, oral glucocorticoid; OLE, open-label extension; Q4W, every 4 weeks; SC, subcutaneous.

was no disease activity (Birmingham Vasculitis Activity Score [BVAS] = 0). A tapering schedule was provided in the study protocol; however, investigators were not required to adhere to it. After 6 months in the OLE period (week 76), investigators could taper non-OGC immunosuppressive therapy in patients according to clinical judgement. The OLE analysis set included all patients who entered the OLE of the study and who received at least 1 dose of benralizumab during the OLE treatment period.

Efficacy outcomes

The outcomes of this analysis of the combined double-blind period and the first year of the OLE period included (1) the proportion of patients achieving remission up to week 104, defined as BVAS = 0 and OGC dose ≤4 mg/d; (2) the proportion of patients achieving European Alliance of Associations for Rheumatology (EULAR)-defined remission [25] up to week 104, defined as BVAS = 0 and OGC dose ≤7.5 mg/d; the rate of remission at both weeks 36 and 48 was also recorded (MANDARA primary endpoint); (3) total accrued duration of remission for the following categories: 0 week, >0 to <12 weeks, 12 to <24 weeks, 24 to <36 weeks, 36 to <52 weeks, 52 to <78 weeks, and >78 weeks; and (4) the proportion of patients who achieved remission within the first 24 weeks of the double-blind period and remained in remission up to week 104.

Outcomes related to relapses included (1) the proportion of patients who experienced a relapse (defined as active vasculitis [BVAS > 0]; or active symptoms of asthma and/or signs with a corresponding worsening in the 6-item Asthma Control Questionnaire [ACQ-6] score; or active nasal and/or sinus disease, with a corresponding worsening in at least 1 of the questions on the Sino-nasal Symptoms Questionnaire, warranting an increase in the dose of OGC therapy to >4 mg/d; or an increased dose or addition of immunosuppressive therapy; or hospitalisation related to the worsening of EGPA); (2) the proportion of patients who experienced a major relapse (defined as any organ- or life-threatening EGPA event; or BVAS ≥6 [involving at least 2 organ systems in addition to any general symptoms when present, eg, myalgia, arthralgia/arthritis, fever >38°C, or weight loss >2 kg]; or an asthma or a sino-nasal relapse that required hospitalisation); and (3) the annualised relapse rate.

Outcomes related to the use of OGCs included (1) the average daily OGC dose (prednisolone/prednisone equivalent) per 4-weekly periods up to weeks 100 to 104; (2) percent reduction in OGC use from baseline (no reduction, <25%, 25% to <50%, 50% to <75%, 75% to <100%, and 100% reduction in the average daily prednisolone/prednisone dose); and (3) cumulative OGC use, which included all OGCs administered regardless of the reason, or only OGCs administered specifically for EGPA. During the study, only systemic glucocorticoids (not inhaled, topical, or intra-articular routes of administration) were considered part of the OGC dose calculations. Outcomes related to the use of nonglucocorticoid immunosuppressive drugs were assessed by the proportion of patients who completely withdrew these immunosuppressive drugs, lowered their dose compared with entry in the OLE period, initiated new immunosuppressive therapies, or increased their dose.

Blood eosinophil count (bEOS) outcomes consisted of the absolute bEOS from baseline through the 52-week double-blind treatment period and up to week 104, as well as the proportion of patients with a bEOS ≤30 cells/μL.

Other outcomes included disease activity assessed using the BVAS; organ damage assessed using the Vasculitis Damage Index (VDI); lung function (prebronchodilator forced expiratory volume in 1 second [pre-BD FEV_1]); asthma symptom control (ACQ-6 scores and asthma response status rates [decrease from baseline in the ACQ-6 score of ≥0.5]); sino-nasal symptom severity (Sino-Nasal Outcome Test-22 [SNOT 22] scores); health-related quality of life (Short Form 36-Item Health Survey version 2 [SF-36v2]); and Work Productivity and Activity Impairment Questionnaire—General Health (WPAI-GH) scores.

Safety outcomes

Safety and tolerability were evaluated based on adverse events (AEs) classified using the Medical Dictionary for Regulatory Activities version 26.1.

Statistical analysis

Analysis included all patients who entered the OLE and received at least 1 dose of study drug during the OLE treatment period. Endpoints were summarised descriptively and analysed using SAS version 9.4 (SAS Institute Inc).

Patient and public involvement

Patient feedback was obtained on the study design. Patients and/or the public were not involved in the conduct, reporting, or dissemination plans of this research.

RESULTS

Patients

In total, 136 patients completed the double-blind period (week 52), and 128 opted to enter the OLE period; 66 patients continued benralizumab (benralizumab/benralizumab) while 62 switched from mepolizumab to benralizumab (mepolizumab/benralizumab). Of these, 61 benralizumab/benralizumab patients and 58 mepolizumab/benralizumab patients completed the first year of the OLE period (week 104; Fig 1B). The mean (SD) total exposure of benralizumab was 933.1 (328.76) days; 117 (91.4%) patients had ≥104 weeks of cumulative exposure. During the OLE period, compliance with study treatment was similar between groups (mean [SD], 98.9% [2.99%] of patients in the benralizumab/benralizumab group and 98.4% [4.24%] in the mepolizumab/benralizumab group).

Baseline demographics and characteristics were generally similar between patients entering the double-blind period and those entering the OLE period, as well as between treatment groups; overall, 60.2% of patients were female, and the mean (SD) age was 52.8 (13.97) years (Table 1). Among those entering the OLE period, the proportion of patients who had fully withdrawn from OGCs at the end of the double-blind period was 40.9% of benralizumab/benralizumab patients and 25.8% of mepolizumab/benralizumab patients, similar to those previously described for the full analysis set [11] (Supplementary Table S1). There was a slight imbalance between treatment groups in the annualised relapse rate during the double-blind period among patients entering the OLE period. A higher incidence of relapses during the double-blind period in the mepolizumab arm was associated with study discontinuation, which may explain why, among patients who continued to the OLE, mepolizumab/benralizumab patients had a lower baseline relapse rate than benralizumab/benralizumab patients.

Table 1
Baseline demographics and disease characteristics of patients with eosinophilic granulomatosis with polyangiitis in the open-label extension period based on or prior to the date of randomisation into the double-blind period

Characteristics	Benralizumab/benralizumab (n = 66)	Mepolizumab/benralizumab (n = 62)	Total (N = 128)
Age, y			
Mean (SD)	52.5 (13.60)	53.0 (14.46)	52.8 (13.97)
Median (min, max)	55.5 (20, 76)	55.5 (19, 79)	55.5 (19, 79)
Female, n (%)	42 (63.6)	35 (56.5)	77 (60.2)
Region, n (%)			
North America	15 (22.7)	14 (22.6)	29 (22.7)
Japan	4 (6.1)	4 (6.5)	8 (6.3)
Rest of the world	47 (71.2)	44 (71.0)	91 (71.1)
EGPA disease type, n (%)			
Relapsing disease	41 (62.1)	44 (71.0)	85 (66.4)
Refractory disease	40 (60.6)	36 (58.1)	76 (59.4)
Relapsing and refractory	16 (24.2)	18 (29.0)	34 (26.6)
Time since diagnosis of EGPA, y			
Mean (SD)	5.41 (5.31)	5.15 (6.17)	5.28 (5.72)
Median (min, max)	3.37 (0.6, 24.0)	2.18 (0.6, 38.0)	2.89 (0.6, 38.0)
ANCA status, n (%)			
Positive at screening	6 (9.1)	4 (6.5)	10 (7.8)
Positive at screening or history	17 (25.8)	18 (29.0)	35 (27.3)
Blood eosinophil count, cells/μL			
Mean (SD)	309.2 (228.86)	334.2 (400.02)	321.3 (322.22)
Median (min, max)	240.0 (30, 920)	205.0 (0, 2670)	225.0 (0, 2670)
EGPA-related disease characteristics, n (%)			
Asthma	66 (100)	62 (100)	128 (100)
Eosinophilia	66 (100)	62 (100)	128 (100)
Biopsy evidence of eosinophilic vasculitis/inflammation[a]	19 (28.8)	31 (50.0)	50 (39.1)
Neuropathy[b]	34 (51.5)	42 (67.7)	76 (59.4)
Nonfixed pulmonary infiltrates	47 (71.2)	37 (59.7)	84 (65.6)
Sino-nasal abnormality	59 (89.4)	58 (93.5)	117 (91.4)
Cardiomyopathy (by ECG/MRI)[c]	17 (25.8)	12 (19.4)	29 (22.7)
Glomerulonephritis	3 (4.5)	1 (1.6)	4 (3.1)
Alveolar haemorrhage	1 (1.5)	2 (3.2)	3 (2.3)
Palpable purpura	7 (10.6)	10 (16.1)	17 (13.3)
Dose of oral glucocorticoids (prednisolone or prednisone)			
Mean (SD), mg/d	11.27 (4.65)	10.92 (6.09)	11.10 (5.38)
Median (min, max), mg/d	10.0 (5.0, 30.0)[d]	9.5 (7.5, 40.0)	10.0 (5.0, 40.0)
≥12 mg/d, n (%)	18 (27.3)	12 (19.4)	30 (23.4)
<12 mg/d, n (%)	48 (72.7)	50 (80.6)	98 (76.6)
Immunosuppressive therapy at baseline, n (%)	23 (34.8)	24 (38.7)	47 (36.7)
Birmingham Vasculitis Activity Score			
Mean (SD)	2.0 (3.21)	1.9 (3.05)	2.0 (3.12)
>0, n (%)	31 (47.0)	28 (45.2)	59 (46.1)
Vasculitis Damage Index score			
Mean (SD)	3.9 (1.72)	4.1 (1.72)	4.0 (1.71)
≥5, n (%)	20 (30.3)	18 (29.0)	38 (29.7)
ACQ-6, mean (SD)	1.39 (1.18)	1.11 (0.95)	1.26 (1.08)
Prebronchodilator FEV_1, L, mean (SD)	2.50 (0.92)	2.59 (0.81)	2.54 (0.87)
Postbronchodilator FEV_1, % PN, mean (SD)	86.92 (20.35)	87.54 (16.75)	87.22 (18.60)

ACQ-6, 6-item Asthma Control Questionnaire; ANCA, antineutrophil cytoplasmic antibodies; ECG, electrocardiogram; EGPA, eosinophilic granulomatosis with polyangiitis; FEV_1, forced expiratory volume in 1 second; MRI, magnetic resonance imaging; PN, percent of predicted normal value.
[a] A biopsy showing histopathological evidence of eosinophilic vasculitis, perivascular eosinophilic infiltration, or eosinophil-rich granulomatous inflammation.
[b] Mono- or polyneuropathy (motor deficit or nerve conduction abnormality).
[c] Established by echocardiography or MRI.
[d] One patient started tapering on the day of visit 2, making the oral glucocorticoid dose 5 mg/d. The screening dose had been stable at 7.5 mg/d.

Remission

The proportion of patients achieving remission (BVAS = 0; OGC dose ≤4 mg/d) at week 52 was 45 (68.2%) patients in the benralizumab/benralizumab group and 44 (71.0%) patients in the mepolizumab/benralizumab group; at week 104, 41 (62.1%) and 42 (67.7%) patients achieved remission, respectively (Fig 2A). The proportion of patients achieving EULAR-defined remission (BVAS = 0; OGC dose ≤7.5 mg/d) [25] is shown in Figure 2B. In total, 28 (42.4%) benralizumab/benralizumab patients and 32 (51.6%) mepolizumab/benralizumab patients were in remission at the end of the double-blind period (at both weeks 36 and 48) and also at the end of the first year of the OLE period (week 104) (Fig 2C).

Approximately half the patients who achieved remission within the first 24 weeks of the double-blind period and completed the OLE year 1 remained in continuous remission through week 104: 14/29 (48.3%) in the benralizumab/benralizumab group and 16/29 (55.2%) in the mepolizumab/benralizumab group.

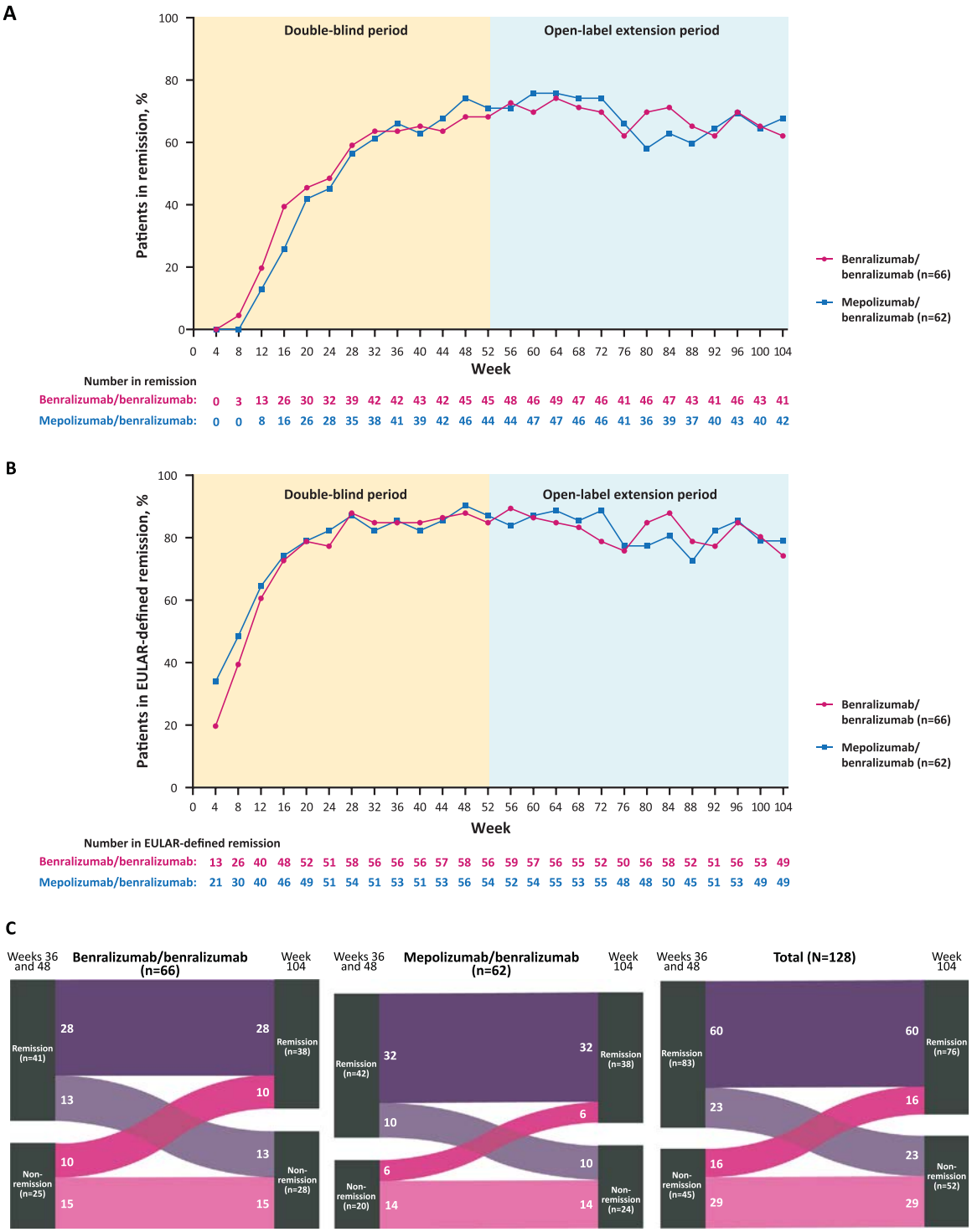

Figure 2. (A) Proportion of patients who achieved remission, (B) European Alliance of Associations for Rheumatology (EULAR)-defined remission during the study, and (C) flow of patients between remission and nonremission states at the end of the double-blind period and the end of the open-label extension period (open-label extension analysis set). Remission was defined as a Birmingham Vasculitis Activity Score (BVAS) = 0 and oral glucocorticoid (OGC) dose ≤4 mg/d at the set time points. EULAR-defined remission was BVAS = 0 and OGC dose ≤7.5 mg/d.

Relapses

During the combined double-blind and OLE periods, 39 (59.1%) benralizumab/benralizumab patients and 35 (56.5%) mepolizumab/benralizumab patients had no relapses. During the first year of the OLE period, 51 (77.3%) benralizumab/benralizumab patients and 42 (67.7%) mepolizumab/benralizumab patients had no relapses; the 15 benralizumab/benralizumab patients with at least 1 relapse experienced a total of 26 relapses, while the 20 mepolizumab/benralizumab patients with at least 1 relapse experienced a total of 37 relapses. Few patients experienced >3 relapses during the first year of the OLE period (2 [3.0%] in the benralizumab/benralizumab group and 1 [1.6%] in the mepolizumab/benralizumab group). During the first year of the OLE period, the majority of relapses involved airway-related manifestations (44 [69.8%] asthma and/or sino-nasal), while 12 (19.0%) relapses involved nonairway manifestations (not asthma or sino-nasal); 7 (11.1%) relapses involved a combination of airway and nonairway manifestations. During the first year of the OLE period, the mean (SD) annualised relapse rate

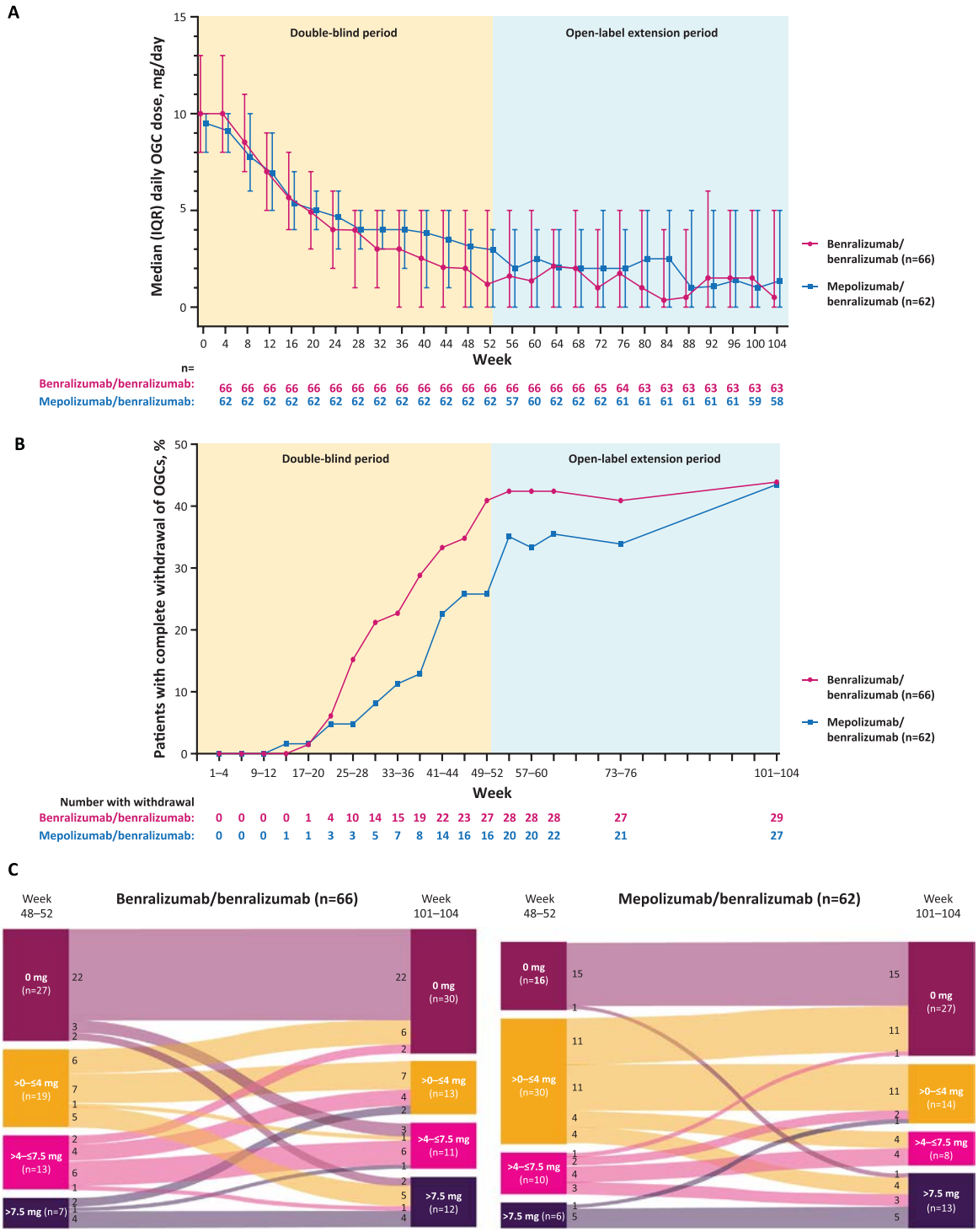

Figure 3. (A) Median (IQR) daily dose of oral glucocorticoids (OGCs), (B) proportion of patients with complete withdrawal of OGCs from baseline, and (C) flow of patients between different OGC doses between the end of the double-blind period and the end of the open-label extension period.

per patient was 0.40 (0.94) and 0.66 (1.15) in benralizumab/benralizumab and mepolizumab/benralizumab patients, respectively. One patient in each group experienced a major relapse. Supplementary Figure S1 shows the number of relapses by treatment group in the 2 years before study entry and on treatment.

Use of OGCs

The patient-level daily dose of OGCs throughout the study is shown as a heatmap in Supplementary Figure S2 (see Supplementary Fig S3 for a colour vision-friendly version) and as a spaghetti plot in Supplementary Figure S4.

During weeks 49 to 52 of the double-blind period, the median dose of OGCs was 1.18 mg/d for benralizumab/benralizumab patients and 2.96 mg/d for mepolizumab/benralizumab patients (Supplementary Table S1). At weeks 101 to 104 of the OLE period, the median dose of OGCs was 0.50 mg/d for benralizumab/benralizumab patients and 1.36 mg/d for mepolizumab/benralizumab patients (Fig 3A).

The percentage reduction from baseline in OGC use is shown in Supplementary Table S2. In the benralizumab/benralizumab patients, complete withdrawal of OGC use was achieved in 27 (40.9%) patients at weeks 49 to 52 and in 29 (43.9%) patients at weeks 101 to 104, demonstrating a durable response of 2 years

of benralizumab treatment (Fig 3B). Of the patients initially receiving mepolizumab, 16 (25.8%) achieved complete withdrawal of OGCs at weeks 49 to 52, and this percentage increased following the switch to benralizumab, reaching 27 (43.5%) at weeks 101 to 104 (Supplementary Fig S2). Of the patients with complete withdrawal of OGCs at weeks 48 to 52, 22/27 (81.5%) benralizumab/benralizumab patients and 15/16 (93.8%) mepolizumab/benralizumab patients were still OGC-free at weeks 101 to 104 (Fig 3C).

During the first year of the OLE period, the median (min, max) cumulative use of OGCs was 950 (0, 5904) mg in the benralizumab/benralizumab group and 791 (0, 4338) mg in the mepolizumab/benralizumab group compared with 1813 (486, 5674) mg and 1794 (640, 7999) mg, respectively, during the double-blind period. This represents a median percentage reduction of 61.0% in the benralizumab/benralizumab group and 62.5% in the mepolizumab/benralizumab group between the 2 study periods (Supplementary Table S3). The median (min, max) cumulative EGPA-related OGC dose was 159 (0, 5551) mg in the benralizumab/benralizumab group and 523 (0, 4262) mg in the mepolizumab/benralizumab group during the first year of the OLE period, compared with 1519 (486, 4761) mg and 1794 (640, 7999) mg, respectively, in the double-blind period. This represents a median percentage reduction of 88.0% and 76.2% in the benralizumab/benralizumab and mepolizumab/benralizumab groups, respectively, between the 2 study periods (Supplementary Table S3). There were differences in the cumulative OGC use between the study periods, but not between the treatment groups. The most common reasons for non−EGPA-related use of OGCs during the double-blind period and first year of the OLE period were AEs, which included COVID-19, adrenal insufficiency, sinusitis and bronchitis, and prophylaxis for adrenal insufficiency (Supplementary Table S4). During the first year of the OLE period, 7/20 patients in the benralizumab/benralizumab group and 9/23 patients in the mepolizumab/benralizumab group stopped or reduced their dose of non-OGC immunosuppressive therapies; 3 and 1 patients initiated immunosuppressive therapies or increased their non-OGC immunosuppressive dose, respectively. Heatmaps depicting patient-level doses of azathioprine, methotrexate, and mycophenolate mofetil and the occurrence of any type of relapse during the double-blind and OLE periods are shown in Supplementary Figure S5.

bEOS

bEOS remained low from week 1 throughout the first year of the OLE period in benralizumab/benralizumab patients (median [IQR], 20.0 [10.0, 40.0] cells/μL at weeks 52 and 100; Fig 4). In mepolizumab/benralizumab patients, further depletion of bEOS was seen at the first time point after switching to benralizumab, from a median (IQR) of 70.0 (40.0, 90.0) cells/μL at week 52 to 20 (10.0, 50.0) cells/μL at week 56; low levels were maintained through week 100 (Fig 4). Similar trends in the proportion of patients with bEOS ≤30 cells/μL in the different arms are shown in Supplementary Figure S6. Supplementary Figure S7 shows bEOS counts in individual patients.

Other outcomes

There were minimal changes in disease activity as assessed by the BVAS (Supplementary Fig S8) and minimal organ damage as assessed by increases in the VDI score (Supplementary Fig S9). Lung function was unchanged in both treatment groups throughout the 2-year treatment period (Supplementary Fig S10).

The mean ACQ-6 scores throughout the study are shown in Supplementary Figure S11A. The ACQ-6 response rate (a decrease from baseline in the ACQ-6 score of ≥0.5) was 45.5% and 40.3% in benralizumab/benralizumab and mepolizumab/benralizumab patients at week 104, respectively (Supplementary Fig S11B).

SNOT-22 scores were similar between groups (Supplementary Fig S12).

SF-36v2 physical and mental component scores remained consistent and were similar between both treatment groups throughout the double-blind and OLE periods (Supplementary Fig S13A,B).

WPAI-GH showed that a larger proportion of benralizumab/benralizumab-treated patients (29/66 [43.9%]) than

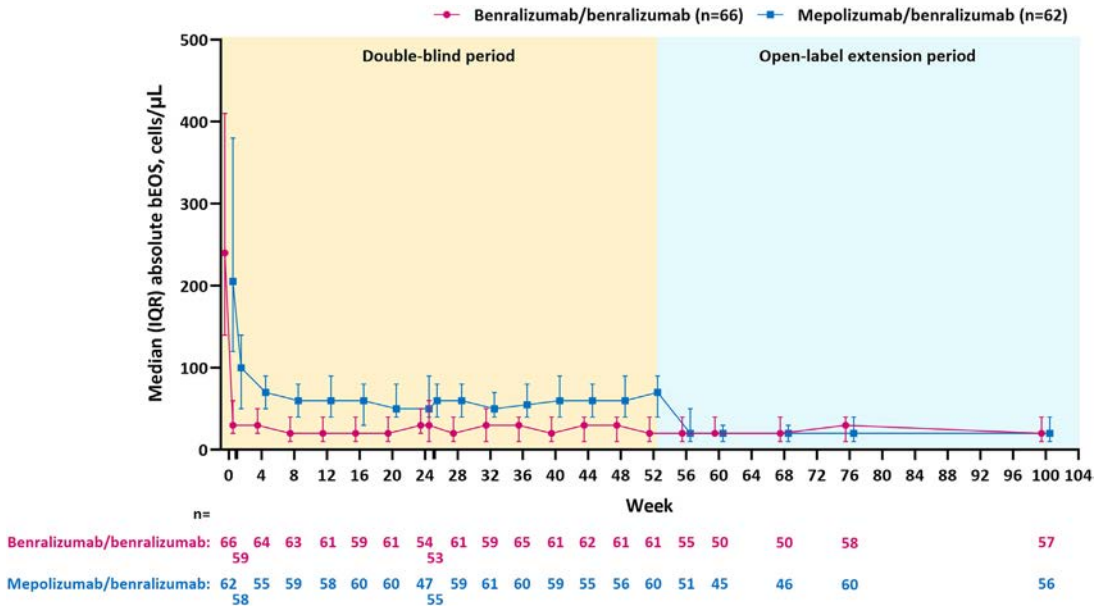

Figure 4. Absolute blood eosinophil count (bEOS) during the double-blind and open-label extension periods.

mepolizumab/benralizumab-treated patients (22/62 [35.5%]) were employed through week 100 (Supplementary Table S5).

Safety

During the double-blind period and first year of the OLE period, AEs were reported in 97.0% (64) of benralizumab/benralizumab patients and 100.0% (62) of mepolizumab/benralizumab patients (Table 2). The most commonly reported AEs in both the double-blind and 1-year OLE periods in the benralizumab/benralizumab and mepolizumab/benralizumab groups were COVID-19, nasopharyngitis, and sinusitis (Table 2 and Supplementary Table S6). Serious AEs were reported in 22.7% (15) of benralizumab/benralizumab patients and 35.5% (22) of mepolizumab/benralizumab patients. Two (3.0%) benralizumab/benralizumab patients and 3 (4.8%) mepolizumab/benralizumab patients experienced AEs leading to the discontinuation of treatment. There was 1 death in the mepolizumab/benralizumab group during the OLE period, which was not considered treatment-related (Table 2).

DISCUSSION

This study reports on a 2-year prospective description of patients with EGPA managed with anti-IL-5/receptor (anti-IL-5/R) therapies, and describes benralizumab treatment over 2 years as well as switching from 1 year of treatment with mepolizumab to 1 year of treatment with benralizumab. Benralizumab was associated with durable responses over the 1 year of treatment beyond the double-blind period, with over 60% of patients in remission at week 104. Overall, approximately 50% of patients achieved remission after 24 weeks of treatment and remained in remission over the next 18 months until week 104. The proportion of patients achieving remission was similar between patients who continued to receive benralizumab and those who switched from mepolizumab to benralizumab. Despite substantial reductions in OGC use, the majority of patients had no relapses over 2 years of treatment, which is similar to data available in a real-world setting following 2 years of treatment with mepolizumab [14] and benralizumab [16]. These high rates of continued remission contrast with relapse rates reported in smaller series of patients with organ-threatening disease treated with immunosuppressive therapies for remission induction, with 4/14 (28.6%) and 6/14 (42.9%) patients who received rituximab and cyclophosphamide, respectively, experienced a relapse following 3 years of treatment [26] and ~70% of azathioprine-treated patients experienced a relapse after up to 24 months of treatment [27]. However, it is difficult to directly compare the study populations between these studies.

The efficacy of 2 years of benralizumab treatment was also measured by patients' ability to completely discontinue OGCs. Over 40% of benralizumab/benralizumab-treated patients fully withdrew from OGCs in the first year, with continued full withdrawal of OGCs in the following year. In mepolizumab/benralizumab-treated patients, the proportion of patients who fully withdrew from OGCs increased after switching to benralizumab, with ~43% achieving discontinuation of OGCs by week 104. This proportion was similar to that in patients who continued benralizumab treatment, suggesting an additional OGC tapering effect in the patients who switched. Further benefits were also seen regarding the cumulative dose of OGCs, with a marked decrease in cumulative OGC dose in the second year of

Table 2
Summary of adverse events during the double-blind and open-label extension periods

Adverse events, n (%)	Open-label extension		Double-blind and open-label extension		
	Benralizumab/benralizumab (n = 66)	Mepolizumab/benralizumab (n = 62)	Benralizumab/benralizumab (n = 66)	Mepolizumab/benralizumab (n = 62)	Total while on benralizumab (N = 128)
Any AE	60 (90.9)	61 (98.4)	64 (97.0)	62 (100)	125 (97.7)
AEs by preferred term[a]					
COVID-19	25 (37.9)	33 (53.2)	35 (53.0)	47 (75.8)	68 (53.1)
Nasopharyngitis	8 (12.1)	15 (24.2)	12 (18.2)	20 (32.3)	27 (21.1)
Sinusitis	16 (24.2)	7 (11.3)	20 (30.3)	10 (16.1)	27 (21.1)
Headache	4 (6.1)	5 (8.1)	13 (19.7)	14 (22.6)	18 (14.1)
Arthralgia	4 (6.1)	4 (6.5)	14 (21.2)	11 (17.7)	18 (14.1)
Influenza-like illness	10 (15.2)	8 (12.9)	13 (19.7)	10 (16.1)	21 (16.4)
Bronchitis	8 (12.1)	3 (4.8)	12 (18.2)	7 (11.3)	15 (11.7)
Upper respiratory tract infection	5 (7.6)	7 (11.3)	7 (10.6)	10 (16.1)	14 (10.9)
Back pain	4 (6.1)	6 (9.7)	6 (9.1)	8 (12.9)	12 (9.4)
Urinary tract infection	4 (6.1)	5 (8.1)	8 (12.1)	6 (9.7)	13 (10.2)
Any serious AE	14 (21.2)	18 (29.0)	15 (22.7)	22 (35.5)	33 (25.8)
Serious AEs by system organ class					
Infections and infestations	6 (9.1)	6 (9.7)	6 (9.1)	9 (14.5)	12 (9.4)
Gastrointestinal disorders	1 (1.5)	4 (6.5)	1 (1.5)	4 (6.5)	5 (3.9)
Immune system disorders	2 (3.0)	3 (4.8)	2 (3.0)	3 (4.8)	5 (3.9)
Injury, poisoning, and procedural complications	2 (3.0)	3 (4.8)	2 (3.0)	3 (4.8)	5 (3.9)
Respiratory, thoracic, and mediastinal disorders	2 (3.0)	3 (4.8)	2 (3.0)	3 (4.8)	5 (3.9)
Nervous system disorders	1 (1.5)	1 (1.6)	3 (4.5)	1 (1.6)	4 (3.1)
Cardiac disorders	1 (1.5)	2 (3.2)	1 (1.5)	2 (3.2)	3 (2.3)
Hepatobiliary disorders	0 (0.0)	2 (3.2)	0 (0.0)	3 (4.8)	2 (1.6)
Endocrine disorders	0 (0.0)	2 (3.2)	0 (0.0)	2 (3.2)	2 (1.6)
Any AE leading to discontinuation of treatment	2 (3.0)	3 (4.8)	2 (3.0)	3 (4.8)	5 (3.9)
Any AE with an outcome of death	0 (0.0)	1 (1.6)	0 (0.0)	1 (1.6)	1 (0.8)

AE, adverse event.
[a] Ten of the most common adverse events are listed (frequency of >3%). Adverse events were classified using the Medical Dictionary for Regulatory Activities version 26.1.

benralizumab treatment and after treatment switch. Although there was no control group of patients treated with mepolizumab for 2 years for comparison, the long-term data from the OLE period of the MIRRA trial of mepolizumab in patients with EGPA were recently published [28]. This analysis showed that long-term discontinuation of OGCs following treatment with mepolizumab was achieved in 21% of patients with EGPA at 22 to 24 months of the OLE period and in 28% of patients at study exit [28]. These proportions are numerically lower than those observed with benralizumab treatment in the current study and reflect a similarly lower proportion of mepolizumab-treated patients in the double-blind period of the MIRRA study who achieved remission and complete withdrawal of OGCs [10] compared with the MANDARA study. These differences are likely due to changes in clinical practice since the publication of MIRRA, with increased confidence among investigators and patients regarding the reduction of OGCs while patients are on mepolizumab. Overall, the data from the randomised controlled setting support the benefits of the anti-IL-5/R therapy class regarding the total burden of OGC use and the potential to reduce OGC-related toxicity in patients with EGPA [5].

bEOS remained low in patients who continued to receive benralizumab. There was further depletion of blood eosinophils in patients who switched from mepolizumab to benralizumab after 4 weeks of switching (the first time point at which this was measured), and this effect was maintained with similar levels in both groups through week 104. This is consistent with the different mechanisms of action of benralizumab and mepolizumab; benralizumab has previously been shown to induce antibody-dependent cell-mediated cytotoxicity of blood eosinophils, leading to a faster and more profound depletion [29]. The correlation between greater eosinophil depletion and clinical benefits in EGPA remains unclear.

Other benefits of 2 years of treatment with these anti-IL-5/R therapies included maintaining asthma control, and lung function was unchanged in the second year of treatment, despite substantial reductions in the use of OGCs. Disease activity remained low, and there was little progression to organ damage. Safety was consistent with the known profile of benralizumab.

The results of this study are broadly consistent with retrospective data collected in real-world settings. Mattioli et al [30] compared mepolizumab and benralizumab in patients with EGPA and found that after 12 months, patients on benralizumab had significantly higher rates of remission (48.1% in the benralizumab group vs 32.4% among patients in the mepolizumab group; $p = .005$); however, there were no differences between the treatment groups in the proportion of patients withdrawing from OGCs (37.5% vs 26.9%, respectively; $p = .192$).

In another study, treatment of EGPA with benralizumab demonstrated that at 2 years, approximately 67.9% (36/53) of patients achieved remission (defined as BVAS = 0 and OGC dose ≤4 mg/d), and 68.3% (28/41) were fully off maintenance OGCs [16]. Another observational, real-world study of 49 patients with EGPA demonstrated that 69.2% (18/26) of patients treated with benralizumab and 43.5% (10/23) of patients treated with mepolizumab achieved remission at 2 years; 32.0% of benralizumab-treated patients and 23.8% of mepolizumab-treated patients discontinued OGC use [13]. Data from the Cottu et al [31] study demonstrated reduced rates of remission (36.7%) in benralizumab-treated patients who were previously administered mepolizumab. However, these patients did not respond to mepolizumab and thus may not be comparable to the mepolizumab/benralizumab group described in MANDARA, as many of the patients in the current study would have attained remission and OGC discontinuation before being switched to benralizumab. It is difficult to directly compare the results of the current study with prior publications due to (1) differences in retrospective observational data vs data from a prospective clinical trial, and (2) differences in the dosing of treatments; the majority of patients in these published real-world studies were treated with lower doses of mepolizumab and a less frequent dosing schedule of benralizumab than was used in MANDARA. Nonetheless, the overall data to date suggest that anti-IL-5/R therapies should now be considered a foundation for the management of EGPA.

Though the majority of patients in this combined 2-year analysis, spanning the 1-year double-blind period and year 1 of the OLE period, achieved remission and a majority experienced no relapses during the second year of treatment, a small proportion continued to experience frequent relapses, suggesting that in some patients, non–eosinophil-mediated inflammatory disease mechanisms remain active or non–eosinophil-based pathologic pathways are involved in the disease process. Further research is needed to understand what may be driving symptoms and disease activity in patients who continue to experience relapses while on benralizumab and mepolizumab, and how to best treat and manage patients who do not respond to anti-IL-5/R therapies.

Strengths of this study include the large sample size for a rare condition, the international representation of the study sites and participants, the prospective protocol-defined data collection, and the high level of retention of patients from the double-blind period to the OLE and during the OLE period.

There are some limitations to this study to consider. There was no mandatory tapering regimen for OGCs and other immunosuppressive drugs. Patients with newly diagnosed (<6 months), more 'vasculitic' disease manifestations or ongoing severe/life-threatening manifestations of EGPA were excluded from the trial, limiting the generalisability of the efficacy and safety profile of anti-IL-5/R therapies to these populations. It is not known if, in a large population, 2 years of mepolizumab therapy would have resulted in the same proportions of patients able to discontinue OGCs as those who switched to or were treated with benralizumab for 2 years in MANDARA. This limitation also applies to the decreases seen in the cumulative OGC burden.

In conclusion, the 2-year data from the phase 3 MANDARA study demonstrate that long-term treatment with benralizumab has a durable effect in achieving remission and tapering of OGCs in patients with EGPA. This tapering of OGCs was possible with low relapse rates and without loss of control of asthma or decline in lung function, suggesting that a substantial reduction of OGCs may be possible in the majority of patients with EGPA treated with anti-IL-5/R therapies.

Competing interests

PAM reports receiving consulting fees from AbbVie, Alpine Pharmaceuticals, Amgen, Argenx, AstraZeneca, Boehringer Ingelheim, Bristol Myers Squibb, CSL Behring, GSK, iCell, Interius BioTherapeutics, Kinevant Sciences, Kyverna, Metagenomi, Neutrolis, Novartis, NS Pharma, Q32 Bio, Quell Therapeutics, Regeneron Pharmaceuticals, Sanofi, Sparrow Pharmaceuticals, Takeda Pharmaceuticals, and Visterra; research support from AbbVie, Amgen, AstraZeneca, Boehringer Ingelheim, Bristol Myers Squibb, Eicos, Electra, GSK, Neutrolis, and Takeda; stock options from Kyverna, Q32, Lifordi, and Sparrow Pharmaceuticals; and royalties from UpToDate. PKN reports that his institution received grant support from AstraZeneca, Cyclomedica, Equillium, Foresee, Genentech, Sanofi, and Teva; he has also

received honoraria from Arrowhead Pharmaceuticals, AstraZeneca, CSL Behring, GSK, and Sanofi. NK reports receiving consulting fees and research support from AbbVie, Bristol Myers Squibb, and Sanofi; consulting fees only from GSK, Mallinckrodt Pharmaceuticals, Otsuka Pharmaceuticals, and Roche. BT reports receiving consulting fees from AstraZeneca, GSK, Novartis, and Vifor Pharma. BH received speaker fees and/or consultancies from AbbVie, Amgen, AstraZeneca, Boehringer Ingelheim, Bristol Myers Squibb, Chugai, GSK, InflaRx, Janssen, MSD, Novartis, Pfizer, Phadia, Roche, and CSL Vifor. AB reports receiving consultancy fees and speaker fees from Amgen, AstraZeneca, Boehringer Ingelheim, Chiesi, GSK, Novartis, and Sanofi Regeneron, and research grants from AstraZeneca, Boehringer Ingelheim, and GSK. DRWJ reports receiving speaker fees and/or consultancies from Amgen, AstraZeneca, Bristol Myers Squibb, Boehringer Ingelheim, ChemoCentryx, Chugai, GSK, Novartis, Roche, Takeda, and Vifor Pharma; advisory board member for Aurinia, Chinook, GSK, and Takeda. DJJ reports consultancy fees and speakers' fees from AstraZeneca, Boehringer Ingelheim, Chiesi, GSK, and Sanofi Regeneron, and research grants from AstraZeneca. FR reports receiving consulting fees from AstraZeneca, GSK, and Merck; royalties from UpToDate; and grant support from the FWO/F.R.S.-FNRS (EOS G0H1222N). CP reports receiving consulting and speaker fees from GSK, Otsuka, Pfizer, and Roche; grants and personal speakers or advisory board fees from Roche; served on advisory boards from AstraZeneca, GSK, and Otsuka; and received educational grants from GSK, Otsuka, and Pfizer. US reports receiving consulting fees from Amgen, Argenx, AstraZeneca, Boehringer Ingelheim, and CSL Vifor, and research grants from Amgen, AstraZeneca, Bristol Myers Squibb, Genentech, GSK, NorthStar Medical Radioisotopes, NS Pharma, and Novartis. LBS, CNH, MJ, CM, SN, ER-S, AS, and CW are or were employees of, and may own stock in, AstraZeneca. CM is currently an employee of Amgen. AS is currently an employee of Boehringer Ingelheim. MEW reports receiving consulting, advisory, or speaking honoraria from the following: Allakos, Amgen, Areteia Therapeutics, Arrowhead Pharmaceuticals, AstraZeneca, Avalo Therapeutics, Celldex, Connect Biopharma, Eli Lilly, Equillium, GSK, Incyte, Kinaset, Kymera, Merck, Phylaxis, Pulmatrix, Rapt Therapeutics, Recludix Pharma, Regeneron Pharmaceuticals, Roche/Genentech, Sanofi/Genzyme, Sentien, Sound Biologics, Tetherex Pharmaceuticals, Uniquity Bio, Upstream Bio, Verona Pharma, and Zurabio.

Acknowledgements

The authors thank the patients and their carers, as well as the site investigators and site staff who participated in this study. We also thank Yunhui Cao (AstraZeneca), Ying Fan (AstraZeneca), Yifan Zhu (ClinChoice Inc), and Sarah Cohen (ClinChoice Inc) for statistical design and analysis support. Medical writing support was provided by Caroline Ridley and Ella Palmer of Springer Health+, Springer Healthcare Ltd, UK, which was funded by AstraZeneca in accordance with Good Publication Practice (GPP 2022) guidelines. These data have been presented at the American Academy of Allergy, Asthma & Immunology (AAAAI)/World Allergy Organization (WAO) 2025 joint meeting [32].

Contributors

Conceptualisation: PAM, PKN, NK, BT, BH, DRWJ, DJJ, FR, and MEW. Data curation: PAM, PKN, NK, BT, BH, AB, DRWJ, DJJ, US, CP, FR, and MEW. Formal analysis: LBS, CNH, MJ, CM, SN, ER-S, AS, and CW. Investigation: PAM, PKN, NK, AB, BT, BH, DRWJ, DJJ, US, CP, FR, and MEW. Methodology: PAM, US, CP, FR, and MEW. Validation: LBS, MJ, and CW. Writing—original draft: all authors. Writing—review and editing: all authors.

Funding

This study was sponsored by AstraZeneca.

Patient consent for publication

Not applicable.

Ethics approval

The trial was approved by institutional review boards and independent ethics committees in participating countries and was conducted in accordance with the ethical principles of the Declaration of Helsinki and is consistent with International Council for Harmonization Good Clinical Practice guidelines, the applicable regulatory requirements, and the AstraZeneca policy on bioethics. All patients provided written informed consent.

Provenance and peer review

Not commissioned; externally peer reviewed.

Data availability statement

Data underlying the findings described in this manuscript may be obtained in accordance with AstraZeneca's data sharing policy described at https://astrazenecagrouptrials.pharmacm.com/ST/Submission/Disclosure.

Data for studies directly listed on Vivli can be requested through Vivli at www.vivli.org. Data for studies not listed on Vivli could be requested through Vivli at https://vivli.org/members/enquiries-about-studies-not-listed-on-the-vivli-platform/. The AstraZeneca Vivli member page is also available, outlining further details: https://vivli.org/ourmember/astrazeneca/.

Supplementary materials

Supplementary material associated with this article can be found in the online version at doi:10.1016/j.ard.2025.06.2131.

REFERENCES

[1] Jennette JC, Falk RJ, Bacon PA, Basu N, Cid MC, Ferrario F, et al. 2012 revised International Chapel Hill Consensus Conference Nomenclature of Vasculitides. Arthritis Rheum 2013;65(1):1–11.
[2] Fijolek J, Radzikowska E. Eosinophilic granulomatosis with polyangiitis - advances in pathogenesis, diagnosis, and treatment. Front Med (Lausanne) 2023;10:1145257.
[3] Grayson PC, Ponte C, Suppiah R, Robson JC, Craven A, Judge A, et al. 2022 American College of Rheumatology/European Alliance of Associations for Rheumatology classification criteria for eosinophilic granulomatosis with polyangiitis. Ann Rheum Dis 2022;81(3):309–14.
[4] Comarmond C, Pagnoux C, Khellaf M, Cordier JF, Hamidou M, Viallard JF, et al. Eosinophilic granulomatosis with polyangiitis (Churg-Strauss): clinical characteristics and long-term followup of the 383 patients enrolled in the French Vasculitis Study Group cohort. Arthritis Rheum 2013;65(1):270–81.
[5] Scherbacher PJ, Hellmich B, Feng YS, Löffler C. Prospective study of complications and sequelae of glucocorticoid therapy in ANCA-associated vasculitis. RMD Open 2024;10(1):e003956.

[6] Daugherty J, Lin X, Baxter R, Suruki R, Bradford E. The impact of long-term systemic glucocorticoid use in severe asthma: a UK retrospective cohort analysis. J Asthma 2018;55(6):651–8.
[7] Samson M, Puéchal X, Devilliers H, Ribi C, Cohen P, Stern M, et al. Long-term outcomes of 118 patients with eosinophilic granulomatosis with polyangiitis (Churg-Strauss syndrome) enrolled in two prospective trials. J Autoimmun 2013;43:60–9.
[8] Strehl C, Bijlsma JW, de Wit M, Boers M, Caeyers N, Cutolo M, et al. Defining conditions where long-term glucocorticoid treatment has an acceptably low level of harm to facilitate implementation of existing recommendations: viewpoints from an EULAR task force. Ann Rheum Dis 2016;75(6):952–7.
[9] Chung SA, Langford CA, Maz M, Abril A, Gorelik M, Guyatt G, et al. 2021 American College of Rheumatology/Vasculitis Foundation guideline for the management of antineutrophil cytoplasmic antibody-associated vasculitis. Arthritis Rheumatol 2021;73(8):1366–83.
[10] Wechsler ME, Akuthota P, Jayne D, Khoury P, Klion A, Langford CA, et al. Mepolizumab or placebo for eosinophilic granulomatosis with polyangiitis. N Engl J Med 2017;376(20):1921–32.
[11] Wechsler ME, Nair P, Terrier B, Walz B, Bourdin A, Jayne DRW, et al. Benralizumab versus mepolizumab for eosinophilic granulomatosis with polyangiitis. N Engl J Med 2024;390(10):911–21.
[12] Spataro F, Solimando AG, Di Girolamo A, Vacca A, Ria R. Efficacy and safety of benralizumab in eosinophilic granulomatosis with polyangiitis: a meta-analysis of eight studies. Eur J Clin Invest 2025;55(2):e14333.
[13] Nolasco S, Portacci A, Campisi R, Buonamico E, Pelaia C, Benfante A, et al. Effectiveness and safety of anti-IL-5/Ralpha biologics in eosinophilic granulomatosis with polyangiitis: a two-year multicenter observational study. Front Immunol 2023;14:1204444.
[14] Bettiol A, Urban ML, Dagna L, Cottin V, Franceschini F, Del Giacco S, et al. Mepolizumab for eosinophilic granulomatosis with polyangiitis: a European multicenter observational study. Arthritis Rheumatol 2022;74(2):295–306.
[15] Bettiol A, Urban ML, Padoan R, Groh M, Lopalco G, Egan A, et al. Benralizumab for eosinophilic granulomatosis with polyangiitis: a retrospective, multicentre, cohort study. Lancet Rheumatol 2023;5(12):e707–15.
[16] Nanzer AM, Maynard-Paquette AC, Alam V, Green L, Thomson L, Lam J, et al. Long-term effectiveness of benralizumab in eosinophilic granulomatosis with polyangiitis. J Allergy Clin Immunol Pract 2024;12(3):724–32.
[17] Menzies-Gow A, Flood-Page P, Sehmi R, Burman J, Hamid Q, Robinson DS, et al. Anti-IL-5 (mepolizumab) therapy induces bone marrow eosinophil maturational arrest and decreases eosinophil progenitors in the bronchial mucosa of atopic asthmatics. J Allergy Clin Immunol 2003;111(4):714–9.
[18] European Medicines Agency. Nucala [Internet]; 2015 [cited 2024 Oct 18]. Available from: https://www.ema.europa.eu/en/medicines/human/EPAR/nucala
[19] Food and Drug Administration. FDA approves first drug for eosinophilic granulomatosis with polyangiitis, a rare disease formerly known as the Churg-Strauss Syndrome [Internet]; 2017 [cited 2017 Dec 12]. Available from: https://www.fda.gov/news-events/press-announcements/fda-approves-first-drug-eosinophilic-granulomatosis-polyangiitis-rare-disease-formerly-known-churg
[20] Hellmich B, Sanchez-Alamo B, Schirmer JH, Berti A, Blockmans D, Cid MC, et al. EULAR recommendations for the management of ANCA-associated vasculitis: 2022 update. Ann Rheum Dis 2024;83(1):30–47.
[21] Kolbeck R, Kozhich A, Koike M, Peng L, Andersson CK, Damschroder MM, et al. MEDI-563, a humanized anti-IL-5 receptor alpha mAb with enhanced antibody-dependent cell-mediated cytotoxicity function. J Allergy Clin Immunol 2010;125(6):1344–1353.e2.
[22] Food and Drug Administration. Fasenra prescribing information [Internet]; 2017 [cited 2024 Sept 18]. Available from: https://www.accessdata.fda.gov/drugsatfda_docs/label/2024/761070s021lbl.pdf
[23] European Commission. Fasenra product information [Internet]; 2018 [cited 2024 Dec 24]. Available from: https://ec.europa.eu/health/documents/community-register/html/h1252.htm
[24] AstraZeneca. Fasenra 30mg subcutaneous injection syringe/pen approved in Japan for eosinophilic granulomatosis with polyangiitis (EGPA) [Internet]; 2024 [cited 2025 Jan 10]. Available from: https://www.astrazeneca.co.jp/media/press-releases1/2024/2024122703.html
[25] Hellmich B, Flossmann O, Gross WL, Bacon P, Cohen-Tervaert JW, Guillevin L, et al. EULAR recommendations for conducting clinical studies and/or clinical trials in systemic vasculitis: focus on anti-neutrophil cytoplasm antibody-associated vasculitis. Ann Rheum Dis 2007;66(5):605–17.
[26] Thiel J, Troilo A, Salzer U, Schleyer T, Halmschlag K, Rizzi M, et al. Rituximab as induction therapy in eosinophilic granulomatosis with polyangiitis refractory to conventional immunosuppressive treatment: a 36-month follow-up analysis. J Allergy Clin Immunol Pract 2017;5(6):1556–63.
[27] Puéchal X, Pagnoux C, Baron G, Lifermann F, Geffray L, Quémeneur T, et al. Non-severe eosinophilic granulomatosis with polyangiitis: long-term outcomes after remission-induction trial. Rheumatology (Oxford) 2019;58(12):2107–16.
[28] Wechsler ME, Silver J, Wolff G, Price RG, Verghis R, Weller PF, et al. Long-term safety and efficacy of mepolizumab in eosinophilic granulomatosis with polyangiitis. Arthritis Rheumatol 2025.
[29] Moran AM, Ramakrishnan S, Borg CA, Connolly CM, Couillard S, Mwasuku CM, et al. Blood eosinophil depletion with mepolizumab, benralizumab, and prednisolone in eosinophilic asthma. Am J Respir Crit Care Med 2020;202(9):1314–6.
[30] Mattioli I, Urban ML, Padoan R, Mohammad AJ, Salvarani C, Baldini C, et al. Mepolizumab versus benralizumab for eosinophilic granulomatosis with polyangiitis (EGPA): a European real-life retrospective comparative study. J Autoimmun 2025;153:103398.
[31] Cottu A, Groh M, Desaintjean C, Marchand-Adam S, Guillevin L, Puechal X, et al. Benralizumab for eosinophilic granulomatosis with polyangiitis. Ann Rheum Dis 2023;82:1580–6.
[32] Wechsler M, Nair P, Khalidi N, Terrier B, Hellmich B, Bourdin A, et al. L07 Two-year efficacy and safety of benralizumab for the treatment of eosinophilic granulomatosis with polyangiitis. J Allergy Clin Immunol 2025;155:AB430.

Ann Rheum Dis 84 (2025) 1900–1908

Contents lists available at ScienceDirect

Annals of the Rheumatic Diseases

journal homepage: https://www.sciencedirect.com/journal/annals-of-the-rheumatic-diseases

Vasculitis

AYLo study—elevated relapse risk and dysregulated proinflammatory signalling in giant cell arteritis patients with mosaic loss of the Y chromosome

Simon M. Petzinna[1,*], Sophie-Marie Kirch[1], Maike S. Adamson[1], De Xi[2], Claus-Jürgen Bauer[1], Lena Kreis[1], Reza Gheitasi[1], Pantelis Karakostas[1], Rayk Behrendt[2], Georg Nickenig[3], Sebastian Zimmer[3], Raul N. Jamin[3], Valentin S. Schäfer[1]

[1] *Medical Clinic III for Oncology, Hematology, Immune-Oncology and Rheumatology, University Hospital of Bonn, Bonn, Germany*
[2] *Institute for Clinical Chemistry and Clinical Pharmacology, University Hospital of Bonn, Bonn, Germany*
[3] *Department of Cardiology, University Hospital of Bonn, Bonn, Germany*

ARTICLE INFO

Article history:
Received 9 February 2025
Received in revised form 19 June 2025
Accepted 20 June 2025

ABSTRACT

Objectives: To assess the prevalence of mosaic loss of the Y chromosome (mLOY) in giant cell arteritis (GCA) and its impact on disease activity.

Methods: Patients diagnosed with GCA were prospectively recruited, and their leukocyte mLOY burden was analysed. The optimal mLOY threshold for predicting relapse was determined using the receiver operating characteristic curve and Youden index. Relapse-free survival was assessed using Kaplan-Meier analysis with the log-rank test. Levels of selected proinflammatory cytokines were quantified using a multiplex array.

Results: A total of 74 GCA patients were enrolled (mean, 76.0 years; SD, 10.7). At inclusion, 25.7% (19/74) of patients exhibited active disease. Relapses occurred in 23.0% of patients. The median mLOY burden was 17.8% (SD, 23.7%). An optimal threshold of 10.2% was identified for predicting relapse. Patients exceeding this cutoff had a significantly higher relapse risk ($P < .001$) with a shorter relapse-free survival (647 vs 992 days; $P < .001$). Multivariable Cox regression confirmed mLOY >10.2% as an independent predictor of relapse (hazard ratio, 17.4; 95% CI, 3.5-86.0; $P = .003$). In multiplex analysis, mLOY was positively associated with interleukin (IL)-6 ($P = .045$; r = 0.24) across the cohort, with elevated IL-6 levels in remission patients with mLOY >10.2% ($P = .010$). In patients undergoing IL-6 receptor inhibitor treatment and in remission, mLOY was significantly positively associated with IL-6 ($P = .002$; r = 0.54) and IL-17A ($P = .026$; r = 0.40).

Conclusions: This study is the first to identify mLOY as a strong, independent predictor of relapse risk and to link mLOY with modulated proinflammatory signalling in GCA. Our findings suggest mLOY as a prognostic biomarker and underscore its possible role in the pathophysiology of GCA.

*Correspondence to Dr Simon M. Petzinna, Medical Clinik III for Oncology, Hematology, Immune-Oncology and Rheumatology, Bonn, Germany.
E-mail address: Simon_Michael.Petzinna@ukbonn.de (S.M. Petzinna).
Simon M. Petzinna, Sophie-Marie Kirch, Raul N. Jamin and Valentin S. Schäfer contributed equally to this work.
Handling editor Josef S. Smolen.

https://doi.org/10.1016/j.ard.2025.06.2133

WHAT IS ALREADY KNOWN ON THIS TOPIC

- Giant cell arteritis (GCA) is a systemic vasculitis affecting individuals over 50 years, characterised by immune dysregulation, particularly involving Th1 and Th17 pathways.
- Mosaic loss of the Y chromosome (mLOY) is the most common somatic mutation in ageing men, associated with cancer, cardiovascular disease, and increased mortality.
- The presence of mLOY in leukocytes disrupts immune homeostasis by altering key Y chromosome genes, contributing to inflammation and the progression of age-related diseases.
- The connection between mLOY and autoimmune diseases, including GCA, is unexplored.

WHAT THIS STUDY ADDS

- This is the first study to identify mLOY as a strong, independent predictor of relapse risk with a highly increased hazard ratio in male GCA patients, with a threshold of 10.2% mLOY burden linked to significantly shorter relapse-free survival.
- A higher mLOY burden correlates with altered inflammatory signalling, including elevated interleukin (IL)-6 and IL-17A levels, particularly under IL-6 receptor inhibition, indicating activation of alternative inflammatory pathways.
- Our findings suggest that mLOY modulates leukocyte-driven inflammation, playing a mechanistic role in disease activity and progression in GCA.

HOW THIS STUDY MIGHT AFFECT RESEARCH, PRACTICE OR POLICY

- The study proposes that mLOY may be more than a simple epiphenomenon of ageing, potentially contributing to the initiation or maintenance of pathological immune responses in GCA.
- The burden of mLOY could serve as a prognostic biomarker in GCA, facilitating earlier identification of high-relapse risk patients.
- Future research should focus on clarifying the molecular and cellular mechanisms by which mLOY exacerbates GCA progression.

INTRODUCTION

As individuals age, they acquire somatic mutations across different cells, a process contributing to what is known as somatic mosaicism. Mosaic loss of the Y chromosome (mLOY) in leukocytes is the most common acquired somatic mutation in ageing men [1], detectable via genome sequencing data or single-nucleotide polymorphism (SNP) arrays [2]. Prior research in population-based studies has established a detection threshold of 10% mLOY [2,3]. Genome-wide association studies showed that mLOY in blood samples is <2% for men under 60 years of age, reaching 15% to 40% in 70- to 85-year-old males [4–7] and 57% in males at 93 years of age [2,7]. Besides age, risk factors include smoking, air pollution, and genetic predisposition [3,6,8].

Pathophysiologically, mLOY is associated with genomic instability, impaired DNA repair, and reduced p53 signalling [2,4,9], as well as increased cancer risk and adverse outcomes in solid and haematological cancer [4,10]. Beyond malignancy, mLOY is associated with age-related conditions such as cardiovascular disease [11], stroke [12], Alzheimer disease [9], chronic kidney disease [13], and increased overall mortality [14]. While epidemiological associations are well-documented, mechanistic insights remain scarce.

Recent studies have highlighted the functional consequences of mLOY in leukocytes, primarily linked to the loss of epigenetic modifiers located on the Y chromosome, such as UTY [15] and KDM5D [16]. Loss of these genes alters chromatin structure, leading to the upregulation of gene expression, particularly in MAPK signalling pathways [11,15,16]. Additionally, mLOY also affects immune homeostasis by altering lymphoid subsets, including (FOXP3+) regulatory T cells (Tregs), terminal effector memory T cells, and interleukin (IL)-C3 subsets [17]. The proinflammatory and profibrotic effects of mLOY suggest a possible role in age-dependent rheumatologic conditions. However, to what extent mLOY occurs in and how it impacts the immunopathology of specific age-dependent rheumatologic conditions has not been studied.

An example of the immunopathologic potential of somatic haematopoietic mutations is VEXAS (vacuoles, E1 enzyme, X-linked, autoinflammatory, somatic) syndrome [18]. Caused by acquired mutations in the UBA1 gene within haematopoietic stem and progenitor cells, VEXAS syndrome manifests with autoinflammatory symptoms that can mimic rheumatologic conditions [18,19]. Vasculitis has increasingly been reported as a clinical manifestation in VEXAS [19]. While cutaneous small-vessel inflammation is most common, data indicate that up to one-quarter of individuals develop large or medium-sized vessel vasculitis [19–21]. Analogously, mLOY may represent a more prevalent form of acquired somatic mosaicism, contributing to age-related immune dysregulation and vasculitis.

Giant cell arteritis (GCA) is thus a promising candidate for further investigation, as it exclusively affects individuals over the age of 50, with a median age of 70 years [22]. It is the most prevalent systemic vasculitis in Western populations, with a lifetime risk of 1.0% in women and 0.5% in men [23]. Severe inflammation, neoangiogenesis, and vascular remodelling in GCA can lead to stenosis, occlusion, and complications [22]. While standalone corticosteroid therapy often results in high-relapse rates, IL-6 receptor blockade has improved outcomes [24]. However, its limited efficacy in a subset of patients suggests the presence of IL-6–independent immunotypes, which, when uncovered, could inform stratification for alternative treatment approaches [25].

Recent evidence underscores the complex innate and adaptive immune dysregulation in GCA [25]. Although initially attributed to Th1+ cell-mediated pathways and subsequent interferon (IFN)-γ–driven immune cell migration, Th17+ cells and associated cytokines (eg, IL-17 and IL-21) are now recognised as pivotal in sustaining inflammation [26,27]. Both Th1+ and Th17+ cells release proinflammatory cytokines [28,29] that contribute to the recruitment of cytotoxic CD8+ T cells [30] and the activation of monocytes, which then differentiate into macrophages, driving vascular damage [31–33]. Understanding the Th1+/Th17+ axis is crucial for explaining the limited efficacy of IL-6 receptor blockade in the treatment of GCA [24,34]. Primarily produced by macrophages in the adventitial layer [31–33], IL-6 is elevated in GCA and drives Th17+ cell development via FOXP3 splicing in Tregs [28,35].

Given the overlapping evidence of mLOY and GCA-associated immune dysregulation, we hypothesise that mLOY may contribute to GCA pathophysiology. Therefore, this study aimed to elucidate the clinical impact, mechanistic relevance, and pathophysiological role of mLOY in GCA.

METHODS

Patient characteristics and clinical assessment

Male patients diagnosed with GCA were recruited for a cross-sectional study conducted at the Department of Rheumatology

and Clinical Immunology, University Hospital Bonn, Germany. Diagnosis was confirmed by a board-certified rheumatologist. Inclusion criteria included age >50 years and fulfilment of the American College of Rheumatology/European Alliance of Associations for Rheumatology classification criteria for GCA [36]. The therapy decision was made by the treating rheumatologist.

Comprehensive demographic and clinical data were assessed at diagnosis, study inclusion, and in the case of relapse. Collected parameters included GCA-related symptoms, disease manifestation, laboratory parameters (including C-reactive protein [CRP] and complete blood count), and glucocorticoid and/or disease-modifying antirheumatic drug (DMARD) therapy. Additionally, data on disease and treatment history, time of diagnosis, follow-up duration, and the frequency and timing of relapses were systematically documented in the AutoimmunitY and Loss of Y (AYLo) trial. The study was registered on ClinicalTrials.gov under the identifier NCT06696027.

Imaging data, including vascular ultrasound, magnetic resonance imaging, and positron emission tomography-computed tomography, were obtained to evaluate vascular involvement. For vascular ultrasound, the Outcome Measures in Rheumatology (OMERACT) GCA Ultrasonography (OGUS) score was calculated as previously described to assess and quantify vascular abnormalities [37,38].

Assessment of mLOY

At the time of inclusion, whole blood was collected and subsequently stored at the Biobank Bonn. DNA elution was conducted using the GeneJET Whole Blood DNA Elution Mini Kit, and DNA concentrations were normalised using a NanoDrop (both Thermo Fisher Scientific). For loss of the Y chromosome (LOY) analysis, a Droplet Digital PCR System (Naica) was used with a 16.000-droplet chip employing a SNP assay targeting a 6 bp difference between the AMELX and AMELY genes (Thermo Fisher Scientific, hCV990000001), with the fluorophore (VIC) dye detecting AMELX and the 6-carboxyfluorescein (FAM) dye detecting AMELY. Analysis was conducted using the manufacturer's software, and the extent of LOY was calculated as 1 −(Concentration AMELY/Concentration AMELX).

Assessment of proinflammatory signalling

To evaluate proinflammatory signalling, cytokine concentration in the serum of GCA patients was assessed after a 1:2 dilution using the LEGENDplex Human Inflammation Panel 1 (13-plex) Assay Kit (BioLegend) according to the manufacturer's instructions. Data analysis was conducted using the LEGENDplex online software (https://legendplex.qognit.com).

Statistical analysis

Statistical analyses were performed utilising SPSS (version 29.0.2.0, IBM), R (version 4.4.2, R Core Team), and GraphPad Prism 10 (GraphPad Software). Continuous data showing a Gaussian distribution are presented as means with SD, and continuous data showing a non-Gaussian distribution are displayed as medians with 95% CIs. Categorical data are expressed as percentages. The Shapiro-Wilk test was used to evaluate the normality of data distributions. For nonnormally distributed continuous variables, comparisons were made using the Mann-Whitney U test; categorical variables were assessed with the chi-square test. Continuous variables following a normal distribution were analysed using the Student *t*-test. Receiver operating characteristic (ROC) curve analysis was performed to evaluate model performance, with Youden index employed to identify the optimal threshold for LOY in predicting relapse. Kaplan-Meier survival analysis with log-rank testing was used to explore univariate relapse-free survival. Multivariable Cox regression analysis was conducted to adjust for potential confounders, with proportional hazard assumptions validated through Schoenfeld residuals. The association between mLOY and cytokine levels was conducted with Pearson correlation (r) after log-transforming the values to minimise outlier influence. A 2-tailed *P* value of <.05 was considered statistically significant. Data visualisation was carried out using GraphPad Prism and SPSS.

Given the number of demographic characteristics assessed in Table 1, we acknowledge the potential for statistical error due to multiple comparisons. However, as the table is primarily descriptive, no formal correction for multiple testing was applied to avoid overlooking potentially meaningful differences in the mLOY-stratified cohorts. This approach aimed to reduce bias in exploratory subgroup analysis, particularly as some of these variables may influence relapse risk.

Patient and public involvement statement

This project was discussed and reviewed in collaboration with patient representatives as part of the Patient Advisory Board of the Department of Rheumatology, University Hospital of Bonn to ensure alignment with patient needs and perspectives.

Ethical approval

The AYLo study was conducted in accordance with the Declaration of Helsinki and received approval from the ethics committee of the University Hospital Bonn, Germany (reference number: 321/22).

RESULTS

Patient characteristics and clinical assessment

The AYLo study included 74 male patients with confirmed GCA. The mean age at diagnosis was 76.0 years (SD, 10.7). Detailed demographics are presented in Table 1.

At diagnosis, visual impairment was the most common GCA-related symptom (48/74). Large vessel involvement was identified in 28 patients, with aortic manifestations in 8. Laboratory analysis showed elevated CRP levels at diagnosis (median, 29.0 mg/L; 95% CI, 0.9-252.8) and normal levels at study inclusion (median, 0.9 mg/L; 95% CI, 0.5-71.4). After diagnosis, all patients had received prednisolone therapy per the Giant-Cell Arteritis Actemra (GiACTA) protocol for 26 weeks, with additional intravenous prednisolone (250 mg for 5 days) in case of visual symptoms.

At inclusion, 25.7% (19/74) of patients exhibited active disease, while 32 patients were receiving prednisolone therapy with a mean cumulative dose of 3231.5 mg (SD, 3357.5). Adjunctive biological DMARD therapy, which was exclusively IL-6 receptor inhibition (tocilizumab), was administered to 32 patients at the time of inclusion.

During follow-up, 23.0% (17/74) of patients experienced at least 1 relapse, with 4.0% (3/74) having multiple relapses. The overall median follow-up time was 360 days (95% CI, 205-434). In patients with mLOY <10.2%, the median follow-up was 384 days (95% CI, 332-547), and 300 days (95% CI, 255-518) in those with mLOY >10.2% (P = .533). No deaths occurred during follow-up.

Table 1
Patient characteristics and clinical assessment

	Overall (n = 74)	mLOY <10.2% (n = 47)	mLOY >10.2% (n = 27)	*P* value
Patient characteristics/clinical assessment				
Age (y), mean (SD)	75.99 (10.7)	73.38 (11.2)	80.27 (8.2)	.006[a]
Follow-up (d), median (95% CI)	360 (205-434)	384 (332-547)	300 (255-518)	.533
Aortal manifestation, n (%)	8 (32)	6 (31.6)	2 (33.2)	.936
Large vessel involvement (yes), n (%)	28 (48.3)	20 (51.3)	8 (42.1)	.512
OGUS (at diagnosis), mean (SD)	0.91 (0.56)	0.93 (0.57)	0.87 (0.56)	.690
Current prednisolone (yes), n (%)	32 (47.1)	20 (46.5)	12 (48.0)	.744
Dose prednisolone (mg), mean (SD)	3231.5 (3357.5)	3306.6 (3673.3)	3107.5 (2822.2)	.813
Current TCZ (yes), n (%)	32 (43.2)	19 (41.3)	13 (50)	.613
Duration TCZ (d), mean (SD)	172.6 (240)	164.1 (223.1)	187.4 (272.9)	.901
CRP at diagnosis (mg/L), median (95% CI)	29.0 (0.9-252.8)	50.0 (1.0-259.9)	16.6 (0.7-162.9)	**.022**[a]
CRP at inclusion (mg/L), median (95% CI)	0.9 (0.55-71.4)	0.75 (0.6-84.0)	1.21 (0.5-38.0)	.949
Leukocytes (G/L), mean (SD)	9.1 (3.8)	9.3 (4.0)	8.7 (3.5)	.502
Symptoms (at diagnosis), n (%)				
Visual impairment (yes)	48 (64.9)	30 (65.2)	18 (64.3)	.935
Shoulder/pelvic pain (yes)	16 (25.0)	11 (28.2)	4 (16.0)	.264
Night sweat (yes)	9 (19.6)	7 (23.3)	2 (12.5)	.378
Weight loss (yes)	13 (27.7)	12 (37.5)	1 (6.7)	**.028**[a]
Fatigue (yes)	8 (22.9)	5 (21.7)	3 (25.0)	.827
Headache (yes)	28 (42.4)	19 (47.5)	9 (34.6)	.301
Claudicatio (yes)	12 (19.4)	8 (20.0)	4 (18.2)	.862
Preconditions, n (%)				
Hypertension (yes)	47 (67.1)	27 (61.4)	20 (76.9)	.181
Diabetes mellitus (yes)	24 (33.8)	13 (28.9)	11 (42.3)	.321
Apoplex/transient ischaemic attack (yes)	9 (12.4)	4 (8.9)	5 (17.9)	.137
Coronary heart disease (yes)	19 (27.9)	11 (26.2)	8 (30.8)	.683
Neurological precondition (yes)	4 (5.5)	3 (6.7)	1 (3.6)	.572
Ophthalmological precondition (yes)	11 (15.2)	5 (11.1)	6 (21.5)	.334
Autoimmune disease (yes)	9 (12.2)	5 (10.9)	4 (14.3)	.663
Malignant disease (yes)	13 (21)	6 (16.2)	7 (28)	.264

CRP, C-reactive protein; mLoY, mosaic loss of Y chromosome; OGUS, Outcome Measures in Rheumatology ultrasonography score; TCZ, tocilizumab.
The table presents an overview of patient characteristics and clinical parameters stratified by the degree of mLoY (mLoY <10.2% vs mLoY ≥10.2%).
[a] $P < .05$ indicates statistical significance and is marked bold.

Assessment of mLOY

The median mLOY burden in whole blood was 17.8% (SD, 23.7%), with 39.2% (29/74) displaying a mLOY >10.0%. Analysis of the ROC curve and Youden index identified an optimal mLOY threshold of 10.2% for predicting GCA relapse, demonstrating adequate model performance (area under the curve [AUC] = 0.706; $P = .006$) (Supplementary Fig). At inclusion, 36.4% (27/74) of patients exceeded this threshold.

Patients with mLOY >10.2% were older (mean, 80.27 vs 73.38 years; $P = .006$) and had significantly lower CRP levels at diagnosis (mean, 16.6 vs 50.0 mg/L; $P = .022$). Total cumulative prednisolone exposure did not significantly differ between groups (mean, 3107.5 mg vs 3306.6 mg; $P = .813$). Comorbidities, including hypertension ($P = .181$), diabetes ($P = .321$), coronary heart disease ($P = .683$), and other cardiovascular conditions, as well as previous autoimmune or malignant diseases, were comparable between groups. Similarly, GCA-related symptoms, such as visual impairment ($P = .935$) and headache ($P = .301$), as well as large vessel involvement ($P = .512$) and vascular ultrasound (OGUS, $P = .690$) results, showed no significant differences.

Within a 3-year follow-up, 43.1% of patients with mLOY >10.2% suffered a relapse compared with only 8.7% of patients with mLOY <10.2% ($P < .001$, univariate Kaplan-Meier log-rank analysis) (Fig 1). The median relapse-free survival was 647 days (95% CI, 468-827) in patients with mLOY >10.2% compared with 992 days (95% CI, 898-1087) in those with mLOY <10.2%. Multivariable Cox regression analysis, adjusted for age and clinical factors associated with relapse risk [39], identified mLOY >10.2% as the sole independent predictor of relapse (hazard ratio [HR], 17.4; 95% CI, 3.5-86.0; $P = .003$) (Fig 2, Supplementary Table S1).

Assessment of proinflammatory signalling

Multiplex analysis revealed a significant association between mLOY and proinflammatory cytokine expression. In the overall cohort, mLOY, as a continuous variable, was positively associated with IL-6 ($P = .045$; r = 0.24; Fig 3). As IL-6 levels are strongly influenced by treatment regimen (eg, IL-6 receptor blockade) and disease activity, we performed stratified subgroup analyses.

Among patients in remission (n = 45), individuals with mLOY levels >10.2% exhibited significantly higher IL-6 concentrations compared with those with a lower mLOY burden ($P = .010$; Table 2). In this subgroup, mLOY burden (as a continuous variable) also showed a positive correlation with IL-6 levels ($P = .046$; r = 0.24). This relationship was most pronounced in patients in remission receiving tocilizumab, where mLOY burden was significantly associated with IL-6 ($P = .002$; r = 0.54) and IL-17A ($P = .026$; r = 0.40). Additionally, trends were observed for IFN-γ ($P = .052$; r = 0.35), tumour necrosis factor (TNF)-α ($P = .104$; r = 0.30), and IL-23 ($P = .063$; r = 0.34), which narrowly missed statistical significance. In contrast, no significant associations between mLOY and cytokine levels were observed in patients with active disease, treatment-free remission, or other treatment regimens (all $P > .05$).

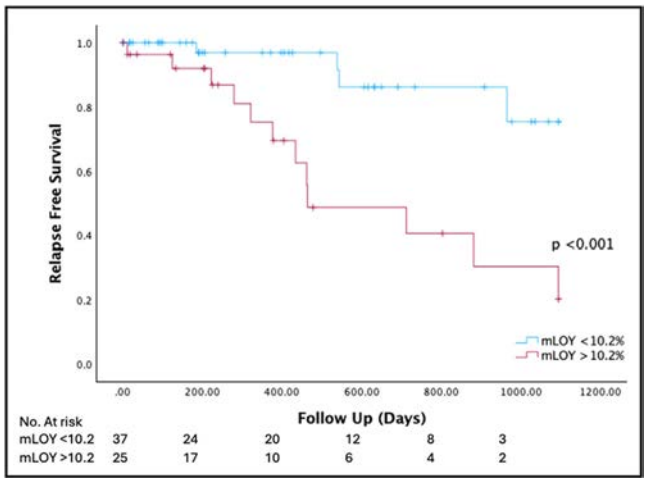

Figure 1. Survival analysis for predicting relapse in patients with giant cell arteritis. The figure depicts the relationship between mosaic loss of Y chromosome (mLOY) burden and relapse risk in giant cell arteritis patients. Kaplan-Meier survival analysis demonstrates that patients with mLOY >10.2% had a significantly higher relapse risk ($P < .001$, univariate log-rank test) and a shorter median relapse-free survival (647 days; 95% CI, 468-827) compared with those with mLOY <10.2% (992 days; 95% CI, 898-1087; $P < .001$).

Furthermore, we investigated whether IL-6 levels at the time of measurement were associated with relapse risk. This analysis was conducted in the overall cohort and across relevant subgroups, stratified by mLOY status, disease activity, and treatment regimen. No statistically significant association between IL-6 levels and relapse risk was observed in any of these analyses (all $P > .05$). The IL-6 levels stratified by tocilizumab treatment and mLOY status are shown in Supplementary Table S2.

DISCUSSION

This is the first study to investigate the role of mLOY in GCA and its impact on disease activity, relapse risk, and its possible role in immunopathology. In our cross-sectional study, we identified a high prevalence of mLOY among male GCA patients, with a median mLOY burden of 17.8% (SD, 23.7%) and 37.8% of patients exhibiting mLOY >10%. This frequency substantially exceeds previously reported rates of 10% to 20% in men over 50 years of age and 15% to 40% in 70- to 85-year-old males [3–7,40]. However, caution is warranted when comparing mLOY prevalence and threshold effects across studies, as detection methodologies vary. Most large-scale cohorts have relied on whole-genome sequencing, which detects mLOY at fractions around 10%, depending on sequencing depth and quality.

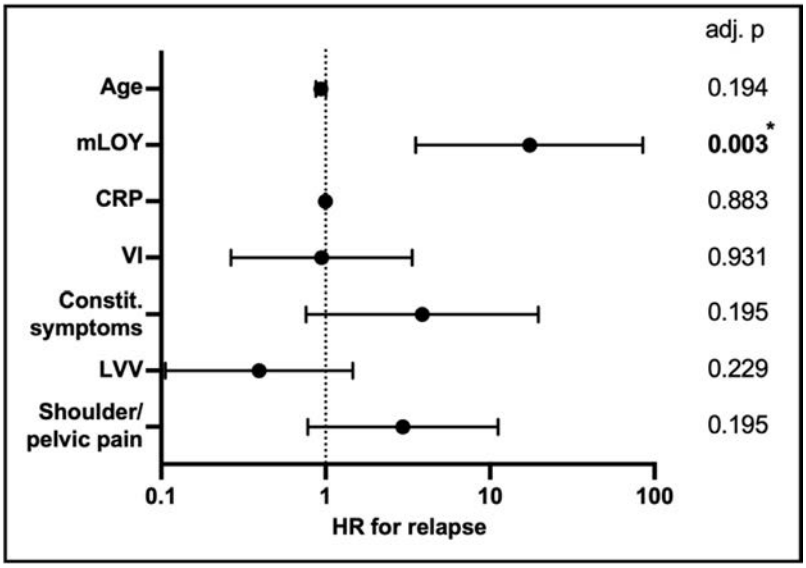

Figure 2. Cox regression analysis of risk factors associated with relapse in giant cell arteritis. This figure presents a forest plot summarising the Cox regression analysis of relapse risk in patients with giant cell arteritis, adjusting for factors potentially associated with relapse risk. The model included 7 variables: age, mosaic loss of the Y chromosome (mLOY) burden >10.2%, C-reactive protein (CRP) levels, visual impairment (VI), constitutional (Constit.) symptoms (fever, night sweats, and weight loss), large vessel vasculitis (LVV), and shoulder or pelvic pain. adj. p, adjusted P value; HR, hazard ratio. *$P < .05$ indicates statistical significance.

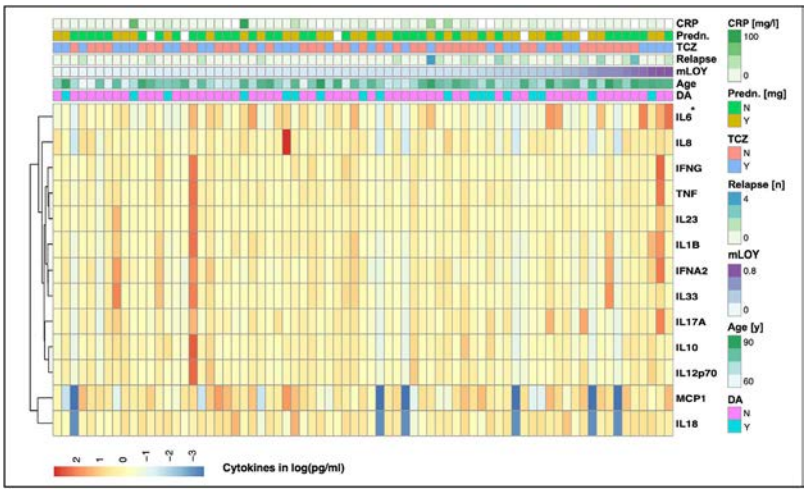

Figure 3. Inflammatory cytokine profile, mosaic loss of the Y chromosome (mLoY), and clinical parameters in giant cell arteritis patients. The figure depicts inflammatory cytokines measured by LegendPlex, shown as a heatmap. Clinical parameters are depicted above the columns. In the overall cohort, mLOY, as a continuous variable, was positively associated with interleukin (IL)-6 ($P = .045$). CRP, C-reactive protein; DA, disease activity; IFN, interferon; MCP, monocyte chemoattractand protein; N, no; Predn., prednisolone; TCZ, tocilizumab; TNF, tumour necrosis factor; Y, yes. *$P < .05$ indicates statistical significance.

Table 2
Inflammatory cytokine profile, mosaic loss of the Y chromosome, and disease activity in giant cell arteritis patients

Cytokine	Active disease			Remission		
	mLOY >10.2% (n = 10)	mLOY <10.2% (n = 8)	*P* value	mLOY >10.2% (n = 16)	mLOY <10.2% (n = 39)	*P* value
IL-1ß	313.6	315.2	.976	298.4	347.1	.307
IFN-α2	622.3	647.8	.875	515.1	618.3	.306
IFN-γ	271.1	254.9	.513	292.4	322.4	.332
TNF-α	266.6	257.6	.817	363.1	268.8	.364
MCP-1	7970.0	6351.0	.664	9390.0	8487.0	.602
IL-6	603.2	483.5	.236	1623.0	911.2	.010[a]
IL-8	935.3	838.3	.670	804.2	850.9	.693
IL-10	620.0	644.5	.868	503.8	596.1	.218
IL-12p70	553.9	668.6	.390	556.3	609.8	.453
IL-17A	532.0	674.7	.334	723.4	567.5	.156
IL-18	9585.0	100,093.0	.875	9225.0	8760.0	.743
IL-23	505.6	471.1	.277	513.4	520.5	.864
IL-33	594.6	544.4	.565	564.2	602.8	.648

IFN, interferon; IL, interleukin; mLOY, mosaic loss of Y chromosome; TNF, tumour necrosis factor.
The table presents the expression levels of 13 human inflammatory cytokines (pg/mL, mean) in relation to mLOY burden (mLOY ≥10.2% vs mLOY <10.2%) and disease activity (active disease vs remission) in patients with giant cell arteritis. A *t*-test was performed to assess differences between these groups. A significant difference was observed in IL-6 among patients in remission.
[a] $P < .05$ indicates statistical significance and is marked bold.

Beyond age, no clinical confounders, including cardiovascular comorbidities, autoimmune diseases, or malignancies, were associated with mLOY status. Furthermore, mLOY burden did not correlate with disease manifestation, including large vessel involvement, vascular imaging abnormalities, visual impairment, or typical GCA symptoms.

Our findings demonstrate a strong association between mLOY and increased relapse risk in male GCA patients. A mLOY threshold of 10.2% was identified as the optimal predictor of relapse, supporting prior research defining 10.0% as a relevant cutoff value [2,3]. Patients with mLOY >10.2% had a significantly elevated relapse risk with a highly increased HR, even after adjusting for age ($P = .003$; HR, 17.4; Fig 2). Importantly, mLOY emerged as the sole significant predictor of relapse in this cohort, while conventional clinical variables showed no association. The median relapse-free survival was significantly shorter in patients with mLOY >10.2% compared with those with mLOY <10.2% (647 vs 992 days; Fig 1). The robustness of the HR for mLOY >10.2% is particularly notable given the slightly shorter median follow-up in this group (384 vs 300 days), which may have led to an underestimation of relapse rates. These findings align with prior studies linking mLOY to adverse outcomes in haematologic, oncologic, and cardiovascular diseases, where mLOY serves as an early biomarker for heightened disease risk and is hypothesised to contribute to disease immunopathogenesis [2,4,10–14]. However, age itself was not associated with relapse risk in our cohort. This apparent discrepancy may be explained by the notion that mLOY reflects biological rather than chronological ageing, marking a subset of older individuals with haematopoietic alterations or immune dysfunction.

In this context, our study reveals that mLOY burden is associated with altered inflammatory signalling. Patients with mLOY >10.2% displayed significantly lower CRP levels at diagnosis. While CRP is typically elevated in inflammatory conditions, in the context of mLOY in GCA, CRP levels appear to be lower in patients with mLOY burden. This paradoxical finding supports previous observations in broader populations, although the underlying mechanisms remain unclear [41].

In contrast, multiplex analysis revealed significant positive associations between mLOY burden and IL-6 levels (Fig 3), a cytokine central to GCA pathogenesis. This finding is consistent with observations in cardiovascular disease and supports a potential link between mLOY and persistent inflammation predisposing to relapse [15]. The association was most pronounced in patients in clinical remission under tocilizumab, where mLOY positively correlated with IL-6 and IL-17A and was narrowly missing significance for IFN-γ, TNF-α, and IL-23. Our results suggest that mLOY-associated immune activation may persist even when the IL-6 pathway is pharmacologically inhibited. Notably, despite elevated IL-6 levels in this subgroup, no direct association with relapse risk was detected. This discrepancy may reflect the multifactorial nature of inflammation in mLOY-positive patients, limitations due to treatment heterogeneity and small subgroup sizes, or the constraints of single-timepoint measurements in capturing the dynamic immunologic changes preceding relapse.

The observed alterations in proinflammatory signalling may stem from several mechanisms. Recent evidence links circulating macrophages to the interplay between mLOY and cardiac disease [42], potentially paralleling altered signalling in GCA. One potential mechanism involves the loss of Y chromosome-encoded ubiquitously expressed epigenetic modifiers, such as UTY and KDM5D, which are critical for chromatin remodelling and transcriptional regulation [15,16]. Dysregulation of these processes in GCA may impair immune homeostasis and perpetuate inflammation via the activation of transcription factors, such as Elk3, Cux1, and Ctcf, as well as toll-like receptor pathways [15]. Enhanced transforming growth factor-β/SMAD signalling due to loss of UTY has been demonstrated to exacerbate cardiac fibrosis in heart failure. Beyond macrophages, mLOY may impact Tregs [17,43]. While mLOY in Tregs has been associated with cancer progression and mortality, its role in GCA remains unclear. In GCA, IL-6–driven alternative splicing of FOXP3 to FOXP3Δ increases IL-17 production in regulatory $CD161^{+}CD25^{-}$ T cells, which are elevated during active disease [25,35]. Tocilizumab reduces these FOXP3Δ2 Tregs, highlighting potential

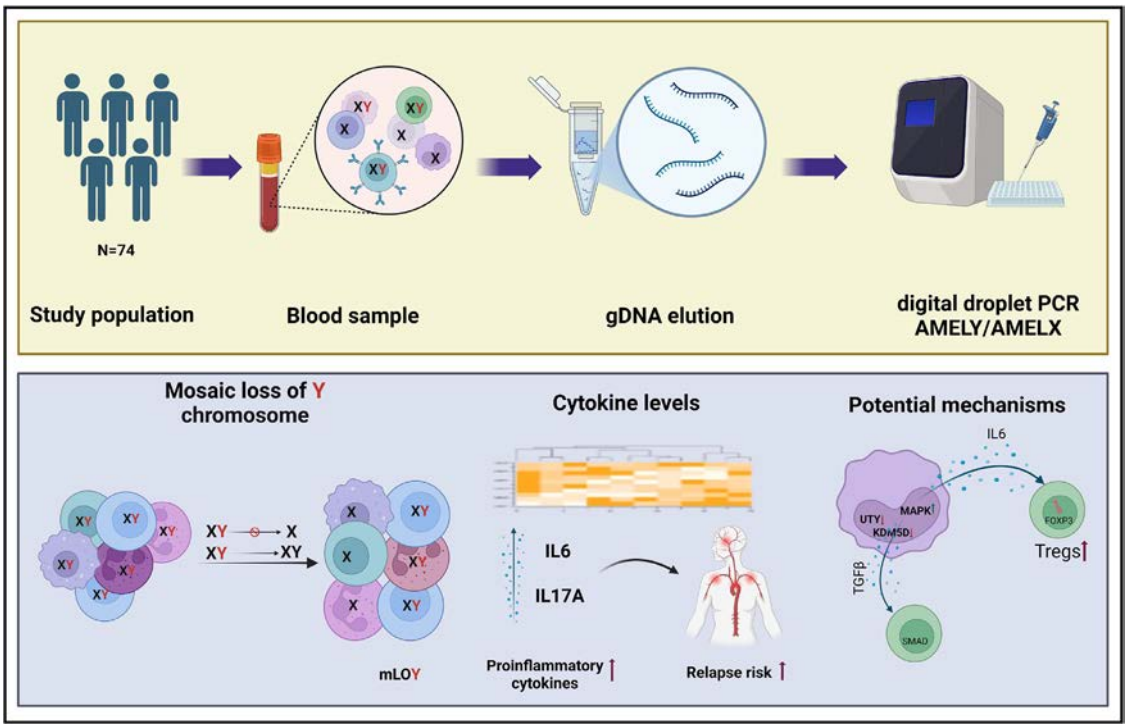

Figure 4. Methodological approach and mosaic loss of the Y chromosome (mLOY) in giant cell arteritis. The figure illustrates the methodological workflow for determining mLOY (upper panel) and its potential pathophysiological implications (lower panel). The upper panel provides a schematic overview of the analytical steps used to assess mLOY in PBMCs. The lower panel depicts the development of mLOY burden in PBMCs, alterations in proinflammatory signalling pathways and relapse risk, and potential mechanisms contributing to disease pathogenesis. gDNA, genomic DNA; IL, interleukin; PBMC, peripheral blood mononuclear cell; PCR, polymerase chain reaction; TGF, transforming growth factor; Treg, regulatory T cell. Created with BioRender.com.

crosstalk between IL-6 signalling and mLOY-related inflammatory pathways [35]. Although IL-33, a cytokine implicated in Treg and Th2 expansion, was not altered in our cohort, its established role in GCA via the induction of IL-2, IL-10, and TGF-β warrants further exploration [44]. A third potential mechanism involves mLOY-associated nuclear factor κB [11] and subsequent CD28-mediated signalling. CD28 signalling promotes early expression of Notch ligands (DLL1, DLL4, and JAG1) on $CD4^+$ T cells [45]. In GCA, Notch signalling drives Th1 and Th17 differentiation by upregulating T-bet and RORγt transcription factors [25]. Our findings position mLOY at the intersection of these immune pathways, suggesting that it may have constitutive proinflammatory effects, thereby contributing to chronic inflammation in GCA (Fig 4). This could be particularly relevant for the ~40% of patients with partial responses to IL-6 receptor blockade [24].

As no studies to date have investigated the role of mLOY in autoimmune diseases, expanding the scope to include other somatic mutations, particularly clonal haematopoietic mutations, may provide further valuable insights into the role of mLOY in GCA. Clonal hematopoiesis of indeterminate potential (CHIP), initially linked to haematologic malignancies, has since been implicated in cardiovascular disease and all-cause mortality in the general population [46–48]. Mechanistically, the increased cardiovascular risk associated with CHIP appears to be driven by sustained proinflammatory signalling through pathways such as the NLRP3 inflammasome, IL-1β, IL-6, and pathogenic T cell differentiation [49–51]. Mutated haematopoietic cells in CHIP evade replicative exhaustion induced by chronic inflammatory signalling, gaining a selective advantage over unaffected cells [8,52]. Importantly, an increased prevalence of clonal haematopoiesis has also been observed in various autoimmune conditions, including GCA. Specific CHIP-associated mutations have been linked to a higher risk of vision loss and paradoxically lower CRP levels in GCA patients [53,54]. These findings correspond with our study's observation of an inverse relationship between mLOY burden and CRP levels.

A plausible unifying mechanism across CHIP, mLOY, and other forms of acquired clonal haematopoiesis, such as that seen in VEXAS syndrome, involves cell-intrinsic immune activation and expansion of dysregulated myeloid or lymphoid lineages, ultimately promoting chronic inflammation and adverse outcomes [18]. While VEXAS represents a monogenic and severe phenotype [18], mLOY may reflect a subtler, yet more prevalent, form of haematopoietic mosaicism that similarly contributes to immune dysregulation in older adults.

Due to the observational nature of this study, causality between mLOY, relapse risk, and cytokine alterations cannot be definitively established. However, our data raise the possibility that mLOY could actively sustain proinflammatory immune responses. In this context, mLOY burden may serve not only as a biomarker of persistent immune activation, but also as a more specific indicator of immune ageing or dysfunction than chronological age itself. Additionally, it may act as a contributor to haematopoietic stress, particularly under IL-6 receptor blockade. The markedly increased relapse risk observed in our study may be explained by a hypothetical bidirectional model, in which chronic inflammation facilitates the expansion of mLOY-positive clones that, in turn, may contribute to immune dysregulation and disease progression in GCA.

Notably, even if mLOY functions solely as a biomarker, its strong association with relapse risk (HR, 17.4) provides clinically significant prognostic value, surpassing established risk factors. For instance, the current literature reports an odds ratio

of 2.04 (P = .001) for large vessel vasculitis, a recognised relapse risk factor [39]. Still, given the small sample size and wide CI, further studies and validation cohorts are needed to refine the exact HR estimate and validate mLOY as a predictive biomarker.

In summary, this study is the first to propose and demonstrate a role for mLOY in the immunopathology of GCA. Our findings indicate that mLOY is not merely an epiphenomenon of ageing but may actively contribute to dysregulated immune responses, as evidenced by markedly elevated relapse rates and distinct cytokine profiles in patients with a high mLOY burden. These results also position mLOY as a promising prognostic biomarker for GCA.

While our cross-sectional design offers important initial insights into the prevalence and immunological correlates of mLOY, it does not permit conclusions about causality or temporal dynamics. To elucidate the mechanistic and predictive relevance of mLOY, prospective longitudinal studies with harmonised follow-up intervals and serial assessment of both mLOY burden and inflammatory markers are warranted. Additionally, future investigations should include cell-type–specific analyses, as the functional impact of mLOY likely varies across immune lineages. This will be particularly important in the context of immunomodulatory therapies, as our data indicate that mLOY-related immune activation may persist despite IL-6 receptor inhibition. Finally, validation in larger, multicentre cohorts, including appropriately matched healthy controls, will be critical to confirm the prognostic value of mLOY and to establish its broader clinical utility for risk stratification, treatment guidance, and disease monitoring in GCA.

Competing interests

The authors report no disclosures relevant to the manuscript.

Acknowledgements

We thank the BioBank Bonn of the University of Bonn Medical Faculty and the University Hospital Bonn for storing the biomaterials used in this study.

Contributors

Conceptualisation: SMP, RNJ, and VSS; Methodology: SMP, RNJ, and VSS; Validation: SMP, S-MK, MSA, DX, RNJ, and VSS; Formal analysis: SMP, S-MK, MSA, DX, RNJ, and VSS; Investigation: SMP, S-MK, MSA, DX, C-JB, LK, PK, RNJ, and VSS; Resources: SMP, RB, GN, SZ, and VSS; Data curation: SMP, S-MK, MSA, DX, LK, RNJ, and VSS; Writing–Original Draft: SMP, S-MK, RNJ, and VSS; Writing–Review & Editing: SMP, S-MK, MSA, DX, C-JB, LK, RG, PK, RB, GN, SZ, RNJ, and VSS; Visualisation: SMP, MSA, RG, RNJ and VSS; Supervision: SMP, RNJ, and VSS; Project administration: SMP, RNJ, and VSS.

Funding

This research received no external funding.

Patient consent for publication

Informed consent was obtained from all patients involved in the study.

Ethics approval

The study received ethical approval from the local ethics committe (Institutional Review Board number #321/22.

Provenance and peer review

Not commissioned; externally peer reviewed.

Data availability statement

Data are available upon reasonable request from the corresponding author.

Supplementary materials

Supplementary material associated with this article can be found in the online version at doi:10.1016/j.ard.2025.06.2133.

Orcid

Simon M. Petzinna: http://orcid.org/0000-0002-4686-1143
Sophie-Marie Kirch: http://orcid.org/0009-0001-8963-2922
Maike S. Adamson: http://orcid.org/0000-0001-6491-9516
Claus-Jürgen Bauer: http://orcid.org/0000-0003-3152-6550
Lena Kreis: http://orcid.org/0009-0004-3810-2229
Raul N. Jamin: http://orcid.org/0009-0003-2084-8463

REFERENCES

[1] Danielsson M, Halvardson J, Davies H, Torabi Moghadam B, Mattisson J, Rychlicka-Buniowska E, et al. Longitudinal changes in the frequency of mosaic chromosome Y loss in peripheral blood cells of aging men varies profoundly between individuals. Eur J Hum Genet 2020;28(3):349–57. doi: 10.1038/s41431-019-0533-z.

[2] Forsberg LA, Halvardson J, Rychlicka-Buniowska E, Danielsson M, Moghadam BT, Mattisson J, et al. Mosaic loss of chromosome Y in leukocytes matters. Nat Genet 2019;51(1):4–7.

[3] Thompson DJ, Genovese G, Halvardson J, Ulirsch JC, Wright DJ, Terao C, et al. Genetic predisposition to mosaic Y chromosome loss in blood. Nature 2019;575(7784):652–7. doi: 10.1038/s41586-019-1765-3.

[4] Forsberg LA, Rasi C, Malmqvist N, Davies H, Pasupulati S, Pakalapati G, et al. Mosaic loss of chromosome Y in peripheral blood is associated with shorter survival and higher risk of cancer. Nat Genet 2014;46(6):624–8. doi: 10.1038/ng.2966.

[5] Dumanski JP, Rasi C, Lönn M, Davies H, Ingelsson M, Giedraitis V, et al. Mutagenesis. Smoking is associated with mosaic loss of chromosome Y. Science 2015;347(6217):81–3. doi: 10.1126/science.1262092.

[6] Zhou W, Machiela MJ, Freedman ND, Rothman N, Malats N, Dagnall C, et al. Mosaic loss of chromosome Y is associated with common variation near TCL1A. Nat Genet 2016;48(5):563–8. doi: 10.1038/ng.3545.

[7] Zink F, Stacey SN, Norddahl GL, Frigge ML, Magnusson OT, Jonsdottir I, et al. Clonal hematopoiesis, with and without candidate driver mutations, is common in the elderly. Blood 2017;130(6):742–52. doi: 10.1182/blood-2017-02-769869.

[8] Wong TN, Miller CA, Jotte MRM, Bagegni N, Baty JD, Schmidt AP, et al. Cellular stressors contribute to the expansion of hematopoietic clones of varying leukemic potential. Nat Commun 2018;9(1):455. doi: 10.1038/s41467-018-02858-0.

[9] Dumanski JP, Lambert JC, Rasi C, Giedraitis V, Davies H, Grenier-Boley B, et al. Mosaic loss of chromosome Y in blood is associated with Alzheimer disease. Am J Hum Genet 2016;98(6):1208–19. doi: 10.1016/j.ajhg.2016.05.014.

[10] Wright DJ, Day FR, Kerrison ND, Zink F, Cardona A, Sulem P, et al. Genetic variants associated with mosaic Y chromosome loss highlight cell cycle genes and overlap with cancer susceptibility. Nat Genet 2017;49(5):674–9. doi: 10.1038/ng.3821.

[11] Sano S, Horitani K, Ogawa H, Halvardson J, Chavkin NW, Wang Y, et al. Hematopoietic loss of Y chromosome leads to cardiac fibrosis and heart failure mortality. Science 2022;377(6603):292–7. doi: 10.1126/science.abn3100.

[12] Dorvall M, Pedersen A, Dumanski JP, Söderholm M, Lindgren AG, Stanne TM, et al. Mosaic loss of chromosome Y is associated with functional outcome after ischemic stroke. Stroke 2023;54(9):2434–7. doi: 10.1161/STROKEAHA.123.043551.
[13] Weyrich M, Cremer S, Gerster M, Sarakpi T, Rasper T, Zewinger S, et al. Loss of Y chromosome and cardiovascular events in chronic kidney disease. Circulation 2024;150(10):746–57. doi: 10.1161/CIRCULATIONAHA.124.069139.
[14] Loftfield E, Zhou W, Graubard BI, Yeager M, Chanock SJ, Freedman ND, Machiela MJ. Predictors of mosaic chromosome Y loss and associations with mortality in the UK. Biobank. Sci Rep. 2018;8(1):12316. doi: 10.1038/s41598-018-30759-1.
[15] Horitani K, Chavkin NW, Arai Y, Wang Y, Ogawa H, Yura Y, et al. Disruption of the Uty epigenetic regulator locus in hematopoietic cells phenocopies the profibrotic attributes of Y chromosome loss in heart failure. Nat Cardiovasc Res 2024;3(3):343–55. doi: 10.1038/s44161-024-00441-z.
[16] Arseneault M, Monlong J, Vasudev NS, Laskar RS, Safisamghabadi M, Harnden P, et al. Loss of chromosome Y leads to down regulation of KDM5D and KDM6C epigenetic modifiers in clear cell renal cell carcinoma. Sci Rep 2017;7:44876. doi: 10.1038/srep44876.
[17] Wójcik M, Juhas U, Mohammadi E, Mattisson J, Drężek-Chyła K, Rychlicka-Buniowska E, et al. Loss of Y in regulatory T lymphocytes in the tumor microenvironment of primary colorectal cancers and liver metastases. Sci Rep 2024;14(1):9458. doi: 10.1038/s41598-024-60049-y.
[18] Beck DB, Ferrada MA, Sikora KA, Ombrello AK, Collins JC, Pei W, et al. Somatic mutations in UBA1 and severe adult-onset autoinflammatory disease. N Engl J Med 2020;383(27):2628–38. doi: 10.1056/NEJMoa2026834.
[19] Beck DB, Bodian DL, Shah V, Mirshahi UL, Kim J, Ding Y, et al. Estimated prevalence and clinical manifestations of UBA1 variants associated with VEXAS syndrome in a clinical population. JAMA 2023;329(4):318–24.
[20] Sullivan MM, Mead-Harvey C, Sartori-Valinotti JC, Kalantari K, Kusne YN, Patnaik MM, et al. Vasculitis associated with VEXAS syndrome. Rheumatology (Oxford) 2025;64:3889–94. doi: 10.1093/rheumatology/keae550.
[21] Grambow-Velilla J, Braun T, Pop G, Louzoun A, Soussan M. Aortitis PET imaging in VEXAS syndrome: a case report. Clin Nucl Med 2023;48(2):e67–8. doi: 10.1097/RLU.0000000000004506.
[22] Dejaco C, Brouwer E, Mason JC, Buttgereit F, Matteson EL, Dasgupta B. Giant cell arteritis and polymyalgia rheumatica: current challenges and opportunities. Nat Rev Rheumatol 2017;13(10):578–92. doi: 10.1038/nrrheum.2017.142.
[23] Buttgereit F, Dejaco C, Matteson EL, Dasgupta B. Polymyalgia rheumatica and giant cell arteritis: a systematic review. JAMA 2016;315(22):2442–58.
[24] Stone JH, Tuckwell K, Dimonaco S, Klearman M, Aringer M, Blockmans D, et al. Trial of tocilizumab in giant-cell arteritis. N Engl J Med 2017;377(4):317–28.
[25] Schäfer VS, Brossart P, Warrington KJ, Kurts C, Sendtner GW, Aden CA. The role of autoimmunity and autoinflammation in giant cell arteritis: a systematic literature review. Autoimmun Rev 2023;22(6):103328. doi: 10.1016/j.autrev.2023.103328.
[26] Espígol-Frigolé G, Planas-Rigol E, Lozano E, Corbera-Bellalta M, Terrades-García N, Prieto-González S, et al. Expression and function of IL12/23 related cytokine subunits (p35, p40, and p19) in giant-cell arteritis lesions: contribution of p40 to Th1- and Th17-mediated inflammatory pathways. Front Immunol 2018;9:809. doi: 10.3389/fimmu.2018.00809.
[27] Deng J, Younge BR, Olshen RA, Goronzy JJ, Weyand CM. Th17 and Th1 T-cell responses in giant cell arteritis. Circulation 2010;121(7):906–15. doi: 10.1161/CIRCULATIONAHA.109.872903.
[28] Mihara M, Hashizume M, Yoshida H, Suzuki M, Shiina M. IL-6/IL-6 receptor system and its role in physiological and pathological conditions. Clin Sci (Lond) 2012;122(4):143–59.
[29] Wen Z, Shen Y, Berry G, Shahram F, Li Y, Watanabe R, et al. The microvascular niche instructs T cells in large vessel vasculitis via the VEGF-Jagged1-notch pathway. Sci Transl Med 2017;9(399):eaal3322.
[30] Hid Cadena R, Reitsema RD, Huitema MG, van Sleen Y, van der Geest KSM, Heeringa P, et al. Decreased expression of negative immune checkpoint VISTA by CD4+ T cells facilitates T helper 1, T helper 17, and T follicular helper lineage differentiation in GCA. Front Immunol 2019;10:1638. doi: 10.3389/fimmu.2019.01638.
[31] Roche NE, Fulbright JW, Wagner AD, Hunder GG, Goronzy JJ, Weyand CM. Correlation of interleukin-6 production and disease activity in polymyalgia rheumatica and giant cell arteritis. Arthritis Rheum 1993;36(9):1286–94.
[32] Burja B, Feichtinger J, Lakota K, Thallinger GG, Sodin-Semrl S, Kuret T, et al. Utility of serological biomarkers for giant cell arteritis in a large cohort of treatment-naïve patients. Clin Rheumatol 2019;38(2):317–29. doi: 10.1007/s10067-018-4240-x.
[33] García-Martínez A, Hernández-Rodríguez J, Espígol-Frigolé G, Prieto-González S, Butjosa M, Segarra M, et al. Clinical relevance of persistently elevated circulating cytokines (tumor necrosis factor alpha and interleukin-6) in the long-term followup of patients with giant cell arteritis. Arthritis Care Res (Hoboken) 2010;62(6):835–41.
[34] Villiger PM, Adler S, Kuchen S, Wermelinger F, Dan D, Fiege V, et al. Tocilizumab for induction and maintenance of remission in giant cell arteritis: a phase 2, randomised, double-blind, placebo-controlled trial. Lancet 2016;387(10031):1921–7.
[35] Miyabe C, Miyabe Y, Strle K, Kim ND, Stone JH, Luster AD, et al. An expanded population of pathogenic regulatory T cells in giant cell arteritis is abrogated by IL-6 blockade therapy. Ann Rheum Dis 2017;76(5):898–905. doi: 10.1136/annrheumdis-2016-210070.
[36] Ponte C, Grayson PC, Robson JC, Suppiah R, Gribbons KB, Judge A, et al. 2022 American College of Rheumatology/EULAR classification criteria for giant cell arteritis. Ann Rheum Dis 2022;81(12):1647–53. doi: 10.1136/ard-2022-223480.
[37] Dejaco C, Ponte C, Monti S, Rozza D, Scirè CA, Terslev L, et al. The provisional OMERACT ultrasonography score for giant cell arteritis. Ann Rheum Dis 2023;82(4):556–64.
[38] Monti S, Ponte C, Schäfer VS, Rozza D, Scirè C, Franchi G, et al. The giant cell arteritis (GCA) ultrasound score (OGUS) at diagnosis and after initial treatment predicts future relapses in GCA patients: results of a multicentre prospective study. Ann Rheum Dis 2025;84:823–32. doi: 10.1016/j.ard.2025.01.018.
[39] Moreel L, Betrains A, Molenberghs G, Vanderschueren S, Blockmans D. Epidemiology and predictors of relapse in giant cell arteritis: a systematic review and meta-analysis. Joint Bone Spine 2023;90(1):105494. doi: 10.1016/j.jbspin.2022.105494.
[40] Ouseph MM, Hasserjian RP, Dal Cin P, Lovitch SB, Steensma DP, Nardi V, et al. Genomic alterations in patients with somatic loss of the Y chromosome as the sole cytogenetic finding in bone marrow cells. Haematologica 2021;106(2):555–64.
[41] Hubbard AK, Brown DW, Zhou W, Lin SH, Genovese G, Chanock SJ, et al. Serum biomarkers are altered in UK Biobank participants with mosaic chromosomal alterations. Hum Mol Genet 2023;32(22):3146–52.
[42] Xu X, Zhou R, Duan Q, Miao Y, Zhang T, Wang M, et al. Circulating macrophages as the mechanistic link between mosaic loss of Y-chromosome and cardiac disease. Cell Biosci 2023;13(1):135. doi: 10.1186/s13578-023-01075-7.
[43] Mattisson J, Halvardson J, Davies H, Bruhn-Olszewska B, Olszewski P, Danielsson M, et al. Loss of chromosome Y in regulatory T cells. BMC Genomics 2024;25(1):243. doi: 10.1186/s12864-024-10168-7.
[44] Desbois AC, Cacoub P, Leroyer AS, Tellier E, Garrido M, Maciejewski-Duval A, et al. Immunomodulatory role of interleukin-33 in large vessel vasculitis. Sci Rep 2020;10(1):6405. doi: 10.1038/s41598-020-63042-3.
[45] Mitra A, Shanthalingam S, Sherman HL, Singh K, Canakci M, Torres JA, et al. CD28 signaling drives notch ligand expression on CD4 T cells. Front Immunol 2020;11:735. doi: 10.3389/fimmu.2020.00735.
[46] Genovese G, Kähler AK, Handsaker RE, Lindberg J, Rose SA, Bakhoum SF, et al. Clonal hematopoiesis and blood-cancer risk inferred from blood DNA sequence. N Engl J Med 2014;371(26):2477–87. doi: 10.1056/NEJMoa1409405.
[47] Jaiswal S, Fontanillas P, Flannick J, Manning A, Grauman PV, Mar BG, et al. Age-related clonal hematopoiesis associated with adverse outcomes. N Engl J Med 2014;371(26):2488–98. doi: 10.1056/NEJMoa1408617.
[48] Jaiswal S, Natarajan P, Silver AJ, Gibson CJ, Bick AG, Shvartz E, et al. Clonal hematopoiesis and risk of atherosclerotic cardiovascular disease. N Engl J Med 2017;377(2):111–21. doi: 10.1056/NEJMoa1701719.
[49] Bick AG, Pirruccello JP, Griffin GK, Gupta N, Gabriel S, Saleheen D, et al. Genetic interleukin 6 signaling deficiency attenuates cardiovascular risk in clonal hematopoiesis. Circulation 2020;141(2):124–31. doi: 10.1161/CIRCULATIONAHA.119.044362.
[50] Sano S, Oshima K, Wang Y, MacLauchlan S, Katanasaka Y, Sano M, et al. Tet2-mediated clonal hematopoiesis accelerates heart failure through a mechanism involving the IL-1β/NLRP3 inflammasome. J Am Coll Cardiol 2018;71(8):875–86.
[51] Svensson EC, Madar A, Campbell CD, He Y, Sultan M, Healey ML, et al. TET2-driven clonal hematopoiesis and response to canakinumab: an exploratory analysis of the CANTOS randomized clinical trial. JAMA Cardiol 2022;7(5):521–8.
[52] Avagyan S, Henninger JE, Mannherz WP, Mistry M, Yoon J, Yang S, et al. Resistance to inflammation underlies enhanced fitness in clonal hematopoiesis. Science 2021;374(6568):768–72. doi: 10.1126/science.aba9304.
[53] Robinette ML, Weeks LD, Kramer RJ, Agrawal M, Gibson CJ, Yu Z, et al. Association of somatic TET2 mutations with giant cell arteritis. Arthritis Rheumatol 2024;76:438–43. doi: 10.1002/art.42738.
[54] Gutierrez-Rodrigues F, Wells KV, Jones AI, Hironaka D, Rankin C, Gadina M, et al. Clonal haematopoiesis across the age spectrum of vasculitis patients with Takayasu's arteritis, ANCA-associated vasculitis and giant cell arteritis. Ann Rheum Dis 2024;83:508–17. doi: 10.1136/ard-2023-224933.

Ann Rheum Dis 84 (2025) 1909–1927

Contents lists available at ScienceDirect

Annals of the Rheumatic Diseases

journal homepage: https://www.sciencedirect.com/journal/annals-of-the-rheumatic-diseases

Autoinflammatory disorders

Efficacy and safety of treatments in familial Mediterranean fever and its complications: a systematic review informing the EULAR/PReS recommendations for familial Mediterranean fever

Erdal Sag [1,*], Teresa Otón [2], Loreto Carmona [2], Seza Ozen [1]

[1] *Department of Paediatric Rheumatology, Hacettepe University, Ankara, Türkiye*
[2] *Instituto de Salud Musculoesquelética, Madrid, Spain*

ARTICLE INFO

Article history:
Received 27 January 2025
Received in revised form 20 May 2025
Accepted 23 May 2025

ABSTRACT

Objectives: To analyse the efficacy and safety of (1) the biological agents and tofacitinib in the treatment of familial Mediterranean fever (FMF); (2) the biological agents and tofacitinib in FMF patients with complications such as amyloidosis; and (3) the colchicine preparations and dosing strategies to serve as evidence supporting the updated European Alliance of Associations for Rheumatology (EULAR) recommendations.

Methods: This was a systematic review (SR) of studies testing pharmacological treatments in FMF patients, including targets, dosing, tapering, and uses in AA amyloidosis. MEDLINE, Embase, and the Cochrane Library were searched, focusing on studies published after October 1, 2014. The Cochrane Risk of Bias tool and the Newcastle-Ottawa Scale were used to assess the risk of bias in the included randomised controlled trials (RCTs) and observational studies, respectively. Due to excess heterogeneity, results were synthesised qualitatively.

Results: This SR included 42 studies for efficacy and safety (n = 1798 patients), 13 for tapering, and 31 for amyloidosis. Based on 6 RCTs of interleukin (IL)-1 blockers and observational studies, these biologicals seem to be effective in decreasing the number of attacks and acute-phase reactants and improving disease activity scores and patient-reported outcomes. They also seem relatively safe. An RCT showed the equivalence of once-daily vs twice-daily doses of colchicine. The evidence of AA amyloidosis was entirely observational but reassuring for a deadly complication.

Conclusions: Biological agents, particularly IL-1 inhibitors, are effective and relatively safe options for FMF patients who do not respond to colchicine. These treatments may be promising alternatives for managing symptoms and preventing comorbidities in both paediatric and adult populations.

*Correspondence to Dr. Erdal Sag, Department of Paediatric Rheumatology, Faculty of Medicine, Hacettepe University, Ankara, 06230 Türkiye.
E-mail address: sag.erdal@gmail.com (E. Sag).
Erdal Sag and Teresa share first authorship.
Handling editor Josef S. Smolen.

https://doi.org/10.1016/j.ard.2025.05.020

WHAT IS ALREADY KNOWN ON THIS TOPIC?

- Familial Mediterranean fever (FMF) is the most common monogenic autoinflammatory disease. Colchicine is the mainstay of treatment, but 5% of patients are resistant to colchicine.

WHAT THIS STUDY ADDS?

- This systematic review provides more comprehensive evidence on the efficacy and safety of the addition of biological DMARDs (Disease Modifying Anti-Rheumatic Drugs) to colchicine treatment in FMF patients.

HOW THIS STUDY MIGHT AFFECT RESEARCH, PRACTICE OR POLICY?

- The addition of biological DMARDs, particularly anti−interleukin-1 agents, seems to be safe and effective in FMF patients who are resistant to colchicine, as well as in patients with amyloidosis and renal transplantation.
- Despite the results of research involving patients with biallelic pathogenic *MEFV* mutations not being very encouraging, tapering strategies for FMF appear to be possible.

INTRODUCTION

Familial Mediterranean fever (FMF) is the most frequent autoinflammatory disease, and it is characterised by recurrent self-limiting attacks of fever, abdominal pain, arthritis, and chest pain [1]. The primary aim of treatment in FMF is to prevent attacks, subclinical inflammation and, more importantly, the life-threatening complication of AA amyloidosis. The first-line treatment is colchicine [2,3]. Unfortunately, 5% to 10% of FMF patients experience intolerance (eg, diarrhoea, elevated liver enzymes, and leukopenia) or resistance to colchicine treatment [4]. In these patients, some clinicians prefer to switch to other colchicine preparations, but usually, they end up starting biological DMARDs (Disease Modifying Anti-Rheumatic Drugs), specifically anti-interleukin (IL)-1 agents. The effect on specific characteristics of the disease, such as protracted myalgia or sacroiliitis, or even in patients with AA amyloidosis, is unclear. Also, considering long-term treatment, some clinicians are considering different colchicine dosing strategies, and others are starting to withdraw biologicals once FMF enters remission or can be controlled with colchicine only. Given all these practices, the European Alliance of Associations for Rheumatology (EULAR) task force on FMF decided not only to update the systematic review (SR) performed in 2014 [2] but also to address these novel clinical questions by reviewing the evidence critically.

Therefore, this review aimed to analyse the efficacy and safety of different treatment strategies in FMF, including tapering, after reaching a positive effect. As a secondary aim, we examined the efficacy and safety of different treatment strategies in patients with specific FMF-related characteristics, including AA amyloidosis.

METHODS

Search strategy

This SR was performed based on the previous SR done for the original recommendations [3]. The reviewers (E.S. and T.O.) established the protocol with a methodologist based on the PICOT (Population, Intervention, Comparison, Outcome, Time) framework [5] (see Supplementary Table S1 for the PICOT questions). Further advice was obtained from an international panel of experts, including the convenor of the consensus. The following bibliographic databases were searched: Medline through PubMed, Embase, and Cochrane Central Trials Register, all up to August 15, 2023. We used comprehensive free text and MeSH (Medical Subject Headings) synonyms for FMF, as well as different treatment options (Supplementary Tables S2-S4). We searched only published articles in English and selected articles from October 1, 2014 (from the last search date of the previous recommendation paper), except for the tapering search, which had no limits.

Eligibility criteria

Studies were eligible for each question if they fulfilled the corresponding PICOT components. As for efficacy and safety of the different treatments, we used a hierarchical approach: we included randomised controlled trials (RCTs), if not available, then quasi-controlled trials (CCTs) were considered. If neither trial was available, we included studies that tested anti−IL-1 treatments in FMF patients with at least 20 patients and any other biological DMARDs in at least 1 FMF patient. Furthermore, studies were eligible if they included at least 1 FMF patient with AA amyloidosis treated with biological DMARDs. SRs were screened, and all eligible trials were cross-checked with the primary studies selected regarding the outcomes. Not only were studies assessing the effect on clinical outcomes targeted, but also laboratory parameters.

Selection and data collection

Two reviewers (E.S. and T.O.) performed the study screening, data collection, and synthesis. Both reviewers independently screened the titles and abstracts of the retrieved articles using the Rayyan web-based software (https://www.rayyan.ai). The full texts of the selected articles were then read in detail, and the eligibility criteria were checked. The PRISMA flow charts (Preferred Reporting Items for Systematic Reviews and Meta-Analyses) were produced with the PRISMA application [6].

The following variables were collected from the included studies: (1) related to the study design, type, and duration of the study; (2) related to the sample studied: number of patients, mean age, gender distribution, and specific subgroups (sacroiliitis, protracted febrile myalgia, and AA amyloidosis); (3) related to the treatment or strategy (tapering) and comparator; (4) efficacy results (as presented in the papers, eg, frequency of attacks, duration and severity of attacks, acute-phase reactants, disease activity scores, such as AIDAI (AutoInflammatory Disease Activity Index), FMF50 (familial Mediterranean fever 50 score), PRAS, or Mor, or 24-hour urinary protein excretion); (5) safety results (total adverse events, serious adverse events, infections, and reasons for treatment discontinuation); and (6) efficacy results related to amyloidosis studies (proteinuria, end-stage renal disease, and death).

Risk of bias assessment and synthesis

We used the Cochrane Risk of Bias (RoB) tool to assess the quality of the included studies on efficacy and safety [7]. The studies on tapering were assessed with the Newcastle-Ottawa Scale [8]. Studies and results were synthesised qualitatively by research question and drug. We planned to perform a meta-analysis only if the design, population, intervention, and outcome measure homogeneity were deemed acceptable.

RESULTS

The searches above identified 1244 records for efficacy and safety, of which 126 were fully assessed for eligibility. After the

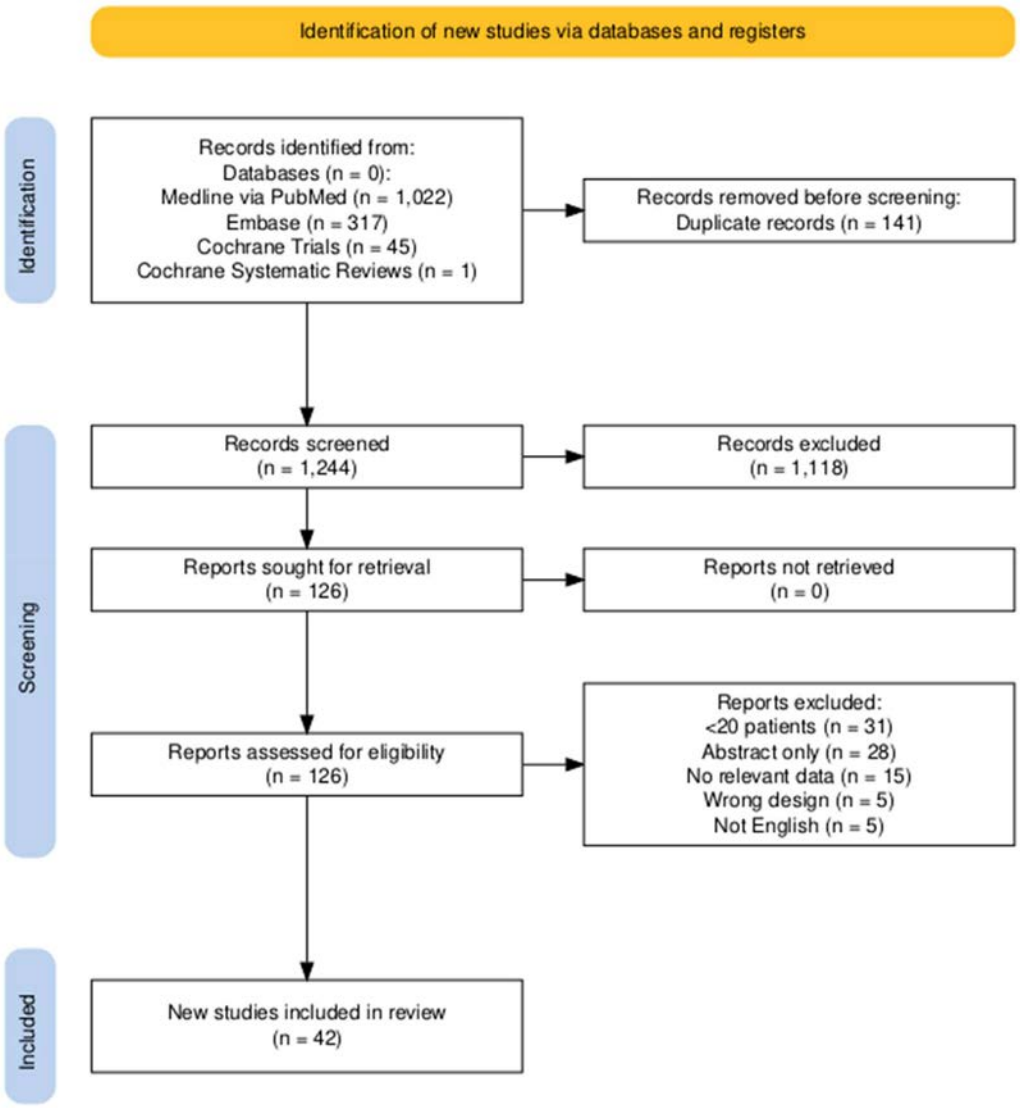

Figure 1. PRISMA flow chart of the review of efficacy and safety of treatments in FMF.

full-text assessment, 84 were excluded, of which 31 were case reports or small case series (less than 20 patients included for anti−IL-1-related studies), 28 were conference abstracts with the same results as another paper included, 15 had no relevant data, 5 had the wrong study design, and 5 were in languages other than English. Finally, 42 articles (Fig 1) provided information on 1798 patients. The search strategy identified 544 records for the tapering of treatments in FMF patients, of which 24 were fully assessed for eligibility. After the full-text assessment, 11 were excluded (Supplementary Table S5), and 13 were included (Fig 2).

For AA amyloidosis secondary to FMF, 45 articles were fully assessed for eligibility. After the full-text assessment, 19 articles were excluded; 10 had no efficacy data, 5 had no definitive treatment related to FMF, 2 were conference abstracts with the same results as a paper, and 2 were not in English. Five more studies were retrieved from the selected SRs by title and abstract; 2 recent studies, including a relatively high number of patients, were included due to expert recommendation. In total, 31 articles were included (Fig 3).

Information on the efficacy and safety of biological agents in FMF was based on 8 clinical trials (n = 277) and 23 longitudinal studies and case series (n = 910). Except for 1 study, all had at least 1 domain with an unclear risk of bias, and 6 studies had all domains with a high risk of bias; thus, we can say that, in general, the studies had a risk of bias (Fig 4 and Supplementary Fig S1).

Efficacy of different biological agents on FMF

Six RCTs with IL-1 blockers (1 anakinra: n = 25 patients; 4 canakinumab: total N = 190 patients; 1 rilonacept: n = 14 patients) [9−14] and 2 RCTs with anti−IL-6 treatments (total N = 48 patients) were identified [15,16]. Apart from these, there were 16 longitudinal studies and case series with anti−IL-1 treatments (including >20 patients; total N = 854 patients) [17−32], 3 case series with anti−IL-6 (total N = 24 patients) [33−35], 3 case series/case reports with tofacitinib (total N = 6 patients) [36−38], and 1 with antitumor necrosis factor (TNF) treatments (n = 26 patients) [39] (Table 1) [9−40]. The endpoints were heterogeneous across studies, with the most frequently used being a decrease in the frequency of attacks and acute-phase reactants. The RCTs with anti−IL-6 treatment could not reach the primary endpoint, but anti−IL-1 treatments seemed effective in decreasing the number of attacks and acute-phase reactants, together with improving the different disease activity scores (such as AIDAI, FMF50, PRAS score, etc) and patient-reported outcomes (patient visual analogue scale [VAS], Child Health Questionnaire [CHQ], health-related quality of life [HRQoL], etc). Table 2 [9−16,40] shows the results of clinical trials; for observational evidence, see Supplementary Table S6. No meta-analysis was deemed reasonable due to the heterogeneity in designs, outcomes, and treatments.

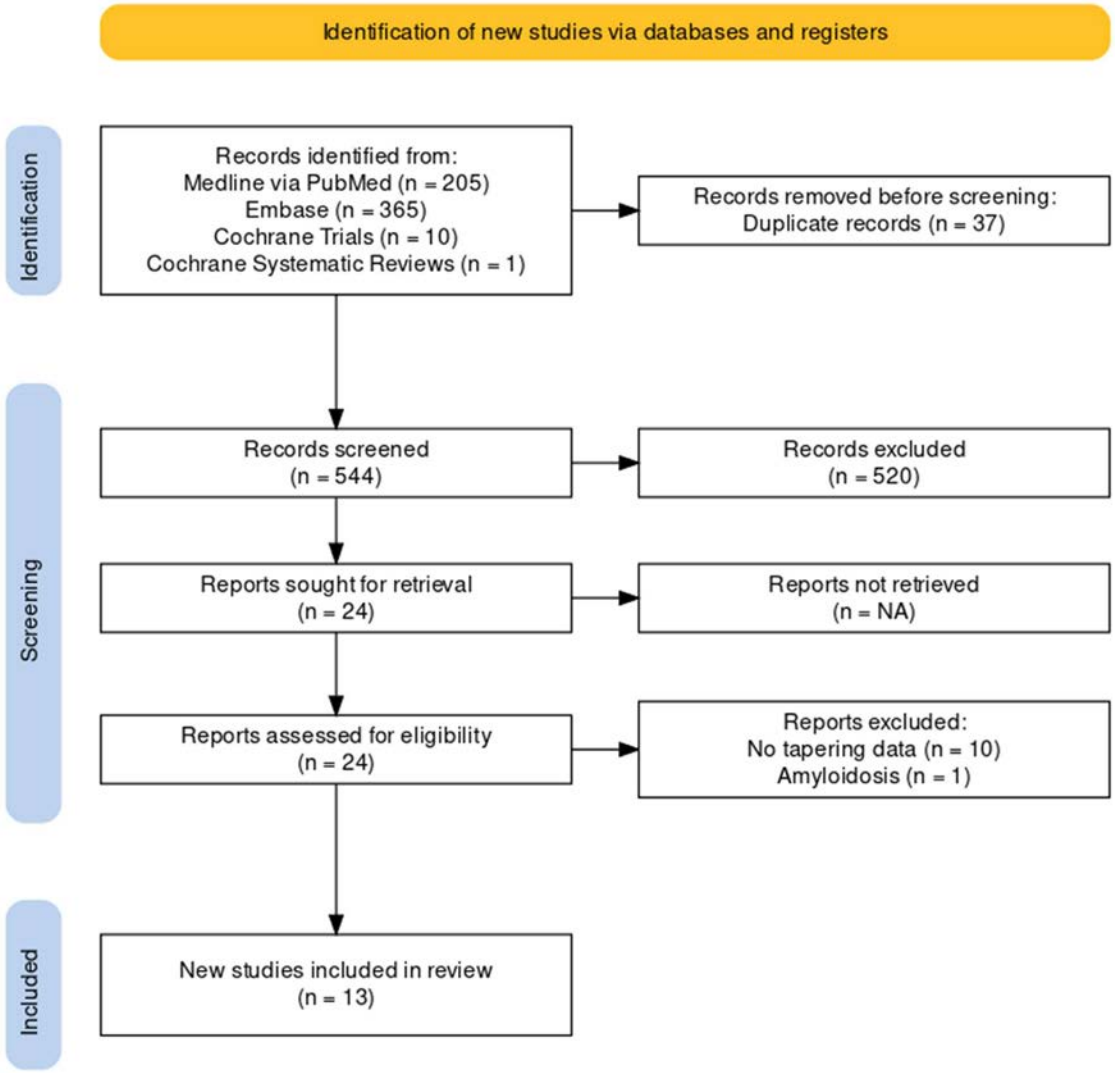

Figure 2. PRISMA flow chart of the tapering review. NA, not available.

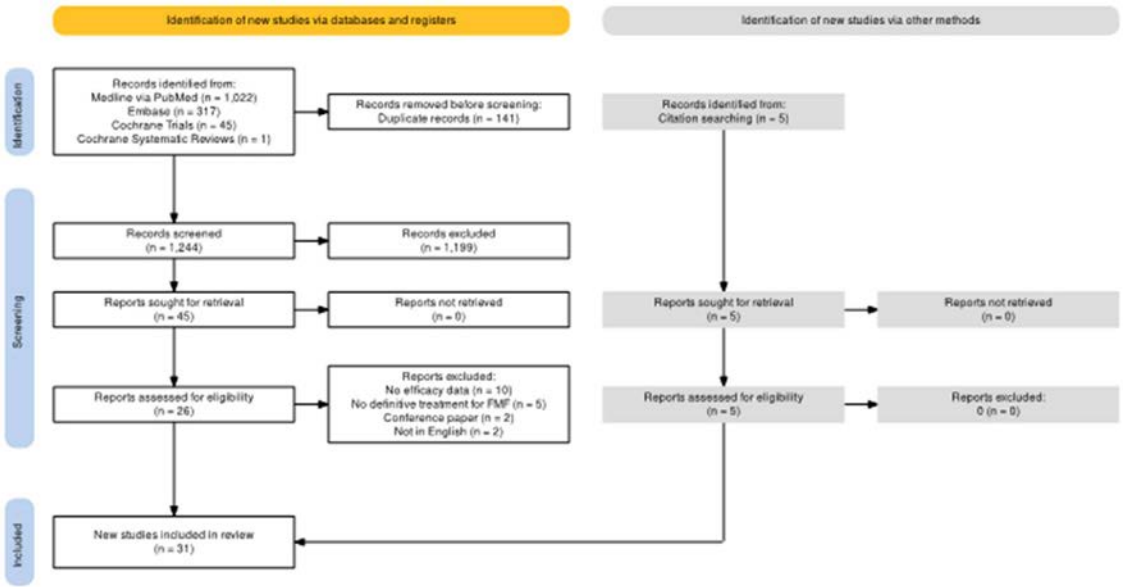

Figure 3. PRISMA flow chart of the review on amyloidosis. FMF, familial Mediterranean fever.

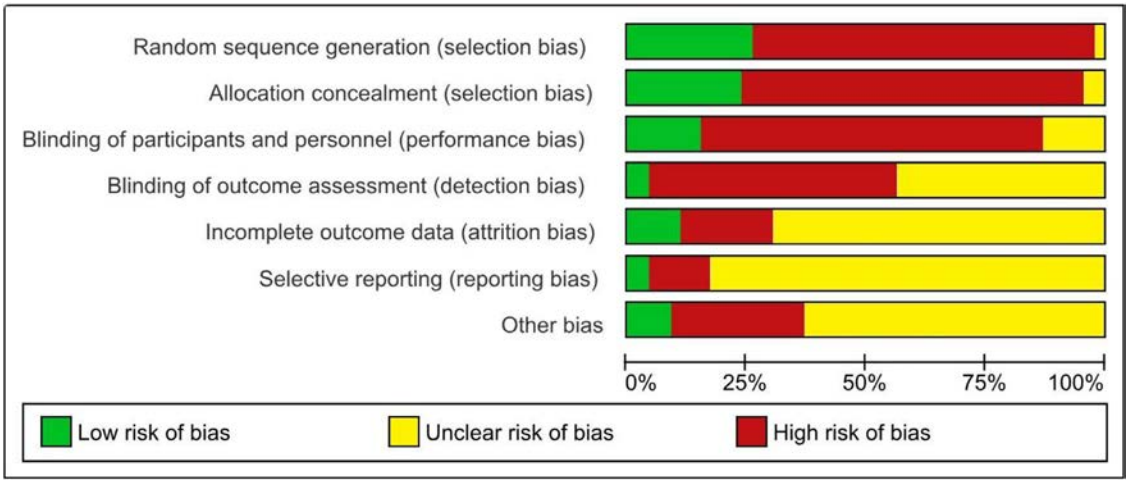

Figure 4. Summary of the risk of bias assessment of the studies included.

Table 1
Characteristics of the studies on biological DMARDs in FMF

Study	Design	N	Age	♀, %	Treatment	Dose	Comparator	Outcome measures
Clinical trials								
IL-1								
Ben-Zvi, 2016 [9]	RCT 16 wk	25[a]	38 ± 10	58	Anakinra	100 mg/d	Placebo	Frequency of attacks Attack site APRs QoL, VAS, modified FMF50 score
Brik, 2014 [10]	CCT[d] 6 mo	7[a]	Median 9.5 (6.8 - 14.9)	29	Canakinumab	150 mg/4 wk	Before-after	Frequency of attacks APR HRQoL (CHQ-PF50) Physician GA
de Benedetti, 2018 [11]	RCT 16 wk	63[a]	23 ± 15	45	Canakinumab	150 mg (or 2 mg/kg < 40 kg) every 4 wk 300 mg (or 4 mg/kg) every 4 wk for a flare 150 mg every 8 wk after a complete response	Placebo	Complete response: Phy GA<2; CRP < 10 mg/L or >70% reduction from baseline Flare: Phy GA > 2 + CRP > 30 mg/L % Phy GA < 2, CRP < 10 mg/L, or SAA < 10 mg/L
Lachmann, 2021 [12]	RCT[e] 52 wk	60[a]	15	48	Canakinumab	150 mg or 300 mg every 4 wk	Placebo	HRQoL (CHQ-PF50, SF-12, health survey-acute version 2, SDS)
Ozen, 2020 [13]	RCT 72 wk[f]	60[a]	Median 18 (14 - 29.5)	47	Canakinumab	150 mg or 300 mg every 4 or 8 wk Cumulative dose: <2700 mg (n = 44) >2700 mg (n = 16)	Placebo	Phy GA APRs
Hashkes 2014 [40]	RCT 24 wk	14	24 ± 12	43	Rilonacept	2.2 mg/kg/wk, max 160 mg	Placebo	Frequency of attacks HRQoL (CHQ)
IL-6								
Henes, 2022 [16]	RCT 32 wk	25[a]	Median 31 (18 - 53)	56	Tocilizumab	8 mg/kg monthly, max 800 mg	Placebo	Complete response at wk 16 (Phy GA < 2; SAA, ESR, and/or CRP < ULN) Serological remission (CRP < 5 mg/L or SAA < 10 mg/L) Improvement VAS, HRQoL (FFbH scale) Phy GA

(*continued*)

Table 1 (*Continued*)

Study	Design	N	Age	♀, %	Treatment	Dose	Comparator	Outcome measures
Koga, 2022 [15]	RCT 24 wk	23[a]	38 ± 15	73	Tocilizumab	162 mg every week	Placebo	No. of attacks at wk 24 Frequency of accompanying symptoms Time between attacks, duration of attacks CRP, SAA SF-36, FMF50 Phy GA
Longitudinal studies and case series								
IL-1								
Akar, 2018 [17]	LOS > 20	172	36	48	Anakinra Canakinumab	Anakinra 100 mg/d (96.4%), 50-300 mg/d Canakinumab 150 mg/4 wk (67%), 150 mg/8 wk (24%), 150 mg/12 wk (9%)	Before-after	Attacks per year APR 24-h urinary protein serum creatinine
Atas, 2021 [18]	LOS > 20	101[a]	37	57	Anakinra Canakinumab	100 mg daily (n = 48), twice daily (n = 4), every other day (n = 23), once every 3 d (n = 9) canakinumab 150 mg monthly (n = 21), bimonthly (n = 3), and quarterly (n = 1)	Before-after	Attacks/3 mo APR Creatinine, albumin AIDAI PGA and modified FMF50
Babaoglu, 2019 [19]	LOS > 20	78[a]	34	60	Anakinra	2-5 d of anakinra (15 on-demand)	Before-after	Frequency of attacks Duration and severity of attacks Patient GA, AIDAI, work productivity
Babaoglu, 2020 [20]	LOS > 20	23[a]	32	65	Canakinumab		Before-after	Frequency of attacks Duration of attacks, severity of attacks Patient GA, AIDAI, work productivity
Cetin, 2015 [21]	LOS > 20	20[a]	Median 23 (14 - 50)	45	Anakinra Canakinumab	100 mg/d 150 mg/8 wk	Before-after	Frequency of attacks
Eroglu, 2015 [22]	Case series	14	13 ± 7		Anakinra Canakinumab Etanercept	Ranging from 1-5 mg/kg/d 2 mg/kg/8-16 wk 0.8 mg/kg/wk	Before-after	AIDAI APR Patient and Phy VAS
Karabulut, 2022 [23]	LOS > 20	30[a]	32 ± 10	70	Canakinumab	150 mg/mo	Before-after	Frequency of attacks Duration of attacks APR PRAS score
Kucuksahin, 2016 [24]	LOS > 20	26	37	65	Anakinra Canakinumab	100 mg/d 150 mg/4 wk	Before-after	APRs Frequency of attacks
Kurt, 2020 [25]	LOS > 20	25[b]	14 ± 2	56	Anakinra Canakinumab	2-5 mg/kg/d 4 mg/kg/mo (max 150 mg)	Before-after	APRs Frequency of attacks Patient VAS, AIDAI, school loss
Marko, 2021 [26]	LOS > 20	44[a]	44 ± 13	55	Anakinra	50-100 mg/d	Before-after	Frequency of attacks Duration of attacks, no. of sites APRs GAS: no. of attacks, duration of attacks, and no. of sites affected
Pinchevski-Kadir, 2023 [27]	LOS > 20	22[a]	13 ± 4	64	Anakinra Canakinumab		Before-after	Response to treatment PRAS severity score Body weight and height
Sag, 2020 [28]	LOS > 20	40	12 ± 5	62	Anakinra Canakinumab	2 mg/kg/d, max 100 mg/d 2 mg/kg/bimonthly, max 150 mg/dose 6 on-demand	Before-after	Frequency of attacks APRs No. of sites

(*continued*)

Table 1 (*Continued*)

Study	Design	N	Age	♀, %	Treatment	Dose	Comparator	Outcome measures
Sahin, 2020 [29]	LOS > 20	65[a]	32 (17-60)	49	Anakinra Canakinumab	100 mg/d 150 mg/8 wk	Before-after	Frequency of attacks Duration of attacks Patient VAS, Phy VAS APRs 24-h urinary protein FMF50 score
Ugurlu, 2020[30]	LOS > 20	44[a]	44 ± 12	50	Anakinra Canakinumab	100 mg/d 150 mg/mo	Before-after	APR Changes in creatinine, creatinine clearance, and 24-h urinary protein QoL
Ugurlu, 2021 [31]	LOS > 20	106[c]	34 ± 10	65	Anakinra	100mg/d (n = 89) 100 mg every other day (n = 14) Other doses (n = 3)	Before-after	Frequency of attacks Patient GA APRs
Varan, 2019 [32]	LOS > 20	44	36 ± 12	57	Anakinra Canakinumab	100 mg/d 150 mg/mo	Before-after	Frequency of attacks Duration of attacks, severity of attacks SF-36
IL-6								
Honda, 2021 [33]	Case	1	20	0	Tocilizumab	162 mg every other week	Before-after	
Ugurlu, 2017 [34]	Case series	12[a]	35.2±10	50	Tocilizumab	8 mg/kg mo	Before-after	APR Changes in creatinine, creatinine clearance 24-h urinary protein
Yilmaz, 2015 [35]	Case series	11	38	9	Tocilizumab	8 mg/kg 4 wk	Before-after	Renal function tests (serum total protein, albumin, serum creatinine, BUN, and 24-h protein excretion)
Others								
Karadeniz, 2020 [36]	Case series	4	48	75	Tofacitinib	5 mg twice/d	Before-after	APRs Patient VAS AIDAI
Garci-Robledo, 2019 [37]	Case	1[a]	16	0	Tofacitinib	5 mg twice/d	Before-after	Remission of clinical symptoms APRs
Gök, 2017 [38]	Case	1	27	100	Tofacitinib	5 mg twice/d	Before-after	APRs VAS-pain Frequency of attacks
Haj-Yahia, 2021 [39]	LOS > 20	26	46 ± 12.5	57.7	Anti-TNF[g]		Before-after	Complete response: <1 FMF attack in 3 mo Nearly complete response: <1 attack/mo but >1 attack per 3 mo

Values are provided either mean ± SD, median or median (IQR). APR, acute-phase reactants; BUN, blood urine nitrogen; CCT, quasi-controlled trial; CHQ-PF50, Child Health Questionnaire-Parent Form 50; CRP, C-reactive protein; DMARD, Disease Modifying Anti Rheumatic Drugs; ESR, erythrocyte sedimentation rate; FFbH, Hannover Functional Ability Questionnaire; FMF, familial Mediterranean fever; FMF50, familial Mediterranean fever 50 score; AIDAI, AutoInflammatory Disease Activity Index; GA, global assessment; GAS, Global Assessment Score; HRQoL, health-related quality of life; IL, interleukin; LOS, longitudinal observational study; PGA, Physician's Global Assessment; Phy, physician; QoL, quality of life; RCT, randomized controlled trial; SAA, serum amyloid A; SDS, Sheehan Disability Scale; SF-12/36, Short Form 12/36; TNF, tumour necrosis factor; ULN, upper limit of normal; VAS, visual analogue scale.

[a] FMF as defined by Tel Hashomer criteria.
[b] By the Yalcinkaya-Ozen criteria.
[c] By the new Eurofever/PRINTO criteria.
[d] Open-label single arm.
[e] Sixteen-week double-blind, placebo-controlled, 24-week withdrawal.
[f] Epoch 4 (weeks 41-113).
[g] Adalimumab, etanercept, infliximab, and golimumab.

Safety of biological agents in FMF

The studies showed a relatively safe profile for the biologicals used in FMF, similar to what is seen in other uses. The most common adverse events were injection site reactions, followed by mild infections, elevated liver enzymes, and transient leukopenia. Although very rare, there were reports of severe adverse events, such as anaphylactoid reactions, severe cytopenia, and pneumonia, where hospitalisation was needed (Table 3) [9–40].

Efficacy and safety of different colchicine preparations and dosing

We evaluated the efficacy and safety of colchicine preparations and dosing options (Table 4) [42–49]. One RCT compared once-daily vs twice-daily dosing [47], 3 studies compared a domestic colchicine product with a different foreign preparation [42–44], 2 studies compared age-related dosing practices [45,46], and 2 studies evaluated compliance and intolerance problems [48,49].

Table 2
Efficacy results of clinical trials testing biological agents in FMF

Study	Treatment	% Reduction after treatment				Other outcome parameters				
		No. attacks	CRP	SAA	ESR					
IL-1										
Ben-Zvi, 2016 [9]	Anakinra	ANA: 63% PBO: 30%	ANA: 83% PBO: 54%	ANA: 89% PBO: 49%			Anakinra		Placebo	
							Before	After	Before	After
						QoL (10 cm VAS)	4 ± 2.3	7.7 ± 2.3	3.9 ± 1.5	4.2 ± 2.9
						Abdominal attacks (/mo)	2.1 ± 1.6	1 ± 1.2	1.7 ± 1.8	1.4 ± 1.1
						Chest attacks (/mo)	1.5 ± 1.6	0.7 ± 0.8	1.4 ± 1.5	1.6 ± 1.4
						Joint attacks (/mo)	3 ± 3.7	0.8 ± 1.6	2.7 ± 2.4	2.1 ± 1.1
						Skin attacks (/mo)	5.1 ± 6.9	0	1.1 ± 1.3	0.3 ± 0.6
						FMF50 score: ANA: 83.3%; PBO: 30.7%				
Brik, 2014 [10]	Canakinumab	89%	98%	99%	80%			Before	After	
						CHQ-PF50 physical domain		21	46	
						Psychosocial domain		31	40	
						Phy GA (0-5)		1.71	4.57	
de Benedetti, 2018 [11]	Canakinumab						Canakinumab, %		Placebo, %	
						Complete response	61		0	
						Patient GA score < 2	65		9	
						CRP < 10 mg/L	68		6	
						SAA < 10 mg/L	26		0	
Lachmann, 2021 [12]	Canakinumab						Baseline	17 wk (Epoch 2)	41 wk (Epoch 3)	
						CHQ-PF50 physical	26	51	50	
						CHQ-PF50 psychological	43	56	51	
						SF-12 physical	38	47	49	
						SF-12 mental	42	46	50	
						SDS global function impairment	18	6	3	
						SDS work/school	6	2	1	
						SDS social life	6	2	1	
Ozen, 2020 [13]	Canakinumab					No flares: total 58%; <2700 mg (59%) vs >2700 mg (57%) 70% entered Epoch 4 on low dose (150 mg q8w) 40% is sufficient to control the disease until the end 44% received an intermediate dose (150 mg q4w or 300 mg q8w) 16% titrated to the highest dose (300 mg q4w) Low Phy GA: total 90% CRP < 10 mg/L target maintained between wk 41-113 SAA 12-23 mg/L (<2700 mg group) vs 36-56 mg/L (>2700 mg group)				
Hashkes, 2014 [40]	Rilonacept	RIL: 76% PBO: 39%					Rilonacept	Placebo	*P*	
						Physical summary score	33.66 ± 16.41	23.7 ± 14.51	.025	
						Psychosocial summary score	51.4 ± 10.31	49.79 ± 12.37	.550	
IL-6										
Henes, 2022 [16]	Tocilizumab						Tocilizumab		Placebo	
						Responder at wk 16, n (%)	2 (15.4)		0	*P* = .089
						Secondary outcome wk 16:	Before	After	Before	After
						Phy GA < 2, n (%)		3 (23.1)		4 (33.3)
						SAA < ULN (10 mg/L), n (%)		7 (53.8)		2 (16.7)
						CRP < ULN (5 mg/L), n (%)		9 (69.2)		3 (25)
						Phy GA (mm)	60.0	29.5	66.5	38.0
						Patient GA (mm)	58.0	33.0	47.0	38.5
						FFbH (%)	91.7	91.7	88.9	86.6
Koga, 2022 [15]	Tocilizumab	TCZ: 93% PBO: 89%	TCZ: 100% PBO: 23%	TCZ: 100% PBO: 5%		Achievement of FMF50 score: TCZ 20% vs PBO 8.3% The change in Phy GA and SF-36 from baseline did not differ between TCZ and PBO.				

ANA, anakinra; CHQ-PF50, Child Health Questionnaire-Parent Form 50; CRP, C-reactive protein; ESR, erythrocyte sedimentation rate; FFbH, Hannover Functional Ability Questionnaire; FMF, familial Mediterranean fever; GA, global assessment; IL, interleukin; PBO, placebo; Phy, physician; q4w, every 4 weeks; q8w, every 8 weeks; QoL, quality of life; RIL, rilonacept; SAA, serum A-amyloid; SDS, Sheehan Disability Scale; SF-12/36, Short Form 12/36; ULN, upper limit of normal; VAS, visual analogue scale; TCZ, tocilizumab.

Table 5 [42–49] shows the results of these studies. Colchicine may cause transient and mild leukopenia, while intolerance is associated with increased attacks, chronic inflammation, and proteinuria [48,49]. In a randomised controlled study, Polat et al. [47] showed that using colchicine daily in a single dose has a similar efficacy without additional safety issues compared with routine twice-daily usage. Bustaffa et al. [45] reported that partial and/or nonresponders to colchicine are mostly undertreated according to the patient's age and body weight. Similarly, Goldberg et al. [46] showed that the efficacy and safety of colchicine are comparable between FMF patients <4 years old and those 4 to 8 years old if they receive appropriate doses according to

Table 3
Safety of biological agents in FMF

Study	Treatment	Total	Serious	Mild infections	Others	Discontinuation
Clinical trials						
IL-1						
Ben-Zvi, 2016 [9]	Anakinra	Total AEs: 94 Drug-related AEs: 16.7%				
Brik, 2014 [10]	Canakinumab	11 AEs in 4 patients		1 moderate streptococcal throat infection		
de Benedetti, 2018 [11]	Canakinumab	Including fever and disease flare 926[a] Excluding fever and disease flare 671[a] Infections 173[a]	Including flares 37.3[a] Excluding flares 30.7[a] Infections 6.6[a]		Abdominal pain 26.3[a] Headache 28.5[a] Diarrhoea 19.7[a] Arthralgia 15.4[a] Injection site reaction 43.9[a]	
Lachmann, 2021 [12]	Canakinumab	NR				
Ozen, 2020 [13]	Canakinumab	<2700 mg group vs >2700 mg group rate (no. of events during 72 wk) **Total AEs:** 1.38[a] vs 1.92[a] Total AEs excluding flares and fever: 1.21[a] vs 1.5[a]	**All** 0.09[a] vs 0.04[a] **Infections:** 0.02[a] vs 0.001[a]	0.37[a] vs 0.33[a]		AEs leading to discontinuation: <0.01[a] vs 0[a] FMF flares: 0.12[a] vs 0.36[a] Abdominal pain: 0.03[a] vs 0.12[a] Headache: 0.06[a] vs 0.06[a] Back pain: 0.03[a] vs 0.05[a] URTIs: 0.04[a] vs 0.08[a] Fever: 0.04[a] vs 0.06[a] Arthralgia: 0.04[a] vs 0.06[a]
Hashkes, 2014 [40]	Rilonacept	NR				
IL-6						
Henes, 2022 [16]	Tocilizumab	52 (26.5%)	1 ileitis	10 (19.6%)	10 (19.6%) FMF flare 9 (17.6%) gastroenterology 6 (11.8%) skin disorder 6 (11.8%) joint complaints 2 (3.9%) cardiac 8 (15.7%) other mild AEs	
Koga, 2022 [15]	Tocilizumab	Tocilizumab 90.9% Placebo: 33.3%	Tocilizumab 18.2% Placebo: 8.3%	2 URTIs 2 folliculitis	8 hypofibrinogenemia 2 injection site reactions 2 headaches	
Observational studies						
Akar, 2018 [17]	Anakinra or Canakinumab	Anakinra: 22 Canakinumab: 4	Anakinra: 1 anaphylactoid reaction, 1 serious neutropenia, 1 pneumonia Canakinumab: 1 fungal pneumonia	1 herpes infection 1 cellulitis	17 injection site reactions (16 anakinra, 1 canakinumab) 1 psoriasis	35 patients discontinued after a mean of 19.2 mo: 11 due to AEs 5 primary and 8 secondary failures 3 patient decisions 2 pregnancies 6 unknown reasons
Atas, 2021 [18]	Anakinra Canakinumab	Anakinra 40.6% Canakinumab 30.4%	Anakinra: 2 anaphylactoid reactions, 1 severe neutropenia, 1 severe skin rash that needed hospitalisation Canakinumab: none		Anakinra: 22 injection side reaction, 12 skin rash, 8 weight gain, 3 increased liver enzymes, 3 mild neutropenia Canakinumab: 6 weight gain, 1 increased liver enzyme	**Anakinra** (38.6% in total) 19.8% side effects, 13.8% insufficient response **Canakinumab** (18.5% in total) 11.1% insufficient response, 7.4% pregnancy
Babaoglu, 2019 [19]	Anakinra	2			2 transient leukopenia	
Babaoglu, 2020 [20]	Canakinumab	NR				
Cetin, 2015 [21]	Anakinra Canakinumab		Anakinra: 1 pneumonia			

(*continued*)

Table 3 (*Continued*)

Study	Treatment	Total	Serious	Mild infections	Others	Discontinuation
Eroglu, 2015 [22]	Anakinra Canakinumab Etanercept	Anakinra: 3 Canakinumab: 1 Etanercept: 1		**Canakinumab:** 1 pneumonia	**Anakinra:** 2 injection site reactions 1 urticarial skin reaction **Etanercept**: 1 neutropenia	
Karabulut, 2022 [23]	Canakinumab	NR				
Kucuksahin, 2016 [24]	Anakinra Canakinumab				3 injection site reactions, 1 mild fatigue	
Kurt, 2020 [25]	Anakinra Canakinumab	Anakinra: 3 Canakinumab: none	1 severe disseminated urticarial rash		2 headaches	
Marko, 2021 [26]	Anakinra		Hospitalisation: drug-related: 3 (7%); 2 respiratory tract infections and 1 acute coronary syndrome followed by an infection with influenza Drug unrelated: 3 (7%); 1 soft tissue bleeding, 1 acute kidney injury, and 1 acute coronary syndrome	Diarrhoea: 2 (4.5%)	Injection site reaction: 11 (25%) Headache: 4 (9%) Alopecia: 3 (7%) Neutropenia: 2 (5%) Leukopenia: 1 (2%)	
Pinchevski-Kadir, 2023 [27]	Anakinra Canakinumab	3			1 local skin reaction 2 abdominal pains	
Sag, 2020 [28]	Anakinra Canakinumab	17		3 mild infections	Anakinra: 11 local skin reactions 2 transient leukopenia Canakinumab: 1 transient thrombocytopenia	
Sahin, 2020 [29]	Anakinra Canakinumab		1 (2.4%) severe neutropenia 1 (2.4%) patient who also had PAN and sacroiliitis **died** due to sepsis	URTI or UTI 7%-30%	8 (19.5%) allergic reaction 1 (2.4%) multiple sclerosis after 2 y of treatment	
Ugurlu, 2020 [30]	Anakinra Canakinumab	2	2 patients **died:** 1 non-Hodgkin lymphoma 1 cardiac amyloidosis			
Ugurlu, 2021 [31]	Anakinra	14			7 skin reaction 3 increased liver enzymes 4 leukopenia	
Varan, 2019 [41]	Anakinra Canakinumab	NR				
IL-6						
Honda, 2021 [33]	Tocilizumab	NR				
Ugurlu, 2017 [34]	Tocilizumab		1 hypertensive encephalopathy	1 URTI 1 UTI	1 diplopia 1 hypertension	
Yilmaz, 2015 [35]	Tocilizumab	2			1 elevated liver enzyme, 1 mild thrombocytopenia	
Other						
Karadeniz, 2020 [36]	Tofacitinib	NR				
Garcia-Robledo, 2019 [37]	Tofacitinib	NR				

(*continued*)

Table 3 (*Continued*)

Study	Treatment	Total	Serious	Mild infections	Others	Discontinuation
Gök, 2017 [38]	Tofacitinib	NR				
Haj-Yahia, 2021 [39]	Anti-TNF (adalimumab, etanercept, infliximab, golimumab)	12		1 pneumonia	5 injection site reactions 3 fevers 2 neurological manifestations (1 drop wrist) 1 abdominal pain	

Unless otherwise noted, rates are presented as the total or percent over the number of patients.
AE, adverse event; FMF, familial Mediterranean fever; IL, interleukin; NR, not reported; PAN, polyarteritis nodosa; TNF, tumour necrosis factor; URTI, upper respiratory tract infection; UTI, urinary tract infection.
[a] Rate per 100 patient-years.

Table 4
Characteristics of studies with different colchicine treatment dosing strategies

Study	Design	Patients	Dose 1		Dose 2	Outcomes measured
Comparison of different colchicine products						
Baglan, 2021 [42]	LOS > 20	35 children[a]	C. Dispert and Kolsin[c] 1.72 mg/m^2/d		C. Opocalcium[d]: 1.74 mg/m^2/d	Frequency of attacks Attack duration APR
Emmungil, 2020 [43]	LOS > 20	50 adults[b]	C. Dispert and Kolsin[c] 1.85 ± 0.47 mg/d		C. Opocalcium[d]: 1.84 ± 0.37 mg/d	Frequency of attacks
Türkucar, 2021 [44]	LOS > 20	29 children[a]	C. Dispert[c]: 1.71 ± 0.45 mg/d		C. Opocalcium[d]: 1.71 ± 0.45 mg/d	Frequency of attacks Attack duration APR FMF severity score
Comparison of age-related dosing						
Bustaffa, 2021 [45]	LOS > 20	125 children 96 adults	Colchicine oral	<5 y 5-10 y 10-18 y >18 y	0.5-0.75 mg/d 0.5-0.8 mg/d 1.0-1.5 mg/d 1 mg/d	Complete response Partial response (<1 episode/mo) Partial response with unknown frequency Resistant (>1 episode/mo)
Goldberg, 2019 [46]	LOS > 20	89 children[a] 41, <4 y 48, 4-8 y	Colchicine oral	<4 y 4-8 y	0.053 (0.039-0.066) mg/kg 0.050 (0.040-0.060) mg/kg	Frequency of attacks Duration of attacks Complete/partial/no response
Comparison of once-daily vs twice-daily dosing						
Polat, 2016 [47]	RCT 24 wk noninferiority	79 children[a]	Colchicine oral 1 × 1 mg		Colchicine oral 2 × 0.5 mg	Mor severity score APRs Safety
Other dose comparisons						
Sag, 2020 [48]	LOS > 20	213 children[a]	Colchicine oral 0.027 mg/kg/d			Safety
Satis, 2020 [49]	LOS > 20	971[b] (172 intolerant)	Colchicine oral 1 (1-2) mg (tolerant)		Colchicine oral 1 (1-1) mg (intolerant)	Safety No. of attacks per year Proteinuria Amyloidosis ADDI

ADDI, autoinflammatory disease damage index; APR, acute-phase reactants; FMF, familial Mediterranean fever; LOS, longitudinal observational study; RCT, randomized controlled trial.
[a] Turkish paediatric criteria (Yalcinkaya-Ozen).
[b] Tel-Hashomer criteria.
[c] Turkish preparation.
[d] Non-Turkish preparation.

their body weight. Interestingly, changing colchicine tablets to different brands improved disease activity and decreased the number of attacks and acute-phase reactants with no safety issues [42–44].

Efficacy and safety of biological agents in FMF-related amyloidosis

No RCT investigated the efficacy and safety of biological agents in patients with FMF-related AA amyloidosis; therefore, the evidence comes from longitudinal case series and case reports (Table 6) [17,18,21,24–26,29,30,34–36,41,50–70]. Twenty studies provided information on patients with FMF-related amyloidosis without renal transplantation, of whom 144 patients had been treated with anti–IL-1 [17,18,21,24–26,41,50–55], 27 with anti–IL-6 [34,35,56–59], and 1 with a JAK (Janus kinase) inhibitor [36]. Additionally, 13 studies provided information on 338 patients undergoing renal transplants due to FMF-related AA amyloidosis: 164 who received IL-1 inhibitors [29,30,60–68], and 174 who received other or mixed treatments [69,70].

Table 5
Efficacy and safety results of studies with different colchicine treatment dosing strategies

Study	Efficacy			Safety			
Comparison of different colchicine products							
Baglan, 2021 [42]		Turkish product	Non-Turkish product	Turkish product	Non-Turkish product		
	Attacks per year	9.85	1.85	Elevated liver enzymes (n = 4) Diarrhoea (n = 4) Leukopenia (n = 3)	No AEs		
	Attack duration (h)	52.14	44.28				
	ESR mm/h	20.69	13.58				
	CRP mg/L	8.76	1.85				
Emmungil, 2020 [43]	0-3 attacks/y, %	16	88	None reported			
	4-6 attacks/y, %	20	10				
	>7 attacks/y, %	64	2				
Türkucar, 2021 [44]	No. of attacks last 6 mo	5.22 ± 2.09	1.17 ± 1.66	None reported			
	Attack duration (h)	48 (48-51)	24 (24-30)				
	FMF severity score	9.26 ± 1.88	5.92 ± 2.08				
	CRP mg/L	1.54 (1.54-1.64)	0.02 (0.03-0.17)				
	ESR mm/h	44 (41.75-44)	23 (21.25-23)				
Comparison of age-related dosing							
Bustaffa, 2021 [45]		Overall, %	<5 y, %	5-10 y, %	10-18 y, %	>18 y, %	Diarrhoea (n = 2)
	Complete response	55.2	66.7	34.4	52.8	60.8	Vomiting (n = 1)
	Partial (<1 episode/ mo)	29.4	16.7	34.4	26.4	30.0	Myalgia (n = 1)
	Partial (unknown frequency)	7.7	0	18.7	13.2	3.1	
	Resistant (>1 episode/mo)	7.7	16.6	12.5	7.6	6.1	
Goldberg, 2019 [46]		<4 y	4-8 y			<4 y, %	4-8 y, %
	Attacks per month	2	1		Total AEs	26.9	30
	Duration (d)	2	2		Severe AEs	0	4
	Complete response, %	61	60.4		Lowered dose due to AEs	12.2	16.7
	Partial response, %	24.4	29.2		Colchicine failure	2.4	0
	No response, %	14.6	10.4				
	Colchicine failure, %	7.3	12.5				
Comparison of once-daily and twice-daily dosing							
Polat, 2016 [47]		Once daily		Twice daily			Once daily, %	Twice daily, %
		Baseline	Second visit	Baseline	Second visit	Anorexia	16.7	16.2
	Fever, %	66.7	19	54.1	16.7	Nausea	2.4	5.4
	Duration of attacks (h)	48 ± 27.25	8.4 ± 21.77	44.57 ± 31.42	5.6 ± 15.13	Diarrhoea	2.4	2.7
	No. of attacks	3	0	3	0	Abdominal pain	11.9	8.1
	ELE, %	7.1	4.8	5.4	0	Vomiting	0	5.4
	Mor score	3.48 ± 1.13	2.81 ± 0.83	3.27 ± 1.07	2.76 ± 0.93	Elevated ALT	7.1	2.7
	High ESR, %	55.9	4.2	56.7	10.8	Elevated AST	11.9	14.3
	Elevated CRP, %	40.5	14.3	37.8	10.8			
Other dose comparisons							
Sag, 2020 [48]				AEs: 23 (10.8%)[a] Moderate: 1 lymphopenia 2 neutropenia	Mild: 7 neutropenia 11 leukopenia 2 lymphopenia and neutropenia		

(*continued on next page*)

Table 5 (*Continued*)

Study	Efficacy				Safety	
		Colchicine tolerant	Colchicine intolerant	All AEs	Permanent cessation n = 18 (10.5%)
Satis, 2020 [49]	-			Diarrhoea n = 99	11 diarrhoea
				Liver toxicity n = 54	4 liver toxicity
	Chronic inflammation, %	15.4	26.1	Leukopenia n = 10	1 leukopenia
	No. of attacks per year	2 (5)	4 (8)	Muscle toxicity n = 5	2 muscle toxicity
	Proteinuria, %	5.9	11.6	Skin reaction n = 2	
	Amyloidosis, %	4.4	13.3	Nausea n = 4	
	ADDI	1 (1)	1 (1)	Infertility n = 2	

ADDI, autoinflammatory disease damage index; AE, adverse event; ALT, Alanine aminotransferase; CRP, C-reactive protein; ELE, erysipelas-like erythema; ESR, erythrocyte sedimentation rate; FMF, familial Mediterranean fever.

[a] All were transient and reversed after dose adjustment.

Two patients died among the nontransplanted patients and 18 among the transplanted patients, all of whom were on IL-1 inhibitors. End-stage renal disease was observed only in 14 amyloidosis patients who had no renal transplantation (Supplementary Fig S1).

Proteinuria decreased in most patients (70.9%) treated with biological agents, regardless of renal transplantation status (Table 7) [17,18,21,24–26,29,30,34–36,41,50–70]. No additional safety issues were reported.

Tapering

Except for 1 [71], all studies were observational, with the majority being retrospective, and they all had a high risk of bias. Five studies analysed the tapering of colchicine (Supplementary Table S7) and 7 of canakinumab (Supplementary Table S8). The studies' descriptions and results are compiled in Supplementary Table S8.

DISCUSSION

In this SR, we showed the efficacy and safety of different biological treatments in colchicine-resistant and intolerant FMF, as well as patients with FMF-related AA amyloidosis. We also evaluated the effect of treatment with varying colchicine preparations and age and bodyweight-related dosing. This information will guide the decisions taken in the EULAR task force on FMF.

FMF is the most common autoinflammatory disease, and the first-line treatment is colchicine. The primary pathogenic mechanism is the overactivation of the pyrin inflammasome, which causes increased proinflammatory cytokines, specifically IL-1 [72]. In light of this mechanism, anti–IL-1 agents were tested in patients in whom colchicine cannot control the disease and subclinical inflammation. The evidence we identified includes RCTs that support using anti–IL-1 treatments in FMF. Other SRs found similar results to ours [73,74], including a Cochrane review [75]. In the review by Kilic et al. [74] and the Cochrane review by Yin et al. [75], the authors performed meta-analyses. The former group pooled observational data without adjustment and with high heterogeneity, and the latter used an endpoint challenging to prove efficacy in FMF: the 'number of participants experiencing an attack'. The studies identified in our SR negatively surprised us with their endpoint heterogeneity, making a proper meta-analysis very challenging.

IL-1 overproduction triggers the production of other inflammatory cytokines, such as IL-6 and TNF-α, leading to the activation of immune cells, including macrophages and T cells; consequently, therapies that block IL-6 have gained attention as potential treatments for autoinflammatory disorders, such as FMF [76]. Besides, IL-6 has been shown to be elevated during attacks [77]. Two recent RCTs on anti–IL-6 treatments in colchicine-resistant FMF patients suggest efficient results [15,16]. Interestingly, JAK inhibitors have also been successfully tested in 3 case series [36–38].

Colchicine resistance is an important problem during the management of the disease [4]. In addition, colchicine is taken orally; thus, adherence should be carefully assessed before deciding on resistance to colchicine. One way to improve adherence may be through using a single dose. An RCT was performed to overcome this problem by offering patients treatment once daily instead of twice daily [47]. Interestingly, there were no differences in efficacy and safety between the groups, supporting that once-daily treatment might be an option for patients who forget to take their medicine. In some countries, there is

Table 6
Characteristic of studies testing treatments for FMF-related amyloidosis

Study	Design	N[a]	Age	% Female	Treatment	Dose
Without renal transplant						
IL-1						
Akar, 2018 [17]	LOS > 20	52	m: 36	48	Anakinra	100 mg/d (96.4%), 50-300 mg/d remaining
					Canakinumab	150 mg/4 wk (67%)/8 wk (24%)/12 wk (9%)
Atas, 2021 [18]	LOS > 20	27	m: 43.3	52	Anakinra	100 mg daily (48%)/twice daily (4%)/2 d (23%)/3 d (9%)
					Canakinumab	150 mg monthly (21%), bimonthly (3%), and quarterly (n = 1)
Cansu, 2021 [50]	Case report	1	40	100	Anakinra	100 mg/2 d
Cetin, 2015 [21]	LOS > 20	2	14 and 32	50	Anakinra	100 mg/d
					Canakinumab	150 mg/8 wk
Kisla-Ekinci, 2019 [51]	Case series	1	14	0	Canakinumab	3 mg/kg/mo
Kucuksahin, 2017 [24]	LOS > 20	7	m: 39.2	86	Anakinra	100 mg/d
					Canakinumab	150 mg/4 wk
Kurt, 2020 [25]	LOS > 20	1		0	Anakinra	2-5 mg/kg/d
					Canakinumab	4 mg/kg/mo (max 150 mg)
Marko, 2021 [26]	LOS > 20	7	m: 44	55	Anakinra	50-100 mg/d
Nalcacıoglu, 2017 [52]	Case report	1	64		Anakinra	1 mg/kg/d
Sargın, 2019 [53]	Case series	7	m: 42	83	Anakinra	100 mg/d
Varan 2019 [41]	Case series	17	21	59	Anakinra	100 mg/d
					Canakinumab	150-300 mg/mo
Yazilitas, 2017 [54]	Case series	3	m: 14.3	100	Canakinumab	
Yildirim, 2021 [55]	Case series	18	m: 35.8 ± 10.2	28	Canakinumab	150 mg/mo
IL-6						
Aikawa, 2019 [56]	Case report	1	53	0	Tocilizumab	162 mg/2 wk
Hamanoue, 2016 [57]	Case report	1	51	0	Tocilizumab	400 mg/mo
Inui, 2020 [58]	Case report	1	51	0	Tocilizumab	8 mg/kg/mo
Serelis, 2019 [59]	Case report	1	32	100	Tocilizumab	8 mg/kg/mo
Ugurlu, 2017 [34]	Case series	12	m: 35.2 ± 10	50	Tocilizumab	8 mg/kg/mo
Yilmaz 2015 [35]	Case series	11	m: 38	9	Tocilizumab	8 mg/kg/4 wk
Others						
Karadeniz 2020 [36]	Case series	1	24	0	Tofacitinib	5 mg twice/d
With renal transplant						
IL-1						
Hasbal, 2019 [60]	Case report	1	24	100	Anakinra	100 mg/d
Mirioglu, 2022 [61]	LOS > 20	36	m: 35.2 ± 12.3	38.9	Anakinra	None specified
					Canakinumab	None specified
Ozcakar, 2018 [62]	Case series	5	m: 21.4	40	Anakinra	1 mg/kg/d
					Canakinumab	2 mg/kg/4-8 wk
Ozcakar, 2016 [63]	Case series	6	m: 16	50	Anakinra	1 mg/kg/d
					Canakinumab	2 mg/kg/4-8 wk
Peces, 2017 [64]	Case series	2	m: 38	0	Anakinra	100 mg/48 h
Sahin, 2020 [29]	LOS > 20	15	m: 32 (17-60)	49.2	Anakinra	100 mg/d
					Canakinumab	150 mg/8 wk
Sendogan, 2019 [65]	Case series	4	m: 36	50	Canakinumab	150 mg/4-8 wk
Şimşek, 2021 [66]	LOS > 20	39	m: 39.3 ± 11.5	43.5	Anakinra	100 mg/d
					Canakinumab	150 mg/4 wk
Trabulus, 2018 [67]	Case series	9	m: 39	44.4	Canakinumab	150 mg/mo
Ugurlu 2020 [30]	LOS > 20	44	m: 43.63 ± 12.17	50	Anakinra	100 mg/d
					Canakinumab	150 mg/mo
Yıldırım, 2018 [68]	Case series	3	m: 54.6	100	Canakinumab	150 mg/mo
Others						
Bektas, 2023 [69]	LOS > 20	137	m: 43	48.2	Anakinra Canakinumab Etanercept Tocilizumab Infliximab Secukinumab Adalimumab	None specified
Schwarz, 2024 [70]	LOS > 20	37	m: 49.4	37.2	Anti−IL-1[b] Anti−IL-6[b] Anti-TNF[b]	None specified

FMF, familial Mediterranean fever; LOS, longitudinal observational study; m, mean; TNF, tumour necrosis factor.
[a] Patients with AA amyloidosis. The studies may investigate many more FMF patients.
[b] No specific drug names.

more than 1 colchicine preparation, in which the colchicine dose remains the same, but the other components or the coating differ. According to 3 interesting studies [42–44], a trial with another colchicine preparation may be justified before moving forward with anti−IL−1 treatment, which is costly in all countries.

AA amyloidosis is the most important morbidity and complication of FMF. In the previous definition of colchicine resistance, amyloidosis was recommended as a reason to intensify treatment [3]. According to our results, biological agents, particularly anti−IL-1 treatments, decrease disease activity,

Table 7
Efficacy and safety of biological agents in FMF-related amyloidosis

Study	Treatment	Site of amyloidosis	Proteinuria mg/d		Other outcome parameters
			Before	After	
Without renal transplant					
IL-1					
Akar, 2018 [17]	Anakinra or Canakinumab	Renal	5458	3557	47 patients had >500 mg/d urinary protein. 77% had a decrease after treatment, and 21% had nondetectable protein. Serum creatinine decreased, but it was not significant.
Atas, 2021 [18]	Anakinra Canakinumab	Renal	3126	730	ANA: 22 patients with proteinuria evaluated. 24-h proteinuria decreased significantly.
Cansu, 2021 [50]	Anakinra	Renal Uterine	3900	7000	Haemodialysis and proteinuria continued, but the follow-up duration was only 2 mo
Cetin 2015 [21]	Anakinra Canakinumab	Renal	**ANA:** 9000/d **CAN:** 25.6 mg/m^2/d	**ANA:** 3700/d **CAN:** 12 mg/m^2/d	
Kisla-Ekinci, 2019 [51]	Canakinumab	Renal			Proteinuria disappeared after 6 doses of monthly canakinumab treatment in a patient with renal amyloidosis.
Kucuksahin, 2016 [24]	Anakinra Canakinumab	Renal (n = 5) Systemic (n = 2)			Two of these patients already had ESRD at the onset of anti−IL-1 treatment, and 1 patient showed stable proteinuria under anti−IL-1 treatment
Kurt, 2020 [25]	Anakinra Canakinumab	Renal			CAN increased attack frequency and proteinuria. ANA decreased the frequency of attacks and proteinuria.
Marko, 2021 [26]	Anakinra	Renal	2500	2200	13 patients with proteinuria, of whom 5 remained stable, 4 improved, and 1 worsened
Nalcacioglu, 2017 [52]	Anakinra	Systemic	118 mg/m^2/d	<20 mg/m^2/d	
Sargin, 2019 [53]	Anakinra	Renal	13,995	2508	
Varan, 2019 [41]	Anakinra Canakinumab	Renal	1606	519	
Yazilitas, 2017 [54]	Canakinumab	Renal			Proteinuria decreased in 2 patients, and 1 had a partial response.
Yildirim, 2021 [55]	Canakinumab	Renal			Patients with GFR ≥ 60 mL/min: 7670 mg/d decreased to 2462 mg/d Patients with GFR < 60 mL/min: 8618 mg/d decreased to 7065 mg/d
IL-6					
Aikawa, 2019 [56]	Tocilizumab	GIS			Abdominal pain and watery diarrhoea resolved after treatment. AA amyloidosis in endoscopic biopsies resolved.
Hamanoue, 2016 [57]	Tocilizumab	Renal GIS	3800	300	Endoscopic biopsy revealed decreased amyloid deposition in the stomach.
Inui, 2020 [58]	Tocilizumab	Renal	3800	1400	Repeat renal biopsies showed a decrease of amyloid area up to approximately 19% of the AA amyloid area of the first biopsy's specimen.
Serelis, 2015 [59]	Tocilizumab	Renal	9000	3600	
Ugurlu, 2017 [34]	Tocilizumab	Renal	6537	4745	
Yilmaz, 2015 [35]	Tocilizumab	Renal			Protein excretion significantly decreased in 4 patients, decreased in 2, and did not change or slightly increased in 4
Others					
Karadeniz, 2020 [36]	Tofacitinib	Renal	36,600	11200	A case of increased proteinuria with CAN and TCZ improved with TOFA
With renal transplant					
IL-1					
Hasbal, 2019 [60]	Anakinra	Renal			Decrease in APRs, attack-free, acute kidney injury during attack resolved after treatment.
Mirioglu, 2022 [61]	Anakinra Canakinumab	Renal	200	200	Overall graft loss 10 (27.8%), 5-y graft survival 94.4%, 10-y graft survival 83.3% Rejections 3 (8.3%) 9 patients in CAN: 8 inadequate response; 1 severe injection site reaction

(*continued on next page*)

Table 7 (*Continued*)

Study	Treatment	Site of amyloidosis	Proteinuria mg/d		Other outcome parameters
			Before	After	
Ozcakar, 2018 [62]	Anakinra Canakinumab	Renal		89.8	Mean age at amyloidosis 10.3 y Mean age at ESRD 15.6 y Mean age at transplant 17.3 y Mean anti−IL-1 treatment duration 41.2 mo None of the patients had proteinuria at the last visit. 2 had steroid-responsive acute rejection at the 4th and 8.5th mo
Ozcakar, 2016 [63]	Anakinra Canakinumab	Renal	190 mg/m^2/h	12 mg/m^2/h	All patients became attack-free 1 had chronic renal failure, 1 had ESRD, and 3 had renal transplantation
Peces, 2017 [64]	Anakinra	Renal	21,500	770	
Sahin, 2020 [29]	Anakinra Canakinumab	Renal	4472	3960	3 patients switched to TCZ (2 refractory arthritis, 1 increased proteinuria with amyloidosis) 1 progressed to ESRD under anti−IL-1 treatment and had a renal transplant
Sendogan, 2019 [65]	Canakinumab	Renal			The patients had no attacks. Their serum CRP and SAA levels normalised; creatinine and proteinuria levels were stable. No graft loss
Şimşek, 2021 [66]	Anakinra Canakinumab	Renal			Vascular amyloid accumulation on pretreatment protocol biopsies of 4 patients persisted in repeated biopsies after IL-1 antagonist treatment. Untreated (n = 30), % / Treated (n = 9), % Acute rejection 13.3 / 22.2 Graft recurrence of amyloidosis 62.5 / 77.7 Graft loss 14.2 / 0 Death 30 / 0
Trabulus, 2018 [67]	Anakinra Canakinumab Canakinumab	Renal Renal Systemic	2381	710	No attacks after treatment
Ugurlu, 2020 [30]	Anakinra Canakinumab	Renal	2361	2596	4 had renal transplants. 1 had CAN, but GFR worsened, and haemodialysis was initiated. 3 had ANA; 1 had renal improvement from stage 3 to 2; 2 had stable disease 5 were on dialysis; 1 with ANA received a transplant; 1 died due to cardiac amyloidosis; 1 stopped ANA due to insufficient response; 2 are still on treatment.
Yildirim, 2018 [68]	Canakinumab	Renal			Abolition of attacks and normalisation of CRP levels; stabilisation of serum creatinine levels
Bektas, 2023 [69]	Anakinra Canakinumab Etanercept Tocilizumab Infliximab Secukinumab Adalimumab	Systemic	4000	500	Chronic renal failure at admission: 61 (47.3%) ESRD at admission: 22 (19.8%) Favourable outcome 83 (61.9%) Poor outcome: 51 (38.1%)
Schwarz, 2024 [70]	Anti−IL-1 Anti−IL-6 Anti-TNF	Renal			Survival rates after transplant: 94% at 1 y, 86% at 5 y. Cumulative incidences of allograft loss: 10.5% at 1 y, 13.0% at 5 y. Histologically proven AA amyloidosis recurrence: 5 (5.8%)

ANA, anakinra; APR, acute-phase reactant; CAN, canakinumab; CRP, C-reactive protein; ESRD, end-stage renal disease; FMF, familial Mediterranean fever; GFR, glomerular flow rate; GIS, gastrointestinal system; IL, interleukin; SAA, serum amyloid A; TCZ, tocilizumab; TNF, tumour necrosis factor; TOFA, tofacitinib.

proteinuria, mortality, and ongoing inflammation, even in renal transplant patients.

Tapering strategies in FMF seem feasible, although the outcome of studies that included patients with biallelic pathogenic *MEFV* mutations was not so promising. As for tapering biologics, there were only studies on canakinumab at the time of the review, with varying intervals and dose protocols. Also, the time when tapering was started differed across studies, making conclusions on tapering difficult.

This study also has some limitations. Although there are some RCTs on this topic, most of the data come from case series, and the risk of bias is relatively high. Even in RCTs, the outcome measures were very heterogeneous, which prevented us from performing a solid meta-analysis. Also, since this review was performed as part of the update to the previous EULAR recommendations, we only started our search after 2014, which might have led us to miss some studies. We had to include 2 more recently published papers beyond the search date limit recommended by the expert panel, as they reported a very high number of patients and had a major impact on our topic of interest.

In conclusion, while patients should remain on colchicine, the addition of biological DMARDs, particularly anti−IL-1 and anti−IL-6 agents, seems effective and relatively safe in FMF patients who are resistant to colchicine, as well as in patients with amyloidosis and renal transplantation. Future trials in FMF should consider an outcome standardisation to facilitate clinical decisions.

Competing interests

ES declare no conflicts of interest. SO has been a consultant for Novartis and the speaker's bureau for Sobi. LC and TO have no conflicts of interest with the review topic and do not prescribe; nevertheless, they work for an institute that delivers services for many stakeholders, including pharmaceutical companies that produce drugs listed here, such as Roche or Novartis.

CRediT authorship contribution statement

Erdal Sag: Writing − review & editing, Writing − original draft, Investigation, Formal analysis, Data curation, Conceptualization. **Teresa Otón:** Writing − review & editing, Investigation, Data curation, Conceptualization. **Loreto Carmona:** Writing − review & editing, Supervision, Methodology, Data curation, Conceptualization. **Seza Ozen:** Writing − review & editing, Supervision, Funding acquisition, Conceptualization.

Contributors

All authors prepared and discussed the research questions under the supervision of SO. ES and TO designed the search strategies, selected the articles, and collected the data. LC supervised all works and helped select articles and visualise data. ES drafted this manuscript. All authors were involved in the discussions and revised the manuscript prior to submission. LC is the guarantor of the content.

Funding

The work received funding from the European Alliance of Associations for Rheumatology (EULAR) under project QoC018.

Patient consent for publication

Not applicable

Ethics approval

Not applicable

Provenance and peer review

Not applicable

Data availability statement

Data are available upon reasonable request. The review was not registered; however, the protocol is available and can be provided upon request from the authors.

Supplementary materials

Supplementary material associated with this article can be found in the online version at doi:10.1016/j.ard.2025.05.020.

Orcid

Erdal Sag: http://orcid.org/0000-0002-6542-2656
Teresa Otón: http://orcid.org/0000-0003-3622-7146
Loreto Carmona: http://orcid.org/0000-0002-4401-2551
Seza Ozen: http://orcid.org/0000-0003-2883-7868

REFERENCES

[1] Sag E, Bilginer Y, Ozen S. Autoinflammatory diseases with periodic fevers. Curr Rheumatol Rep 2017;19(7):41. doi: 10.1007/s11926-017-0670-8.
[2] Demirkaya E, Erer B, Ozen S, Ben-Chetrit E. Efficacy and safety of treatments in Familial Mediterranean fever: a systematic review. Rheumatol Int 2016;36(3):325–31. doi: 10.1007/s00296-015-3408-9.
[3] Ozen S, Demirkaya E, Erer B, Livneh A, Ben-Chetrit E, Giancane G, et al. EULAR recommendations for the management of familial Mediterranean fever. Ann Rheum Dis 2016;75(4):644–51. doi: 10.1136/annrheumdis-2015-208690.
[4] Özen S, Sag E, Ben-Chetrit E, Gattorno M, Gül A, Hashkes PJ, et al. Defining colchicine resistance/intolerance in patients with familial Mediterranean fever: a modified-Delphi consensus approach. Rheumatology (Oxford) 2021;60(8):3799–808. doi: 10.1093/rheumatology/keaa863.
[5] Schardt C, Adams MB, Owens T, Keitz S, Fontelo P. Utilization of the PICO framework to improve searching PubMed for clinical questions. BMC Med Inform Decis Mak 2007;7:16. doi: 10.1186/1472-6947-7-16.
[6] Haddaway NR, Page MJ, Pritchard CC, McGuinness LA. PRISMA2020: an R package and Shiny app for producing PRISMA 2020-compliant flow diagrams, with interactivity for optimised digital transparency and Open Synthesis. Campbell Syst Rev 2022;18(2):e1230. doi: 10.1002/cl2.1230.
[7] Higgins JP, Altman DG, Gøtzsche PC, Jüni P, Moher D, Oxman AD, et al. The Cochrane Collaboration's tool for assessing risk of bias in randomised trials. BMJ 2011;343:d5928. doi: 10.1136/bmj.d5928.
[8] Wells G, Shea B, O'Connell D, Peterson J, Welch V, Losos M, et al. The Newcastle-Ottawa Scale (NOS) for assessing the quality of nonrandomised studies in meta-analyses [Internet]; 2013 [cited 2024 Sept 8]. Available from: http://www.ohri.ca/programs/clinical_epidemiology/oxford.asp
[9] Ben-Zvi I, Kukuy O, Giat E, Pras E, Feld O, Kivity S, et al. Anakinra for colchicine-resistant familial mediterranean fever: a randomized, double-blind, placebo-controlled trial. Arthritis Rheumatol 2017;69(4):854–62. doi: 10.1002/art.39995.
[10] Brik R, Butbul-Aviel Y, Lubin S, Ben Dayan E, Rachmilewitz-Minei T, Tseng L, et al. Canakinumab for the treatment of children with colchicine-resistant familial Mediterranean fever: a 6-month open-label, single-arm pilot study. Arthritis Rheumatol 2014;66(11):3241–3. doi: 10.1002/art.38777.
[11] De Benedetti F, Gattorno M, Anton J, Ben-Chetrit E, Frenkel J, Hoffman HM, et al. Canakinumab for the treatment of autoinflammatory recurrent fever

syndromes. N Engl J Med 2018;378(20):1908–19. doi: 10.1056/NEJMoa1706314.
[12] Lachmann HJ, Lauwerys B, Miettunen P, Kallinich T, Jansson A, Rosner I, et al. Canakinumab improves patient-reported outcomes in children and adults with autoinflammatory recurrent fever syndromes: results from the CLUSTER trial. Clin Exp Rheumatol 2021;39(5):51–8 Suppl 132. doi: 10.55563/clinexprheumatol/e92f7o.
[13] Ozen S, Ben-Cherit E, Foeldvari I, Amarilyo G, Ozdogan H, Vanderschueren S, et al. Long-term efficacy and safety of canakinumab in patients with colchicine-resistant familial Mediterranean fever: results from the randomised phase III CLUSTER trial. Ann Rheum Dis 2020;79(10):1362–9. doi: 10.1136/annrheumdis-2020-217419.
[14] Hashkes PJ, Spalding SJ, Giannini EH, Huang B, Johnson A, Park G, et al. Rilonacept for colchicine-resistant or -intolerant familial Mediterranean fever: a randomized trial. Ann Intern Med 2012;157(8):533–41. doi: 10.7326/0003-4819-157-8-201210160-00003.
[15] Koga T, Sato S, Hagimori N, Yamamoto H, Ishimura M, Yasumi T, et al. A randomised, double-blind, placebo-controlled phase III trial on the efficacy and safety of tocilizumab in patients with familial Mediterranean fever. Clin Exp Rheumatol 2022;40(8):1535–42. doi: 10.55563/clinexprheumatol/fgx9vv.
[16] Henes JC, Saur S, Kofler DM, Kedor C, Meisner C, Schuett M, et al. Tocilizumab for the treatment of familial Mediterranean fever-a randomized, double-blind, placebo-controlled phase II study. J Clin Med 2022;11(18):5360. doi: 10.3390/jcm11185360.
[17] Akar S, Cetin P, Kalyoncu U, Karadag O, Sari I, Cınar M, et al. Nationwide experience with off-label use of interleukin-1 targeting treatment in familial Mediterranean fever patients. Arthritis Care Res (Hoboken) 2018;70(7):1090–4. doi: 10.1002/acr.23446.
[18] Atas N, Eroglu GA, Sodan HN, Ozturk BO, Babaoglu H, Satis H, et al. Long-term safety and efficacy of anakinra and canakinumab in patients with familial Mediterranean fever: a single-centre real-life study with 101 patients. Clin Exp Rheumatol 2021;39(5):30–6 Suppl 132. doi: 10.55563/clinexprheumatol/815tdt.
[19] Babaoglu H, Varan O, Kucuk H, Atas N, Satis H, Salman R, et al. On demand use of anakinra for attacks of familial Mediterranean fever (FMF). Clin Rheumatol 2019;38(2):577–81. doi: 10.1007/s10067-018-4230-z.
[20] Babaoglu H, Varan O, Kucuk H, Atas N, Satis H, Salman R, et al. Effectiveness of canakinumab in colchicine- and anakinra-resistant or -intolerant adult familial Mediterranean fever patients: a single-center real-life study. J Clin Rheumatol 2020;26(1):7–13. doi: 10.1097/RHU.0000000000000873.
[21] Cetin P, Sari I, Sozeri B, Cam O, Birlik M, Akkoc N, et al. Efficacy of interleukin-1 targeting treatments in patients with familial Mediterranean fever. Inflammation 2015;38(1):27–31. doi: 10.1007/s10753-014-0004-1.
[22] Eroglu FK, Beşbaş N, Topaloglu R, Ozen S. Treatment of colchicine-resistant familial Mediterranean fever in children and adolescents. Rheumatol Int 2015;35(10):1733–7. doi: 10.1007/s00296-015-3293-2.
[23] Karabulut Y, Gezer HH, Duruoz MT. Canakinumab is effective in patients with familial Mediterranean fever resistant and intolerant to the colchicine and/or anakinra treatment. Rheumatol Int 2022;42(1):81–6. doi: 10.1007/s00296-021-04997-y.
[24] Kucuksahin O, Yildizgoren MT, Ilgen U, Ates A, Kinikli G, Turgay M, et al. Anti-interleukin-1 treatment in 26 patients with refractory familial Mediterranean fever. Mod Rheumatol 2017;27(2):350–5. doi: 10.1080/14397595.2016.1194510.
[25] Kurt T, Aydın F, Nilüfer Tekgöz P, Sezer M, Uncu N. Çelikel Acar B. Effect of anti-interleukin-1 treatment on quality of life in children with colchicine-resistant familial Mediterranean fever: a single-center experience. Int J Rheum Dis 2020;23(7):977–81. doi: 10.1111/1756-185X.13891.
[26] Marko L, Shemer A, Lidar M, Grossman C, Druyan A, Livneh A, et al. Anakinra for colchicine refractory familial Mediterranean fever: a cohort of 44 patients. Rheumatology (Oxford) 2021;60(6):2878–83. doi: 10.1093/rheumatology/keaa728.
[27] Pinchevski-Kadir S, Gerstein M, Pleniceanu O, Yacobi Y, Vivante A, Granat OE, et al. Effect of interleukin-1 antagonist on growth of children with colchicine resistant or intolerant FMF. Pediatr Rheumatol Online J 2023;21(1):4. doi: 10.1186/s12969-022-00784-6.
[28] Sag E, Akal F, Atalay E, Akca UK, Demir S, Demirel D, et al. Anti-IL1 treatment in colchicine-resistant paediatric FMF patients: real life data from the HELIOS registry. Rheumatology (Oxford) 2020;59(11):3324–9. doi: 10.1093/rheumatology/keaa121.
[29] Şahin A, Derin ME, Albayrak F, Karakaş B, Karagöz Y. Assessment of effectiveness of anakinra and canakinumab in patients with colchicine-resistant/unresponsive familial Mediterranean fever. Adv Rheumatol 2020;60(1):12. doi: 10.1186/s42358-020-0117-1.
[30] Ugurlu S, Ergezen B, Egeli BH, Selvi O, Ozdogan H. Safety and efficacy of anti-interleukin-1 treatment in 40 patients, followed in a single centre, with AA amyloidosis secondary to familial Mediterranean fever. Rheumatology (Oxford) 2020;59(12):3892–9. doi: 10.1093/rheumatology/keaa211.
[31] Ugurlu S, Ergezen B, Egeli BH, Selvi O, Ozdogan H. Anakinra treatment in patients with familial Mediterranean fever: a single-centre experience. Rheumatology (Oxford) 2021;60(5):2327–32. doi: 10.1093/rheumatology/keaa596.
[32] Varan O, Kucuk H, Babaoglu H, Atas N, Salman RB, Satis H, et al. Effect of interleukin-1 antagonists on the quality of life in familial Mediterranean fever patients. Clin Rheumatol 2019;38(4):1125–30. doi: 10.1007/s10067-018-4384-8.
[33] Honda N, Yokogawa N, Koga T, Endo Y, Matsubara S. Protracted febrile myalgia syndrome treated with tocilizumab. J Clin Rheumatol 2021;27(3):e95. doi: 10.1097/RHU.0000000000001271.
[34] Ugurlu S, Hacioglu A, Adibnia Y, Hamuryudan V, Ozdogan H. Tocilizumab in the treatment of twelve cases with AA amyloidosis secondary to familial Mediterranean fever. Orphanet J Rare Dis 2017;12(1):105. doi: 10.1186/s13023-017-0642-0.
[35] Yilmaz S, Cinar M, Simsek I, Erdem H, Pay S. Tocilizumab in the treatment of patients with AA amyloidosis secondary to familial Mediterranean fever. Rheumatology (Oxford) 2015;54(3):564–5. doi: 10.1093/rheumatology/keu474.
[36] Karadeniz H, Güler AA, Atas N, Satış H, Salman RB, Babaoglu H, et al. Tofacitinib for the treatment for colchicine-resistant familial Mediterranean fever: case-based review. Rheumatol Int 2020;40(1):169–73. doi: 10.1007/s00296-019-04490-7.
[37] Garcia-Robledo JE, Aragón CC, Nieto-Aristizabal I, Posso-Osorio I, Cañas CA, Tobón GJ. Tofacitinib for familial Mediterranean fever: a new alternative therapy? Rheumatology (Oxford) 2019;58(3):553–4. doi: 10.1093/rheumatology/key384.
[38] Gök K, Cengiz G, Erol K, Ozgocmen S. Tofacitinib suppresses disease activity and febrile attacks in a patient with coexisting rheumatoid arthritis and familial Mediterranean fever. Acta Reumatol Port 2017;42(1):88–90.
[39] Haj-Yahia S, Ben-Zvi I, Lidar M, Livneh A. Familial Mediterranean fever (FMF)-response to TNF-blockers used for treatment of FMF patients with concurrent inflammatory diseases. Joint Bone Spine 2021;88(5):105201. doi: 10.1016/j.jbspin.2021.105201.
[40] Hashkes PJ, Spalding SJ, Hajj-Ali R, Giannini EH, Johnson A, Barron KS, et al. The effect of rilonacept versus placebo on health-related quality of life in patients with poorly controlled familial Mediterranean fever. Biomed Res Int 2014;2014:854842. doi: 10.1155/2014/854842.
[41] Varan Ö, Kucuk H, Babaoglu H, Guven SC, Ozturk MA, Haznedaroglu S, et al. Efficacy and safety of interleukin-1 inhibitors in familial Mediterranean fever patients complicated with amyloidosis. Mod Rheumatol 2019;29(2):363–6. doi: 10.1080/14397595.2018.1457469.
[42] Baglan E, Ozdel S, Bulbul M. Do all colchicine preparations have the same effectiveness in patients with familial Mediterranean fever? Mod Rheumatol 2021;31(2):481–4. doi: 10.1080/14397595.2020.1790139.
[43] Emmungil H, İlgen U, Turan S, Yaman S, Küçükşahin O. Different pharmaceutical preparations of colchicine for familial Mediterranean fever: are they the same? Rheumatol Int 2020;40(1):129–35. doi: 10.1007/s00296-019-04432-3.
[44] Türkuçar S, Otar Yener G, Adıgüzel Dundar H, Acari C, Makay B, Yüksel S, et al. Comparison of different pharmaceutical preparations of colchicine in children with familial Mediterranean fever: is colchicine opocalcium a good alternative? Balkan Med J 2021;38(1):29–33. doi: 10.1007/s00296-019-04432-3.
[45] Bustaffa M, Mazza F, Sutera D, Carrabba MD, Alessio M, Cantarini L, et al. Persistence of disease flares is associated with an inadequate colchicine dose in familial Mediterranean fever: a national multicenter longitudinal study. J Allergy Clin Immunol Pract 2021;9(8):3218–3220.e1. doi: 10.1016/j.jaip.2021.03.048.
[46] Goldberg O, Levinsky Y, Peled O, Koren G, Harel L, Amarilyo G. Age dependent safety and efficacy of colchicine treatment for familial Mediterranean fever in children. Semin Arthritis Rheum 2019;49(3):459–63. doi: 10.1016/j.semarthrit.2019.05.011.
[47] Polat A, Acikel C, Sozeri B, Dursun I, Kasapcopur O, Gulez N, et al. Comparison of the efficacy of once- and twice-daily colchicine dosage in pediatric patients with familial Mediterranean fever—a randomized controlled noninferiority trial. Arthritis Res Ther 2016;18:85. doi: 10.1186/s13075-016-0980-7.
[48] Sag E, Bayindir Y, Adiguzel A, Demir S, Bilginer Y, Aytac S, et al. Colchicine and leukopenia: clinical implications. J Pediatr 2020;224:166–170.e1. doi: 10.1016/j.jpeds.2020.03.065.
[49] Satiş H, Armağan B, Bodakçi E, Ataş N, Sari A, NŞ Yaşar Bilge, et al. Colchicine intolerance in FMF patients and primary obstacles for optimal dosing. Turk J Med Sci 2020;50(5):1337–43. doi: 10.3906/sag-2001-261.

[50] Cansu DÜ, Teke HÜ, Arik D, Korkmaz C. Menorrhagia due to uterine amyloidosis in familial Mediterranean fever: case-based review. Rheumatol Int 2021;41(1):205–11. doi: 10.1007/s00296-020-04721-2.
[51] Kisla Ekinci RM, Balci S, Dogruel D, Altintas DU, Yilmaz M. Canakinumab in children with familial Mediterranean fever: a single-center, retrospective analysis. Paediatr Drugs 2019;21(5):389–95. doi: 10.1007/s40272-019-00354-6.
[52] Nalcacioglu H, Ozkaya O, Genc G, Ayyildiz S, Kefeli M, Elli M, et al. Efficacy of anakinra in a patient with systemic amyloidosis presenting as amyloidoma. Int J Rheum Dis 2018;21(2):552–9. doi: 10.1111/1756-185X.13250.
[53] Sargin G, Kose R, Senturk T. Anti-interleukin-1 treatment among patients with familial Mediterranean fever resistant to colchicine treatment. Retrospective analysis. Sao Paulo Med J 2019;137(1):39–44. doi: 10.1590/1516-3180.2018.0311101218.
[54] Yazıltaş F, Aydoğ Ö, Özlü SG, Çakıcı EK, Güngör T, Eroğlu FK, et al. Canakinumab treatment in children with familial Mediterranean fever: report from a single center. Rheumatol Int 2018;38(5):879–85. doi: 10.1007/s00296-018-3993-5.
[55] Yildirim T, Yilmaz R, Saglam A, Uzerk-Kibar M, Jabrayilov J, Erdem Y. Baseline renal functions predict the effect of canakinumab on regression of proteinuria in patients with familial Mediterranean fever. Nefrologia (Engl Ed) 2021;41(6):632–9. doi: 10.1016/j.nefroe.2022.01.002.
[56] Aikawa E, Shimizu T, Koga T, Endo Y, Umeda M, Hori T, et al. Atypical familial Mediterranean fever complicated with gastrointestinal amyloidosis diagnosed due to paroxysmal arthralgia and intractable diarrhea, successfully treated with tocilizumab. Intern Med 2019;58(12):1781–5. doi: 10.2169/internalmedicine.2277-18.
[57] Hamanoue S, Suwabe T, Hoshino J, Sumida K, Mise K, Hayami N, et al. Successful treatment with humanized anti-interleukin-6 receptor antibody (tocilizumab) in a case of AA amyloidosis complicated by familial Mediterranean fever. Mod Rheumatol 2016;26(4):610–3. doi: 10.3109/14397595.2014.908810.
[58] Inui K, Sawa N, Suwabe T, Mizuno H, Yamanouchi M, Hiramatsu R, et al. Long term administration of tocilizumab improves renal amyloid A (AA) amyloidosis deposition in familial Mediterranean fever. Mod Rheumatol Case Rep 2020;4(2):310–1. doi: 10.1080/24725625.2020.1739193.
[59] Serelis J, Christaki S, Skopouli FN. Remission of nephrotic syndrome due to AA-amyloidosis, complicating familiar Mediterranean fever, with tocilizumab. Clin Exp Rheumatol 2015;33(6):S169.
[60] Hasbal NB, Koc Y, Sevinc M, Unsal A, Basturk T. A familial Mediterranean fever patient with double homozygous mutations treated with anakinra after kidney transplantation. Nefrologia (Engl Ed) 2020;40(5):563–4. doi: 10.1016/j.nefro.2019.03.012.
[61] Mirioglu S, Dirim AB, Bektas M, Demir E, Tor YB, Ozluk Y, et al. Efficacy and safety of interleukin-1 blockers in kidney transplant recipients with familial Mediterranean fever: a propensity score-matched cohort study. Nephrol Dial Transplant 2023;38(5):1327–36. doi: 10.1093/ndt/gfac335.
[62] Özçakar ZB, Keven K, Çakar N, Yalçınkaya F. Transplantation within the era of anti-IL-1 therapy: case series of five patients with familial Mediterranean fever-related amyloidosis. Transpl Int 2018;31(10):1181–4. doi: 10.1111/tri.13312.
[63] Özçakar ZB, Özdel S, Yılmaz S, Kurt-Şükür ED, Ekim M, Yalçınkaya F. Anti-IL-1 treatment in familial Mediterranean fever and related amyloidosis. Clin Rheumatol 2016;35(2):441–6. doi: 10.1007/s10067-014-2772-2.
[64] Peces R, Afonso S, Peces C, Nevado J, Selgas R. Living kidney transplantation between brothers with unrecognized renal amyloidosis as the first manifestation of familial Mediterranean fever: a case report. BMC Med Genet 2017;18(1):97. doi: 10.1186/s12881-017-0457-9.
[65] Sendogan DO, Saritas H, Kumru G, Eyupoglu S, Sadioglu RE, Tuzuner A, et al. Outcomes of canakinumab treatment in recipients of kidney transplant with familial Mediterranean fever: a case series. Transplant Proc 2019;51(7):2292–4. doi: 10.1016/j.transproceed.2019.03.049.
[66] Simsek C, Karatas M, Tatar E, Yildirim AM, Alkan FT, Uslu A. The efficacy of interleukin-1 antagonist drugs in combination with colchicine in patients with FMF-AA with colchicine resistance after kidney transplantation: a study with histopathologic evidence. Clin Transplant 2021;35(6):e14309. doi: 10.1111/ctr.14309.
[67] Trabulus S, Korkmaz M, Kaya E, Seyahi N. Canakinumab treatment in kidney transplant recipients with AA amyloidosis due to familial Mediterranean fever. Clin Transplant 2018;32(8):e13345. doi: 10.1111/ctr.13345.
[68] Yildirim T, Yilmaz R, Uzerk Kibar M, Erdem Y. Canakinumab treatment in renal transplant recipients with familial Mediterranean fever. J Nephrol 2018;31(3):453–5. doi: 10.1007/s40620-018-0475-5.
[69] Bektas M, Koca N, Oguz E, Sari S, Dagci G, Ince B, et al. Characteristics and course of patients with AA amyloidosis: single centre experience with 174 patients from Turkey. Rheumatology (Oxford) 2024;63(2):319–28. doi: 10.1093/rheumatology/kead465.
[70] Schwarz C, Georgin-Lavialle S, Lombardi Y, Marion O, Jambon F, Legendre C, et al. Kidney transplantation in patients with AA amyloidosis: outcomes in a French multicenter cohort. Am J Kidney Dis 2024;83(3):329–39. doi: 10.1053/j.ajkd.2023.07.020.
[71] Ozen S, Kone-Paut I, Hofer M, van Der Hilst J, Gül A, Brogan P, et al. Efficacy, safety, pharmacokinetics and pharmacodynamics of canakinumab in patients with colchicine-resistant FMF: results from the phase 3 cluster trial. Pediatr Rheumatol 2017;15(Suppl 2):65. doi: 10.1186/s12969-017-0186-9.
[72] Lancieri M, Bustaffa M, Palmeri S, Prigione I, Penco F, Papa R, et al. An update on familial Mediterranean fever. Int J Mol Sci 2023;24(11):9584. doi: 10.3390/ijms24119584.
[73] Kuemmerle-Deschner JB, Gautam R, George AT, Raza S, Lomax KG, Hur P. A systematic literature review of efficacy, effectiveness and safety of biologic therapies for treatment of familial Mediterranean fever. Rheumatology (Oxford) 2020;59(10):2711–24. doi: 10.1093/rheumatology/keaa205.
[74] Kilic B, Guler Y, Azman FN, Bostanci E, Ugurlu S. Efficacy and safety of anti-interleukin-1 treatment in familial Mediterranean fever patients: a systematic review and meta-analysis. Rheumatology (Oxford) 2024;63(4):925–35. doi: 10.1093/rheumatology/kead514.
[75] Yin X, Tian F, Wu B, Xu T. Interventions for reducing inflammation in familial Mediterranean fever. Cochrane Database Syst Rev 2022;3(3)CD010893. doi: 10.1002/14651858.CD010893.pub4.
[76] Koga T, Kawakami A. Interleukin-6 inhibition in the treatment of autoinflammatory diseases. Front Immunol 2022;13:956795. doi: 10.3389/fimmu.2022.956795.
[77] Oktem S, Yavuzsen TU, Sengül B, Akhunlar H, Akar S, Tunca M. Levels of interleukin-6 (IL-6) and its soluble receptor (sIL-6R) in familial Mediterranean fever (FMF) patients and their first degree relatives. Clin Exp Rheumatol 2004;22(4 Suppl 34):S34–6.

Ann Rheum Dis 84 (2025) 1928–1937

Contents lists available at ScienceDirect

Annals of the Rheumatic Diseases

journal homepage: https://www.sciencedirect.com/journal/annals-of-the-rheumatic-diseases

Autoinflammatory disorders

Transcriptome analysis of unmedicated heterozygous familial Mediterranean fever patients reveals a type I interferon signature driving increasing Pyrin expression

Erdal Sag[1,2], Gozde Imren[3], Lieselotte Vande Walle[4], Elif Arslanoglu Aydin[5], Yagmur Bayindir[1], Veysel Cam[1], Dilara Unal[1], Hulya Ercan Emreol[1], Ayşenur Pac Kısaarslan[6], Semanur Ozdel[5], Ozge Basaran[1], Beren Karaosmanoglu[3], Mehmet Alikasifoglu[3], Yelda Bilginer[1], Mohamed Lamkanfi[4], Ekim Z. Taskiran[3], Seza Ozen[1,2,*]

[1] *Department of Pediatrics, Division of Pediatric Rheumatology, Hacettepe University Faculty of Medicine, Ankara, Türkiye*
[2] *Translational Medicine Laboratories, Pediatric Rheumatology Unit, Hacettepe University, Ankara, Türkiye*
[3] *Department of Medical Genetics, Hacettepe University Faculty of Medicine, Ankara, Türkiye*
[4] *Laboratory of Medical Immunology, Department of Internal Medicine and Paediatrics, Ghent University, Ghent, Belgium*
[5] *Department of Pediatric Rheumatology, Etlik City Hospital, Ankara, Türkiye*
[6] *Department of Pediatric Rheumatology, Erciyes University, Kayseri, Türkiye*

ARTICLE INFO

Article history:
Received 8 May 2025
Received in revised form 22 July 2025
Accepted 2 August 2025

ABSTRACT

Objectives: Familial Mediterranean fever (FMF) is traditionally viewed as an autosomal recessive autoinflammatory disorder. However, a significant subset of patients harbouring a single pathogenic *MEFV* mutation exhibit a clinical phenotype indistinguishable from that of homozygous patients. We aimed to compare the transcriptomic profiles of patients carrying a single pathogenic mutation who exhibit the classical FMF phenotype with those of healthy carriers (with 1 pathogenic mutation), as well as with homozygous or compound heterozygous patients (with 2 pathogenic mutations), to identify differential molecular signatures and potential diagnostic pathways.

Methods: Peripheral blood mononuclear cells (PBMCs) from 10 patients with FMF (phenotypic carriers/homozygotes) and 5 healthy *MEFV* mutation carriers were isolated during asymptomatic, treatment-naïve phases. Transcriptome profiling employed globin mRNA-depleted, strand-specific Qiaseq libraries sequenced on Illumina NextSeq 500/550 (paired-end). Differential expression analysis applied TMM (trimmed mean of M values) based-normalised negative binomial models ($|\log_2 FC| > 1$, adjusted $^*P^* < .01$), with Reactome pathway enrichment. For immunoblotting, interferon (IFN)-α-stimulated monocytes/PBMCs of healthy individuals were lysed, denatured, and probed with antibodies targeting key proteins (IRF-3, IFN-stimulated gene 15 [ISG15], Pyrin, STAT1, AIM2, caspase-5, β-actin). CXCL10 levels were quantified using Luminex.

Results: PBMC profiling revealed 147 differentially expressed genes. Pathway analyses highlighted enrichment in type I IFN signalling and inflammasome-related pathways, with marked upregulation of type I ISGs: *ISG15*, *IFIT2*, *STAT1*, and the inflammasome sensor Pyrin

*Correspondence to Prof Seza Ozen, Department of Pediatrics, Division of Pediatric Rheumatology, Hacettepe University Faculty of Medicine, Ankara, Türkiye.
E-mail address: sezaozen@gmail.com (S. Ozen).
Erdal Sag and Gozde Imren contributed equally to this work.
Handling editor Josef S. Smolen.

https://doi.org/10.1016/j.ard.2025.08.001

encoded by the *MEFV* gene, mutated in FMF. Moreover, functional assays demonstrated that type I IFN stimulation increases Pyrin protein levels in PBMCs and isolated monocytes, revealing cross-talk between IFN responses and inflammasome signalling.

Conclusions: These findings suggest that type I IFN signalling acts as a critical 'second hit', amplifying Pyrin expression in heterozygous individuals and enabling disease manifestation despite a single *MEFV* mutation. This study offers an explanation for the much-debated issue of the carriers expressing disease phenotypes in diseases such as FMF and presents novel insights for precision diagnosis and therapeutic intervention.

WHAT IS ALREADY KNOWN ON THIS TOPIC

- Although familial Mediterranean fever (FMF) is largely autosomal recessively inherited, heterozygous carriers may express the disease phenotype. However, the underlying mechanism driving the disease phenotype in heterozygous patients has remained elusive.

WHAT THIS STUDY ADDS

- In this manuscript, transcriptomic profiling of peripheral blood mononuclear cells from treatment-naïve patients and well-considered control groups reveals a prominent upregulation of type I interferon (IFN) signalling pathways in patients with heterozygous FMF. Our results indicate that the second hit required for this inflammatory disease is the increased expression of type I IFN, which promotes upregulated expression of the inflammasome sensor Pyrin (which is encoded by the *MEFV* gene that is mutated in FMF).

HOW THIS STUDY MIGHT AFFECT RESEARCH, PRACTICE OR POLICY

- Clinically, these findings underscore the possibility that a chronic type I IFN response may act as a critical modifier in FMF by amplifying the pathogenic effects of a single *MEFV* mutation. This 'second hit' mechanism not only explains the clinical presentation observed in heterozygous patients but also holds significant translational relevance by improving diagnostic accuracy. Establishing IFN signalling as a biomarker could refine patient stratification and aid in tailoring therapeutic interventions. Our data will also shed light on similar cases for other autoinflammatory diseases, such as the heterozygotes with disease in mevalonate kinase deficiency.

INTRODUCTION

Familial Mediterranean fever (FMF) is the most common monogenic autoinflammatory disease globally and has emerged as a paradigm in the study of innate immune dysregulation [1]. Predominantly affecting populations of Mediterranean, Middle Eastern, and North African ancestry, clinical hallmarks of FMF are recurrent episodes of fever, serositis, and systemic inflammation, which, if left untreated, can culminate in the life-threatening complication of AA amyloidosis. Although mutations in the *MEFV* gene—typically inherited in an autosomal recessive manner—form the genetic cornerstone of FMF, the disease exhibits striking clinical heterogeneity. This variability is particularly evident in a significant subset of patients: approximately 10% to 15% of individuals diagnosed with FMF in specialised centres harbour only a single pathogenic *MEFV* mutation, yet their clinical manifestations mirror those seen in biallelic cases [2]. This observation has fuelled debate regarding the pathogenic relevance of heterozygous mutations and prompted their formal recognition in diagnostic frameworks such as the Eurofever criteria for paediatric autoinflammatory syndromes [3].

Despite advances in our understanding, several challenges persist in our understanding of the aetiology and clinical management of FMF. Heterozygous carriers and patients with variants of unknown significance pose a diagnostic dilemma. Physicians must differentiate between FMF and other periodic fever syndromes—such as PFAPA (Periodic Fever, Aphthous stomatitis, Pharyngitis, Adenitis) especially in children who present with isolated febrile episodes [4]. The uncertainty surrounding the disease trajectory in these patients has profound implications for genetic counselling and the initiation of lifelong treatments like colchicine. Moreover, even though the risk of amyloidosis in heterozygotes remains rare, its potential occurrence underscores the pressing need for more precise biomarkers that can predict disease penetrance and progression.

In this study, we aimed to elucidate the molecular underpinnings that contribute to the phenotype in heterozygous FMF by leveraging transcriptomic profiling of peripheral blood mononuclear cells (PBMCs). By focusing on treatment-naïve patients with a single pathogenic *MEFV* mutation who met the Eurofever criteria [3], we performed a comprehensive comparison with asymptomatic healthy carriers of pathogenic *MEFV* alleles and patients with homozygous FMF. This approach, which minimised the confounding effects of colchicine therapy, allowed us to capture intrinsic disease-related molecular signatures. Notably, our multiomics integration strategy—combining RNA sequencing with targeted protein validation—revealed a distinctive activation of type I interferon (IFN) signalling pathways, which appear to upregulate Pyrin and core inflammasome components.

Our findings not only offer mechanistic insights into the genotype-phenotype discordance observed in patients with heterozygous FMF but also highlight type I IFN signatures as promising biomarker candidates for refining diagnostic precision and therapeutic decision-making. In bridging the gap between genetic predisposition and clinical outcome, this study paves the way for more personalised management strategies in FMF, ultimately contributing to improved patient care in this complex and heterogeneous disorder.

METHODS

Patients and sample collection

PBMCs were collected from a cohort comprising 10 patients with FMF and 5 healthy carriers. Patients with FMF, recruited from the Departments of Pediatric Rheumatology at Hacettepe University Faculty of Medicine, Etlik City Hospital, and Erciyes University Faculty of Medicine, fulfilled the 2019 Eurofever/-PRINTO classification criteria for FMF [3], regardless of whether they were homozygous or heterozygous for the pathogenic mutation. Demographic and clinical data, including laboratory parameters, were retrospectively compiled from medical records. Blood sampling was scheduled during the patients' asymptomatic periods and before the onset of colchicine

therapy. Venous blood was drawn directly into EDTA tubes and processed within 30 to 45 minutes. PBMCs were isolated using the Ficoll-based density gradient method, aliquoted, and stored at −80°C. The collection and storage protocols received approval from the Hacettepe University Ethics Committee for Non-Interventional Clinical Trials (GO 2021/03-14), and informed written consent was obtained from patients or their legal guardians. Clinical parameters, such as erythrocyte sedimentation rate, C-reactive protein, and complete blood counts, were documented at the time of blood collection.

Participants were classified into 3 groups:

- *Group 1*: patients exhibiting the clinical FMF phenotype with a single pathogenic mutation that are free of confounding diagnoses such as PFAPA, and who at the time of sampling had not received any treatment for their FMF phenotype.
- *Group 2*: healthy heterozygous carriers of a pathogenic *MEFV* mutation that do not present with clinical disease.
- *Group 3*: patients with homozygous and compound heterozygous FMF who at the time of sampling had not received any treatment.

MEFV gene analysis identified homozygous/compound heterozygous exon 10 mutations in 5 patients, while another 5 patients with FMF and the healthy carriers harboured heterozygous exon 10 mutations (8 with M694V/- and 2 with V726A/-). A summary of demographic and clinical features is provided in Table 1. All patients were treatment naïve at the time of inclusion, with acute-phase reactants generally within normal ranges at sampling.

Transcriptome profiling

Total RNA was extracted from PBMCs (total) using the Norgen Total RNA Purification Kit (Norgen). RNA quantity and quality were assessed with a Qubit Fluorometer (Thermo Fisher Scientific). Pooled RNA from each group (totalling 1000 ng per pool) underwent library preparation using the Qiaseq Stranded mRNA RNA Library Kit (Qiagen), following depletion of globin mRNA with the Qiaseq Fast Select Globin mRNA Removal Kit. Library quality was verified using the QIAxcel DNA High Resolution Kit. Sequencing was performed on the Illumina NextSeq 500/550 platform employing the High Output Kit v2.5 (300 cycles) to generate 2 × 74 bp paired-end reads per sample. Raw data were processed with GenerateFASTQ v2.5.56.27, and downstream analysis was conducted using CLC Genomic Workbench. Quality control steps—including adapter trimming and alignment—were performed under criteria of up to 2 mismatches, a minimum 80% similarity fraction, and a maximum of 10 hits per read. Reads were aligned to the human reference genome (hg19). Differential gene expression analysis applied TMM (trimmed mean of M values)-based normalisation and used a general linear model with a negative binomial distribution. Genes with a FDR adjusted *P* value below .01 and an absolute $\log_2$ fold change exceeding 1 were considered significantly differentially expressed. Furthermore, gene expression within enriched pathways was analysed using the ExpressAnalyst platform, with over-representation analysis based on the Reactome database and visualised through Ridgeline diagrams.

Protein expression analysis in PBMCs and primary monocytes

For protein studies, PBMCs were isolated from buffy coats of healthy donors who do not carry any *MEFV* mutations at Ghent University using Ficoll-Hypaque density gradient centrifugation (227288, Greiner Bio-One). Monocytes were purified with the Pan Monocyte Isolation Kit (130-096-537, Miltenyi Biotec) according to manufacturer instructions. After isolation, cells were cryopreserved in 90% fetal bovine serum (FBS) and 10% dimethyl sulfoxide until further use. Upon thawing, cells were washed in cold DPBS (CA PBS-1A, Capricorn Scientific) and seeded at a density of 1.5×10^6 cells per well in RPMI 1640 medium (CA RPMI-STA, Capricorn Scientific) supplemented with 10% endotoxin-free, heat-inactivated FBS (S-FBS-SA-015, Bodinco), 100 U/mL penicillin, and 100 µg/mL streptomycin

Table 1
The demographic and clinical features of healthy donors and patients with FMF included in the transcriptomic analysis

Groups	Gender	Age (y)	Age at disease onset (y)	Duration of the disease (y)	Presenting features	MEFV mutation	CRP level(mg/dL) (0-0.8)	WBC (/mm^3)
Group 1 (patients with heterozygote FMF)	F	9	6	2	Fever, abdominal pain	M694V/-	<0.3	5880
	F	8.5	8	0.5	Fever, arthritis, abdominal pain	V726A/-	<0.3	5460
	F	16	15	1	Fever, abdominal pain	V726A/-	<0.3	5800
	F	9.3	9.1	0.17	Abdominal pain, protracted febrile myalgia	M694V/-	0.65	15,000
	M	3	2.7	0.25	Fever, abdominal pain, arthralgia	M694V/-	0.15	11,360
Group 2 (healthy carriers)	F	8.3				M694V/-	0.47	7880
	F	11				M694V/-	0.02	4700
	M	11				M694V/-	0.16	7100
	F	15				M694V/-	0.05	7960
	F	4				M694V/-	0.2	5100
Group 3 (patients with homozygote FMF)	M	6.4	5	1.4	Fever, abdominal pain	M694V/M694V	<0.3	6010
	M	14.5	6	8.5	Fever, abdominal pain, arthralgia	M694V/M694V	<0.3	6260
	M	6.8	4	2.8	Fever, abdominal pain	M680I/M680I	0.14	6780
	M	15.5	14	1.5	Fever, abdominal pain, chest pain, arthritis	M680I/V726A	0.4	5820
	M	6.6	2	4.6	Fever, abdominal pain, chest pain	V726A/M694V	0.3	6120

CRP, C-reactive protein; FMF, familial Mediterranean fever; WBC, white blood cell.

(LO DE17-602E, Lonza). Cells were then stimulated with 1000 U/mL of type I IFN-α. The study protocol for acquisition and storage was approved by the Medical Ethics Committee of the Red Cross and Ghent University (G20241030A).

Immunoblotting

Cell lysates were prepared by incubating the cells in NP-40 lysis buffer (20 mM Tris-HCl pH 7.4, 200 mM NaCl, 1% Nonidet P-40), followed by denaturation with sample buffer (M00676, GenScript) at 95°C for 10 minutes. Proteins were separated by SDS-PAGE and transferred onto PVDF membranes. Membranes were blocked with 5% nonfat dry milk in TBS containing 0.1% Tween-20 (TBST), and then probed with primary antibodies diluted in either 5% BSA or 5% nonfat dry milk in TBST, as specified by the manufacturers. Washing steps were performed with 1× TBST. The primary antibodies included IRF-3 (11904, Cell Signaling), IFN-stimulated gene 15 (ISG15) (2743, Cell Signaling), Pyrin (58525, Cell Signaling), STAT1 (14994, Cell Signaling), AIM2 (12948, Cell Signaling), caspase-5 (46680, Cell Signaling/Abcam), and β-actin (SC-47778HRP, Santa Cruz Biotechnology). Detection was performed using a Peroxidase-AffiniPure Goat anti-rabbit secondary antibody (111-035-144, Jackson Immunoresearch Laboratories) in conjunction with enhanced chemiluminescence (34580, Thermo Fisher Scientific).

Cytokine analysis

CXCL10 levels in the culture supernatants were quantified using a magnetic bead-based multiplex assay on the Luminex platform (Bio-Rad), following the manufacturer's protocol.

Statistical analysis

Data analyses were conducted using GraphPad Statistics for MAC (Version 6.0). Baseline characteristics were summarised with medians and IQR for continuous variables, and proportions for categorical variables. A P value of .05 was set as the threshold for statistical significance. Cytokine data were further analysed using Prism 10.0.2 (GraphPad), with results expressed as mean ± SEM from 3 or more independent biological replicates. Following confirmation of normal distribution via the Shapiro-Wilk test, a 1-way analysis of variance with Bonferroni's multiple-comparison test was employed for group comparisons.

RESULTS

A total of 10 patients with FMF (6 males/4 females) and 5 control subjects (1 male/4 females) were enrolled in the study. The median age was 9 years (IQR 8.5-9.3) for patients with heterozygous FMF (group 1), 11 years (IQR 8.3-11.0) for healthy carriers (group 2), and 6.8 years (IQR 6.6-14.5) for patients with homozygous and compound heterozygous FMF (group 3). The median disease duration was 0.5 years (IQR 0.25-1.0) in group 1 and 2.8 years (IQR 1.5-4.6) in group 3 (Table 1).

PBMCs were isolated from all subjects, and transcriptomic profiling was performed. Importantly, all patients were treatment naïve at the time of inclusion to eliminate potential confounding effects of colchicine on NF-κB and inflammasome signalling [5,6].

Differential gene expression analysis comparing patients with heterozygous FMF to healthy heterozygous carriers revealed 147 significantly altered genes (FDR $\leq$ 0.001; $|\log_2 FC| \geq 1$), with 96 genes upregulated and 51 downregulated (Fig 1A, Table 2). Notably, the upregulated genes included key ISG such as *ISG15, IFIT2, IFIT3, USP18*, and *STAT1*.

Gene ontology enrichment analysis identified significant over-representation of biological processes related to type I IFN response, cytokine-mediated signal transduction, and inflammatory responses (P-adj < .01) (Fig 1B). At the cellular component level, enrichment was noted in cytoplasmic inflammasome complexes and IFN-stimulated gene complexes, while molecular function analysis highlighted an increase in enzymatic activities linked to JAK-STAT signalling (Fig 1B). These findings collectively indicate a marked activation of type I IFN signalling in patients with heterozygous FMF compared to healthy carriers. Furthermore, Reactome pathway analysis confirmed significant activation of the type I IFN response pathway (P-adj < .01), with pronounced upregulation in both IFN-α and IFN-β gene clusters (Fig 1C).

The protein-protein interaction network generated using STRING database (Search Tool for the Retrieval of Interacting Genes/Proteins) analysis further underscored these findings, revealing robust interconnections among differentially expressed genes involved in innate immune responses (Fig 2). Within this network, proteins directly associated with the IFN response, such as STAT1, IRF7, ISG15, IFIT2, and OAS1, were tightly linked by an extensive protein interaction network, underscoring the systematic enhancement of the IFN response in patients with heterozygous FMF. These IFN-stimulated genes were not upregulated in homozygous and compound heterozygous patients (Fig 3).

In addition to IFN-related changes, significant upregulation was observed in inflammasome-associated genes. Genes implicated in the noncanonical inflammasome pathway, such as *CASP5* and *GBP1*, as well as the bacterial type III secretion system sensor *NLRC4* were differentially expressed between patients with heterozygous FMF and healthy carriers (Table 2). Notably, expression of the *MEFV* gene, which encodes the inflammasome sensor Pyrin, was significantly upregulated (P-adj < .05). This observation is consistent with previous reports documenting IFN-α-induced upregulation of *MEFV* mRNA in primary monocytes [7], and it suggests that IFN signalling may drive inflammasome activation via enhanced Pyrin expression.

Building on these insights, we hypothesised that type I IFN-mediated inflammatory activation serves as a 'second hit' in heterozygous *MEFV* carriers, increasing expression of mutant Pyrin and consequently triggering the inflammatory cascade characteristic of FMF in heterozygous patients.

To explore this hypothesis further and validate these transcriptomic findings at the protein level, we investigated the expression of selected proteins following type I IFN stimulation in PBMCs and isolated monocytes from healthy donors. Since FMF-associated mutations are coding variants, usually located in exon 10, we do not expect a differential response to type I IFN stimulation between wild-type and mutant *MEFV* alleles. We included healthy donors who do not carry any *MEFV* mutations for these setups. Stimulation with recombinant IFN-α elicited a robust, time-dependent increase in the secretion of the IFN-responsive chemokine CXCL10 (Fig 4A), which emerged as a central node within our STRING network (Fig 2). Kinetic analyses further demonstrated significant upregulation of key inflammasome proteins, including Pyrin (*MEFV*), caspase-5 (*CASP5*), the dsDNA sensor AIM2, as well as IFN signalling mediators STAT1 and ISG15 in IFN-α-stimulated monocytes (Fig 4B), while IRF3 levels remained unchanged, consistent with our transcriptome data. Similarly, IFN-α treatment of PBMCs from healthy

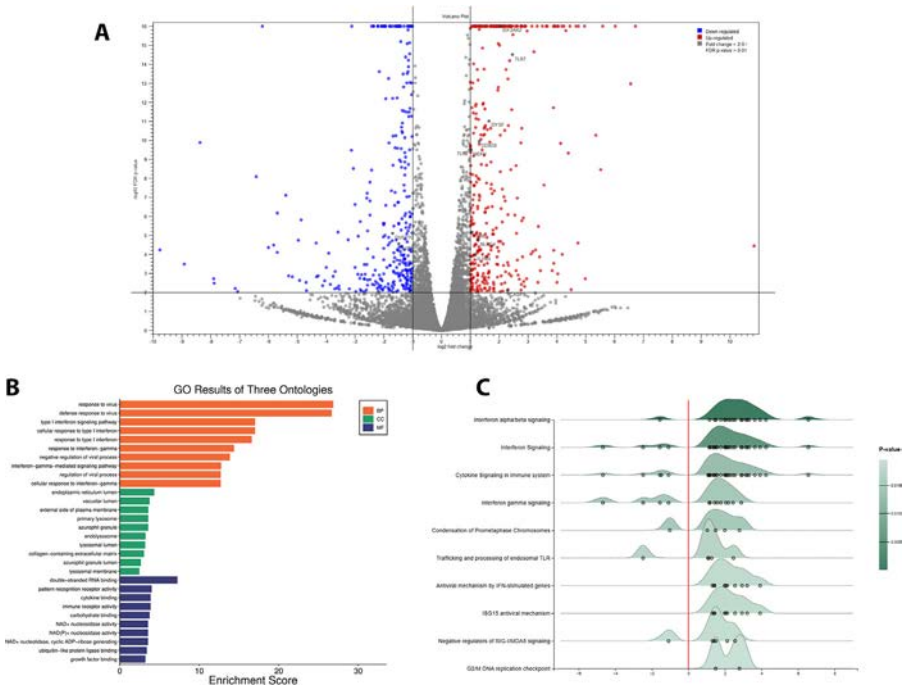

Figure 1. Transcriptome analysis reveals a type I interferon signature in unmedicated patients with heterozygous familial Mediterranean fever (FMF). (A) The volcano plot illustrates differentially expressed genes (DEGs), marking upregulated genes in red and downregulated ones in blue, for those with a False discovery rate (FDR) adjusted *P* value <.01 and a fold change >2. The plot's vertical axis, showing the −log10 (*P* value), indicates the level of statistical significance, with higher values denoting greater significance. (B) This bar chart displays the gene ontology (GO) enrichment results across 3 ontologies: Biological processes (BPs), cellular components (CCs), and molecular functions (MFs). Bars are colour-coded to represent each ontology category: BPs in orange, CCs in green, and MFs in blue. The enrichment score on the *x*-axis quantifies the degree to which each term is over-represented in the dataset, with higher scores indicating greater enrichment. (C) This Ridgeline diagram presents the ordering of pathways according to their significance in the analysis, as determined by *P* values from the Reactome database, with the most significant pathways displayed at the top. Pathways are colour-coded, with darker shades indicating lower, more significant *P* values. The density plots illustrate the distribution of DEGs within each pathway, highlighting the log2 fold change (log_2FC) values to show overall upregulation or downregulation. Each DEG is marked as a point along the baseline of its corresponding density plot, providing a visual representation of gene expression trends within significant biological pathways.

donors resulted in elevated CXCL10 release and increased expression of Pyrin and STAT1, with no change in IRF3 expression (Fig 4C,D).

In summary, these results confirm that type I IFN stimulation leads to the upregulation of a specific set of proteins implicated in the FMF inflammatory pathway and support our model in which chronic IFN signalling acts as a critical 'second hit' that exacerbates mutant Pyrin expression, thereby determining the FMF phenotype in heterozygous patients.

DISCUSSION

Our study is the first to offer a mechanistic basis for the observation that heterozygous carriers of what is traditionally viewed as an autosomal recessive disease can display the FMF phenotype. It has long been recognised that FMF does not follow a strictly recessive inheritance model [8]. Our results offer a molecular explanation for these observations and lend support to a gene-dosage effect in the clinical expression of FMF. Specifically, our data indicate that type I IFN signalling provides a critical 'second hit' that amplifies *MEFV* gene expression and triggers the downstream inflammatory cascade in heterozygous carriers. This aligns with earlier reports demonstrating that IFN-α enhances *MEFV* mRNA levels in monocytes [7], and extends this paradigm by implicating additional inflammatory modifiers that act in concert with a single mutated allele.

Clinically, these insights are highly relevant for rheumatologists who frequently encounter patients with heterozygous FMF presenting with inflammatory episodes. The dilemma of initiating lifelong colchicine therapy—despite its associated side effects—hinges on whether a single mutation is sufficient to drive pathology. Our study provides molecular evidence that heterozygous patients exhibit a unique transcriptomic and proteomic signature characterised by heightened type I IFN activity. This 'second hit' mechanism may help to resolve diagnostic uncertainty, enabling clinicians to better stratify patients based on their risk for disease progression and tailor therapeutic strategies accordingly. Such an approach could minimise unnecessary treatment exposure while preventing severe sequelae like AA amyloidosis.

Previous studies have focused on characterising the disease manifestation in patients with heterozygous FMF at the genetic level. Booty et al [9] evaluated patients with FMF with a single mutation and found that haplotype analysis failed to identify a common genetic marker that might convey a second FMF allele.

Table 2
Inflammasome-related differentially expressed genes with fold changes and False discovery rate (FDR) *P* value

Name	Log_2 fold change	FDR *P* value
DUSP10	−1.69	7.97E-06
IL1B	−1.48	2.92E-05
TLR2	1.00	2.99E-10
MEFV	1.03	3.29E-10
TLR8	1.07	6.85E-06
IL1RN	1.17	1.07E-04
NLRC4	1.27	1.83E-05
DDX58	1.31	1.13E-10
DYSF	1.65	9.65E-12
EIF2AK2	2.04	6.73E-29
CASP5	2.29	7.99E-03
TLR7	2.46	3.16E-15

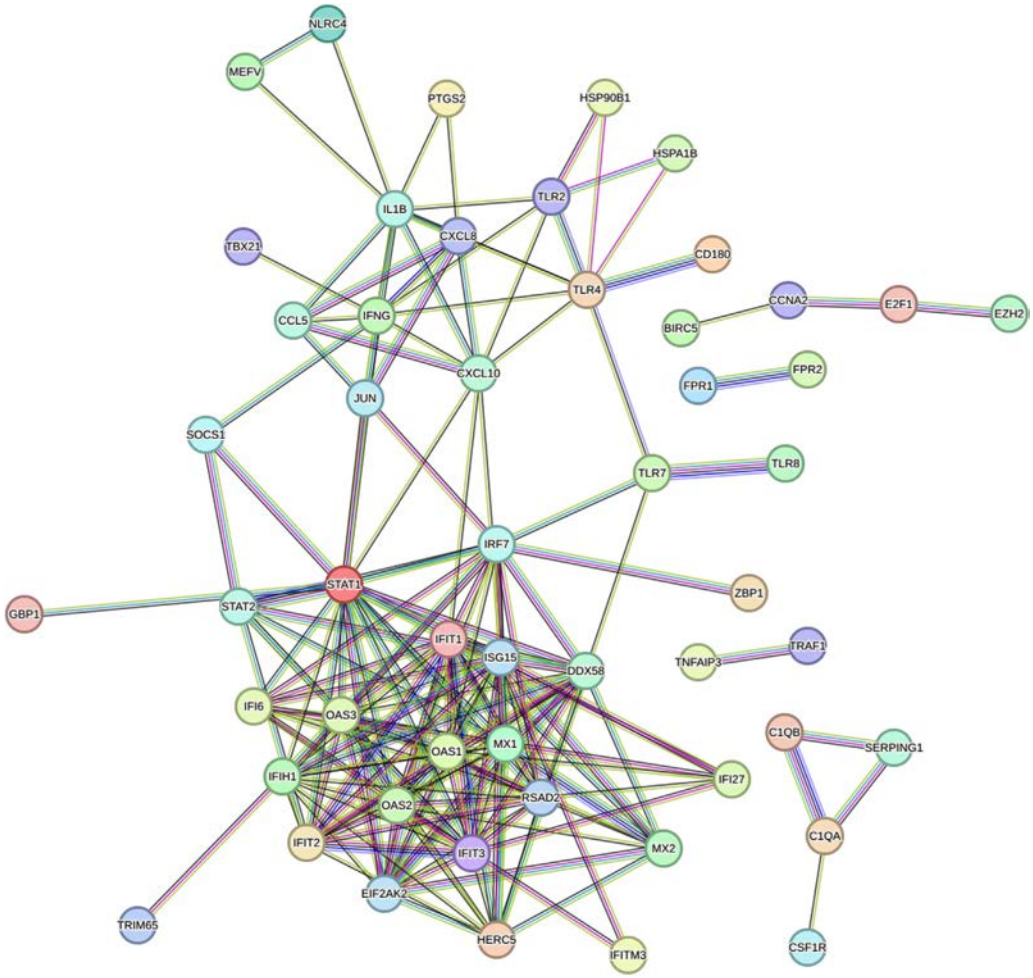

Figure 2. Protein-protein interaction network of innate immune system-related differentially expressed genes (DEGs). The network diagram of STRING database (Search Tool for the Retrieval of Interacting Genes/Proteins) analysis shows the upregulated genes associated with the innate immune system. Nodes represent proteins, and edges indicate protein-protein interactions with the following colour codes: gene neighbourhood (green), gene fusion (red), gene co-occurrence (blue), text-mining (light green), coexpression (black), experimentally determined (pink), and curated from databases (sky blue).

Similarly, Marek-Yagel et al [10] were unable to detect additional mutations, large genomic deletions, or duplications in their cohort of 18 patients with heterozygous FMF. Further investigations examining single-nucleotide polymorphisms along the cDNA ruled out allelic silencing as a cause for the phenotype. Based on these findings, we proposed that patients with heterozygous FMF may be exposed to a combination of environmental cues and genetic polymorphisms that predispose them to disease through the action of additional inflammatory pathways on the mutant disease allele—a concept reflecting an environmental 'second hit' operating in a polygenic manner to drive the clinical expression in these patients in response to such modifying triggers. Our transcriptomic analysis was designed to delineate these molecular signatures. Whereas homozygotes experience inflammation primarily due to the presence of 2 pathogenic mutations, heterozygotes appear to require an extra inflammatory stimulus, as evidenced by enhanced cytokine signalling pathways and increased Pyrin mRNA and protein expression. Our data suggest that type I IFN signalling functions as the converging mechanism for this critical 'second hit', driving *MEFV* upregulation and triggering the FMF phenotype in heterozygous patients, a necessity not observed in patients with biallelic mutations.

We explored possible differences in IFN-related gene expression between patients carrying the M694V and V726A variants. Although our sample size does not allow for robust statistical comparisons, we did not observe a consistent or significant difference in the IFN signature between these genotypes within our cohort.

Type I IFN signalling interacts with inflammasome activation in a complex manner, influencing key mediators such as IL-1β, caspase-1, and gasdermin D (GSDMD) through both stimulatory and inhibitory mechanisms. Specifically, type I IFN can diminish pro-IL-1β expression while concurrently upregulating anti-inflammatory mediators like IL-1Ra and IL-10 [11]. In human monocyte-derived macrophages, IFN-α treatment progressively elevates *CASP1* and *GSDMD* mRNA levels [12]. Studies in murine macrophages indicate that type I IFN downregulates pro-IL-1β and curtails caspase-1 activation by modulating NLRP3 at the translational level [13], whereas in human monocytes and epithelial cells, chronic IFN-α exposure or cGAS-STING pathway activation has been shown to enhance NLRP3 inflammasome activity [14–16]. Together, these findings illustrate a multifaceted regulatory network in which type I IFN orchestrates inflammasome responses.

Interestingly, our findings point to a novel connection between IFN-mediated signalling and inflammasome activation in patients with FMF. Contrary to our initial expectation that NF-κB and type II IFN responses would dominate, we observed a robust type I IFN signature in patients with heterozygous FMF, characterised by elevated expression of IFN-stimulated genes (*ISG15, IFIT2, STAT1*) that coincides with upregulation of *MEFV* mRNA levels.

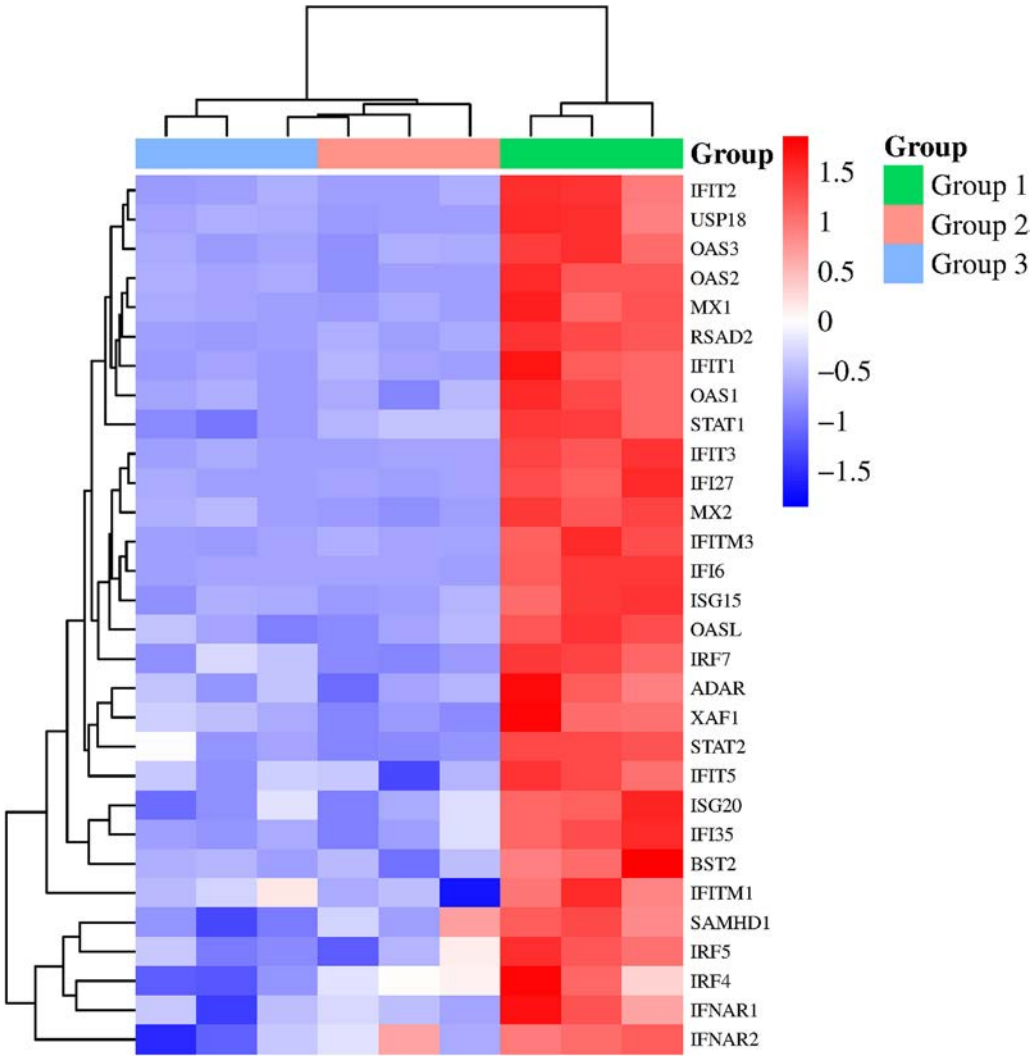

Figure 3. Interferon pathway-related genes specifically upregulated in patients with heterozygous familial Mediterranean fever (FMF). Heatmap showing the expression profiles of selected interferon-related genes that are significantly upregulated (False discovery rate (FDR) p-value < 0.01, $\log_2$-Fold Change ≥ 1) in peripheral blood mononuclear cells (PBMCs) samples of group 1 compared to group 2 and group 3. Normalised $\log_2$-transformed expression values were *z*-score-scaled across genes. Rows represent genes and columns represent individual samples. Hierarchical clustering was applied to both genes and samples. Colour intensity represents relative gene expression: blue indicates lower, and red indicates higher expression relative to the gene-wise mean. Sample groups are colour-coded as follows: group 1 (green), group 2 (red), and group 3 (blue). *Group 1*: patients exhibiting the clinical FMF phenotype with a single pathogenic mutation. *Group 2*: healthy heterozygous carriers of a pathogenic *MEFV* mutation that do not present with clinical disease. *Group 3*: homozygous and compound patients with heterozygous FMF.

This suggests that type I IFN may drive Pyrin inflammasome activation and autoinflammation in heterozygous patients. Furthermore, network analyses based on our transcriptomic data, together with a reported *in silico* model of the Pyrin inflammasome pathway that highlights the roles of NF-κB and JAK1/TYK2 signalling [17] further substantiate IFN signalling as a critical modifier in FMF pathogenesis. Consistent herewith this, we showed that type I IFN stimulation increases Pyrin protein levels in a time-dependent manner in human monocytes and PBMCs, thus linking type I IFN pathways to Pyrin inflammasome-driven autoinflammation. The elevated IFN responses, particularly in patients with heterozygous FMF, potentially act as a secondary modifier that increases *MEFV* expression or inflammasome activity beyond the threshold required for disease manifestation. This offers a mechanistic explanation for variable penetrance and may have therapeutic implications. In fact, there are 3 case series with 6 patients with colchicine-resistant FMF in whom tofacitinib effectively suppresses inflammatory markers and provides remission in clinical symptoms [18–20].

We have to stress that patients with heterozygous FMF did not exhibit type I IFN levels comparable to those observed in monogenic interferonopathies. The observed IFN signature was modest, likely serving as a modulatory factor that primes mutant FMF allele-driven inflammatory responses rather than directly driving the hallmark clinical features of interferonopathy. Consequently, patients do not typically develop classic interferonopathy manifestations, such as cytopenia.

It is also important to note that our strategy of enrolling treatment-naïve patients circumvents potential confounding effects of colchicine on NF-κB and inflammasome signalling pathways [5,6]. This careful patient selection likely accounts for the absence of immunosuppressive signatures in our transcriptome data, in contrast to findings from recent studies of FMF monocytes from 7 homozygous patients on anti-inflammatory therapy—predominantly colchicine—which reported downregulation of immune-related pathways during remission and the intervals between flares [21]. Such differences

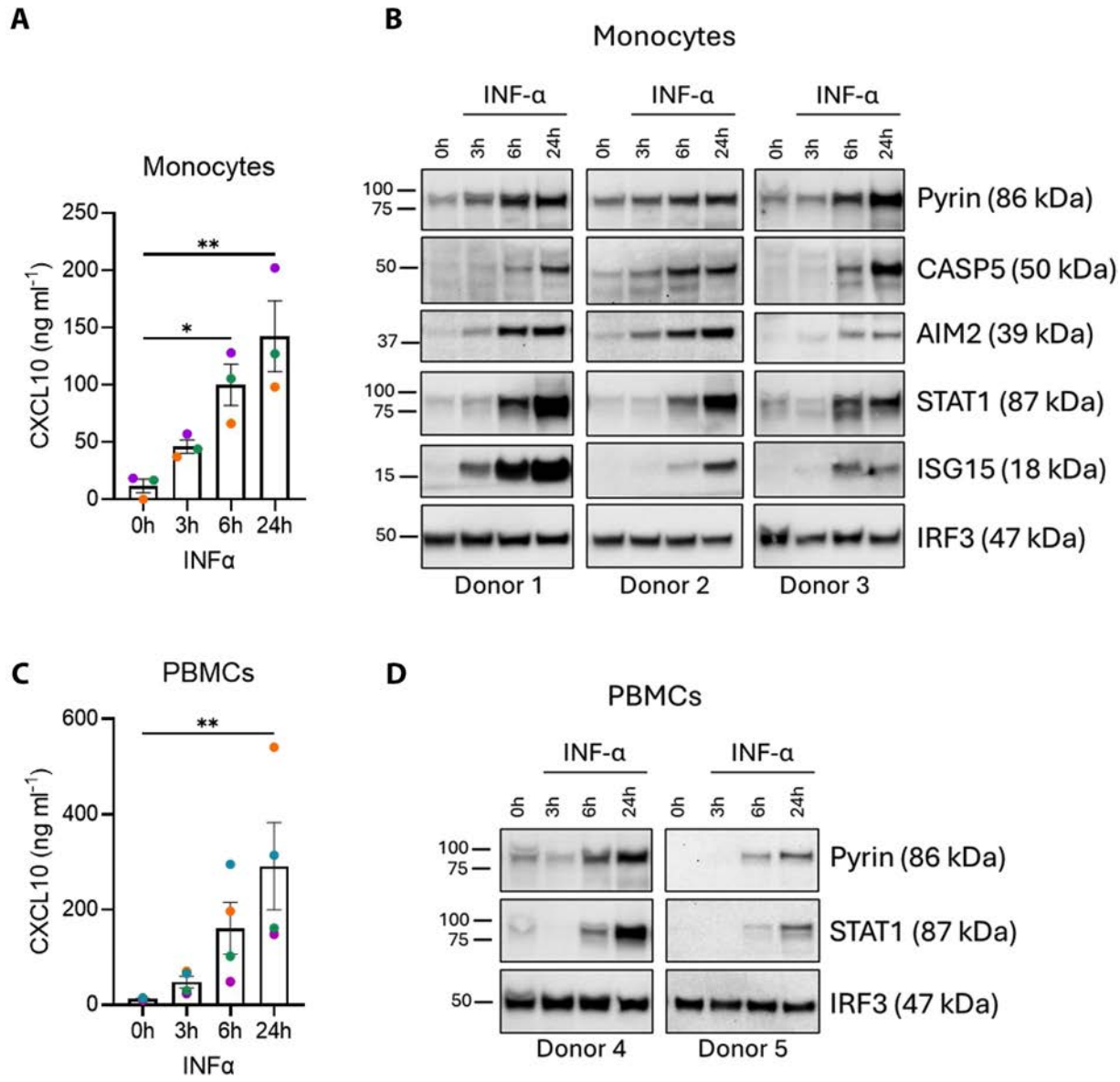

Figure 4. Validation of type I interferon (IFN)-induced protein expression in monocytes and peripheral blood mononuclear cells (PBMCs) from healthy donors. (A-D) Primary human monocytes (A, B) or PBMCs (C, D) from healthy donors who do not carry any MEFV mutations were stimulated with 1000 U/mL IFN-α for the indicated times. Supernatants were analysed for CXCL10 secretion (A, C). Data are presented as mean ± SEM from n = 3 (monocytes) or n = 4 (PBMCs) biological replicates. Statistical significance was determined by 1-way analysis of variance with Bonferroni's multiple comparisons test ($P \leq .01$; $P \leq .05$). Cell lysates were immunoblotted for the indicated proteins (B, D). Representative immunoblots from 3 independent healthy donors (monocytes) and 2 independent healthy donors (PBMCs) are shown.

underscore the critical value of analysing treatment-naïve patient samples to accurately capture the intrinsic molecular mechanisms driving FMF.

While elevated type I IFN may act as a 'second hit' driving disease in a subset of heterozygous individuals, the low penetrance of FMF in heterozygous individuals (2%-5%) remains incompletely explained. We hypothesise that only heterozygotes exhibiting an IFN signature manifest the FMF phenotype, likely requiring additional genetic or epigenetic modifiers (eg, variations in *MEFV* expression, regulatory variants, other inflammatory genes, or early-life exposures) to reach the disease threshold. It is tempting to speculate that the modest IFN signature observed becomes pathogenic only in the context of such susceptibility factors, highlighting the complex interplay determining heterozygote disease expression and underscoring the need for future studies to define these modifiers.

In summary, our study provides compelling evidence that type I IFN-mediated inflammatory activation can serve as a 'second hit' in patients with heterozygous FMF, bridging the gap between genetic predisposition and clinical manifestation. By demonstrating that treatment-naïve heterozygous patients have a distinctive IFN-associated molecular signature—including robust upregulation of *MEFV* and other ISGs—we not only challenge traditional views of autosomal recessive inheritance in FMF but also pave the way for enhanced patient stratification and the development of targeted therapies. These findings have far-reaching implications for understanding the pathogenesis of autoinflammatory diseases and ultimately improving clinical management through a precision medicine approach.

Limitations

One limitation of our study could be that although the healthy heterozygotes did not describe any attacks, they may have them in the future since they are still very young. Our findings also need to be validated in non-Turkish populations.

Longitudinal analysis in these heterozygotes may serve to strengthen our hypothesis. Furthermore, it might be worth analysing the IFN signature in asymptomatic homozygous individuals, which may provide valuable insights into disease penetrance and potential compensatory mechanisms, but such cases are extremely rare, especially in Turkey, where most of the individuals have exon 10 mutations.

CONCLUSIONS

Our findings identify a novel feedforward loop linking type I IFN signalling to MEFV upregulation, suggesting IFN-α may potentiate Pyrin inflammasome activation in heterozygous carriers as a plausible 'second hit' mechanism driving inflammation in patients with heterozygous FMF. The upregulation of IFN-related genes appears to amplify inflammatory cascades, including the induction of *MEFV* expression, providing mechanistic insight into the pathogenesis of FMF in this subgroup. These results underscore the importance of IFN signalling in modulating FMF phenotypes and may guide future diagnostic and therapeutic strategies.

Competing interests

All authors declare they have no competing interests.

CRediT authorship contribution statement

Erdal Sag: Writing – original draft, Software, Methodology, Investigation, Formal analysis, Data curation, Conceptualization. **Gozde Imren:** Writing – original draft, Validation, Investigation, Formal analysis, Data curation. **Lieselotte Vande Walle:** Writing – review & editing, Validation, Formal analysis, Data curation. **Elif Arslanoglu Aydin:** Writing – review & editing, Data curation. **Yagmur Bayindir:** Writing – review & editing, Data curation. **Veysel Cam:** Writing – review & editing, Data curation. **Dilara Unal:** Writing – review & editing, Data curation. **Hulya Ercan Emreol:** Writing – review & editing, Data curation. **Ayşenur Pac Kısaarslan:** Writing – review & editing, Data curation. **Semanur Ozdel:** Writing – review & editing, Data curation. **Ozge Basaran:** Writing – review & editing, Data curation. **Beren Karaosmanoglu:** Writing – review & editing, Data curation. **Mehmet Alikasifoglu:** Writing – review & editing, Data curation. **Yelda Bilginer:** Writing – review & editing, Supervision, Data curation. **Mohamed Lamkanfi:** Writing – original draft, Validation, Methodology, Funding acquisition, Conceptualization. **Ekim Z. Taskiran:** Writing – original draft, Supervision, Software, Methodology, Formal analysis, Data curation, Conceptualization. **Seza Ozen:** Writing – original draft, Supervision, Resources, Project administration, Methodology, Funding acquisition, Conceptualization.

Acknowledgements

The authors thank TUBITAK for their support.

Funding

This study was supported by the Scientific and Technological Research Council of Turkey (TUBITAK) under Grant Number 120C127 as part of the 2247-A National Outstanding Researchers Program and by research grants from Ghent University (BOF23/GOA/001) and the Fund for Scientific Research (FWO)-Flanders (GOI5722N and G017121N).

Patient consent for publication

Informed written consent was obtained from patients or their legal guardians.

Ethics approval

The collection and storage protocols received approval from the Hacettepe University Ethics Committee for Non-Interventional Clinical Trials (GO 2021/03-14) and the Medical Ethics Committee of the Red Cross and Ghent University (G10141030A).

Provenance and peer review

Not comissioned, externally peer-reviewed.

Orcid

Erdal Sag: http://orcid.org/0000-0002-6542-2656
Seza Ozen: http://orcid.org/0000-0003-2883-7868

REFERENCES

[1] Sag E, Bilginer Y, Ozen S. Autoinflammatory diseases with periodic fevers. Curr Rheumatol Rep 2017;19(7):41.
[2] Çakan M, Alkaya A, Koru L, Öksel B, Akgün Ö, Tunce E, et al. The journey of MEFV heterozygous children: with or without colchicine. Eur J Pediatr 2024;184(1):40.
[3] Gattorno M, Hofer M, Federici S, Vanoni F, Bovis F, Aksentijevich I, et al. Classification criteria for autoinflammatory recurrent fevers. Ann Rheum Dis 2019;78:1025–32.
[4] Ozen S, Bilginer Y. A clinical guide to autoinflammatory diseases: familial Mediterranean fever and next-of-kin. Nat Rev Rheumatol 2014;10(3):135–47.
[5] Ding AH, Porteu F, Sanchez E, Nathan CF. Downregulation of tumor necrosis factor receptors on macrophages and endothelial cells by microtubule depolymerizing agents. J Exp Med 1990;171(3):715–27.
[6] Van Gorp H, Saavedra PH, de Vasconcelos NM, Van Opdenbosch N, Vande Walle L, Matusiak M, et al. Familial Mediterranean fever mutations lift the obligatory requirement for microtubules in Pyrin inflammasome activation. Proc Natl Acad Sci USA 2016;113(50):14384–9.
[7] Centola M, Wood G, Frucht DM, Galon J, Aringer M, Farrell C, et al. The gene for familial Mediterranean fever, MEFV, is expressed in early leukocyte development and is regulated in response to inflammatory mediators. Blood 2000;95(10):3223–31.
[8] Jamilloux Y, Lefeuvre L, Magnotti F, Martin A, Benezech S, Allatif O, et al. Familial Mediterranean fever mutations are hypermorphic mutations that specifically decrease the activation threshold of the Pyrin inflammasome. Rheumatology (Oxford) 2018;57(1):100–11.
[9] Booty MG, Chae JJ, Masters SL, Remmers EF, Barham B, Le JM, et al. Familial Mediterranean fever with a single MEFV mutation: where is the second hit? Arthritis Rheum 2009;60(6):1851–61.
[10] Marek-Yagel D, Berkun Y, Padeh S, Abu A, Reznik-Wolf H, Livneh A, et al. Clinical disease among patients heterozygous for familial Mediterranean fever. Arthritis Rheum 2009;60(6):1862–6.
[11] Mayer-Barber KD, Yan B. Clash of the Cytokine Titans: counter-regulation of interleukin-1 and type I interferon-mediated inflammatory responses. Cell Mol Immunol 2017;14(1):22–35.
[12] Díaz-Pino R, Rice GI, San Felipe D, Pepanashvili T, Kasher PR, Briggs TA, et al. Type I interferon regulates interleukin-1beta and IL-18 production and secretion in human macrophages. Life Sci Alliance 2024;7(6):e202302399.
[13] Guarda G, Braun M, Staehli F, Tardivel A, Mattmann C, Förster I, et al. Type I interferon inhibits interleukin-1 production and inflammasome activation. Immunity 2011;34(2):213–23.
[14] Liu X, Yang P, Wang C, Li F, Kijlstra A. IFN-alpha blocks IL-17 production by peripheral blood mononuclear cells in Behcet's disease. Rheumatology (Oxford) 2011;50(2):293–8.
[15] Hong SM, Lee J, Jang SG, Lee J, Cho ML, Kwok SK, et al. Type I interferon increases inflammasomes associated pyroptosis in the salivary glands of patients with primary Sjogren's syndrome. Immune Netw 2020;20(5):e39.

[16] Gaidt MM, Ebert TS, Chauhan D, Ramshorn K, Pinci F, Zuber S, et al. The DNA inflammasome in human myeloid cells is initiated by a STING-cell death program upstream of NLRP3. Cell 2017;171(5):1110–24 .e18.
[17] Veyssiere M, S Sadat Aghamiri, A Hernandez Cervantes, consortium ImmunAID, Henry T, Soumelis V. A mathematical model of familial Mediterranean fever predicts mechanisms controlling inflammation. Clin Immunol 2023;257:109839.
[18] Karadeniz H, Güler AA, Atas N, Satış H, Salman RB, Babaoglu H, et al. Tofacitinib for the treatment for colchicine-resistant familial Mediterranean fever: case-based review. Rheumatol Int 2020;40(1):169–73.
[19] Garcia-Robledo JE, Aragón CC, Nieto-Aristizabal I, Posso-Osorio I, Cañas CA, Tobón GJ. Tofacitinib for familial Mediterranean fever: a new alternative therapy? Rheumatology (Oxford) 2019;58(3):553–4.
[20] Gok K, Cengiz G, Erol K, Ozgocmen S. Tofacitinib suppresses disease activity and febrile attacks in a patient with coexisting rheumatoid arthritis and familial Mediterranean fever. Acta Reumatol Port 2017;42(1):88–90.
[21] Röring RJ, Li W, Liu R, Bruno M, Zhang B, Debisarun PA, et al. Epigenetic, transcriptional, and functional characterization of myeloid cells in familial Mediterranean fever. iScience 2024;27(4):109356.

Ann Rheum Dis 84 (2025) 1938–1947

Contents lists available at ScienceDirect

Annals of the Rheumatic Diseases

journal homepage: https://www.sciencedirect.com/journal/annals-of-the-rheumatic-diseases

Osteoarthritis

Osteoarthritis risk associated with romosozumab compared with teriparatide in individuals with osteoporosis: a target trial emulation study

Masaki Hatano[1,*], Yusuke Sasabuchi[2], Akira Okada[3], Yuya Kimura[4], Hisatoshi Ishikura[5], Takeyuki Tanaka[5], Taku Saito[5], Sakae Tanaka[5], Hideo Yasunaga[1]

[1] *Department of Clinical Epidemiology and Health Economics, School of Public Health, The University of Tokyo, Tokyo, Japan*
[2] *Department of Real-world Evidence, Graduate School of Medicine, The University of Tokyo, Tokyo, Japan*
[3] *Department of Prevention of Diabetes and Lifestyle-Related Diseases, Graduate School of Medicine, The University of Tokyo, Tokyo, Japan*
[4] *Department of Health Services Research, Graduate School of Medicine, The University of Tokyo, Tokyo, Japan*
[5] *Department of Orthopaedic Surgery, Faculty of Medicine, The University of Tokyo, Tokyo, Japan*

ARTICLE INFO

Article history:
Received 20 February 2025
Received in revised form 5 June 2025
Accepted 6 June 2025

ABSTRACT

Objectives: To compare osteoarthritis among individuals with osteoporosis initiating romosozumab vs an active comparator.

Methods: This new user comparative effectiveness study, emulating a target trial, included individuals aged ≥50 years in the administrative claims database from 2019 to 2022. Individuals who initiated romosozumab were compared with those who initiated teriparatide. The primary outcome was the incidence of osteoarthritis, while secondary outcomes included joint-specific osteoarthritis (knee, hip, and hand) at 1 year. Inverse probability of treatment weighting (IPTW) was applied to balance baseline characteristics between romosozumab and teriparatide users, and inverse probability of censoring weighting (IPCW) was employed to account for informative censoring. Absolute risk reduction (ARR) and relative risk (RR) at 1 year were estimated using a weighted Kaplan-Meier estimator.

Results: A total of 22,145 individuals were included in the study (87% female; mean age, 80 years). After IPTW-IPCW adjustment, romosozumab was associated with a lower risk of osteoarthritis compared with teriparatide (ARR, 1.1% [95% CI, 0.5%-1.8%]; RR, 0.79 [0.66, 0.89]). Joint-specific analyses showed the following results: knee osteoarthritis: ARR, 0.8% (95% CI, 0.3%-1.5%), RR, 0.79 (0.66, 0.92); hip osteoarthritis: ARR, 0.2% (95% CI, 0.0%-0.5%), RR, 0.68 (0.37, 1.05); and hand osteoarthritis: ARR, 0.2% (95% CI, 0.0%-0.4%), RR, 0.61 (0.35, 1.06).

Conclusions: Romosozumab was associated with a lower risk of osteoarthritis than teriparatide among individuals with osteoporosis, particularly for knee osteoarthritis. Similar trends were observed for hip and hand osteoarthritis; however, the differences were not significant.

*Correspondence to Dr Masaki Hatano, Department of Clinical Epidemiology and Health Economics, School of Public Health, The University of Tokyo, Tokyo, Japan.
E-mail address: h-masaki@g.ecc.u-tokyo.ac.jp (M. Hatano).

Handling editor Josef S. Smolen.

https://doi.org/10.1016/j.ard.2025.06.2124

WHAT IS ALREADY KNOWN ON THIS TOPIC

- Osteoporosis contributes to a distinct subtype of osteoarthritis characterised by subchondral bone fragility, progressive bone loss, and high remodelling rates.
- Romosozumab, an osteoanabolic agent that inhibits sclerostin, has demonstrated efficacy in improving bone mass and skeletal strength. However, its impact on osteoarthritis risk remains unclear due to conflicting preclinical evidence and a paucity of human studies.

WHAT THIS STUDY ADDS

- This new user comparative effectiveness study, designed as a target trial emulation, included adults who were newly prescribed either romosozumab or teriparatide for osteoporosis management.
- After inverse probability treatment weighting and inverse probability of censoring weighting, romosozumab use was associated with a 21% lower risk of incident osteoarthritis compared with teriparatide use in individuals with osteoporosis.

HOW THIS STUDY MIGHT AFFECT RESEARCH, PRACTICE OR POLICY

- These findings suggest that romosozumab may serve as a potential therapeutic option for individuals with osteoporosis, offering dual benefits in both osteoporosis treatment and osteoarthritis risk reduction.

INTRODUCTION

Osteoarthritis has been recognised as a condition influenced by osteoporosis, contributing to a distinct subtype of the disease [1]. Osteoarthritis preceded by osteoporosis is characterised by subchondral bone fragility and distinctive bone loss, accompanied by high remodelling rates [2–5]. These subchondral bone alterations play a pivotal role in the development and progression of osteoarthritis [2–5]. Thus, improving bone mass and strength is essential in managing individuals with osteoporosis who are at risk of developing osteoarthritis. Recent studies have emphasised potential links between antiosteoporotic drugs and osteoarthritis outcomes. For example, denosumab, an antiresorptive agent that inhibits the receptor activator of nuclear factor kappa-B ligand, has demonstrated structural benefits in erosive hand osteoarthritis, a condition considered a distinct osteoporotic subtype of osteoarthritis [6–8].

Osteoanabolic drugs enhance bone mass by directly stimulating bone formation. By targeting and modulating subchondral bone alterations, these drugs have the potential to reduce the risk of osteoarthritis development in individuals with osteoporosis [9,10]. Romosozumab, a monoclonal antibody that targets sclerostin, has been approved as a novel osteoanabolic drug due to its dual mechanism of action, promoting bone formation while simultaneously inhibiting bone resorption [11]. In previous randomised trials, a 12-month course of romosozumab was shown to increase areal bone mineral density at the spine and hip in postmenopausal women with osteoporosis compared with teriparatide [12–14].

Despite these benefits, preclinical studies present conflicting evidence regarding the effects of romosozumab on osteoarthritis. While some findings suggest that sclerostin exerts cartilage-protective properties [15,16], others indicate that antisclerostin antibodies may benefit joint health by promoting bone repair and preventing local bone loss and cartilage damage [17–20]. Nevertheless, human studies investigating whether romosozumab use is associated with the risk of osteoarthritis in populations with osteoporosis remain limited [21,22]. These conflicting preclinical findings and the scarcity of human evidence highlight the need for further research to clarify the role of romosozumab in joint health and its potential impact on osteoarthritis risk in individuals with osteoporosis.

Teriparatide, another widely used osteoanabolic drug, has long been established as a standard treatment for osteoporosis [23]. In Japan, teriparatide, like romosozumab, is specifically indicated for individuals with osteoporosis at high risk of fracture [24]. Therefore, teriparatide was selected as the comparator drug in this study to reduce confounding by indication.

To address this critical knowledge gap, we employed a new user cohort design, emulating a target trial, to evaluate the risk of incident osteoarthritis in individuals with osteoporosis who initiated treatment with romosozumab vs teriparatide using a nationwide administrative claims database.

METHODS

Data source

The source population for the target trial was derived from the DeSC database (DeSC Healthcare Inc). The details of this database have been described elsewhere [25]. Briefly, the database contains administrative claims submitted to health insurers by clinics, hospitals, and pharmacies from April 2014 to November 2022. It encompasses data from 3 types of insurers: health insurance for employees of large companies, national health insurance for nonemployees, and the Advanced Elderly Medical Service System for individuals aged ≥75 years [25]. The database also includes information on annual health check-ups, covering approximately 30% of individuals registered within it. Health check-up data include information on the date, participant demographics (including age, sex, height, and weight), clinical laboratory test results, and lifestyle factors collected through questionnaires.

In the DeSC database, diagnoses are recorded using the International Classification of Diseases, 10th Revision (ICD-10) codes. Prescribed medications are classified according to the World Health Organization Anatomical Therapeutic Chemical (WHO-ATC) system, while procedures are documented using Japanese procedure codes.

Study design and population

We emulated a target trial for the outcomes of interest using an active comparator and a new user cohort study design, incorporating the inverse probability of treatment weighting (IPTW) and the inverse probability of censoring weighting (IPCW) (see Supplementary Table S1 for the framework of the target trial emulation) [26]. Individuals aged ≥50 years who initiated their first-ever use of romosozumab or teriparatide between March 1, 2019, and November 30, 2022, were eligible for inclusion (see Supplementary Fig S1). The study commenced in March 2019, the year romosozumab was first approved in Japan. The target trial index date was defined as the earliest first-ever prescription date of the drug of interest during the study period. The drug of interest included romosozumab (210 mg once monthly) and the comparator, teriparatide, which was administered at one of 3 dosing regimens: 20 μg once daily, 28.2 μg twice weekly, or

56.5 μg once weekly. A 12-month run-in period preceding the index date was used to determine eligibility for cohort entry. Exclusion criteria included the following: simultaneous initiation of both study drugs, lack of insurance enrolment for at least 12 months prior to the index date, initiation of the study drug during hospitalisation, absence of an osteoporosis diagnosis before the index date, history of osteoarthritis, conditions that could lead to secondary osteoarthritis, hyperparathyroidism, or cancer before the index date, prior total knee, hip, hand, or finger replacement before the index date, and lack of follow-up. We did not exclude individuals with injuries associated with osteoarthritis to ensure the inclusion of individuals with a history of insufficiency fractures. Diagnoses were confirmed based on the presence of at least 2 ICD-10 codes recorded (see Supplementary Table S2). The Japanese procedural codes corresponding to the exclusion criteria are listed in Supplementary Table S3.

Exposure and comparison

The exposure group comprised individuals initiating romosozumab (WHO-ATC code: M05BX06) (romosozumab group), while the comparison group consisted of those initiating teriparatide (WHO-ATC code: H05AA02) (teriparatide group) during the study period. Drug use was defined based on the observational analogue of per-protocol effects. Thus, individuals were followed until the earliest occurrence of one of the following events: the study endpoint, treatment discontinuation, switching to the other study drug, initiation of an additional antiosteoporosis drug (including bisphosphonates, denosumab, or selective oestrogen receptor modulators), outcome-related joint replacement, 1 year after the index date, death, or the end of the study period (November 30, 2022). Treatment discontinuation was defined as the absence of drug administration within 60 days following the expected date of the next administration. This expected date was determined by adding the number of days supplied to the most recent administration date of the study drug. Individuals who discontinued the study drug were monitored until the last expected administration date, extended by a 60-day grace period. Switching to the other study drug or initiating another antiosteoporosis drug resulted in immediate censoring.

Outcomes and covariates

The primary outcome was the new occurrence of knee, hip, or hand osteoarthritis. The secondary outcomes were the new occurrences of knee, hip, and hand osteoarthritis separately. Osteoarthritis was defined as the presence of at least 1 ICD-10 code accompanied by at least 1 specific treatment prescribed within 14 days of the initial consultation date (see Supplementary Table S4). We also assessed negative control outcomes between the 2 treatment groups to examine potential unmeasured systematic biases. These included decubitus ulcers, defined as the presence of at least 1 ICD-10 code, and cataract surgery, identified using Japanese procedure codes [27]. The ICD-10 and Japanese procedure codes for the outcomes are listed in Supplementary Table S5.

Diagnostic information and healthcare utilisation measures were collected during the run-in period, including each component of the Charlson Comorbidity Index [28,29], each component of the claims-based Frailty Index [30], hypertension, time since the first recorded diagnosis of osteoporosis, sarcopenia, hip fractures, vertebral fractures, and other insufficiency fractures (fractures of the radius/ulna, pelvis, humerus, or femur). Hip and vertebral fractures were defined as diagnoses requiring specific treatment. Additionally, we recorded the number of outpatient and orthopaedic visits, hospital admissions, and whether individuals had undergone bone biomarker testing or dual-energy X-ray absorptiometry. Injuries that could contribute to secondary osteoarthritis, including individuals who had undergone knee, hip, or hand injury-related surgery, were also documented before the index date. The ICD-10 codes and Japanese procedural codes for covariates (excluding the Charlson Comorbidity Index) are listed in Supplementary Table S6. The claims-based Frailty Index ranges from 0 to 1, with higher values reflecting greater levels of frailty. Following prior studies [30], we categorised frailty status into 3 groups: 'robust' (<0.15), 'prefrail' (0.15-0.25), and 'frail' (>0.25).

Prescription histories were assessed for the 6 months preceding the index date. This included medications such as insulin, hyperglycaemic drugs, beta-blockers, calcium channel blockers, angiotensin-converting enzyme inhibitors/angiotensin receptor blockers, diuretics, antiplatelet drugs, anticoagulants, cardiac glycosides, antidepressants, systemic corticosteroids, nonsteroidal anti-inflammatory drugs, calcium, vitamin D, vitamin K, and chondroitin. Additionally, we documented the use of antiosteoporosis drugs, including bisphosphonates, denosumab, and selective oestrogen receptor modulators during the run-in period. The WHO-ATC codes for these covariates are listed in Supplementary Table S7.

Statistical analysis

To account for the nonrandom allocation of individuals to treatment groups, we applied stabilised IPTW to estimate the average treatment effect on the entire population. The weights were derived using logistic regression, with the administration of romosozumab as the dependent variable and covariates including age, sex, the Charlson Comorbidity Index score, frailty status based on the claims-based Frailty Index, diagnostic and prescription history, healthcare utilisation measures, and calendar year of drug initiation. We also applied IPCW to address potential biases arising from treatment assignment and informative censoring. To calculate the IPCW for the observational time, we used Cox proportional hazards models to estimate the probabilities of treatment changes, adjusting for covariates at the index date. The balance of baseline characteristics between the romosozumab and teriparatide groups was assessed using the standardised mean difference (SMD), with an SMD > 0.1 indicating considerable imbalance.

Absolute and relative treatment effects were estimated for each outcome following IPTW and IPCW adjustment. We used a weighted nonparametric Kaplan-Meier estimator to calculate the absolute risk reduction (ARR) for each outcome within 1 year following romosozumab or teriparatide treatment. Additionally, we estimated the relative risk (RR) at 1 year by comparing the cumulative incidence in the romosozumab group to that in the teriparatide group. To derive 95% CIs, we employed a nonparametric bootstrap approach with 100 samples. Weighted cumulative incidence curves were plotted to visualise the outcomes over time. There was no missing data for the covariates.

We conducted several subgroup and sensitivity analyses to investigate potential treatment effect modifications. To evaluate the potential impact of age on the treatment effect [31,32], we conducted analyses stratified by age (≥80 years and <80 years). To examine the biological impact of initiating romosozumab in relation to a history of insufficiency fractures [32,33], considered a surrogate for osteoporosis severity, we reanalysed the

data, stratifying individuals by the presence or absence of insufficiency fractures during the run-in period. Additionally, to assess the biological impact of initiating romosozumab concerning prior osteoporosis treatment history [32], individuals were categorised into treatment-naïve and treatment-experienced groups. Treatment-naïve individuals were defined as those who initiated romosozumab or teriparatide as their first antiosteoporosis drug and had no recorded use of denosumab, bisphosphonates, or selective oestrogen receptor modulators during the run-in period. Treatment-experienced individuals were defined as those with a history of prior use of any of these drugs before initiating romosozumab or teriparatide.

Eight sensitivity analyses were conducted to confirm the robustness of our findings. First, to account for longer-term outcomes, we evaluated the association between romosozumab and teriparatide with respect to the primary outcome over a 2-year follow-up period using an observational approach analogous to intention-to-treat effects. In this analysis, individuals were followed throughout the entire study period without censoring, even if they discontinued the study drug or switched to another antiosteoporotic drug during follow-up. Second, to test whether the primary outcome was influenced by injuries that could contribute to secondary osteoarthritis, we conducted the same analyses after excluding individuals with any recorded injuries associated with secondary osteoarthritis. Third, given that alternative dosing regimens for teriparatide are approved exclusively in Asia, we performed an additional sensitivity analysis restricted to teriparatide users receiving daily dosing. Additionally, we calculated the average monthly dosage for romosozumab and teriparatide in both the main and sensitivity analyses as the total number of days supplied divided by each individual's follow-up time, up to a maximum of 1 year. Fourth, the robustness of our findings was assessed by reanalysing the outcomes using propensity score overlap weighting instead of IPTW [34]. Fifth, to assess the potential impact of body mass index (BMI) data on our results, we performed analyses restricted to individuals for whom BMI data were available from health check-up records during the run-in period. Sixth, to strengthen the validity of identifying incident osteoarthritis, we reanalysed our data using an extended 24-month run-in period to further ensure the identification of true incident osteoarthritis cases. Seventh, we performed an analysis restricted to individuals who initiated treatment with either romosozumab or teriparatide from March 2020 onwards, 1 year after both drugs became simultaneously available in clinical practice. This approach aimed to minimise potential confounding arising from differences in individual characteristics associated with the early adoption of newly approved medications [35]. Eighth, we used an alternative outcome algorithm to evaluate the possibility that results might vary depending on the outcome definitions [36]. We performed the analysis by redefining the primary outcome as the presence of at least 2 ICD-10 codes for osteoarthritis recorded, together with at least 1 specific treatment.

To address the potential bias associated with using teriparatide as the sole comparator, particularly given emerging evidence suggesting that teriparatide may reduce osteoarthritis risk [37], we conducted a supplementary analysis using the following oral bisphosphonates: alendronate (35 mg once weekly; WHO–ATC M05BA04), ibandronate (100 mg once monthly; WHO–ATC M05BA06), risedronate (17.5 mg once weekly or 75 mg once monthly; WHO–ATC M05BA07), and minodronate (50 mg once monthly; WHO–ATC M05BA), which are reported to have neutral or minimal effects on osteoarthritis progression [38]. The primary outcome was assessed using both per-protocol and intention-to-treat analyses. All statistical analyses were performed using Stata version 18 (Stata Corporation).

Patient and public involvement

Our dataset included only deidentified patients, and data use agreements precluded us from contacting these individuals. Additionally, our funding did not support patient or public involvement.

RESULTS

Participant characteristics

The study cohort included individuals diagnosed with osteoporosis between April 1, 2014, and November 30, 2022. Among these, we identified 8504 new users of romosozumab and 13,641 new users of teriparatide who were free of known osteoarthritis and had not used either study drug at baseline (Fig 1). Table 1 presents the baseline characteristics of the romosozumab and teriparatide groups before IPTW. Overall, the mean age was 79.9 years (SD, 7.5), and 19,167 (86.6%) individuals were female. The mean follow-up time was 233 days (SD, 129) in the romosozumab group and 209 days (SD, 132) in the teriparatide group. The most common reason for censoring was reaching 1 year after baseline, followed by administrative censoring (see Supplementary Table S8 for the distribution of censoring events). There was negligible imbalance (SMD < 0.1) between the groups after IPTW (Table 1 and Supplementary Fig S2).

Primary outcome

Table 2 presents the results of the primary outcome analysis. After IPTW-IPCW adjustment, the cumulative incidence of osteoarthritis within 1 year of follow-up was 3.9% for the romosozumab group and 5.0% for the teriparatide group (Table 2). The romosozumab group had a significantly lower incident risk of osteoarthritis compared with the teriparatide group (ARR, 1.1% [95% CI, 0.5%-1.8%]; RR, 0.79 [0.66, 0.89]) (Table 2). Figure 2A shows that the cumulative incidence curve for the romosozumab group consistently indicated a lower incidence of osteoarthritis than that of the teriparatide group throughout the follow-up period.

Secondary outcomes

Table 2 presents the results of the secondary outcomes. After IPTW-IPCW adjustment, the cumulative incidence of knee osteoarthritis within 1 year of follow-up was 3.2% for the romosozumab group and 4.1% for the teriparatide group (Table 2). The cumulative incidence of hip osteoarthritis was 0.5% for the romosozumab group and 0.7% for the teriparatide group (Table 2). The cumulative incidence of hand osteoarthritis was 0.3% for the romosozumab group and 0.5% for the teriparatide group (Table 2). The romosozumab group had a significantly lower incident risk of knee osteoarthritis compared with the teriparatide group (knee osteoarthritis: ARR, 0.8% [95% CI, 0.3%-1.5%]; RR, 0.79 [0.66, 0.92]) (Table 2). Similar trends were observed for hip and hand osteoarthritis; however, the differences were not significant (hip osteoarthritis: ARR, 0.2% [95% CI, 0.0%-0.5%]; RR, 0.68 [0.37, 1.05]; hand osteoarthritis: ARR, 0.2% [95% CI, 0.0%-0.4%]; RR, 0.61 [0.35, 1.06]) (Table 2). Figure 2B-D shows that the cumulative incidence curves for the

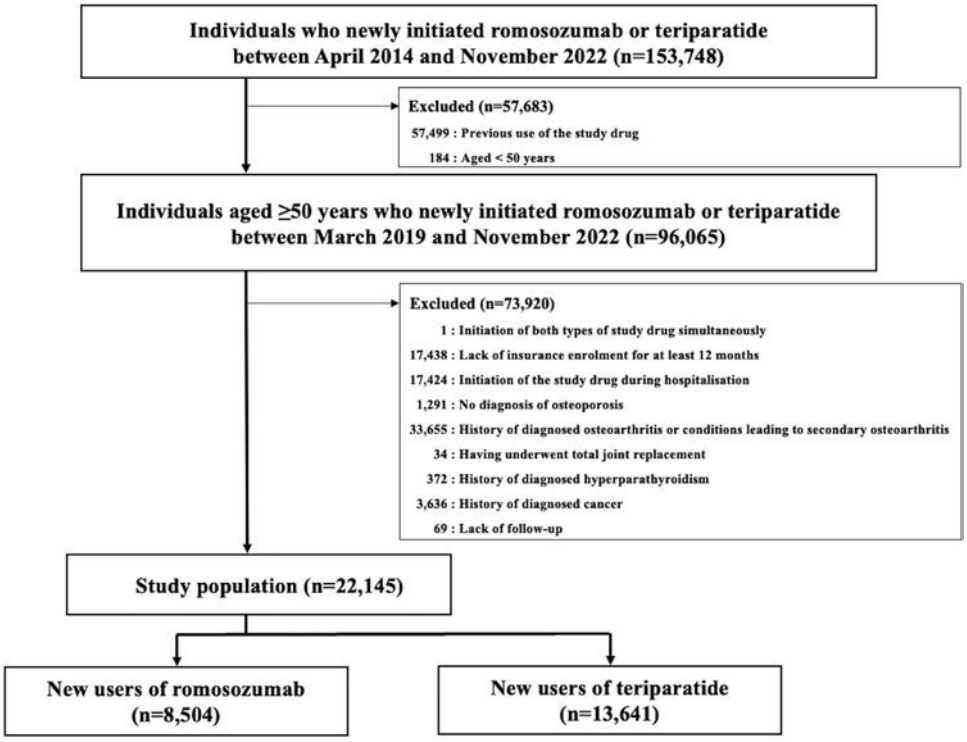

Figure 1. Study flow chart.

romosozumab group consistently indicated a lower incidence of knee, hip, and hand osteoarthritis than those of the teriparatide group throughout the follow-up period.

Subgroup and sensitivity analyses

Across the subgroup analyses, similar trends were observed for the primary outcome (Table 3). In the sensitivity analyses, the lower risk associated with romosozumab remained generally consistent (Supplementary Tables S9-S16). However, statistical significance was not achieved in the 2-year follow-up intention-to-treat analysis, the analysis using a 24-month run-in period, or the analysis restricted to patients receiving daily teriparatide.

Negative control outcomes and supplementary analysis

For the negative control outcomes, no significant differences were found in the risk of decubitus ulcers (ARR, 0.3% [95% CI, −0.3% to 0.8%]; RR, 0.90 [0.75, 1.13]) or cataract surgery (ARR, 0.1% [95% CI, −0.2% to 0.4%]; RR, 0.89 [0.61, 1.23]) (Supplementary Table S17).

In our supplementary analysis (Supplementary Table S18), the per-protocol analysis showed a cumulative incidence of osteoarthritis of 4.3% for the romosozumab group vs 5.5% for the oral bisphosphonate group (ARR, 1.2% [95% CI, 0.7%-1.9%]; RR, 0.78 [0.65, 0.87]). In the intention-to-treat analysis (2-year follow-up), the incidence was 7.4% vs 10.0% (ARR, 2.6% [95% CI, 1.4%-4.0%]; RR, 0.74 [0.61, 0.86]), again indicating a lower risk of osteoarthritis with romosozumab compared with oral bisphosphonates.

DISCUSSION

In this new user comparative effectiveness study, designed to emulate a target trial, romosozumab use was associated with a 21% reduction in incident osteoarthritis compared with teriparatide use in individuals with osteoporosis at 1 year in the per-protocol analysis. The ARR was estimated to be 1.1% fewer cases of osteoarthritis annually. Romosozumab was associated with a lower risk of knee osteoarthritis than teriparatide. A similar pattern was observed for osteoarthritis of the hip and hand; however, the differences were not significant.

Additionally, sensitivity analysis restricted to individuals receiving daily teriparatide—the standard recommended dosing regimen—demonstrated a similar protective trend against osteoarthritis; however, it did not reach statistical significance. The point estimates remained similar to those of the primary analysis; however, the CIs were wider in the sensitivity analysis, possibly owing to the smaller sample size in the teriparatide group and the imbalance in group sizes between the romosozumab and teriparatide groups [39]. As teriparatide users in the sensitivity cohort had a higher average dosage than those in the primary analysis (Supplementary Table S19), dosage differences may have partly influenced the varying precision between these analyses [40].

Comparison with previous studies

Evidence directly comparing the effects of romosozumab and teriparatide on osteoarthritis is scarce. A few large randomised clinical trials involving 7180 and 4093 participants suggested that romosozumab may slightly reduce the risk of osteoarthritis compared with placebo (7.8% vs 8.8%) and alendronate (6.8% vs 7.2%) over 12 months [21,22]. However, these trials lacked prespecified evaluation criteria for osteoarthritis, raising concerns that osteoarthritis was underreported as an adverse event. In contrast, this emulated trial study focused on osteoarthritis as the primary outcome in individuals with osteoporosis, providing a clinically relevant endpoint with a specific comparison to teriparatide.

Our study results should be interpreted in light of previous evidence from bisphosphonate studies, in which observational

Table 1
Characteristics of individuals who initiated romosozumab or teriparatide before and after inverse probability treatment weighting

	Before IPTW			After IPTW		
	Romosozumab group	Teriparatide group	SMD	Romosozumab group	Teriparatide group	SMD
Total no. of individuals, n	8504	13,641		8500	13,671	
Age (y), mean (SD)	80.4 (7.4)	79.6 (7.6)	0.100	79.9 (7.5)	79.9 (7.6)	−0.003
Sex (male), n (%)	890 (10.5)	2088 (15.3)	−0.145	1151 (13.5)	1834 (13.4)	0.004
Claims-based Frailty Index, n (%)			0.018			−0.003
Robust	6530 (76.8)	10,591 (77.6)		6555 (77.1)	10,526 (77.0)	
Prefrail	1603 (18.8)	2471 (18.1)		1578 (18.6)	2551 (18.7)	
Frail	371 (4.4)	579 (4.2)		366 (4.3)	594 (4.4)	
Charlson Comorbidity Index, n (%)			−0.007			0.003
0	3165 (37.2)	5045 (37.0)		3122 (36.7)	5039 (36.9)	
1	2289 (26.9)	3684 (27.0)		2299 (27.1)	3692 (27.0)	
2	1478 (17.4)	2396 (17.6)		1493 (17.6)	2388 (17.5)	
3	832 (9.8)	1254 (9.2)		800 (9.4)	1308 (9.6)	
≥4	740 (8.7)	1262 (9.3)		786 (9.3)	1245 (9.1)	
Osteoporosis duration, mean (SD)	3.0 (4.0)	2.5 (3.9)	0.135	2.7 (3.9)	2.7 (4.1)	0.001
Calendar year of drug initiation, n (%)			0.074			−0.005
2019	2209 (26.0)	3240 (23.8)		2065 (24.3)	3306 (24.2)	
2020	2041 (24.0)	4338 (31.8)		2466 (29.0)	3949 (28.9)	
2021	2932 (34.5)	4494 (32.9)		2859 (33.6)	4610 (33.7)	
2022	1322 (15.5)	1569 (11.5)		1110 (13.1)	1806 (13.2)	
Comorbidities, n (%)						
Hypertension	5012 (58.9)	7993 (58.6)	0.007	5023 (59.1)	8048 (58.9)	0.005
Myocardial infarction	131 (1.5)	325 (2.4)	−0.061	181 (2.1)	282 (2.1)	0.005
Heart failure	1724 (20.3)	3011 (22.1)	−0.044	1840 (21.6)	2947 (21.6)	0.002
Cerebrovascular disease	1450 (17.1)	2352 (17.2)	−0.005	1487 (17.5)	2368 (17.3)	0.005
Peripheral vascular disease	1089 (12.8)	1757 (12.9)	−0.002	1095 (12.9)	1747 (12.8)	0.003
Chronic pulmonary disease	1524 (17.9)	2525 (18.5)	−0.015	1561 (18.4)	2500 (18.3)	0.002
Renal failure	393 (4.6)	605 (4.4)	0.009	388 (4.6)	619 (4.5)	0.002
Liver disease	1237 (14.5)	2056 (15.1)	−0.015	1262 (14.9)	2036 (14.9)	−0.001
Sarcopenia	201 (2.4)	299 (2.2)	0.012	192 (2.3)	312 (2.3)	−0.002
Hip fracture	412 (4.8)	412 (3.0)	0.094	319 (3.8)	535 (3.9)	−0.009
Vertebral fracture	533 (6.3)	855 (6.3)	0.000	539 (6.3)	862 (6.3)	0.001
Other insufficiency fractures	627 (7.4)	958 (7.0)	0.014	606 (7.1)	981 (7.2)	−0.002
Knee injury	186 (2.2)	267 (2.0)	0.016	168 (2.0)	275 (2.0)	−0.003
Hip injury	738 (8.7)	840 (6.2)	0.096	610 (7.2)	1009 (7.4)	−0.008
Hand injury	136 (1.6)	226 (1.7)	−0.005	139 (1.6)	227 (1.7)	−0.002
Medications, n (%)						
Denosumab	650 (7.6)	268 (2.0)	0.268	354 (4.2)	599 (4.4)	−0.010
Bisphosphonates	2443 (28.7)	3087 (22.6)	0.140	2143 (25.2)	3429 (25.1)	0.003
SERM	615 (7.2)	966 (7.1)	0.006	600 (7.1)	972 (7.1)	−0.002
Vitamin D agents	3777 (44.4)	4227 (31.0)	0.280	3076 (36.2)	4964 (36.3)	−0.003
Calcium agents	363 (4.3)	307 (2.3)	0.114	259 (3.1)	425 (3.1)	−0.003
Vitamin K agents	84 (1.0)	125 (0.9)	0.007	81 (1.0)	129 (0.9)	0.001
Insulin	220 (2.6)	393 (2.9)	−0.018	232 (2.7)	377 (2.8)	−0.002
Hyperglycaemic drugs	860 (10.1)	1539 (11.3)	−0.038	926 (10.9)	1485 (10.9)	0.001
Antiplatelet drugs	1595 (18.8)	2832 (20.8)	−0.05	1714 (20.2)	2721 (19.9)	0.007
Anticoagulant drugs	437 (5.1)	800 (5.9)	−0.032	482 (5.7)	781 (5.7)	−0.002
Cardiac glycosides	49 (0.6)	108 (0.8)	−0.026	60 (0.7)	95 (0.7)	0.002
Diuretic drugs	864 (10.2)	1507 (11.0)	−0.029	908 (10.7)	1463 (10.7)	−0.001
Beta-blockers	810 (9.5)	1582 (11.6)	−0.067	917 (10.8)	1473 (10.8)	0.000
Calcium channel blockers	3036 (35.7)	4955 (36.3)	−0.013	3101 (36.5)	4955 (36.3)	0.005
ACE inhibitors/ARB	2627 (30.9)	4228 (31.0)	−0.002	2637 (31.0)	4240 (31.0)	0.000
Antidepressants	531 (6.2)	914 (6.7)	−0.019	567 (6.7)	908 (6.6)	0.001
NSAIDs	4652 (54.7)	8567 (62.8)	−0.165	5090 (59.9)	8165 (59.7)	0.003
Systemic corticosteroids	1135 (13.3)	1941 (14.2)	−0.026	1194 (14.1)	1906 (13.9)	0.003
Chondroitin	10 (0.1)	33 (0.2)	−0.029	20 (0.2)	27 (0.2)	0.008
Healthcare utilisation measures						
Mean (SD) no. of orthopaedic department visits per year	2.2 (5.3)	2.1 (5.6)	0.027	2.2 (5.1)	2.2 (5.7)	0.002
Mean (SD) no. of hospital admissions per year	0.7 (1.5)	0.6 (1.4)	0.051	0.7 (1.4)	0.7 (1.5)	−0.001
No. of outpatient visits per year, n (%)			−0.027			0.002
<12	1840 (21.6)	2879 (21.1)		1799 (21.2)	2909 (21.3)	
12-24	3191 (37.5)	4978 (36.5)		3137 (36.9)	5031 (36.8)	
>24	3473 (40.8)	5784 (42.4)		3564 (41.9)	5731 (41.9)	
Dual X-ray absorptiometry, n (%)	4037 (47.5)	5162 (37.8)	0.196	3541 (41.7)	5721 (41.9)	−0.004
Bone biomarkers, n (%)	4029 (47.4)	5490 (40.2)	0.144	3681 (43.3)	5928 (43.4)	−0.001

ACE inhibitor/ARB, angiotensin-converting enzyme inhibitor/angiotensin receptor blocker; IPTW, inverse probability of treatment weighting; NSAID, nonsteroidal anti-inflammatory drug; SERM, selective oestrogen receptor modulator; SMD, standardised mean difference.

Table 2
Effects of romosozumab on outcomes relative to teriparatide: per-protocol analyses

	No. of individuals	Cumulative incidence risk, %	% Absolute risk reduction (95% CI)[a]	Relative risk (95% CI)[a]
Primary outcome				
Osteoarthritis				
Teriparatide group	13,671	5.0	Reference	Reference
Romosozumab group	8500	3.9	1.1 (0.5, 1.8)	0.79 (0.66, 0.89)
Secondary outcomes				
Knee osteoarthritis				
Teriparatide group	13,671	4.1	Reference	Reference
Romosozumab group	8500	3.2	0.8 (0.3, 1.5)	0.79 (0.66, 0.92)
Hip osteoarthritis				
Teriparatide group	13,671	0.7	Reference	Reference
Romosozumab group	8500	0.5	0.2 (0.0, 0.5)	0.68 (0.37, 1.05)
Hand osteoarthritis				
Teriparatide group	13,671	0.5	Reference	Reference
Romosozumab group	8500	0.3	0.2 (0.0, 0.4)	0.61 (0.35, 1.06)

[a] Absolute risk reduction > 0 (or <0) and a relative risk < 1 (or >1) indicate that individuals for whom romosozumab was initiated had a lower (higher) risk of the outcomes than those for whom teriparatide was initiated.

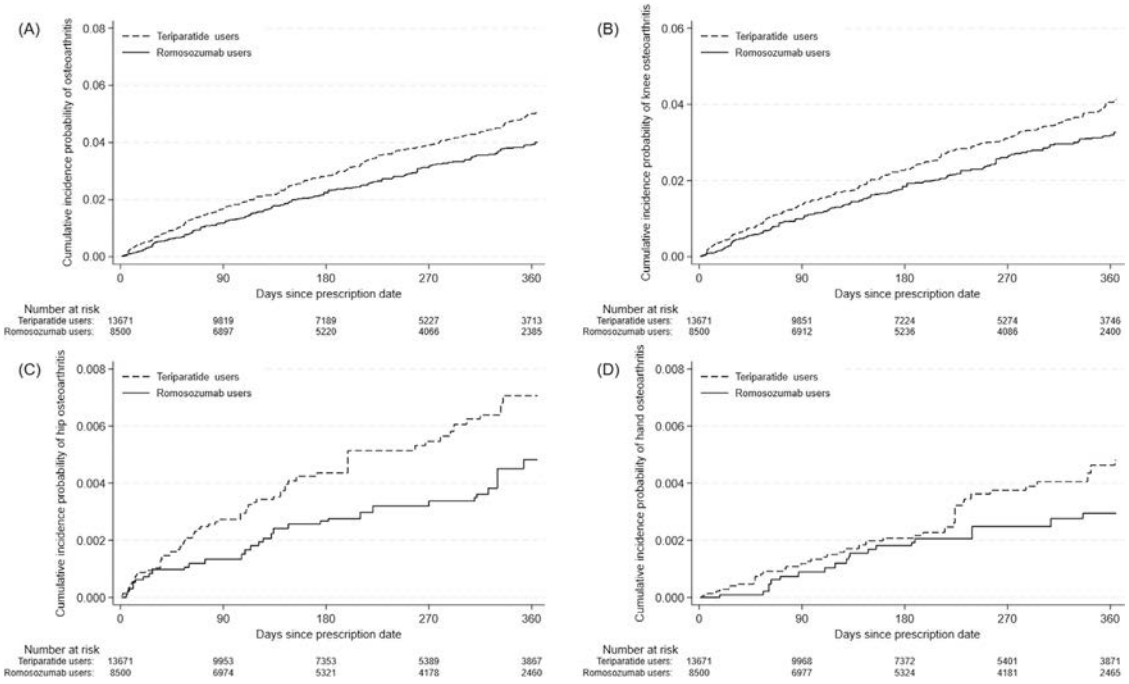

Figure 2. Cumulative incidence probability of outcomes after inverse probability treatment weighting. Cumulative incidence probability of osteoarthritis (A), knee osteoarthritis (B), hip osteoarthritis (C), and hand osteoarthritis (D) after inverse probability treatment weighting are presented.

Table 3
Subgroup analyses of the comparative effects of romosozumab vs teriparatide: per-protocol analyses

	Cumulative incidence					
	Romosozumab		Teriparatide			
	No. of individuals	Risk, %	No. of individuals	Risk, %	% Absolute risk reduction (95% CI)[a]	Relative risk (95% CI)[a]
Age (y)						
<80	3685	4.1	6370	4.8	0.7 (−0.4, 1.5)	0.85 (0.71, 1.09)
≥80	4816	3.7	7298	5.0	1.2 (0.3, 2.3)	0.75 (0.57, 0.94)
History of insufficiency fractures						
Without history	4676	4.4	7655	5.8	1.4 (0.4, 2.6)	0.75 (0.59, 0.92)
With history	3827	3.3	6009	4.0	0.6 (−0.5, 1.6)	0.84 (0.66, 1.16)
Prior osteoporosis treatment history						
Treatment-naïve	4976	4.2	9517	4.8	0.5 (−0.3, 1.5)	0.89 (0.70, 1.07)
Treatment-experienced	3535	3.4	4131	5.3	1.9 (0.4, 2.9)	0.64 (0.49, 0.91)

[a] Absolute risk reduction > 0 (or <0) and a relative risk < 1 (or >1) indicate that individuals for whom romosozumab was initiated had a lower (higher) risk of the outcomes than those for whom teriparatide was initiated.

studies showed promising associations with reduced osteoarthritis incidence, but subsequent randomised controlled trials showed no significant efficacy [38]. Such discrepancies are likely due to selection bias, immortal time bias, and other methodological limitations inherent in observational research, particularly when comparing drug initiators with noninitiators [26]. However, our study applied a rigorous pharmacoepidemiological methodology, ie, a new user cohort design emulating a target trial, which is recognised for strengthening causal inference and reducing biases such as selection bias and immortal time bias [26].

Biological mechanisms

The biological mechanisms underlying the effects of romosozumab remain unclear; however, its dual actions involving osteoblast-mediated bone formation and the suppression of bone resorption may provide protective effects against osteoarthritis [12,13,17–20]. In weight-bearing joints affected by osteoporosis, compromised subchondral bone integrity alters load distribution, increasing stress on cartilage and causing microfractures and collapse [41,42]. By inhibiting sclerostin and activating Wnt/β-catenin signalling, romosozumab could improve cortical and trabecular bone quality and enhance joint stability, which might explain the observed reduction in osteoarthritis development in this study [43,44]. Additionally, romosozumab may have protective effects in hand osteoarthritis similar to denosumab [6]. The antiresorptive activity of romosozumab, mediated through Wnt/β-catenin pathways, could protect hand joints by reducing osteoclast-driven erosion; however, the precise mechanisms may differ from those described for denosumab [21,22]. These hypothetical mechanisms require further validation through future basic and clinical studies.

Notably, the protective effect of romosozumab emerged relatively early, which may not be owing to structural modifications in joint tissues alone, as such changes typically require long periods to become apparent. An alternative explanation is that romosozumab may prevent osteoarthritis-related pain before detectable structural changes, potentially through mechanisms involving the early stabilisation of subchondral bone [45].

Implications for clinical practice

Our study provides real-world evidence suggesting the benefit of romosozumab, an agent combining anabolic and antiresorptive effects, in improving bone strength and possibly reducing osteoarthritis risk in individuals with osteoporosis. Given the paucity of effective preventive options for osteoarthritis in osteoporotic populations and the practical challenges inherent in conducting randomised controlled trials in this clinical setting, observational evidence such as that provided by this study may contribute to informing potential therapeutic strategies. The observed protective effect of romosozumab against osteoarthritis risk appears consistent across clinically relevant factors, including age, history of recent insufficiency fractures, and prior osteoporosis treatments, all of which are essential considerations when selecting osteoporosis management strategies [32,33]. However, the absolute reduction in osteoarthritis risk observed in this study was modest, suggesting that the clinical significance of this observed association may be limited. In the 2-year intention-to-treat analysis, the reduction in osteoarthritis incidence observed at 1 year in the per-protocol analysis was attenuated, possibly owing to romosozumab discontinuation. As intention-to-treat analyses between active treatments of differing durations or adherence can underestimate true efficacy [46], our 2-year intention-to-treat results should be interpreted carefully, acknowledging that the actual efficacy of romosozumab may be greater than what is observed.

Given the observational nature of this study and the potential for residual confounding, including confounding by indication, our findings should be carefully interpreted. Although our findings provide valuable initial evidence regarding romosozumab's potential dual skeletal benefits, definitive conclusions regarding its efficacy in preventing osteoarthritis require confirmation through randomised controlled trials designed to evaluate structural and symptomatic outcomes. Moreover, our reliance on a healthcare insurance claims database limits inferences about osteoarthritis progression, as imaging findings and detailed clinical symptom data were not available. In light of these constraints, future clinical trials, especially in individuals with established osteoarthritis and osteoporosis, are warranted to determine whether romosozumab can provide clinically meaningful benefits in slowing or preventing osteoarthritis progression.

Strengths and weaknesses of the study

This study has several notable strengths. First, we employed an active comparator and a new user design within an emulated target trial framework, IPTW, to mitigate the risk of confounding by indication and unmeasured clinical characteristics. Second, the inclusion of sensitivity analyses and control outcomes strengthens the internal validity of this study, ensuring a rigorous assessment of the primary findings. The consistency of the results with our primary analysis further underscores their robustness. Third, the main analyses were conducted on a cohort that excluded individuals with conditions that could lead to secondary osteoarthritis. This approach allowed for a more precise evaluation of the natural history of osteoarthritis development while minimising the risk of outcome misclassification. Finally, to the best of our knowledge, no previous studies have investigated the effects of romosozumab on osteoarthritis risk in individuals with osteoporosis. These findings underscore the potential role of romosozumab as a therapeutic option for this population, particularly in the context of osteoarthritis risk reduction.

Despite these strengths, the study has some limitations. First, the incidence of osteoarthritis may not have been fully captured due to the relatively short follow-up period, as romosozumab is approved for use only up to 12 months. Longer follow-up studies are warranted to assess the long-term effects of romosozumab on osteoarthritis following treatment cessation. Second, the database lacked detailed information on dual X-ray absorptiometry and bone biomarkers. Consequently, incident hip and vertebral fractures occurring within 1 year before treatment initiation were used as surrogate indicators of osteoporosis severity and were adjusted for in the analysis. Third, residual or unmeasured confounding factors may have biased our findings, especially as patient or physician preferences could still influence treatment choices. Fourth, the database did not contain information on over-the-counter medication use, which may have led to an underestimation of osteoarthritis incidence, potentially influencing the study results. Fifth, the absence of BMI data, a well-established risk factor for osteoarthritis, limits our findings. To address this limitation, we conducted a sensitivity analysis using BMI data from health check-ups performed during the run-in period. Although the number of eligible individuals with health check-ups was smaller, the results were consistent with our

main findings, suggesting that the absence of comprehensive BMI data may not have substantially biased our main results. Sixth, reliance on ICD-10 diagnostic codes may have led to the underreporting of osteoarthritis cases, potentially biasing our findings [47]. Previous research has demonstrated substantial underreporting when using claims data alone, particularly for mild or asymptomatic osteoarthritis cases and for types less likely to prompt healthcare visits, such as hand and generalised osteoarthritis [47]. Although comprehensive validation studies specific to Japanese claims data are currently unavailable, similar underreporting is likely. Therefore, caution is necessary when interpreting our findings, as the true incidence of osteoarthritis may be underestimated.

Conclusions

This target trial emulation study suggests that romosozumab treatment is associated with a lower osteoarthritis risk than teriparatide treatment in individuals with osteoporosis. This association was consistently observed for knee osteoarthritis. Similar trends were observed for hip and hand osteoarthritis; however, the trends were not significant. These findings suggest that romosozumab is a promising therapeutic option for addressing osteoporosis and preclinical osteoarthritis related to osteoporosis, potentially offering dual skeletal benefits in high-risk populations.

Competing interests

HY reports receiving an institutional grant from the Ministry of Health, Labour and Welfare, Japan (23AA2003). YS discloses that DeSC Healthcare, Inc, provided financial support for the present manuscript.

CRediT authorship contribution statement

Masaki Hatano: Writing – original draft, Methodology, Formal analysis, Data curation, Conceptualization. **Yusuke Sasabuchi:** Writing – review & editing, Supervision, Methodology, Conceptualization. **Akira Okada:** Writing – review & editing, Supervision, Methodology, Conceptualization. **Yuya Kimura:** Writing – review & editing, Methodology, Conceptualization. **Hisatoshi Ishikura:** Writing – review & editing, Supervision, Conceptualization. **Takeyuki Tanaka:** Writing – review & editing, Methodology, Conceptualization. **Taku Saito:** Writing – review & editing, Supervision, Conceptualization. **Sakae Tanaka:** Writing – review & editing, Supervision, Conceptualization. **Hideo Yasunaga:** Writing – review & editing, Supervision, Resources, Project administration, Funding acquisition, Conceptualization.

Funding

This study was funded by a grant from the Ministry of Health, Labour and Welfare, Japan (23AA2003). The funding source had no role in the study design, data collection, analysis, interpretation, or decision to submit this article for publication.

Patient consent for publication

Not applicable.

Ethics approval

This study was approved by the Institutional Review Board at the University of Tokyo (approval number: 2021010NI [April 23, 2021]). The requirement for informed consent was waived as all data were deidentified.

Provenance and peer review

Not commissioned; externally peer reviewed.

Data availability statement

The data supporting this study were provided by DeSC Healthcare, Inc, under a licensing agreement. Data will be made available upon reasonable request to the corresponding author, subject to approval from DeSC Healthcare, Inc.

Supplementary materials

Supplementary material associated with this article can be found in the online version at doi:10.1016/j.ard.2025.06.2124.

Orcid

Masaki Hatano: http://orcid.org/0000-0002-7096-5604
Yuya Kimura: http://orcid.org/0000-0003-1649-0596

REFERENCES

[1] Herrero-Beaumont G, Roman-Blas JA. Osteoarthritis: osteoporotic OA: a reasonable target for bone-acting agents. Nat Rev Rheumatol 2013;9(8):448–50. doi: 10.1038/nrrheum.2013.113.
[2] Roman-Blas JA, Castañeda S, Largo R, Lems WF, Herrero-Beaumont G. An OA phenotype may obtain major benefit from bone-acting agents. Semin Arthritis Rheum 2014;43(4):421–8. doi: 10.1016/j.semarthrit.2013.07.012.
[3] Bultink IEM, Lems WF. Osteoarthritis and osteoporosis: what is the overlap? Curr Rheumatol Rep 2013;15(5):328. doi: 10.1007/s11926-013-0328-0.
[4] Chu L, Liu X, He Z, Han X, Yan M, Qu X, et al. Articular cartilage degradation and aberrant subchondral bone remodeling in patients with osteoarthritis and osteoporosis. J Bone Miner Res 2020;35(3):505–15. doi: 10.1002/jbmr.3909.
[5] Bellido M, Lugo L, Roman-Blas JA, Castañeda S, Caeiro JR, Dapia S, et al. Subchondral bone microstructural damage by increased remodelling aggravates experimental osteoarthritis preceded by osteoporosis. Arthritis Res Ther 2010;12(4):R152. doi: 10.1186/ar3103.
[6] Wittoek R, Verbruggen G, Vanhaverbeke T, Colman R, Elewaut D. RANKL blockade for erosive hand osteoarthritis: a randomized placebo-controlled phase 2a trial. Nat Med 2024;30(3):829–36. doi: 10.1038/s41591-024-02822-0.
[7] Bergink AP, Rivadeneira F, Bierma-Zeinstra SM, Zillikens MC, Ikram MA, Uitterlinden AG, et al. Are bone mineral density and fractures related to the incidence and progression of radiographic osteoarthritis of the knee, hip, and hand in elderly men and women? The Rotterdam study. Arthritis Rheumatol 2019;71(3):361–9. doi: 10.1002/art.40735.
[8] McAlindon TE, Driban JB, Roberts MB, Duryea J, Haugen IK, Schaefer LF, et al. Erosive hand osteoarthritis: incidence and predictive characteristics among participants in the osteoarthritis initiative. Arthritis Rheumatol 2021;73(11):2015–24. doi: 10.1002/art.41757.
[9] Bellido M, Lugo L, Roman-Blas JA, Castañeda S, Calvo E, Largo R, et al. Improving subchondral bone integrity reduces progression of cartilage damage in experimental osteoarthritis preceded by osteoporosis. Osteoarthritis Cartilage 2011;19(10):1228–36. doi: 10.1016/j.joca.2011.07.003.
[10] Lewiecki EM. Role of sclerostin in bone and cartilage and its potential as a therapeutic target in bone diseases. Ther Adv Musculoskelet Dis 2014;6(2):48–57. doi: 10.1177/1759720X13510479.
[11] Tanaka S, Matsumoto T. Sclerostin: from bench to bedside. J Bone Miner Metab 2021;39(3):332–40. doi: 10.1007/s00774-020-01176-0.
[12] Keaveny TM, Crittenden DB, Bolognese MA, Genant HK, Engelke K, Oliveri B, et al. Greater gains in spine and hip strength for romosozumab compared

with teriparatide in postmenopausal women with low bone mass. J Bone Miner Res 2017;32(9):1956–62. doi: 10.1002/jbmr.3176.
[13] Genant HK, Engelke K, Bolognese MA, Mautalen C, Brown JP, Recknor C, et al. Effects of romosozumab compared with teriparatide on bone density and mass at the spine and hip in postmenopausal women with low bone mass. J Bone Miner Res 2017;32(1):181–7. doi: 10.1002/jbmr.2932.
[14] Langdahl BL, Libanati C, Crittenden DB, Bolognese MA, Brown JP, Daizadeh NS, et al. Romosozumab (sclerostin monoclonal antibody) versus teriparatide in postmenopausal women with osteoporosis transitioning from oral bisphosphonate therapy: a randomised, open-label, phase 3 trial. Lancet 2017;390(10102):1585–94. doi: 10.1016/S0140-6736(17)31613-6.
[15] Chan BY, Fuller ES, Russell AK, Smith SM, Smith MM, Jackson MT, et al. Increased chondrocyte sclerostin may protect against cartilage degradation in osteoarthritis. Osteoarthritis Cartilage 2011;19(7):874–85. doi: 10.1016/j.joca.2011.04.014.
[16] Hartley A, Gregson CL, Paternoster L, Tobias JH. Osteoarthritis: insights offered by the study of bone mass genetics. Curr Osteoporos Rep 2021;19(2):115–22. doi: 10.1007/s11914-021-00655-1.
[17] Chen XX, Baum W, Dwyer D, Stock M, Schwabe K, Ke HZ, et al. Sclerostin inhibition reverses systemic, periarticular and local bone loss in arthritis. Ann Rheum Dis 2013;72(10):1732–6. doi: 10.1136/annrheumdis-2013-203345.
[18] Agholme F, Li X, Isaksson H, Ke HZ. Aspenberg P. Sclerostin antibody treatment enhances metaphyseal bone healing in rats. J Bone Miner Res 2010;25(11):2412–8. doi: 10.1002/jbmr.135.
[19] Fessel J. There are many potential medical therapies for atraumatic osteonecrosis. Rheumatology (Oxford) 2013;52(2):235–41. doi: 10.1093/rheumatology/kes241.
[20] Ozawa Y, Takegami Y, Osawa Y, Asamoto T, Tanaka S, Imagama S. Anti-sclerostin antibody therapy prevents post-ischemic osteonecrosis bone collapse via interleukin-6 association. Bone 2024;181:117030. doi: 10.1016/j.bone.2024.117030.
[21] Cosman F, Crittenden DB, Adachi JD, Binkley N, Czerwinski E, Ferrari S, et al. Romosozumab treatment in postmenopausal women with osteoporosis. N Engl J Med 2016;375(16):1532–43. doi: 10.1056/NEJMoa1607948.
[22] Saag KG, Petersen J, Brandi ML, Karaplis AC, Lorentzon M, Thomas T, et al. Romosozumab or alendronate for fracture prevention in women with osteoporosis. N Engl J Med 2017;377(15):1417–27. doi: 10.1056/NEJMoa1708322.
[23] Kendler DL, Marin F, Zerbini CAF, Russo LA, Greenspan SL, Zikan V, et al. Effects of teriparatide and risedronate on new fractures in post-menopausal women with severe osteoporosis (VERO): a multicentre, double-blind, double-dummy, randomised controlled trial. Lancet 2018;391(10117):230–40. doi: 10.1016/S0140-6736(17)32137-2.
[24] Reid IR, Billington EO. Drug therapy for osteoporosis in older adults. Lancet 2022;399(10329):1080–92. doi: 10.1016/S0140-6736(21)02646-5.
[25] Okada A, Yasunaga H. Prevalence of noncommunicable diseases in Japan using a newly developed administrative claims database covering young, middle-aged, and elderly people. JMA J 2022;5(2):190–8. doi: 10.31662/jmaj.2021-0189.
[26] Hernán MA, Robins JM. Using big data to emulate a target trial when a randomized trial is not available. Am J Epidemiol 2016;183(8):758–64. doi: 10.1093/aje/kwv254.
[27] McGrath LJ, Spangler L, Curtis JR, Ehrenstein V, Sørensen HT, Saul B, et al. Using negative control outcomes to assess the comparability of treatment groups among women with osteoporosis in the United States. Pharmacoepidemiol Drug Saf 2020;29(8):854–63. doi: 10.1002/pds.5037.
[28] Charlson ME, Pompei P, Ales KL, MacKenzie CR. A new method of classifying prognostic comorbidity in longitudinal studies: development and validation. J Chronic Dis 1987;40(5):373–83. doi: 10.1016/0021-9681(87)90171-8.
[29] Quan H, Sundararajan V, Halfon P, Fong A, Burnand B, Luthi JC, et al. Coding algorithms for defining comorbidities in ICD-9-CM and ICD-10 administrative data. Med Care 2005;43(11):1130–9. doi: 10.1097/01.mlr.0000182534.19832.83.
[30] Nakatsuka K, Ono R, Murata S, Akisue T, Fukuda H. Claims-based Frailty Index in Japanese older adults: a cohort study using LIFE study data. J Epidemiol 2024;34(3):112–8. doi: 10.2188/jea.JE20220310.
[31] Prieto-Alhambra D, Judge A, Javaid MK, Cooper C, Diez-Perez A, NK Arden. Incidence and risk factors for clinically diagnosed knee, hip and hand osteoarthritis: influences of age, gender and osteoarthritis affecting other joints. Ann Rheum Dis 2014;73(9):1659–64. doi: 10.1136/annrheumdis-2013-203355.
[32] Cosman F, Lewiecki EM, Eastell R, Ebeling PR, Jan De Beur S, Langdahl B, et al. Goal-directed osteoporosis treatment: ASBMR/BHOF task force position statement 2024. J Bone Miner Res 2024;39(10):1393–405. doi: 10.1093/jbmr/zjae119.
[33] Anastasilakis AD, Yavropoulou MP, Palermo A, Makras P, Paccou J, Tabacco G, et al. Romosozumab versus parathyroid hormone receptor agonists: which osteoanabolic to choose and when? Eur J Endocrinol 2024;191(1) R9-21. doi: 10.1093/ejendo/lvae076.
[34] Thomas LE, Li F, Pencina MJ. Overlap weighting: a propensity score method that mimics attributes of a randomized clinical trial. JAMA 2020;323(23):2417–8. doi: 10.1001/jama.2020.7819.
[35] Schneeweiss S, Gagne JJ, Glynn RJ, Ruhl M, Rassen JA. Assessing the comparative effectiveness of newly marketed medications: methodological challenges and implications for drug development. Clin Pharmacol Ther 2011;90(6):777–90. doi: 10.1038/clpt.2011.235.
[36] Lu Y, Ganz ML, Robinson RL, Zagar AJ, Okala S, Hartrick CT, et al. Use of electronic health data to identify patients with moderate-to-severe osteoarthritis of the hip and/or knee and inadequate response to pain medications. BMC Med Res Methodol 2023;23(1):156. doi: 10.1186/s12874-023-01964-y.
[37] Li G, Liu S, Xu H, Chen Y, Deng J, Xiong A, et al. Potential effects of teriparatide (PTH (1-34)) on osteoarthritis: a systematic review. Arthritis Res Ther 2023;25(1):3. doi: 10.1186/s13075-022-02981-w.
[38] Vaysbrot EE, Osani MC, MC Musetti, McAlindon TE, Bannuru RR. Are bisphosphonates efficacious in knee osteoarthritis? A meta-analysis of randomized controlled trials. Osteoarthritis Cartilage 2018;26(2):154–64. doi: 10.1016/j.joca.2017.11.013.
[39] Hazra A. Using the confidence interval confidently. J Thorac Dis 2017;9(10):4125–30. doi: 10.21037/jtd.2017.09.14.
[40] Chiba K, Okazaki N, Kurogi A, Watanabe T, Mori A, Suzuki N, et al. Randomized controlled trial of daily teriparatide, weekly high-dose teriparatide, or bisphosphonate in patients with postmenopausal osteoporosis: the TERABIT study. Bone 2022;160:116416. doi: 10.1016/j.bone.2022.116416.
[41] Lajeunesse D, Reboul P. Subchondral bone in osteoarthritis: a biologic link with articular cartilage leading to abnormal remodeling. Curr Opin Rheumatol 2003;15(5):628–33. doi: 10.1097/00002281-200309000-00018.
[42] Qu Y, Chen S, Han M, Gu Z, Zhang Y, Fan T, et al. Osteoporosis and osteoarthritis: a bi-directional Mendelian randomization study. Arthritis Res Ther 2023;25(1):242. doi: 10.1186/s13075-023-03213-5.
[43] Galea GL, Lanyon LE, Price JS. Sclerostin's role in bone's adaptive response to mechanical loading. Bone 2017;96:38–44. doi: 10.1016/j.bone.2016.10.008.
[44] Yee CS, Xie L, Hatsell S, Hum N, Murugesh D, Economides AN, et al. Sclerostin antibody treatment improves fracture outcomes in a type I diabetic mouse model. Bone 2016;82:122–34. doi: 10.1016/j.bone.2015.04.048.
[45] Laslett LL, Doré DA, Quinn SJ, Boon P, Ryan E, Winzenberg TM, et al. Zoledronic acid reduces knee pain and bone marrow lesions over 1 year: a randomised controlled trial. Ann Rheum Dis 2012;71(8):1322–8. doi: 10.1136/annrheumdis-2011-200970.
[46] Hernán MA, Robins JM. Per-protocol analyses of pragmatic trials. N Engl J Med 2017;377(14):1391–8. doi: 10.1056/NEJMsm1605385.
[47] Arslan IG, Damen J, de Wilde M, van den Driest JJ, Bindels PJE, van der Lei J, et al. Incidence and prevalence of knee osteoarthritis using codified and narrative data from electronic health records: a population-based study. Arthritis Care Res (Hoboken) 2022;74(6):937–44. doi: 10.1002/acr.24861.

Ann Rheum Dis 84 (2025) 1948–1950

Contents lists available at ScienceDirect

Annals of the Rheumatic Diseases

journal homepage: https://www.sciencedirect.com/journal/annals-of-the-rheumatic-diseases

Letter

Genetic susceptibility to membranous lupus nephritis: a genome-wide association study

Dear Editor,

We present a comprehensive genome-wide association study (GWAS) of lupus nephritis (LN) subtypes, focusing on the distinction between membranous lupus nephritis (MLN) and proliferative lupus nephritis (PLN). LN affects approximately 40% to 60% of systemic lupus erythematosus patients, with 10% progressing to end-stage kidney disease. Despite the widely used International Society of Nephrology/Renal Pathology Society (ISN/RPS) classification system, the molecular pathogenesis of LN subtypes remains unclear, necessitating further genetic exploration [1–3].

Our study included 2041 biopsy-proven LN patients and 524 healthy controls from 2 cohorts in China (Supplementary Methods). All patients and controls provided written informed consent, and the study protocol was approved by the Ethical Committee of the Peking University First Hospital (2020–Y158) and the First Affiliated Hospital of Zhengzhou University (2019-KY-0033-002). Patients were classified according to the ISN/RPS system, with MLN defined as Class V, PLN as Class III or IV, and mixed proliferative LN as Class III or IV + V. Genotyping was performed using the Illumina Global Screening Array, followed by imputation using the Michigan Imputation Server. After quality control, we analysed 6 million single nucleotide polymorphisms (SNPs). GWAS was conducted using logistic regression in PLINK 1.9, with meta-analysis performed in METAL [4]. Heterogeneity between discovery and validation phases was assessed using Cochran's Q and I^2 statistics for MLN-specific signals. We used FINEMAP for fine-mapping and various databases for functional annotation of SNPs.

Clinically, class V patients exhibited a distinct profile compared to class III/IV, including older age of onset, lower blood pressure, higher proteinuria but better renal function, and less severe immunological abnormalities (Supplementary Tables S1-S4 and Figs S1-S2). These findings suggest that class V may have a different underlying pathophysiology and a potentially more indolent course than class III/IV. This is further supported by the long-term follow-up data, which demonstrated significantly better renal outcomes for class V patients compared to class III/IV (hazard ratio 0.14, 95% CI 0.03-0.59, $P = .007$).

Our GWAS identified 3 loci (*HLA-DQA1, GTF2IRD1* and *BLK*) significantly associated with LN compared to healthy controls ($P < 5 \times 10^{-8}$). Additionally, *PLD4* was found to be associated with LN, albeit at a less stringent significance level ($5 \times 10^{-8} < P < 5 \times 10^{-2}$) (Supplementary Figs S3-S5).

To further explore the genetic underpinnings of class V LN, we conducted GWAS using 2 comparison groups. First, we compared the genetic profiles of LN subgroups to those of healthy controls. This analysis revealed that *HLA-DQA1* is associated with both class V and class III/IV LN, while *GTF2IRD1, BLK*, and *PLD4* are associated with class III/IV (Table). Notably, GTF2IRD1 and BLK also showed associations with class V, although these did not reach genome-wide significance due to possible sample size limitations, with a significance level of $5 \times 10^{-8} < P < 5 \times 10^{-2}$ (Supplementary Table S5 and Figs S5-S6).

Second, when comparing MLN (class V) to PLN (class III/IV), *BLK* and *PLD4* showed associations with class V at a suggestive significance level ($5 \times 10^{-8} < P < 5 \times 10^{-2}$). These genes exhibit a gradient in minor allele frequencies (class III/IV > class V > healthy controls), suggesting they may be related to disease activity rather than subtype-specific effects. However, a notable exception is the rs609157 variant in the 3p25.3 region, which emerged as a potential genetic marker specifically associated with class V at genome-wide significance ($P = 3.04 \times 10^{-8}$). This SNP consistently showed association across different analytical approaches (Supplementary Tables S5-S6), with fine-mapping indicating it has the highest posterior probability (67.9%) of being the causal variant.

The rs609157-T allele is in linkage disequilibrium with the wild-type *IRAK2* allele (rs708035-T; D' = 1.0, $r^2 = 0.63$), whereas rs609157-C associates with the gain-of-function D431E variant (rs708035-A). This linkage pattern indicates that carriers of rs609157-T predominantly inherit the wild-type IRAK2 configuration, which shows reduced nuclear factor (NF)-κB activation compared to the D431E variant [5]. Blood expression quantitative trait locus (eQTL) analyses (eQTLGen Consortium, n = 31,684) confirm that rs609157-T correlates with lower *IRAK2* expression ($\beta = -0.15$, $P = 1.65 \times 10^{-32}$). The D431E variant enhances NF-κB signalling through accelerated TRAF6 ubiquitination and IκBα degradation, leading to elevated IL-6 production [5]. While rs708035-A acts as an eQTL for *IRAK2* in blood, brain and pancreas, neither SNP shows significant IRAK2 expression associations in kidney tissue (the Nephrotic Syndrome Study Network (NEPTUNE), n = 240; or Kidney eQTL Atlas, n = 686) (Supplementary Table S7 and Figs S7-S11). Protein–protein interaction analysis supports IRAK2's role in NF-κB pathway activation, interacting with key proteins like MYD88, IL1R1, TRAF6 and TLR4. For *IRAK2*, the allele associated with class V risk corresponds to a lower pathogenicity allele, consistent with protective effects observed for genes like *BLK* and *PLD4*

Yang Liu, Ting Gan and Yuan-yuan Qi contributed equally to this work. Ying Tan, Swapan K. Nath, Hong Zhang, and Xu-jie Zhou contributed equally as joint senior authors.

https://doi.org/10.1016/j.ard.2025.05.015
Received 24 December 2024; Revised 20 May 2025; Accepted 23 May 2025

Table
Identified loci associated with biopsy-proven lupus nephritis

CHR	BP (hg19)	SNP	Risk allele	LN MAF (%) (n = 2041)	MLN MAF (%) (n = 395)	MPLN+PLN MAF (%) (n = 1518)	Control MAF (%) (n = 524)	OR1	*P1*	OR2	*P2*	OR3	*P3*	OR4	*P4*	Gene
6	32601129	rs9272159	A	25.88	27.01	25.69	13.21	**2.30 (1.89-2.80)**	$\mathbf{1.36 \times 10^{-17}}$	**2.45 (1.92-3.11)**	$\mathbf{2.82 \times 10^{-13}}$	**2.38 (1.87-2.78)**	$\mathbf{1.96 \times 10^{-16}}$	1.07 (0.90-1.29)	4.07×10^{-1}	*HLA-DQA1*
7	73994733	rs17145600	T	29.10	28.75	29.14	20.46	**1.59 (1.35-1.88)**	$\mathbf{2.22 \times 10^{-8}}$	1.54 (1.25-1.91)	3.90×10^{-5}	**1.58 (1.34-1.87)**	$\mathbf{4.78 \times 10^{-8}}$	0.98 (0.82-1.16)	8.33×10^{-1}	*GTF2IRD1*
8	11338561	rs1531577	T	82.62	80.25	83.12	72.65	**1.79 (1.53-2.10)**	$\mathbf{3.77 \times 10^{-13}}$	1.51 (1.21-1.88)	1.60×10^{-4}	**1.83 (1.55-2.16)**	$\mathbf{1.93 \times 10^{-13}}$	**0.82 (0.67-1.01)**	4.17×10^{-2}	*BLK*
14	105391005	rs2841277	T	69.46	64.56	70.56	61.19	1.44 (1.25-1.66)	3.31×10^{-7}	1.15 (0.95-1.39)	1.39×10^{-1}	**1.51 (1.31-1.75)**	$\mathbf{2.00 \times 10^{-8}}$	**0.76 (0.64-0.89)**	9.86×10^{-4}	*PLD4*
3	10304829	rs609157	T	2.29	4.95	1.72	1.83	1.25 (0.76-2.06)	8.08×10^{-1}	**2.64 (1.53-4.57)**	1.67×10^{-4}	1.12 (0.66-1.88)	8.16×10^{-1}	**3.11 (2.04-4.73)**	$\mathbf{3.04 \times 10^{-8}}$	*IRAK2*

BP, base pair; CHR, chromosome; LN, lupus nephritis; MAF, mean allele frequency; MLN, membranous lupus nephritis; MPLN, mixed proliferative lupus nephritis; PLN, proliferative lupus nephritis; SNP, single nucleotide polymorphism.
Boldface values in the table footnote, linked to the $P < 5 \times 10^{-8}$ criterion, indicate that the corresponding results meet the threshold for genome-wide significance.
OR1 and p1: OR (95% CI) and *P* value for lupus nephritis versus healthy control (HC); OR2 and p2: OR and *P* value for MLN (class V) versus HC; OR3 and p3: OR and *P* value for MPLN (mix class III + V, IV + V) + PLN (class III, IV) versus HC; OR4 and p4: OR and *P* value for MLN versus non-MLN (class I, II, III, IV, VI and III + V, IV + V).

when comparing class V to class III/IV. This finding is consistent with GWAS results from primary membranous nephropathy (eg, *NFKB1* and *IRF4*) [6], suggesting shared mechanisms and potential therapeutic targets. However, further studies are needed to explore how rs609157-T and its linked missense variant influence immune responses in class V. While the rs609157-T allele indicates differences in pathophysiology between class V and class III/IV, it does not confer protection but points to distinct regulatory pathways requiring further investigation. Class III/IV renal tissues show greater NF-κB pathway activation than class V, potentially reflecting reduced IRAK2 expression and a milder inflammatory environment in class V [7].

This study highlights the distinct clinical, prognostic, and genetic profiles of class V and class III/IV LN. Notably, the risk allele associated with class V appears to reduce NF-κB activation, which is consistent with previous observations that class V involves less inflammation compared to class III/IV. While this association may contribute to understanding the unique clinical and pathological features of class V, it does not establish a direct mechanistic link, and pathogenesis may involve more complex regulation of inflammatory pathways than currently appreciated. The observed odds ratios (OR) >2.0 in MLN and PLN comparisons are intriguing, but we stress that the limited sample size of the MLN subgroup (resulting in 40-60% reduced power to detect ORs <1.5 compared to the full cohort) necessitates cautious interpretation. The tissue-specific expression patterns of IRAK2—robust eQTLs in blood but not in kidney tissue—raise interesting questions about the locus's primary effects, which may be mediated through systemic immune cell signalling rather than direct renal modulation. However, compartment-specific studies are required to investigate this further. Current kidney transcriptomic datasets confirm *IRAK2* expression in infiltrating macrophages and neutrophils but lack sufficient resolution to compare MLN and PLN subtypes directly. Future research should focus on class-stratified kidney biopsies, especially examining glomerular and tubulointerstitial compartments, and conduct targeted molecular analyses in subtype-defined renal tissue to clarify these genetic associations. *IRAK2* should therefore be considered a candidate locus of interest for MLN, pending further validation in independent cohorts. While our findings raise the possibility of novel therapeutic avenues—such as kidney-targeted immunomodulation—these implications remain speculative and should be explored in future studies. Ultimately, the translation of these genetic insights into clinical applications will require functional validation and replication in larger, multiethnic cohorts, as well as mechanistic studies to elucidate how these variants influence cellular processes across disease subtypes and tissue microenvironments.

Competing interests

None declared.

Acknowledgements

We wish to thank all the patients, and staffs from all the units that participated in the study.

Funding

Support was provided by National Key Research and Development Program of China (2024YFC2511000); National Science Foundation of China (82370709, 82470751, 82470752); Beijing Nova Program Interdisciplinary Cooperation Project

(20230484426); Beijing Natural Science Foundation (7242143); National High Level Hospital Clinical Research Funding (Interdisciplinary Clinical Research Project of Peking University First Hospital, 2024IR35, 2022CR41); Chinese Academy of Medical Sciences (CAMS) Innovation Fund for Medical Sciences (2019-I2M-5-046, 2020-JKCS-009); China International Medical Foundation (Z-2017-26-2202-2); the Self-Topic Fund of the State Key Laboratory of Vascular Homeostasis and Remodeling; and the Joint Institute (JI) Collaboration Scholars Program at the University of Michigan Medical School. The funder had no role in study design, data collection and analysis, decision to publish, or preparation of the manuscript.

Patient consent for publication

All patients and controls provided written informed consent.

Ethics approval

The study protocol was approved by the Ethical Committee of the Peking University First Hospital (2020−Y158) and the First Affiliated Hospital of Zhengzhou University (2019-KY-0033-002).

Provenance and peer review

Commissioned; externally peer reviewed.

Data availability statement

Summary statistics are available under reasonable request to the corresponding author.

Supplementary materials

Supplementary material associated with this article can be found in the online version at doi:10.1016/j.ard.2025.05.015.

Orcid

Yang Liu: http://orcid.org/0000-0001-9125-5786
Lizhong Wang: http://orcid.org/0000-0002-3571-8771
Xu-jie Zhou: http://orcid.org/0000-0002-7215-707X

REFERENCES

[1] Ward F, Bargman JM. Membranous lupus nephritis: the same, but different. Am J Kidney Dis 2016;68(6):954–66.
[2] Kostopoulou M, Mukhtyar CB, Bertsias G, Boumpas DT, Fanouriakis A. Management of systemic lupus erythematosus: a systematic literature review informing the 2023 update of the EULAR recommendations. Ann Rheum Dis 2024;83(11):1489–501.
[3] Kidney Disease: Improving Global Outcomes (KDIGO) Lupus Nephritis Work Group. KDIGO 2024 Clinical Practice Guideline for the management of LUPUS NEPHRITIS. Kidney Int 2024;105(1S):S1–69.
[4] Kiryluk K, Sanchez-Rodriguez E, Zhou XJ, Zanoni F, Liu L, Mladkova N, et al. Genome-wide association analyses define pathogenic signaling pathways and prioritize drug targets for IgA nephropathy. Nat Genet 2023;55(7):1091–105.
[5] Zhang W, He T, Wang Q, Li X, Wei J, Hou X, et al. Interleukin-1 receptor-associated kinase-2 genetic variant rs708035 increases NF-κB activity through promoting TRAF6 ubiquitination. J Biol Chem 2014;289(18):12507–19.
[6] Xie J, Liu L, Mladkova N, Li Y, Ren H, Wang W, et al. The genetic architecture of membranous nephropathy and its potential to improve non-invasive diagnosis. Nat Commun 2020;11(1):1600.
[7] Gilmore AC, Wilson HR, Cairns TD, Botto M, Lightstone L, Bruce IN, et al. Immune gene expression and functional networks in distinct lupus nephritis classes. Lupus Sci Med 2022;9(1):e000615.

Yang Liu[1], Ting Gan[1], Yuan-yuan Qi[2], Meng Tan[1], Lin-lin Xu[1], Yang Li[1], Jiong Liu[1], Shu Qu[1], Lizhong Wang[3,4,5], Gang Chen[3,4,5], Ji-cheng Lv[1], Zhan-Zheng Zhao[2], Wenjian Bi[6], Peipei Zhang[7], Ming-hui Zhao[1], Ying Tan[1], Swapan K. Nath[8], Hong Zhang[1], Xu-jie Zhou[1,*]

[1] *Renal Division, Peking University First Hospital; Kidney Genetics Center, Peking University Institute of Nephrology; Key Laboratory of Renal Disease, National Health Commission; Key Laboratory of Chronic Kidney Disease Prevention and Treatment (Peking University), Ministry of Education; and State Key Laboratory of Vascular Homeostasis and Remodeling, Peking University; Beijing, People's Republic of China*
[2] *Department of Nephrology, The First Affiliated Hospital of Zhengzhou University, Zhengzhou, Henan Province, People's Republic of China*
[3] *Hunan Provincial Key Lab on Bioinformatics, School of Computer Science and Engineering, Central South University, Changsha, People's Republic of China*
[4] *WeGene, Shenzhen Zaozhidao Technology Co. Ltd., TianAn CyberTech Plaza I, Futian Dist., Shenzhen, People's Republic of China*
[5] *Shenzhen WeGene Clinical Laboratory, Haikexing Industrial Park, Pingshan Dist., Shenzhen, People's Republic of China*
[6] *Department of Medical Genetics, School of Basic Medical Sciences, Peking University, Beijing, People's Republic of China*
[7] *Department of Biochemistry and Molecular Biology, School of Basic Medical Sciences, Peking University Health Science Center, Beijing, People's Republic of China*
[8] *Arthritis and Clinical Immunology Research Program, Oklahoma Medical Research Foundation, Oklahoma City, OK, USA*

*__Correspondence to__ Dr. Xu-jie Zhou, Renal Division, Peking University First Hospital, Kidney Genetic Center, Peking University Institute of Nephrology, Beijing, People's Republic of China.
E-mail address: zhouxujie@bjmu.edu.cn (X.-j. Zhou).

Ann Rheum Dis 84 (2025) e57–e59

Contents lists available at ScienceDirect

Annals of the Rheumatic Diseases

journal homepage: https://www.sciencedirect.com/journal/annals-of-the-rheumatic-diseases

Correspondence

Correspondence on 'In immune-mediated necrotising myopathy, anti-HMGCR antibodies inhibit HMGCR activity, leading to the sarcoplasmic accumulation of lipid droplets and myofibres necrosis' by Giannini et al.

With much interest, we read the article by Giannini et al [1] recently published in *ARD* lending further evidence to the hypothesis that anti-HMG-CoA reductase (HMGCR) autoantibodies are pathogenic in immune-mediated necrotising myopathy (IMNM) and not a mere bystander product of a given immune process. The authors provide interesting *in vitro* data that anti-HMGCR autoantibodies interfere with HMGCR activity and have a myopathic effect [2]. Their study is inspired by a recent article by Pinal-Fernandez et al [3] published in 2024, who showed that the autoantibodies are internalised into the cytoplasm of myofibres from patients with anti-HMGCR-associated IMNM. They also found *APOA4.6* was the only differentially expressed gene in their transcriptomic study, but internalisation of antibodies from anti-HMGCR-positive patients into cultured myoblasts did not lead to an increase in *APOA4* expression. Studying the extent of sarcoplasmic lipid droplets (LDs) in myofibres of patients with anti-HMGCR autoantibodies using Oil Red O, the authors identified 90% (18/20) of muscle biopsies from anti-HMGCR-positive patients had excess lipid accumulation compared with 8.3% (10/110) of patients with other types of myositis ($P < .001$). HMGCR dysfunction was deemed to induce accumulation of acetyl-CoA and the production of excess lipids [3]. Oil Red O stains were used in the present paper by Giannini et al [1] as well, and the authors describe 10-fold higher LD accumulation in patients with anti-HMGCR-associated IMNM compared with those with other immune-mediated and without neuromuscular diseases. However, their quantification method, using a semiquantitative scoring system [4] that was not developed for LD accumulation, may lack accuracy. We previously determined that Oil Red O stains are not suited to precisely identify the quality and quantity of LDs [5].

It seems very likely that autoantibody-mediated inhibition of HMGCR leads to triacylglyceride accumulation in the cytoplasm. HMG-CoA is formed by the condensation of 3 moles of acetyl-CoA and is then reduced by HMGCR to mevalonate, which is subsequently introduced into isoprene biosynthesis to finally become cholesterol. A block (via the autoantibody) may actually lead to accumulation of acetyl-CoA, which is instead channelled towards fatty acid synthesis followed by triacylglyceride biosynthesis. However, it remains unclear how LDs are involved in this conundrum. Hence, the complex interplay between LDs and cellular toxicity, particularly within the domains of mitochondrial and cytosolic compartments, remains poorly explored [6]. This is particularly important when it comes to establishing a hypothetical link between the necrotising aspect and the metabolic aspect of the disease.

Analysing microphotographs obtained by 2D electron microscopy, we provide a precise method to quantify the volume density of LDs in muscle fibres *in situ* [7]. This method not only offers unprecedented quality and quantification possibilities, but also informs about additionally altered subcellular structures such as mitochondria, endoplasmic reticulum or autophagolysosomal mechanisms and their spatial relationships in individual muscle fibres.

Quantification of LDs in muscle fibres of one patient's vastus lateralis muscles with HMGCR autoantibodies versus those of an anti-signal recognition particle autoantibody-positive patient and a nondiseased control as well as a patient with genetically proven multiple acyl-CoA dehydrogenase deficiency shows that the LDs can be precisely identified and quantified by calculation of the volume density of LD/entire muscle volume. In addition, qualitative data such as interaction with other subcellular organelles (eg, mitochondria) and quality of sarcomere integrity, etc. can be validated (Fig, Supplementary Fig and electronic Supplementary Material).

Handling editor Josef S. Smolen.

Nathalie Focks and Oliver Baum share first authorship.

Carsten Dittmayer and Werner Stenzel share last authorship.

https://doi.org/10.1016/j.ard.2025.07.006
Received 4 July 2025; Accepted 5 July 2025

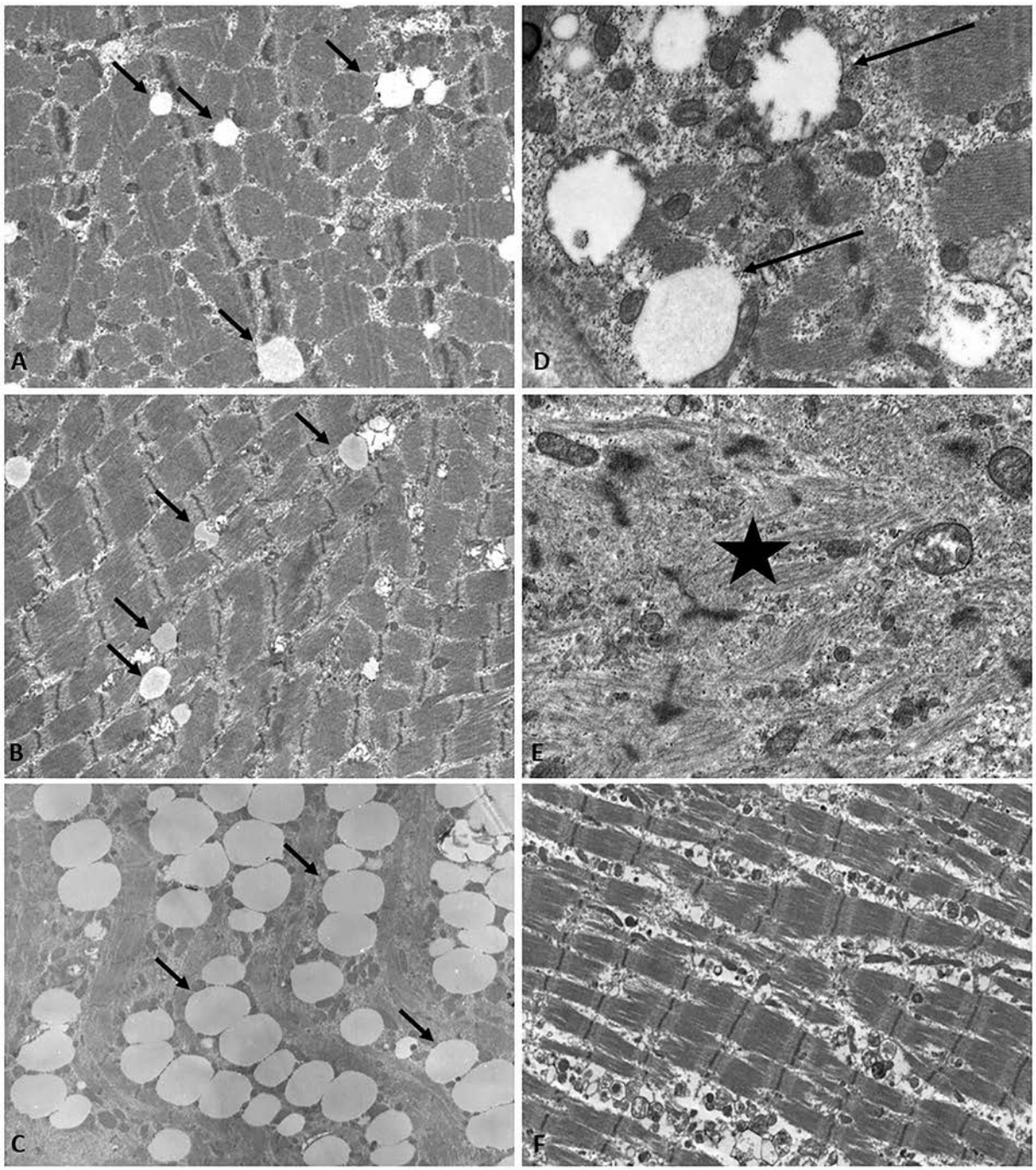

Figure. (A) Electron microscopic visualisation of skeletal muscle from a patient with anti-HMGCR+ IMNM. Lipid droplets are faint grey (black arrow). Original magnification, × 3000. (B) Electron microscopic visualisation of skeletal muscle from a patient with anti-SRP+ IMNM. Lipid droplets are faint grey (black arrow). Original magnification, × 3000. (C) Electron microscopic visualisation of skeletal muscle from a patient with riboflavin-responsive MADD. Lipid droplets are faint grey (black arrow). Original magnification, × 3000. (D) Mitochondria in close contact with lipid droplets in a patient with anti-HMGCR+ IMNM. Original magnification, × 20,000. (E) Disrupted sarcomere structures* in a patient with anti-HMGCR+ IMNM. Original magnification, × 20,000. (F) Diffuse accumulation of minute autophagolysosomal compartments within the sarcoplasm of a patient with anti-HMGCR+ IMNM. Original magnification, × 4000. HMGCR, 3-hydroxy-3-methylglutaryl-coenzyme A reductase; IMNM, immune-mediated necrotising myopathy; MADD, multiple acyl-CoA dehydrogenase deficiency; SRP, signal recognition particle.

Funding

The authors have no funding to report.

Competing interests

WS is affiliated with Charité University Hospital, Berlin. Germany. WS reports a relationship with World Muscle Society that includes: board membership. WS has no patents pending.

Patient consent for publication

Patient consent for publication was obtained.

Ethics approval

The Charité – Universitätsmedizin Berlin ethics committee has granted ethical approval (EA2/163/17 and EA1/019/22) for this study.

Provenance and peer review

Externally peer reviewed.

Supplementary materials

Supplementary material associated with this article can be found in the online version at doi:10.1016/j.ard.2025.07.006.

Orcid

Werner Stenzel: http://orcid.org/0000-0002-1143-2103

REFERENCES

[1] Giannini M, Quiring G, Oulad-Abdelghani M, Lannes B, Allenbach Y, Benveniste O, et al. In immune-mediated necrotising myopathy, anti-HMGCR antibodies inhibit HMGCR activity, leading to the sarcoplasmic accumulation of lipid droplets and myofibres necrosis. Ann Rheum Dis Published online May 22, 2025. doi: 10.1016/j.ard.2025.04.027.

[2] Allenbach Y, Arouche-Delaperche L, Preusse C, Radbruch H, Butler-Browne G, Champtiaux N, et al. Necrosis in anti-SRP$^+$ and anti-HMGCR$^+$ myopathies: role of autoantibodies and complement. Neurology 2018;90(6):e507–17. doi: 10.1212/WNL.0000000000004923.

[3] Pinal-Fernandez I, Muñoz-Braceras S, Casal-Dominguez M, Pak K, Torres-Ruiz J, Musai J, et al. Pathological autoantibody internalisation in myositis. Ann Rheum Dis 2024;83(11):1549–60. doi: 10.1136/ard-2024-225773.

[4] Olivier PA, De Paepe B, Aronica E, Berfelo F, Colman R, Amato A, et al. Idiopathic inflammatory myopathy: interrater variability in muscle biopsy reading. Neurology 2019;93(9):e889–94. doi: 10.1212/WNL.0000000000008005.

[5] Kleefeld F, von Renesse A, Dittmayer C, Harms L, Radke J, Radbruch H, et al. Successful plasmapheresis and immunoglobulin treatment for severe lipid storage myopathy: doing the right thing for the wrong reason. Neuropathol Appl Neurobiol 2022;48:e12731. doi: 10.1111/nan.12731.

[6] Smolková K, Gotvaldová K. Fatty acid trafficking between lipid droplets and mitochondria: an emerging perspective. Int J Biol Sci 2025;21(5):1863–73. doi: 10.7150/ijbs.105361.

[7] Dittmayer C, Goebel HH, Heppner FL, Stenzel W, Bachmann S. Preparation of samples for large-scale automated electron microscopy of tissue and cell ultrastructure. Microsc Microanal 2021;27(4):815–27. doi: 10.1017/S1431927621011958.

Nathalie Focks[1], Oliver Baum[2], Felix Kleefeld[1,3], Eleonora Torchia[1,4], Hans-Hilmar Goebel[1], Carsten Dittmayer[5], Werner Stenzel[1,*]

[1] *Department of Neuropathology, Charité – Universitätsmedizin Berlin, Berlin, Germany*

[2] *Department of Physiology, Charité – Universitätsmedizin Berlin, Berlin, Germany*

[3] *Department of Neurology, Bergmannsheil, Bochum, Germany*

[4] *Department of Neuroscience, Università Cattolica del Sacro Cuore, Rome, Italy*

[5] *Department of Pathology, Charité – Universitätsmedizin Berlin, Berlin, Germany*

*__Correspondence to__ Dr Werner Stenzel, Department of Neuropathology, Charité – Universitätsmedizin Berlin, Berlin, Germany.
E-mail address: werner.stenzel@charite.de (W. Stenzel).

Ann Rheum Dis 84 (2025) e60–e61

Contents lists available at ScienceDirect

Annals of the Rheumatic Diseases

journal homepage: https://www.sciencedirect.com/journal/annals-of-the-rheumatic-diseases

Response

Response to: 'Lipid droplets at center stage in IMNM? - An ultrastructural 2D large scale quantification' by Focks et al. New insights into pathology, serology, and pathophysiology highlight IMNM as a heterogeneous group of inflammatory myopathies

We read with great interest the comment by Focks et al [1], reporting quantitative and qualitative ultrastructural modifications of skeletal muscle fibres, obtained through large-scale 2-dimensional automated electron microscopy, in a patient with anti-HMGCR immune-mediated necrotising myopathy (IMNM) compared with 3 others (1 with anti-signal recognition particle (SRP) IMNM, 1 with multiple acyl-CoA dehydrogenase deficiency, and 1 without neuromuscular disease). The increased volume density of lipid droplets in the muscle fibres of anti-HMGCR patients is consistent with both (1) our findings [2] and those of others [3], as observed through optical microscopy, and (2) our demonstration that anti-HMGCR antibodies block HMGCR activity within the muscle fibres of these patients [2]. In addition, the observation by Focks et al [1] that mitochondria are in close contact with lipid droplets, along with the diffuse accumulation of minute autophagolysosomal compartments within the sarcoplasm, may shed new light on the pathophysiology of anti-HMGCR IMNM. Altogether, the clinical, serological, pathological, and pathophysiological hallmarks of patients with anti-HMGCR IMNM further delineate this condition as a distinct myopathy within the IMNM spectrum, an entity originally defined at the 2003 European Neuromuscular Centre (ENMC) workshop [4] and revised in 2016 [5].

Beyond this, we would like to emphasise that, based on similar methodological approaches, additional subgroups have recently been identified within the IMNM spectrum, suggesting that IMNM is actually more heterogeneous than the 3 categories proposed in the 2016 ENMC classification (anti-SRP+, anti-HMGCR+, and seronegative).

Scleromyositis, for instance, is an increasingly recognised inflammatory myopathy, characterised by a high rate of multisystem involvement, notably cardiac and pulmonary, which correlates with a poor prognosis [6]. Several autoantibodies have been specifically associated with this disease, some of which may exert a pathogenic effect [3,7]. In up to half of the cases, no autoantibodies are detected, making diagnosis particularly challenging. At the pathological level, approximately one-third of scleromyositis patients fulfil the ENMC criteria for IMNM [8,9]. Nonetheless, in line with capillaroscopic studies [10], electron microscopy performed by Focks et al [1] and others [11–14] has revealed distinctive capillary alterations in these patients, including basement membrane thickening and reduplication. The histopathological distinction of this entity is further supported by characteristic findings of skeletal muscle immunostaining [7,15]. Together, these clinical, serological, and pathological features delineate scleromyositis as a distinct myopathy within the classical IMNM spectrum.

More recently, immune-mediated megaconial myopathy has been reported as a newly recognised separate entity based on the observation of 5 patients with seronegative IMNM, all of whom exhibited giant mitochondria in skeletal muscle fibres, but no pathogenic variants in *CHKB*, a gene in which such electron microscopy findings were previously considered pathognomonic. These myopathic features, combined with a positive response to immunomodulatory treatment and the presence of pancreatic disease in all patients, support the recognition of this condition as another distinct subtype within the IMNM spectrum [16].

Altogether, these observations advocate for a refinement of the IMNM framework, integrating advances in pathology (including electron microscopy), autoantibody profiling, and pathophysiology, in order to achieve the level of precision needed for optimal patient management and to guide future research.

FUNDING

This research did not receive any specific grant from funding agencies in the public, commercial, or not-for-profit sectors.

Patient consent for publication

Not applicable.

Ethics approval

Not applicable.

Provenance and peer review

Not commissioned; externally peer reviewed.

https://doi.org/10.1016/j.ard.2025.07.027
Received 22 July 2025; Revised 28 July 2025; Accepted 29 July 2025

Competing interests

All authors declare they have no competing interests.

Orcid

Margherita Giannini: http://orcid.org/0000-0002-4834-5804

REFERENCES

[1] Focks N, Baum O, Kleefeld F, Torchia E, Goebel HH, Dittmayer C, Stenzel W. Lipid droplets at center stage in IMNM? - An ultrastructural 2D large scale quantification. Ann Rheum Dis 2025 in press.
[2] Giannini M, Quiring G, Oulad-Abdelghani M, Lannes B, Allenbach Y, Benveniste O, et al. In immune-mediated necrotising myopathy, anti-HMGCR antibodies inhibit HMGCR activity, leading to the sarcoplasmic accumulation of lipid droplets and myofibres necrosis. Ann Rheum Dis 2025 in press.
[3] Pinal-Fernandez I, Muñoz-Braceras S, Casal-Dominguez M, Pak K, Torres-Ruiz J, Musai J, et al. Pathological autoantibody internalisation in myositis. Ann Rheum Dis 2024;83(11):1549–60.
[4] Hoogendijk JE, Amato AA, Lecky BR, Choy EH, Lundberg IE, Rose MR, et al. 119th ENMC international workshop: trial design in adult idiopathic inflammatory myopathies, with the exception of inclusion body myositis, 10−12 October 2003, Naarden, The Netherlands. Neuromuscular Disord 2004;14(5):337–45.
[5] Allenbach Y, Mammen AL, Benveniste O, Stenzel W. Immune-Mediated Necrotizing Myopathies Working Group. 224th ENMC International Workshop: clinico-sero-pathological classification of immune-mediated necrotizing myopathies Zandvoort, The Netherlands, 14-16 October 2016. Neuromuscul Disord 2018;28(1):87–99.
[6] Giannini M, Ellezam B, Leclair V, Lefebvre F, Troyanov Y, Hudson M, et al. Scleromyositis: a distinct novel entity within the systemic sclerosis and autoimmune myositis spectrum. Implications for care and pathogenesis. Front Immunol 2022;13:974078.
[7] Holzer MT, Uruha A, Roos A, Hentschel A, Schänzer A, Weis J, et al. Anti-Ku + myositis: an acquired inflammatory protein-aggregate myopathy. Acta Neuropathol 2024;148(1):6.
[8] Lefebvre F, Giannini M, Ellezam B, Leclair V, Troyanov Y, Hoa S, et al. Histopathological features of systemic sclerosis-associated myopathy: a scoping review. Autoimmun Rev 2021;20(7):102851.
[9] Lim J, Rietveld A, De Bleecker JL, Badrising UA, Saris CGJ, van der Kooi AJ, et al. Seronegative patients form a distinctive subgroup of immune-mediated necrotizing myopathy. Neurol Neuroimmunol Neuroinflamm 2019;6(1):e513.
[10] Piette Y, Reynaert V, Vanhaecke A, Bonroy C, Gutermuth J, Sulli A, et al. Standardised interpretation of capillaroscopy in autoimmune idiopathic inflammatory myopathies: a structured review on behalf of the EULAR study group on microcirculation in Rheumatic Diseases. Autoimmun Rev 2022;21(6):103087.
[11] Siegert E, Uruha A, Goebel HH, Preuße C, Casteleyn V, Kleefeld F, et al. Systemic sclerosis-associated myositis features minimal inflammation and characteristic capillary pathology. Acta Neuropathol 2021;141(6):917–27.
[12] Ellezam B, Leclair V, Troyanov Y, Meyer A, Hudson M. Landon-Cardinal O. Capillary basement membrane reduplication in myositis patients with mild clinical features of systemic sclerosis supports the concept of 'scleromyositis.'. Acta Neuropathol 2021;142(2):395–7.
[13] Ellezam B, Leclair V, Troyanov Y, Bersali I, Giannini M, Hoa S, et al. Capillary pathology with prominent basement membrane reduplication is the hallmark histopathological feature of scleromyositis. Neuropathol Appl Neurobiol 2022;27:e12840.
[14] Corallo C, Cutolo M, Volpi N, Franci D, Aglianò M, Montella A, et al. Histopathological findings in systemic sclerosis-related myopathy: fibrosis and microangiopathy with lack of cellular inflammation. Ther Adv Musculoskelet Dis 2017;9(1):3–10.
[15] Lessard LER, Robert M, Fenouil T, Mounier R, Landel V, Carlesimo M, et al. Contribution of major histocompatibility complex class II immunostaining in distinguishing idiopathic inflammatory myopathy subgroups: a histopathological cohort study. J Neuropathol Exp Neurol 2024;83(12):1060–75.
[16] Santilli AR, Ni O, Milone M, Selcen D, Mehrabyan AC, Seth A, et al. Immune-mediated megaconial myopathy: a novel subtype of autoimmune myopathy. Neurology 2024;103(10):e210001.

Margherita Giannini[1,2,*], Giulia Quiring[2], Bernard Geny[1,3], Alain Meyer[1,2]
[1] *UR3072, Centre de Recherche en Biomédecine, Université de Strasbourg, Strasbourg, France*
[2] *Explorations fonctionnelles musculaires, Service de physiologie, Centre de référence des maladies autoimmunes rares, Hôpitaux Universitaires de Strasbourg, Strasbourg, France*
[3] *Service de physiologie et Explorations fonctionnelles, Hôpitaux Universitaires de Strasbourg, Strasbourg, France*

*__Correspondence to__ Dr Margherita Giannini.
E-mail address: gianninim@unistra.fr (M. Giannini).

Ann Rheum Dis 84 (2025) e62–e63

Contents lists available at ScienceDirect

Annals of the Rheumatic Diseases

journal homepage: https://www.sciencedirect.com/journal/annals-of-the-rheumatic-diseases

Correspondence

Correspondence on 'Janus kinase inhibitors enhance prostanoid biosynthesis in human whole blood *in vitro*: implications for cardiovascular side effects and prevention strategies' by Alabbasi et al

Dear Editor,

We read with great interest the recent study by Alabbasi et al [1], entitled 'Janus kinase inhibitors enhance prostanoid biosynthesis in human whole blood *in vitro*: implications for cardiovascular side effects and prevention strategies.' The authors reported that Janus kinase inhibitors (JAKis) increased thromboxane (TX)A_2 and prostaglandin (PG)E_2 biosynthesis *in vitro* in human whole blood and hypothesised that low-dose aspirin (ASA) may help mitigate these prothrombotic effects. However, we would like to raise several methodological concerns.

First, the analysis of variance (ANOVA) did not match the study design. Whole blood from the same donors was used across multiple JAKi concentrations, constituting a classic within-subject (repeated-measures) design. Nonetheless, the authors analysed these data using one-way ANOVA, which assumes that all groups are independent [2]. This violates the assumption of independence and ignores the correlation structure inherent in repeated measurements from the same biological source. Furthermore, this situation may underestimate the variability attributable to individual donors, potentially exaggerating the consistency of the observed effects across subjects. As a result, the derived *P* values may be artificially low, increasing the likelihood of false-positive findings [2]. More appropriate approaches would include repeated-measures ANOVA or linear mixed-effects modelling, which accounts for intradonor variability by including random intercepts for each subject [3]. Without this correction, conclusions about dose-response relationships and statistical significance may not be reliable.

Second, the authors used ASA at a final concentration of 100 μM in their *in vitro* experiments to demonstrate the suppression of TXB_2 biosynthesis and then extrapolated the observed inhibitory effects to support the use of 'low-dose ASA' in clinical settings. This inference is pharmacologically unjustified. A 100 μM plasma concentration corresponds to intravenous or high-dose ASA administration, whereas standard low-dose ASA (75-100 mg/d) produces peak plasma concentrations between 1 and 7 μM [4]. At these lower levels, COX-1 inhibition in platelets is well-documented [5], but its effects on JAKi-enhanced TXB_2 and PGE_2 biosynthesis are not established. The inhibition of COX-2–dependent TXB_2 and PGE_2 synthesis generally requires much higher systemic ASA concentrations. Thus, the observed suppression of both TXB_2 and PGE_2 at 100 μM ASA may reflect COX-2 involvement, which is unlikely to be inhibited under standard clinical ASA dosing regimens. Without *in vitro* validation at physiologic ASA levels or *in vivo* confirmation, the translational claim overstates the clinical applicability of the experimental results and may mislead readers into assuming that low-dose ASA offers protective cardiovascular benefits in JAKi-treated populations.

Third, the concentration range shown in Figure 1 as '0.04-20 mM' is inconsistent with the Methods description in the Abstract, where the range is given as '0.04-20 μM.' Although this may seem like a minor typographical issue, a 1000-fold difference in concentration is substantial. A value of 20 mM lies well outside the pharmacologically relevant range and would likely produce off-target or cytotoxic effects in most biological systems. Such inconsistencies between the figure and text undermine clarity and may mislead readers regarding the actual dosing used in the experiments.

Lastly, while the study provides valuable mechanistic insights into the use of *in vitro* whole blood assays, the translational relevance of these findings remains uncertain. The complex dynamics of *in vivo* inflammation, endothelial interactions, hepatic metabolism, and platelet turnover are not captured in this model. Moreover, limited information was provided about the clinical status, disease activity, or background medications of the patient groups, which could significantly influence prostanoid biosynthesis. Although the authors propose oxidative stress as a contributing mechanism, the evidence based on 8-iso-$PGF_2\alpha$ measurements was derived from a small subset of samples, limiting the strength of this conclusion.

Clarification of these issues is essential to ensure valid interpretation and to facilitate accurate clinical translation of the findings.

Contributors

All authors have contributed intellectually to the correspondence letter.

Handling editor. Josef S. Smolen.

https://doi.org/10.1016/j.ard.2025.05.018
Received 17 May 2025; Accepted 20 May 2025

Funding

The authors declare that they have not received a specific grant for this research from any funding agency in the public, commercial, or not-for-profit sectors.

Competing interests

None declared.

Patient consent for publication

Not applicable.

Ethics approval

Not applicable.

Provenance and peer review

Not commissioned; externally peer reviewed.

Data availability statement

No data are available.

Declaration of generative AI and AI-assisted technologies in the writing process

During the preparation of this work, the authors used ChatGPT-4o (OpenAI) in order to assist with spelling, grammar, and language refinement. After using this tool, the authors reviewed and edited the content as needed and took full responsibility for the content of the publication.

Orcid

Jian Huang: http://orcid.org/0000-0003-3504-6319

REFERENCES

[1] Alabbasi S, Tacconelli S, de Vries M, Gunnarsson I, Oke V, Kvarnström M, et al. Janus kinase inhibitors enhance prostanoid biosynthesis in human whole blood *in vitro*: implications for cardiovascular side effects and prevention strategies. Ann Rheum Dis 2025:S0003-4967(25)00882-9. In press. doi: 10.1016/j.ard.2025.03.014.

[2] Kim TK. Understanding one-way ANOVA using conceptual figures. Korean J Anesthesiol 2017;70:22–6. doi: 10.4097/kjae.2017.70.1.22.

[3] Muhammad LN. Guidelines for repeated measures statistical analysis approaches with basic science research considerations. J Clin Invest 2023;133:e171058. doi: 10.1172/JCI171058.

[4] Dovizio M, Tacconelli S, Sostres C, Ricciotti E, Patrignani P. Mechanistic and pharmacological issues of aspirin as an anticancer agent. Pharmaceuticals (Basel) 2012;5:1346–71. doi: 10.3390/ph5121346.

[5] Patrignani P, Filabozzi P, Patrono C. Selective cumulative inhibition of platelet thromboxane production by low-dose aspirin in healthy subjects. J Clin Invest 1982;69:1366–72. doi: 10.1172/jci110576.

Jian Huang [1,*], Seher Sener [2]

[1] *Clinical Laboratory Center, The First Affiliated Hospital of Guangxi Medical University, Nanning, China*

[2] *Division of Pediatric Rheumatology, Department of Pediatrics, Adana City Training and Research Hospital, Adana, Turkiye*

*__Correspondence to__ Dr. Jian Huang, Clinical Laboratory Center, The First Affiliated Hospital of Guangxi Medical University, Qingxiu District, Nanning, China.

E-mail address: huangjian_chn@163.com (J. Huang).

Ann Rheum Dis 84 (2025) e64–e66

Contents lists available at ScienceDirect

Annals of the Rheumatic Diseases

journal homepage: https://www.sciencedirect.com/journal/annals-of-the-rheumatic-diseases

Response

Response to correspondence: "Janus kinase inhibitors enhance prostanoid biosynthesis in human whole blood *in vitro*: implications for cardiovascular side effects and prevention strategies"

We appreciate the opportunity to respond and clarify the points raised.

1. Statistical analysis approach

Whole blood assays serve as capacity indices for prostanoid biosynthesis, and the aim of the present study was to assess the pharmacodynamics of Janus kinase (JAK) inhibitors in relation to prostanoid biosynthesis at varying concentrations of the drugs. This study was not designed to investigate differences in drug responses between healthy individuals and patients. This study included a single independent variable (drug concentration) and aimed to determine whether varying levels of this variable significantly influence a dependent variable, such as prostanoid biosynthesis. A one-way analysis of variance (ANOVA) is deemed appropriate for verifying this hypothesis. The 3 primary assumptions inherent in ANOVA were fulfilled: the responses of each factor level conformed to a normal distribution, these distributions exhibited homogeneity of variance (ie, the ratio of the smallest to the largest sample SDs was maintained between 0.5 and 2), and the data demonstrated independence. Whole blood samples obtained from various individuals were put into tubes or wells and independently stimulated with lipopolysaccharide (LPS) or allowed to clot. In the latter scenario, endogenous thrombin was generated, leading to variability in thrombin production across samples. Thus, different whole blood samples were independently prepared and treated with the inhibitors, thereby confirming that the assumption of data independence is upheld.

To enhance transparency, in the LPS-stimulated whole blood assay, we also reported unadjusted *P* values (from paired *t*-tests) in the table and underlined those that remained significant following the conservative Bonferroni correction. This dual reporting approach provides a balanced view: unadjusted *P* values may reveal trends and potential effects of other JAK inhibitors beyond tofacitinib that merit further investigation in additional individuals (thus reducing the risk of false negatives), while Bonferroni-corrected values offer stringent control over false positives. In the abstract and highlights, we emphasise findings that remained statistically significant following Bonferroni correction.

2. Interpretation of aspirin concentration and clinical relevance

In this *in vitro* study, we utilised biomarkers of platelet cyclooxygenase (COX)-1 activity, such as the assessment of thromboxane B_2 (TXB_2) generation in human whole blood allowed to clot for 1 hour at 37°C and leukocyte COX-2 activity in LPS-stimulated whole blood incubated at 37°C for 24 hours. These models have been extensively used to examine the effects of drugs that modulate the COX pathway of prostanoid generation, thereby gathering information on their pharmacodynamics [1–4]. The TXB_2 generated in serum after allowing whole blood to clot at 37°C is a biomarker of platelet capacity to generate TXA_2 from COX-1 activity in response to thrombin. Paola Patrignani contributed to the development of this assay, which was used to define the dose of aspirin for cardiovascular disease prevention [2]. Evidence suggests that serum TXB_2 that originates from platelets (i) in mice with specific deletion of COX-1 (*PTGS1*) in megakaryocytes/platelets, serum TXB_2 is almost completely inhibited (>95%) [5]; (ii) the administration of very low doses of aspirin, such as 0.45 mg/kg (approximately 30 mg/d), is associated with very low circulating levels of the active drug but leads to complete inhibition of serum TXB_2 levels after a week due to the cumulative inhibition of COX-1 in platelets [2]. The contribution of platelets is also supported by the time-dependent recovery of serum TXB_2, which requires approximately 10 days, corresponding to the entry of new platelets into circulation with intact COX-1 activity. Platelets do not express COX-2, at least under physiological conditions, but only COX-1 [6]. The cumulative inhibition of COX-1 by aspirin occurs because platelets lack a nucleus and have a limited capacity for de novo protein synthesis. Additionally, it is important to note that aspirin is an irreversible inhibitor of platelet COX-1 due to the acetylation of COX-1 at serine 529 [7]. After dosing with low-dose aspirin in humans, the inhibitory effect of aspirin occurs primarily in the presystemic circulation, while systemic levels of the drug contribute to this effect to a lesser extent [7,8]. This explains why achieving nearly complete inhibition of serum TXB_2 *in vitro* by aspirin requires higher concentrations of the drug. Patrignani's group published several papers reporting the characterisation of the concentration-dependent inhibition of serum TXB_2 by aspirin. The maximal inhibitory effect (>95%), like that obtained *in*

DOI of original article: http://dx.doi.org/10.1016/j.ard.2025.05.018.

https://doi.org/10.1016/j.ard.2025.06.2122
Received 5 June 2025; Accepted 7 June 2025

vivo after chronic dosing with low-dose aspirin, is achieved at 100 μM [9,10]. At this concentration, an almost maximal level of platelet COX-1 acetylation is attained [7]. Additionally, extra COX-1 arachidonic acid metabolites, such as 12S-hydroxyeicosatetraenoic acid, which is derived from platelet type 12-lipoxygenase and produced at high concentrations in serum, are not significantly affected [11]. Thus, employing 100 μM of aspirin, as detailed in the study by Alabbasi et al [12], effectively targets platelet COX-1 activity and TXA_2 production *in vitro*, mirroring the selective COX-1 inhibition of platelet COX-1 obtained *in vivo* with low doses of aspirin.

The other assay used in this study involved generating prostaglandin E_2 (PGE_2) and TXB_2 in whole blood after stimulation with LPS for 24 hours. In this assay, the primary targets of LPS are leukocytes, which produce prostanoids via COX-2 following time-dependent expression in response to LPS stimulation [3,13]. In this system, COX-2–dependent prostanoids become detectable in a time-dependent manner, linked to COX-2 induction, which occurs through both transcriptional and posttranscriptional mechanisms. Most of the aspirin added at time zero is profoundly inactivated before the high expression of COX-2 occurs in leukocytes. Aspirin is unstable in plasma due to esterases converting it to salicylate, a weak inhibitor of COX isozymes that requires concentrations in the millimolar range [9]. Additionally, acetylated COX-2 at serine 516, caused by aspirin, can be resynthesised for de novo protein synthesis in nucleated cells, such as blood leukocytes. Thus, in LPS-stimulated whole blood, PGE_2 is primarily produced by induced leukocyte COX-2. In isolated monocytes, we previously showed that 100 μM of aspirin caused incomplete inhibition of COX-2–dependent PGE_2 production [9]. As shown in Figure 6 in the paper by Alabbasi et al [12], aspirin caused partial inhibition of COX-2–dependent PGE_2 at 100 μM both without and with tofacitinib. These data suggest that tofacitinib promotes increased COX-2–dependent PGE_2 production, while aspirin partially inhibits this effect by inhibiting COX-2 activity. In LPS-stimulated whole blood, TXB_2 can arise from COX-2, but COX-1 contributions from platelets and monocytes can also occur. The finding that aspirin was more effective in inhibiting TXA_2 than PGE_2 suggests an inhibitory effect on platelet TXA_2 generation.

Overall, these data indicate that platelet TXA_2 can be produced in response to the platelet agonist thrombin in platelets, as well as from leukocytes and platelets in response to LPS. JAK inhibitors modified the regulation of prostanoid biosynthesis in response to proaggregatory and inflammatory stimuli. Aspirin was able to largely eliminate the contribution of platelets to the increased TXA_2 biosynthesis induced by JAK inhibitors.

3. Concentration typographical error

We thank the correspondents for identifying the inconsistency in the reported concentration range. The correct range used in the experiments is 0.04 to 20 μM, as stated in the abstract, Methods section, and figures.

4. *In vitro* model limitations and translational relevance

According to the conclusions of the paper by Alabbasi et al [12], a mechanistic study should be conducted *in vivo* in patients before recommending aspirin to mitigate the potential increased risk of cardiovascular events associated with JAK inhibitors. In the study by Alabbasi et al [12], most of the data on JAK inhibitors were obtained from healthy subjects, as we aimed to avoid the possibility that the response could be influenced by the disease condition. We also demonstrated that patients' whole blood undergoes altered prostanoid generation in response to JAK inhibitors. The findings of this study provide a rationale for designing a clinical trial involving patients receiving JAK inhibitors to confirm the altered generation of prostanoids and investigate whether low-dose aspirin can mitigate it. Our preliminary data suggest that an increase in oxidative stress biomarkers in response to JAK inhibitors requires validation in a mechanistic clinical study involving patients.

We believe this response provides the necessary clarification regarding the points raised.

Competing interests

PP reports financial support was provided by Queen Mary University of London Faculty of Medicine and Dentistry. The other authors declare they have no competing interests.

CRediT authorship contribution statement

Helena Idborg: Conceptualization, Writing – original draft, Writing – review & editing. **Per-Johan Jakobsson:** Conceptualization, Writing – review & editing, Supervision. **Paola Patrignani:** Conceptualization, Writing – original draft, Writing – review & editing, Supervision.

Funding

This study was supported by the Stockholm county research council FoUI-987035, Swedish research council 2023-02305, Ulla and Gustafaf Ugglas foundation 2023 (2023-02503), Swedish Rheumatism Association (grantR-995601), The Swedish Cancer Society 222092, and King Gustaf V's 80 Years Foundation. Part of this work was conducted on behalf of the Aspirin for Cancer Prevention Group, Wolfson Institute of Preventive Medicine, Queen Mary School of Medicine and Dentistry, University of London (UK) to PP.

Patient consent for publication

Not applicable.

Ethics approval

Not applicable.

Provenance and peer review

Not commissoned; externally peer reviewed.

Orcid

Helena Idborg: http://orcid.org/0000-0003-4041-4729

REFERENCES

[1] Patrono C, Patrignani P, Rodríguez LA. Cyclooxygenase-selective inhibition of prostanoid formation: transducing biochemical selectivity into clinical read-outs. J Clin Invest 2001 Jul;108(1):7–13.
[2] Patrignani P, Filabozzi P, Patrono C. Selective cumulative inhibition of platelet thromboxane production by low-dose aspirin in healthy subjects. J Clin Invest 1982 Jun;69(6):1366–72.
[3] Patrignani P, Panara MR, Greco A, Fusco O, Natoli C, Iacobelli S, et al. Biochemical and pharmacological characterization of the cyclooxygenase

activity of human blood prostaglandin endoperoxide synthases. J Pharmacol Exp Ther 1994 Dec;271(3):1705–12.
[4] Patrignani P, Patrono C. Cyclooxygenase inhibitors: from pharmacology to clinical read-outs. Biochim Biophys Acta 2015 Apr;1851(4):422–32.
[5] Bruno A, Contursi A, Tacconelli S, Sacco A, Hofling U, Mucci M, et al. The specific deletion of cyclooxygenase-1 in megakaryocytes/platelets reduces intestinal polyposis in $Apc^{Min/+}$ mice. Pharmacol Res 2022 Nov;185:106506.
[6] Patrignani P, Sciulli MG, Manarini S, Santini G, Cerletti C, Evangelista V. COX-2 is not involved in thromboxane biosynthesis by activated human platelets. J Physiol Pharmacol 1999 Dec;50(4):661–7.
[7] Patrignani P, Tacconelli S, Piazuelo E, Di Francesco L, Dovizio M, Sostres C, et al. Reappraisal of the clinical pharmacology of low-dose aspirin by comparing novel direct and traditional indirect biomarkers of drug action. J Thromb Haemost 2014 Aug;12(8):1320–30.
[8] Pedersen AK, FitzGerald GA. Dose-related kinetics of aspirin. Presystemic acetylation of platelet cyclooxygenase. N Engl J Med 1984 Nov 8;311 (19):1206–11.
[9] Dovizio M, Bruno A, Tacconelli S, Patrignani P. Mode of action of aspirin as a chemopreventive agent. Recent Results Cancer Res 2013;191:39–65.
[10] Hofling U, Tacconelli S, Contursi A, Bruno A, Mucci M, Ballerini P, et al. Characterization of the acetylation of cyclooxygenase-isozymes and targeted lipidomics of eicosanoids in serum and colon cancer cells by the new aspirin formulation IP1867B versus aspirin *in vitro*. Front Pharmacol 2022;13:1070277.
[11] Tacconelli S, Fullone R, Dovizio M, Pizzicoli G, Marschler S, Bruno A, et al. Pharmacological characterization of the biosynthesis of prostanoids and hydroxyeicosatetraenoic acids in human whole blood and platelets by targeted chiral lipidomics analysis. Biochim Biophys Acta Mol Cell Biol Lipids 2020 Dec;1865(12):158804.
[12] Alabbasi S, Tacconelli S, de Vries M, Gunnarsson I, Oke V, Kvarnström M, et al. Janus kinase inhibitors enhance prostanoid biosynthesis in human whole blood *in vitro*: implications for cardiovascular side effects and prevention strategies. Ann Rheum Dis 2025 May 5.
[13] Bergqvist F, Sundström Y, Shang MM, Gunnarsson I, Lundberg IE, Sundström M, et al. Anti-inflammatory properties of chemical probes in human whole blood: focus on prostaglandin E_2 production. Front Pharmacol 2020;11:613.

Helena Idborg [1,2,*], Per-Johan Jakobsson[1,2,1], Paola Patrignani[3,4,#]

[1] *Division of Rheumatology, Department of Medicine, Solna, Karolinska Institutet, and Karolinska University Hospital, Stockholm, Sweden*
[2] *Center for Molecular Medicine, Stockholm, Sweden*
[3] *Systems Pharmacology and Translational Therapeutics Laboratory, Center for Advanced Studies and Technology (CAST), G. d'Annunzio University, Chieti, Italy*
[4] *Department of Neuroscience, Imaging and Clinical Science, G. d'Annunzio University Medical School, Chieti, Italy*

*__Correspondence to__ Dr. Helena Idborg. (H. Idborg).
E-mail address: helena.idborg@ki.se (H. Idborg).
[#]Shared last authorship.